Journal of Biological Regulators & Homeostatic Agents
Volume 29, No. 4, October - December, 2015

CONTENTS

JOURNAL OF BIOLOGICAL REGULATORS & HOMEOSTATIC AGENTS Vol. 29, no. 4, 745-753 (2015)

EDITORIAL

mTORC2-Akt SIGNALING AXIS IS IMPLICATED IN MYOCARDIAL COMPENSATION AND FIBROSIS

M. DANY[1], H.H. RIMMANI[1], S.A. MATAR[1] and I. HAJJ HUSSEIN[2]

[1]College of Medicine, Medical University of South Carolina, Charleston, USA; [2]School of Medicine, Oakland University William Beaumont, Rochester, USA

Received October 4, 2015 – Accepted October 27, 2015

mTOR signaling has long been implicated in the mechanisms of cardiomyocyte survival in response to volume or pressure overload. Several studies have focused on the significance of mTORC1 in cardiomyocyte survival, questioning the role of mTORC2. mTORC2–Akt signaling is an emerging axis implicated in cardiomyocyte compensation and thus heart failure. Upon being subjected to chronic stress, cardiomyocytes activate mTORC2–Akt signaling pathway to promote survival by activating the ubiquitin proteasome system, inducing the degradation of pro-apoptotic proteins, and altering the actin cytoskeleton. Given the importance of mTORC2 in cardiomyocyte survival, studies suggest that loss of mTORC2 signaling would result in loss of cardiomyocytes, fibrosis, and heart failure. This review serves to elaborate on how mTORC2-Akt signaling plays a role in cardiomyocyte growth and survival under stress and how the loss of the axis would result in fibrosis and heart failure.

When cardiomyocytes are subjected to pressure or volume overload, a hypertrophic growth mechanism instigates to allow the cells to survive and maintain ventricular function. However, when the overload increases or persists for a long time, as in aortic valve stenosis or hypertension, the growth mechanism fails to compensate and tissue remodeling occurs leading to loss of cardiomyocytes, fibrosis, and congestive heart failure (1).

Recent studies have attempted to shed light on the signaling pathways involved in the initial compensatory growth mechanism and the alterations that take place during the transition to the non-adaptive state. One pathway implicated in cardiomyocyte survival in response to hemodynamic overload is mTOR signaling (2, 3). mTOR (mammalian target of Rapamycin) is a serine/threonine kinase that acts as a sensor of intracellular energy and nutritional status, thus regulating energy production, protein synthesis, ribosomal biogenesis, and cell growth (4). In addition to hemodynamic overload, mTOR signaling was found to be protective in the process of ischemic preconditioning where the cardiomyocytes act to prevent their own death. To function as a pro-survival kinase, mTOR associates with other proteins to form two independent complexes, mTORC1 and mTORC2 (5). Even though evidence suggests that both complexes 1 and 2 promote cardiomyocyte survival during pressure overload, each complex signals independently and has its own set of protein composition (4, 6). Specifically, mTORC1 regulates cell growth by activating p70S6 kinase (S6K1), 4E

Key words: mTORC2, Akt, heart compensation, heart failure

Mailing address:
Mohammed Dany,
Medical Scientist Training Program,
College of Medicine,
Medical University of South Carolina,
Charleston, SC, 29425, USA
e-mail: dany@musc.edu

0393-974X (2015)

Binding Protein (4EBP), and Protein phosphatase 2A. On the other hand, mTORC2 promotes cell growth by altering the actin cytoskeleton and activating Protein Kinase B (Akt) (4, 5). The protein composition of each complex regulates their response to the inhibitor Rapamycin: mTORC1 contains Raptor and is sensitive to Rapamycin; mTORC2 contains Rictor and is not sensitive to Rapamycin (6, 7).

Many studies highlighted the importance of mTORC1 in promoting survival of cardiomyocytes; however, when Rapamycin was used as a treatment modality *in vivo*, some studies reported that it was effective while others showed that it was not effective in abolishing cardiac hypertrophy (8). Because of the insensitivity of mTORC2 to Rapamycin, speculations concerning the role of the second leg of mTOR signaling started to form. Recently, several studies attempted to describe the mechanism by which mTORC2 promotes growth and survival in overloaded cardiomyocytes. This review serves to elaborate on how mTORC2 plays a role in cardiomyocyte growth and survival under stress and how Akt is involved in this signaling pathway.

The activation of mTORC2

A number of factors can activate mTOR signaling. A very common pathway is through the binding of soluble growth factors, such as insulin and insulin growth factor (IGF), to cell surface receptors causing phosphorylation of insulin substrate receptor (IRS). This recruits phospho-inositide-3-kinase (PI3K) that will generate phospho-inositide-3-phosphate (PIP3). PIP3 is able to recruit and activate Akt, which then activates mTORC1 (3). At the same time, PIP3 will also activate mTORC2. Interestingly, it is well established that mTORC2 also activates Akt (6, 9). Since Akt activates mTORC1 and mTORC2 activates Akt, one can speculate whether mTORC2 activates mTORC1. Studies, however, show that mTORC2 activates a different pool of Akt that is not involved in mTORC1 activation (10). mTORC1 and mTORC2 can also be activated during starvation, changes in energy status, and stress as in pressure or volume overload in cardiomyocytes (13).

mTOR complex 2 activates Akt

Several studies showed that mTOR signaling activates Akt in several cell lines, including cardiomyocytes (2, 9). Akt, also known as Protein Kinase B, promotes survival and anti-apoptotic signals by inducing ribosomal biogenesis, protein synthesis, transcription, and other mitogenic functions (11). It has three isoforms, Akt 1,2 and 3, with Akt1 being very prevalent in the heart (11). Akt protein has two critical residues that need to be phosphorylated for it to be active: Threonine 308 and Serine 473. It is known that PDK1 (PI3K-dependent kinase) is responsible to phosphorylate Akt at the T308 residue in the activation loop. Recently, it was shown that mTORC2 is the one required to phosphorylate Akt at the S473 residue in the hydrophobic site (9). Indeed, activation of mTOR signaling by agonist stimulation (insulin treatment) induced the phosphorylation of Akt (2). Likewise, shRNA mediated silencing of Rictor, a component in mTORC2, abrogated Akt phosphorylation. Pharmacological inhibition of mTORC1 alone by Rapamycin increased the activation of p-Akt, however inhibition of both mTORC1 and mTORC2 by Torin-1 prevents insulin mediated Akt phosphorylation (2). One study addressed the surprising outcome of increased p-Akt after Rapamycin treatment to the loss of negative regulation of S6K1 on IRS-1 and Rictor: when mTORC1 activates S6K1, S6K1 leads to the phosphorylation of IRS-1 and Rictor at critical sites that inactivates them. Rapamycin blocks mTORC1 and thus activates IRS-1 and Rictor, both of which are required to switch on the mTORC2/Akt signaling pathway (2). All the mentioned studies lead to the conclusion that mTORC2, and not mTORC1, is specific for phosphorylating and activating Akt.

PKCε activation by mTORC2 is required to phosphorylate and activate Akt

A detailed study on how mTORC2 signaling activates Akt showed that this process is dependent on Protein Kinase C epsilon PKCε**.** PKCε is a pro-survival kinase in cardiomyocytes (12). Adult feline cardiomyocytes transfected with a vector containing dominant negative PKCε had lower levels of Akt phosphorylation without a change in mTOR phosphorylation levels, suggesting that PKCε plays a role upstream of Akt but downstream of mTORC2 (2).

IPKCε was recently established to be downstream of mTORC2. Silencing of Rictor by shRNA abolished

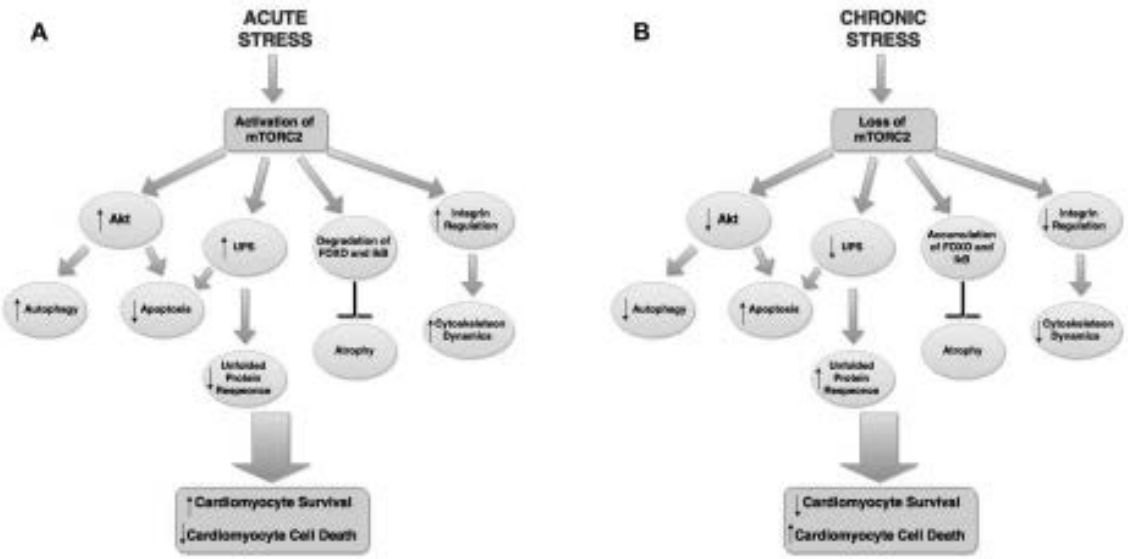

Fig. 1. *The role of mTORC2 in acute vs chronic stress in cardiomyocytes.* ***A)*** *mTORC2 is activated in acute stress to result in cardiomyocyte survival. This is via activation of Akt signaling to promote survival autophagy and inhibit apoptosis; activation of the unfolded protein response; degradation of FOXO and IkB to prevent atrophy; and increases cytoskeletal dynamics via altering integrins.* ***B)*** *Chronic exposure of cardiomycoytes to stress such as pressure or volume overload, results in loss of mTORC2 signaling to result in cardiomyocyte cell death and fibrosis, via loss of Akt and unfolded protein response and activation of FOXO and IkB to promote atrophy.*

the phosphorylation of PKCε S729. In addition, pharmacological inhibition of both mTORC1 and mTORC2 using Torin-1 blocked the phosphorylation of PKCε. However, pharmacological inhibition of mTORC1 alone by Rapamycin did not decrease the levels of active p-PKCε S729 (2). This suggests that PKCε is regulated specifically by mTORC2.

mTORC2, hence, activates PKCε which in turn can activate Akt. The complex comprising Rictor, PKCε, and Akt was detected by immunoprecipitation in cardiomyocytes stimulated by insulin after pulling down one of the components and blotting for the other two. The formation of this complex is PI3Kdependent, as inhibition of PI3K prevented the ability of insulin to induce the formation of the complex. Moreover, Raptor, a component of mTORC1, was not detected in the complex, confirming that mTORC2, and not mTORC1, specifically regulates PKCε/Akt axis (2).

mTORC2-mediated activation of Akt is required for cardiomyocyte growth and survival during hemodynamic overload

In acute stress, mTORC2 activates Akt which promotes regeneration and prevents apoptotic and autophagic cell death (11). Recent studies addressed the question whether Akt is required for hypertrophy and survival in cardiomyocytes during hemodynamic overload (14). *In vivo*, cells of a right ventricle subjected to pressure overload had much higher levels of p-Akt S473 compared to cells of a normally loaded left ventricle in the same heart. Another study showed that mice with overexpression of Akt had hearts with significantly larger size and higher contractility compared to control mice. Moreover, Akt-deficient mice had an exaggerated hypertrophic response and pronounced fibrosis upon subjecting the heart to pressure overload. The Akt-deficient mice did not develop swim-training-induced physiological heart hypertrophy and their cardiomyocytes did not show an induction in protein synthesis when stimulated with IGF-1. This suggests that Akt phosphorylation and subsequent activation have important physiological roles that allow cardiomyocytes under stress to induce protein synthesis and other protective processes for the cells to grow, survive, and compensate in order maintain a

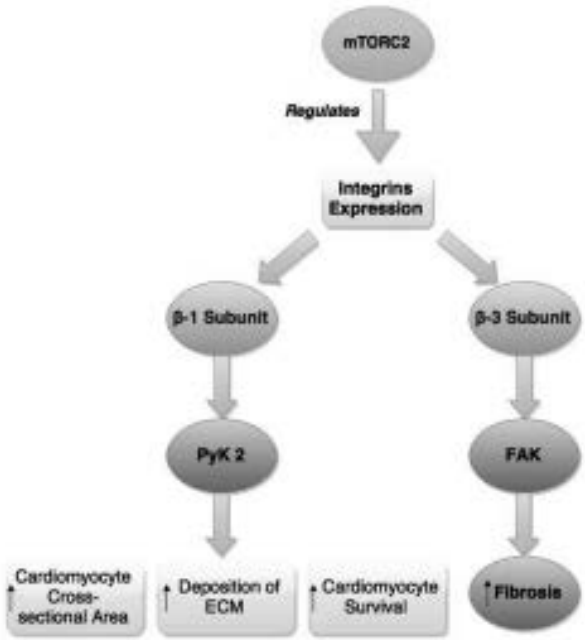

Fig.2. *The role of integrins in mTORC2 mediated cardiomyocyte survival. mTORC2 signaling regulates integrins expression in both cardiomyocytes and fibroblasts of the myocardium. It can either result in cardiomyocyte survival through the β-3 subunit or Focal Adhesion Kinase (FAK) dependent fibrosis through the β-2 subunit.*

normal ventricular function.

Interestingly, the cellular location of Akt is of great importance in the context of cardiomyocyte hypertrophy. Some studies believe that Akt localization to the nucleus enhances the cardiomyocyte response to hemodynamic overload and improves systolic function. This sheds light that Akt activation by mTORC2 in the nucleus might be more beneficial than cytoplasmic activation (15). The importance of Akt nuclear localization and the mechanism inside the nucleus is not yet fully understood.

mTORC2/Akt axis promotes survival in cardiomyocytes by activating the ubiquitin proteasome system

The ubiquitin-proteasome system (UPS) serves to degrade proteins by tagging them with ubiquitin moieties to end up in proteasomes. These proteins are usually denatured, misfolded, or short-lived (16). During stress conditions, there is an increase in the accumulation of such proteins, which is harmful for the cell because unfolded proteins induce ER stress and apoptotic signals. When cardiomyocytes are under stress, as in pressure overload, one way to survive cell death is to activate the UPS system to degrade the accumulating deleterious proteins (17).

There is strong evidence suggesting that the mTORC2/Akt axis plays an important role in activating the UPS system. Inhibiting mTOR or Akt resulted in a decrease in ubiquitin-mediated proteolysis. Interestingly, inhibition of UPS resulted in a decrease in mTOR and Akt phosphorylation. This shows that UPS functions both upstream and downstream of mTORC2, and that there is some sort of a feedback loop. Some studies also show that the two systems are highly interconnected and that the amino acids generated from UPS-mediated degradation of proteins can be used to synthesize proteins that support mTORC2 (16-18).

The UPS system is very relevant in the context of cardiac hypertrophy. Upon pharmacological inhibition of proteasomal degradation, the hypertrophic growth of cardiomyocytes was prevented in response to stress (18). At the same time, hearts with congestive heart failure have much higher levels of ubiquitin-tagged deleterious proteins accumulating in their cells, suggesting that the degradation process is suppressed in the de-compensating state, and that heart failure is preceded by UPS dysfunction (18) (Fig. 1 A.).

mTORC2/Akt axis promotes survival in cardiomyocytes by inducing the degradation of pro-apoptotic proteins

mTORC2 and Akt activation can also regulate the phosphorylation and ubiquitination of the pro-apoptotic proteins FOXO and IkB (19, 23).

FOXO is a transcription factor that activates the expression of genes implicated in cell atrophy. These include atrogenes (e.g. MURF1), regulators of the breakdown of myofibrils, and Atrogin 1, an inhibitor of calcineurin, a Ca2+ dependent phosphatase that promotes hypertrophy (20, 21). In addition, FOXO activates the expression of LC3B and Bnip3, both of which are required for autophagy programmed cell death (22). Upon mTORC2 activation of Akt, FOXO

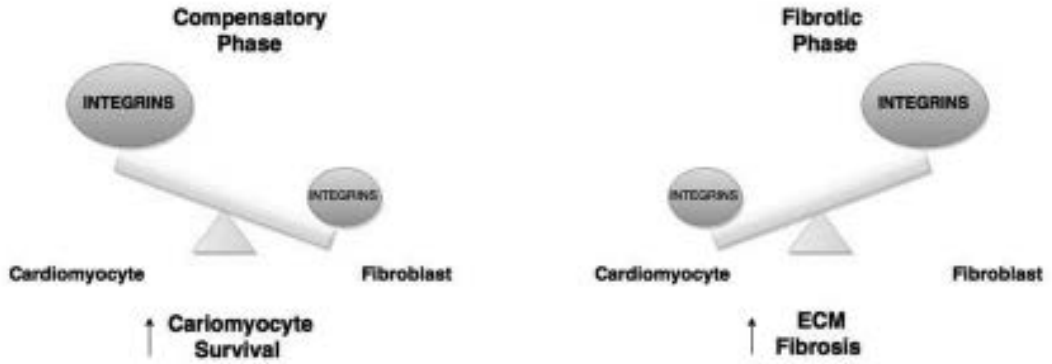

Fig. 3. *Proposed mechanism for the role of integrins in fibroblasts versus cardiomyocytes in compensatory phase or heart failure. We propose that there exists a delicate balance in the integrins expression between the cardiomyocytes and fibroblasts. A disruption of the balance results in either myocardial compensation or fibrosis. In acute stress, there is increased integrins expression in cardiomyocytes to result in cardiomyocyte survival. However, in chronic stress the balance of integrin expression is swayed towards fibroblasts resulting in increased deposition of ECM, atrophy, and fibrosis.*

becomes phosphorylated, leading to its expulsion from the nucleus and its subsequent degradation (18). Again, studies showed that FOXO inactivation is dependent on mTORC2 and not on mTORC1 (421).

IkB is the inhibitor of NFkB transcription factor, which is required for hypertrophic growth. Akt signaling inactivates IkB leading to an increase in the activity of NFkB and therefore initiating hypertrophy (23). Overexpression of IkB mutant that cannot be inactivated by phosphorylation prevented the development of stress-induced hypertrophy (23). Hence, mTORC2/Akt activates NFkB and leads to its nuclear localization where it acts as a transcription factor for several survival genes.

mTORC2 promotes cardiomyocyte survival by altering the actin cytoskeleton

Another mechanism by which mTORC2 promotes survival in stressed cardiomyocyctes is by affecting the dynamics of the cytoskeleton to result in an increased spatial cell growth (24). Studies showed that mTORC2 activation initiated the formation of actin fibers. In the same context, the silencing of Rictor or mTOR using siRNA resulted in defective actin fiber assembly (25). The mechanism is through mTORC2 activation of Rho 1 GTPase. Rho 1 in turn activates PKC1 and MAPK, both of which are required for actin polymerization and cell spreading. Rac-1, a protein important for hypertrophy, also plays a role in this pathway (24,25). However, it is still unclear how mTORC2 controls this process and how it acts as a switch for Rho GTPases.

Mechanisms by which the loss of mTORC2 results in loss of cardiomyocytes

Loss of cardiomyocytes and development of fibrosis underlie the development of congestive heart failure and increased mortality (26). We have shown so far that activation of mTORC2 signaling promotes cardiomyocyte survival; thus, it is important to understand the mechanisms of how the loss of mTORC2 can lead to cardiomyocyte cell death and fibrosis (Fig. 1B.).

As mentioned earlier, Akt is a mitogenic factor that can inhibit apoptotic cell death pathways. As such, if mTORC2 activity is lost in chronic pressure overload, it is expected that Akt phosphorylation and activation would become abolished, leading to the removal of suppression on the apoptotic pathways. In addition, Akt is known to suppress autophagy, a self-digestion mechanism (27). During autophagy, phagophore membranes engulf organelles and large molecules

to form autophagosomes (28). These can then fuse with lysosomes to form autophagolysososmes in which hydrolytic enzymes digest and hydrolyze the organelles (26-28). Even though autophagy promotes survival in some cases by providing amino acids to the cell, chronic activation of autophagy leads to autosis - a.k.a. autophagy programmed cell death (28). This is because an increase in autophagy will deplete the cell from its essential organelles resulting in cell death (27, 28). Hence, loss of mTORC2/Akt axis can lead to cell death by promoting apoptotic and autophagic cell death.

Moreover, loss of mTORC2/Akt axis can lead to the dysregulation of the ubiquitin proteasome system UPS (17). The inactivation of UPS causes the accumulation of deleterious proteins that are unfolded or denatured which can lead to initiation of apoptotic signals and ER stress, which itself can cause cell death (28). As mentioned earlier, studies have shown that heart failure is preceded by UPS dysfunction.

In addition, loss of mTORC2/ Akt axis can lead to upregulation of FOXO and IkB factors, which results in cardiomyocyte atrophy and death. FOXO and IkB are usually tagged for degradation downstream of mTORC2/Akt signaling. However, when this signaling is lost in chronic pressure overload, FOXO becomes more stable to act as a transcription factor for atrogenes that degrade myofibrils and atrophins that cause atrophy (20). Stability of IkB also increases, leading to decreased NFkB mediated survival signals (23).

Finally, loss of mTORC2 leads to defects in the actin cytoskeleton, which is crucial for cell survival. Another class of proteins called integrins also regulate the cytoskeletal dynamics via cytoskeletal associated proteins and kinases (29). Integrin signaling is critical for cardiomyocyte survival (29). Studies show that signaling pathways of mTORC2 and integrins are interlinked, where it is suspected that mTORC2 might be upstream of β1 and β3 integrin activation (30). Hence, loss of mTORC2 can lead to perturbations in integrin signaling resulting in loss of caridomyocytes (Fig. 2).

Loss of mTORC2 can promote cardiac fibrosis

Apart from cardiomyocytes, the heart tissue is comprised of other cell types such as fibroblasts, endothelial cells, and smooth muscle cells (31). As such, it is important to consider the roles of these cells in pressure overload. Cardiac fibrosis in heart failure ensues when fibroblasts excessively proliferate and increase their release of extracellular matrix proteins, such as collagen, fibronectin, and laminin (32). This causes increased stiffness, perivascular scarring, and myocardial dysfunction (33).

Studies have shown that integrins and their associated signaling pathways play an important role in the pathological fibrosis observed in heart failure (34, 35). Integrins are receptors on the cell surface known for their bidirectional signaling that links extracellular and intracellular events. Thus, they are important for cell migration, adhesion, proliferation, and ECM deposition. Integrins are composed of two proteins, alpha and beta, that form a heterodimer, and that recruit other proteins, such as non receptor tyrosine kinases, to form adhesion focal contacts (30).

The expression of β1 and β3 integrins is altered in fibroblasts isolated from fibrotic myocardium. Evidence suggests that both integrins are required for proper proliferation, migration, and adhesion of fibroblasts for them to deposit the ECM fibrotic proteins (31, 32). Consistently, the downstream mediators of β integrin, such as Focal Adhesion Kinase FAK, contribute to fibrogenesis (32). For instance, silencing of FAK using siRNA alleviated the fibrosis in myocardium subjected to chronic pressure overload, and FAK-deficient mice had better systolic function in response to chronic pressure overload compared with control mice (32). Furthermore, β1 integrin seems to also be required for pressure overload induced fibrosis (31). Mice deficient with β1 integrin had a decrease in myocyte cross sectional area and deposition of ECM proteins. This process is shown to be dependent on PDGFR localization of Pyk2 non-tyrosine kinase (31) (Fig. 2).

We already mentioned that both integrins and mTORC2 are important for cytoskeletal dynamics during hypertrophy. Alteration of integrins or mTORC2 signaling leads to defects in the cytoskeleton. In fact, a study showed that mTORC2 regulates the expression of β1 and β3 integrins (36). We can expect that loss of mTORC2 signaling in chronic pressure overload might lead to a perturbation in β1 and β3 expression, both of which are implicated in fibrosis.

What is intriguing is that both integrins β1 and β3 are required for survival in the compensatory phase but are also required for fibrosis-mediated heart failure. Our hypothesis on this dilemma is that there is a critical balance that decides the outcome of the functions of the involved integrins: survival of cardiomyocytes versus fibrotic deposition by fibroblasts. During the compensatory phase, mTORC2 might activate integrins to function physiologically, that is to promote survival in cardiomyocytes, by preventing the activation of calpain (37), and promote the physiological deposition of ECM by fibroblasts to form a proper scaffold for the engagement and survival of cardiomyocytes. However, upon loss of mTORC2, this balance might be altered: the integrins might be suppressed in cardiomyocytes (allowing calpain and others to induce cell death); however, their functions might become exaggerated in fibroblasts resulting in pathological deposition of ECM, tissue remodeling, and fibrosis (Fig. 3). This should be studied more extensively for the dilemma to be resolved.

CONCLUSION

mTORC2 plays a significant role in the hypertrophic response of cardiomyocytes to stress. mTORC2 and integrin signaling pathways interact to modify the cytoskeleton in cardiomyocytes and activate fibroblasts, as part of the growth compensatory mechanism. Interestingly, mTORC1 is not involved in the hypertrophic compensatory response even though mTORC1 can also activate some subtypes of Akt. mTORC2 activation turns on Akt-1 signaling directly via phosphorylation and/or indirectly via Protein Kinase C epsilon PKCε. mTORC2/Akt-mediated cardiomyocyte survival is dependent on the UPS system, expulsion of FOXO, inactivation of IkB, and pathways implicated in programmed cell death. The field of mTORC2 in cardiac hypertrophy and fibrosis is very promising and many of the unanswered questions, if addressed, can help in establishing novel therapeutic strategies for heart failure that target the mTORC2/Akt and integrin pathways.

REFERENCES

1. Wencker D, Chandra M, Nguyen K, Miao W, Garantziotis S, Factor SM, Shirani J, Armstrong RC, Kitsis RN. A mechanistic role for cardiac myocyte apoptosis in heart failure. J Clin Invest 2003; 111:1497-504.
2. Moschella PC, McKillop J, Pleasant DL, Harston RK, Balasubramanian S, Kuppuswamy D. mTOR complex 2 mediates Akt phosphorylation that requires PKCε in adult cardiac muscle cells. Cell Signal 2013; 25:1904-12.
3. Laser M, Kasi VS, Hamawaki M, Cooper G, Kerr CM, Kuppuswamy D. Differential activation of p70 and p85 S6 kinase isoforms during cardiac hypertrophy in the adult mammal. J Biol Chem 1998; 273:24610-9.
4. Wullschleger S, Loewith R, Hall MN. TOR signaling in growth and metabolism. Cell 2006; 124:471-84.
5. Park IH, Erbay E, Nuzzi P, Chen J. Skeletal myocyte hypertrophy requires mTOR kinase activity and S6K1. Exp Cell Res 2005; 309:211-19.
6. Guertin DA, Stevens DM, Thoreen CC, Burds AA, Kalaany NY, Moffat J, Brown M, Fitzgerald KJ, Sabatini DM. Ablation in mice of the mTORC components raptor, rictor, or mLST8 reveals that mTORC2 is required for signaling to Akt-FOXO and PKCalpha, but not S6K1. Dev Cell 2006; 11:859-71.
7. Jacinto E, Loewith R, Schmidt A, Lin S, Rüegg MA, Hall A, Hall MN. Mammalian TOR complex 2 controls the actin cytoskeleton and is rapamycin insensitive. Nat Cell Biol 2004; 6:1122-28.
8. Shioi T, McMullen JR, Tarnavski O, Converso K, Sherwood MC, Manning WJ, Izumo S. Rapamycin attenuates load-induced cardiac hypertrophy in mice. Circulation 2003; 107:1664-70.
9. Sarbassov DD, Guertin DA, Ali SM, Sabatini DM. Phosphorylation and regulation of Akt/PKB by the rictor-mTOR complex. Science 2005; 307:1098-10.
10. Shiojima I, Walsh K. Role of Akt signaling in vascular homeostasis and angiogenesis. Circ Res 2002; 90:1243-50.
11. Fujio Y, Nguyen T, Wencker D, Kitsis R.N, Walsh K. Akt promotes survival of cardiomyocytes in vitro and protects against ischemia-reperfusion injury in mouse heart. Circulation 2000; 101:660-67.
12. Pende M. mTOR, Akt, S6 kinases and the control of skeletal muscle growth. Bull Cancer 2006; 93:E39.
13. Inagaki K, Churchill E, Mochly-Rosen D. Epsilon protein kinase C as a potential therapeutic target for

the ischemic heart. Cardiovasc Res 2006; 70:222-30.
14. Condorelli G, Drusco A, Stassi G, et al. Akt induces enhanced myocardial contractility and cell size in vivo in transgenic mice. Proc Natl Acad Sci 2002; 99:12333-38.
15. Rota M, Boni A, Urbanek K, et al. Nuclear targeting of Akt enhances ventricular function and myocyte contractility. Circ Res 2005; 97:1332-41.
16. Pickart CM. Mechanisms underlying ubiquitination. Annu Rev Biochem 2001; 70:503-33.
17. Depre C, Wang Q, Yan L, et al. Activation of the cardiac proteasome during pressure overload promotes ventricular hypertrophy. Circulation 2006; 114:1821-8.
18. Meiners S, Dreger H, Fechner M, et al. Suppression of cardiomyocyte hypertrophy by inhibition of the ubiquitin-proteasome system. Hypertension 2008; 51:302-8.
19. Plas DR, Thompson CB. Akt activation promotes degradation of tuberin and FOXO3a via the proteasome. J Biol Chem 2003; 278:12361-6.
20. Sacheck JM, Ohtsuka A, McLary SC, Goldberg AL. IGF-I stimulates muscle growth by suppressing protein breakdown and expression of atrophy-related ubiquitin ligases, atrogin-1 and MuRF1. Am J Physiol Endocrinol Metab 2004; 287:E591.
21. Li HH, Willis MS, Lockyer P, Miller N, McDonough H, Glass DJ, Patterson C. Atrogin-1 inhibits Akt-dependent cardiac hypertrophy in mice via ubiquitin-dependent coactivation of Forkhead proteins. J Clin Invest 2007; 117:3211-23.
22. Mammucari C, Milan G, Romanello V, et al. FoxO3 controls autophagy in skeletal muscle in vivo. Cell Metab 2007; 6:458-71.
23. Li Y, Ha T, Gao X, Kelley J, Williams DL, Browder IW, Kao RL, Li C. NF-kappaB activation is required for the development of cardiac hypertrophy in vivo. Am J Physiol Heart Circ Physiol 2004; 287:H1712.
24. Jacinto E, Loewith R, Schmidt A, Lin S, Ruegg MA, Hall A, Hall MN. Mammalian TOR complex 2 controls the actin cytoskeleton and is rapamycin insensitive. Nat Cell Biol 2004; 6:1122-8.
25. Sarbassov DD, Ali SM, Kim DH, Guertin DA, Latek RR, Erdjument-Bromage H, Tempst P, Sabatini DM. Rictor, a novel binding partner of mTOR, defines a rapamycin-insensitive and raptor independent pathway that regulates the cytoskeleton. Curr Biol 2004; 14:1296-302.
26. Bronzwaer JG, Paulus WJ. Matrix, cytoskeleton, or myofilaments: which one to blame for diastolic left ventricular dysfunction? Prog Cardiovasc Dis 2005; 47:276-84.
27. Hou X, Hu Z, Xu H, Xu J, Zhang S, Zhong Y, He X, Wang N. Advanced glycation endproducts trigger autophagy in cadiomyocyte via RAGE/PI3K/AKT/mTOR pathway. Cardiovasc Diabetol 2014; 13:78.
28. Dany M, Ogretmen B. Ceramide induced mitophagy and tumor suppression. Biochim Biophys Acta. 2015; 1853:2834-45.
29. Manso AM, Kang SM, Ross RS. Integrins, focal adhesions, and cardiac fibroblasts. J Investig Med 2009; 57:856-60.
30. Sheppard D. In vivo functions of integrins: lessons from null mutations in mice. Matrix Biol 2000; 19:203-9.
31. Balasubramanian S, Quinones L, Kasiganesan H, et al. β3 integrin in cardiac fibroblast is critical for extracellular matrix accumulation during pressure overload hypertrophy in mouse. PLoS One 2012; 7:e45076.
32. Manso AM, Kang SM, Plotnikov SV, Thievessen I, Oh J, Beggs HE, Ross RS. Cardiac fibroblasts require focal adhesion kinase for normal proliferation and migration. Am J Physiol Heart Circ Physiol 2009; 296:H627-38.
33. Camelliti P, Borg TK, Kohl P. Structural and functional characterization of cardiac fibroblasts. Cardiovasc Res 2005; 65:40-51.
34. Shai SY, Harpf AE, Babbitt CJ, Jordan MC, Fishbein MC. Cardiac myocyte-specific excision of the beta1 integrin gene results in myocardial fibrosis and cardiac failure. Circ Res 2002; 90:458-64.
35. Willey CD, Balasubramanian S, Rodriguez Rosas MC, Ross RS, Kuppuswamy D. Focal complex formation in adult cardiomyocytes is accompanied by the activation of beta3 integrin and c-Src. J Mol Cell Cardiol 2003; 35:671-83.
36. Masri J, Bernath A, Martin J, Jo OD, Vartanian R, Funk A, Gera J. mTORC2 activity is elevated in gliomas and promotes growth and cell motility via overexpression of rictor. Cancer Res 2007; 67:11712-20.
37. Suryakumar G, Kasiganesan H, Balasubramanian

S, Kuppuswamy D. Lack of beta3 integrin signaling contributes to calpain-mediated myocardial cell loss in pressure-overloaded myocardium. J Cardiovasc Pharmacol 2010; 55:567-73.

JOURNAL OF BIOLOGICAL REGULATORS & HOMEOSTATIC AGENTS Vol. 29, no. 4, 755-760 (2015)

EDITORIAL

LINK OF OBESITY AND GASTROINTESTINAL CANCER: CROSSROAD OF INFLAMMATION AND OXIDATIVE STRESS

X-D. YANG[1], S. JIANG[2], G. WANG[1], R. ZHANG[1], J. ZHANG[1] and J-S. ZHU[1]

[1]Department of Gastroenterology, Shanghai Jiao Tong University Affiliated Shanghai Sixth People's Hospital, Shanghai, China; [2]Emergency Department, East Hospital Affiliated Tongji University School of Medicine, Shanghai, China

Received August 8, 2015 – Accepted September 22, 2015

The first two authors contributed equally to this article

Obesity incidence has reached pandemic levels, and is accompanied by high incidence and poor prognosis of various types of cancers including gastrointestinal ones. Underlying mechanisms include elevated levels of insulin, IGF-I, and altered adipokine concentration, mainly towards leptin and adiponectin levels. However, it is not yet thoroughly understood. It is now widely known that obesity is associated with chronic low-grade inflammation, characteristic of altered immune cell infiltration in adipose tissue, and changed inflammatory cytokines and chemokines: tumor necrosis factor alpha (TNF-a), IL-6, and the chemoattractant monocyte chemoattractant protein 1 (MCP-1) and others, all together eventually promoting caner pathogenesis. Moreover, accumulating reports have shown that excess adipose tissue in obese individuals resulted in elevated levels of systematic oxidative stress, another way of promoting cancer development and progression. In general, altered immunological milieu and oxidative stress in obesity are important determinants for tumorigenesis.

Epidemiological data has demonstrated that overweight and obesity strongly increase the incidence and mortality of many kinds of malignancies, including gastrointestinal cancers (1). Obesity is associated with low-grade chronic inflammation, widely regarded as an important factor in cancer etiology and oxidative stress facilitating tumorigenesis (2). In this article, the role of inflammation and oxidative stress in obesity-associated gastrointestinal cancer is discussed.

Obesity and gastrointestinal cancer prognosis and inflammation

Obesity has been considered as a risk factor for some chronic diseases including cancer. It has been reported that overweight contributes to colon cancer and oesophageal adenocarcinoma (3) and represents an increased risk for gastric cancer and pancreatic cancer (4). A meta-analysis including 20,678 patients demonstrates that obesity increases surgical difficulty and complications and impairs the long-term survival of patients with gastric cancer (5) as well as leading to the poor outcome and recurrence in colorectal cancer (6).

Obesity is associated with chronic inflammation, characterized by increased circulating fatty acids and immune cell infiltration in adipose tissues that

Key words: obesity, gastrointestinal cancer, inflammation, oxidative stress

Mailing address: Dr. Jing Zhang,
Department of Gastroenterology,
Shanghai Jiao Tong University
Affiliated Shanghai Sixth People's Hospital,
No. 600 Yishan Road, Shanghai 200233, China
Tel.: +86 21 64369181 Fax: +86 21 64837019
e-mail: jing5522724@163.com

0393-974X (2015)

DISCLOSURE: ALL AUTHORS REPORT NO CONFLICTS OF INTEREST RELEVANT TO THIS ARTICLE.

cause the activation of inflammatory signaling. Epidemiology data indicates that 25% of cancers are correlated with chronic inflammation and 15% of cancer deaths are related to inflammation (7). The relationships between obesity, inflammation and cancer show the importance of inflammation in obesity -associated cancer.

Chronic inflammation and obesity

Adipose tissue contains several types of cells, such as adipocytes, immune, endothelial cells, which release many inflammatory cytokines and chemokines, including IL-6, IL-17, tumor necrosis factor alpha (TNF-a), and monocyte chemotatic protein 1 (MCP-1) in obesity patients (8). Hypoxia is important for chronic inflammation and adiponectin inhibition in adipose tissue (9). HIF-1a modulates the expression of tumor-related genes involved in angiogenesis, cell survival, and tumor invasion (10) and interacts with the NF-kB inflammatory pathway, promoting the cancer progression (11).

Leptin and adiponectin

Adipose tissues synthesize and secrete many polypeptide growth factors and cytokines, including adipokines, participating in altering metabolic cellular function and altering leptin and adiponectin levels (12). Leptin exerts pro-inflammatory effects and regulates immune surveillance of colon cancer via increasing cytokine release from macrophages and insulin resistance (13). In obese diabetic and nondiabetic subjects, adiponectin inhibits NF-kB -dependent expression of the inflammatory cytokines such as TNF-alpha, IFN-gamma and interleukin (IL)-6, and increases the activity of IL-10 and TIMP1 mediated by the AMPK pathway (14). Chronic inflammation induces the carcinogenesis of gastrointestinal cancers, and the anti-inflammatory effect of adiponectin may have a role in limiting the development of these cancers.

Altered immune cells

Immune cells including macrophages, lymphocytes, mast cells, eosinophils neutrophils and foam cells, infiltrate the adipose tissue, secrete inflammatory cytokines, growth factors and reactive oxygen species, induce DNA damage and chromosomal instability, thereby contributing to the tumorigenesis (15). Macrophages and monocytes belong to the innate immune system in adipose tissue, and neutrophils and mast cells are implicated in promoting inflammation during obesity, whereas eosinophils and myeloid-derived suppressor cells exert a protective role (16). Obesity induces a phenotypic switch from an anti-inflammatory M2-polarized state to a pro-inflammatory M1 state, and neutrophils can trigger the inflammation cascade associated with obesity (17). Mast cells, like macrophages, are inflammatory cells and have been demonstrated to be higher in obese individuals than lean ones (18). In addition, lymphocytes, including T and B lymphocytes and natural-killer cells are found to be involved in inflammation associated with obesity (19). Convincing evidence suggested that CD4+ T cells are key factors in regulating disease progression induced by obesity (20) and Th1 cells take a pro-inflammatory role, while Th2 cells are regarded to be anti-inflammatory (21).

Altered inflammation molecular

Obesity-induced chronic inflammation participates in the tumor pathogenesis based on the high levels of inflammatory cytokines and enzymes (IL-6, TNF-a, and MCP-1), and reactive oxygen intermediators and pro-inflammatory mediators (NF-kB, STAT3 and COX-2) (22). IL-6, a cytokine secreted by many tissues, interacts with its receptor and leads to the subsequent phosphorylation of some tumor-promoting transcription factors such as STAT3, resulting in gene translation (23), tumorigenesis of colon cancer (24) and promoting angiogenesis (25). TNF-a can trigger the acute inflammation reaction by activation of macrophages and monocytes, while obesity-associated infiltration of macrophages in adipose tissue causes the elevated level of TNF-a (26). TNF-a/TNFR axis regulates tumor cell proliferation, survival and differentiation via intracellular signaling pathways (27). MCP-1 is highly-expressed in obese individuals via inflammatory infiltration and activation of the monocytes (28) and accelerates macrophage infiltration and tumor proliferation through activation of the PI3K/AKT pathway in prostate cancer (29). Obesity-induced inflammation contributes to colorectal cancer progression via upregulation of the TNF-a, IL-6, and MCP-1 expression (30),

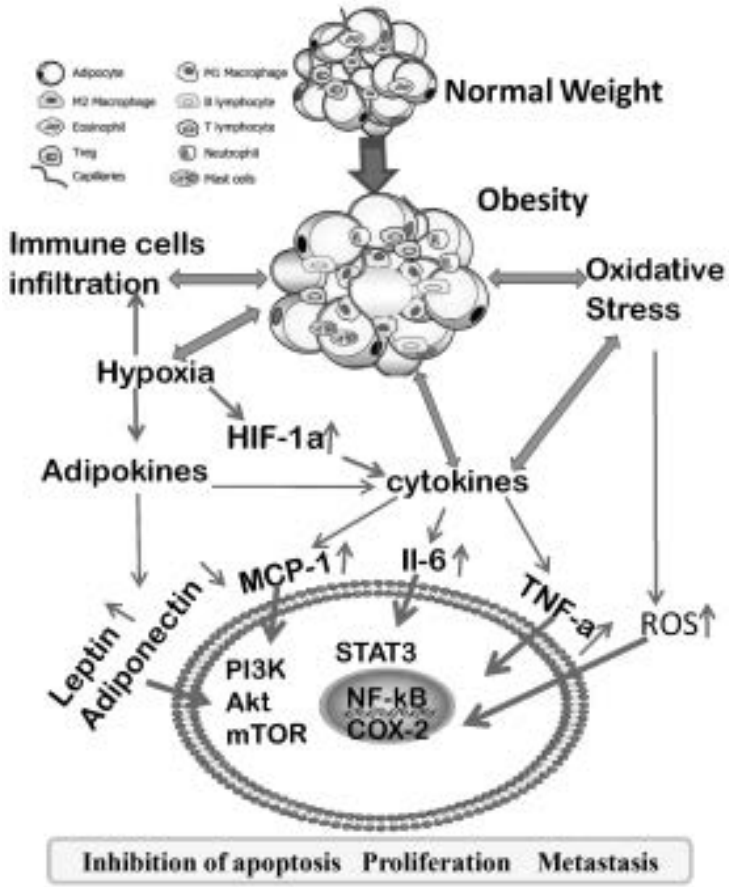

Fig. 1. *Inflammation and oxidative stress contribute to cancer progression. In obese individuals, adipocytes, preadipocytes, and infiltrated immune cells release adipokines and inflammatory cytokines and chemokines, influencing cell survival and migration via several signaling pathways including the PI3K/AKT/mTOR pathway, proinflammatory NF-kB, COX-2, and signal transducer STAT3.*

which stimulates the proliferation and decreases the apoptosis in gastric cancer cells (31, 32). IFN-γ, a prototypical Th1 cytokine, takes an important role in inflammatory response that accompanies obesity. Earlier study indicated higher levels of IFN-γ in adipose tissue extracts from obesity animals than lean ones, and IFN-γ can stimulate chemokine expression such as MCP-1(33). Moreover, IFN-γ can interact with macrophages, NK cells by up-regulating many gene products and eliciting oxidative burst (34).

Oxidative stress and obesity

In obesity, there is an imbalance between enhanced reactive oxygen species (ROS) production and lowered antioxidant activity resulting in oxidative stress and injury (35). Obesity-associated oxidative stress is related with fat accumulation by increasing Nox activity and endoplasmic reticulum (ER) stress (36), altered post-prandial ROS production, hyperleptinemia, low antioxidant defenses, and chronic inflammation (37). Adipose tissue inflammation leads to increasing circulating concentration of pro-inflammatory cytokines, and other inflammatory factors such as hormone-like molecules, NF-kB and activator protein-1 (AP-1), which stimulate ROS and nitrogen oxide by macrophages and monocytes (38-40). Obesity diminishes antioxidant production by reducing superoxide dismutase (SOD), glutathione peroxidase (GPx) and catalase (CAT) (39). `

Oxidative stress and inflammation are two critical factors contributing to the pathogenesis of obesity-associated cancer. Systematic oxidative stress can cause DNA damage and genomic instability, stimulating the activation of oncogenes and inactivation of the tumor suppressor genes by altered modification of oxidative DNA (41). In addition, ROS disrupts the epigenetic model by inducing hypermethylation and histone modifications promoting cancer development (42). These studies suggest the association between oxidative stress/ chronic inflammation and carcinogenesis.

Crosstalk of cytokines, immune cells, adipocytes and epithelial cells

Inflammatory cytokines promote immune cell infiltration in adipose tissue, resulting in secretion of the inflammatory cytokines. Adipokine production is regulated by the level of immune cell infiltration in adipose tissue, induced by hypoxia suffered from effective oxygen diffusion in obesity (43). Adipose tissue is infiltrated with macrophages, which is correlated with the degree of adiposity. Peripheral monocytes are triggered by inflammatory cytokines such as MCP-1 and TNF-a, and differentiated into activated macrophages (44), exerting great effects on adipocyte function (45). Co-culturing adipocytes with macrophage result in enhanced production of adipokine and inflammatory cytokines from adipocytes (46).

In obese patients, activated macrophages modify the inflammatory tumor microenvironment by increasing the production of cytokines and angiogenic factors through NF-κB-dependent pathway, which is activated by many stimulators including bacterial and viral stimuli, growth factors, and inflammatory cytokines (TNF-a, IL-6, and IL-1β). The above changes can then induce gene expression alteration and further regulate cell proliferation, apoptosis, inflammation, metastasis, and angiogenesis (47). Activation of NF-κB as a common characteristic of many tumors is positively associated with insulin resistance, and increases circulating leptin, insulin, and IGF-1 (48). Cyclooxygenase-2, an important cancer–related inflammatory mediator is upregulated in most tumors and it catalyzes the synthesis of the potent inflammatory lipid metabolite. Moreover, cyclooxygenase-2 overexpression is an indicator of poor prognosis in multiple cancers (49).

CONCLUSION

Epidemiological data demonstrate the relationship between obesity and increased risk of various gastrointestinal cancers, therefore a thorough understanding of the biological processes linking obesity and cancer may be important for strategies in the prevention of the oncogenic events. In obese patients, adipocytes, preadipocytes, and altered surrounding stromal immune cells release adipokines and inflammatory cytokines and chemokines, including IL-17, IL-22, TNF-a, IL-6, and the chemoattractant monocyte chemoattractant protein 1 (MCP-1) in hypoxia adipose tissue, leading to a microenvironment where high levels of oxidative stress and related DNA damage cause obese-associated cancer progression (Fig. 1). Comprehensive understanding of the mechanisms of obesity-associated cancers is helpful to prevent and treat cancer.

ACKNOWLEDGEMENTS

This study was supported by National Nature Science Foundation of China (No. 81573747, 81302093 and 81272752).

REFERENCES

1. Renehan AG, Tyson M, Egger M, Heller RF, Zwahlen M. Body-mass index and incidence of cancer: a systematic review and meta-analysis of prospective observational studies. Lancet 2008; 371:569-78.
2. Vermorken AJ, Zhu J, Andres E. Obesity and colorectal cancer risk: the role of oxidative stress. Gut 2014; 63:529-30.
3. Singh S, Sharma AN, Murad MH, Buttar NS, El-Serag HB, Katzka DA, Iyer PG. Central adiposity is associated with increased risk of esophageal inflammation, metaplasia, and adenocarcinoma: a systematic review and meta-analysis. Clin Gastroenterol Hepatol 2013; 11:1399-1412.e7.
4. Aune D, Greenwood DC, Chan DS, et al. Body mass index, abdominal fatness and pancreatic cancer risk: a systematic review and non-linear dose-response

meta-analysis of prospective studies. Ann Oncol 2012; 23:843-52.
5. Bickenbach KA, Denton B, Gonen M, Brennan MF, Coit DG, Strong VE. Impact of obesity on perioperative complications and long-term survival of patients with gastric cancer. Ann Surg Onocl 2013; 20:780-7.
6. Bardou M, Barkun AN, Martel M. Obesity and colorectal cancer. GUT 2013; 62:933-47.
7. Vendramini-Costa DB, Carvalho JE. Molecular link mechanisms between inflammation and cancer. Curr Pharm Des 2012; 18:3831-52.
8. Balistreri CR, Caruso C, Candore G. The role of adipose tissue and adipokines in obesity-related inflammatory diseases. Mediators Inflamm 2010; 2010:802078.
9. Ye J, Gao Z, Yin J, He Q. Hypoxia is a potential risk factor for chronic inflammation and adiponectin reduction in adipose tissue of ob/ob and dietary obese mice. Am J Physiol Endocrinol Metab 2007; 293:E1118-28.
10. Semenza GL. Targeting HIF-1 for cancer therapy. Nat Rev Cancer 2003; 3:721-32.
11. Hursting SD, Berger NA. Energy balance, host-related factors, and cancer progression. J Clin Oncol 2010; 28:4058-65.
12. Margetic S, Gazzola C, Pegg GG, Hill RA. Leptin: a review of its peripheral actions and interactions. Int J Obes Relat Metab Disord 2002; 26:1407-33.
13. Drew JE. Molecular mechanisms linking adipokines to obesity-related colon cancer: focus on leptin. Proc Nutr Soc 2012; 71:175-80.
14. Dalamaga M, Diakopoulos KN, Mantzoros CS. The role of adiponectin in cancer: a review of current evidence. Endocr Rev 2012; 33:547-94.
15. Winer DA, Winer S, Shen L, et al. B cells promote insulin resistance through modulation of T cells and production of pathogenic IgG antibodies. Nat Med 2011;17:610-7.
16. Wu l, Van Kaer L. Contribution of lipid-reactive natural killer T cells to obesity-associated inflammation and insulin resistance. Adipocyte 2013; 2:12-16.
17. Elgazar-Carmon V, Rudich A, Hadad N, Levy R. Neutrophils transiently infiltrate intra-abdominal fat early in the course of high-fat feeding. J Lipid Res 2008; 49:1894-903.
18. Stienstra R, van Diepen JA, Tack CJ, et al. Inflammasome is a central player in the induction of obesity and insulin resistance. Proc Natl Acad Sci U S A 2011; 108: 15324-9.
19. Sell H, Eckel J. Adipose tissue inflammation: novel insight into the role of macrophages and lymphocytes. Curr Opin Clin Nutr Metab Care 2010; 13:366-70.
20. Winer S, Chan Y, Paltser G, et al. Normalization of obesity-associated insulin resistance through immunotherapy. NAT MED 2009;15:921-9.
21. Guevara-Aguirre J, Rosenbloom AL. Obesity, diabetes and cancer: insight into the relationship from a cohort with growth hormone receptor deficiency. Diabetologia 2015;58:37-42.
22. Aggarwal BB. Inflammation, a silent killer in cancer is not so silent! Curr Opin Pharmacol 2009; 9:347-50.
23. Sriuranpong V, Park JI, Amornphimoltham P, et al. Epidermal growth factor receptor-independent constitutive activation of STAT3 in head and neck squamous cell carcinoma is mediated by the autocrine/paracrine stimulation of the interleukin 6/gp130 cytokine system. Cancer Res 2003; 63:2948-56.
24. Li YY, Hsieh LL, Tang RP, Liao SK, Yeh KY. Interleukin-6 (IL-6) released by macrophages induces IL-6 secretion in the human colon cancer HT-29 cell line. Hum Immunol 2009; 70:151-8.
25. Rose DP, Komninou D, Stephenson GD. Obesity, adipocytokines, and insulin resistance in breast cancer. Obes Rev 2004; 5:153-65.
26. Tzanavari T, Giannogonas P, Karalis KP. TNF-alpha and obesity. Curr Dir Autoimmun 2010; 11:145-56.
27. Tao T, Ji Y, Cheng C, Yang H, Liu H, Sun L, Qin Y, Yang J, Wang H, Shen A. Tumor necrosis factor-alpha inhibits Schwann cell proliferation by up-regulating Src-suppressed protein kinase C substrate expression. J Neurochem 2009; 111:647-55.
28. Catalan V, Gomez-Ambrosi J, Ramirez B, et al. Proinflammatory cytokines in obesity: impact of type 2 diabetes mellitus and gastric bypass. Obes Surg 2007; 17:1464-74.
29. Loberg RD, Day LL, Harwood J, Ying C, John . LN. St, Giles R, Neeley CK, Pienta KJ. CCL2 is a potent regulator of prostate cancer cell migration and

proliferation. Neoplasia 2006; 8:578-86.
30. Chen ZY, He WZ, Peng LX, Jia WH, Guo RP, Xia LP, Qian CN. A prognostic classifier consisting of 17 circulating cytokines is a novel predictor of overall survival for metastatic colorectal cancer patients. Int J Cancer 2015; 136:584-92.
31. Golan R, Shelef I, Rudich A, et al. Abdominal superficial subcutaneous fat: a putative distinct protective fat subdepot in type 2 diabetes. Diabetes Care 2012; 35:640-7.
32. Hanahan D, Weinberg RA. Hallmarks of cancer: the next generation. Cell 2011; 144:646-74.
33. Rocha VZ, Folco EJ, Sukhova G, Shimizu K, Gotsman I, Vernon AH, Libby P. Interferon-gamma, a Th1 cytokine, regulates fat inflammation: a role for adaptive immunity in obesity.Circ Res 2008;103:467-76.
34. Ellis TN, Beaman BL. Interferon-γ activation of polymorphonuclear neutrophil function. Immunology 2004; 112(1): 2-12.
35. Tang J, Yan H, Zhuang S. Inflammation and oxidative stress in obesity-related glomerulopathy. Int J Nephrol 2012; 2012:608397.
36. Mlinar B, Marc J. New insights into adipose tissue dysfunction in insulin resistance., Clin Chem Lab Med 2011; 49:1925-35.
37. Bondia-Pons I, Ryan L, Martinez JA. Oxidative stress and inflammation interactions in human obesity. J Physiol Biochem 2012; 68:701-11.
38. Balistreri CR, Caruso C, Candore C. The role of adipose tissue and adipokines in obesity-related inflammatory diseases. Mediators Inflamm 2010; 2010:802078.
39. Fernandez-Sanchez A, Madrigal-Santillan E, Bautista M, et al. Inflammation, oxidative stress, and obesity. Int J Mol Sci 2011:12:3117-32.
40. Bryan S, Baregzay B, Spicer D, Singal PK, Khaper N. Redox-inflammatory synergy in the metabolic syndrome. Can J Physiol Pharmacol 2013; 91:22-30.
41. Vucenik, Stains JP. Obesity and cancer risk: evidence, mechanisms, and recommendations. Ann N Y Acad Sci 2012; 1271:37-43.
42. Dandona P, Aljada A, Chaudhuri A, Mohanty P, Garg R. Metabolic syndrome: a comprehensive perspective based on interactions between obesity, diabetes, and inflammation. Circulation 2005; 111:1448-54.
43. Xu H, Barnes GT, Yang Q, et al. Chronic inflammation in fat plays a crucial role in the development of obesity-related insulin resistance. J Clin Invest 2003; 112:1821-30.
44. Curat CA, Miranville A, Sengenes C, Diehl M, Tonus C, Busse R, Bouloumie A. From blood monocytes to adipose tissue-resident macrophages: induction of diapedesis by human mature adipocytes. Diabetes 2004; 53:1285-92.
45. Wellen KE, Hotamisligil GS. Obesity-induced inflammatory changes in adipose tissue. J Clin Invest 2003; 112:1785-8.
46. Bassols J, Ortega FJ, Moreno-Navarrete JM, Peral B, Ricart W, Fernandez-Real JM. Study of the proinflammatory role of human differentiated omental adipocytes. J Cell Biochem 2009; 107:1107-17.
47. Subbaramaiah K, Howe LR, Bhardwaj P, et al. Obesity is associated with inflammation and elevated aromatase expression in the mouse mammary gland. Cancer Prev Res (Phila) 2011; 4:329-46.
48. Renehan AG, Roberts DL, Dive C. Obesity and cancer: pathophysiological and biological mechanisms. Arch Physiol Biochem 2008; 114:71-83.
49. Koki A, Khan NK, Woerner BM, et al. Cyclooxygenase-2 in human pathological disease. Adv Exp Med Biol 2002; 507:177-84.

JOURNAL OF BIOLOGICAL REGULATORS & HOMEOSTATIC AGENTS Vol. 29, no. 4, 761-769 (2015)

EDITORIAL

FRAGILITY FRACTURES: CLINICAL AND THERAPEUTIC ASPECTS

N. MALAVOLTA[1], E. ROSSI[1], A. BUFFA[1] and A. FALCHETTI[2]

[1]St Orsola-Malpighi Hospital, University of Bologna, Department of Medical and Surgical Sciences, Division of Internal Medicine, Bologna, Italy; [2]Hercolani Center, Bologna, Italy

Received March 3, 2015 – Accepted September 30, 2015

Osteoporosis is the most important bone metabolic disorder characterized by reduction of bone mass and micro-architectural deterioration associated to an increased risk for fragility fractures. It involves millions of worldwide-dispersed individuals of both sexes and, consequently, the elevated morbidity and mortality of fractured subjects and the increased socio-economic costs suggest it must be faced as a major health problem. Thus, there is a need for either a precocious identification of subjects with fragile "bones" or the institution of specific diagnostic-therapeutical strategies. Improvement in bone pathophysiology knowledge, together with progress in pharmaceutical development has led to an opportunity for early identification and therapy of subjects at high risk of fragility fractures. In this review, we briefly describe the recent acquisitions in bone pathophysiology as well as in the anti-fracture drug development with a brief excursus on those already well established.

It is well known that the exclusion of high trauma fractures may underestimate the prevalence of bone fragility fractures in the general population. Due to the difficulty to quantize the degree of trauma, low bone mass may also contribute to fractures following a severe trauma. Osteoporosis (OP) is a metabolic skeletal disorder in which bone strength is compromised, predisposing the affected individual to fragility fractures. Fragility fractures, occurring as a result of bone micro-architectural deterioration as well as low bone mass, are associated with substantial pain and suffering, disability and even death for the affected patients, and with elevated socio-economic costs, since fractures are a strong source of morbidity and mortality for the patient. OP, defined by low Bone Mineral Density (BMD) (2.5 standard deviations below peak gender specific BMD or T-score), is a progressive disease with high prevalence, affecting 30% of women and approximately 13% of men by the time they reach 90 years of age. The prevalence of OP in Europe was estimated at 27.6 million (22 million women and 5.6 million men over the age of 50) in 2010 (1). In Italy, over 3 million people suffer from OP and 465,000 fragility fractures were estimated in 2010 (Table I) (3). The major concern with low BMD is the high risk of fractures of nonvertebral bones such as the wrist or hip. A hip fracture may require extended hospital stay, surgical repair and rehabilitation therapy, and is associated with increased risk of death (4). In addition, OP can lead to vertebral fractures, identified by clinical assessment through decreased patient height or with vertebral compression radiologically assessed (5). However, only 50% of these are usually diagnosed

Key words: osteoporosis, fragility fracture, medical treatment

Mailing address:
Nazzarena Malavolta, M.D.
St Orsola-Malpighi Hospital,
University of Bologna,
Via Albertoni, 15,
40138, Bologna, Italy
e-mail: nazzarena.malavolta@aosp.bo.it

0393-974X (2015)

DISCLOSURE: ALL AUTHORS REPORT NO CONFLICTS OF INTEREST RELEVANT TO THIS ARTICLE.

and consequently they are underestimated and undertreated. It has to be stressed that more than 80% of postmenopausal women with fractures had DXA T-scores better than -2.5 SD, falling into the osteopenic range (6). These findings have clearly suggested the existence of risk factors, other than reduced BMD, for fragility fractures, and also the need for their recognition in order to use them in the clinical assessment for early identification of the subjects at risk. Osteoporotic fractures have a strong impact on quality of life, morbidity and mortality, since they: i) limit mobility and ability of daily tasks; and ii) involve the loss of years of healthy life [Disability Adjusted Life Years (DALYs)] more than common types of cancer, except for lung cancer. Moreover, women over 45 years spend more days in hospital due to OP-related complications compared to diabetes, myocardial infarction and breast cancer. Other than pain, subjects with fragility fractures may suffer for disability, loss of independence, and affection of mental wellbeing, contributing to reduction of quality of life (7). Other negative aspects on the quality of life are summarized in Table II (8). Today, we have appropriate tools, and new ones will be found in the future, that allow us to identify early the risk factors for fracture, either due to the reduction of bone mass or related to the predisposing conditions, independently by BMD values (e. g., familial history of fractures, alcohol and/or tobacco abuse, glucorticoids prolonged therapy) (FRAX algorithm at http://www.shef.ac.uk/FRAX). Specifically, modifiable risk factors, such as an inadequate calcium and vitamin D daily intake, smoking, sedentary lifestyle, and environmental risk of falling have always to be looked for. For all these described negative aspects on quality of life and health care costs, the creation of specific strategies and dedicated clinical pathways for the prevention, early diagnosis and treatment of bone fragility is mandatory. To facilitate this, it is essential to always keep high the level of information on this condition, encouraging both the development of a specific "bone" culture in professional health givers and offering broad disclosure to the general population, using a simple and clear language. Keeping in mind that the recommendations given in Table III are of universal value and that drug therapy should always be combined with appropriate and adequate physical activity, we briefly review the drugs currently in use for the prevention/reduction of the risk of fragility fracture, concluding with a mention of the promising innovative molecules still under study.

ANTI-FRACTURE THERAPIES FALL INTO TWO MAIN CATEGORIES: ANTI-RESORPTIVE AND ANABOLIC

We have to consider that for most of the anti-resorptive drugs: i) out of 100 patients starting anti-fracture therapy, less than 50% are still on therapy after 12 months; ii) the ideal level of adherence (80%) has been reached in less than 50% of patients; and iii) the percentage of those who complied with the rules of assumption cannot be defined (9). In Italy, the following data was reported: a) the adherence to drugs for osteoporosis in the first half of 2013 was 49% (at 6 months); and b) approximately 13% of subjects followed the therapy in an occasional manner (10). Finally, we stress that adequate vitamin D repletion is necessary for an equally appropriate response to treatment with anti-resorptive agents (11).

Bisphosphonates (BPs). Bisphosphonates are the first line treatment for OP and are approved for use in postmenopausal, glucocorticoid-induced and male OP. In particular, alendronate is still considered to have the better cost/effective ratio both for primary and secondary prevention of fragility fractures (12) (Table IV). Alendronate, risedronate, and zoledronic acid decreased fracture risk at the spine, nonvertebral sites, and the hip alone, whereas ibandronate reduced vertebral but not nonvertebral fractures. However, BP treatment has some questions and concerns (13). Firstly, BPs reduce nonvertebral and hip fractures by 20-40%, while reducing vertebral fractures by approximately 60–70% (14, 15). Secondly, when orally administered (daily/weekly/monthly), the drugs predispose to esophageal irritation and gastrointestinal side effects, leading to their discontinuation in up to 20% of subjects. Intravenous (quarterly/yearly) BP infusion may be associated with an acute phase reaction that leads to transient flu-like symptoms in about 20–30% of cases, although these symptoms tend to be more pronounced after the first dose. Thirdly, BPs are not advised in those with severe

Table I. *Incidence of fragility fractures occurred in Italy in 2010.*

Age (years)	Hip	Vertebra	Forearm	Other	All
Women					
50-74	12,298	18,582	32,856	44,355	108,091
75+	55,297	29,339	28,667	100,888	214,191
Total	67,595	47,921	61,523	145,243	322,282
Men					
50-74	6,345	11,053	6,721	40,133	64,252
75+	16,598	12,488	3,435	46,345	78,866
Total	22,944	23,540	10,156	86,478	143,118

Table II. *Impact on quality of life, morbidity and mortality.*

Negative psychological aspects	- Occurrence or worsening of pre-existing anxiety, depression, social withdrawal and isolation. All this helps to increase the costs of pharmaceutical expenditure due to the treatments for these conditions - about 40% of women with osteoporosis exhibit depression symptoms - 58% of women suffer for the sense of poor welfare - 41% of women have a reduction in quality of life
Pain	It is referred by 50% of women with OP, 26% of which suffers for more than 10 hours/day
Mortality in Europe	24% of women and 33% of men die within the next year by a hip fracture
Among those who survive	40% are unable to walk independently, and up to 80% will not able to perform basic activities of daily living (30% live in care centers in the years following fracture)

Table III. *Interventions to preserve bone strength to be recommended to the general population.*

1. Adequate daily intake of calcium and vitamin D
2. Regular load and muscle strengthening exercises
3. Cessation of tobacco use
4. Identification and treatment of alcoholism
5. Identification and prevention of the risk factors for falls

renal dysfunction (eGFR/35 ml/min/1.73m^2). Lastly, uncommon long-term treatment may be linked to an increased incidence of atypical femoral fracture and osteonecrosis of the jaw (16, 17), although such disturbances are still classified as rare events. In summary, the use of BPs only as treatment for OP is "imperfect" and there is an important need for the development of newer drugs that reduce fractures with equivalent or greater efficacy than BPs.

Estrogens. They were commonly used to treat OP, prior to BPs. Although findings published by the Women's Health Initiative revealed that estrogenic molecules were efficacious in improving both BMD and preventing osteoporotic fractures, their use dramatically declined as the same study also demonstrated an association with increased risk

Table IV. *Principal conclusions on drug efficacy/effectiveness.*

Drug name	Outcome	Strength of Evidence	Magnitude of Effect
Alendronate, Ibandronate, Risedronate, Zoledronic acid, Denosumab, Teriparatide, Raloxifene	Vertebral fractures in women with OP	Strong	Number needed to treat, 60-89 to prevent 1 fracture over 1-3 years of treatment
Alendronate, Risedronate, Zoledronic acid, Denosumab, Teriparatide	Non vertebral fractures in women with OP	Strong	Number needed to treat, 50-60 to prevent 1 fracture over 1-3 years of treatment

of breast cancer and cardiovascular event (18, 19). Future epidemiological and clinical studies could partially reverse these, in some aspects contradictory, observations.

Selective Estrogen Receptors Molecules (SERMs). Non-steroidal SERMs, specifically raloxifene (RLX) and bazedoxifene (BDX), have beneficial skeletal effects, capable of inducing tissue-specific estrogen receptor activity (20), therefore, they do not exhibit the same adverse effects as estradiol on the breast, endometrium and heart. In fact, RLX reduces the risk of breast cancer by 65%, and its use is associated with a 30–50% reduction of risk of vertebral fracture, although this may not be comparable to the 50% fracture risk reduction observed in BP clinical trials due to differences in population selection and severity of the OP considered (21, 22). In phase 3 clinical studies, BDX, a newly generated SERM, demonstrated a significant reduction of risk of incident vertebral fractures versus placebo, as well as positive effects on both BMD and bone turnover. In particular, in a subgroup analysis of women at high risk for fragility fracture, BDX significantly reduced the risk of nonvertebral fracture versus both placebo and raloxifene. BDX resulted generally safe and well-tolerated in women with and at risk for OP, with no evidence of endometrial or breast stimulation (23). More recently, BDX, together with conjugated estrogen, has been able to reduce climateric symptoms, also reducing bone turnover and preserving BMD (24).

Denosumab. It is a fully human monoclonal antibody that opposes the Receptor Activator of Nuclear Factor Kappa B Ligand (RANKL) and, consequently, inhibits osteoclast function and survival, to combat the excessive bone loss in OP. RANKL is produced by osteoblast, mesenchymal cells of bone environment, and the latest investigations have indicated that also osteocytes are a major RANKL source (25, 26). The reduction of estrogens in menopause, hyperparathyroidism and glucocorticoid prolonged use increase RANKL production, enhancing osteoclast recruitment and function. The 3-year randomized placebo-controlled study, the FREEDOM trial, is the largest study to date with the enrollment of 7,808 women between 60 and 90 years of age with T scores ranging from -2.5 to -4.0 SD (DXA at the spine or total hip). The participants were randomized to receive either denosumab (60 mg dose, biannually as a subcutaneous injection) or placebo. When fracture reduction at 36 months was assessed, denosumab was found to significantly reduce the incidence of new vertebral fractures compared to placebo (with a cumulative incidence of 7.2% placebo *vs* 2.3% denosumab, and a relative decrease of 68%, $p<0.0001$) as also nonvertebral (1.2 *vs* 0.7%, 40%, $p = 0.04$) and hip fractures (8.0 *vs* 6.5%, 20%, $p = 0.01$). After 36 months, denosumab also increased BMD and decreased bone turnover. The participants assigned to the denosumab arm experienced a relative increase of 9.2% at the lumbar spine, and 6% at the total hip BMD, in respect to

placebo (27). Previously, it had been reported that a focal thinning at the level of upper femoral head/neck junction and cortical lateral trochanter may be predictive of hip fracture (28) and more recently it was reported that denosumab increases the thickness of the cortical femur, with general and focal effects, thus suggesting a possible explanation of its anti-fracturative efficacy at the hip level (29).

Anabolic treatment: Teriparatide

Teriparatide (TPTD) is a recombinant form of human PTH (1-34 N-terminal fragment) approved for use in post-menopausal women with OP and in both men and women suffering from glucocorticoid-induced OP. Drug use is currently extended to 2 years. TPTD induces the largest increase in BMD to date when compared to any other anti-osteoporosis therapy and reduces the risk of vertebral and nonvertebral fracture in post-menopausal women with previous vertebral fracture. The pivotal trial showed a 65% reduction in the risk of new radiographic vertebral fractures (9.7% increase in lumbar spine BMD *vs* 1.1% placebo) and a 53% reduction in nonvertebral fractures in patients treated with TPTD, 20 mcg/day, as a subcutaneous injection, for 12 months compared to placebo (30). The "Direct Assessment of Nonvertebral Fractures in Community Experience (DANCE)" study evaluated the occurrence of nonvertebral fragility fractures (NVFX) in 4,000 men and women receiving TPTD for OP in a real-world setting for up to 24 months and they were followed-up for 24 months after treatment cessation. The incidence of new NVFX decreased for patients receiving TPTD treatment for longer than 6 months and this trend persisted throughout the cessation phase (31). Studies assessing the effect of TPTD on glucocorticoid-induced OP are in keeping with the trend whereby the greatest increase in BMD occurs in the lumbar region, followed by a less marked increase in the region of the hip. Furthermore, they show that TPTD is able to induce an early rise in markers of bone formation, along with a slower increase in resorptive markers, reinforcing the concept of the 'anabolic window', in which there is an initial uncoupling of bone turnover in favor of bone formation (32). Currently, new routes of administration for TPTD and human PTH fragments (daily systemic, once-weekly subcutaneous injection, oral formulation) are under investigations. A recent updated systematic review on the comparative benefits of the above reported pharmacological treatments for low bone density (33) (Table IV).

NOVEL THERAPIES

The new knowledge of bone biology, skeletal dynamics, and bone anabolic and catabolic pathways has opened the way to new and increasingly selective, bone cell-specific, therapies for OP. Here, we briefly review inhibitors of cathepsin K and blockers of sclerostin activity.

Cathepsin K inhibitors

Cathepsin K (Cat K) is a cysteine-rich protease highly expressed in osteoclasts. Cat K is responsible for the degradation of the bone matrix and it may also have an important role in bone resorption. As occurred in other human disease, also in this case the understanding of the molecular mechanisms underlying rare diseases of the skeleton has allowed the elucidation of the role of this protease in the pathophysiology of bone. The genetic deficiency of Cat K accounts for pycnodysostosis (34, 35), a rare human skeletal disease characterized by short stature, high bone mass with skeletal fragility, and Cat K-deficient mice strains show osteopetrosis and increased bone formation rate (36). On the contrary, overexpression of Cat K is associated with high bone turnover (37). Given that the protease Cat K is central to enzymatic bone degradation, its inhibitors represent a novel therapeutic approach in the treatment of OP. Currently, the only agent under clinical evaluation is odanacatib, a Cat K antibody. A phase II trial conducted with odanacatib (50 mg/week) on 399 post-menopausal women with low BMD (T scores of between -2 and -3.5 SD) found that after 24 months of oral therapy, BMD was increased by 5.7% at the lumbar spine, 4.1% at the total hip and 4.7% at the femoral neck compared to placebo. Further to this, a dose-dependent decrease of resorption markers was noted, along with a transient and moderate decline in formation markers without suppression of bone formation rate. Cutaneous lesions resembling scleroderma were not observed and adverse outcomes were similar to those of placebo (38). A large phase III trial has

now been completed. A pre-planned interim analysis demonstrated anti-fracture efficacy and a favorable benefit/risk profile. Because of safety findings, the trial is currently being extended for a minimal total period of observation of 5 years (39). The mechanism of action of odanacatib is unique and preserves bone formation. In fact, since this agent interferes with the process of resorption, rather than impairing osteoclast viability, the signaling between osteoclasts and osteoblasts is preserved and bone formation unaffected. This uncoupling action of the drug contrasts that of denosumab and BPs, two anti-resorptives that function by reducing osteoclast differentiation and promoting apoptosis, respectively (40).

Inhibitors of Wnt antagonists: sclerostin antibody

As mentioned above for Cat K, rare human mutations accounting for opposite bone phenotypes occurrence, osteoporosis-pseudoglioma syndrome and high–bone mass syndrome (*LRP5* gene) (41), sclerosteosis and Van Buchem disease (42, 43) (*SOST* gene) provided the evidence that they all resided in components of the, so-called canonical WNT signaling machinery. Mouse genetics confirmed the importance of canonical Wnt signaling in the homeostatic regulation of bone metabolism, with activation of the pathway leading to increased, and inhibition leading to decreased bone mass and strength. Moreover, several genome-wide association studies on human general populations confirmed and highlighted the importance of WNT signaling for bone (44). The pathway is now the target for therapeutic intervention to restore bone strength in patients at risk for fracture.

Sclerostin

The observation that *SOST* gene, encoding for sclerostin, inactivation occurs in sclerosteosis and van Buchem disease, two rare diseases characterized by high bone mass, has provided the rationale for targeting sclerostin in OP (43). Sclerostin is expressed by osteocytes and is a physiological regulator of bone formation, negatively regulated by loading and PTH. Sclerostin acts by blocking WNT binding to low-density lipoprotein receptor-related protein 5, LRP-5, thereby inhibiting WNT signaling, which results in decreased osteoblast differentiation and survival and altered bone formation. Thus, since sclerostin inhibits bone formation, targeting sclerostin using a sclerostin antibody results in increased bone formation and bone mass.

A human monoclonal sclerostin antibody, called AMG 785 or romosozumab, which inhibits the binding of sclerostin to LRP5/6 molecules, members of WNT pathway, has been developed and evaluated as part of a randomized, double-blind, placebo controlled phase I trial. The study recruited 72 postmenopausal women and men and demonstrated a 5.3% increase in BMD at the lumbar spine and 2.8% at the total hip after 85 days in participants given a solitary subcutaneous dose of 10 mg/kg compared to placebo. Furthermore, bone formation markers [procollagen type I N-terminal propeptide (P1NP), osteocalcin, bone-specific ALP] increased while resorption markers [serum carboxy-terminal collagen crosslinks (CTX)] decreased, indicating an uncoupling action and a large anabolic window, possibly due to cross talk with RANKL/osteoprotegerin (OPG) with a subsequent increase in OPG (45). OPG is a decoy receptor, produced by osteoblasts/stromal cells of bone environment, for RANKL that, preventing RANKL-dependent osteoclastogenesis, reduces the production of osteoclasts by inhibiting the differentiation of osteoclast precursors. In the phase II dose-ranging study, romosozumab was compared with alendronate and TPTD in 419 post-menopausal women with OP. The bone turnover markers confirmed the unique profile obtained by sclerostin inhibition in pre-clinical models, namely an increase in bone formation and a concomitant decrease of bone resorption. BMD gains after one year with romosozumab (210 mg monthly) were three times greater compared with alendronate and nearly double compared with TPTD for lumbar spine, and were twice as high as with alendronate or TPTD at hip (46). Phase III clinical trials comparing romosozumab with placebo (registration trial) or alendronate for facture prevention in osteoporosis are still ongoing.

CONCLUSIONS

Currently, no treatment “eliminates” an already present osteoporosis and fracture risk can be reduced but not removed. An early identification of fracture

risk factors can prevent osteoporosis in most people, and for patients with OP medical intervention can stop the progression. It has to be taken into account that when we face a secondary osteoporosis, an appropriate therapy for the primary pathology has to be provided in association with an anti-fracture agent. Therapy for OP should be individualized and based on the clinical scenario for each patient, with the risks and benefits of treatment discussed between the physician and the patient. Where we are now? We briefly summarize the state of the art in a dichotomist way: bad news and good news. Bad news consists of: i) the still reduced number of patients receiving therapy; ii) under-recognition of patients at risk of fractures; iii) poor compliance of both adherence to therapy and perception of the patient's risk/benefit; and iv) the growing concerns of patients about the side effects of treatments. Good news can be described as follows: i) excellent diagnostic tools available; ii) the possibility to assess fracture risk with BMD and/or clinical risk factors (FRAX algorithm); iii) individualized safe and effective treatments available and new ones expected; iv) a better understanding of the pathogenesis of bone metabolic disorders occurred in recent years; and v) initiatives to improve disclosure on OP and fracture risks are in continuous expansion. Recent discoveries in the field of bone cell biology have led to the development of novel therapeutic compounds for osteoporosis and fracture prevention, the goal of all treatment. As soon as these molecules pass from pre-clinical studies to clinical practice, patients will receive an increasingly individualized therapy, targeted to their specific clinical requirements. However, drug therapy alone, unsupported by any appropriate preventive measures, such as adherence to appropriate lifestyle, an adequate vitamin D status and appropriate and regular physical activity, will not be sufficient to improve the quality of life and maintain/increase strength and endurance of our skeleton.

REFERENCES

1. Hernlund E, Svedbom A, Ivergård M, et al. Osteoporosis in the European Union: medical management, epidemiology and economic burden. Arch Osteoporos 2013; 8:136.
2. Kanis JA, Borgström F. SCOPE: a scorecard for osteoporosis in Europe. Arch Osteoporos 2013; 18:144.
3. Svedbom A, Hernlund E, Ivergard M, et al. Epidemiology and economic burden of osteoporosis in Italy. Arch Osteoporos 2013; 8:137.
4. Wiktorowicz ME, Goeree R, Papaioannou A, Adachi JD, Papadimitropoulos E. Economic implications of hip fracture: health service use, institutional care and cost in Canada. Osteoporos Int 2001; 12:271-78.
5. Cauley JA, Hochberg MC, Lui LY, Palermo L, Ensrud KE, Hillier TA, Nevitt MC, Cummings SR. Long-term risk of incident vertebral fractures. JAMA 2007; 298:2761-67.
6. Siris ES, Chen YT, Abbott TA, Barrett-Connor E, Miller PD, Wehren LE, Berger ML. Bone mineral density thresholds for pharmacological intervention to prevent fractures. Arch Intern Med 2004; 164(10):1108-12.
7. Johnell O, Kanis A. An estimate of the worldwide prevalence and disability associated with osteoporotic fractures. Osteoporos Int 2006; 17(12):1726-33.
8. Bianchi ML, Orsini MR, Saraifoger S, Ortolani S, Radaelli G, Betti S. Quality of life in post-menopausal osteoporosis. Health Qual Life Outcomes 2005; 3:78.
9. Crandall CJ, Newberry SJ, Diamant A, et al. Treatment to prevent fractures in men and women with low bone density or osteoporosis: 2012 update of a 2007 report. Agency for Healthcare Research and Quality U. S. Department of Health and Human Services 2012.
10. AIFA, L'uso dei farmaci in Italia. Rapporto nazionale gennaio-settembre 2012. http://www.agenziafarmaco.gov.it/it/content/luso-dei-farmaci-italia-rapporto-osmed-gennaio-settembre-2012.
11. Adami S, Giannini S, Bianchi G, Sinigaglia L, Di Munno O, Fiore CE, Minisola S, Rossini M. Vitamin D status and response to treatment in post-menopausal osteoporosis. Osteoporos Int 2009; 20(2):239-44.
12. http://www.nice.org.uk Alendronate, etidronate, risedronate, raloxifene and strontium ranelate for the primary prevention of osteoporotic fragility fractures in postmenopausal women (amended). Issued: October 2008 last modified: January 2011 and Alendronate, etidronate, risedronate, raloxifene,

strontium ranelate and teriparatide for the secondary prevention of osteoporotic fragility fractures in postmenopausal women (amended). Issued: October 2008 last modified: January 2011.
13. Ishtiaq S, Fogelman I, Hampson G. Treatment of post-menopausal osteoporosis: beyond bisphosphonates. J Endocrinol Invest 2015; 38:13-29.
14. Black DM, Delmas PD, Eastell R, et al. Once-yearly zoledronic acid for treatment of postmenopausal osteoporosis. N Engl J Med 2007; 356:1809-22.
15. Orwoll E, Ettinger M, Weiss S, et al. Alendronate for the treatment of osteoporosis in men. N Engl J Med 2000; 343:604-10.
16. Shane E, Burr D, Ebeling PR, et al. Atypical subtrochanteric and diaphyseal femoral fractures: report of a task force of the American Society for Bone and Mineral Research. J Bone Miner Res 2010; 25:2267-94.
17. Khosla S, Burr D, Cauley J, et al. Bisphosphonate-associated osteonecrosis of the jaw: report of a task force of the American Society for Bone and Mineral Research. J Bone Miner Res 2007; 22:1479-91.
18. Rossouw JE, Anderson GL, Prentice RL, et al. Risks and benefits of estrogen plus progestin in healthy postmenopausal women: principal results from the Women's Health Initiative randomized controlled trial. JAMA 2002; 288:321-33.
19. Cauley JA, Robbins J, Chen Z, et al. Effects of estrogen plus progestin on risk of fracture and bone mineral density: the women's health initiative randomized trial. JAMA 2003; 290:1729–1738.
20. McDonnell DP. Mining the complexities of the estrogen signaling pathways for novel therapeutics. Endocrinology 2003; 144:4237-40.
21. Dickler MN, Norton L. The MORE trial: multiple outcomes for raloxifene evaluation. Breast cancer as a secondary end point: implications for prevention. Ann N Y Acad Sci 2001; 949:134-42.
22. Seeman E, Crans GG, Diez-Perez A, Pinette KV, Delmas PD. Anti vertebral fracture efficacy of raloxifene: a metaanalysis. Osteoporos Int 2006; 17:313-16.
23. Palacios S. Efficacy and safety of bazedoxifene, a novel selective estrogen receptor modulator for the prevention and treatment of postmenopausal osteoporosis. Curr Med Res Opin 2010; 26(7):1553-63.
24. Pinkerton JV1, Harvey JA, Lindsay R, Pan K, Chines AA, Mirkin S, Archer DF; SMART-5 Investigators. Effects of bazedoxifene/conjugated estrogens on the endometrium and bone: a randomized trial. J Clin Endocrinol Metab 2014; 99(2):E189-98.
25. Nakashima T, Hayashi M, Fukunaga T, et al. Evidence for osteocyte regulation of bone homeostasis through RANKL expression. Nat Med 2011; 17(10):1231-34.
26. Xiong J, Onal M, Jilka RL, Weinstein RS, Manolagas SC, O'Brien CA. Matrix-embedded cells control osteoclast formation. Nat Med 2011; 17(10):1235-41.
27. Cummings SR, Black DM, Thompson DE, et al. Effect of alendronate on risk of fracture in women with low bone density but without vertebral fractures: results from the Fracture Intervention Trial. JAMA 1998; 280:2077-82.
28. Johannesdottir F, Poole KE, Reeve J, et al. Distribution of cortical bone in the femoral neck and hip fracture: a prospective case-control analysis of 143 incident hip fractures; the AGES-REYKJAVIK Study. Bone 2011; 48(6):1268-76.
29. Poole KE, Treece GM, Gee AH, Brown JP, McClung MR, Wang A, Libanati C. Denosumab rapidly increases cortical bone in key locations of the femur: a 3D bone mapping study in women with osteoporosis. J Bone Miner Res 2015; 30(1):46-54.
30. Neer RM, Arnaud CD, Zanchetta JR, et al. Effect of parathyroid hormone (1-34) on fractures and bone mineral density in postmenopausal women with osteoporosis. N Engl J Med 2001; 344:1434-41.
31. Silverman S, Miller P, Sebba A. The Direct Assessment of Nonvertebral Fractures in Community Experience (DANCE) study: 2-year nonvertebral fragility fracture results. Osteoporos Int 2013; 24:2309-17.
32. Rehman Q, Lang TF, Arnaud CD, Modin GW, Lane NE. Daily treatment with parathyroid hormone is associated with an increase in vertebral cross-sectional area in postmenopausal women with glucocorticoid-induced osteoporosis. Osteoporos Int 2003; 14:77-81.
33. Crandall CJ, Newberry SJ, Diamant A. Comparative Effectiveness of Pharmacologic Treatments to Prevent Fractures. Ann Intern Med 2014; 161:711-23.
34. Gelb BD, Moissoglu K, Zhang J, Martignetti JA,

Brömme D, Desnick RJ. Cathepsin K: isolation and characterization of the murine cDNA and genomic sequence, the homologue of the human pycnodysostosis gene. Biochem Mol Med 1996; 59(2):200-206.

35. Schilling AF, Mülhausen C, Lehmann W, Santer R, Schinke T, Rueger JM, Amling M. High bone mineral density in pycnodysostotic patients with a novel mutation in the propeptide of cathepsin K. High bone mineral density in pycnodysostotic patients with a novel mutation in the propeptide of cathepsin K. Osteoporos Int 2007; 18(5):659-69.
36. Pennypacker B, Shea M, Liu Q, Masarachia P, Saftig P, Rodan S, Rodan G, Kimmel D. Bone density, strength, and formation in adult cathepsin K (-/-) mice. Bone 2009; 44(2):199-207.
37. Kiviranta R, Morko J, Uusitalo H, Aro HT, Vuorio E, Rantakokko J. Accelerated turnover of metaphyseal trabecular bone in mice overexpressing cathepsin K. J Bone Miner Res 2001; 16(8):1444-52.
38. Bone HG, McClung MR, Roux C, et al. Odanacatib, a cathepsin K inhibitor for osteoporosis: a two year study in postmenopausal women with low bone density. J Bone Miner Res 2010; 25:937-47.
39. Papapoulos S, Bone HB, Dempster DW, et al. Phase 3 fracture trial of odanacatib for osteoporosis. Baseline characteristics and study design. Arthritis Rheum 2013; 65(S):S515-16.
40. Rachner TD, Khosla S, Hofbauer LC. New horizons in osteoporosis. Lancet 2011; 377:1276-87.
41. Levasseur R, Lacombe D, de Vernejoul MC. LRP5 mutations in osteoporosis-pseudoglioma syndrome and high-bone-mass disorders. Joint Bone Spine 2005; 72(3):207-14.
42. Fosmoe RJ, Holm RS, Hildreth RC. Van Buchem's disease (hyperostosis corticalis generalisata familiaris). A case report. Radiology 1968; 90(4):771-74.
43. Johnson ML Unlocking the Sost Gene. J Bone Miner Res 2015; doi: 10.1002/jbmr.2459. [Epub ahead of print].
44. Baron R, Rawadi G, Roman-Roman S. Wnt signaling: a key regulator of bone mass. Curr Top Dev Biol 2006; 76:103-27.
45. Padhi D, Jang G, Stouch B, Fang L, Posvar E. Single dose placebo controlled randomized study of AMG 785, a sclerostin monoclonal antibody. J Bone Miner Res 2011; 26:19-26.
46. McClung MR, Grauer A, et al. Romosozumab in postmenopausal women with low bone mineral density. N Engl J Med 2014; 370:412-20.

JOURNAL OF BIOLOGICAL REGULATORS & HOMEOSTATIC AGENTS Vol. 29, no. 4, 771-785 (2015)

EDITORIAL

CLINICAL APPLICATION OF SHOCK WAVE THERAPY IN MUSCULOSKELETAL DISORDERS: PART II RELATED TO MYOFASCIAL AND NERVE APPARATUS

R. SAGGINI[1], A. DI STEFANO[2], A. SAGGINI[3] and R.G. BELLOMO[4]

[1]Department of Medical Science Oral and Biotechnology "G. D'Annunzio" University, Chieti, Italy; [2]School of Specialties in Physical Medicine and Rehabilitation "G. D'Annunzio" University, Chieti, Italy; [3]Department of Dermatology, University of Rome Tor Vergata, Rome, Italy; [4]Department of Medicine and Science of Aging, "G. D'Annunzio" University, Chieti, Italy

Received May 4, 2015 – Accepted October 26, 2015

Shock waves have been widely recognized in literature as a biological regulator; accordingly we carried out a review on the effect of shock waves on the mesenchymal cells in their various expressions: bone, muscle, ligament and tendon tissue. To date, the application of Shock Wave Therapy (SWT) in musculoskeletal disorders has been primarily used in the treatment of tendinopathies (proximal plantar fasciopathy, lateral elbow tendinopathy, calcific tendinopathy of the shoulder, and patellar tendinopathy, etc.) and bone defects (delayed and non-union of bone fractures, avascular necrosis of femoral head, etc.). Although the mechanism of their therapeutic effects is still unknown, the majority of published papers have shown the positive and beneficial effects of using SWT as a treatment for musculoskeletal disorders, with a success rate ranging from 65% to 91%, while the complications are low or negligible. The purpose of this paper is to present the published data on the clinical application of SWT in the treatment of myofascial and nerve disorders. With the help of the relevant literature, in this paper we outline the indications and success rates of SWT, as well as the adequate SWT parameters (e.g., rate of impulses, energy flux density) defined according to the present state of knowledge.

During the last decade myofascial and nerves disorders have found a possible key to their resolution in Extracorporeal Shock Wave Therapy (ESWT). Our objective is to highlight the literature on this topic and discuss the specific characteristics involved.

SHOCK WAVE THERAPY FOR TENDINOPATHIES

Although the Shock Wave Therapy (SWT) mechanism of action on tendinopathies has not yet been fully understood, many authors (1-10) found good results in the use of SWT pogenitor cells (12). Both tendon cells and the collagen structure are potential targets of ESWT, particularly in later degenerative phases. However, it is not clear whether Shock Waves (SW) activate tendon cells directly, or regulate the pathogenetic alteration of the Extracellular Matrix (ECM) homeostasis that occurs in tendinopathies. Early *in vivo* experimental studies showed typical histomorphological patterns

Key words: muscular fascial diseases, tendon, entrapment syndromes, shock wave, biological regulator

Mailing address: Prof. Raoul Saggini,
Department of Medical Science Oral and Biotechnology,
"G. D'Annunzio" University,
V.le Abruzzo 322
66100 Chieti Scalo, Italy
Tel.: +39 0871 3553005/3553007
e-mail: saggini@unich.it

0393-974X (2015)

DISCLOSURE: ALL AUTHORS REPORT NO CONFLICTS OF INTEREST RELEVANT TO THIS ARTICLE.

characterized by a reversible inflammatory reaction (mostly dose-dependent) in tendon cells after SWT. A neovascular proliferation on the bone-tendon junction associated with the release of proangiogenic regulatory factors [NO synthase (NOS) and Vascular Endothelial Growth factor (VEGF)] and Proliferating Cell Nuclear Antigen (PCNA) have also been demonstrated (13). *In vitro*, the dose-dependent effect of SW at low energies results in a proliferative action as well as an increase in the gene expression of collagen types I and III and Transforming growth factor beta 1 (TGF-β1), followed by the production of NO and collagen (14).

NO is a highly reactive molecule and, in tendon healing, all 3 isoforms of the activating enzyme NOS are expressed by fibroblasts. NO enhances ECM synthesis and is overexpressed in injured as well as in overused tendon models (15). Nevertheless, NO itself may lead to an oxidant status, revealed by high levels of malondialdehyde, which is an end product of lipid peroxidation (16). It has not been clarified whether SW regulate the levels of NO on tendons toward physiological values. The regulatory effect of SW has been observed in the expression of tenocytic markers such as scleraxis, tenomodulin, tenascin-C, and type I and III collagens, as well as in interleukin (IL)-6 and Matrix Metalloproteinases (MMPS) 1 and 13 in cultures of pathologic tenocytes (17). Although supported by clinical data, the validity, effectiveness and reliability of ESWT in the treatment of tendinopathies do not always meet the criteria of evidence-based medicine. This is mainly due to an objective difficulty in comparing data from non-homogeneous studies, which have adopted various types of SW generators, with differing energy parameters and treatment protocols (18, 19). The data published regarding patellar tendinopathy are particularly controversial. Even though some studies describe the efficacy of ESWT (24–26), others report no significant difference between ESWT and placebo in inducing angiogenesis and clinical improvement (20).

Some studies reported that SWT can significantly increase the diffusion of cytokines across vessel walls into the pain-generating region, thereby stimulating the tendon healing response (21), significantly reduce the non-myelinated sensory fibers, and release of calcitonin gene-related peptide, and substance P (11). Taken together, these data indicate that, as expressed above for bone tissue, tendon tissue can convert SWT stimulation into biochemical signals by means of TGF-β1 and insulin-like growth factor (IGF)-I (21). Other authors have demonstrated that SWT acts on the pain system by means of hyper stimulation analgesia, which involves stimulation of a brainstem feedback loop through serotonergic activation via the dorsal horn that exerts descending inhibitory control over pain (22).

UPPER LIMB TENDINOPATHIES

Calcific tendinopathy of the shoulder

The first reports regarding the effectiveness of SWT on calcific tendinopathy of the shoulder date back to the first half of the 1990s, when preliminary data coming from non-controlled trials showed the efficacy and safety of this approach (23). Subsequently, several authors focused their attention on this topic; in particular the efficacy of SWT, its dose-dependent effect, and its safety have been the object of a number of randomized controlled trials. Rompe et al. randomized 100 patients with calcific tendinopathy of the rotator cuff, with pain for more than 12 months and with a history of previous unsuccessful conservative treatments, to either a low-dose SWT group (1 session of 1500 pulses at 0.06 mJ/mm2 - no anesthesia before treatment) or a high-dose SWT group (1 session of 1500 pulses at 0.28 mJ/mm2 – local anesthesia needed). Constant and Murley score (CS), radiographic and clinical control were assessed after 6 and 24 months. The authors found improvement in both groups, with significant results achieved with high energy dose (24).

It should be noted that some studies have shown the dose-dependent effect of SWT on calcific tendinopathy of the shoulder (3, 25). Loew et al. (25) found that both low- and high-dose SWT are more effective compared to no treatment in terms of function and reabsorption of calcifications, but higher doses show more efficacy than lower ones. Three months after therapy, patients receiving 2 sessions of 2000 pulses at 0.3 mJ/mm2 achieved a CS of 71% of normal values, compared to 53% of those receiving 1 session of 2000 pulses at 0.1 mJ/mm2.

Similar results came from the only multicenter randomized controlled trial published on this topic (3), in which the difference of mean improvement in CS between high- and low-dose SWT in a follow-up after 3 months was at 37%, increasing to 48% and 49% at 6 and 12 months. Ioppolo et al. recently published a randomized controlled trial designed to compare 2 different ranges of Energy Flux Density (EFD) in the treatment of calcific tendinopathy of the shoulder (4); 46 patients were randomized to receive high-dose (4x2400 pulses at 0.20 mJ/mm2) or low-dose SWT (4x2400 pulses at 0.10 mJ/mm2). Significant clinical improvement based on mean Constant Scores was observed after 6 months in patients receiving high-dose SWT (mean score=79.43±10.33) compared with low-dose SWT (57.91±6.53). Likewise, after 6 months, a significant decrease in Visual Analogue Scale (VAS) scores was found in high-dose SWT compared with low-dose SWT. Calcific deposits disappeared in the same percentage of patients in both groups.

Albert et al. (26) randomized 80 patients with calcifying tendinopathy of the rotator cuff to high-dose SWT (2x2500 pulses at 0.45 mJ/mm2) or to low-dose SWT (2x2500 pulses at 0.06 mJ/mm2). Despite the fact that high-energy SWT significantly improves symptoms in refractory calcific tendinopathy of the shoulder, it was found that the size of the calcific deposit had not changed in the majority of patients after a three-month follow-up.

A recent systematic review and meta-analysis (27) evaluated the effectiveness of SWT in improving function and reducing pain in patients with calcific tendinopathy of the shoulder, and the rate of disappearance of calcifications after therapy at 6 month follow-up, founding a pooled total resorption ratio of 27.19 and a pooled partial resorption ratio of 16.22.

Galasso et al. (28) assessed the short-term outcomes of ESWT for the treatment of chronic non-calcific tendinopathy of the supraspinatus: 20 patients with non-calcifying supraspinatus tendinopathy (NCST) were randomized into an active or a sham treatment group. Effectiveness was determined by the comparison of the mean improvement in the Constant and Murley score (CMS) between the treatment and the placebo groups after three months. At the final follow-up, significant improvement in the total CMS score and most of the CMS subscales was observed in the ESWT group when compared to the baseline values. Significantly higher total CMS, and significantly higher scores for CMS pain and ROM were observed in the ESWT group when compared to the placebo. No serious adverse effects were noted after ESWT. They concluded that patients with NCST may benefit from low energy ESWT, at least in the short-term, and that ESWT is likely to play a key-role in successful treatment.

Saggini et al. (29, 30) assessed the mid- and long-term effects of ESWT on shoulder tendinopathy in two randomized controlled trials. In the first study in 2010 (29), they evaluated two groups of patients, recruited on the basis of each subject choosing to undergo either the conservative treatment (arm A) or the surgical one (arm B).

Arm A included 30 subjects randomized into three groups: A1, A2, A3, each one made up of 10 subjects. Group A1 were treated with 3 SW sessions, 1 per week (Evotron, Electroidraulic Spark Gap device, 5 mm focal depth, medium EFD 0.132 mJ/mm2, 600 shock waves for each session), 9 Multi Joint System-MJS sessions, 3 per week, and specific nutritional supplement. Group A2 received SW plus MJS. Group A3 received SW treatment only.

Arm B included 50 patients (randomized into two groups, B1 and B2) who had undergone rotator cuff surgery and acromionplasty for non-massive lesions without important gleno-humeral instability, with either open or arthroscopic procedures. Subjects in Group B1 underwent a specific rehabilitation program after acromionplasty; group B2 took part in the same program but a nutritional supplement was also given to them. The analysis of the results in Arm A highlighted that, in terms of reducing pain, the main benefits were found in group A1 where the supplement was given. From the analysis of the data in arm B, in both groups an improvement of the first 4 items of the assessment was found. In group B1, 84% of patients declared to be satisfied with the improvement whereas 16% were dissatisfied; in group B2, where the nutritional supplement was given, 92% were satisfied and 8% were dissatisfied. The author concluded that an integrated rehabilitative approach, whether conservative or post-surgical, should provide particular attention to the optimization of the articular and metabolic

balance in order to better achieve functional recovery in rotator cuff syndrome.

In a subsequent 2012 study (30), Saggini et al. assessed the long-term results of rehabilitative management with extracorporeal shockwave therapy in rotator cuff syndrome with partial tears; 108 patients with pain from 6 weeks to 24 months were recruited. All patients underwent 3 sessions (1/week) of extracorporeal shock waves, associated with therapeutic exercise to increase range ofmotion (R.O.M.) and postural rebalancing (24 sessions, 3/ week). An Electrohydraulic Spark Gap device was used for the shockwaves (therapeutic waves at 5 mm focal depth, medium strength power at 0.132 mJ/ mm2, 600 waves per session).Before treatment, all subjects were assessed by a clinical examination with VAS and CMS. At the end of the shock wave therapy, they were reassessed after three weeks, 2 months, 4 months and 6 months. At the end of each year, from 2005 to 2009, a telephone interview was conducted to evaluate changes in pain and function and the efficacy of treatment. Results showed significant improvement in pain level, reduction in the rate of drug consumption and an increase in R.O.M. Even in the long-term follow-up after 5 years, 85% of subjects reported subjective satisfaction and well-being.

Lateral elbow tendinopathy

The therapeutic use of SWT on lateral epicondylitis has been a focus of research since the mid 90s. Several studies investigated the efficacy of SWT on lateral elbow pain; however, its usefulness still remains controversial. Rompe et al. (31) evaluated the efficacy of low-EFD SWT (3 sessions, at weekly intervals, of 1000 pulses of 0.08 mJ/mm2) delivered on the lateral epicondyle, compared to a sham therapy involving 50 subjects experiencing pain for >12 months and who had previously received unsuccessful conservative treatments. In the follow-up, after 12 weeks, the reduction in pain was significantly greater in the treatment group, with a good to excellent outcome in 56% of patients. Similar results were obtained by the same researchers in 100 patients with chronic and recalcitrant lateral elbow pain, who were randomized to a low-dose SWT protocol or to a sham protocol. In the follow-up after 24 weeks, patients in the SWT group showed a decrease in pain compared to baseline, ranging from 64.5% for pressure pain to 78.9% for night pain. At the same time, patients in the sham group showed no improvement of pain scores (32) - on the contrary, it even worsened. In a selected population of recreational tennis players with chronic (>12 months) elbow pain of at least moderate intensity (pain ≥4 on a 10 cm VAS), unresponsive to conservative treatments, the efficacy of 3 weekly sessions of 2000 pulses at 0.09 mJ/ mm2 was compared to that of a sham treatment (3 weekly sessions of 20 pulses at 0.09 mJ/mm2) (32): 78 patients were randomized to either the treatment group or sham group, and assessed 3 months after therapy for pain during resisted wrist extension and functionality with the Upper Extremity Function Scale. A significant decrease in pain during resisted wrist extension and an improvement in the Upper Extremity Scale were observed in the treatment group compared to the sham group

Pettrone et al. (33), recruited 108 patients with chronic lateral epicondylitis, unresponsive to previous conservative treatments, and randomized them into a treatment group, receiving three consecutive weekly sessions of low-dose SWT (2000 pulses at 0.06 mJ/mm2), and a placebo group. Three months after therapy, 60% of patients receiving SWT experienced a reduction of at least 50% of baseline pain, compared to 30% of those receiving placebo. A number of trials, however, did not find similar positive results. Speed et al. (34) randomly assigned 75 patients experiencing lateral elbow pain for more than 3 months to a treatment group, receiving 3 monthly sessions of medium dose SWT (1500 pulses at 0.18 mJ/mm2) or to a sham group (1500 pulses at 0.04 mJ/mm2). In the follow-up after 3 months, 35% of those assigned to the treatment group and 34% of patients in the sham groups showed more than 50% improvement from baseline pain. In this case, contrarily to all the other studies found in the relevant literature and to general manufacturers' indications, monthly sessions were used. Such distance between two consecutive treatments might have contributed to failure in the SWT group.

Doubts about the present results were also described in a systematic review of nine placebo-controlled trials involving 1,006 participants, in which the authors found a "Platinum" level of

evidence showing that SWT provides little or no benefit in terms of pain and function in lateral elbow pain (35). However, too many discrepancies exist in the current literature as to the duration of the disorder, the type of disorder, the frequency and total dose of SWT, the length of time between SWT administration, the type of management and control group, the timing of the follow-up and the outcomes assessed, to appropriately consider a pooled meta-analysis of SWT for lateral elbow tendinopathy (36). It seems, in fact, that low energy SWT delivered without local anesthesia in patients with chronic lateral epicondylitis (which is recalcitrant to conservative treatments) is more effective than placebo in improving symptoms (6, 44-46, 50). Correct selection of patients (i.e. selecting patients who have been excluded from surgery and are suitable for treatment according to the level of chronicity of the disease), as well as of treatment protocols (whether performing the treatment once or twice a week instead of once a month), is thereby crucial in order to obtain positive results in these patients.

In 2012, Özçakar et al. compared - clinically and ultrasonographically - the therapeutic effects of physical therapy modalities (hot pack, ultrasound therapy, and friction massage), local corticosteroid injection, and extracorporeal shock wave treatment (ESWT) in lateral epicondylitis (LE) (37). In that study, fifty-nine elbows of 59 patients with LE were randomized into three treatment groups receiving either physical therapy, a single corticosteroid injection, or ESWT. The VAS was used to assess pain intensity, Jamar hydraulic dynamometer was used for grip strength, finger dynamometer was used for pinch strength (before treatment, and then on the first, third, and sixth months of treatment). All subjects were also assessed with ultrasonography before and 6 months after treatment. In all groups, VAS scores in patients were found to have decreased significantly at the first, third, and sixth months of treatment. In respect to grip strength evaluations, the increase after treatment was significant only in the first month in group II; in the first and third months in group I; and in the first, third, and sixth months of treatment in group III. Pinch strength and ultrasonographical findings did not change during follow-up in any group. The authors concluded that physical therapy modalities, corticosteroid injection, and ESWT all have favorable effects on pain and grip strength in the early period of LE treatment. The increase in grip strength lasts longer with ESWT. On the other hand, they found no change in ultrasonographic imaging in the first six months of these treatment methods.

Kim et al. (38) assessed the effectiveness of initial ESWT compared to local steroid injection for patients newly diagnosed with lateral or medial epicondylitis, and found greater improvement in the ESWT group compared to those subjects who underwent corticosteroid injections in terms of Nirschl score and Roles and Maudsley score. They concluded that ESWT can be a useful treatment option in patients for whom local steroid injection is difficult.

In a recent study, Moretti et al. (39) assessed the correlation between clinical and functional measures and strength recovery after ESWT on 26 patients with epicondylitis. It showed an improvement in VAS values and Mayo Elbow Performance Index scores for the pathologic limb and a concomitant decrease in grip strength, especially in the dominant limb, probably related to the effects of ESWT, which reduce spasticity in painful hypertonic muscles.

LOWER LIMB TENDINOPATHIES

In a systematic review (40) Barton et al. stated that ESWT can be considered an effective intervention in lower limb tendinopathy and should be considered as a treatment for Greater Trochanteric Pain Syndrome (GTPS), Patellar Tendinopathy (PT), and Achilles Tendinopathy (AT), particularly after failure of other non-operative treatments.

Patellar tendinopathy

Some studies found significant improvement of clinical outcomes in patients with patellar tendinopathy treated with SWT with a success rate ranging from 73.5% to 87.5% (9, 41-44) whereas in other studies no improvement was evidenced (46). The athletes in all these studies were all still actively taking part in sports activities (basketball, volleyball or handball).

Peers et al. (43) compared surgical treatment and low-EFD SWT in 15 patellar tendinopathies. SWT was administered in 3 sessions of 0.08 mJ/mm2. In the follow-up after 2 years, no significant

differences in VAS or Victorian Institute of Sport Assessment (VISA) questionnaire scores were found between groups, but the surgical treatment group had a longer absence from work after surgery. Despite the retrospective nature of the study, the authors concluded that SWT was an effective alternative to surgical treatment when conservative treatments fail in chronic patellar tendinopathy.

In a randomized controlled study, Wang et al. (9) assessed the efficacy and safety of a single SWT treatment compared to a standard conservative treatment in patients with patellar tendinopathy. A single session of SWT with an EFD of 0.18 mJ/mm2 was administered to 30 tendons, while 24 tendons received standard conservative treatment. Follow-ups, scheduled after 1, 3, 6, 12, 24 and 36 months, showed a significant improvement in function as shown in their VISA and VAS scores. Moreover, ultrasonographic examination revealed a significant increase in vascularity of the tendon and a reduction of tendon thickness in patients who underwent SWT compared with those who underwent conservative treatment.

In an observational study on 83 tendons with tendinopathy for at least 3 months, refractory to conservative treatments, Vulpiani et al. (41) performed 3 to 5 sessions of SWT with an EFD ranging from 0.08-0.44 mJ/mm2. Results showed an improvement in the average score of VAS already in the first month after treatment, with a constant increase in the short-term (6-12 months), medium-term (13-24 months) and long-term (>24 months) follow-ups.

Saggini et al. (45) carried out a perspective non-randomized study on soccer players with Jumper's knee; 42 male soccer players were assessed after a treatment protocol consisting of 1 session with focused ESWT per week combined with 3 physiotherapy sessions per week, for 3 consecutive weeks, based on mechanotransduction. For ESWT, Evotron Spark Gap Electrohydraulic equipment was used; 5 mm focal depth, average energy of 0.132 mJ/mm2, 800 shots (240 sw/min) during each ESWT session, at a shot frequency of 4 Hz, and with an energy flow density of 0.10–0.14 mJ/mm2; total absorbed energy per session was 3.30 mJ. Physiotherapy sessions consisted of eccentric training combined with simultaneous administration of high efficiency focused acoustic waves (VISS system). Their condition was assessed before treatment, at the end of the rehabilitation period (3 weeks) and after 2 , 4 and 6 months from the end of treatment by clinical examination, instrumental analysis, VAS for pain assessment and VISA score. A mid- and long-term follow-up by telephone interview was conducted every year, for five years after treatment. Upon therapeutic protocol completion, significant improvement was recorded in both mean pain VAS and mean VISA score compared to baseline values. Follow-up controls after 2, 4 and 6 months confirmed the improvement in mean pain VAS and VISA score. At the last telephone interview the majority of patients reported to consider/acknowledge ESWT as an effective treatment and described a significant improvement in their functional abilities, a significant reduction in drug consumption, and 88% of subjects continued to play competitive soccer.

Achilles tendinopathy

Many studies investigated the effect of SWT on Achilles tendinopathy, and most reported favorable results with similar success rate to patellar tendinopathy (1, 6, 46).

Furia carried out two separate case controlled studies (1, 46) investigating the efficacy of SWT for both chronic insertional and non-insertional Achilles tendinopathy. In the first study, 35 patients with insertional Achilles tendinopathy were treated with a single session of SWT (3000 pulses and EFD of 0.21 mJ/mm2), and 33 patients with conventional treatments. SWT was administered either with a local anesthesia field block (12 patients) or with a regional block (23 patients). VAS and RMS were used for evaluation. Twelve months after treatment, 83% of patients in the SWT group and 39% of those in the conventional treatment group showed an improvement of their symptoms according to the RMS. The VAS scores after 1, 3, and 12 months for SWT conventional treatment were 4.2 and 8.2, 2.9 and 7.2, and 2.8 and 7.0, respectively.

The second of these studies investigated the efficacy of SWT in patients with non-insertional chronic Achilles tendinopathy. The procedures used to administer the SWT were the same used in the study described above. Thirty-four patients were treated with SWT and 34 with conventional treatments. VAS

and RMS were again used to evaluate the outcome. Twelve months after treatment, 85% of patients in the SWT group and 27% of those in the conventional treatment group showed an improvement of their symptoms according to the RMS. VAS scores after 1, 3, and 12 months for SWT and conventional treatment were 4.4 and 8.4, 2.9 and 6.5, and 2.2 and 5.6, respectively.

In a non-randomized observational study, Vulpiani (10) assessed the efficacy of SWT on 127 Achilles tendons with tendinopathy. Patients were treated in 3 to 5 sessions, at 2/7-day intervals, with 1500-2500 pulses for each session and an EFD ranging from 0.08 to 0.40 mJ/mm2. Results were satisfactory on VAS score in 47.2% of cases (60 of 127 tendons) in the follow-up after 2 months, in 73.2% of cases (93 of 127 tendons) in the medium-term follow-up (13–24 months), and in 76% of cases (92 of 121 tendons) in the long-term follow-up (>24 months).

In a randomized triple-arm study, Rompe et al. (47) compared 25 patients in a wait-and-see policy, 25 patients treated by eccentric exercises and 25 patients treated with SWT. SWT was administered in 3 sessions at weekly intervals with 2000 pulses for each session with an EFD of 0.1 mJ/mm². Four months after baseline, 15 of 25 (60%) patients in the eccentric exercises group, 13 of 25 (52%) patients in the SWT group, and 6 of 25 (24%) patients in the wait-and-see group reported symptoms indicating that they had "completely recovered" or felt "much improved" for all outcome measures. No difference was found between the eccentric and SWT groups. However, both of these groups showed better results than the wait-and-see group. The same authors (7) compared 25 patients treated by eccentric exercises with 25 patients treated with SWT, and the results showed that SWT was better than eccentric exercises in the treatment of patients with chronic recalcitrant Achilles tendinopathy.

Costa et al. (48) reported no treatment efficacy in 49 patients with Achilles tendinopathy treated with SWT. SWT was administered in 3 sessions at 1-month intervals with 1500 pulses and an EFD of 0.2 mJ/mm². Patients with insertional and non-insertional forms of Achilles tendinopathy were included in this study. Baseline VAS score was 55 for both SWT and control groups. The score after intervention was 34 points in the SWT group and 50 in the control group.

Although the authors affirm that their results do not support the use of SWT in the management of patients with chronic Achilles tendinopathy, their study could be biased: i) a too small cohort of patients to detect a significant treatment effect (the authors affirm in their conclusion that: "the confidence intervals include the potential for a clinically relevant treatment effect"); ii) the practice of monthly intervals between sessions is not recommended. Although to date there is no consensus on the procedures for SWT use, it is, in fact, widely accepted that weekly intervals between sessions lead to better results (29, 31, 47, 49, 53, 58, 71); and iii) the inclusion of both non-insertional and insertional Achilles tendinopathy as a single group may have decreased the positive effects of SWT.

In a systematic review, Al-Abbad and Simon (49) found satisfactory evidence of the effectiveness of low-energy ESWT in the treatment of chronic insertional and non-insertional Achilles tendinopathies at follow-up after a minimum of 3 months before considering surgery if other conservative management fails. However, combining ESWT with eccentric loading appears (even based on this evidence) to show superior results.

Plantar fasciitis

The safety and efficacy of SWT in the management of chronic plantar fasciopathy has been reported by several randomized clinical trials. These studies have shown that low-energy SWT, when directly applied to the tender point at the medial calcaneal tubercle, and performed without local anesthesia, leads to significant and persistent improvement of recalcitrant plantar fasciopathy symptoms within a reasonable time frame (50-52). Rompe et al. (8, 50, 51), and more recently Dizon et al. (52), reviewed the results of using SWT to treat chronic plantar fasciopathy. Rompe et al. (50) firstly investigated the efficacy of SWT in the plantar fasciopathy in 30 patients randomized in either SWT group (N.=15) or placebo group (N.=15). The SWT was administered in 3 sessions at weekly intervals with 1000 pulses in each session with an EFD of 0.06 mJ/mm2, without local anesthesia. Twelve weeks after the last treatment, only patients in the SWT group experienced a significant reduction of pain and improvement of function. After this, they (51) also evaluated 45 running athletes with chronic

plantar fasciopathy. Athletes were either assigned to a treatment group that received 3 sessions of 2100 pulses of 0.09 mJ/mm2 without local anesthesia or to a placebo treatment. After 24 weeks, 60% versus 27% of patients reported >50% reduction of pain on first walking in the morning.

Buchbinder et al. (53), in a randomized controlled trial, investigated 166 patients with acute or chronic (symptoms ranging from 8 to 980 weeks) plantar fasciopathy. Patients were randomly assigned to receive active or placebo SWT. In the active group, 3 sessions at weekly intervals, with 2000 or 2500 pulses per session and an EFD varying from 0.02 mJ/mm2 to 0.33 mJ/mm2 were administered. Patients in the placebo group received 3 sessions at weekly intervals with only 100 pulses per session with an EFD of 0.02 mJ/mm2. After 6 and 12 weeks, there were significant improvements in overall, morning, and activity pain, walking ability in both groups, without significant statistical differences between the groups.

Kubo et al. (54) investigated the relationship between magnetic resonance imaging (MRI) findings before extracorporeal shockwave therapy (ESWT) and the treatment outcome of ESWT in chronic plantar fasciitis. The study examined 50 feet with chronic plantar fasciitis. The scores before and after ESWT in the follow-up after six months were investigated using the Japanese Society for Surgery of the Foot (JSSF) Ankle-Hindfoot Scale and the VAS. MRI before ESWT was used for image evaluation. MRI revealed thickening of the plantar fascia (PF), and an investigation was conducted regarding the findings of a high-signal-intensity area (HSIA) inside the PF, the edema near the PF, and the bone marrow edema (BME) of the calcaneus. The average JSSF score and VAS score improved significantly during follow-up. In total, 44 feet were deemed to have improved. MRI revealed that the average amounts of PF thickening did not significantly differ between the improved group and the non-improved group. HSIA, edema near the PF, and BME were observed in 36, 41, and 11 feet in the improved group, respectively; and 2, 4, and 2 feet in the non-improved group, respectively.

OTHER TENDINOPATHIES

Several studies reported a positive effect of shock-wave therapy in other tendinopathies such as greater-trochanter pain syndrome (GTPS) chronic proximal hamstring tendinopathy (PHT) and medial tibial stress syndrome (MTSS) (55).

Medial tibial stress syndrome

MTSS is a benign, though painful, condition, and a common problem found in runners. It is prevalent among military personnel, runners, and dancers, showing an incidence of 4% to 35%. Conservative treatment is almost always successful and includes several options, though none has proven more superior than resting. Prevention programs do not seem to influence the rate of MTSS, though shock-absorbing insoles have reduced MTSS rates in military personnel, and ESWT has shortened the duration of symptoms.

Moen et al. (56) compared the results of two treatment regimen for MTSS, one with and the other without additional shockwave therapy. The participants were 42 athletes with MTSS. Patients from one hospital were treated with a graded running program, while patients from the other hospital were treated with a 6-phase graded running program and ESWT (5 treatment sessions. Session 1: 1,000 shocks with an energy flux density of 0.10 mJ/mm2, 2.5 shocks per second. Session 2: 1,500 shocks, 0.15 mJ/mm2, 2.5 shocks p/s. Session 3: 1,500 shocks, 0.20 mJ/mm2, 2.5 shocks p/s. Session 4:1,500 shocks, 0.25 mJ/mm2, 2.5 shocks p/s. Session 5: 1,500 shocks, 0.30 mJ/mm2, 2.5 shocks p/s (five sessions in 9 weeks). The time to full recovery was significantly faster in the ESWT group compared with the patients who only performed a graded running program, respectively 59.7±25.8 and 91.6±43.0 days (p=0.008). The authors concluded that MTSS patients may benefit from ESWT in addition to a graded running program and that ESWT can be considered as good additional treatment. However, further investigation in a prospective controlled trial with the addition of randomization and double blinding assessment is needed.

SWT for muscle disorders

There are few studies on the treatment of muscle lesions and disorders with ESWT. We describe below what is reported in literature.

Myofascial pain syndrome

Ji et al. (57) assessed the effect of ESWT in

myofascial pain syndrome of upper trapezius with VAS and pressure threshold by digital algometer; 22 patients with shoulder pain were recruited. The ESWT was applied by using a Dornier AR2® (MedTech, Munchen, Germany). The participants were randomly assigned to a treated group or a control group. One doctor examined the taut band of one side of the upper trapezius and applied ESWT for 700 impulses to the taut band and 300 impulses surrounding the taut band. The treated group had 0.056 mJ/mm2 applied as low energy while the control group had 0.001 mJ/mm2 applied, an ineffective level of ESWT that can, however, make the participants unaware of being part of the control group by the sound of shock during treatment. There were 4 treatment sessions: 2 sessions per week for 2 weeks and no other treatment of myofascial pain syndrome such as medication, physical therapy and exercise. There was no significant difference of pre-VAS and pre-threshold between the two groups. Post-VAS was instead significantly different between the two groups ($p<0.05$). The pressure threshold rose significantly only in the treated group ($p<0.05$). The authors concluded that ESWT was effective in relieving pain for myofascial pain syndrome in the upper trapezius after 4 treatments over two weeks. The effect of ESWT in myofascial pain syndrome might be pain relief by regulating the concentration of pain-related substances, promoting angiogenesis and increasing perfusion at ischemic tissues. They also considered the need for future studies with more patients with diverse characteristics such as age and sex, and assessment within further duration.

Jeon et al. (58) investigated the effect of extracorporeal shock wave therapy (ESWT) on 30 patients with myofascial pain syndrome (MPS) in trapezius muscle. They were randomly divided into two groups, one ESWT group (n=15), and one trigger point injection (TPI)+transcutaneous electrical nerve stimulation (TENS) group (n=15). For a total of 3 weeks, ESWT was carried out with 1500 pulses each time at one week interval totaling 4500 pulses, TPI once a week totaling three times and TENS five times a week totaling three weeks. The changes in pain threshold (lb/cm2) showed the values of 6.86±1.35 before the first therapy, 11.43±0.27 after the first therapy, and 12.57±0.72 after the third therapy, while TPI+TENS group showed the values of 6.20±1.92 before first therapy, 8.80±0.48 after first therapy, and 9.60±2.19 after third therapy, and the changes between the groups were significantly different ($p=0.045$). The changes in visual analogue scale were estimated to be 6.86±0.90 before first therapy, 2.86±0.90 after first therapy, and 1.86±0.69 after third therapy in the ESWT group, whereas the figures were estimated to be 7.20±1.30 before first therapy, 4.60±0.55 after first therapy, and 2.80±0.84 after third therapy in the TPI+TENS group. The changes between the groups were significantly different. The changes in the McGill pain questionnaire and pain rating scale between the groups were not significantly different. Nor were the changes in neck ROM significantly different between the groups. The authors concluded that ESWT is as effective in causing reduction in pain and improvement in neck range of motion as TPI and TENS in patients with myofascial pain syndrome in trapezius muscle. In addition, execution of ESWT is deemed to be helpful in diagnosing myofascial pain syndrome as it would enable the confirmation of referred pain occurrence and muscular twitching response, which are the standards for the diagnosis of myofascial pain syndrome.

In a recent study, Moghtaderi et al. (59) assessed the effectiveness of ESWT on myofascial pain related to plantar fasciitis by comparing the treatment of gastro-soleus trigger points and heel region with the treatment of the heel region alone; 40 patients with a clinical diagnosis of plantar fasciitis were randomly divided into two groups. The case group received ESWT for the heel region and for the gastro-soleus trigger points. The control group received ESWT for the heel region only. The protocol was the same for both groups and they were treated with three sessions every week. The pain score by VAS and the modified RMS were assessed before the first session and 8 weeks after the last session. In the second assessment (8 weeks after the last session), the authors found a more significant improvement both in pain and function in the case group. The authors concluded that combining ESWT for both plantar fasciitis and gastro-soleus trigger points in treating patients with plantar fasciitis is more effective than utilizing it solely for plantar fasciitis.

Myositis ossificans

Myositis ossificans (MO) is common in sports

activity and can be the result of direct trauma or to repeated micro-injuries. The traditional therapeutic approach relies on several treatments, such as physical therapy, with low evidence of their proven clinical efficacy. The latest therapeutic option is surgical removal, often associated with significant loss of functional integrity. There are few articles in literature on the treatment of post-traumatic MO. Buselli et al. (60) reported a case series of 24 sportsmen, with post-traumatic MO, treated with ESWT and physiotherapy. A control group was absent. The ESWT was generated by two electro-hydraulic systems, Evotron or Ossatron OSA 40 by HMT (Switzerland); 100 pulses per cm2 of ossification were administered every 2 weeks for three sessions (range from 0.13 to 0.23 mJ/mm2, mean 0.15±0.02 mJ/mm2) taking as an example the energy flux density (EFD) used in the treatment of calcified tendons. After the first session, the patients started a rehabilitation program consisting of one daily session 6 days a week. The authors found a significant progressive decrease in the intensity of pain measured using the VAS scale and Fischer's algometer and an improvement of the ROM in all the patients. They also found a complete clinical and functional resolution in 21 of the 24 patients, with a return to sport-specific training after 7.17±3.05 weeks, to sport-specific activity after 11.32±4.06 weeks and to competitive activity after 13.05±4.17 weeks. Except for three patients, all had made a complete return to the previous sport activity within 12 months. Only a partial reduction of the ossification was observed in the X-ray images but all the patients showed signs of functional improvement immediately after therapy. Two months after therapy, a normal range of motions and no signs of weakness were noticed. Three months after treatment, 87.5% of patients resumed regular sports activities. The results of this clinical experience revealed that at first the administration of physiotherapy alone had been unsuccessful and only when the shock waves were associated, the management of MO became efficient; the injury tissue benefited from the SW for the biologic stimulus and from the physiotherapy for the physical one. However, this experience was a preliminary case study. The authors proposed to continue the study with the adoption of a randomization into two groups to compare the effects of the cooperation of ESWT and physiotherapy *vs* only physiotherapy which seems to be necessary for classification of ESWT as evidence-based medicine.

Based on Buselli's article, in 2011 Torrance and deGraauw (61) described the case of a 20 year-old male semiprofessional rugby player with progressive pain and loss of range of motion after sustaining a severe, right quadriceps contusion nine weeks earlier with subsequent myositis ossificans, which was confirmed during radiographic examination. A trial of shockwave therapy was started 10 weeks after the injury. The first EWST treatment (Masterpuls MP100, Storz Medical) consisted of 100 pulses at 1.5 bar (1 bar = 0.1 MPa = 0.1 N/mm2) delivered to each of five locations over the mass: two at the proximal end, one in the middle and two at the distal end. Two days later, the patient reported that he had experienced about 12 hours of soreness after the treatment but presently felt great and had no night pain. Objectively, his ROM increased to 115° (baseline 90°). He had a second shockwave treatment for 100 impulses at 3.0 bar over every square centimeter of the mass (2500 pulses). After one week (11 weeks post-injury), he reported that he was able to walk for over an hour with no pain and had no night pain. The ROM of his knee was not restricted and was equal to the contralateral side (125°). He had a final treatment of 2500 pulses over 25 points and was advised that he could start shallow, body weight squats and 45° knee flexion lunges. He was advised to gradually increase his ROM with the lunges and squats before adding resistance. Two weeks after the last ESWT session (13 weeks post-injury), he reported that he was running an average of four km/day and had just played his first 60-minute touch rugby session with no pain. The following week he was running over 5 km in 25 minutes with speed intervals of up to 85% capacity and playing touch rugby three times a week. He reported full ROM with only some muscle fatigue that seemed to be similar in both legs, possibly due to deconditioning; 17 weeks after his injury, he reported he was playing touch rugby at full pace, his timed sprints were back to pre-injury levels, and his squat and deadlifts were back to full strength and ROM. He reported being unrestricted in training with the rest of the team and felt that he had made a full recovery.

According to Buselli, they concluded that ESWT may be a promising treatment modality for the

management of pain and loss of ROM that results from Myositis ossificans. Although the results have not yet been confirmed in a controlled trial, the appreciable improvement in pain scores and ROM in elite and sub-elite athletes after only 3 treatments of ESWT in a relatively short period of time is encouraging. ESWT is an attractive modality for the treatment of Myositis ossificans given that it is non-invasive, affordable and with few side effects.

NERVE ENTRAPMENT

Carpal tunnel syndrome

Carpal tunnel syndrome (CTS) is the most frequent entrapment neuropathy affecting people worldwide. Although surgery represents the gold-standard in CTS therapy, 82 several conservative approaches exist, including physical agents (62, 63). SWT has been recently reported to be effective in the treatment of CTS. In a group of 36 patients with CTS, a single session of 1000 pulses of SWT delivered over the carpal tunnel with the probe oriented perpendicular to the patient's palm, was found to be as effective as a single corticosteroid injection in relieving symptoms and improving nerve conduction. The energy level was set at the maximum level tolerated by the patient (0.09 to 0.29 mJ/mm2).

The mechanisms of action of SWT in CTS may only be speculated. It has been recently demonstrated that chronic compression of a nerve, as occurs in CTS, leads to an increased release of neuropeptides which triggers vasodilation mediated by cyclic-GMP and by endothelial nitric oxide (NO). From this point of view, low energy flux density levels (0.03 to 0.08 mJ/mm2) of SWT significantly reduce the number of cutaneous nerve fibers and the immune-reactivity to the CGRP-Calcitonin gene-related peptide (30, 31). SWT is also known to induce a short-term anti-inflammatory effect and a long-term tissue regeneration effect, both of which are mediated by NO induction.

Romeo et al. (64) also studied the effect of ESWT in pillar pain after carpal tunnel release. He investigated the efficacy of low-energy, flux density-focused ESWT in the treatment of pillar pain; 40 patients with pillar pain for a period of at least six months after carpal tunnel release surgery were treated with ESWT. Three treatments of ESWT, performed at weekly intervals using an electromagnetic device (MODULITH, SLK, Storz Medical, Tagerwilen, Switzerland), with an average of 2800 shocks at very low EFD of 0.03 mJ/mm2 and a repetition frequency of 4 Hz, were made. They placed the shockwave probe directly onto the area of subcutaneous swelling and skin redness or, if no redness or edema were present, in the area between the thenar and hypothenar eminences. Since the aim of the therapy was to treat the deep scar tissue, the pulses were focused superficially under sonographic control. Results showed that in all of the patients treated there was a marked improvement: the mean VAS score decreased from 6.18 (±1.02) to 0.44 (±0.63) 120 days after treatment, and redness and swelling of the surgical scar had also decreased significantly.

CONCLUSIONS

Over the last decade several reviews have been made on ESWT for myofascial and nerve disorders, which have show controversial evidence on its efficacy. However, the evidence found in the literature of the last five years has led us to develop a new review to better understand and describe the phenomena of ESWT treatment and its effects. Significant results have been found especially in tendon disorders, for example, Achille's and patellar tendinopathy and in myofascial structure pain. The data show that results are comparable to those obtained with surgery, yet avoid the possible consequences related to the surgical intervention itself. At present, it is possible to say that ESWT can be a tool of significant efficacy in the context of conservative-therapeutic treatment (especially rehabilitative) in many myofascial and nerve disorders. However, more precision is required regarding the parameters of pulses, especially the flux density in order to reach the appropriate results. It should be emphasized that, currently, the evidence is for a weekly or biweekly treatment (rather than a diluted administration over time, i.e. monthly) according to the devices, in order to transfer the correct amount of energy on the tissues.

REFERENCES

1. Furia JP. High energy extracorporeal shock wave therapy as a treatment for insertional Achilles tendinopathy. Am J Sports Med 2006; 34:733-40.

2. Furia JP, Rompe JD, Cacchio A, Del Buono A, Maffulli N. A single application of low-energy radial extracorporeal shock wave therapy is effective for the management of chronic patellar tendinopathy. Knee Surg Sports Traumatol Arthrosc 2013; 21:346-50.
3. Gerdesmeyer L, Wagenpfeil S, Haake M, et al. Extracorporeal shock wave therapy for the treatment of chronic calcifying tendonitis of the rotator cuff: a randomized controlled trial. JAMA 2003; 290:2573-80.
4. Ioppolo F, Tattoli M, Di Sante L, et al. Extracorporeal shock-wave therapy for supraspinatus calcifying tendinitis: a randomized clinical trial comparing two different energy levels. Phys Ther 2012; 92:1376-78.
5. Rompe JD, Decking J, Schoellner C, Theis C. Repetitive low energy shock wave treatment for chronic lateral epicondylitis in tennis players. Am J Sports Med 2004; 32:734-43.
6. Rompe JD, Furia J, Maffulli N. Eccentric loading compared with shock wave treatment for chronic insertional Achilles tendinopathy. J Bone Joint Surg Am 2008; 90:52-61.
7. Rompe JD, Furia J, Maffulli N. Eccentric loading versus eccentric loading plus shock-wave treatment for midportion Achilles tendinopathy: a randomized controlled trial. Am J Sports Med 2009; 37:463-70.
8. Rompe JD, Furia JP, Weil L, Maffuli N. Shock wave therapy for chronic plantar fasciopathy. Br Med Bull 2007; 81-82:183-208.
9. Wang CJ, Ko JY, Chan YS, Weng LH, Hsu SL. Extracorporeal shockwave for chronic patellar tendinopathy. Am J Sports Med 2007; 35:972-8.
10. Vulpiani MC, Trischitta D, Trovato P, Vetrano M, Ferretti A. Extracorporeal shockwave therapy (ESWT) in Achilles tendinopathy. A long-term follow-up observational study. J Sports Med Phys Fitness 2009; 49:171-6.
11. Romeo P, Lavanga V, Pagani D, Sansone V. Extracorporeal shock wave therapy in musculoskeletal disorders: a review. Med Princ Pract 2014; 23(1):7-13.
12. Bi Y, Ehirchiou D, Kilts TM, et al. Identification of tendon stem/progenitor cells and the role of the extracellular matrix in their niche. Nat Med 2007; 13:1219-27.
13. Wang CJ, Yang KD, Wang FS, et al. Shock wave therapy indices neovascularization at the tendon-bone junction: a study in rabbits. J Orthop Res 2003; 21:984-89.
14. Vetrano M, D'Alessandro F, Torrisi MR, et al. Extracorporeal shock wave therapy promotes cell proliferation and collagen synthesis of primary cultured human tenocytes. Knee Surg Sports Traumatol Arthrosc 2011; 19:2159-68.
15. Bokhari AR, Murrel GAC. The role of nitric oxide in tendon healing. J Shoulder Elbow Surg. 2012; 21:238-44.
16. Devrim E, Erten S, Erguder Image B, Namuslu M, Turgay M, Durak I. Malonildialdehyde and nitric oxide levels in erythrocytes from patients with systemic sclerosis. Med Princ Pract 2008; 17:349-50.
17. Leone L, Vetrano M, Ranieri D, et al. Extracorporeal shock wave treatment (ESWT) improves in vitro functional activities of ruptured human tendon-derived tenocytes. PLoS One 2012; 7:e49759.
18. Lee SY, Cheng B, Grimmer-Somers K. The midterm effectiveness of extracorporeal shockwave therapy in the management of chronic calcific shoulder tendinitis. J Shoulder Elbow Surg 2011; 20:845-54.
19. Galasso O, Amelio E, Riccelli DA, et al. Short-term outcomes of extracorporeal shock wave therapy for the treatment of chronic non-calcific tendinopathy of the supraspinatus: a double-blind, randomized, placebo-controlled trial. BMC Musculoskelet Disord 2012; 13:86.
20. Zwerver J, Hartgens F, Verhagen E, et al. No effect of extracorporeal shockwave therapy on patellar tendinopathy in jumping athletes during the competitive season: a randomized clinical trial. Am J Sports Med 2011; 39:1191-99.
21. Chen YJ, Wang CJ, Yang KD, et al. Extracorporeal shock waves promote healing of collagenaseinduced Achilles tendinitis and increase TGF-beta1 and IGF-I expression. J Orthop Res 2004; 22:854-61.
22. Abrahamsson SO. Similar effects of recombinant human insulin-like growth factor-I and II on cellular activities in flexor tendons of young rabbits: experimental studies in vitro. J Orthop Res 1997; 15:256-62.
23. Loew M, Jurgowski W, Mau HC, Thomsen M.

Treatment of calcifying tendinitis of rotator cuff by extracorporeal shock waves: a preliminary report. J Shoulder Elbow Surg 1995; 4:101-6.
24. Rompe JD, Burger R, Hopf C, Eysel P. Shoulder function after extracorporal shock wave therapy for calcific tendinitis. J Shoulder Elbow Surg 1998; 7:505-9.
25. Loew M, Daecke W, Kusnierczak D, Rahmanzadeh M, Ewerbeck V. Shock-wave therapy is effective for chronic calcifying tendinitis of the shoulder. J Bone Joint Surg Br 1999; 81:863-7.
26. Albert JD, Meadeb J, Guggenbuhl P, et al. High-energy extracorporeal shock-wave therapy for calcifying tendinitis of the rotator cuff: a randomized trial. J Bone Joint Surg Br 2007; 89:335-41.
27. Ioppolo F, Tattoli M, Di Sante L, et al. Clinical improvement and resorption of calcifications in calcific tendinitis of the shoulder after shock wave therapy at 6 months' follow-up: a systematic review and meta-analysis. Arch Phys Med Rehabil 2013; 94:1699-706.
28. Galasso O, Amelio E, Riccelli DA, Gasparini G. Short-term outcomes of extracorporeal shock wave therapy for the treatment of chronic non-calcific tendinopathy of the supraspinatus: a double-blind, randomized, placebo-controlled trial. BMC Musculoskelet Disord 2012; 13:86.
29. Saggini R, Cavezza T, Di Pancrazio L, Pisciella V, Saladino G, Zuccaro MC, Bellomo RG. Treatment of lesions of the rotator cuff. Journal of Biological Regulators & Homeostatic Agents 2010; 24:453-59.
30. Saggini R, Coco V, Di Pancrazio L, Megna M, Iodice P, Bellomo RG. Long-term results of rehabilitative management with extracorporeal shockwave therapy in rotator cuff disease with partial tears. Eur J Inflamm 2012; 10(3):483-90.
31. Rompe JD, Hopf C, Kullmer K, Heine J, Burger R, Nafe B. Low energy extracorporal shock wave therapy for persistent tennis elbow. Int Orthop 1996; 20:23-27.
32. Rompe JD, Hope C, Kullmer K, Heine J, Burger R. Analgesic effect of extracorporeal shock-wave therapy on chronic tennis elbow. J Bone Joint Surg Br 1996; 78:233-37.
33. Pettrone FA, McCall BR. Extracorporeal shock wave therapy without local anesthesia for chronic lateral epicondylitis. J Bone Joint Surg Am 2005; 87:1297-304.
34. Speed CA, Nichols D, Richards C, et al. Extracorporeal shock wave therapy for lateral epicondylitis: a double blind randomised controlled trial. J Orthop Res 2002; 20:895-98.
35. Buchbinder R, Green SE, Youd JM, Assendelft WJ, Barnsley L, Smidt N. Shock wave therapy for lateral elbow pain. Cochrane Database Syst Rev 2005; 4:CD003524.
36. Rompe JD, Maffulli N. Repetitive shock wave therapy for lateral elbow tendinopathy (tennis elbow): a systematic and qualitative analysis. Br Med Bull 2007; 83:355-78.
37. Gündüz R, Malas FÜ, Borman P, Kocaoğlu S, Özçakar L. Physical therapy, corticosteroid injection, and extracorporeal shock wave treatment in lateral epicondylitis. Clinical and ultrasonographical comparison. Clin Rheumatol 2012; 31(5):807-12.
38. Lee SS, Kang S, Park NK, Lee CW, Song HS, Sohn MK, Cho KH, Kim JH. Effectiveness of initial extracorporeal shock wave therapy on the newly diagnosed lateral or medial epicondylitis. Ann Rehabil Med 2012; 36(5):6817.
39. Notarnicola A, Quagliarella L, Sasanelli N, Maccagnano G, Fracella MR, Forcignanò MI, Moretti B. Effects of extracorporeal shock wave therapy on functional and strength recovery of handgrip in patients affected by epicondylitis. Ultrasound Med Biol 2014; 40(12):283040.
40. Mani-Babu S, Morrissey D, Waugh C, Screen H, Barton C. The effectiveness of extracorporeal shock wave therapy in lower limb tendinopathy: a systematic review. Am J Sports Med 2014; 9.
41. Vulpiani MC, Vetrano M, Savoia V, Di Pangrazio E, Trischitta D, Ferretti A. Jumper's knee treatment with extracorporeal shock wave therapy: a long-term follow-up observational study. J Sports Med Physical Fitness 2007; 47:323-8.
42. Zwerver J, Dekker F, Pepping GJ. Patient guided Piezo-electric extracorporeal shockwave therapy as treatment for chronic severe patellar tendinopathy: a pilot study. J Back Musculoskeletal Rehab 2010; 23:111-5.
43. Peers KH, Lysens RJ, Brys P, Bellemans J. Cross-sectional outcome analysis of athletes with chronic

patellar tendinopathy treated surgically and by extracorporeal shock wave therapy. Clin J Sport Med 2003; 13:79-83.
44. Zwerver J, Hartgens F, Verhagen E, van der Worp H, van den Akker-Scheek I, Diercks RL. No effect of extracorporeal shockwave therapy on patellar tendinopathy in jumping athletes during the competitive season: a randomized clinical trial. Am J Sports Med 2011; 39:1191-9.
45. Saggini R, Di Stefano A, Galati V, Panelli E, Valeri M, Di Pancrazio L, Iodice P, Bellomo RG. Long term effectiveness of combined mechanotransduction treatment in Jumper's knee. European Journal of Inflammation 2012; 10(3):515-24.
46. Furia JP. High-energy extracorporeal shock wave therapy as a treatment for chronic noninsertional Achilles tendinopathy. Am J Sports Med 2008; 36:502-8.
47. Rompe JD, Furia JP, Maffulli N. Eccentric loading, shockwave treatment or a wait-and-see policy for tendinopathy of the main body of the tendo Achilles: a randomized controlled trial. Am J Sports Med 2007; 35:374-83.
48. Costa ML, Shepstone L, Donell ST, Thomas TL. Shock wave therapy for chronic Achilles tendon pain: a randomized placebocontrolled trial. Clin Orthop Relat Res 2005; 440:199-204.
49. Al-Abbad H, Simon JV. The effectiveness of extracorporeal shock wave therapy on chronic Achilles tendinopathy: a systematic review. Foot Ankle Int 2013; 34(1):33-41.
50. Rompe JD, Hopf C, Nafe B, Burger R. Low-energy extracorporeal shock wave therapy for painful heel: a prospective controlled single-blind study. Arch Orthop Trauma Surg 1996; 115:75-9.
51. Rompe JD, Decking J, Schoellner C, Nafe B. Shock wave application for chronic plantar fasciitis in running athletes. A prospective, randomized, placebo-controlled trial. Am J Sports Med 2003; 31:268-75.
52. Dizon JN, Gonzalez-Suarez C, Zamora MT, Gambito ED. Effectiveness of extracorporeal shock wave therapy in chronic plantar fasciitis: a metaanalysis. Am J Phys Med Rehabil 2013; 92:606-20.
53. Buchbinder R, Ptasznik R, Gordon J, Buchanan J, Prabaharan V, Forbes A. Ultrasound-guided extracorporeal shock wave therapy for plantar fasciitis: a randomized controlled trial. JAMA 2002; 288:1364-72.
54. Maki M, Ikoma K, Imai K, Kido M, Hara Y, Arai Y, Fujiwara H, Kubo T. Correlation between the outcome of extracorporeal shockwave therapy and pretreatment MRI findings for chronic plantar fasciitis. Mod Rheumatol 2014; 17:1-4.
55. Winters M, Eskes M, Weir A, Moen MH, Backx FJ, Bakker EW. Treatment of medial tibial stress syndrome: a systematic review. Sports Med 2013; 43(12):1315-33.
56. Moen MH, Rayer S, Schipper M, Schmikli S, Weir A, Tol JL, Backx FJ. Shockwave treatment for medial tibial stress syndrome in athletes; a prospective controlled study. Br J Sports Med 2012; 46(4):253-7.
57. Ji HM, Kim HJ, Han SJ. Extracorporeal shock wave therapy in myofascial pain syndrome of upper trapezius. Ann Rehabil Med 2012; 36(5):675-80.
58. Jeon JH, Jung YJ, Lee JY, Choi JS, Mun JH, Park WY, Seo CH, Jang KU. The effect of extracorporeal shock wave therapy on myofascial pain syndrome. Ann Rehabil Med 2012; 36(5):665-74.
59. Moghtaderi A, Khosrawi S1, Dehghan F1. Extracorporeal shock wave therapy of gastroc-soleus trigger points in patients with plantar fasciitis: A randomized, placebo-controlled trial. Adv Biomed Res 2014; 3:99.
60. Buselli P, Coco V, Notarnicola A, Messina S, Saggini R, Tafuri S, Moretti L, Moretti B. Shock waves in the treatment of post-traumatic myositis ossificans. Ultrasound Med Biol 2010; 36(3):397-409.
61. Torrance DA, Degraauw C. Treatment of post-traumatic myositis ossificans of the anterior thigh with extracorporeal shock wave therapy. J Can Chiropr Assoc 2011; 55(4):240-6.
62. Casale R, Damiani C, Maestri R, Wells CD. Pain and electrophysiological parameters are improved by combined 830-1064 high-intensity LASER in symptomatic carpal tunnel syndrome versus transcutaneous electrical nerve stimulation. A randomized controlled study. Eur J Phys Rehabil Med 2013; 49:205-11.
63. Seok H, Kim SH. The effectiveness of extracorporeal shock wave therapy vs. local steroid injection for management of carpal tunnel syndrome: a

randomized controlled trial. Am J Phys Med Rehabil 2013; 92:327-34.
64. Romeo P, d'Agostino MC, Lazzerini A, Sansone VC. Extracorporeal shock wave therapy in pillar pain after carpal tunnel release: a preliminary study. Ultrasound Med Biol 2011; 37(10):1603-8.

JOURNAL OF BIOLOGICAL REGULATORS & HOMEOSTATIC AGENTS Vol. 29, no. 4, 787-791 (2015)

EDITORIAL

ROLE OF TNF IN MAST CELL NEUROINFLAMMATION AND PAIN

Y. GU[1], D-K. YANG, E. SPINAS[3], S.K. KRITAS[4], A. SAGGINI[5], A. CARAFFA[6], P. ANTINOLFI[6], R. SAGGINI[7] and P. CONTI[8]

[1]Radiotherapy Ward 3, The First Affiliated Hospital of Zhengzhou, Zhengzhou, Henan, China; [2]Compositive Thermotherapy Center, The First Affiliated Hospital of Zhengzhou University, Zhengzhou, Henan, China; [3]Department of Surgery and dontostomatological Sciences, University of Cagliari, Italy; [4]Department of Microbiology and Infectious Diseases, School of Veterinary Medicine, Aristotle University of Thessaloniki, Macedonia, Greece; [5]Department of Dermatology, University of Rome Tor Vergata, Rome, Italy; [6]Orthopedic Division, University of Perugia, Perugia, Italy; [7]Department of Neurosciences and Imaging, Faculty of Medicine and Surgery, G. D'Annunzio University Chieti-Pescara, Chieti, Italy; [8]Immunology Division, Post Graduate School of Medicine, Chieti, Italy

Received September 30, 2015 - Accepted December 1, 2015

Inflammatory mediators, such as cytokines, chemokines and arachidonic acid compounds, lead to vascular permeability and dilation and increase sensitization and pain receptors. Proinflammatory cytokines, including tumor necrosis factor, are involved in the etiology of clinical neurological disorders. These cytokines activate nuclear factor-κB (NF-κB) which leads to the activation of different inflammatory genes. TNF implicated in neurological disorders has an important role in the activation of microglia and astrocytes. The inhibition of TNF may lead to the decrease of microglia activation and can be useful for therapeutic intervention. TNF, at the site of nerve injury may activate mast cells (MCs) which mediate pathologic events such as headache and pain. TNF is the only cytokine stored in mast cells and can be rapidly released along with biogenic amines after MC stimulation. Activation of MCs leads to NF-κB and AP1 generation with release of many cytokines including TNF, IL-33 and IL-1. In this paper we discuss the role of TNF in MC activation, mediating pain and neurological disorders.

Inflammatory signs are provoked by inflammatory mediators which cause directly or indirectly the generation of inflammatory cytokines/chemokines and arachidonic acid compounds (prostaglandin, leukotrienes and lipoxins), which all provoke vascular permeability, vascular dilatation, increase and sensitization of pain receptors (1). Central and peripheral nervous systems respond to acute and chronic stress involving the above-mentioned inflammatory molecules and others, which are detrimental for cellular homeostasis and health (2).

Proinflammatory cytokines, such as interleukin (IL)-1β, IL-6, IL-18, IL-33 and tumor necrosis factor (TNF) are involved in the etiologies of clinical neurological disorders (3).

Chronic stress may alter constitutive (COX-1) and inducible (COX-2) enzymes which are implicated in the regulation and activity of HPA axis (4).

Key words: mast cell, cytokine, inflammation, TNF

Mailing address:
Dr D-K. Yang,
Compositive Thermotherapy Center,
The First Affiliated Hospital
of Zhengzhou University,
Zhengzhou, Henan,
450052, China

0393-974X (2015)

Prostaglandins may regulate cytokine production via a cellular cAMP-dependent mechanism, while TNF induces the generation of IL-1 (and *vice versa*), IL-6 and several chemokines, for example IL-8 (a CXC chemokine). It is well known that non-steroidal anti-inflammatory drugs inhibit prostaglandin generation - a process that provokes an increase of pro-inflammatory TNF in gastric mucosa. Inflammatory cytokines, such as TNF, IL-1, IL-18, activate NF-κB which leads to the activation of different inflammatory genes (5).

A number of inflammatory cytokines such as IL-1, IL-6, IL-18, IL-33, IL-8, and TNF have been implicated in neurological chronic inflammatory disorders (6). TNF has an important role within the central nervous system (CNS); it activates microglia and astrocytes. In addition, TNF increases amino-3-hydroxy-5-methyl-4-isoxazolepropionic acid (AMPA) receptor density on the cell surface and at the same time decreases expression of γ-aminobutyric acid receptor cells, which are involved in neurotoxicity. TNF can be inhibited by a number of endogenous compounds such as cortisol, cAMP, prostaglandins and anti-TNF monoclonal antibody (6). The inhibition of TNF may lead to the decrease of microglia activation which can be useful for therapeutic intervention. For instance, when injected into nerve, TNF is believed to activate resident synovial cells to produce collagenase that mediates destruction of cartilage, and may be implicated in neuropathic pain, hyperalgesia and neurological complications (7). In response to nervous tissue damage, activation of resident recruited mast cells (MCs) leads to the production of inflammatory mediators such as TNF, IL-1 family cytokines (IL-18 and IL-33) and other inflammatory cytokines along with chemokines such as MCP-1 and RANTES which recruit additional MC population (8). The recruitment of MCs causes changes in vascular and electrophysiologic activity in pain fibers. There is an important ability of TNF to activate cells of peripheral nervous system (PNS) and CNS including neurons, glia, endothelial cells, and MCs (9).

The effect of TNF at the site of nerve injury initiates the activation of MCs which mediates pathologic events associated with headache, and play an important role in pain formation. The generation of the proinflammatory cytokines, including TNF, provokes sensitization and activation of sensory neurons and glia, which leads to neuropathic pain. In the brain, within minutes of nerve activation TNF is up-regulated in MCs and other resident cells such as macrophages, with immediate effects on electrophysiology and permeability associated with chronic pain.

TNF receptors (TNFR1 and TNFR2) can be activated by many physiological and non-physiological compounds which lead to phosphorylation of extracellular signal-regulated kinases (ERKs), p38 MAPK, and Jun N-terminal kinase (JNK), which may activate NF-κB transcription pathways. p38 pathway phosphorylates and increases the activity of transcription factors NF-κB, ELK-1 with an increasing of TNF generation and other inflammatory cytokines (10).

TNFR1 is more related to signal transduction pathways and mediates pro-inflammatory effects and pain; while TNFR2 has resulted to be neuroprotective. In addition, TNF not only functions as a signal molecule of the immune system, but may also act as an activator of vagal afferent fibers in CNS, resulting as a neurogenic stressor, along with IL-1 (11). In fact, it has been reported that TNF causes a time-dependent sensitization of neuroendocrine processes and sickness behaviors (11). Moreover, TNF is up-regulated in the serum of multiple sclerosis (MS) patients; while CSF, TGF-b and IL-10 are over-expressed during the remission of MS.

It is well known that treatment with anti-TNF is associated with a beneficial effect on the pathophysiology of PNS and CNS. Therefore, antagonists against the inflammatory cytokine TNF and IL-1-inducing TNF have beneficial effects in neuropathological and other inflammatory disorders. Compounds such as monoclonal antibody that targets inflammatory cytokines IL-1 and TNF receptors, may alleviate symptoms in patients with inflammatory diseases such as neuroinflammation and migraine (12).

TNF is the only cytokine that can be stored in the granules of MCs and, like biogenic amines and enzymes, can also be rapidly released after MC stimulation (13). Activation of MCs leads to NF-κB and AP-1 generation, and production of many cytokines such as TNF, GM-CSF, IL-33, IL-6, IL-5, IL-4, IL-1, and IL-13 as well as various chemokines

e.g. MIP-1alpha, MIP-1beta and MCP-1 (CCL2). MCP-1 is a member of the CC subfamily chemokines, characterized by two adjacent cysteine residues which display chemotactic activity for monocytes, MCs and basophils, but not for neutrophils (8). MCP-1 binds to chemokine receptors CCR2 and CCR4, and has been implicated in the pathogenesis of neuroinflammatory diseases characterized by infiltrate MCs and/or macrophages. We previously reported, for the first time, that injection of chemokines RANTES and MCP-1 in rat skin provokes the recruitment of inflammatory cells, including MCs, release of cytokines and activation of transcription of histidine decarboxylase, the enzyme responsible for the production of histamine from histidine, involved in anaphylactic shock (8). This effect is absent in genetically MC-deficient W/Wv mice.

MCs develop from a common circulating $CD34^+$/c-kit^+/ $CD13^+$/$FceRI^-$ hematopoietic progenitor representing single lineage and they act by degranulation and secreting preformed and newly chemical mediators, cytokines and other various effector molecules (14). They are observed at sites of inflammation and injury in the brain and spinal cord. MC mediators, including TNF, are involved in the blood-brain barrier permeability, an effect that affects brain function and can stimulate the hypothalamic-pituitary-adrenal axis. Moreover, it has been found that tyrosine-kinase inhibitors targeting the c-Kit mast cell receptor play a therapeutic role and are effective in treating some autoimmune diseases (15). MCs are also important for maturation of Th17 cells and are recognized as key cells in autoimmune disorders (16). Their aggregation induces PI3K, ERK, JNK, NF-κB and PKC activation, resulting in several responses, including the immediate release of potent inflammatory mediators and leading to differential release of distinct mediators without degranulation (10). However, Src family kinase Lyn is a negative regulator of inflammatory MC activation.

Neurological diseases are associated with several cytokines characterized by up-regulation of proinflammatory cytokines such as TNF and other cytokines with an immune response which down-regulate TGF-beta and IL-10 (17). It has been reported that TNF is up-regulated in the serum of patients with neurological disorders, while CSF, TGF-b and IL-10 are over-expressed during the remission of diseases (18). Microglial cells play an important role in the injuries of the brain affecting both neurons and oligodendrocytes and display surface receptors and antigens shared by macrophages.

Macrophages have two sub-populations: M1 and M2. Both take part in the inflammatory process, although with opposite roles. M1 macrophages activated via toll-like receptor (TLR) or IFN-gamma, generate high levels of IL-12, IL-23, IL-6, IL-1, and TNF; while activated M2 macrophages by regulatory mediators, such as certain cytokines, produce TGF-beta IL-4, IL-13, and IL-10 which can deactivate M1 macrophages, all contributing to inflammation (19).

Dinarello and associates demonstrated that IL-1 induces TNF which induces activation of intracellular signaling molecules such as Janus Kinases (JAK), c-Jun N-terminal Kinase (JNK), p38, ERK, Signal Transducer and Activator of Transcription (STAT), and NF-κB (20).

The neuropeptide substance P, in combination with some inflammatory cytokines, may produce a synergistic effect on TNF generation in MC activation, this is because two independent mechanisms could be involved, one is immediate and the other through the transcription factors (unpublished data). Neuropeptides, such as substance P, NGF and neurotensin, can activate MCs and lead to MC-dependent immune cell infiltration directly through the synthesis of TNF and some other cytokines/chemokines (21). In addition, CRH-R1-activated MCs release CRH which is implicated in the production of TNF from cultured microglia, and induces rapid phosphorylation of extracellular signal-regulated protein kinase (ERK) and p38 mitogen-activated protein kinase (p38 kinases). These effects can be inhibited by some specific inhibitors of ERK or p38 protein kinase (22). In addition, CRH, through c-Fos and cAMP pathways participate in the developing of astrocytes in cerebella cultures (22).

Involvment of CRH in brain disorders: CRH→CRHR→Mast cell or Microglia actvation →TNF, IL-6, IL-8 and IL-33 release→Inflammatory cell recruitment→INFLAMMATION

The effects of TNF also include the stimulation of histamine from MCs which contribute to the immediate inflammatory reactions (12). Moreover, TNF is a mediator of acute phase response which

may promote the generation of histamine, an effect inhibited by H_1 and H_2 histamine antagonists. The histamines generated by MCs are found in CNS and in the parenchyma of the brain in response to neurological disorders. Histamine is also generated by neurons affecting neurological dysfunctions. Therefore, TNF may sensitize CNS functioning through the stimulation of either neurons or MCs, resulting in histamine production, which affect central neurochemical functioning.

In the light of these concepts expressed above, targeting MCs and/or TNF receptors suggests a promising treatment for neuroinflammatory disorders and pain.

These studies indicate that inflammation is commonly detectable in neurological disorders and is characterized by immune cell infiltration including MCs and cytokine secretion such as TNF. However, future studies are needed to elucidate the true role of MCs and TNF in the development and progression of neurological inflammation.

*This paper was written on the basis of a survey of PUBMED and the data obtained in the Laboratory of "Molecular Immunopharmacology and Drug Discovery Laboratory", Tufts University School of Medicine, Boston, MA, USA.

REFERENCES

1. Szekanecz Z, Koch AE. Vascular endothelium and immune responses: implications for inflammation and angiogenesis. Rheum Dis Clin North Am 2004; 30(1):97-114. Review.
2. Johnson AC, Greenwood-Van Meerveld B. Stress-induced pain: a target for the development of novel therapeutics. J Pharmacol Exp Ther 2014; 351(2):327-35.
3. Covelli V, Passeri ME, Leogrande D, Jirillo E, Amati L. Drug targets in stress-related disorders. Curr Med Chem 2005; 12(15):1801-9.
4. Gądek-Michalska A, Tadeusz J, Rachwalska P, Bugajski J. Cytokines, prostaglandins and nitric oxide in the regulation of stress-response systems. Pharmacol Rep 2013; 65(6):1655-62.
5. Schrör K, Rauch BH. Aspirin and lipid mediators in the cardiovascular system. Prostaglandins Other Lipid Mediat 2015; pii: S1098-8823(15)30005-8.
6. Garraway SM, Woller SA, Huie JR, et al. Peripheral noxious stimulation reduces withdrawal threshold to mechanical stimuli after spinal cord injury: role of tumor necrosis factor alpha and apoptosis. Pain 2014; 155(11):2344-59.
7. Myers RR, Shubayev VI. The ology of neuropathy: an integrative review of the role of neuroinflammation and TNF-α axonal transport in neuropathic pain. J Peripher Nerv Syst 2011; 16(4):277-86.
8. Conti P, Pang X, Boucher W, Letourneau R, Reale M, Barbacane RC, Thibault J, Theoharides TC. Impact of Rantes and MCP-1 chemokines on in vivo basophilic cell recruitment in rat skin injection model and their role in modifying the protein and mRNA levels for histidine decarboxylase. Blood 1997; 89(11):4120-7.
9. Jin Y, Silverman AJ, Vannucci SJ. Mast cells are early responders after hypoxia-ischemia in immature rat brain. Stroke 2009; 40(9):3107-12.
10. Ibeas E, Fuentes L, Martín R, Hernández M, Nieto ML. Inflammatory protein sPLA(2)-IIA abrogates TNFalpha-induced apoptosis in human astroglioma cells: Crucial role of ERK. Biochim Biophys Acta 2009; 1793(12):1837-47.
11. Anisman H, Merali Z, Hayley S. Sensitization associated with stressors and cytokine treatments. Brain Behav Immun 2003; 17(2):86-93.
12. Perini F, D'Andrea G, Galloni E, Pignatelli F, Billo G, Alba S, Bussone G, Toso V. Plasma cytokine levels in migraineurs and controls. Headache 2005; 45(7):926-31.
13. Zhang B, Weng Z, Sismanopoulos N, et al. Mitochondria distinguish granule-stored from de novo synthesized tumor necrosis factor secretion in human mast cells. Int Arch Allergy Immunol 2012; 159(1):23-32.
14. Toniato E, Spinas E, Saggini A, et al. Immunomodulatory effects of vitamin d on skin inflammation. J Biol Regul Homeost Agents 2015; 29(3):563-7.
15. Spinas E, Kritas SK, Saggini A, et al. Role of mast cells in atherosclerosis: a classical inflammatory disease. Int J Immunopathol Pharmacol 2014; 27(4):517-21.
16. Milovanovic M, Volarevic V, Radosavljevic G, Jovanovic I, Pejnovic N, Arsenijevic N, Lukic ML. IL-

33/ST2 axis in inflammation and immunopathology. Immunol Res 2012; 52(1-2):89-99.
17. Spinas E, Saggini A, Kritas SK, et al. Crosstalk between vitamin b and immunity. J Biol Regul Homeost Agents 2015; 29(2):283-88.
18. Karaduman B, Uraz A, Altan GN, Balos Tuncer B, Alkan O, Gonen S, Pehlivan S, Centiner D. Changes of tumor necrosis factor-a, interleukin-10, and tartrate-resistant acid phosphatase5b in the crevicular fluid in relation to orthodontic movement. Eur J Inflamm 2015; 13(1):3-13.
19. Kratochvill F, Neale G, Haverkamp JM, et al. TNF Counterbalances the Emergence of M2 Tumor Macrophages. Cell Rep 2015; 12(11):1902-14.
20. Dinarello CA, van der Meer JW. Treating inflammation by blocking interleukin-1 in humans. Semin Immunol 2013; 25(6):469-84.
21. Sismanopoulos N, Delivanis DA, Mavrommati D, Hatziagelaki E, Conti P, Theoharides TC. Do mast cells link obesity and asthma? Allergy 2013; 68(1):8-15.
22. Stevens SL, Shaw TE, Dykhuizen E, Lessov NS, Hill JK, Wurst W, Stenzel-Poore MP. Reduced cerebral injury in CRH-R1 deficient mice after focal ischemia: a potential link to microglia and atrocytes that express CRH-R1. J Cereb Blood Flow Metab 2003; 23(10):1151-9.

SELECTIVE INHIBITORS OF AURORA KINASES INHIBIT PROLIFERATION, REDUCE CELL VIABILITY AND IMPAIR CELL CYCLE PROGRESSION IN PAPILLARY THYROID CARCINOMA CELLS

E. BALDINI[1], C. TUCCILLI[1], N. PRINZI[1], S. SORRENTI[2], A. ANTONELLI[3], P. FALLAHI[3], C. MIAN[4], S. BAROLLO[4], A. CATANIA[2], S. MORRONE[1], F. TARTAGLIA[2], D. MASCAGNI[1], C. COCCARO[1], M. PEPE[1], A. FILIPPINI[2], M. D'ARMIENTO[1] and S. ULISSE[1]

[1]Department of Experimental Medicine, "Sapienza" University of Rome, Italy; [2]Department of Surgical Sciences, "Sapienza" University of Rome, Italy; [3]Department of Internal Medicine, University of Pisa, Italy; [4]Department of Medicine, University of Padua, Italy

Received June 17, 2015 – Accepted August 7, 2015

The first two authors contributed equally to the manuscript

The three members of the Aurora kinase family, Aurora-A, -B and -C, regulate several aspects of the mitotic process, and their aberrant expression and/or function causes mitotic abnormalities leading either to cell death or aneuploidy. They are found overexpressed in several human malignancies, including the papillary thyroid carcinoma (PTC). In the present study, we sought to establish whether Aurora kinase inhibition could be of any therapeutic value in the treatment of aggressive forms of PTC, enduring to radioactive iodide (RAI) ablation. To this end, the effects of selective inhibitors of Aurora-A (MLN8237) and Aurora-B (AZD1152) were analyzed on 3 human PTC cell lines expressing either wild-type (K1 and TPC1) or mutant p53 (BCPAP). The two inhibitors were capable of reducing cell proliferation in a time- and dose-dependent manner, with IC_{50} comprised between 65.4 and 114.9 nM for MLN8237, and between 26.6 and 484.6 nM for AZD1152. Immunofluorescence experiments confirmed that AZD1152 inhibited Aurora-B phosphorylation of histone H3 on Ser10, however, it did not affect Aurora-A autophosphorylation. MLN8237 inhibited Aurora-A autophosphorylation as expected, but at concentrations required to achieve the maximum antiproliferative effects it also abolished H3 (Ser10) phosphorylation. Time-lapse videomicroscopy evidenced that both inhibitors prevented the completion of cytokinesis, and cytofluorimetric analysis showed accumulation of cells in G2/M phase and/or polyploidy. Apoptosis was induced in all the cells by both inhibitors independently from the p53 status. In conclusion, in the present preclinical study MLN8237 and AZD1152 have emerged as promising drug candidates for RAI-insensitive PTC.

Thyroid cancer (TC) is the 18th most common cancer in Europe, and the 16th most common cancer worldwide (1). Papillary thyroid carcinoma (PTC), resulting from follicular thyroid cells, is the most

Key words: papillary thyroid cancer, Aurora kinases, Aurora kinase inhibitors, MLN8237, AZD1152, therapy, cell cycle

Mailing address: Prof. Salvatore Ulisse,
Department of Experimental Medicine,
"Sapienza" University of Roma,
Viale Regina Elena, 324 00161 - Roma, Italy
Tel.: +39 0649972607
Fax: +39 0649972606
e-mail: salvatore.ulisse@uniroma1.it

0393-974X (2015)

DISCLOSURE: ALL AUTHORS REPORT NO CONFLICTS OF INTEREST RELEVANT TO THIS ARTICLE.

common TC type, and its incidence has been shown to increase over the last decades (2). The classic tissutal structure of PTC is characterized by branching papillae lying on a central fibrovascular stalk. There are also several histopathological variants, each of which shows a combination of specific growth patterns, cell types and stromal changes and, in some cases, a worse prognosis (3). Initial treatment of PTC patients includes total thyroidectomy followed, in most cases, by adjuvant therapy with radioactive iodine [(RAI (^{131}I)]. Patient follow-up includes radioiodine scanning 6-12 months after surgery, periodic ultrasound of the thyroid bed and cervical lymph node compartments, and measurement of basal and recombinant human TSH-stimulated thyroglobulin (Tg) serum level. The prognosis of PTC is usually favorable, with a 10-year-survival rate of apptoximately 90%. However, about 5% of patients develop more aggressive and metastatic forms, which do not respond to RAI (4-7). External beam radiation, suppressive therapy with thyroid hormone and cytotoxic chemotherapies show no prolonged responses in advanced non-iodine avid TC, and patients eventually succumb to the disease (4). A number of oncogenes have been associated with TC progression, against which many targeted agents are currently available and many others are being investigated. In particular, early oncogenic mutations comprise gene rearrangements of tyrosine kinase receptors, such as RET/PTC and NTRK1 (neurotrophic receptor-tyrosine kinase 1), or activating point mutations of proteins mediating cellular responses to growth and differentiation signals, including RAS and BRAF, or the oncogenic fusion protein PAX8-PPARg, that suppresses wild-type PPARg function in a dominant-negative manner (8). A class of targeted drugs known as tyrosine-kinase inhibitors (TKIs) has raised considerable interest as a feasible therapeutic choice for RAI-unresponsive TC. Most TKIs prevent the activation of more than one cellular pathway/receptor, such as the mitogen-activated protein kinase (MAPK), phosphoinositide 3-kinase/AKT (PI3K-AKT), vascular endothelial growth factor receptor (VEFGFR), endothelial growth factor receptor (EGFR), or mitogen activated protein kinase enzyme (MET). The availability of multitargeted TKIs has allowed beneficial and generally well-tolerated therapy for TC patients with progressive disease. Among these, sorafenib and lenvatinib mesylate have been recently approved by the Food and Drug Administration for the treatment of epithelial RAI-resistant TC. However, different clinical studies performed on patients with the same histotype of TC reported marked differences in relation to survival, which can be explained by the biological heterogeneity of tumors. Moreover, TKIs are usually tumoristatic rather than tumoricidal, therefore requiring repeated administrations, resulting over time in the appearance of significant toxicities, as well as in development of therapeutic resistance (9).

In recent years, a number of gene expression studies have demonstrated deregulation in TC of genes involved in cell cycle progression and chromosome segregation, among which the Aurora kinases (10). The latter, namely Aurora-A, -B and -C, are serine/threonine kinases essential in all mitotic steps, from prophase to anaphase (10). In particular, Aurora-A localizes to centrosomes where it participates in their duplication, maturation and separation, drives the timing of mitotic entry, and is essential for spindle assembly (10). Aurora-B, together with the proteins INCENP, Survivin and Borealin, forms the Chromosomal Passenger Complex (CPC), which shows dynamic locations reflecting its diverse functions as the mitosis proceed. Along the entire chromatin CPC modifies histones during the onset of mitosis, in the inner centromeres it corrects chromosome–microtubule attachment errors and activates the spindle assembly checkpoint (SAC) during prometaphase, it constructs and regulates the contractile apparatus in the central spindle from the metaphase–anaphase transition up to telophase/cytokinesis (10). Aurora-C is highly similar to Aurora-B and joins the CPC, but it has been found expressed substantially only in germ cells during spermatogenesis and oogenesis, including meiosis, and in some cancer cell lines (10).

Aberrant expression and/or function of one or more Aurora kinases is often observed in solid tumors, and correlates positively with aneuploidy, defective mitotic spindles, and resistance to apoptosis (10, 11).

Regarding TC, we previously demonstrated an increase in both mRNA and protein levels of Aurora-A and -B in human cell lines derived from differentiated and undifferentiated TC compared to

normal thyrocytes and cells of follicular adenoma (12, 13). In a more recent work carried out on 87 PTC, we showed that the expression of Aurora-A and -B was either up- or down-regulated at mRNA level in the majority of tissues analyzed (14). Moreover, in a preclinical context, we ascertained the efficacy of different small molecule inhibitors of Aurora kinases in preventing cell growth and survival of various human cell lines derived from anaplastic thyroid carcinoma (ATC), the most aggressive form of TC and overall one of the most lethal cancers (15-18).

Taken together, the above observations indicate the Aurora kinases as potential therapeutic targets in RAI-insensitive PTC. Taking as experimental model three PTC-derived cell lines, in the present study we exploited the therapeutic potential of two selective inhibitors of Aurora-A and Aurora-B by evaluating their effects on proliferation, cell cycle and survival. Moreover, we sought to verify whether the p53 status of PTC cells could influence the effectiveness of these inhibitors.

MATERIALS AND METHODS

Cell cultures

The B-CPAP cell line, derived from a poorly differentiated PTC, was purchased from the German Collection of Microorganisms and Cell Cultures (DMSZ, Braunschweig, Germany). It has a near-diploid karyotype with hexaploid sidelines, and harbors the $BRAF^{V600E}$ and the $TP53^{D259Y}$ mutations (19). The K1 cell line, originated from a primary PTC, was obtained from the European Collection of Cell Culture (ECACC, Salisbury, UK). It has a near tetraploid karyotype and harbors the $BRAF^{V600E}$ and the $PI3KCA^{E542K}$ mutations. Prof. Massimo Santoro (University of Naples, Federico II, Italy) kindly provided the TPC1 cell line, derived from a metastasis of a well-differentiated PTC. It is near-diploid, and harbors the RET/PTC1 rearrangement. Both TPC1 and K1 possess wild type p53 protein. The cells were cultured in RPMI supplemented with 10% FBS and 2 mM L-glutamine, and used at passages 3-6 for all the experiments described below. In order to avoid potential interactions and/or interferences with the Aurora inhibitors, no antibiotic was added to the medium.

Aurora kinase inhibitors

MLN8237 (Alisertib) is an Aurora-A inhibitor with IC_{50} of 1.2 nM, having >200-fold higher selectivity for Aurora-A than Aurora-B (20). AZD1152 (Barasertib) is an Aurora-B inhibitor with IC_{50} of 0.37 nM, about 3000-fold more selective for Aurora-B over Aurora-A (21). Both were acquired from Selleck Chemicals (Houston, USA). Stock solutions 10 mM were prepared by diluting the powder in dimetilsulfoxide (DMSO), aliquoted and stored at -80°C until use.

Proliferation assay

The time- and dose-dependent effects of the inhibitors on cell proliferation were evaluated by colorimetric assay. First, cells were seeded in 96-multiwell culture plates and treated with different concentrations of MLN8237 (5-1000 nM) or AZD1152 (10-2000 nM) for 4 days. Controls were performed by administrating DMSO at the highest concentration used for treatments (0.02% DMSO in the control for AZD1152, and 0.01% DMSO in the control for MLN8237), and all the media were replaced every 48 h. The proliferation was measured by detecting cellular incorporation of BrdU (5-bromo-2-deoxyuridine) with the Cell Proliferation ELISA BrdU kit (Roche Diagnostics, Mannheim, Germany). Based on these results, the lowest doses exerting maximum antiproliferative effects, i.e. 500 nM MLN8237 or 50 nM AZD1152 for TPC1, 500 nM AZD1152 for BCPAP or 1 mM AZD1152 for K1, were employed in time-response experiments (1-6 days).

Immunofluorescence

Cells were cultured on glass coverslips and treated with different concentrations of AZD1152 (10-2000 nM), MLN8237 (10-1000 nM) or vehicle for 24 h, then fixed in cold methanol for 5 min. The coverslips were rinsed with phosphate buffered saline (PBS) containing 0.1% Tween 20 (PBS-T), saturated with 3% bovine serum albumin (BSA) in PBS-T for 1 h, and incubated overnight with antibodies anti-phospho-Aurora-A/B/C 1:100 (Cell Signaling Technology, Danvers, MA, USA), anti-phospho histone H3 (Ser10) 1:1000 (Cell Signaling Technology, Danvers, MA, USA), and anti-β-tubulin 1:2000 (Sigma-Aldrich, Milano, Italy) in PBS-T plus 1% BSA. After washing, the coverslips were incubated with TRITC- and FITC-conjugated secondary antibodies 1:100 (Jackson Laboratories, West Grove, PA, USA) in PBS-T with 1% BSA for 1 h, washed and then mounted in Vectashield medium (Vector Laboratories, Burlingame, KS, USA) containing 1 μg/ml DAPI. The cells were observed with a Motic-BA410 microscope and photographed with a Moticam Pro 285A digital camera (Motic Asia, Hong Kong).

Western blot

Cells were treated with MLN8237 or DMSO for 24 h, then protein extracts were prepared and Western blot was carried out as previously described (16). The primary antibodies employed were the above-mentioned anti-

phospho-histone H3 (Ser10) 1:1000 and anti-β-tubulin 1:10000. After washing, the membranes were incubated with appropriate horseradish peroxidase-conjugated secondary antibodies 1:1000 (Thermo Fisher Scientific, Rockford, IL, USA), and developed using the LiteAblot EXTEND or PLUS chemiluminescent substrates (Euroclone, MI, Italy).

Time-lapse analysis

Cells were cultured in a Petri dish until 50% of confluence, then medium was replaced with fresh medium containing 50 nM AZD1152 for TPC1, 500 nM AZD1152 for BCPAP, 1 mM AZD1152 for K1, or 500 nM MLN8237 or DMSO, and the dish placed inside an incubation chamber at 37°C and 5% CO_2 under a Leica DM-IRBE microscope. Images were acquired every 5 min for 24 h by a Moticam 5 photo camera (Motic Asia, Hong Kong).

Flow cytometric analysis

Cells were treated for 48h with 500 nM MLN8237 or with 50 nM AZD1152 for TPC1, 500 nM AZD1152 for BCPAP, 1 mM AZD1152 for K1 or DMSO, then collected in PBS by scraping, centrifuged at 1200 r.p.m. for 5 min, and fixed in 70% ice-cold ethanol for 1 h. After centrifugation and washing with PBS, cells were incubated with 0.5 mg/ml RNAse at 37°C for 1 h, labeled with 10 μg/ml propidium iodide and analyzed with a FACScalibur Flow cytometer and CellQUEST software (BD Biosciences, San Jose, CA, USA), counting no less than 15.000 events for each sample.

Apoptosis assay

The induction of apoptosis following cell exposure to the inhibitors was evaluated by means of the Cell Death Detection ELISA^{PLUS} kit (Roche Diagnostics, Mannheim, Germany). Cells were seeded in 96-multiwell culture plates, treated with 500 nM MLN8237 or with 50 nM AZD1152 for TPC1, 500 nM AZD1152 for BCPAP, 1 mM AZD1152 for K1 or DMSO, and incubated from 1 to 4 days. Samples were analyzed daily following the manufacturer's instructions. Briefly, culture medium was removed and cells incubated for 30 min in lysis buffer, then lysates were collected, centrifuged at 200 × g for 10 min, and 20 μl of supernatants were transferred into the streptavidin-coated multiwell for analysis. Eighty μl of the immunoreagent were added to each well, and then the multiwell was incubated for 2 h at room temperature on a shaker under gentle shaking. After rinsing, 100 μl of substrate solution was added to each well, and the plate incubated on a shaker until the color developed. After adding the stop solution, absorbance at 405 nm was measured in a multiplate reader (DAS, Rome, Italy).

Statistical analysis

All the results were obtained from three independent experiments, and are expressed as mean±S.E.M. Dose-response curves were analyzed by curve fitting with four-parameter logistic functions using the ALLFIT program. One-way Anova followed by the Bonferroni post-Anova test, using the SPSS software (Armonk, New York, USA), evaluated the statistical significance of data.

RESULTS

Dose- and time-dependent effects of MLN8237 and AZD1152 on the proliferation of PTC-derived cells

Aurora inhibitors were administered to the cells at different doses and times of incubation. As shown in Fig. 1, both drugs were capable of reducing the growth of all three cell lines in a dose-dependent manner up to 80-95%, with IC_{50} ranges of 26.6-484.5 nM for AZD1152 and of 65.4-114.9 nM for MLN8237 (see Table I). The proliferation decreased significantly after only 24 h of treatment, and reached the minimum rate within 48-96 h (Fig. 2).

Selectivity of the Aurora inhibitors at effective antiproliferative doses

In order to ascertain that the inhibitors were actually selective for Aurora-A or Aurora-B at doses exerting optimal antiproliferative effects, immunofluorescence (IF) experiments were performed. Similar results were obtained for all the cell lines, represented in Figs. 3 and 4 by B-CPAP cells. Phosphorylation of H3 on Ser10, specifically due to Aurora-B, disappeared following treatment with AZD1152 at doses consistent with the trend of the dose-response proliferation curve. At 250 nM AZD1152, some spots of residual H3 (Ser10) phosphorylation were still present (data not shown), disappearing completely at 500 nM. On the contrary, no effect on the auto-phosphorylation of Aurora-A was observed even at the highest dose used (Fig. 3). On the other hand, besides inhibiting Aurora-A auto-phosphorylation as expected, MLN8237 also impaired H3 (Ser10) phosphorylation starting from the dose 250 nM (Fig. 4). Western blot (WB) experiments confirmed the decay of H3 (Ser10) phosphorylation in all three cell lines with increasing doses of MLN8237 (Fig. 5). In both IF and WB the B-CPAP cells appeared to be slightly less sensitive to inhibition of Aurora-B, yet this was not reflected

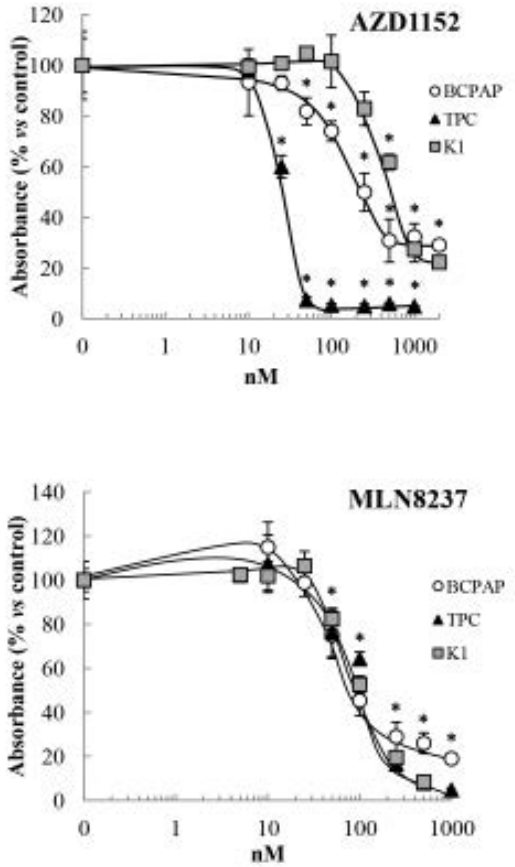

Fig. 1. *Dose-dependent effects of the Aurora kinase inhibitors MLN8237 and AZD1152 on PTC cell proliferation. Cells were treated with different concentrations of MLN8237 (5-1000 nM) or AZD1152 (10-2000 nM) or with DMSO alone (control) for 4 days, after which cell proliferation was measured by colorimetric assay. Data are representative of one out of three similar experiments. * p<0.01.*

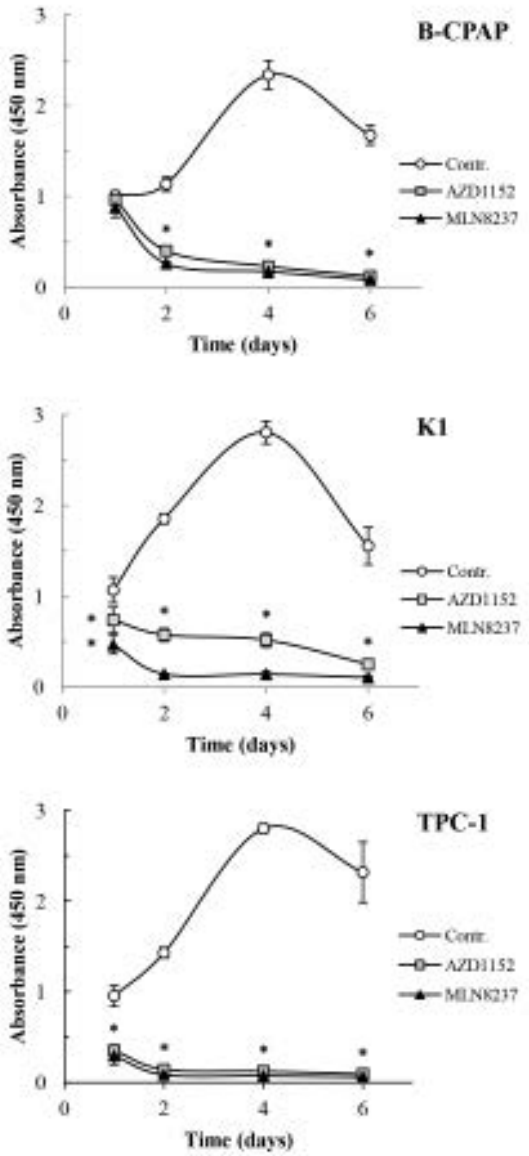

Fig. 2. *Time-dependent effects of the Aurora kinase inhibitors MLN8237 and AZD1152 on PTC cell proliferation. Cells were treated with 500 nM MLN8237 or with 50 nM AZD1152 for TPC1, 500 nM AZD1152 for BCPAP or 1 mM AZD1152 for K1, or DMSO alone (control) from 1 to 6 days, then proliferation was measured by colorimetric assay. Data are representative of one out of three similar experiments.* p<0.01.*

in a lower antiproliferative efficacy of the MLN8237 on this line, as shown by the IC_{50} values (Table I).

Effects of MLN8237 and AZD1152 on PTC cell division

The IF experiments were also aimed to observe mitosis of PTC cells lacking of either Aurora-A or Aurora-B activity. In cells treated with AZD1152 the spindle structures were mostly bipolar, while in those treated with MLN8237 they were drastically altered, often with multiple minispindles and amplified centrosomes occurring in the same cell (Figs. 3 and 4). Moreover, in cell cultures exposed to either AZD1152 or MLN8237 no anaphase, telophase

Table I. *Estimated IC_{50} for MLN8237 and AZD1152 in the different PTC-derived cell lines.*

	AZD1152	MLN8237
B-CPAP	123.7±28.7	65.4±5.3
K1	484.6±71.0	95.3±8.8
TPC1	26.6±0.7	114.9±9.8

Cell proliferation was evaluated by means of BrdU incorporation as specified in the Materials and Methods section. The IC_{50} values were calculated with data from three independent experiments using the ALLFIT software.

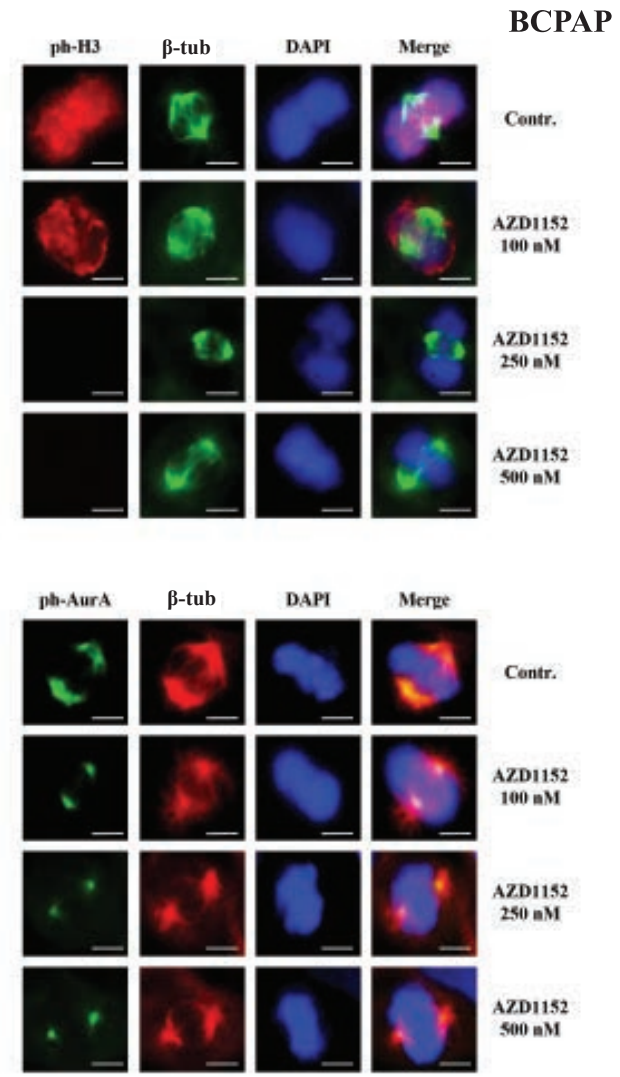

Fig. 3. *Immunofluorescence of PTC cells treated with AZD1152. B-CPAP cells cultured on coverslips were exposed to increasing doses of AZD1152 for 24 h, then fixed in cold methanol for 5 min and subjected to IF experiments. Ph-Aur-A: auto-phosphorylated Aurora-A; Ph-H3: histone H3 phosphorylated on Ser10; β-tub: beta-tubulin.*

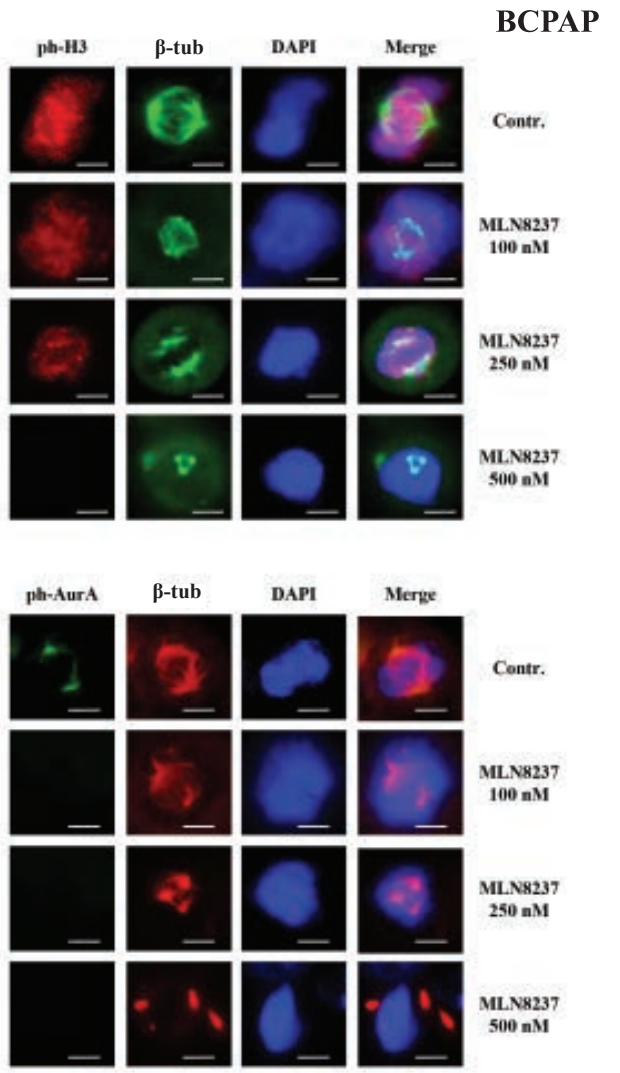

Fig. 4. *Immunofluorescence of PTC cells treated with MLN8237. B-CPAP cells cultured on coverslips were exposed to increasing doses of MLN8237 for 24 h, then fixed in cold methanol for 5 min. and subjected to IF experiments. Ph-AurA: auto-phosphorylated Aurora-A; Ph-H3: histone H3 phosphorylated on Ser10; β-tub: beta-tubulin.*

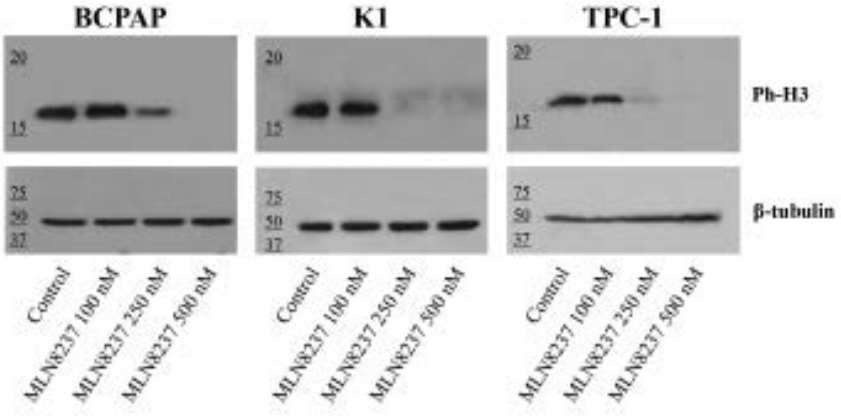

Fig. 5. *Dose-dependent selectivity of MLN8237 in PTC cells. PTC cells were treated with increasing doses of MLN8237 for 24 h, then total protein extracts were analysed by Western blot for detecting the disappearance of H3 phosphorylation. Ph-H3: histone H3 phosphorylated on Ser10.*

or cytokinesis could be detected. Similarly, image sequences acquired from time lapse videomicroscopy showed that cells treated with AZD1152 or MLN8237 entered mitosis but were unable to divide, eventually returning to interphase (Fig. 6).

Effects of MLN8237 and AZD1152 on cell cycle progression and survival of PTC cells

The cytofluorometric analysis showed that polyploid subpopulations were present in all the cell lines cultured in standard conditions. This is not surprising since B-CPAP cells are described to have a near-diploid karyotype with hexaploid sidelines, K1 cell karyotype is characterized by both structural and numerical chromosome changes, and the chromosome number of TPC1 cells was reported to vary from 28 to 139, with a modal number of 49 (22, 23).

As expected, based on the previous findings, after 48 h of treatment with either AZD1152 or MLN8237, all three cell types displayed accumulation in G2/M phase and/or increase of ploidy (Fig. 7). The induction of apoptosis in treated cells was monitored daily by measuring the intracellular DNA fragmentation in a quantitative sandwich-enzyme immunoassay. At 72-h incubation a significant enrichment of apoptotic cells was detected in all the cultures, more pronounced for TPC1. Consistently with the shorter doubling time of this line (~ 20 h) compared to K1 (~ 40 h) and B-CPAP (~ 36 h), TPC1 cells arrive sooner to accumulate a quantity of intracellular material incompatible with their survival, which may explain the higher proportion of dying cells observed for this line (Fig. 8).

DISCUSSION

To date, treatment options for patients with progressive, RAI-resistant TC remain limited. The most relevant therapeutic results have been obtained with TKIs, which, however, do not go beyond disease stabilization or partial responses. Overall, considering the discrepancy of several clinical reports about their efficacy, the ability of these drugs to improve TC patient survival is not even clear.

In recent years, the Aurora kinases, which play key roles in mitotic progression, have sparked a growing interest as potential targets for anticancer therapy. A number of phase I and II clinical trials have been performed with several small molecule inhibitors of one or more Aurora kinases on multiple cancer types, and many others are ongoing at present

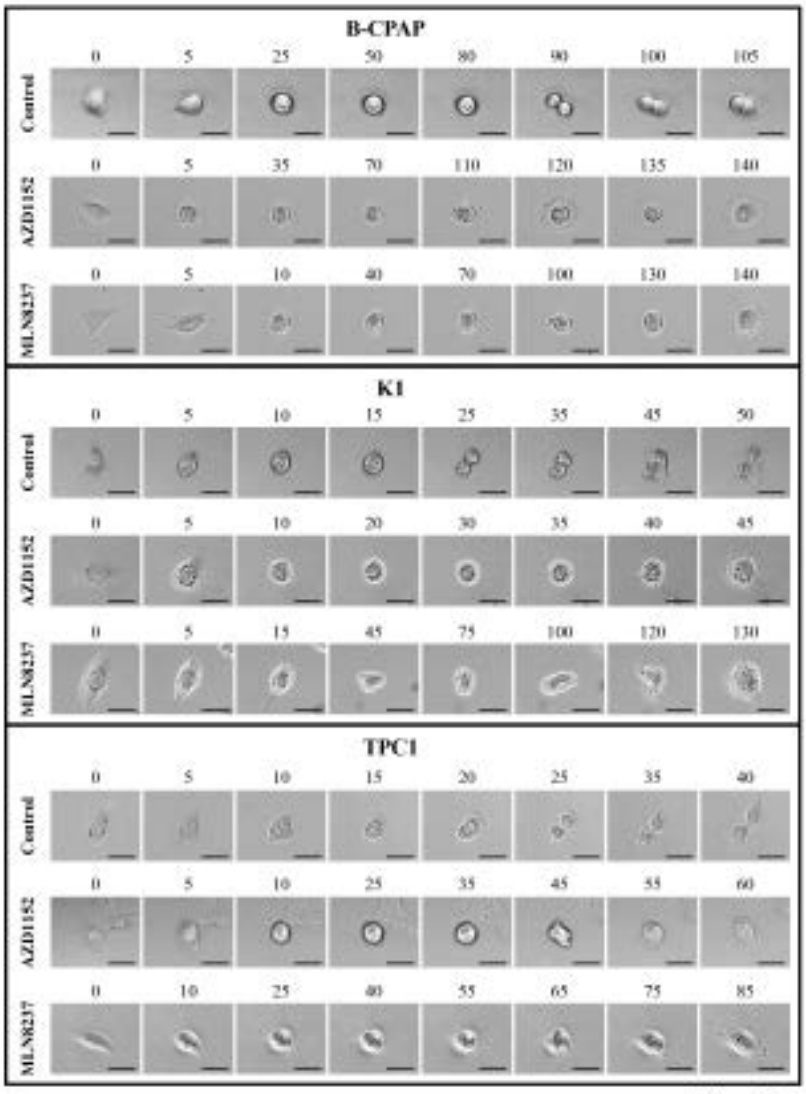

Fig. 6. *Time-lapse videomicroscopy of PTC cells cultured with MLN8237 or AZD1152. Cells were cultured in a Petri dish and treated with a drug effective dose or DMSO. Immediately after (time 0), dishes were placed into an incubation chamber, and images were acquired every 5 min for 24 h with a photographic microscope camera. Numbers above images represent the minutes elapsed from the time 0.*

(24-26). At cellular levels, these drugs allow entry into mitosis, but dramatically disrupt the process leading to imbalanced chromosomal segregation or endoreduplication. In particular, selective inhibition of Aurora-A causes activation of the spindle assembly checkpoint (SAC) and provisional block of cells in G2/M, followed by either mitotic slippage or cell division, while selective inhibition of Aurora-B impairs SAC and abolishes cytokinesis with consequent generation of tetraploid cells.

As stated above, in previous reports we documented the efficacy of different Aurora inhibitors, both general and selective, in damaging cell growth and survival of cell lines derived from anaplastic thyroid carcinoma (ATC). In the present work, we tested two selective Aurora inhibitors on cancer cell lines derived from differentiated papillary thyroid carcinoma (PTC). In particular, we chose a

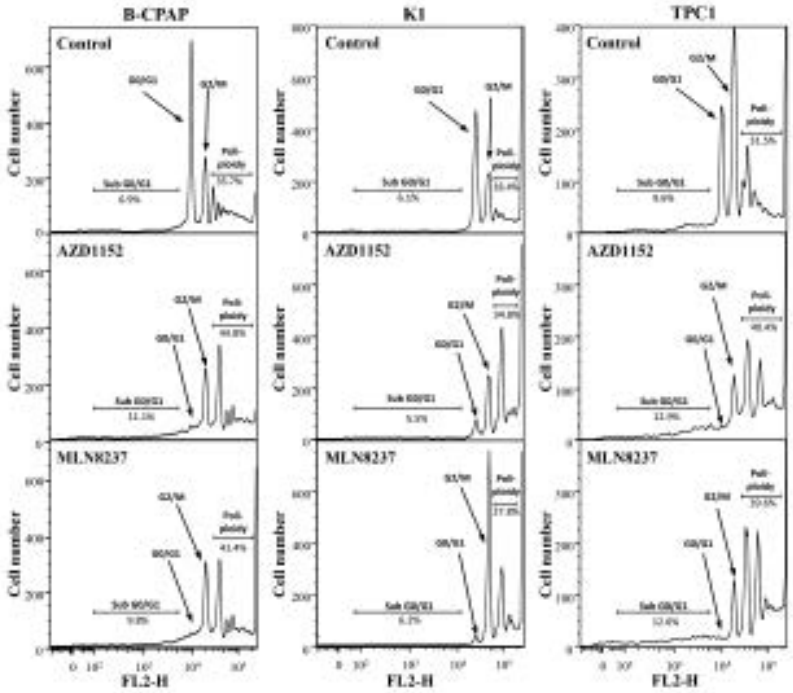

Fig. 7. *Cytofluorometric analysis of PTC cells treated with MLN8237 or AZD1152. Cells were cultured for 48 h with effective doses of each inhibitor or DMSO, then collected, fixed in 70% ice-cold ethanol, depleted of RNA, labeled with propidium iodide and finally examined by flow cytometry.*

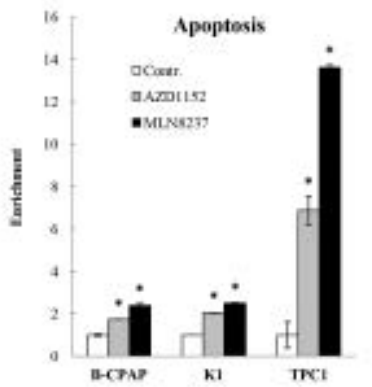

Fig. 8. *Apoptosis induction of PTC cells treated with MLN8237 or AZD1152. Cells were exposed to effective doses of each inhibitor or DMSO from 1 to 4 days, and DNA fragmentation was measured daily by colorimetric assay. Significant enrichment of apoptotic cells appeared at 72 h. The results are expressed as fold change of treated cells vs control cells.* $p<0.01$.*

cell line derived from a primary PTC (K1), a cell line derived from the metastasis of a well-differentiated PTC (TPC1), and a third cell line originated from a metastasizing poorly differentiated PTC (B-CPAP) in order to evaluate the potential drug sensitivity of PTC at different levels of progression.

Our findings demonstrated that both MLN8237, targeting Aurora-A, and ADZ1152, targeting Aurora-B, are highly effective in reducing cell proliferation in a dose- and time-dependent manner. The IC_{50} range calculated by BrdU incorporation assay was broad for AZD1152 (26.6-484.6 nM), but quite narrow for MLN8237 (65.4-114.9 nM). However, MLN8237 produced the maximum effect at concentrations that inhibited both Aurora-A and Aurora-B. In all cell types apoptosis appeared within 3 days of incubation with both inhibitors.

Among the identified substrates of the Aurora kinases, p53 is considered to be one of those that most affect cell responses to Aurora inhibitors,

as the p53-dependent postmitotic checkpoint is activated after defective cytokinesis arresting cells in a pseudo-G_1 state. Both Auroras phosphorylate p53 and are thought to have a prevalent role in reducing p53 transactivation activity and protein stability. Silencing of Aurora-A in wt-p53 cancer cells results in higher p53 protein level, cell-cycle arrest at G2/M, and sensitization to the cytotoxic effects of cisplatinum (27). Similarly, pharmacologic inhibition of Aurora B in wt-p53 cancer cells was shown to elevate p53 protein level and expression of target genes, enhancing p53 tumor suppressor function (28).

In view of these findings, one might assume that the effectiveness of Aurora inhibitors is greater in cells with inactivating mutations of p53, because reversible activation of the postmitotic checkpoint by p53 in wt cells can protect them from the effects of an incorrect division. However, recent studies that analyzed a panel of commonly used tumor-derived cell lines having either wt, mutant or deleted p53 gene demonstrated that cells treated with VX-680, a pan-inhibitor of Aurora, underwent extensive endoreduplication independent from p53 status (29). In cells with functional p53, this occurred despite the protein being activated and its target genes (i.e. p21, PUMA and MDM2) upregulated, indicating that the action of p53 is not sufficient to avoid endoreduplication. Analogous results were obtained by challenging with AZD1152 wt p53-containing HCT116 cells of colorectal carcinoma (30).

All the epithelial TC cells previously tested by us were characterized by inactivating mutations of the transcription factor p53. Therefore, in the present study we chose PTC cell lines having either wt or mutated p53. In agreement with the above reports, we found no differences in terms of sensitivity, polyploidization or apoptosis induction following exposure to Aurora inhibitors between wt-p53 PTC cells (K1 and TPC1) and those with mutated p53 (B-CPAP). Thus, our experimental data support the hypothesis that the Aurora kinases represent a potential therapeutic target for the therapy of PTC unresponsive to RAI treatment regardless of p53 status.

In conclusion, in the present preclinical study we demonstrated that Aurora kinase inhibition might represent a therapeutic strategy for RAI-insensitive PTC.

ACKNOWLEDGEMENTS

This work was supported by the Italian Ministero dell'Istruzione, dell'Università e della Ricerca (PRIN 2010-2011, protocol n. 2010BX2SNA_002).

REFERENCES

1. Ferlay J, Steliarova-Foucher E, Lortet-Tieulent J, Rosso S, Coebergh JW, Comber H, Forman D, Bray F. Cancer incidence and mortality patterns in Europe: estimates for 40 countries in 2012. Eur J Cancer 2013; 49:1374-403.
2. Davies L, Welch HG. Increasing incidence of thyroid cancer in the United States, 1973-2002. Jama 2006; 295:2164-7.
3. Nikiforov YE, Ohori NP. Papillary Carcinoma. In Diagnostic pathology and molecular genetics of the thyroid. YE Nikiforv, PW Biddinger, LDR Thompson, eds. Wolters Kluver-Lippincott Williams & Wilkins, Philadelphia, 2009; p 160-213.
4. Busaidy NL, Cabanillas ME. Differentiated thyroid cancer: management of patients with radioiodine nonresponsive disease. J Thyroid Res 2012; 2012:618985.
5. Handkiewicz-Junak D, Czarniecka A, Jarząb B. Molecular prognostic markers in papillary thyroid cancer: current status and future directions. Mol Cell Endocrinol 2010; 322:8-28.
6. Ulisse S, Baldini E, Sorrenti S, et al. High expression of the urokinase plasminogen activator and its cognate receptor associates with advanced stages and reduced disease-free interval in papillary thyroid carcinoma. J Clin Endocrinol Metab 2011; 96:504-8.
7. Ulisse S, Baldini E, Sorrenti S, et al. In papillary thyroid carcinoma BRAFV600E is associated with increased expression of the urokinase plasminogen activator and its cognate receptor, but not with disease-free interval. Clin Endocrinol 2012; 77:780-86.
8. The cancer Genome Atlas Research Network. Integrated genomic characterization of papillary thyroid carcinoma. Cell 2014; 159:676-90.
9. Antonelli A, Fallahi P, Ulisse S, et al. New targeted therapies for anaplastic thyroid cancer. Anticancer Agents Med Chem 2012; 12:87-93.

10. Baldini E, D'Armiento M, Ulisse S. A new aurora in anaplastic thyroid cancer therapy. Int J Endocrinol 2014; 2014:816430 doi: 10.1155/2014/816430.
11. Nikonova AS, Astsaturov I, Serebriiskii IG, Dunbrack RL Jr, Golemis EA. Aurora A kinase (AURKA) in normal and pathological cell division. Cell Mol Life Sci 2013; 70:661-87.
12. Sorrentino R, Libertini S, Pallante PL, et al. Aurora B overexpression associates with the thyroid carcinoma undifferentiated phenotype and is required for thyroid carcinoma cell proliferation. J Clin Endocrinol Metab 2005; 90:928-35.
13. Ulisse S, Delcros JG, Baldini E, et al. Expression of Aurora kinases in human thyroid carcinoma cell lines and tissues. Int J Cancer 2006; 119:275-82.
14. Baldini E, Tuccilli C, Prinzi N, et al. Deregulated expression of Aurora kinases is not a prognostic biomarker in papillary thyroid cancer patients. PLoS One 2015; 10:e0121514.
15. Baldini E, Tuccilli C, Prinzi N, et al. Effects of selective inhibitors of Aurora kinases on anaplastic thyroid carcinoma cell lines. Endocr Relat Cancer 2014; 21:797-811.
16. Baldini E, Sorrenti S, D'Armiento E, et al. Effects of the Aurora kinases pan-inhibitor SNS-314 mesylate on anaplastic thyroid cancer derived cell lines. Clin Ter 2012; 163:e307-13.
17. Arlot-Bonnemains Y, Baldini E, Martin B, et al. Effects of the Aurora kinase inhibitor VX-680 on anaplastic thyroid cancer-derived cell lines. Endocr Relat Cancer 2008; 15:559-68.
18. Baldini E, Tuccilli C, Prinzi N, et al. The dual Aurora kinase inhibitor ZM447439 prevents anaplastic thyroid cancer cell growth and tumorigenicity. J Biol Regul Homeost Agents 2013; 27:705-15.
19. Saiselet M, Floor S, Tarabichi M, Dom G, Hébrant A, van Staveren WC, Maenhaut C. "Thyroid cancer cell lines: an overview". Front Endocrinol 2012; 3:133.
20. Manfredi MG, Ecsedy JA, Chakravarty A, et al. Characterization of Alisertib (MLN8237), an investigational small-molecule inhibitor of aurora A kinase using novel in vivo pharmacodynamic assays. Clin Cancer Res 2011; 17:7614-24.
21. Wilkinson RW, Odedra R, Heaton SP, et al. AZD1152, a selective inhibitor of Aurora B kinase, inhibits human tumor xenograft growth by inducing apoptosis. Clin Cancer Res 2007; 13:3682-8.
22. Maric I, Viaggi S, Caria P, Frau DV, Degan P, Vanni R. Centrosomal and mitotic abnormalities in cell lines derived from papillary thyroid cancer harboring specific gene alterations. Mol Cytogenet 2011; 4:26.
23. Chang J, Sui Z, Ma T, Ma K, Zhang X, Wang J, Dong K, Yao Q. Establishment and characterization of two cell lines derived from human transitional cell carcinoma. Chin Med J 1995; 108:522-7.
24. Mehra R, Serebriiskii IG, Burtness B, Astsaturov I, Golemis EA. The role of targeting of Aurora kinase in head and neck cancer. Lancet Oncol 2013; 14:e425-35.
25. Dees EC, Cohen RB, von Mehren M, et al. Phase I study of aurora A kinase inhibitor MLN8237 in advanced solid tumors: safety, pharmacokinetics, pharmacodynamics, and bioavailability of two oral formulations. Clin Cancer Res 2012; 18:4775-84.
26. Schwartz GK, Carvajal RD, Midgley R, et al. Phase I study of barasertib (AZD1152), a selective inhibitor of Aurora B kinase, in patients with advanced solid tumors. Invest New Drugs 2013; 31:370-80.
27. Katayama H, Sasai K, Kawai H, et al. Phosphorylation by aurora kinase A induces Mdm2-mediated destabilization and inhibition of p53. Nat Genet 2004; 36:55-62.
28. Gully CP, Velazquez-Torres G, Shin JH, et al. Aurora B kinase phosphorylates and instigates degradation of p53. Proc Natl Acad Sci U S A 109:E1513-22, 2012.
29. Harrington EA, Bebbington D, Moore J, et al. VX-680, a potent and selective small-molecule inhibitor of the Aurora kinases, suppresses tumor growth in vivo. Nat Med 2004; 10:262-7.
30. Nair JS, Ho AL, Tse AN, Coward J, Cheema H, Ambrosini G, Keen N, Schwartz GK. Aurora B kinase regulates the postmitotic endoreduplication checkpoint via phosphorylation of the retinoblastoma protein at serine 780. Mol Biol Cell 2009; 20:2218-28.

LYMPHATIC EDEMA OF THE LOWER LIMBS AFTER ORTHOPEDIC SURGERY: RESULTS OF A RANDOMIZED, OPEN-LABEL CLINICAL TRIAL WITH A NEW EXTENDED-RELEASE PREPARATION

G. LESSIANI[1], P. IODICE[2], E. NICOLUCCI[3] and M. GENTILI[3]

[1]Vascular Medicine Unit, Private Hospital "Villa Serena", Città Sant'Angelo (PE), Italy;
[2]Orthopedic Rehabilitation Unit, Private Hospital "Villa Serena", Città Sant'Angelo (PE), Italy;
[3]Institute of Cognitive Sciences and Technologies, National Research Council, Rome, Italy

Received February 5, 2015 – Accepted September 4, 2015

The lymphedema is a high interstitial protein concentration edema, caused by impaired lymphatic transport capacity. It can be primary or secondary. The secondary form may be caused by a lesion of the lymphatic vessels and/or lymph nodes during diagnostic or therapeutic procedures such as surgical interventions. Often, in clinical practice, there is lymphedema after orthopedic surgery, even in minor orthopedic surgery. Lymphedema, typically presents symptoms of swelling, pain, inflammation, and itching, and it can generate, over the years, acute disability in the affected limbs. The standard therapy is mainly represented by medical treatment, such as manual lymphatic drainage and compression with bandages and stockings. In literature it is documented that lymphedema is responsive to alpha and the gamma benzopyrones. The aim of this study was to determine the effectiveness of delayed extended-release formulation of a compound containing apha-benzo-pyrone (Coumarin), benzo-gamma-pyrone (Troxuretina) and oligomeric proanthocyanidins from *Vitis vinifera* (OPC), in addition to compression therapy, in the reduction of lymphatic edema after prosthetic hip and knee surgery. In the group treated, after 30 days, a reduction was observed of the edema of 4.8% in the ankle area ($p<0.008$) and 2.7% in the calf area ($p< 0.013$). The control group showed no significant reduction. The treated group showed a marked reduction of all the secondary symptoms considered in the study, although variations were not significant. The results show that the compound used was effective in reducing edema after major orthopedic surgery, and consequently in alleviating some related symptoms, such as pain, itching, and burning. As an edema has extensive inflammatory components in patients with reduced mobility, the final data seems interesting, however, further investigations and a better follow-up are required.

The lymphedema is a high interstitial protein concentration edema, caused by impaired lymphatic transport capacity (1, 2). The reduced ability of lymphatic transport can be congenital or acquired.

The secondary lymphedema may be due to a lesion of the lymphatic vessels and/or lymph nodes caused by diagnostic or therapeutic processes. A previous study, in patients with aorto-bifemoral aneurysm by-pass, documented an incidence of injuries to the lymphatic system in 8.1% of cases (3). Literature data provide evidence that it is possible to have lymphedema in 29% of patients submitted

Key words: lymphedema, orthopedic surgery, alpha- benzopyrones, gamma benzopyrones

Mailing address:
Dr Gianfranco Lessiani,
Vascular Medicine Unit,
Villa Serena Hospital,
Viale L. Petruzzi, 42
65013 Città Sant'Angelo (Pe), Italy
e-mail: g.lessiani@libero.it

0393-974X (2015)

DISCLOSURE: ALL AUTHORS REPORT NO CONFLICTS OF INTEREST RELEVANT TO THIS ARTICLE.

to radical inguinal lymph node dissection (4). Moreover, the incidence of lymphatic complications after urology or gynecology surgery, ranges between 20% and 40%, according to published studies (5). The complications that occur in the lymphatic system can be different: lymphorrhagia, lymphocele, or lymphedema. Significant data can be found in literature concerning breast cancer surgery, that report lymphatic lesions after mastectomy in 37% of patients (6, 7, and 8). The radiation therapy in these cases is an aggravating element (9).

Despite the increasing number of orthopedic operations, there are few data regarding the incidence of lymphedema after surgery.

The lymphatic edema also determines symptoms such as pain, heaviness, burning, and itching, which may limit the rehabilitation program and, furthermore, may affect the patient's quality of life. The aim of this study was to determine whether the use of a compound, containing benzo-alpha-pyrone (Coumarine), benzo-gamma-pyrone (Troxuretina) and OPC (oligomeric proanthocyanidins from V*itis vinifera*), could effectively reduce post-surgical lymphatic edema, as well as attenuating related symptoms.

MATERIALS AND METHODS

Sixty patients affected by post-surgical lymphatic edema in lower limb were enrolled in the study. The surgery consisted in hip/knee replacement, and all operations were carried out in Villa Serena, Città Sant'Angelo, Italy during the period from May to November 2013 after approval by the local Ethics committee. All patients signed an informed consent.

The inclusion criteria were: over 18 years of age, acute lymphatic edema after major orthopedic surgery.

The exclusion criteria were: under 18 years of age, severe heart failure, severe kidney failure, verified allergy to any component used in the study, presence of neoplasia, thrombosis of the deep and/or superficial veins (ongoing or previous), diabetes

All the anthropometric, clinical and instrumental data of patients are shown in Table I. The patients were divided into two homogeneous groups. No significant differences related to the clinical and anthropometric characteristics were detected. There were differences concerning the number of subjects who underwent knee or ankle surgery in the two groups. Seven patients dropped out of the study, 4 for complications directly linked with surgery (3 for DVT; 1 for infection) and 3 for personal reasons.

Fifty-three patients were randomized (simple computer system randomization) into two groups. Thirty-six in group A (treatment) underwent anti-thrombotic prophylaxis with low molecular weight heparin (Enoxapaina 4000 IU / day sc) starting 12 hours before surgery and used anti-thrombus elastic stockings (18-21 mmhg compression). From day 7 the formulation of the study was administered according to the dosage of 1 pill of 750 mg (50 mg *Melilotus officinalis* c tit. 20% coumarin, 50 mg *Vitis vinifera* titrated. 5% polyphenols, 200 mg troxerutin).

Seventeen patients in group B (control) underwent anti-thrombotic prophylaxis with low molecular weight heparin (enoxaparin 4000 IU/day sc) starting 12 h before surgery and wore anti-thrombus elastic stockings (18-21 mmhg compression).

Before surgery (T0), and after 7 (T1) and 30 days (T2) for all patients measurement were taken of the circumferences (cm) of ankle and calf (using specific anatomical landmarks), and evaluation was made of the perception of pain, itching, and burning using the visual analogical scale (VAS). Eco Colour Doppler was also carried out to exclude possible deep venous thrombosis (DVT).

Statistical analysis

To compare differences between the two groups, the Mann-Whitney test, Fisher's test and Pearson's c^2 were used. The differences before and after treatment were analyzed with the Wilcoxon signed-rank test. Unless otherwise specified, the data were expressed as mean ± standard deviation (SD). The value of $p<0.05$ was considered as statistically significant.

RESULTS

To evaluate the edema, the percentage was used of volume reduction, in centimeters, of the ankle and the calf. Data were recorded 7 and 30 days after surgery for both the operated limb and the controlateral one. Volume reduction:

Group A (treatment): At T1 circumference of the operated limb, compared to T0, showed an increase of 9.6±4.1% in the ankle and 4.2±2.8% in the calf. After 30 days, T2, we found a reduction of the size of 4.8±3% in the ankle and 2.7±2% in the calf.

Group B (control): At T1 our data showed an increase of 8.3±3.8% in the ankle and 5.1±3.1% in the calf diameter. After 30 days (T2), there was a reduction of 2.3±2.8% and 0.5±7.3% in the size of

Table I. *Clinical characteristics of patients at baseline.*

Variable	*Untreated*	*Treated*	*P value*[1]
N	17	36	
Age, years	73±8	69±10	0.167
Male gender, n (%)	7 (41.2)	8 (22.2)	0.167
BMI, Kg/m²	29.4±4.5	27.8±4.1	0.211
Chronic venous disease, n (%)			0.095
CEAP 2, n (%)	1 (5.9)	1 (2.8)	
CEAP 3, n (%)	2 (11.8)	8 (22.2)	
CEAP 4-6, n (%)	0	4 (11.1)	
Lymphedema, n (%)	2 (11.8)	8 (22.2)	0.471
Surgery site			0.736
Hip, n (%)	8 (47.1)	21 (58.3)	
Knee, n (%)	9 (52.9)	13 (36.1)	
Other, n (%)	0	2 (5.6)	

[1]*By Mann-Whitney or Kruskal Wallis test, as appropriate.*
BMI, body mass index; CEAP, clinical-etiology-anatomy-pathophysiology classification

Table II. *Ankle and calf circumferences of operated and control limbs at baseline and after 7 and 30 days follow-up.*

	Timepoint	*Untreated*	*Treated*	*P value*[1]
Operated limb				
Ankle	Baseline, cm	22.6±2.2	23.2±2.3	0.386
	After 7 days, cm	24.4±2.2**	25.4±2.4**	0.156
	% change[2]	8.3±3.8	9.6±4.1	0.268
	After 30 days, cm	23.5±1.8*	24.1±2.3**	0.501
	% change[2]	-2.3±2.8	- 4.8±3.0	0.013
Calf	Baseline, cm	36.6±2.8	36.5±4.0	0.484
	After 7 days, cm	38.3±3.0**	38.0±4.0**	0.618
	% change[2]	5.1±3.1	4.2±2.8	0.532
	After 30 days, cm	38.2±2.7*	37.0±4.0**	0.085
	% change[2]	0.5±7.3	- 2.7±2.0	0.008
Control limb				
Ankle	Baseline, cm	22.6±2.3	23.2±2.1	0.302
	After 7 days, cm	22.5±2.3	23.1±2.1	0.232
	% change[2]	- 0.5±1.5	-0.1±0.8	0.284
	After 30 days, cm	22.1±1.6	23.2±2.1	0.135
	% change[2]	0.3±1.2	0.1±0.8	0.377
Calf	Baseline, cm	36.6±2.7	36.5±3.9	0.612
	After 7 days, cm	36.5±2.7	36.5±3.9	0.744
	% change[2]	- 0.4±1.1	0	0.05
	After 30 days, cm	36.3±2.7	36.5±3.9	0.865
	% change[2]	0.2±0.7	0.1±1.3	0.404

[1]*By Mann-Whitney U-test.* [2]*% change vs previous time-point.*
**P = 0.01, **P < 0.0001 vs baseline, by Wilcoxon Signed Ranks test.*

Table III. *Lymphedema-related symptoms at baseline and after 7 and 30 days follow-up.*

Symptoms	*Timepoint*	Untreated	Treated	P value[1]
Pain	Baseline, score	8.2±1.7	8.0 ± 2.1	0.959
	After 30 days, score	4.2±1.4*	3.7±1.5**	0.177
	Δ change[2]	3.9±0.7	4.2±1.3	0.140
Itch	Baseline, score	2.5±2.8	2.3±3.0	0.636
	After 30 days, score	1.6±1.7**	1.0±1.4**	0.174
	Δ change[2]	0.9±1.3	1.3±1.7	0.606
Burning	Baseline, score	3.4±3.2	3.6±3.4	0.769
	After 30 days, score	1.7±1.6*	1.7±1.7*	0.967
	Δ *change*[2]	1.7±1.6	1.9±1.8	0.795

[1]*By Mann-Whitney U-test.* [2]*% change vs previous time-point.*
**P = 0.01, **P < 0.0001 vs baseline, by Wilcoxon Signed Ranks test.*

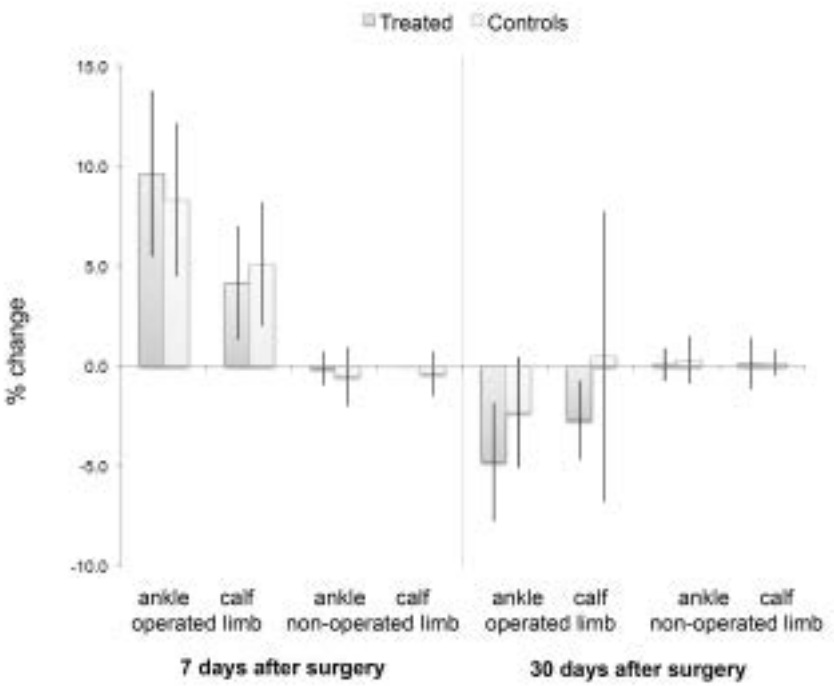

Fig. 1. *Percentage change vs baseline of ankle and calf circumferences of operated and control limbs after 7 and 30 days follow-up.*

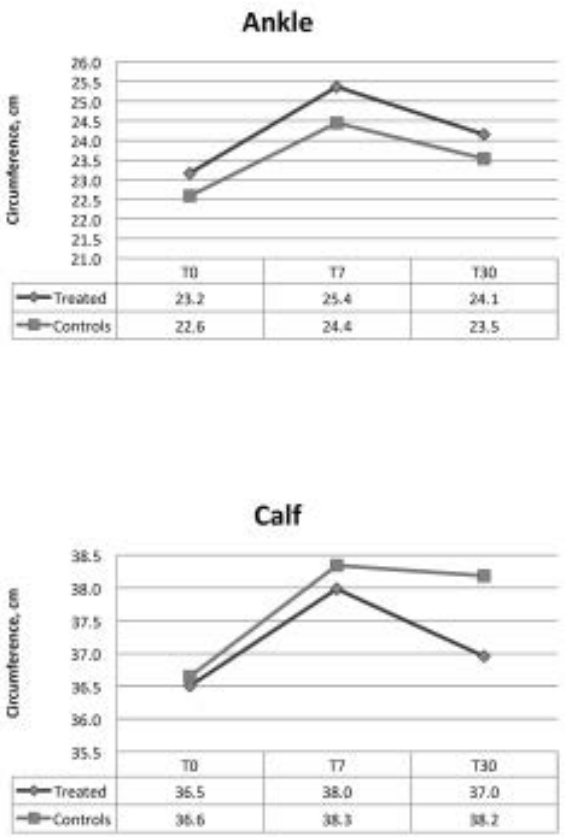

Fig. 2. *Ankle and calf circumference of the operated limb at baseline (T0) and after 7 (T7) and 30 days (T30) follow-up.*

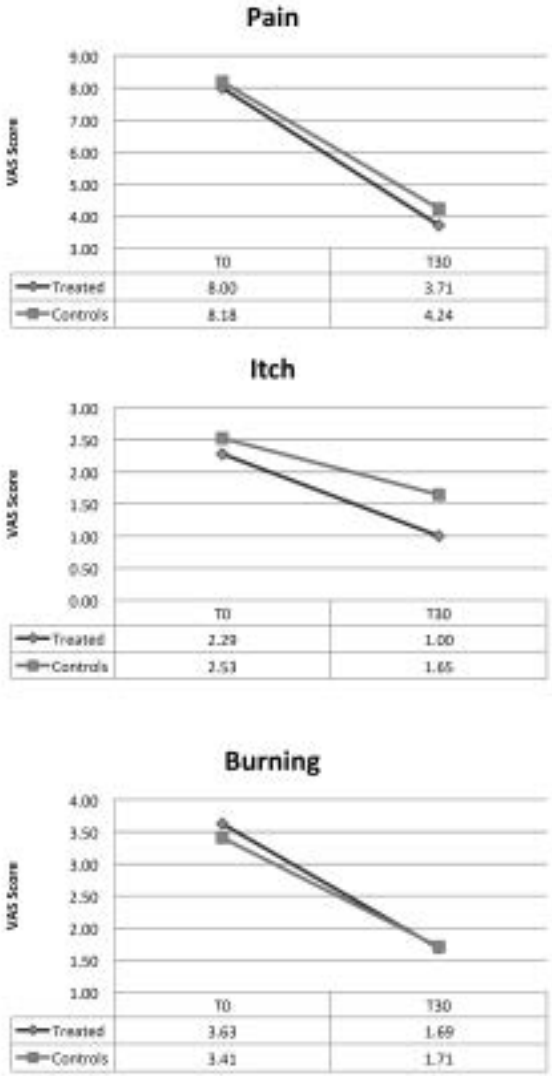

Fig. 3. *Lymphedema-related symptoms of the operated limb at baseline (T0) and after 30 days (T30) follow-up.*

ankle and calf respectively.

Therefore, after 30 days, there was a clear difference between the two groups in terms of reduction of circumference. The treated group presented a systematically greater reduction in edema dimension (calf, $P<0.008$; ankle, $P<0.013$) (Table II; Fig. 1).

Signs and symptoms

After 30 days (T2) VAS data showed a reduction of all symptoms (pain, burning and itching) in the treatment group compared to the control group. However, the data are not statistically significant for any of the symptoms analyzed (Table III).

In the group treated with the compound, we did not find significant adverse events or different clinical situations compared to the control group. The treatment was well tolerated by all patients and therefore there were no temporary or definitive suspensions of the treatment during the study.

DISCUSSION

Secondary lymphatic edema due to surgery is quite common in clinical practice. Several data in literature are related to trauma of the lymphatic system in patients who had undergone surgical oncology (9, 10).

It is well known, in clinical practice, that an edema can be a complication of orthopedic surgery and may appear in the early days after the surgical operation. Sometimes it may be a conditioning element for the rehabilitation program. However, there are no data in literature on the real incidence of surgery on lymphedema.

The cornerstone of lymphedema treatment includes: skin care, compression therapy (bandages/stockings) and manual lymphatic drainage, as well as physical exercise. This therapy plan is defined as combined physical therapy (11, 12). However, pharmacological therapy is an integral part of the treatment of lymphatic edema. Coumarine, chemically 5-6 benzo-alpha-pyrone, is a molecule extracted from the medicinal plant *melilotus* used for a long time to remove tissue from the interstices of the high liquid component colloid-osmotic swelling up the edema. Its use is indicated in the additional treatment of lymphedema in some of the major guidelines (13).

Studies conducted for over a decade by a number of researchers have documented that coumarine efficacy is carried out through two different main mechanisms: i) proteolytic activity which consists of the ability to activate macrophages of Coumarine 1-2, which favours the removal or reabsorption (pro-macrophage) of the protein-macromolecules entrapped in the interstitial tissue; ii) stimulating propulsive activity on lymphatic vessel, through a direct action on smooth muscle of the lymphatic valve canals, stimulating their activity driving and accelerating lymphatic drainage. These functions are mediated by the metabolite 7-hydroxy-coumarine after hepatic transformation, which has a short half-life (14-19). In the present study, a compound was used in which the Troxerutin and OPC *vitis vinifera* had an immediate release process, while the coumarine was released gradually over a prolonged time.

Several studies, both *in vitro* and *in vivo*, on animals and humans, have shown the effect of Benzo-pyrones (BP), and in particular of coumarine, on the activity of the lymphatic system.

In literature, clinical studies have demonstrated the efficacy of BP in the treatment of edema. Desprez-Curley et al. (1985), in a study of mastectomy patients operated and treated with coumarine showed, using a volume reduction and isotopic lymphography, a significant reduction of edema (-52% at 6 months, 70.55% at 12 months and 72.7% at 16 months). The same Authors, in another study on post-mastectomy patients treated with coumarine, showed a reduction of edema of 0.2% after 6 months (20). From a meta-analysis conducted by Casley-Smith et al. on lymphedema treatment with coumarine in different doses, there was an overall reduction in the edema volume average of 49% (after one year) (21). However, some clinical trials on the effects of drug therapy in lymphedema have shown conflicting results (22, 23). Moreover, a Cochrane review, given the heterogeneity of the studies in literature, has been unable to provide definitive information on the pharmacological treatment of lymphedema (24).

According to previous studies, there were side effects in 1.5-5% of cases, mainly depending on the gastrointestinal system (diarrhea, nausea). For synthetic coumarine the risk of severe liver injury (0.3% of cases) has also been described (25).

The natural form of coumarine is derived from the extraction of the active ingredient from *melilotus officinalis* and differs from the synthetic aspects of pharmacodynamics and toxicology, but has the same propulsive activities on lymphatic vessel and proteolytic activities and does not seem to show hepatotoxicity. Even in the natural form the effectiveness has been documented, in addition to physical therapy, to decrease symptoms, and on the reduction of the edema (27, 28). In our study, we evaluated the early edema that can occur in the first few days after orthopedic surgery.

The patients studied wore anti-thrombus stockings from the day of surgery until mobilization. Later, none of them could wear stockings for several reasons: excessive swelling, limitation of action, skin inflammation, etc. Our data show a decrease of edema of 4.8±3% and 2.7±2% in ankle and calf, respectively, in the treated group compared to a decrease of edema of 2.3±2.8% and 0.5±7.3% in control group. The differences between the two groups were significant in both ankle and calf, respectively $p<0.008$ and $p<0.013$ (Fig. 2). Reduction of the volume of the limb in the treated group was minor compared to that shown in other studies in the literature. However, we must consider the specific characteristics of our study, acute edema, inflammation, immobility or reduced mobility, as

well as a short period of treatment, 3 weeks compared with 6-12 months of similar studies.

Furthermore, data of the evaluation of symptoms with VAS (28), after the treatment period, showed an important, although not significant, reduction in the treated group. Moreover, patients reported a strong compliance with the rehabilitative therapy especially concerning the reduction of secondary symptoms and an increased mobility of limb (Fig. 3). Symptoms such as burning, itching and pain are also due to other conditions that coexist in these patients, such as extensive inflammation and hematoma. Our study showed some limitations, the small size of population, the lack of a control group with placebo (not open), the short term of treatment and the absence of adequate follow-up. All these elements would have strengthened the results presented in this study.

In contrast, however, our data demonstrate the effectiveness of the preparation proposed, even at short term, in patients who presented a resistant edema due to reduced mobility or to the presence of extensive tissue inflammation. For these patients our treatment may represent a complementary therapy to the common rehabilitative program.

REFERENCES

1. ISL. The diagnosis and treatment of lymphedema. Lymphology 2009; 42:51-60.
2. Foldi M, Foldi E. Foldi's Textbook of Lymphology. Elsevier. San Francisco 2009.
3. Schmidt KR, Welter H, Pfeiffer KJ, Becker HM. Lymphangiographische Untersuchungen zum Extremitatenodem nach rekonstruktiven Gefabeingriffen im Femoropoplitealbereich. Fortschr Rontgenstr 1978; 128:94-202.
4. Serpel JW, Carne PW, Bailey M. Radical lymph node dissection for melanoma. ANZ J Surg 2003; 73:294-299.
5. Wernecke K, Heckemann R, Jakuboswki HD. Perienale Raumforderungen nach Nierentransplanation. Fortschr Rontgenstr 1982; 137:403-9.
6. Armer J, Fu MR, Wainstock JM, Zagar E, Jacobs LK. Lymphedema following breast cancer treatment including sentinel lymph node biopsy. Lymphology 2004; 37:73-91.
7. Golsham M, Martin WJ, Dowlatshahi K. Sentinel lymph node biopsy lowers the rate of lymphedema when compared with standartd axillary lymph node dissection. Am Surg 2003: 69:209-11.
8. Larger I, Guller U, Berclaz G, et al. Morbidity of sentinel lymph node biopsy (SLN) alone versus SLN and completion axillary lymph node dissection after breast cancer surgery: a prospective Swiss multicenter study on 659 patients. Ann Surg 2007; 245:452-61.
9. Schijven MP, Vingerhoets AJ, Rutten HJ, Nieuwenhuijeren GA, Roumen RM, Van Bussel ME, Voogd AC. Comparison of morbidity between axillary lymph node dissection and sentinel node biopsy. Eur J Surg Oncol 2003; 29:341-350.
10. Recht A, Houliahan MJ. Axillary Lymph nodes and breast cancer. Cancer 1995; 76:1491-512.
11. Boris M, Weindorf S, Lasinkski S. Persistence of lymphedema reduction after noninvasive complex lymphedea therapy. Oncology (Huntingt.) 1997; 11:99-109.
12. Casley-Smith JR, Casley-Smith JR. Modern treatment of lymphedema I: complex physical therapy: the first 200 Australian limbs. Australas J Dermatol 1992; 33:61-68.
13. Agus GB, Allegra C, Arpaia G, De Franciscis S, Gasbarro V. Malattie delle vene e dei Linfatici, Linee Guida del Collegio Italiano di Flebologia (revisione 2013). Acta Phlebologica 2013; 14(S1)2.
14. Mislin H. Die Wirkung von cumarin aus Melilotus officinalis auf die funktions des lymphangions. Arzn : Forsch (Drug Res)1971; 21:852-53.
15. Krajnovic P. Ricerche farmacologiche relative all'influenza di sostanze farmacologiche sulla circolazione linfatica. Artz Forsch.1969; 23:381.
16. Clement DL. Management of venous edema: Insights from an international task force. Angiology 2000; 51:13-17.
17. Knight KR, Khazanchi RK, Pederson WC, McCann JJ, Coe SA, O'brien BM. Coumarin and 7 hydroxycoumarin treatment of canine obstructive lymphoedema. Clinic Sci.1989; 77:69-76
18. Casley-Smith JR, Morgan RG, Piller NB. Treatmemt of lymphedema of the arms and the legs with 5,6-benzo-alpha-pyrone. N Engl J Med 1993; 329:1158-63

19. Casley-Smith JR, Casley–Smith JR. Modern treatment of lymphoedema, II: The benzopyrones. Autralas J Dermatol 1992; 33:69-74.
20. Desprez-Curely JP, Cluzan R, Pecking A. Benzopyrones and post mastectomy lymphedemas. Double-blind trial placebo versus sustained release coumarin with trioxyethylrutin. In Casley-Smith JR, Piller NB, eds. Progress in lymphology X Adelaide: Univ Adelaide Press 1985; 156-58.
21. Casley-Smith JR, Morgan RG, Piller NB. Treatment of lymphedema of the arms and legs with 5,6-benzo-alpha-pyrone. N Eng J Med 1993; 329:1158-63.
22. Burgos A, Alcaide A, Alcoba C, et al. Comparative study of the clinical efficacy of two different coumarin dosages in the managment of arm lymphedema after treatment for breast cancer. Lymphology 1999; 32:3-10.
23. Loprizi CL, Kugler JW, Sloan JA, et al. Lack of effect of coumarin in women with lymphedema after treatment for breast cancer. N Engl J Med 1999; 340(5):346-50.
24. Badger C, Preston N, Seers K, Mortimer P. Benzopyrones for reducing and controlling lymphoedema of the limbs. Cochrane Database Syst Rev 2004; (2):CD003140.
25. Casley-Smith JR, Casley-Smith JR. Frequency of coumarin hepatotoxicity. Med J Aust 1995; 162:391.
26. Michelini S, Campisi C, Failla A, Boccardo F, Moneta G. Combination treatment of lymphedema; our experiences. Minerva Cardioangiol1998; 46(10):395-6.
27. Campisi C, Boccardo F, Macciò A, Zilli A, Michelini S. Natural coumarins in lymphatic microsurgery. Lymphology 2002; 35:635-39.
28. Rodriguez CS. Pain measurement in the elderly: a review. Pain Manag Nurs 2001; 2:38-46.

OSTEOGENIC DIFFERENTIATION AND GENE EXPRESSION OF DENTAL PULP STEM CELLS UNDER LOW-LEVEL LASER IRRADIATION: A GOOD PROMISE FOR TISSUE ENGINEERING

A. BALLINI[1], F. MASTRANGELO[2], G. GASTALDI[2], L. TETTAMANTI[3], N. BUKVIC[4], S. CANTORE[1], T. COCCO[1], R. SAINI[5], A. DESIATE[6], E. GHERLONE[2] and S. SCACCO[1]

[1]Department of Basic Medical Sciences, Neuroscience and Sense Organs, University of Bari Aldo Moro Bari, Italy; [2]Unit of Dentistry, IRCCS San Raffaele Scientific Institute, Vita e Salute San Raffaele University, Milano, Italy; [3]Department of Periodontology and Oral Implantology, Rural Dental College Loni Maharashtra, India; [4]University Hospital Bari-Policlinics, Medical Genetics Unit Bari, Italy; [5]Department of Oral Science, Insubria University of Varese, Varese, Italy; [6]Department of Interdisciplinary Medicine, University of Bari Aldo Moro Bari, Italy.

Received September 18, 2015 – Accepted November 2, 2015

The effects of low-level laser therapy (LLLT) has been the focus of recent studies as being assumed responsible for promoting photostimulatory and photobiomodulatory effects *in vivo* and *in vitro,* increasing cell metabolism, improving cell regeneration and invoking an anti-inflammatory response. A positive effect of LLLT on the bone proliferation of some cell types has been observed, but little is known about its effect on dental pulp stem cells (DPSCs). Here, we accurately describe the technical procedure to isolate mesenchymal DPSCs, and assay their osteogenic capacity when irradiated with an LLLT source. These preliminary results show that LLLT irradiation influences the *in vitro* proliferation of DPSCs and increases the expression of essential proteins for bone formation, although it is necessary to carry out further experiments on other cell types and to uniform the methodological designs.

Biostimulation of human tissues through low-level laser therapy (LLLT) is currently used in medicine in wound healing therapy (1). Several experimental studies *in vivo* and *in vitro* showed that LLLT enhances healing processes (2-5) and regeneration of nerves (6), increases collagen synthesis, expression of procollagen type I and II mRNA (7) and the formation of new capillaries, modulates inflammation and relieves pain (8). The additional calcium transported into the cytoplasm is believed to trigger mitosis and/or enhance cell proliferation (9). However, this stimulation is only achieved in a certain dosage range: too low dosage does not determine any effect and a too high dosage is less effective, while a much too high dosage can lead to inhibitory effects (10). In particular, stimulation of osteoblast proliferation, is of great clinical interest in the regeneration of lost bone (11), particularly for bony defects around dental elements and implants.

In 1995, Barushka et al. (12) reported the use of LLLT to promote bone repair. They showed that LLLT could induce osteoblastic activity and bone

Keywords: dental pulp stem cells, low level laser therapy, RUNX2, osterix, osteoblasts,

Mailing address: Prof. Filiberto Mastrangelo,
Unit of Dentistry,
IRCCS San Raffaele Scientific Institute,
Vita e Salute San Raffaele University,
Via Olgettina,60,
20132 Milano, Italy
e-mail: filibertomastrangelo@hotmail.com

0393-974X (2015)

repair at the site of injury. *In vitro* observation on bone showed that LLLT modulates inflammation (13), enhances the osteogenic differentiation of murine mesenchymal stem cells (14), significantly increases cellular proliferation and healing (15), and bone nodule formation and alkaline phosphatase (ALP) activity (16). In addition, *in vivo* studies on bone regeneration after LLLT treatment showed increased bone deposition after tooth extraction, suggesting enhancing effects of LLLT on ossification (17).

Stem cell research goes far beyond the scientific and therapeutic potential of regenerative medicine (18). Dental Pulp Stem Cells (DPSC) are a heterogeneous population of cells that exhibit some characteristics of bone marrow mesenchymal stem cells (BMMSCs), including the production of fibroblast-like cells that are clonogenic and have a high proliferation rate (19). Furthermore, when cultured under osteogenic conditions DPSCs are capable of forming organized mineral matrix nodules; these results differ from those of BMMSCs which form sparse nodules of calcium phosphate (20-22).

The biostimulatory effects of LLLT on stem cell precursors of osteoblast-like cells could reduce the timing of bony-integration of fixtures, also thanks to implant surface treatments that promote the attachment of these cells (23). The purpose of this experimental study was to evaluate the response to LLLT on DPSC cells, comparing, proliferation, differentiation and osteogenic potential of lasered versus non-lasered cultures.

MATERIALS AND METHODS

Patients and cell cultures

Human DPSCs were isolated and cultivated as reported in our previous study (19-20). Normal human third molar follicles were collected from healthy patients, aged 18-28 years, who underwent extractions for orthodontic reasons. This work was conducted according to the recommendations of the Declaration of Helsinki; all patients gave informed consent.

DPs were digested for 1 h at 37°C in agitation in a solution of 3 mg/ml type I collagenase plus 4 mg/ml dispase (Gibco Ltd., Uxbridge, UK). Single-cell suspensions were obtained by passing the cells through a 70-µm BD Falcon strainer (Falcon) (Becton & Dickinson, Sunnyvale, CA, USA).

After filtration, single cell suspensions were seeded in a 25 cm^2 culture flask and cultured with α-MEM supplemented with 5% fetal bovine serum (FBS), 100 U/ml penicillin-G, 100 µg/ml streptomycin and 0.25 µg/ml fungizone (Gibco Limited, Uxbridge, United Kingdom). The flasks were incubated at 37°C with 5% CO_2 and the medium was changed every 3 days. In order to study DPSCs proliferation rate, 2 x 10^5 cells were plated in a six well plate, detached and counted after 3, 5 and 7 days of culture (Fig. 1).

For the induction of osteoblastic differentiation, cells were grown in an osteogenic medium consisting of α-MEM supplemented with 2% FBS, 10^{-8} M dexamethasone and 50 µg/ml ascorbic acid (Sigma Aldrich, Milan, Italy).

Cellular phenotyping by alkaline phosphatase staining

Identification of the cellular population as osteoblasts was performed before starting all experiments.

The staining for the alkaline phosphatase activity (ALP) was used as an early marker of the osteoblastic character of emerged cells before and after growing them in a differentiating medium. Emerged cells were pooled in a single suspension and seeded in 6-well plates at a density of 100,000 cells/plate. The day of medium replacement was considered as day zero. ALP activity was evaluated at day zero and after 5 and 10 days of growth in the differentiation medium. At each time cells were fixed and incubated for 30 minutes in Tris buffer 0.2 M, pH 8.3 with AS-MX phosphate as a substrate and Fast Blue as a stain (Sigma, St.Louis, MO, USA). The ALP positive cells were blue/purple stained. All experiments were conducted in triplicate.

Synthesis of nodes of mineralized matrix

For the evaluation of DPSCs' ability to form mineralized nodules *in vitro,* they were cultured them for 30 days in the osteogenic medium supplemented with 10 mM β -glycerophosphate (Sigma Aldrich, Milan, Italy) and for 5 weeks to stimulate matrix synthesis and nodes of mineralization deposition. The osteogenic medium was changed twice a week and after 5 weeks of treatment, cells were stained according to Von Kossa protocol (24). Briefly, cells were fixed in a solution of 2% paraformaldehyde, 2% sucrose for 10 minutes, washed 3 times with distilled water and stained with a 5% solution of AgNO3. The staining consisted of 30 minutes incubation at room temperature in the dark and 3 rinses with distilled water followed by an exposition to artificial intense light for 1 hour. Pictures were acquired using a digital camera connected to Axiovert 200 Inverted Fluorescence Microscope and analyzed. All experiments were conducted in triplicate.

RNA extraction and qPCR

RNA was isolated from cells at confluence according to TRIzol technology and reverse transcribed by using RevertAid™ M-MuLV Reverse Transcriptase enzyme (Fermentas). The expression of RUNX-2 (NM_004348) and OSTERIX (NM_152860) genes was evaluated on cDNAs from cultures at day zero, and after 3, 6 and 12 hours in differentiation medium referring expression data to GAPDH as housekeeping gene using a TaqMan assay. Probes for OSTERIX (Osx: Hs00541729_m1), RUNX-2 (Runx-2: Hs00231692_m1) and GAPDH [TaqMan® GAPDH Control Reagents (Human)] were purchased from Applied Biosystem.

Oxygen consumption

The respiratory activity was measured polarographically in 75 mM sucrose, 5 mM KH2PO4, 40 mM KCl, 0.5 mM EDTA, 3 mM MgCl2, 30 mM Tris-HCl, pH 7.4 buffer with a Clark-type oxygen electrode at 37°C. After endogenous oxygen consumption measurement, mitochondrial respiration was uncoupled with CCCP (0.2 µM) (Carbonyl cyanide-m-chloro-phenyl-hydrazone) and cells digitonized (20µg/106cells) for measurement of succinate (5 mM) and ascorbate (10 mM)/TMPD (0.4 mM) dependent respiration. All experiments were conducted in triplicate.

Biostimulation

The irradiation procedure was performed with a diode laser device (5 WATT, DEKA-Italy) using a 980 µm optical fiber to irradiate the whole culture dish, positioned at 1 cm distance from cell layer. Cells underwent a single 60 seconds exposure to a 980 nm continuous wave with a power output of 0.1W and an irradiation dosage of 3 J/ cm2. Cellular phenotyping by alkaline phosphatase staining, cellular differentiation by alkaline phosphatase activity, synthesis of nodes of mineralized matrix, RNA extraction and qPCR were performed in parallel on primary DPSCs grouped in lasered and not-lasered cells.

Statistical analysis

Statistical analyses were performed for *in vitro* proliferation with the Statistical Package for the Social Sciences (spssx/pc) software (SPSS, Chicago, IL, USA). The differences were evaluated by Student's *t*-Test. The results were considered statistically significant at $p<0.05$.

RESULTS

Microscopic examination was performed daily. After 2 weeks DPSCs reached confluence in the dish. The cells were stained for histochemical alkaline phosphatase (ALP) and were characterized as osteoblasts. Parallel experiments were conducted on lasered and non-lasered cultures in order to compare several parameters.

DPSCs irradiated by LLLT express higher levels of ALP

The histochemical staining was performed on lasered and non-lasered cultures, showing greater expression agents in DPSCs treated with laser compared with control cultures which resulted more evident during differentiation.

DPSCs irradiated by LLLT are more efficient in forming bone mineral matrix nodules

In order to evaluate the capacity of the synthesis of bone mineral matrix nodules, at confluence the cells were stimulated to produce and to mineralize the matrix. Both lasered and non-lasered cultures formed mineral matrix nodules. The specific staining confirmed that the lasered cell protocol was more efficient than in the controls. With the image analyzer we quantified the percentage of the area mineralized: it resulted as 85±1 in cells treated with LLLT compared with 44±2 in the control cells (Fig. 2).

Down-regulation of RUNX-2 and OSTERIX in DPSCs in lasered cultures

To verify the effect of laser therapy on molecular expression of RUNX-2 and OSTERIX, the master genes of osteoblast differentiation, relative quantification analysis was performed by real-time PCR. The analysis showed that RUNX-2 gene expression was significantly down-regulated after laser stimulation compared to control cells. In particular, the down-regulation was significant after 3 hours from treatment and RNA levels continually decreased after 6 and 12 hours.

$2^{-\Delta\Delta Ct}$ values were < 0.5 at all times analysed, specifically RUNX-2 gene was significantly reduced after 3 hours and its levels reduced over time.

OSTERIX gene expression was comparable in treated and untreated cells after 3 hours of stimulation but its levels significantly decreased after 6 and 12 hours (Table I). OSTERIX is a RUNX-2 downstream gene and its transcription was consequently reduced by RUNX-2 down-regulation (Fig. 3A), and not by laser stimulation. In fact, OSTERIX expression was

Table I. *RUNX-2 and OSTERIX gene expression in treated and untreated cells after 3, 6 and 12 hours from LLLT stimulation-RT-PCR.*

RUNX2		**A**	**B**	**ΔCT_A**	**ΔCT_B**	**$2^{-\Delta\Delta CT}{}_{medi}$**
CTR	GAPDH	26.03	25.39	25.31	16.55	
	RUNX2	51.34	41.94			
TREATED						
3 h	GAPDH	25.63	25.57	25.61	21.04	ΔCT3H -ΔCTCTRL=0.004
	RUNX2	51.24	46.43			
6 h	GAPDH	25.32	26.44	28.71	21.40	ΔCT6H -ΔCTCTRL=0.034
	RUNX2	54.03	47.84			
12 h	GAPDH	25.85	26.57	28.86	23.38	ΔCT12H-ΔCTCTRL=0.008
	RUNX2	54.71	49.95			

OSTERIX		**A**	**B**	**ΔCT_A**	**ΔCT_B**	**$2^{-\Delta\Delta CT}{}_{medi}$**
CTR	GAPDH	21.53	21.21	26.50	28.27	
	OSX	48.03	49.48			
TREATED						
3 h	GAPDH	21.01	21.36	30.37	28.99	ΔCT3H -ΔCTCTRL=0.006
	OSX	51.38	50.35			
6 h	GAPDH	20.78	21.23	30.58	31.19	ΔCT6H -ΔCTCTRL=0.013
	OSX	51.36	52.42			
12 h	GAPDH	22.42	21.38	30.54	31.64	ΔCT12H-ΔCTCTRL=0.096
	OSX	52.96	53.02			

The value 2– ΔΔCT compared with benchmarks: ≤ 0.5: down-regulated gene ≥ 1.5: up-regulated gene

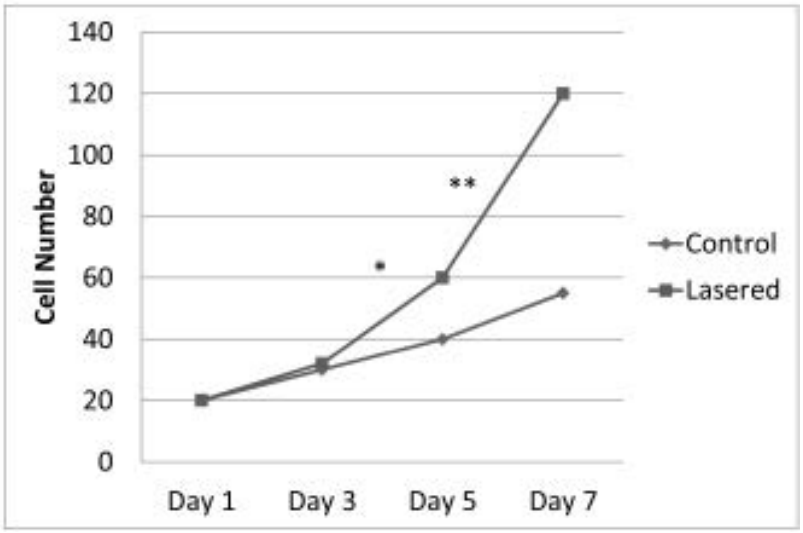

Fig. 1. *DpSC proliferation in vitro. Proliferation of DPSC (lasered vs control) after three, five and seven days of culture. Significant differences were evaluated by student's t-test and indicated as: (*) P<0.01; (**) P<0.001.*

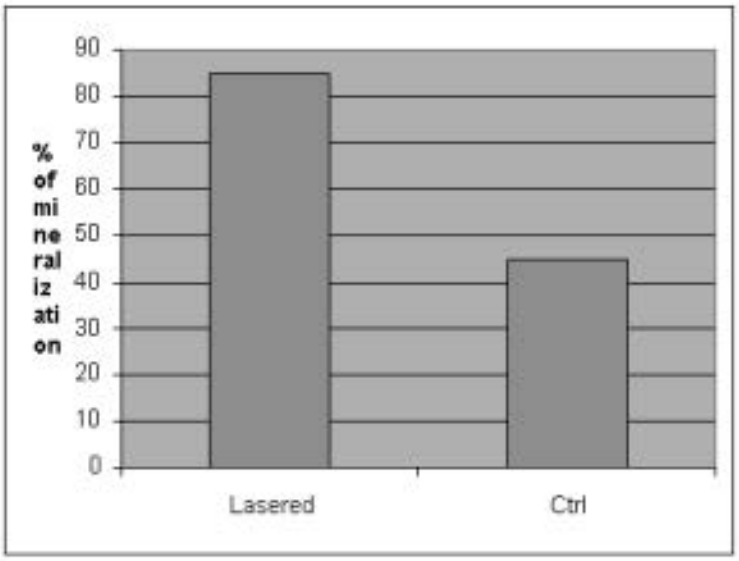

Fig. 2. *ALP expression. The values represented are expressed as a percentage of the total mineralized area in DPSC (lasered vs controls) cell cultures.*

not reduced at the same time as RUNX-2 (Fig. 3-B). These results seem to be in contrast with osteoblast promoting differentiation by laser stimulation but it is significant to analyse RUNX-2 function in osteoblast growth and differentiation. The bone specific expression of RUNX-2 is regulated during the cell cycle, in fact RUNX-2 levels are inversely linked to cell growth and S/G2/M phase progression.

Our results showed that LLLT stimulation initially promotes DP cell proliferation that provokes a down-regulation in osteoblast differentiation but this inhibition is temporarily limited. RUNX-

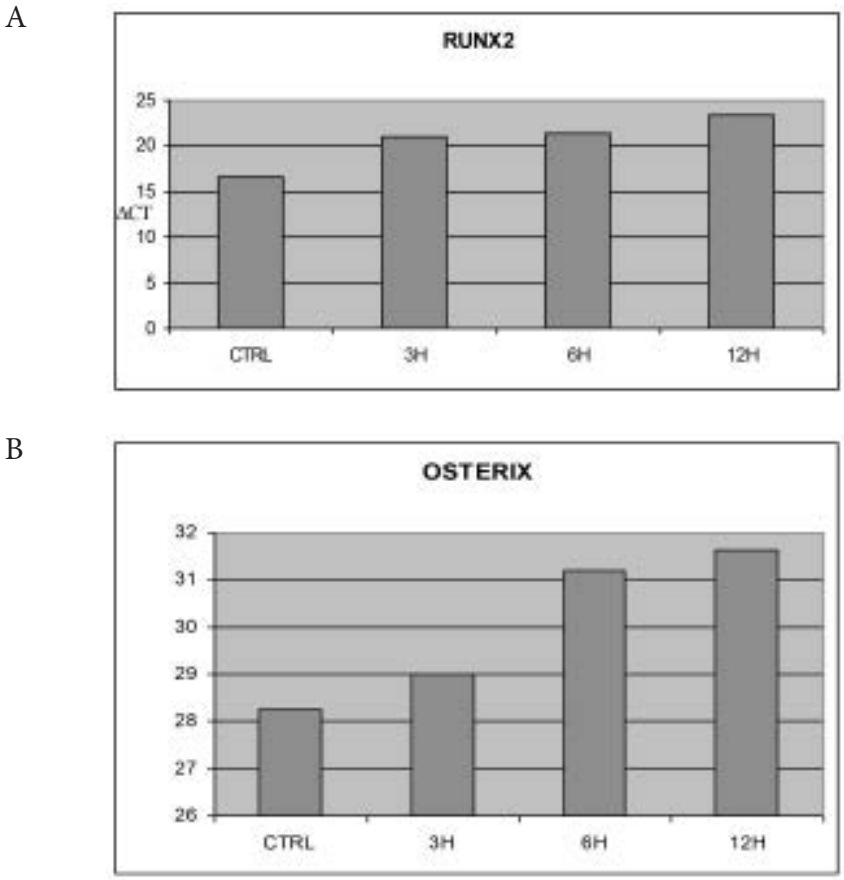

Fig. 3. ***A, B****) RUNX-2 and OSTERIX expression at day zero and after 3, 6 and 12 hours. Real Time-PCR analysis from RNA isolated from cell cultures showing at day zero, and after 3, 6 and 12 hours a down regulation of RUNX-2 (A). OSTERIX expression was not reduced at the same time as RUNX-2 (B).*

2 expression is only reduced and not abrogated so that the maintenance of minimal RUNX-2 levels probably promotes the consequent exit from the cell cycle and the increase of cell differentiation.

The final effect of laser stimulation is an increase of cell number and expansion of osteoblast-like cells from DPSCs cultures.

As evidenced by the above data, it was observed that the expression of the two genes, particularly RUNX-2, is positively influenced by the differential stimulus with a peak of expression of RUNX-2 after one week, followed by a subsequent decrease (Fig. 4 A-B).

LLLT induces a greater number of cells to enter the G2 phase of cellular cycle

The cytofluorimetric analysis of the cellular cycle showed that, compared to controls, a single laser stimulation induces changes in cell turnover. Also a higher percentage of cells coming into the G2 phase of the cell cycle was observed. (Fig. 5 A-B-C).

DISCUSSION

Recently, we have assisted in the spread of new techniques for regenerative surgery and laser sources in medical practice, especially in dentistry (23, 25-28). The use of mesenchymal stem cells derived from dental tissues, which are easy to access for dentists and oral surgeons, with their high proliferation features and capacity to differentiate into osteoblasts, offers a great potential for the future of clinical dentistry (29, 30).

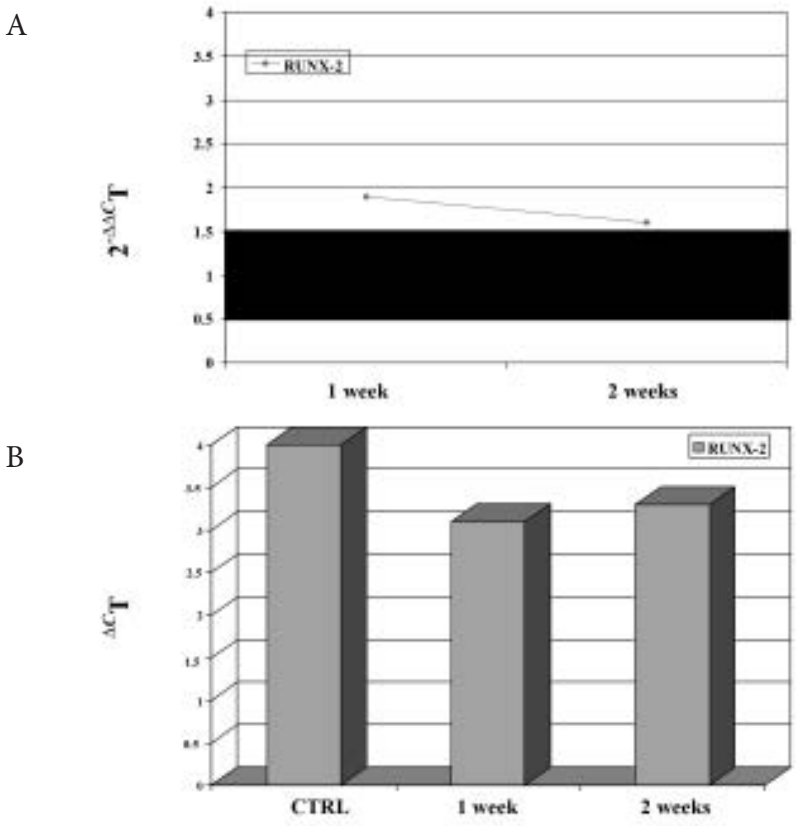

Fig. 4. ***A, B****) RUNX-2 expression AT 1 and 2 weeks. RUNX-2, is positively influenced by the differential stimulus with a peak of expression of RUNX-2 after one week, followed by a subsequent decrease.*

The ability of DPSCs to differentiate into osteoblasts is certain: once they are cultured in osteogenic induction medium, several clusters of cells adhere, assume an osteoblast-like morphology and express the typical osteoblastic markers such as ALP and Coll I (19, 20). Moreover DPSCs form mineralized matrix nodules showing a mature osteoblast exclusive feature (30). In this scenario, LLLT-DPSCs have to be considered ideal stem cells to be used for tissue engineering since they are characterized by a high proliferation rate, multidifferentiation ability, easy accessibility, high viability, opportunity to be safely cryopreserved and the expression of mesenchymal markers.

In our study, both lasered and non-lasered cultures showed good growth activities during the entire observation period and it should be noted that the application of laser irradiation did not cause cell damage. In the treated cultures in respect to the control group, it was possible to observe an increase of proliferation through the use of a marker of osteoblasts, the alkaline phosphatase, an early marker of osteoblast differentiation (16, 23).

The increase of alkaline phosphatase was more significant at 5 and 10 days of differentiation. We also demonstrated an increase in forming bone mineral matrix nodules. In all the experiments RT-PCR showed a down-regulation of RUNX-2 (gene that codifies for a transcription factor that promotes maturation and cellular differentiation), index of differentiation and stop of progression of the cellular cycle in G1 phase (proliferation), with an increase

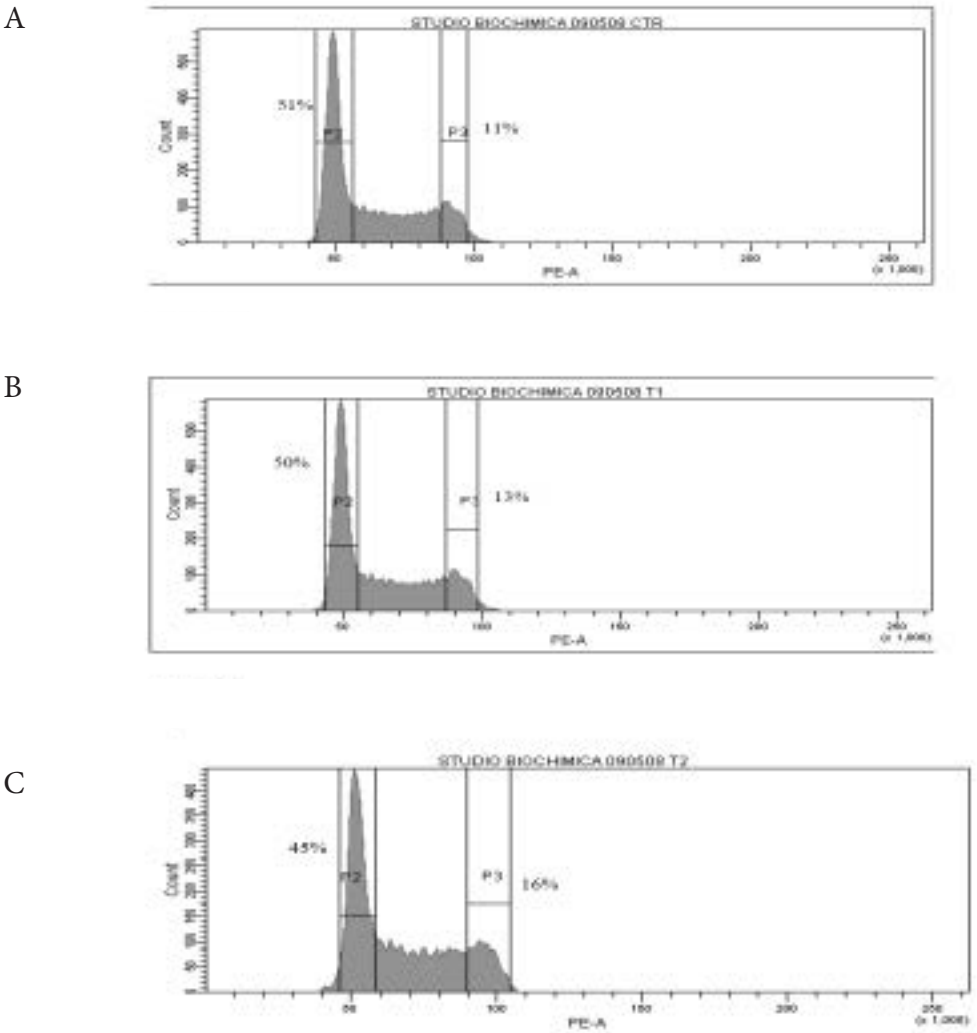

Fig. 5. *Cell cycle study. Cytofluorometry analysis of cell cycle showed that, compared to the control, a single laser stimulation induces changes in cell turnover so that a greater percentage of Osteoblasts enters the cell cycle G2 phase.* ***A****) CTRL;* ***B****) lasered t1;* ***C****) lasered t2.*

in lasered DPSCs at 12 hours. OSTERIX showed the same expression, being RUNX-2 transcribed upstream of OSTERIX.

In confirmation of previous data (23), after a single stimulation with LLLT in the culture with differential medium for one and two weeks, we observed that the two genes, particularly RUNX-2, were positively influenced by the differentiation process, with a peak of expression of RUNX-2 at one week, followed by a subsequent decrease, suggesting the requirement of a weekly laser stimulation to obtain a meaningful result both *in vitro* and *in vivo* (13).

The results of cytofluorimetric analysis of cellular cycle underlined that, compared to controls, a single laser stimulation induces changes in cell turnover so that a greater percentage of osteoblasts from DPSCs enters the G2 phase of the cellular cycle, expression of an increasing of proliferation (23). At the most basic level, LLLT acts by inducing a photochemical reaction in the cell, a process referred to as biostimulation or photobiomodulation (12). Within the cell, there is strong evidence to

suggest that LLLT acts on the mitochondria to increase adenosine triphosphate (ATP) production, modulation of reactive oxygen species (ROS), and the induction of transcription factors (9). Several transcription factors are regulated by changes in the cellular redox state. Among them redox factor-1 (45) dependent activator protein-1 (AP-1) (a heterodimer of c-Fos and c-Jun), nuclear factor kappa B (NF-κB), p53, activating transcription factor/cAMP-response element–binding protein (ATF/CREB), hypoxia-inducible factor (HIF)-1, and HIF-like factor (15). These transcription factors then cause protein synthesis that triggers further effects down-stream, such as increased cell proliferation and migration, modulation in the levels of cytokines, growth factors and inflammatory mediators, and increased tissue oxygenation.

Stimulatory effects of LLLT on bone formation have been reported, but the regulatory mechanisms involved are unclear. In a previous study we also reported stimulatory effects of bone formation by LLLT, with increased cellular proliferation, ALP activity, and Ca accumulation using a quantitative bone nodule formation assay (23). These results suggest that LLLT stimulates both proliferation and differentiation of osteoblastic cells *in vitro*, resulting in enhanced bone formation.

The RUNX-2 independent pathway, which is partly regulated by OSTERIX, could be necessary but not sufficient for osteogenesis *in vivo*. In other words, as reported by other authors (13), both RUNX-2 -dependent and -independent pathways could be required for bone formation.

In conclusion, association between laser-mediated photobiostimulation on dental stem cells, due to osteoblast differentiation, increasing the processes of growth and proliferation of these cells, could further reduce bone integration timing in dental practice. Moreover DPSCs could be used for bone regeneration of the stomatognathic and other systems, and represent an excellent cell source for tissue engineering therapy.

REFERENCES

1. Loreti EH1, Pascoal VL, Nogueira BV, Silva IV, Pedrosa DF. Use of laser therapy in the healing process: a literature review. Photomed Laser Surg 2015; 33:104-16.
2. Chung H, Dai T, Sharma SK, Huang Y, Carroll JD, Hamblin MR The nuts and bolts of low-level laser (light) therapy. Ann Biomed Eng. 2012; 40: 516-33.
3. Pinheiro AL, Pozza DH, Oliveira MG, Weissmann R, Ramalho LM. Polarized light (400-2000 nm) and non-ablative laser (685 nm): a description of the wound healing process using immunohistochemical analysis. Photomed Laser Surg 2005; 23:485-92.
4. Posten W, Wrone DA, Dover JS, Arndt KA, Silapunt S, Alam M. Low-level laser therapy for wound healing: mechanism and efficacy. Dermatol Surg 2005; 31:334-40.
5. Herascu N, Velciu B, Calin M, Savastru D, Talianu C. Low level laser therapy (LLLT) efficacy in post-operative wounds. Photomed Laser Surg 2005; 23:70-73.
6. Miloro M, Halkias, LE, Mallery S. Low-level laser effect on neural regeneration in gore-tex tubes. Oral Surg Oral Med Oral Pathol Oral Radiol Endod 2002; 93:27-31.
7. Saperia D, Glassberg E, Lyons AF, Abergel RP, Dwyer RM, Uitto J. Demonstration of elevated type I and type III procollagen mRNA levels in cutaneous wounds treated with Helium-Neon laser. Proposed mechanism for enhanced wound healing. Biochem Biophys Res Commun 1986; 138:1123-28.
8. Kemmotsu O, Sato K, Furomido H, Harada K, Takigawa C, Kaseno S. Efficacy of low reactive level laser therapy for pain attenuation of postherpetic neuralgia. Laser Ther 1991; 3:1-75.
9. Karu T. Photobiology of low-power laser effects. Health Phys 1989; 56:691-704.
10. Sattayut S, Hughes F, Bradly P. 820 nm gallium aluminium arsenide laser modulation of prostaglandin E2 production in interleukin-1 stimulated myoblasts. Laser Ther 1999; 11:88-95.
11. Nissan J, Assif D, Gross MD, Yaffe A, Binderman I. Effect of low intensity laser irradiation on surgically created bony defects in rats. J Oral Rehabil 2006; 33:619-24.
12. Barushka O, Yaakobi T, Oron U. Effect of low-energy laser irradiation on the process of bone repair in the rat tibia. Bone 1995; 16:47-51.
13. Matsubara T, Kida K, Yamaguchi A, et al. BMP2 regulates Osterix through Msx2 and Runx2 during

osteoblast differentiation. J Biol Chem 2008; 283:29119-25.
14. Abramovitch-Gottlib L, Gross T, Naveh D, Geresh S, Rosenwaks S, Bar I, Vago R. Low level laser irradiation stimulates osteogenic phenotype of mesenchymal stem cells seeded on a three dimensional biomatrix. Lasers Med Sci 2005; 20:138-46.
15. Chen AC-H, Arany PR, Huang Y-Y, Tomkinson EM, Saleem T, Yull FE, Blackwell TS, Hamblin MR. Low level laser therapy activates NF-κB via generation of reactive oxygen species in mouse embryonic fibroblasts. Proc SPIE 2009;7165:71650-59.
16. Haxsen V, Schikora D, Sommer U, Remppis A, Greten J, Kasperk C. Relevance of laser irradiance threshold in the induction of alkaline phosphatase in human osteoblast cultures. Lasers Med Sci 2008; 23:381-84.
17. Takeda Y. Irradiation effect of low-energy laser on alveolar bone after tooth extraction: experimental study in rats. Int J Oral Maxillofac Surg 1988; 17:388-91.
18. Giorgini E, Conti C, Ferraris P, Sabbatini S, Tosi G, Centonze M, Grano M, Mori G. FT-IR microscopic analysis on human dental pulp stem cells. Vibrat Spectrosc 2011; 57:30-34.
19. Mori G, Centonze M, Brunetti G, et al. Osteogenic properties of human dental pulp stem cells. J Biol Regul Homeost Agents 2010; 24:167-174.
20. Mori G, Brunetti G, Oranger A, et al. Dental pulp stem cells: osteogenic differentiation and gene expression. Ann N Y Acad Sci 2011; 1237:47-52.
21. Quaranta N, Buccoliero C, De Luca C, Mori G, Brunetti G, Colucci S, Colaianni G, Grano M. The effects of bone pâté on human osteoblasts cell cultures. Eur Arch Otorhinolaryngol 2015. [Epub ahead of print].
22. Mori G, D'Amelio P, Faccio R, Brunetti G. Bone-immune cell crosstalk: bone diseases. J Immunol Res 2015; 2015:108451.
23. Grassi FR, Ciccolella F, D'Apolito G, et al. Effect of low-level laser irradiation on osteoblast proliferation and bone formation. J Biol Regul Homeost Agents 2011; 25:603-14.
24. Puchtler H, Meloan SN. Demonstration of phosphates in calcium deposits: a modification of von Kossa's reaction. Histochemistry 1978; 56:177-85.
25. Ballini A, Cantore S, Capodiferro S, Grassi FR. Esterified hyaluronic acid and autologous bone in the surgical correction of the infra-bone defects. Int J Med Sci 2009; 6:65-71.
26. Ballini A, Capodiferro S, Toia M, Cantore S, Favia G, De Frenza G, Grassi FR. Evidence-based dentistry: what's new?. Int J Med Sci 2007; 6:174-8.
27. Brunetti G, Oranger A, Carbone C, et al. Osteoblasts Display Different Responsiveness to TRAIL-Induced Apoptosis During Their Differentiation Process. Cell Biochem Biophys 2013; 67:1127-36.
28. Scattarella A, Ballini A, Grassi FR, et al Treatment of oroantral fistula with autologous bone graft and application of a non-reabsorbable membrane. Int J Med Sci 2010; 7:267-71.
29. Mori G, Ballini A, Carbone C, et al. Osteogenic differentiation of dental follicle stem cells. Int J Med Sci 2012; 9:480-7.
30. Ballini A, De Frenza G, Cantore S, Papa F, Grano M, Mastrangelo F, Tetè S, Grassi FR. *In vitro* stem cell cultures from human dental pulp and periodontal ligament: new prospects in dentistry. Int J Immunopathol Pharmacol 2007; 20:9-16.

LETTER TO THE EDITOR

THE PROFILE OF MELATONIN RECEPTORS GENE EXPRESSION AND GENES ASSOCIATED WITH THEIR ACTIVITY IN COLORECTAL CANCER: A PRELIMINARY REPORT

E. ZIÓŁKO[1], T. KOKOT[1], A. SKUBIS[2], B. SIKORA[2], J. SZOTA-CZYŻ[2], C. KRUSZNIEWSKA-RAJS[2], J. WIERZGOŃ[3], U. MAZUREK[2], E. GROCHOWSKA-NIEDWOROK[4] and M. MUC-WIERZGOŃ[1]

[1]School of Public Health in Bytom, Silesian Medical University, Department of Internal Medicine, Poland; [2]Department of Molecular Biology, School of Pharmacy with the Division of Laboratory Medicine in Sosnowiec, Silesian Medical University, Poland; [3]Department of Oncologic and Reconstructive Surgery Gliwice, Maria Sklodowska-Curie Memorial Cancer Center and Institute of Oncology, Poland; [4]Department of Human Nutrition, School of Public Health, Silesian Medical University, Poland

Received May, 25, 2015 – Accepted August 5, 2015

The antiproliferative and immunomodulatory effects of melatonin (MLT) have been demonstrated in a variety of neoplasms including colorectal cancer (CRC). In humans and other mammals, MLT acts on target tissues through membrane and retinoid nuclear receptors. The aim of this study was to evaluate transcription activity of melatonin receptors and genes associated with regulation of their activity in colorectal adenocarcinoma tissues in relation to clinical stage of cancer. A total of 24 pairs of surgically removed tumoral and healthy (marginal) tissue samples from colorectal cancer patients at clinical stages I-II and III-IV were collected. As an additional control, twenty normal samples were taken from people whose large intestine tissues were reported as non-tumoral after colonoscopy. Expression of mRNA genes was studied by microarray HG-U133A analysis. The analysis of gene expression profile was performed using commercially available oligonucleotide microarrays of HG-U133A. High increase of MT1 mRNA expression levels in all cancerous samples *vs* non-cancerous tissues was observed. The MT2 mRNA expression levels increased slightly in marginal and malignant samples. Among the genes participating in the cascade of signal transfer in cells activated by MLT via melatonin receptors, we found encoding genes (GNA11, OXTR, TPH1) only for differentiating stage III - IV of CRC. Monitoring the expression levels of genes that are related to melatonin receptors may offer a strategy to anticipate tumour development and estimate the molecular changes that occur during carcinogenesis. The mechanism behind this association needs further elucidation.

Several years of research into the association between the initiation of carcinogenesis and the presence of melatonin suggest the possibility of using melatonin for tumour prevention (1). The activity of melatonin

Key words: melatonin, receptors, gene expression, colorectal cancer

Mailing address: Prof. Małgorzata Muc-Wierzgoń,
School of Public Health in Bytom,
Silesian Medical University,
Dept. of Internal Medicine, Żeromskiego 7 st,
41-902 Bytom 41-902, Poland
Tel./fax +48/32 2812122
e-mail: mwierzgon@sum.edu.pl

0393-974X (2015)

DISCLOSURE: ALL AUTHORS REPORT NO CONFLICTS OF INTEREST RELEVANT TO THIS ARTICLE.

in suppressing tumour development is based on its inhibition of processes such as tumour transformation, angiogenesis, and metastasis (2-3). The antiproliferative and immunomodulatory effects of melatonin have been investigated in various types of neoplasms including melanoma, breast, prostate, ovarian, hepatocellular, pancreatic, biliary and colorectal cancer (4-5). In humans and other mammals, two G-protein-bound specific high affinity receptors, named MT1 and MT2 (encoded by MTNR1A, MTNR1B, respectively) mediate most of the melatonin physiological and pharmacological actions (5). These subtypes are 60% homologous at the amino-acid level. These receptors can be pharmacological goals for regulation of immune and endocrine functions, anti-cancer activity, circadian rhythm, cardiovascular physiology, aging (5, 6). Besides, as a lipophilic molecule, melatonin easily diffuses through the cell membrane, and it binds to nuclear receptors (Retinoid Z Receptors 7/Retinoid Orphan Receptors) subfamilies with three subtypes (α, β, γ) (7).

In gastrointestinal tract, melatonin is produced locally by serotonin-rich enterochromaffin (EC) cells of the mucosa and submucosa of the human jejunum and colon (8). Its concentrations can be 10- to 100-fold higher in the intestine than in serum and depends on food intake and digestion. MT1 and MT2 receptors have been identified in the intestinal epithelium, vessel, submucosal and myenteric plexus of the human colon (5, 7, 8, 9). Compared to MT1, the expression of MT2 receptors is not affected by food intake. Numerous basic and clinical studies have focused on the role of MLT and its receptors in prevention, diagnosis and treatment of colorectal cancer (1, 4, 5, 7-10).

In the present study, we studied the difference in melatonin receptor gene expression and genes associated with regulation of their activity in colorectal adenocarcinoma tissues in relation to clinical stage of cancer.

MATERIALS AND METHODS

Tissue sampling

A total of 24 pairs of surgically removed tumoral and healthy (marginal) tissues samples from colorectal cancer patients at clinical stages I-II and III-IV were collected. The patients were aged between 55-71 years and had not received any chemotherapy or radiotherapy treatment. As second control, twenty normal samples were taken from subjects whose large intestine tissues were reported as non-tumoral after colonoscopy. Healthy control tissue specimens (marked K2) were obtained from an area 10 mm outside of the histologically negative margin. As second control, ten normal samples (marked K1) were taken from subjects whose large intestine tissues were reported as non-tumoral after colonoscopy. The tumor specimens were divided into two groups according to the 7th edition of the AJCC/UICC staging system of CRC: stages I and II (marked LGC) and stages III and IV (marked HGC) - (11). Samples were placed in RNA later reagents and stored at – 80°C.

The study protocol was approved by the Bioethics Committee of the Medical University of Silesia (KNW/0022/KB1/42/14), and informed consent was obtained from all patients.

Methods

The isolation of RNA from CRC and normal tissues (Invitrogen Life Technologies, USA) and its subsequent molecular analysis (Gene Expression Analysis Technical Manual procedures) were performed according to the manufacturer's instructions. Microarray data analysis was performed using the GeneSpring 11.5 platform (Agilent Technologies UK Limited, South Queensferry, UK) and Significance Analysis of Microarrays (SAM).

Differentially expressed genes were identified in LGC and HGC specimens compared to the expression patterns of the two controls (K1 and K2, respectively). Differences in gene expression were evaluated using univariate analysis of variance ANOVA and Tukey's post-hoc multiple comparisons test, both with Benjamini-Hochberg correction. Following this, a Venn diagram was created to show the logical relationships between the groups of differentially expressed genes that were analysed.

RESULTS

Comparison analysis was carried out of the transcriptomes that were identified by microarray (Affymetrix. Out of the collection of 22 283 ID mRNA that were located on the HG-U133A microarray, 66 ID mRNA were selected using the NetAffxTM database. Selected transcriptomes contained genes that encoded melatonin membrane receptors and were associated with the regulation of their activity.

The profiling analysis identified differences in MT1 and MT2 gene expression levels between each of the groups as illustrated in Fig. 1. Expression of MT1 mRNA was the lowest in normal samples (K1),

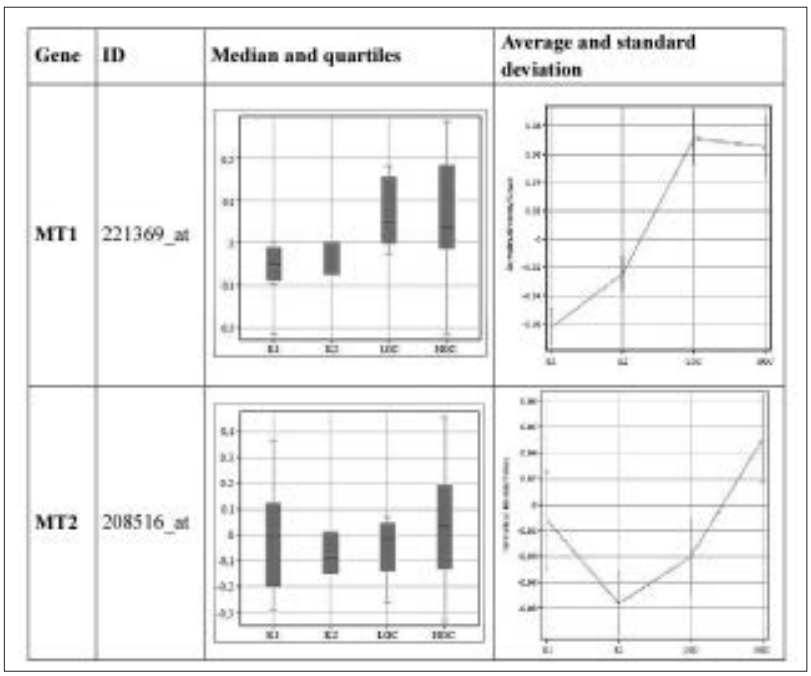

Fig. 1. *Comparison of MT1 and MT2 gene expression levels in colorectal cancer tissues (LGC and HGC) and two control groups (K1, K2).*

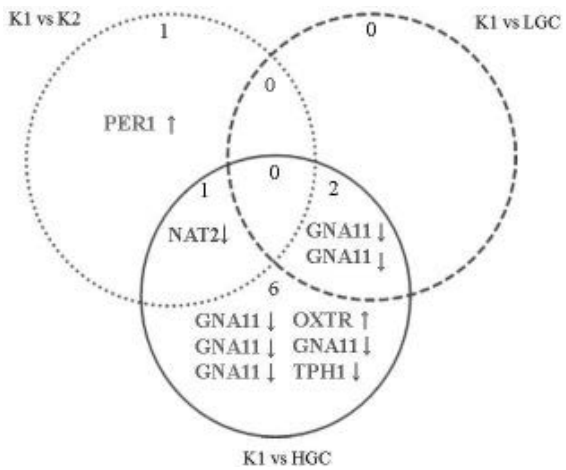

Fig. 2. *Venn diagram indicating the specificity of mRNA genes in relation to the different transcriptomes (LGC, HGC, K1,K2). Results were based on mRNA ID profiles that were selected by post-hoc analysis using Tukey's post-hoc multiple comparison test with Benjamini-Hochberg correction.*

increasing linearly in K2 and LGC specimens. The highest signal of the MT1 transcript was found in samples from patients at clinical stages I-II (LGC). The MT2 mRNA expression increased slightly from K2 to HGC samples. Analysing two control groups only, we observed the high expression of MT2 mRNA in normal tissues (K1) which decreased in marginal samples (K2).

To determine statistically significant differences in gene expression, one-way ANOVA was conducted

Table I. *Differential genes associated with the activity melatonin membrane receptors expression in colorectal adenocarcinomas samples (LGC and HGC), marginal (K2) and normal tissues (K1).*

Trancriptomes groups	mRNA				
	Number	ID	Gene	P value	Expression
K2 *vs* K1	1	36829_at	PER1	6.231329E-4	↑
K2 *vs* K1 LGC *vs* K1	1	206797_at	NAT2	5.652934E-6	↓
HGC *vs* K1	6	40562_at	GNA11	4.6385213E-4	↓
		564_at	GNA11	2.465538E-5	↓
		204248_at	GNA11	2.8779446E-5	↓
		206825_at	OXTR	0.0010466689	↑
		213766_x_at	GNA11	9.252449E-6	↓
		214601_at	TPH1	0.0058652	↓
LGC *vs* K1 HGC *vs* K1	2	213944_x_at	GNA11	8.1121715E-7	↓
		214679_x_at	GNA11	1.323198E-7	↓
LGC *vs* K1	0	-	-	-	-
LGC *vs* K1 HGC vs K1 K2 *vs* K1	0	-	-	-	-

with Benjamini-Hochberg correction. P-values of less than 0.05 were considered significant. A total of 10 genes were revealed that could be used to distinguish the groups. The number of differentiable genes decreased at lower p-values. Tukey's post-hoc analysis test was used to identify differences in gene expression between individual groups (Table I, Fig. 2). Based on the above results, it can be concluded that none of the genes were present in any of the experimental groups. There were six genes that had differentiable levels of expression between HGC versus the control: GNA11, OXTR, and TPH1 genes.

DISCUSSION

In our study, we found a high increase of MT1 mRNA expression levels in all cancerous samples *vs* non-cancerous tissues. The MT2 mRNA expression levels increased slightly in marginal and malignant samples. These findings are similar or opposed to the results of some studies (12-15). Karasek et al. in 2002 (12) demonstrated the expression of mRNA

encoding of both MT1 and MT2 melatonin receptors in colon 38 cancer cells. The significant decrease of MT1 mRNA expression levels in cancerous *vs* non-cancerous tissues observed by Nemeth et al. (15) assessed MT1 transcript levels with RT-PCR in colon adenocarcinomas and normal colonic mucosa of 39 patients. The Authors suggested that hormonal factors and organ differences may play an important role in the activity of MT1 gene expression.

The study group showed large differences in terms of age, gender, clinical status (comorbidities, medications, diet etc.), nutritional status, type of work (shift system) (17). All summarized factors affect the activity of the melatonergic system (16). Furthermore, the microenvironmental regulation of colorectal cancer growth, invasion and metastasis play an important role in melatonin receptor expression (7, 8, 12, 13). Several reports have shown that the genetic variation of the melatonin receptor type 1B gene (SNP- single nucleotide polymorphism) is associated with fasting glucose and type 2 diabetes (18, 19), and the carbohydrate disorders, overweight, obesity, are important metabolic risk factors for colorectal cancer (20). Perhaps in patients with colorectal cancer coexisting with overweight/obesity and glucose intolerance there is also a single nucleotide polymorphism described in/or other as yet unknown genetic variations in one or two MLT receptors.

At the same time, our study showed that among the genes participating in the cascade of signal transfer in cells activated by MLT via melatonin receptors, we found encoding genes (GNA11, OXTR, TPH1) only for differentiating stage III - IV of CRC.High stage colorectal cancer is distinguished by a decreased expression of the GNA11 and TPH1 genes. GNA 11, one of genes of melatonin signal transmitters, encodes Gαq, a member of the q class of G-protein alpha-subunits which are involved in mediating signals between G-protein-coupled receptors (GPCRs) and downstream effectors (21). Mutations of GNA11 lead to changes in the mitogen-activated protein kinases (MAPK) signaling pathway, which results in the development of malignant tumour cells and a disruption of apoptosis, leading to unlimited cell proliferation. TPH1 encodes the tryptophan hydroxylase enzyme. This enzyme transforms tryptophan into hydroxytryptophan and also has a role in melatonin biosynthesis (8). Down-regulation of TPH1 expression leads to a disruption of serotonin biosynthesis and, as a result, a decreased level of melatonin. The oxytocin receptor (OXTR) gene was found to have increased expression in high stage tumour. To date, the mechanisms of regulation of gene expression for both the OXTR and melatonin receptors are poorly understood. MT2 receptor and OXTR both can bind the Gq α subunit and thus activate similar downstream signaling pathways, providing a potential for cross-talk between the two signaling pathways (22).

Monitoring the expression of melatonin membrane, nuclear RZR/ROR receptors genes and genes that are related to melatonin receptors may offer a strategy to anticipate tumour development and estimate the molecular changes that occur during colorectal carcinogenesis. The mechanism behind this association needs further elucidation.

REFERENCES

1. Mediavilla MD, Sanchez-Barcelo EJ, Tan DX, Manchester L, Reiter RJ. Basic mechanisms involved in the anti-cancer effects of melatonin. Curr Med Chem 2010; 17:4462-81.
2. Hill SM, Frasch T, Xiang S, Yuan L, Duplessis T, Mao L. Molecular mechanisms of melatonin anticancer effects. Integr Cancer Ther. 2009; 8(4):337-46.
3. Bella G, Mascia F, Gualano L, Bella L. Melatonin anticancer effects: review. Int J Mol Sc 2013; 14:2410-30.
4. Viswanathan AN, Schernhammer ES. Circulating melatonin and the risk of breast and endometrial cancer in women. Cancer Lett 2009; 281(1):1-7.
5. Dubocovich ML, Markowska M. Functional MT1 and MT2 melatonin receptors in mammals. Endocrine 2005; 27:101-10.
6. Xin Z, Jiang S, Jiang P, et al. Melatonin as a treatment for gastrointestinal cancer: a review. J Pinel Res 2015; 58:375-87
7. Slominski RM, Reiter RM, Schlabritz-Loutsevitch N, Ostrom R, Slominski AT. Melatonin membrane receptors in peripheral tissues: Distribution and functions. Mol Cell Endocrinol 2013; 351:152-66.
8. Söderquis F, Hellström PM, Cunningham JM. Human Gastroenteropancreatic Expression of Melatonin and Its Receptors MT1 and MT2. PLoS One 2015; 10(3):e0120195.

9. Konturek SJ, Konturek PC, Brzozowski T, Bubenik GA. Role of melatonin in upper gastrointestinal tract. J Physiol Pharmacol 2007; 58:23-52.
10. Glenister R, McDaniel K, Francis H, et al. Therapeutic actions of melatonin on gastrointestinal cancer development and progression. Transl Gastrointest Cancer 2013; 2(1):11–20.
11. Edge SB, Compton CC, The American Joint Committee on Cancer: the 7th edition of the AJCC Cancer Staging Manual and the future of TNM, Ann Surg Oncol 2010; 17(6):1471–74.
12. Karasek M, Carrillo-Vico A, Guerrero JM, Winczyk K, Pawlikowski M. Expression of melatonin MT(1) and MT(2) receptors, and ROR alpha(1) receptor in transplantable murine Colon 38 cancer. Neuro Endocrionol Lett 2002; 1:55-60.
13. Danielczyk K, Dzięgiel P.MT1 melatonin receptors and their role in the oncostatic action of melatonin. Post Hig Med Dośw 2009; 63:425-34.
14. Nasrabadi NN, Ataee R, Abediankenari S, Shokrzadeh M, Najafi M, Hoseini SV, Jan HH. Expression of MT2 Receptor in Patients with Gastric Adenocarcinoma and its Relationship with Clinicopathological Features. J Gastrointest Canc 2013; DOI 10.1007/s12029-013-9552-0.
15. Nemeth C, Humpeler S, Kallay E, Mesteri I, Svoboda M, Rögelsperger O, Klammer N, Thalhammer T, Ekmekcioglu C. Decreased expression of the melatonin receptor 1 in human colorectal adenocarcinomas. J Biol Regul Homeost Agents 2011; 25(4):531-42.
16. León J, Casado J, Carazo A, Sanjuán L, Maté A, Muñoz de Rueda P, Cueva P, Quiles R, Ruíz S, Ruíz-Extremera A, Salmerón J. Gender-related invasion differences associated with mRNA expression levels of melatonin membrane receptors in colorectal cancer. Mol Carcinog 2012; (8):608-18.
17. Seithikurippu R. Pandi-Perumal A, Trakht I , Venkataramanujan S, Spence W, Maestroni G, Zisapel N, Cardinali D. Physiological effects of melatonin: Role of melatonin receptors and signal transduction pathways.Prog.Neurobiol 2008; 85:335-353.
18. Reiling E, Riet E, Groenewoud MJ, et al. Combined effects of single-nucleotide polymorphisms in GCK, GCKR, G6PC2 and MTNR1B on fasting plasma glucose and type 2 diabetes risk. Diabetologia 2009; 52(9):1866-70
19. Salman M, Dasgupta S, Cholendra A, Venugopal PN, Lakshmi GL, Xaviour D, Rao J, D'Souza CJ. MTNR1B gene polymorphisms and susceptibility to Type 2 Diabetes: A pilot study in South Indians. Gene. 2015; 566(2):189-93.
20. Muc-Wierzgon M, Nowakowska-Zajdel E, Dzięgielewska-Gęsiak S, Kokot T, Klakla K, Fatyga E. Specific metabolic biomarkers as risk and prognostic factors in colorectal cancer. Word J Gastroenterol 2014; 20:9759-9774
21. Xu W, Wei B,Gao F, Zhang Z, Jonas J. Oncogenic GNAQ and GNA11 Mutations in Uveal Melanoma in Chinese. PLOS One 2014; DOI: 10.1371/journal.pone.0109699.
22. Sharkey J, Puttaramu,R, Word RA, Olcese J. Melatonin synergizes with oxytocin to enhance contractility of human myometrial smooth muscle cells. J Clin Endocrinol Metab 2009; 94(2):421–427.

JOURNAL OF BIOLOGICAL REGULATORS & HOMEOSTATIC AGENTS Vol. 29, no. 4, 829-833 (2015)

LETTER TO THE EDITOR

LRIG1 EXPRESSION DURING HOMEOSTASIS AND SKIN WOUND HEALING IN MICE

S. MURAD[1], A. ANWAR[1], Z.Z. PIRACHA[1] and A. SULTAN[2]

[1]Molecular Immunology Laboratory, Health Care Biotech, Atta-ur-Rahman School of Applied Biosciences, National University of Sciences and Technology (NUST), Islamabad, Pakistan; [2]Biochemistry Department, Quaid-e-Azam University, Islamabad, Pakistan

Received May 18, 2015 – Accepted August 28, 2015

Leucine-rich repeats and immunoglobulin-like domains (LRIG)-1 belong to the family of proteins known to be expressed in skin. Ablation of LRIG1 in mice results in epidermal hyperplasia and its aberrant expression levels have been reported in pathological conditions such as psoriasis, thus evident of an indispensible role of LRIG1 in maintaining epidermal homeostasis. In order to gain insight into the homeostatic expression of LRIG1 and in various stages of cutaneous wound healing, LRIG1 expression was immunohistochemically analyzed in full thickness skin wounds in mice. The full thickness skin wounds were established on the dorsal back of Balb/c mice (n=6). LRIG1 expression at various post wounding days (1, 2, 3, 6 and 14) was determined through Immunohistochemical analysis (IHC) of the murine skin sections. The injury caused a sharp decline in LRIG1 expression in the basal epidermal cells and appendages surrounding the wound which correlates with the re-epithelialization phase of healing. LRIG1 expression remained down regulated during most of the wound healing stages. LRIG1$^+$ cells were found to re-populate the neo-epidermis on day 14, suggesting an important homeostatic role of LRIG1 in skin.

Wound healing is a physiological response to tissue injury. It is a complex, coordinated chain of sequential events divided into the homeostasis, inflammatory, proliferative, and remodeling phase (1). Various cell populations such as keratinocytes, fibroblasts, macrophages, neutrophils and fibroblasts contribute towards bridging the gap formed due to the tissue loss. Various membrane-expressed and soluble proteins such as cytokines and growth factors provide necessary signals both for the *de novo* cellular recruitment and activation as well as necessary regulation and apoptosis of cell populations, contributing towards sequential processes of tissue repair and subsequent gain of homeostasis, respectively (1). The essential role of epidermal growth factor receptor (EGFR) and its ligands during various stages of tissue repair and regeneration, including inflammation, wound contraction, proliferation, migration, and angiogenesis, is well-established (2-4). More than a decade ago, human leucine-rich repeats immunoglobulin-like domain-1 (LRIG-1) was discovered as a negative regulator of EGFR (5). A growing number of studies support its regulatory role in various tumors. LRIG1 belongs to the family of proteins found to be expressed in various organs including skin (6, 7). The role of LRIG1 has

Key words: LRIG1, skin, expression, injury, mice

Mailing address: Sheeba Murad , PhD
Molecular Immunology Lab, Health Care Biotech,
Atta-ur-Rahman School of Applied Biosciences,
National University of Sciences & Technology (NUST),
Islamabad 44000, Pakistan
Tel.: +92 51 9085 6139 Fax: +92 51 9085 6102
e-mail: s.mall@asab.nust.edu.pk

0393-974X (2015)

been implicated in the regulation of wound healing; however, there is a lack of data regarding the cutaneous expression of LRIG1 at various wound healing stages. Therefore, in order to evaluate the expression of LRIG1 during various stages of cutaneous wound healing, the immunohistochemical analysis of LRIG1 at selected post wounding days was performed on mice.

MATERIALS AND METHODS

Full-thickness 5-mm wounds were made on the shaved dorsal back skin of 10-12-week-old adult BALB/c female mice with the help of a punch biopsy instrument. In order to analyze the LRIG-1 expression in three different wound healing stages, inflammation, re-epithelialization, remodelling phases, the skin biopsies of the wounded area along with the unwounded marginal skin (>1mm) were harvested on selected days - 0, 1, 2, 3, 6 and 14 post-wounding. A total of six wounds were examined in female mice in two set of experiments (n= 2+4). The wound contraction was monitored both macroscopically and microscopically. The percentage wound contraction was measured according to the formula: Area of original wound (Lx W) − area of actual wound (Lx W) /area of original wound × 100.

For histological analysis, the excised skin was sectioned into two halves. After the overnight fixation in 10% formalin, the tissues were embedded and later sliced into 5-µ thick sections. For LRIG1 expression analysis at different post wounding days, the sections were immunohistochemically stained, using the following antibodies; LRIG1primary antibody (ab36707, Abcam UK, 1:100), HRP labelled secondary antibody (ab6721, Abcam UK, 1:50) and were co-stained with haematoxylin. Stained skin sections were later evaluated in the blinded fashion. Different skin compartments including epidermis, dermis, hair follicles and sebaceous glands were analyzed (Fig. 1). Positive staining was marked by the presence of a brown signal. On the basis of the staining intensity, LRIG1 expression was scored on the scale of 1-4 (where 1 represents little or no expression and four represents strongest/intense expression) (Fig. 1).

RESULTS

Wound contraction was evaluated both dermascopically and histologically. Fig. 1a represents immunohistochemical analysis of LRIG1 protein expression before and after the induction of wounds. The analysis was carried out on selected post-wounding days; 1, 2, 3, 6 and 14, representing various wound healing stages. The change in the patterns of LRIG1 expression is depicted in Fig. 1b. Percentage wound closure was measured at different post wounding days, through vernier calliper and were further confirmed through haematoxylin and eosine (H&E) staining. More than 70% of the wound closure took place by day 6 and by post wounding day 10-12, the wound closure was 100%. A dry scab started to form on post wounding days 2-3 and by day 5 and 6, it had been shed. The histological analysis showed that on day 2, eschar starts to form with a granulation tissue exactly underneath it. From post wounding day 3 to 6, the size of the granulation tissue increases and neo- epidermis starts to form, bridging the wound margins. At day 14, most of the granulation tissue resolved, however the neo-epidermis was observed to be relatively thicker than the normal epidermis and excessive appendages such as hair follicles and sebaceous glands were observed to be progressively maturing.

Reduced LRIG1 expression in response to mechanical injury

In order to determine the LRIG1 protein expression, the skin sections were taken at the time of wounding designated as day 0 and subsequent post wounding days; 1, 2, 3, 6 and 14. Excised skin sections were then processed for the immunohistochemical (IHC) analysis of LRIG1. A high LRIG-1 expression was detected in the basal epidermal layer in the normal skin and in the compartments of appendages, such as hair follicles, as reported earlier (Fig. 1) (7-9). Further wound healing stages were marked by a gradual decline in the LRIG1 expression in the surrounding wound margins and appendages. LRIG1 expression was neither detected in the newly regenerated skin nor in the granulation tissue.

Repopulation of LRIG1^{+} cells during re-modelling phase/ after healing phase

By post wounding day 14, the repopulation of the new epidermis and dermis with LRIG1^{+hi} cell population was observed. At this stage, most of the granulation tissue had resolved and appendages seemed to be maturing (Fig. 1a). Post wounding day 14 generally marks the remodelling phase which is the last phase of healing.

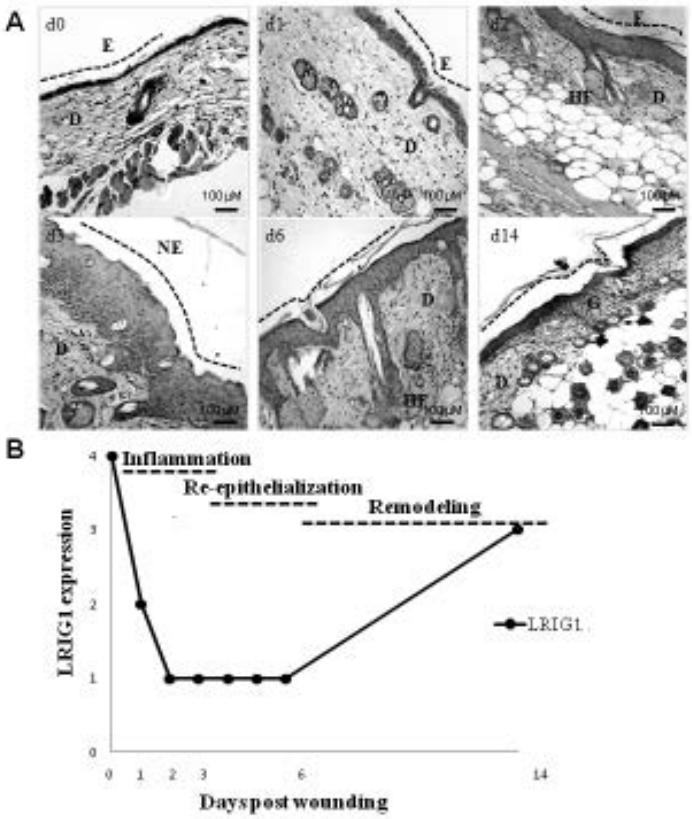

Fig. 1. *Immunohistochemical analysis of LRIG1 expression before and after the full thickness wound induction in murine skin.* ***A****) Representative images (100X) displaying the wound edges on selected post wounding days; 0,1,2,3,6 and 14. Sections were stained with anti- LRIG1 antibody (shown by darker area) counterstained by Haematoxylin. Arrows and abbreviation indicate E: Epidermis, D: Dermis, NE: New Epidermis, G: Granulation tissue, HF: Hair Follicles. n= 6* ***B****) Graphical representation of LRIG1 expression dynamics during selected post wounding days.*

DISCUSSION

The development and maintenance of mammalian skin requires a tight balance between cellular proliferation, differentiation and apoptosis controlled by diverse array of signalling molecules. Likewise, such balance is also required in response to injury and in regaining the homeostasis. The process of wound healing comprises overlapping series of coordinated and sequential steps controlled by various signalling molecules and proteins expressed by cells. LRIG1 has been identified as one of the diverse array of proteins that are expressed during the developmental stages as well as in the adult skin. It is a transmembrane protein (can solubilize) found to be expressed by cells in different organs including skin (6-9). Understanding the dynamics of LRIG1 expression in response to cutaneous injury and at selected post wounding days would further our insight into its role in the physiology of wound healing. LRIG1 expression was observed in the upper dermal layer especially in the cells surrounding the appendages (Fig. 1A). Highest expression was observed on day 0 when punch wounds were introduced on the lower back skin of mice. A notable decrease was observed in the area surrounding the wound within 24-48 hours after wounding (Fig. 1A, B). Various pathological skin conditions marked by abnormal growth or cell proliferation, such as epidermal hyper proliferation in psoriasis, are reported to have aberrant expressions of LRIG1. LRIG1 has been found to mark an important multipotent stem cell (SC) compartment in skin (6-9). The physiological levels of LRIG1 expression are required to maintain

a quiescent and homeostatic state while its loss has been related to the proliferation stages (10-12). The regenerative potential of SCs may vary widely; from the physiological cellular turnover to repair responses against mechanical damage and tissue injuries. LRIG1 is one of the few markers found to be expressed by the groups of basal stem cells in human inter-follicular epidermis (IFE) and in appendages such as the bulge region of the hair follicle (HF) (Fig. 1) or more specifically in the upper pilosebaceous unit of HF (13-16). Fate mapping studies are indicative of the potential of bulge cells to form hair follicle, IFE and sebaceous glands (SGs). Therefore, owing to the multipotency and enormous regenerative potential, the bulge cells have been an intense area of research. These cells are not essential for the maintenance of the IFE but are generally quiescent and take part in the repair of a tissue injury. Upon wounding, the quiescent stem cells in the bulge region are activated, giving rise to the short-lived transient amplifying (TA) cells which migrate rapidly towards the skin lesions and participate actively in the repair of the damaged epidermis (13-16). The reported decrease in the LRIG1 expression from the cells in the basal epidermis and in the HF in response to the mechanical injury reported in the current study (Fig. 1) could be the result of the re-programming of the stem cells and their differentiation into TA cells, thus contributing towards the repair of the injured epidermis. LRIG1 is implicated in maintaining the stem cell quiescence or non-dividing state while its suppression is associated with increased proliferation. LRIG1 over-expression in primary keratinocytes has been shown to decrease the keratinocyte proliferation while its down-regulation results in accelerated proliferation (16, 17). LRIG1-deficiency in mice has been shown to lead to an epidermal hyperplasia causing a psoriasis-like skin lesion and increased EGFR signalling in keratinocytes (10). Therefore, the decrease in levels of LRIG1 (Fig. 1) may be indicative of the loss of stem cell-quiescence status.

Regeneration of the epidermis after wounding requires activation and recruitment of various SCs and TA cells either residing in the surrounding epidermis and the adnexal structures such as the hair follicle, sweat gland or from bone marrow. However, the evidence is conflicting regarding the exact nature and location of these stem cells (17, 18). The current observation of the re-population of the maturing granulation tissue on post-wounding day 14 with $LRIG1^+$ cells suggests the *de novo* recruitment of $LRIG1^+$ stem cells (Fig. 1). Whether these cell populations are bone marrow cells recruited to replenish the exhausted supply of SCs requires further investigation.

There is mounting evidence which indicates an important regulatory role of LRIG1 especially in maintaining the normal skin homeostasis. This endogenous regulatory role of LRIG1 is currently being used to design novel therapeutics in order to intervene in abnormal growth signalling in malignancies (19). The highest expression of LRIG1 before and two weeks after wounding is indicative of its importance in the regain of homeostasis. The current study lends further support to the studies showing a regulatory role of LRIG1 with possible implications in the tissue engineering and regenerative medicines.

ACKNOWLEDGEMENTS

We are grateful to the National University of Sciences and Technology (NUST) recurring budget and Higher Education Commission (HEC) for providing the necessary funds and platform for performing the study. We are also thankful to the National Institute of Health Sciences (NIH) for allowing the use of their facilities.

REFERENCES

1. Werner S, Grose R. Regulation of wound healing by growth factors and cytokines. Physiol Rev 2003; 83(3):835-70
2. Repertinger SK, Campagnaro E, Fuhrman J, El-Abaseri T, Yuspa SH, Hansen LA. EGFR enhances early healing after cutaneous incisional wounding. J Invest Dermatol 2004; 123(5):982-89.
3. Greenhalgh DG. The role of growth factors in wound healing. J Trauma 1996; 41:159-67.
4. Nakamura Y, Sotozono C, Kinoshita S. The epidermal growth factor receptor (EGFR): role in corneal wound healing and homeostasis. Exp Eye Res 2001; 72:511-17.
5. Gur G, Rubin C, Katz M, et al. LRIG1 restricts growth

factor signaling by enhancing receptor ubiquitylation and degradation EMBO J 2004; 23(16):3270-81.

6. Nilsson J, Vallbo C, Guo D, Golovleva I, Hallberg B, Henriksson R, Hedman H. Cloning, characterization, and expression of human LIG1. Biochem Biophys Res Commun 2001; 284(5):1155-61
7. Nilsson J, Starefeldt A, Henriksson R, Hedman H. LRIG1 protein in human cells and tissues. Cell Tissue Res 2003; 312(1):65-71.
8. Jensen KB, Watt FM. Single-cell expression profiling of human epidermal stem and transit-amplifying cells: Lrig1 is a regulator of stem cell quiescence. Proc Nat1 Acad Sci USA 2006; 103(32):11958-63.
9. Jensen KB, Collins CA, Nascimento E, Tan DW, Frye M, Itami S, Watt FM. Lrig1 expression defines a distinct multipotent stem cell population in mammalian epidermis, Cell Stem Cell 2009; 4:427-39.
10. Nakamura T, Hamuro J, Takaishi M, et al. LRIG1 inhibits STAT3-dependent inflammation to maintain corneal homeostasis. J Clin Invest 2014; 124(1):385-97.
11. Y Wang, E J Poulin and R J Coffey. LRIG1 is a triple threat: ERBB negative regulator, intestinal stem cell marker and tumour suppressor. Br J Cancer 2013; 108:1765-70.
12. Suzuki Y, Miura H, Tanemura A, et al. Targeted disruption of LIG-1 gene results in psoriasiform epidermal hyperplasia. FEBS Lett 2002; 521:67-71.
13. Page ME, Lombard P, Ng F, Göttgens B, Jensen KB. The epidermis comprises autonomous compartments maintained by distinct stem cell populations. Cell Stem Cell 2013; 13(4):471-82.
14. Ito M, Liu Y, Yang Z, Nguyen J, Liang F, Morris RJ, Cotsarelis G. Stem cells in the hair follicle bulge contribute to wound repair but not to homeostasis of the epidermis. Nat Med 2005; 11:1351-54.
15. Powell AE, Wang Y, Li Y, et al. The pan-ErbB negative regulator Lrig1 is an intestinal stem cell marker that functions as a tumor suppressor. Cell 2012; 149(1):146-58.
16. Cotsarelis G, Sun TT, Lavker RM. Label-retaining cells reside in the bulge area of pilosebaceous unit: implications for follicular stem cells, hair cycle, and skin carcinogenesis. Cell 1990; 61(7):1329-37
17. Lavker RM, Sun TT. Epidermal stem cells: properties, markers, and location. Proc Natl Acad Sci USA 2000; 97:13473-75.
18. Ghazizadeh S, Taichman LB. Multiple classes of stem cells in cutaneous epithelium: a lineage analysis of adult mouse skin. EMBO J 2001; 20:1215-22.
19. Chang L, Shi R, Yang T, et al. Restoration of LRIG1 suppresses bladder cancer cell growth by directly targeting EGFR activity. J Exp Clin Cancer Res 2013; 8:32-101.

JOURNAL OF BIOLOGICAL REGULATORS & HOMEOSTATIC AGENTS Vol. 29, no. 4, 835-840 (2015)

LETTER TO THE EDITOR

EFFECTS OF VASCULAR ENDOTHELIAL GROWTH FACTOR-B ON THE BIOELECTRIC ACTIVITY OF RAT ATRIAL MYOCARDIUM UNDER NORMAL CONDITIONS AND DURING GRADUAL STRETCHING

R.S. OVCHINNIKOV[1,2], V.M. MITROKHIN[1*] and M.I. MLADENOV[1,3*]

[1]Department of Fundamental and Applied Physiology, Russian National Research Medical University, Moscow, Russia; [2]Federal Scientific Clinical Center for Specialized Types of Medical Assistance and Medical Technologies of the Federal Medical and Biological Agency, Russia, Moscow, Russia; [3]Faculty of Natural Sciences and Mathematics, Institute of Biology, "Ss. Cyril and Methodius" University, Skopje, Macedonia

Received May 25, 2015 – Accepted November 11, 2015

[*]These authors contributed equally as senior authors to this paper

Using a microelectrode technique we studied the effects of vascular endothelial growth factor-B on the activity of rat atrial myocardium under normal conditions and after gradual stretching of the tissue. It was shown that vascular endothelial growth factor-B increased duration of the action potential only at the level of 90% re-polarization. Effects on the frequency and force of contraction were absent. The repetition frequency of the action potentials did not change. Close observation of the vascular endothelial growth factor-B-induced mechanisms and stretch-induced alteration in action potential durations to 90% of repolarization, confirmed the existence of a link between the examining growth factor-B and stretch induced mechanisms.

Members of the vascular endothelial growth factor (VEGF) family, currently comprise 5 mammalian proteins (VEGF-A; VEGF-B; VEGF-C; VEGF-D; VEGF-F). VEGF-B exists as 2 isoforms generated by alternative splicing (1). Both isoforms bind to the VEGF receptor (VEGFR)-1, but not to the major mitogenic endothelial cell receptors VEGFR-2 or VEGFR-3 (2).

VEGF-B has a wide tissue distribution, being most abundant in the myocardium, skeletal muscles, vascular smooth muscles, and brown adipose tissue (3, 4). Mice lacking VEGF-B are viable and fertile and display only a mild phenotype in the heart. This is manifested as an atrial conduction abnormality characterized by a prolonged PQ interval in 1 strain (C57Bl background) (5), or as a smaller heart size with impaired recovery after myocardial ischemia in another strain (129/SvJ or 129/SvJC57Bl/6J background) (6). Such conduction abnormality, specifically for the development of cardiac hypertrophy, is very likely triggered by mechanical stress (7). However, the involvement of growth promoting factors (such as VEGF-B), cannot be ruled out (8). Sadoshima and Izumo carried out an experiment in which they transferred a stretch-conditioned medium, derived from stretched cardiomyocytes, to non-stretched

Key words: action potential, atrium, heart, vascular endothelial growth factor B, stretch

Mailing address: Mitko I. Mladenov, PhD
Department of Fundamental and Applied Physiology,
Russian National Research Medical University,
Ostrovitjanova 1,
Moscow 117997, Russia
Tel.: +7095 131 4863 Fax: +7095 131 4863
e-mail: m.mitko@gmail.com

0393-974X (2015)

DISCLOSURE: ALL AUTHORS REPORT NO CONFLICTS OF INTEREST RELEVANT TO THIS ARTICLE.

cardiomyocytes. Such a transfer induces hypertrophy in the recipient non-stretched cardiomyocytes, which indicates a secretion of some molecules during stretching (8). Later, Thieri et al. (3) confirmed that cardiac myocytes and other cell types, such as cardiac fibroblasts, endothelial cells, and vascular smooth muscle cells, may secrete growth promoting factors after mechanical stress stimulus, which induces hypertrophy of cardiomyocytes in an autocrine/paracrine way.

Besides the described role of VEGF-B regarding its involvement in the induction of heart hypertrophy, there is no data on its direct cardiotropic action. The fact that stretch by itself induced VEGF-B release from one side and altered the activity of mechanically gated channels (MGCs) (9) from the other side helps us to propose that VEGF-B may interact with MGCs and participate in the regulation of mechano-electrical feedback. Furthermore, basing on the fact that the modulation of cardiac electrical activity in a cardiac mechanical environment (mechano-electric feedback) depends to a large extent on the variable filling pressure of the heart (10), the aim of this study was to investigate the influence of VEGF-B on the bio-electric activity of rat's right atrial preparations (RAPs), under normal conditions and conditions of myocardial stretch.

MATERIALS AND METHODS

Animals and experimental design

Male Wistar rats (n = 28) were used for all protocols and were maintained on a 12:12 light:dark cycle and fed with standard rat chow and water, *ad libitum*. All experimental procedures were conducted in accordance with the Guiding Principles for Care and Use of Laboratory Animals approved by the Russian Center for Bioethics. All protocols were approved by the Animal Bioethics Committee at the Russian National Research Medical University, in accordance with the International Guiding Principles for Biomedical Research Involving Animals published by the US National Institutes of Health (NIH Publication No. 85-23, revised 1996). The animals were sacrificed by decapitation without preliminary anaesthesia, the chest was immediately opened and the heart quickly excised.

Intracellular recordings of action potential in isolated rat RAPs

Action potential (AP) recordings of rat RAPs are described in detail in the study published by Kamkin and Cow (11). The RAP, including the auricle, the crista terminalis, the intercaval region, and the sinoatrial node was isolated and pinned to the bottom of an experimental chamber (3 ml) supplied with physiological salt solution (PSS) at 10 ml min^{-1} (37.5°C). After 30 min of equilibration, trans-membrane potentials were recorded with floating glass micro-electrodes (20-30 MΩ) filled with 3 M KCl as described earlier (11). The signal was filtered at 5 KHz and digitized using an ADC PowerLab 4/35 (AD Instruments, Australia) with a sampling frequency of 20 KHz and analysed using the software package LabChart (v. 8 AD Instruments, Australia). Spontaneously occurring APs were recorded from the endocardial surface of the auricle. Stable impalements were maintained during the entire period of drug action. Changes in the resting potential (RP), AP amplitude (APA) and the AP durations to 25 (APD25), 50 (APD50) and 90% of re-polarization (APD90) were analysed. In order to avoid false positives, 10 APs were taken at each time-point (0, 10, 20, 35 min) and averages calculated.

Recording of contractile activity and tissue stretch

The preparations were fixed horizontally with two clips made from tungsten wire connected to a force transduction system (Plug-sys 603, Hugo Sachs Elektronik, Germany) and a programmable electric micro-manipulator (Sutter MP285; Sutter, Novato, CA, USA; accuracy 0.2 μm), respectively. The latter was used for the adjustment of preload and stretch, respectively. Developed active force (AF), was measured at a baseline preload of 1 mN, which was usually about 0.30±0.01 mN. A preload of 1 mN, which is called resting force (RF), corresponded to a lengthening of the preparation by approximately 6% of its initial length.

To simulate changes in right atrial pressure, we used the steps of stretch applied by the micro-manipulator. This stimulus was used to provoke the electro-physiological response of the cardiomyocytes. Each step was applied for approximately 5 s. Since the relationship between the length changes and stretch force differs among preparations, the increase in isometric force amplitude (ΔAF) was used to standardize the mechanical test stimulus (for details see 12).

Solutions and drugs

PSS had the following composition (in mM): NaCl, 137; KCl, 5.4; $CaCl_2$, 1.0; $MgCl_2$, 0.5; Na-HEPES, 5.0; Glucose, 5.5, bubbled with O_2 and pH adjusted to 7.4 with NaOH. VEGF-B was dissolved in a perfusion solution at a concentration of 50 ng/ml. Rat recombinant VEGF-B were obtained from Invitrogen (Carlsbad, CA, USA). The MGC inhibitor Gd^{3+}, and all other compounds in PSS were

purchased from Sigma-Aldrich (St. Louis, MO, USA). O_2 (99.9 % pure), was from Technical Gases (Moscow, Russian Federation).

Statistical analysis

Data for the RPs and APs are presented as means ± standard error (SE). In order to avoid the effect of the beat-to-beat variability, the values of the APs from the entire recording were presented as a means ± standard deviation (SD). Multiple comparisons were made using the analysis of variance (ANOVA) with the post hoc test of Bonferroni, performed in selected instances to evaluate further differences between group pairs. Only 2-tailed probabilities were used for testing statistical significance. Probability values < 0.05 were regarded as statistically significant. All analyses were performed with Graph Pad Prism 4.0 (San Diego, CA, USA).

RESULTS

Bio-electrical activity of RAPs under control and conditions of stretch

The effect of stretching on the bio-electrical activity of RAPs is described in detail in our previous study (12). In control conditions there were

Table I. *Effects of VEGF-B on RP and AP.*

Parameter				
	Baseline	VEGF, 10 min	VEGF, 20 min	VEGF, 35 min
RP	-84 ± 1.6	-84.2 ± 1.4	-81.1 ± 1.3	-81 ± 2.9
AP	112 ± 1.5	112 ± 1.5	117± 1.8	118 ± 1.1

RP: resting potential; AP: action potential; RP and AP: mean values ± SE in mV.

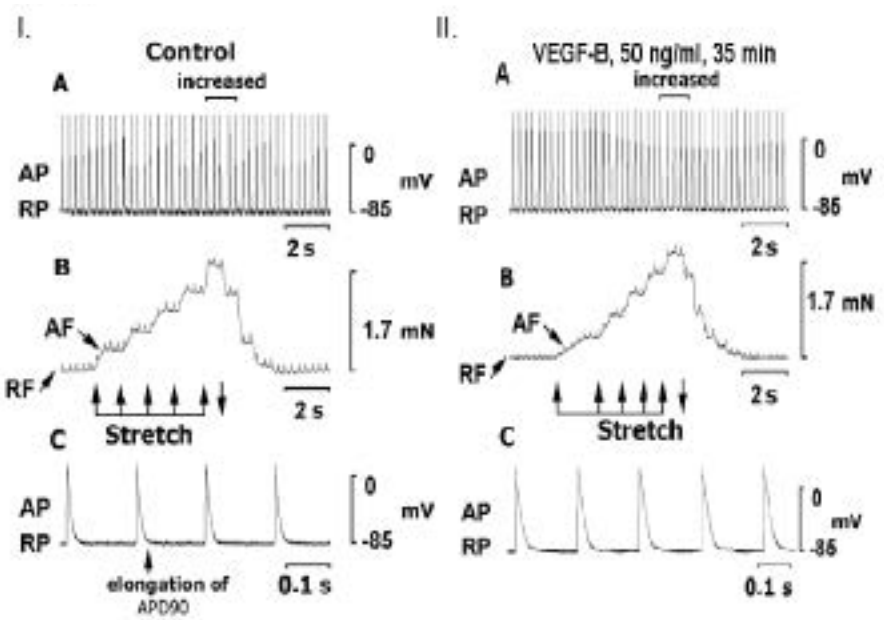

Fig. 1. *Effects of VEGF-B on bio-electrical activity of rat right atrium.* ***A****) control;* ***B****) 35 min perfusion with VEGF-B;* ***C****) superimposed action potentials from (A) and (B);* ***D****) (a,b,c) APD25, APD50, APD90, values at 0, 10, 20 and 35 min of the recording, respectively. Fragments of the original records are presented. RP: resting potential; AP: action potential.*

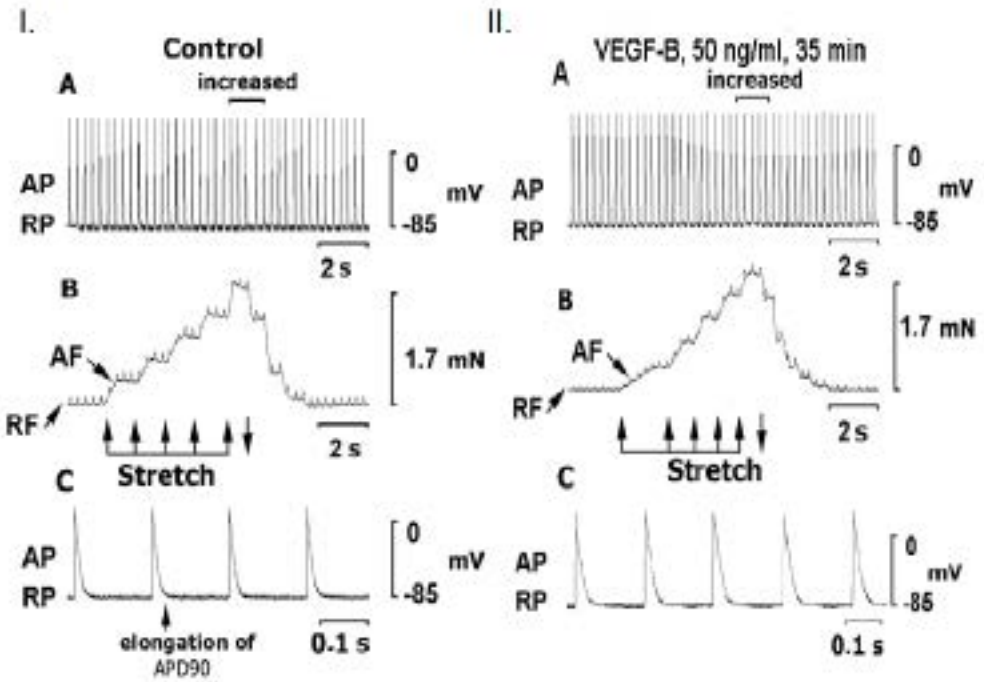

Fig. 2. ***I.*** *Effects of stretching on the bio-electric and mechanical activity of rat right atrium.* ***II.*** *Effects of stretching on bio-electric and mechanical activity of rat right atrium in the presence of VEGF-B.* ***I*** *and* ***II****: **A**) synchronous recording of bio-electrical activity; **B**) force of contraction; **C**) enlarged fragment of the curve shown in A. Fragments of the original records are presented. RF: resting force; AF: active force; RP: resting potential; AP: action potential.*

no significant changes during the first hour of the experiment in all tested parameters. On the other hand, irregular episodes of AP prolongation were observed as a consequence of the stretch application (for details see 12).

The effect of Gd^{3+} on stretch-induced electrical activity

In order to check whether stretch-induced electrical activity is a result of MGCs or not, we performed separated experiments (n=14), with the employment of gadolinium (Gd^{3+}) as a specific antagonist of the MGCs. The effect of Gd^{3+} at a concentration of 40 μM, on the stretch-induced electrical activity, was described in detail in our previous studies (11, 12). Briefly, all stretch-induced depolarizations (SIDs), hump-like SIDs, and extra APs were completely abolished after 10-min perfusion with Gd^{3+}, without significant alteration of contractile activity (12). Hence, we confirmed that under our experimental conditions, MGC activation is caused by stretching (12).

The effect of VEGF-B on stretch-induced electrical activity

Analysis of the electrical activity of RAPs showed that VEGF-B did not change the RP and the APAs (-84.0±1.6 and 112.6±1.5 mV before the start of perfusion, 81.0±2.9 mV and 118.0±1.1 mV, after 35-min perfusion, respectively; n=14). Furthermore, analysis of the APDs showed that the VEGF-B perfusion during 35 min caused significant increase in the APD90, $p<0.001$ (Fig. 1, C and D). Actually, in case of perfusion with VEGF-B, the APD90 increased about 8%, while stretching in the presence of VEGF-B caused an additional 5% increase (Fig. 2, II). There were no registered changes in any other tested parameters during VEGF-B perfusion (Table I).

DISCUSSION

Alterations in the AP waveforms were considered

as SIDs, which in several cases were transformed into hump-like SIDs. Taking into account that SIDs and hump-like SIDs led to an extra AP generation only when occurring at the level of APD90, in this study we discuss only the abnormalities occurring at this level.

Since there were no abnormalities like hump-like depolarizations, changes in repetition frequency of APs or force of contraction during perfusion with VEGF-B, we assumed that the significant increase in APD90 is result of the VEGF-B-reduced activity of potassium channels (K^+). The basis of such an assumption came from the study of Xu et al. (13), who reported an indirect action of the VEGF-B upon K^+ currents. The fact that elongation took place only at APD90 indicates for VEGF-B ability to reduce inward rectifier K^+ current, as an outward current which generates resting membrane potential and modulates the final depolarization phase of the AP (13, 14). In addition, data published by Gupta and Maitland (15), indicating that the prolonged action of VEGF-B led to a rate of deceleration and brady-arrhythmia, additionally confirmed our findings. Such an elongation in APD90, probably prolongs Ca^{2+} entry into the cytoplasm and induces an increase in the intracellular Ca^{2+} concentration, which corresponds with an appropriate increase in the cardiac output (15).

On the other hand, the mechanical stretching during tissue perfusion with VEGF-B had no effect on the studied parameters (Fig. 2, IIC). Taking that tissue stretching (16-19) activates NO sinthases (NOS) and increases NO concentration, we expected that the final effect on the myocardial bioelectrical activity would be determined by the level of intracellular NO. According to the results obtained in this study, it seems that intracellular NO level induced by stretching is balanced by VEGF-B-induced cation influx (15). Such a balance is probably the reason for the prevention of the abnormalities in the heart rhythm (11) in the stretched RAPs. Additional support comes from the fact that the stretch did not cause any change in the repetition frequencies of the APs in the presence of VEGF-B.

In general, the data presented here elucidate the earliest mechanisms of VEGF-B involvement in APD90 elongation, described as a basic precondition for the development of myocardial hypertrophy. Taking the relevance of these findings in rodents in regard to humans (5), this could be another important area for future investigation.

Limitations

Details concerning mechano-induced alterations of the membrane potential in the stretched atrial myocardium are given in our previous studies (16-19).

The concentrations of VEGF-B used here, chosen to demonstrate more efficiently the VEGF-B action, may appear greater than those found in the patho-physiological conditions in plasma. However, higher plasma levels of VEGF-B are related to APD elongation and myocardial hypertrophy (3), which was the reason why we established a procedure to test the effects of an extremely high dose of VEGF-B.

The concentration of Gd^{3+} used in this study was based on the experiences from our previous studies. Bearing in mind that Gd^{3+} in a concentration of 10 mmol/l did not block completely the MGCs (12), we increased its concentration in order to ensure that the recorded electrical activity was a 100% result of the MGC activity.

Future studies addressing the effects of VEGF-B on isolated cardiomyocytes, will provide data that will allow quantification of the effect of the limitations discussed.

ACKNOWLEDGEMENTS

The Authors would like to thank Prof. Dr. A.G. Kamkin for critical evaluation of the manuscript. The Department of Fundamental and Applied Physiology (Professor and Chairman-Andre Kamkin) was supported by the Ministry of Healthcare of the Russian Federation. The Order of Ministry of Healthcare of the Russian Federation No. 200030056 from 19 August 2015, the Period of Financing 2015–2017.

REFERENCES

1. Olofsson B, Pajusola K, von Euler G, Chilov D, Alitalo K, Eriksson U. Genomic organization of the mouse and human genes for vascular endothelial growth factor B (VEGF-B) and characterization of a second splice isoform. J Biol Chem 1996;

271:19310-17.
2. Olofsson B, Korpelainen E, Pepper MS, et al. Vascular endothelial growth factor B (VEGF-B) binds to VEGF receptor-1 and regulates plasminogen activator activity in endothelial cells. Proc Natl Acad Sci USA 1998; 95:11709-14.
3. Thieri K, Bry M, Ollila MH, et al. Overexpression of vascular endothelial growth factor-B in mouse heart alters cardiac lipid metabolism and induces myocardial hypertrophy. Circ Res 2008; 103:1018-26.
4. Aase K, Lymboussaki A, Kaipainen A, Olofsson B, Alitalo K, Eriksson U. Localization of VEGF-B in the mouse embryo suggests a paracrine role of the growth factor in the developing vasculature. Dev Dyn 1999; 215:12-25.
5. Aase K, von Euler G, Li X, et al. Vascular endothelial growth factor-B deficient mice display an atrial conduction defect. Circ 2001; 104:358-64.
6. Bellomo D, Headrick JP, Silins GU, et al. Mice lacking the vascular endothelial growth factor-B gene (Vegfb) have smaller hearts, dysfunctional coronary vasculature, and impaired recovery from cardiac ischemia. Circ Res 2000; 86:29-35.
7. Ruwhof C, van der Laarse A. Mechanical stress-induced cardiac hypertrophy: mechanisms and signal transduction pathways. Cardiovas Res 2000; 47:23-37.
8. Sadoshima J, Izumo S. Mechanical stretch rapidly activates multiple signal transduction pathways in cardiac myocytes: potential involvement of an autocrine/ paracrine mechanism. EMBO J 1993; 12:1681-92.
9. Kazanski V, Kamkin A, Makarenko E, Lysenko N, Lapina N, Kiseleva I. The role of nitric oxide in the regulation of mechanically gated channels in the heart, in: Kamkin A, & Kiseleva I, (Eds.), Mechanosensitivity and mechanotransduction, Springer 2011; pp. 109-40.
10. Lab MJ. Mechanoelectric feedback (transduction) in heart: concepts and implications. Cardiovas Res 1996; 32:3-14.
11. Kamkin A, Kiseleva I, Wagner KD, Leiterer KP, Theres H, Scholz H, Günther J, Lab JM. Mechano-electric feedback in the right atrium after left ventricular infarction in rats. J Mol Cell Cardiol 2000; 32:465-77.
12. Abramochkin VD, Kuzmin SV, Mitrokhin MV, Kalugin L, Dvorzhak A, Makarenko YE, Schubert R, Kamkin A. TNF-α provokes electrical abnormalities in rat atrial myocardium via a NO-dependent mechanism. Eur J Physiol 2013; 465:1741-52.
13. Xu JY, Zheng P, Shen DH, Yang SZ, Zhang LM, Huang YL, Sun FY. Vascular endothelial growth factor inhibits outward delayed-rectifier potassium currents in acutely isolated hippocampal neurons. Neuroscience 2003; 118:59-67.
14. Giles WRB, Imaizumi Y. Comparison of potassium currents in rabbit atrial and ventricular cells. J Physiol 1988; 405:123-45.
15. Gupta R, Maitland ML. Sunitinib, hypertension, and heart failure: a model for kinase inhibitor-mediated cardiotoxicity. Curr Hypertens Rep 2011; 13:430-35.
16. Mitrokhin MV, Mladenov IM, Kamkin GA. Effects of interleukin-6 on the bio-electric activity of rat atrial tissue under normal conditions and during gradual stretching. Immunobiology 2015; 220:1107-12.
17. Aksyonov A, Mitrokhin MV, Mladenov IM. Effects of interleukin-2 on bioelectric activity of rat atrial myocardium under normal conditions and during gradual stretching, Immunol Lett 2015; 167:23-28.
18. Ovchinnikov SR, Mitrokhin MV, Mladenov IM. Effects of interleukin-17A on the bioelectric activity of rat atrial myocardium under normal conditions and during gradual stretching, Cytokine 2015; http://dx.doi.org/10.1016/j.cyto.2015.06.016.
19. Mitrokhin MV, Mladenov IM, Kamkin GA. IL-1 provokes electrical abnormalities in rat atrial myocardium. Int Immunopharm 2015; 28:780-84.

LETTER TO THE EDITOR

PRE-HOSPITAL EMERGENCY VALUES OF HYPERTONIC-HYPERONCONIC LIMITED RESUSCITATION FOR TRAUMATIC SHOCK

S-P. HAN[1], G-T. WANG[2], S-S. ZHANG[1], Q. LIU[1] and L. WANG[1]

[1]Zhengzhou People's Hospital Affiliated to Southern Medical University, Zhengzhou City, Henan Province, PR China; [2]Southern Medical University, Guangdong Province, PR China

Received April 29, 2015 – Accepted July 6, 2015

Traumatic shock is a serious threat to life and health. The aim of this study is to investigate the effect of different resuscitation fluid compositions on the emergency resuscitation for patients with traumatic shock. Sixty patients were enrolled and divided into two groups, Group A and Group B. The patients in Group A were treated with resuscitation fluid, with 2:1 ratio of crystal (0.9% sodium chloride injection) and colloid (hydroxyethyl starch 40 injection). The patients in Group B were treated with hypertonic sodium chloride hydroxyethyl starch 40 injection (HSH40). Both vital signs and fluid dosage were monitored and recorded. At the beginning of resuscitation (T_0) and 30 min (T_1), 60 min (T_2) and 120 min (T_3) after resuscitation, indicator parameters including hemoglobin (HB), hematocrit (HCT), prothrombin time (PT), arterial blood lacic acid (LA) and C-reactive protein (CRP) were monitored and recorded. Tissue oxygenation and hemodynamic profile were also analyzed. At T_1, T_2 and T_3 after fluid resuscitation, the heart rates of the patients in Group B were lower than those in Group A, whereas the average arterial pressure in Group B was significantly higher than that in Group A. Notably, significant decreases of HB and HCT were detected at T_1, T_2 and T_3 compared with T_0 in Group A. In contrast, no significant difference was shown in detected HCT at T_2 and T_3 compared with T_0 in Group B, while the detected HB value was smaller. a statistically significant decrease of LA was detected at T_1, T_2 and T_3 in Group A and Group B compared with that at T_0. At T_2 and T_3 in Group A and Group B, a statistically significant increase of PT was detected compared with the beginning of resuscitation. At T_2 and T_3 after resuscitation, CRP in both Group A and Group B was significantly increased compared with that upon admission to hospital, and was lower in Group B than in Group A.

Traumatic shock represents a notoriously challenging threat to life and health. Ranked as the fourth cause of death in China, acute traumatic or trauma-hemorrhagic (hereinafter referred to as acute traumatic) shock has received extensive clinical and managerial attention and is currently an important component of the national disease control program. Identifying effective approaches to improve the emergency resuscitation before hospitalization has increasingly become the focus of study in emergency medicine. In particular, limited resuscitation is a crucial clinical strategy for acute traumatic shock in pre-hospital emergency treatment. However, selection of the resuscitation fluid remains largely

Key words: limited resuscitation, traumatic shock, hypertonic sodium chloride hydroxyethyl starch 40 injection

Mailing address: Dr Si-sen Zhang,
Huanghe Road no.33,
Jinshui District,
Zhengzhou City,
Henan Province, 450003, China
Tel.: +860371 63945120 Fax: +860371 63945120
e-mail: zhangsisen215@163.com

0393-974X (2015)

DISCLOSURE: ALL AUTHORS REPORT NO CONFLICTS OF INTEREST RELEVANT TO THIS ARTICLE.

controversial in the clinical first-aid field. To comprehensively tackle this problem, we built upon the results from multiple previous studies (1, 2) concerning pre-hospital emergency for acute traumatic shock, and set out to monitor and analyze the tissue oxygenation, microcirculation and hemodynamics, which combined can reveal the effect of different compositions of resuscitation fluids on emergency resuscitation for acute traumatic shock.

MATERIALS AND METHODS

Sixty patients (36 male and 24 female) with acute traumatic shock, treated in the emergency department of the Zhengzhou People's Hospital affiliated to the Southern Medical University between November 2013 and June 2014, were selected for this study (20 multiple trauma cases, 14 closed abdominal trauma cases, 10 thoracic blunt trauma cases, 6 thoraco-abdominal injury cases and 10 limb injury cases). The protocol was approved and supervised by the Ethics committee of Zhengzhou People's Hospital. Detailed operating rules and regulations had been fully explained to the patients or their family members, who all signed informed consents.

The inclusion and exclusion criteria were previously described (1-2). Grouping criteria were as follows: patients with acute traumatic shock, with shock index > 0.5, or systolic pressure < 90 mmHg along with diastolic pressure < 60 mmHg. Exclusion criteria were as follows: allergic constitution and allergic to resuscitation fluid; hepatic renal dysfunction and coagulation disorder. Patients who met the above-described criteria were randomly divided into Group A and Group B with 30 cases in each group. Limited fluid resuscitation was adopted. The resuscitation fluid was used in Group A, with a ratio of 2:1 between crystal (0.9% sodium chloride injection) and colloid (hydroxyethyl starch 40 injection); Group B was treated with hypertonic sodium chloride hydroxyethyl starch 40 injection (HSH40).

Rescue methods

Clinical assessment was performed immediately upon diagnosis. The air passage was opened after shock had been definitely diagnosed so as to maintain the fluent respiratory tract. Vital signs were monitored, and the venous channel quickly established. Limited resuscitation was performed, with an infusion speed of 15-20 ml/min. Blood pressure reached the control level of "mean arterial pressure (MAP) > 60 mmHg, for maintaining more than 30 min, with the recovery of peripheral circulation". Those deemed in need of surgery were hospitalized as soon as possible to receive emergency operative treatments. After surgery, all patients remained in the intensive care unit to consolidate the outcome.

Detection methods and indicators

Both the vital signs (blood pressure, heart rate, breathing and transcutaneous oxygen saturation) and fluid dosages were monitored and recorded every 5 min. At the beginning of resuscitation (T_0) as well as 30 min (T_1), 60 min (T_2) and 120 min (T_3) after resuscitation, the following indicators were monitored and recorded: mean artery pressure (MAP), heart rate (HR), urine volume (UV), blood platelet (Plt), hemoglobin (HB), hematocrit (HCT), prothrombin time (PT), arterial blood lactic acid (LA), oxygenation index (OI), C-reactive protein (CRP), renal function, and electrolyte. Meanwhile, tissue oxygenation and hemodynamic profile were analyzed.

Statistical analysis

SPSS17.0 software was adopted for statistical analysis. All quantitative data were expressed as mean ± standard deviation (SD), *t*-test was employed for the comparisons among groups, and χ^2 test was used for all the enumeration data. Differences were considered statistically significant if $P < 0.05$ in two-tailed tests.

RESULTS

No significant differences were identified in respect to age, weight, height and time at the beginning of resuscitation for the patients between Group A and Group B ($P > 0.05$). However, as shown in Fig. 1a, the HR and MAP values for the patients between T_0 and T_1, T_2 or T_3 after the resuscitation had been initiated in both Group A and Group B demonstrated statistically significant differences ($P < 0.05$). Similarly, as displayed in Fig. 1b, the HR and MAP values for the patients at T_0 of resuscitation between Group A and Group B illustrated statistically significant differences ($P < 0.05$). Moreover, at T_1, T_2 and T_3 after resuscitation, the HR values in Group B were smaller than those in Group A, whereas the MAP values in Group B were remarkably larger than those in Group A ($P < 0.05$).

As shown in Fig 1, c and d, at T_1, T_2 and T_3 in Group A, the HB and HCT values were significantly decreased compared with those at T_0 of resuscitation ($P < 0.05$). However, at T_2 and T_3 in Group B, no statistically significant difference was found for the HCT values compared with that at T_0 of resuscitation ($P > 0.05$), although the detected HB values were

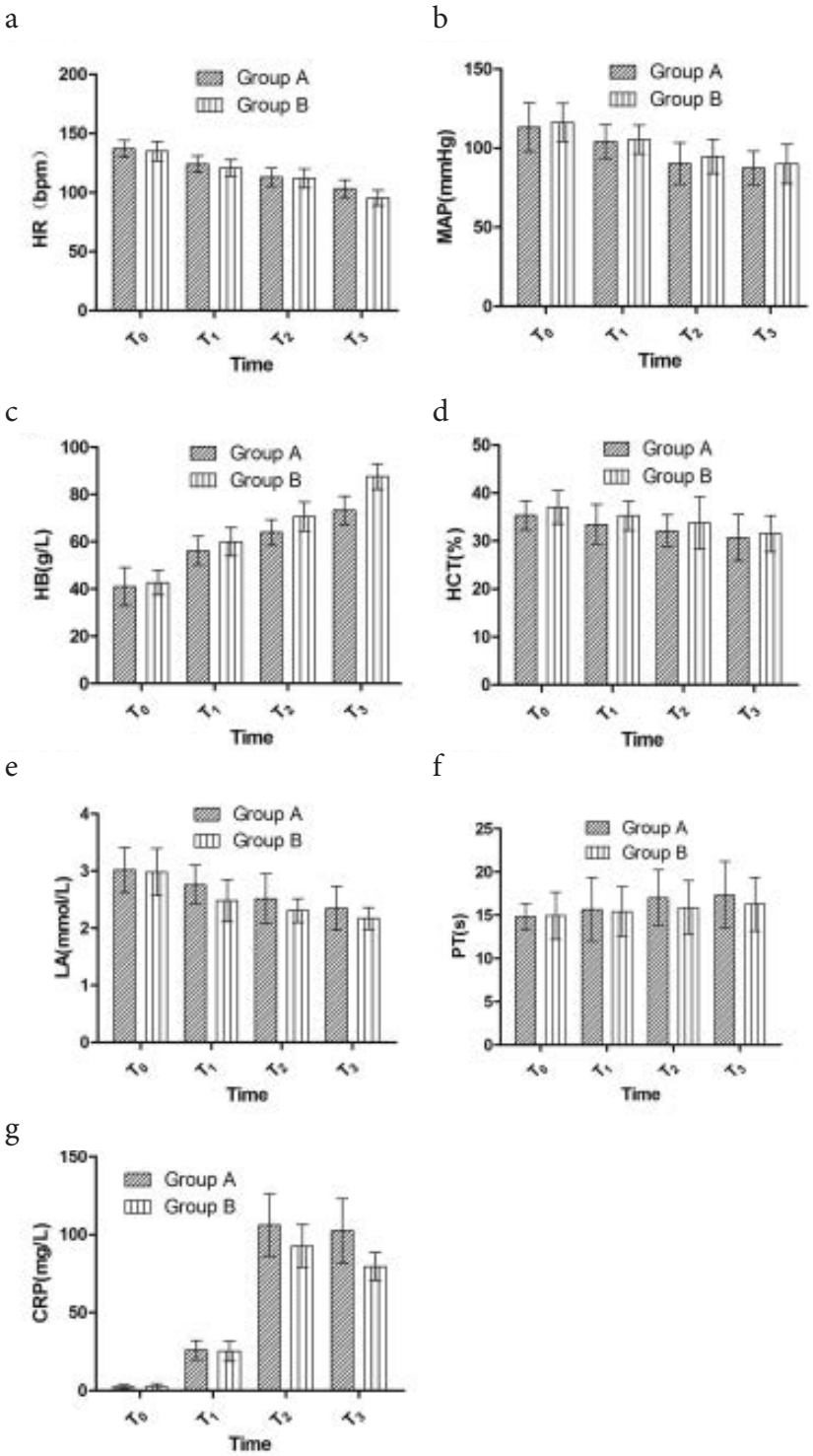

Fig. 1. *Both vital signs (blood pressure, heart rate, breathing and transcutaneous oxygen saturation) and fluid dosage were monitored and recorded every 5 min. At the beginning of resuscitation (T_0) as well as 30 min (T_1), 60 min (T_2) and 120 (T_3) after resuscitation, the following detection indicators were monitored and recorded: heart rate (HR) (**a**), mean artery pressure (MAP) (**b**), hemoglobin (HB) (**c**), hematocrit (HCT) (**d**), arterial blood lacic acid (LA) (**e**), prothrombin time (PT) (**f**), and C-reactive protein(CRP) (**g**).*

significantly lower ($P < 0.05$). Notably, the HR and MAP values for the patients between T_0 of resuscitation and T_1, T_2 and T_3 after resuscitation in both Group A and Group B showed no statistically significant differences ($P > 0.05$).

As demonstrated in Fig. 1e, significantly decreased LA values were detected at T_1, T_2 and T_3 compared with T_0 of resuscitation in Group A ($P < 0.05$). Additional between-group comparisons indicated that there was a greater decrease of LA in Group B than in Group A ($P < 0.05$).

As illustrated in Fig. 1f, significantly increased PT values were detected at T_1, T_2 and T_3 compared with T_0 of resuscitation in Group A ($P < 0.05$). Additional between-group comparisons indicated that there was a similar decrease of PT between Group A and Group B ($P > 0.05$).

As shown in Fig. 1g, the CRP values in both Group A and Group B showed a significant increase at T_2 and T_3 after resuscitation when compared with that upon admission to hospital. In addition, the CRP values in Group B were significantly lower than those in Group A ($P < 0.05$).

DISCUSSION

Volume resuscitation is a crucial part of emergent and critical care medicine. The current study focused on hypertonic sodium chloride hydroxyethyl starch 40 injection (HSH40), which is a patented new drug designated as "*Huomu*" in Chinese. HSH40 was originally developed by Dr Chaoying Zhao, with a chemical composition of 4.2% sodium chloride and 7.6 % hydroxyethyl.

Shock-induced pathophysiological alterations are primarily associated with microcirculation, body fluid metabolism and visceral organs (such as liver and kidney). The major advantage with the HSH40 fluid is its robust capacity to rapidly increase the effective volume of circulating blood, thereby unravelling the clinical obstacle that results from a decrease in extracellular fluid and an increase in intracellular fluid at the shock stage, which has been a challenging difficulty facing the traditional isotonic solution resuscitation (6).

The clinical efficacy of HSH40 on blood coagulation may be a combined consequence of influencing hemodilution, hypertonic sodium chloride and hydroxyethyl starch. Zhang YM et al. (11) have demonstrated the safety, effectiveness and reliability of HSH40 for traumatic shock patients, which may considerably improve the disease state and reduce the recovery time. HSH40 can thus be utilized in combination with other treatments to improve the rates of recovery in patients with traumatic shock. In an animal experiment by Esnault et al. (12), the hypertonic saline compound liquid was shown to exert an anti-shock effect on treating severe chest trauma, with a suppressive function against lung tissue inflammation.

It is widely recognized that the systemic and local defense functions may decline after acute traumatic shock, which may help facilitate bacterial and endotoxin translocation in gastrointestinal tract, respiratory tract and other organs and increase the risks of exogenous and endogenous infection. Our results showed that the CRP concentration was significantly increased in the patients with acute traumatic shock, indicating induced production of CRP and other inflammatory factors as a result of stress factors, such as trauma and surgery. Notably, there was a smaller increase for the CRP rate in the patients from the HSH40 group than from the control group. Compared with previous studies, our treatment approach demonstrated much improved outcomes and significantly diminished complications (16-20). However, given the small sample size in our study, the results need to be independently confirmed by further studies. Furthermore, the prognosis of these patients should be observed for a longer period of time.

In summary, our results demonstrated that blood transfusion and plasma transfusion cannot be administrated in pre-hospital or hospitalized emergency cases. When limited resuscitation was selected for patients with acute traumatic shock, HSH40 was more efficient in terms of its capacity to correct tissue hypoperfusion and suppress stress-induced inflammatory reactions, thus imparting a better preventive effect on the heart, brain, lung and other important organs (13, 14).

ACKNOWLEDGEMENTS

Thanks to Henan Province Medical Science and Technology Key Projects Programs (201303221), Zhengzhou Talents of Science and Technology Plan

Project of Henan Province (131PLJRC682) and Zhengzhou Science and Technology Key Projects Programs of Henan Province (20130595) for their financial support. Thanks to Zhengzhou People's Hospital of affiliated to Southern Medical University for their material support.

REFERENCES

1. Harlak A, Can MF, Mentes O, Ersoz N, Kurt B, Turker T, Yagci G, Tufan T. Does the type of resuscitative fluid affect healing of colonic anastomosis in experimentally induced hemorrhagic shock in rats? Med Princ Pract 2009; 18(4):255-60.
2. Du Z, Liu J, Jia H, Xu W, Zhao X. Three hydrogen-rich solutions protect against intestinal injury in uncontrolled hemorrhagic shock. Int J Clin Exp Med 2015; 8(5):7620-6.
3. Kutcher ME, Howard BM, Sperry JL, et al. Evolving beyond the vicious triad: Differential mediation of traumatic coagulopathy by injury, shock, and resuscitation. J Trauma Acute Care Surg 2015; 78(3):516-23.
4. Delano MJ, Rizoli SB, Rhind SG, et al. Prehospital resuscitation of traumatic hemorrhagic shock with hypertonic solutions worsens hypocoagulation and hyperfibrinolysis. Shock 2015; 44(1):25-31.
5. Esnault P, Prunet B, Cotte J, Cungi PJ, Alonso A, Montcriol A. Hydroxyethyl starch 130/0.4 or hypertonic saline solution to decrease inflammatory response in hemorrhagic shock? Crit Care 2013; 17(5):457.
6. Qureshi AI, Malik AA, Adil MM, Defillo A, Sherr GT, Suri MF. Hematoma enlargement among patients with traumatic brain injury: analysis of a prospective multicenter clinical trial. J Vasc Interv Neurol 2015; 8(3):42-9.
7. Strauss RG, Pennell BJ, Stump DC. A randomized, blinded trial comparing the hemostatic effects of pentastarch versus hetastarch. Transfusion 2002; 42(1):27-36.
8. De Lorenzo C, Calatzis A, Welsch U, Heindl B. Fibrinogen concentrate reverses dilutional coagulopathy induced in vitro by saline but not by hydroxyethyl starch 6%. Anesth Analg 2006; 102(4):1194-200.
9. Roche AM, James MF, Bennett-Guerrero E, Mythen MG. Calcium supplementation of saline-based colloids does not produce equivalent coagulation profiles to similarly balanced salt preparations. J Cardiothorac Vasc Anesth 2006; 20(6):807-11..
10. Krausz MM, Bashenko Y, Hirsh M. Crystalloid and colloid resuscitation of uncontrolled hemorrhagic shock following massive splenic injury. Shock 2001; 16(5):383-8.
11. Zhang YM, Gao B, Wang JJ, Sun XD, Liu XW. Effect of Hypotensive Resuscitation with a Novel Combination of Fluids in a Rabbit Model of Uncontrolled Hemorrhagic Shock. PLoS One 2013; 8(6):e66916.
12. Esnault P, Prunet B, Cotte J, Cungi PJ, Alonso A, Montcriol A. Hydroxyethyl starch 130/0.4 or hypertonic saline solution to decrease inflammatory response in hemorrhagic shock? Crit Care 2013; 17(5):457.
13. Neff, TA, Doelberg M, Jungheinrich C, Sauerland A, Spahn DR, Stocker R. Repetitive large-dose infusion of the novel hydroxyethyl starch 130/0.4 in patients with severe head injury. Anesth Analg 2003; 96(5):1453-59.
14. Hanart, C, Khalife M, De Villé A, Otte F, De Hert S, Van der Linden P. Perioperative volume replacement in children undergoing cardiac surgery: albumin versus hydroxyethyl starch 130/0.4. Crit Care Med 2009; 37(2):696-701.
15. Sloan EP, Koenigsberg M, Clark JM, Desai A. The use of the Revised Trauma Score as an entry criterion in traumatic hemorrhagic shock studies: data from the DCLHb clinical trials. Prehosp Disaster Med 2012; 27(4):330-44.
16. Lienhart HG, Wenzel V, Braun J, et al. [Vasopressin for therapy of persistent traumatic hemorrhagic shock: The VITRIS.at study]. Anaesthesist 2007; 56(2):145-8, 150.
17. Miller JB, Donnino MW, Rogan M, Goyal N. Relative adrenal insufficiency in post-cardiac arrest shock is under-recognized. Resuscitation 2008; 76(2):221-5.
18. Pinto FC, Oliveira MF, Prist R, Silva MR, Silva LF, Capone Neto A. Effect of volume replacement during combined experimental hemorrhagic shock and traumatic brain injury in prostanoids, brain

pathology and pupil status. Arq Neuropsiquiatr 2015; 73(6):499-505.

19. Caputo ND, Kanter M, Fraser R, Simon R. Comparing biomarkers of traumatic shock: the utility of anion gap, base excess, and serum lactate in the ED. Am J Emerg Med 2015; pii: S0735-6757(15)00352-6.
20. Kabu S, Jaffer H, Petro M, Dudzinski D, Stewart D, Courtney A, Courtney M, Labhasetwar V. Blast-associated shock waves result in increased brain vascular leakage and elevated ROS levels in a rat model of traumatic brain injury PLoS One 2015; 10(5):e0127971.

JOURNAL OF BIOLOGICAL REGULATORS & HOMEOSTATIC AGENTS Vol. 29, no. 4, 847-851 (2015)

LETTER TO THE EDITOR

EFFECT OF NEW-PATTERN OBSTETRICAL NURSING IN REDUCING CESAREAN DELIVERY RATE

Y. JIANG and XW. LIU

Department of Obstetrics, Beijing Obstetrics and Gynecology Hospital, Capital Medical University, Beijing, China

Received June 15, 2015 – Accepted September 7, 2015

Spontaneous labor is the preferred delivery way ensuring health of fetus. However, recently, more and more puerperae tend to choose cesarean. However, cesarean delivery is likely to induce various short-term and long-term potential complications, severely threatening maternal and child health. To discuss the clinical effects of new-pattern obstetrical nursing in reducing cesarean delivery rate, 680 primiparas who delivered between December 2011 and December 2013 were selected from Beijing Obstetrics and Gynecology Hospital, Capital Medical University, China as research subjects. They were randomly divided into an observation group (n=340) and a control group (n=340). Primiparas in the observation group were taken care of by new-pattern nursing measures during pregnancy and the puerperal period, while primiparas in the control group received traditional nursing measures. Cesarean delivery rate was compared between two groups. Cesarean delivery rate was statistically significant between the observation group and the control group (21.8% *vs* 32.9%) (P<0.05). Also, it was found that, the incidence rate of perioperative complications of the observation group was much lower than the control group, and the difference was statistically significant (P<0.05). The findings suggest that new-pattern obstetrical nursing is effective in reducing the cesarean delivery rate, therefore is worth promoting and applying in clinical practice.

Currently, some females do not have a thorough understanding of delivery. Fear of pain produced in the delivery process is considered as the major reason for the increasingly higher cesarean delivery rates. Cesarean section is not beneficial to the physical recovery of puerperae after delivery and increases the risk for complications (1, 2). It has been reported that the incidence rate of short- and long-term complications has a positive correlation to the cesarean delivery rate (3). It has also been proved that higher cesarean delivery rate can result in higher incidence rate of late complications (4). Studies (5, 6) have confirmed that, puerperae undergoing cesarean delivery have a 2~4-fold higher possibility of death than puerperae choosing spontaneous labor, and the fatality rate of the newborn is also higher. All this evidence suggests the choice of delivery way is crucial to puerperae and these subjects should choose spontaneous labor (7). Therefore, it is of great significance to inform the puerperae and their family members of the advantages and disadvantages of spontaneous labor, carry out preparatory work for puerperae and lower the cesarean

Key words: new-pattern obstetrical nursing, cesarean delivery rate, complications

Mailing address: Dr Xiaowei Liu,
Department of Obstetrics,
Beijing Obstetrics and Gynecology Hospital,
Capital Medical University,
No.251, Yaojiayuan Street,
Chaoyang, Beijing 100026, China
e-mail: xwlyjy@163.com

0393-974X (2015)

DISCLOSURE: ALL AUTHORS REPORT NO CONFLICTS OF INTEREST RELEVANT TO THIS ARTICLE.

delivery rate in the process of nursing.

To further explore the effect of new-pattern obstetrical nursing in lowering cesarean delivery rate, 680 puerperae who delivered in the obstetrics and gynecology department of Beijing Obstetrics and Gynecology Hospital, Capital Medical University between December 2011 and December 2013 were retrospectively reviewed in this study.

MATERIALS AND METHODS

In the study, 680 primiparae who delivered in Beijing Obstetrics and Gynecology Hospital, Capital Medical University between December 2011 and December 2013 were selected as research subjects. They were aged from 21 to 35 years (average 28.7 ± 3.4 years) and had been pregnant for 36 to 41 weeks (average 38.2±5.5 weeks). Their body mass index (BMI) was between 31 and 42 kg/m^2 (average 39.6±0.8 kg/m^2). All subjects signed informed consent before the study and the study was approved by the medical ethics committee of Beijing Obstetrics and Gynecology Hospital. All of them satisfied natural delivery indications, and had not developed any systemic diseases. They were randomly divided into an observation group and a control group, 340 cases in each group. In the control group, age, gestational time and BMI were 20~32 years (average 27.5±4.4 years), 37~41 weeks (average 39.7±5.3 weeks) and 33~43 (average 37.5±1.1 kg/m^2), respectively, while in the observation group, the corresponding data were 21~34 years (average 29.0±3.2 years), 36~40 weeks (average 37.7±5.9 weeks) and 32~41 kg/m^2 (average 39.9±0.2 kg/m^2). No statistical difference was found in age, gestational weeks and BMI between the two groups; therefore, the results were comparable.

Study method

Puerperae in the control group received traditional nursing. They were examined by obstetricians after being admitted to hospital; their physiological status was observed every day, as well as blood pressure and fetal heart. Furthermore, they received daily nursing (8, 9). The new-pattern nursing was carried out as follows. Firstly, a cozy family-style delivery room and individualized nursing were provided for puerperae. After the puerperae were admitted into the delivery room, obstetric nurses introduced themselves first to narrow the distance between them. In addition, those nurses kept communicating with the puerperae before delivery. The second step was health education. Full-time obstetric nurses informed the puerperae and their family members of the advantages of natural delivery as well as disadvantages of cesarean delivery in forms of issuing promotional materials, face-to-face instruction and compact disc. Moreover, puerperae were evaluated based on health condition, self-care ability, personality, habits, cultural background and support from family and society in order to provide individualized scientific guidance. Next was psychological support. The puerperae were given parturient information, progress of labor, possible discomfort and coping skills; health problems and the target objective were discussed actively and effectively, in order to reduce the anxiety of puerperae and their family members, encourage puerperae to establish confidence for natural delivery and also establish a good doctor-patient relationship. Furthermore, puerperae were asked to sign natural delivery agreement with primary nurses and doctors after physical and obstetric examination. Puerpurea and their family members were all involved in the formulation and implementation of the nursing plan, which was beneficial to build trust and a dependency relationship with medical workers, reduce anxiety and depression of puerperae as well as improve adaption ability, self-care ability and subjective initiative of puerperae. Different nursing measures were used in different labor stages. A one-to-one delivery responsibility system was adopted in the whole process. In the first labor stage, family members of puerperae were permitted to enter the delivery room to provide emotional support and encourage puerperae to eat and rest. When the uterus cervix had widened 3 cm, obstetrical nurses offered timely delivery information to guide puerperae to relax and breathe and help improve their tolerance to pain by massaging the lumbosacral portion or hypogastria. The next step was the enhancement of self-efficacy. Means of motivation, social support and substitute experience were used to improve self-efficacy of puerperae coping with delivery pressure, which was useful for improving spontaneous labor rate, shortening duration of labor and reducing incidence rate of fetal intrauterine distress. To find or prevent perinatal and pregnancy complications early, high-risk pregnant women were taken care of by specially-assigned persons. Moreover, obstetrical nurses help them to cope with labor pain by means of asking them to take deep breaths, touching the lumbosacral portion and telling stories. To help the puerperae pass the delivery period comfortably, painless labor technology was used in the delivery process. Complications which might occur to mother and newborn in the perinatal period were monitored closely.

Observation index

The incidence rate of complications in the near future, cesarean delivery rate and duration of labor were compared between the two groups.

Statistical analysis

SPSS 19.0 statistics were used for data processing. Measurement data were expressed by mean ± standard deviation and controlled by *t* test, and enumeration data

expressed as percentages were also compared. Differences were statistically significant if P<0.05.

RESULTS

Comparison of choice of parturition before and after nursing

Results showed that choice of parturition was remarkably different before and after nursing (P<0.05); besides, fewer puerperae in the group receiving new-pattern obstetrical nursing chose cesarean delivery, compared to the group receiving traditional nursing. Details are shown in Table I.

Comparison of cesarean delivery rate in the two groups

The data show that puerperae who chose cesarean delivery in the observation group were remarkably fewer than in the control group, and the difference was statistically significant (P<0.05) (Table II).

Comparison of duration of labor in the two groups

Puerperae in the control group and observation group had obvious differences in the duration of labor. Puerperae in the observation group mostly completed delivery with 6~12 h, while most puerperae in the control group spent 12~24 h (Table III).

Comparison of incidence of complications after delivery in two groups

Table IV demonstrates that no significant differences were observed in indexes of average bleeding volume, anemia and apnea rate of newborns between the cesarean delivery and natural delivery groups (P>0.05). None of the puerperae in the two groups suffered severe complications, such as disseminated intravascular coagulation (DIC), uterine arterial embolization, hysterectomy and maternal death.

Table I. *Comparison of delivery means selection before and after nursing in two groups.*

Group	Number of cases	Delivery means selection before nursing (cesarean delivery/vaginal delivery)	Delivery means selection after nursing (cesarean delivery/vaginal delivery)
Control group	340	153/187	112/288
Observation group	340	144/196	72/266
χ^2		0.48	10.68
P		0.48	0.00

Table II. *Comparison of choice of delivery way in two groups.*

Group	Cesarean delivery rate	Spontaneous labor
Observation group (n=340)	72 (21.2%)	268 (78.8%)
Control group (n=340)	112 (32.9%)	228 (67.1%)

Table III. *Comparison of total duration time of labor in two groups.*

	6~12 h	12~24 h	Number of cases	Percentage of over 12 h (%)
Observation group	173 (51%)	167 (49%)	340	49.00
Control group	126 (37%)	214 (63%)	340	63.00

n(%)

Table IV. *Comparison of incidence of complications after delivery in two groups.*

Complication	Cesarean delivery (n =340)	Natural delivery (n =340)	χ^2 or t	p
Average bleeding volume (ml)	217.2±17.3	207.5±57.4	0.873	0.407
DIC	0	0		
Uterine arterial embolization	0	0		
Hysterectomy	0	0		
Maternal death	0	0		
Moderate anemia	20(5.9)	13(3.8)	3.362	0.407
Neonatal asphyxia rate	1(0.029)	0	1.001	0.317

n, n (%), (mean ± standard deviation)

DISCUSSION

Pregnancy and delivery are normal and natural physiological processes for females. However, under the influence of improper publicity regarding delivery pain and lack of delivery experience more and more primiparas are inclined to choose caesarean delivery (10, 11). Some evidence (12, 13) has suggested that innovated obstetrical nursing can help puerperae and their family members to correctly understand the complications of caesarean delivery and the scientific and humanistic nursing which can help puerperae overcome the psychological burden and establish confidence for natural delivery (14). Moreover, creative obstetrical nursing can support puerperae at psychological, physical and mental levels (15, 16). In this study, we compared the parturition rate in observation and control groups and found fewer puerperae in the observation group, which adopted new-pattern obstetrical nursing, chose cesarean delivery compared to the control group; and there was a statistically significant difference ($P<0.05$). Additionally, it was found that puerperae in the observation group delivered in shorter time, recovered better after delivery and were less likely to have complications compared to the control group.

To sum up, the new-pattern obstetrical nursing has proved to be able to convince puerperae and their family members to choose spontaneous labor, make spontaneous labor smoother and thus lower the cesarean delivery rate

Therefore, the new pattern obstetrical nursing as a high-quality nursing mode satisfying psychological and physical demands should be applied more in clinical practice.

REFERENCES

1. Zongo A, Dumont A, Fournier P, Traore M, Kouanda S, Sondo B. Effect of maternal death reviews and training on maternal mortality among cesarean delivery: post-hoc analysis of a cluster-randomized controlled trial. Eur J Obstet Gynecol Reprod Biol 2015; 185:174-80.
2. Cyr RM. Myth of the ideal cesarean section rate: Commentary and historic perspective. Am J Obstet Gynecol 2006; 194(4):932-36.
3. Rabilloud M, Ecochard R, Guilhot J, Toselli A, Mabriez JC, Matillion Y. Study of the variations of the cesarean sections rate in the Rhône-Alpes region (France): Effect of women and maternity service characteristics. Eur J Obstet Gynecol Reprod Biol 1998; 78(1):11-17.
4. Kilsztajn S, Carmo MS, Machado LC, Lopes ES, Lima LZ. Caesarean sections and maternal mortality in Sao Paulo. Eur J Obstet Gynecol Reprod Biol 2007; 132(1):64-69.
5. Penna L, Arulkumaran S. Cesarean section for non-medical reasons. Int J Gynaecol Obstet 2003; 82(3):399-409.
6. Kasai EK, Nomura RMY, Benute G, Lucia MCS de,

Zugaib M. Women's opinions about mode of birth in Brazil: a qualitative study in a public teaching hospital. Midwifery 2010; 26(3):319-26.
7. Freitas PF, Drachler ML, Leite JC, Marshall T. Inequalities in cesarean delivery rates by ethnicity and hospital accessibility in Brazil. Int J Gynecol Obstet 2009; 107(3):198-201.
8. Lowe NK. A Review of factors associated With dystocia and cesarean section in nulliparous women. J Midwifery Womens Health 2007; 52(3):216-28.
9. Turan C, Kutlay B. Cesarean section rates and perinatal outcomes in resident and midwife attended low risk deliveries. Eur J Obstet Gynecol Reprod Biol 1995; 62(1):3-5.
10. Blanchette H. Comparison of obstetric outcome of a primary-care access clinic staffed by certified nurse-midwives and a private practice group of obstetricians in the same community. A J Obstet Gynecol 1995; 172(6):1864-71.
11. Sakala C. Medically unnecessary cesarean section births: Introduction to a symposium. Soc Sci Med 1993; 37(10):1177-98.
12. DeMott RK, Sandmire HF. The Green Bay cesarean section study. II. The physician factor as a determinant of cesarean birth rates for failed labor. Am J Obstet Gynecol 1992; 166(6):1799-810.
13. Flamm BL, Lim OW, Jones C,Fallon D, Newman LA, Mantis JK. Vaginal birth after cesarean section: Results of a multicenter study. Am J Obstet Gynecol 1988; 158(5):1079-84.
14. Macones GA, Peipert J, Nelson DB, et al. Maternal complications with vaginal birth after cesarean delivery: A multicenter study. Am J Obstet Gynecol 2005; 193(5):1656-62.
15. Sakala C. Midwifery care and out-of-hospital birth settings: How do they reduce unnecessary cesarean section births? Soc Sci Med 1993; 37(10):1233-50.
16. LoCicero AK. Explaining excessive rates of cesareans and other childbirth interventions: Contributions from contemporary theories of gender and psychosocial development. Soc Sci Med 1993; 37(10):1261-69.

JOURNAL OF BIOLOGICAL REGULATORS & HOMEOSTATIC AGENTS Vol. 29, no. 4, 853-858 (2015)

LETTER TO THE EDITOR

EXPRESSION AND CLINICAL SIGNIFICANCE OF P53, O6-METHYLGUANINE-DNA METHYLTRANSFERASE AND EPIDERMAL GROWTH FACTOR RECEPTOR IN GLIOMA

XR. FU, ZC. SUN and Y. CHANG

Oncology Department, The First Affiliated Hospital of Zhengzhou University, Henan, China

Received May 5, 2015 – Accepted July 29, 2015

The first two authors contributed equally to the work

Glioma is a serious life-threatening disease, the pathogenesis of which remains to be investigated. The objective of the present investigation was to explore the expression and clinical significance of tumor suppressor gene (P53), O6-methylguanine-DNA methyltransferase (MGMT) and epidermal growth factor receptor (EGFR) in glioma. Immunohistochemical staining was applied to study the clinical characteristics of 40 samples from glioma patients, detect the expression of and analyse the relationship between P53, MGMT and EGFR and glioma. The results demonstrated that the positive expression rate of P53 was 47.5% in 40 cases of glioma samples, of which the expression of P53 in the high grade glioma was higher than that of the low grade samples ($P < 0.05$); the positive expression rate of MGMT was 37.5%, but there was no significant significance of MGMT expression between the high grade glioma and the low grade glioma ($P > 0.05$); the positive expression rate of EGFR was 55%, of which the expression of EGFR of the high grade glioma was higher than that of the low grade glioma ($P < 0.05$). There was no significant difference in the expressions of P53, MGMT and EGFR in the glioma patients of different ages, gender and with different tumor sizes. The expressions of P53 and MGMT were negatively correlated ($P < 0.05$). The expressions of P53 and EGFR were positively correlated ($P < 0.05$). In conclusion, P53, EGFR and MGMT could play a role in the occurrence, development and deterioration of glioma.

Glioma is a common primary intracranial central nervous system tumor. The malignant degree, recurrence and the mortality rate of glioma patients are high. Treatment of the disease is very difficult, as if the tumor suppressor gene P53 (P53) is mutated, it will lose tumor suppressor function. The mutated P53 has cell malignant transforming ability. O6-methylguanine-DNA methyltransferase (MGMT) is a DNA repair enzyme. MGMT not only is related to drug resistance against alkylating agents in glioma, but is also is associated with the malignant transformation of glioma. Epidermal growth factor receptor (EGFR) is a transmembrane glycoprotein with kinase activity. EGFR participates in regulating the occurrence, repair, survival, angiogenesis, invasion and metastasis of tumor cells.

Key words: cancer, occurrence and development, P53, O6-methylguanine-DNA methyltransferase (MGMT), epidermal growth factor receptor (EGFR), glioma

Mailing address: Dr XR. Fu,
Oncology Department,
The First Affiliated Hospital
of Zhengzhou University,
Zhengzhou, 450052, China
Tel.: +371 65528998 Fax: +371 65528998
e-mail: editfxr@163.com

0393-974X (2015)

This study detected and analyzed the expressions of the proteins P53, MGMT and EGFR of cerebral glioma samples from 40 patients by using immunohistochemical analysis in order to explore their effects on glioma.

MATERIALS AND METHODS

Cerebral glioma samples and the relevant clinical data were collected from 40 cases of glioma patients (26 male, 14 female; ages 10-74 years, average age 44.5 years) from March 2013 to September 2014 from the First Affiliated Hospital of Zhengzhou University. All the patients gave their informed consent to participate in this study.

The clinical data of the patients were as follows: 40 cases of glioma were pathologically diagnosed. According to the classification criteria of the nervous system tumors of World Health Organization (WHO) in 2000, this study had histologically classified and graded all the neoplasms: 18 cases in the low grade malignant group (I/II grade) and 22 cases in the high grade malignant group (III/IV grade). None of the patients had received any radiation therapy or chemical therapy after registration in the First Affiliated Hospital of Zhengzhou University. All the samples had been prepared by using Hematoxylin and Eosin (HE) staining method, and the samples were diagnosed again by a pathologist.

Main reagents and methods

The main reagents included rat anti-human P53 monoclonal antibody, rat anti-human MGMT monoclonal antibody, and rat anti-human EGFR monoclonal antibody. S-100 protein (SP) reagent kit; 3,3'-diaminobenzidine tetrahydrochloride (DAB) enzyme substrate chromogenic reagent kit. The above reagents were purchased from Beijing ZSGB-BIO ORIGENE company. SP immunohistochemical staining method was applied in the present study. Paraffin samples with 4 μm thickness were prepared, and the samples were then subjected to Immunohistochemical staining analysis.

Staining intensity was scored as follows: 0 point for colorless, 1 point for light yellow, 2 points for tan color, and 3 points for brown color. The positive rate of cells was scored as follows: 0 point for negative, 1 point for positive rate of cells of no less than 10%, 2 points for positive rate of cells of between 11% and 50%, 3 points for positive rate of cells of between 51% and 75%, 4 points for positive rate of cells of more than 75%. The results of more than 3 points was regarded as a positive immune reaction. Five samples were randomly selected for high magnification analysis (10 x 40 times), and the positive rate of stained cells was calculated. P53 protein positive straining was the sample with yellow nucleus or tan particles. MGMT protein positive staining was the sample with slurry yellow nucleus or tan particles. EGFR protein positive staining was the sample with yellow or tan granule cell membrane or cytoplasm.

Statistical analysis

SPSS 15.0 software was used for analysis. *Chi*-squared and Spearman's correlation analysis ($P < 0.05$) were used to analyze the expressions of P53, MGMT and EGFR in the glioma patients with different degrees of malignant glioma, tumor sizes, expression differences and correlation between indicators of different ages and genders.

RESULTS

The positive expression rates of P53, MGMT and EGFR in glioma were 47.5%, 37.5% and 55%, respectively. P53-positive expression rate of glioma tissues with low grade of I and II stage was 27.8%, and P53-positive expression rate of glioma tissues with high grade of III and IV stage was 63.6%. P53-positive expression rate in the high grade glioma was higher than that in the low grade glioma ($P < 0.05$). MGMT-positive expression rate of low grade I and II stage in glioma tissues was 44.4%, and the high level of that in glioma tissue was 31.8%. There was no significant difference in the MGMT positive expressions of the high and low grade gliomas ($P > 0.05$). EGFR-positive expression rate in the low grade I and II stages of glioma tissue was 33.3%, and EGFR-positive expression rate in the high grade III and IV stages in glioma tissues was 72.7%. EGFR-positive expression rate in the high grade glioma tissues was higher than that in the low grade glioma tissues ($P < 0.05$), as shown in Table I.

In 26 cases of male patients with glioma, the positive expression rate of P53 was 46.2%, and the positive expression rate of MGMT was 38.5%. In comparison, the positive expression rate of EGFR was 57.7%; in 14 cases of female patients, the positive expression rate of P53 was 50%, MGMT positive expression rate was 35.7%, and EGFR positive expression rate was 57.7%. In the 28 cases of patients aged under 50 years, P53-positive expression rate was 46.4%, MGMT-positive expression rate was 28.6%, and EGFR-positive expression rate was 50%; in the 12 cases of patients

aged over 50 years, P53-positive expression rate was 50%, MGMT-positive expression rate was 58.3%, EGFR-positive expression was observed in 8 cases, and the rate was 66.7%. In 14 cases of patients with glioma of maximum diameter less than 5 cm, P53-positive expression rate was 28.6%, MGMT-positive expression rate was 42.9%, and EGFR-positive expression rate was observed in 5 cases, and the rate was 35.7%. In 26 cases of patients with maximum diameter of no less than 5 cm, P53-positive expression rate was 57.7%, MGMT-positive expression rate was 34.6%, and EGFR-positive expression rate was 65.4%. There was no significant difference of the expressions of P53, MGMT and EGFR in glioma patients of different gender, different ages (over or under 50 years), and tumor size less than or more

Table I. *Expression of P53, MGMT and EGFR in glioma.*

	P53					MGMT					EGFR				
Grade	Positive (n)	Negative (n)	Positive rate	χ^2	P	Positive (n)	Negative (n)	Positive rate	χ^2	P	Positive (n)	Negative (n)	Positive rate	χ^2	P
I or Ⅱ	5	13	27.8%			8	10	44.4%			6	12	33.3%		
III or IV	14	8	63.6%	5.105	0.024	7	15	31.8%	0.673	0.412	16	6	72.7%	6.208	0.013
Total	19	21	47.5%			15	25	37.5%			22	18	55.0%		

Table II. *P53, MGMT and EGFR expression in different clinical features of patients with glioma. n (%).*

			P53				MGMT				EGFR			
	Grouping	n	Positive (n)	Positive expression rate	χ^2	P	Positive (n)	Positive expression rate	χ^2	P	Positive (n)	Positive expression rate	χ^2	P
Gender	Male	26	12	46.2%	1	0.539	10	38.5%	0.029	0.864	15	57.7%	0.218	0.641
	Female	14	7	50.0%			5	35.7%			7	50.0%		
Age (years)	< 50 years	28	13	46.4%	0.143	0.836	8	28.6%	3.175	0.075	14	50.0%	0.590	0.533
	≥ 50 years	12	6	50.0%			7	58.3%			8	66.7%		
Tumor size (cm)	< 5 cm	14	4	28.6%	2.037	0.154	6	42.9%	0.264	0.608	5	35.7%	3.237	0.072
	≥ 5 cm	26	15	57.7%			9	34.6%			17	65.4%		

Table III. *Correlation between P53, MGMT and EGFR.*

		MGMT		r	P	EGFR		r	*P*
		Positive (n)	Negative (n)			Positive (n)	Positive (n)		
	Positive (n)	4	15			16	3		
P53				-0.323	0.042			0.558	0.000
	Positive (n)	11	10			6	15		
	Positive (n)	6	16						
EGFR				-0.234	0.147				
	Positive (n)	9	9						

than 5 cm, ($P > 0.05$), as illustrated in Table II.

In glioma tissues, P53-positive expression was negatively correlated with MGMT-positive expression (r = -0.323, $P < 0.05$). P53-positive expression was positively correlated with DGFR-positive expression (r = 0.559, $P < 0.05$). MGMT positive expression was not correlated with EGFR positive expression (r = -0.234, $P > 0.05$), as shown in Table III.

DISCUSSION

The functions of P53 gene include DNA binding, controlling of cell cycle, DNA repair, cell apoptosis, participating in cell differentiation and gene plasticity regulation. P53 protein was mainly induced by programmed cell death to enhance cell apoptosis, and then it served as the tumor suppressor (1). Mutated P53 not only did not have tumor suppressor function, but also had cell malignant transformation ability, leading to spreading of malignant tumors. The protein conformation of mutated P53 protein could change with increased stability and prolonged half-life. The expression rate of P53 in this study was 27.8% in the low grade I/II glioma ; and the expression rate of P53 in this study was 63.6% in the high grade glioma for III/IV grade. The expression rate of P53 in the high grade glioma was significantly higher than that of the low grade glioma, which prompted wild type P53 gene inactivation and participation in the occurrence and development of glioma, which might be one of the indicators of poor prognosis.

MGMT is a DNA repair protein, which could remove the 6th part of DNA guanine oxygen and mutate alkyl adduct, and could restore the damage of guanine in order to protect cells from alkylating agents. Therefore, the high expression of MGMT would affect the curative effect of alkylating agents, and MGMT was the molecular basis for drug resistance of cells against alkylating agent drugs. Research data confirmed that MGMT expression in glioma tissues could significantly influence the treatment effect of alkylating agents, and then affect the prognosis of the patients with glioma (2). This study indicated that the expression of MGMT had no relationship with age and gender of the glioma patients, indicating that MGMT expression might have no relationship with endocrine hormone levels. In this study, MGMT positive expression rate exhibited no significant difference in different degrees of malignant glioma, which was similar with the study of Ji and Zhou (3). Different research institutes had different results on MGMT expression in glioma. Some results showed that the MGMT

positive expression rate of the high grade glioma was significantly lower than that in the low grade glioma (4, 5), whereas other scholars had different results. Sun YH, et al. (6) suggested that MGMT expression in the high grade glioma was significantly higher than that of the low grade glioma, and the positive expression increased with the rising of the malignant degrees of glioma. It was supposed that MGMT was correlated with the malignant degree of tumor, and the survival time of the patients with MGMT positive expression was significantly lower than that of the MGMT negative expression patients. Why were the two experimental results different? The reason might be related to the heterogeneity of distribution and expression of MGMT in different tumor tissues. In the same section of this research, the staining and distribution of MGMT positive stained cells were not evenly distributed. At the same time, it can also be analyzed from the MGMT effect on the target cells.

MGMT had the function to repair the damaged DNA, but it had varied effects on different cells (7). For tumor cells, DNA repair in tumor cells could enable drug resistance of tumor cells against alkylating agent chemotherapy. One study (8) proved that the glioma patients with MGMT negative expression had achieved promising curative effects under therapy with temozolomide alkylating agent drug. If MGMT was applied on the non-tumor cells of the patients, it could protect cells from the outside carcinogenic factors of alkylating agents. However, this hypothesis needs to be further investigated.

EGFR is expressed and produced by proto-oncogene cerbB-1. Over-expression of EGFR or/ and mutation of EGFR in tissue cells enabled replication of cell DNA and excessive cell division, resulting in incontrollable cell growth and malignant transformation. Studies in the literature (9-11) indicated that there was high expression of EGFR in many malignant tumors, such as lung cancer, gastric cancer, nasopharyngeal carcinoma. It prompted the occurrence of many tumors which had a certain relationship with the expression of EGFR. The present study showed that EGFR positive expression rate in the high grade glioma was significantly higher than that in the low grade glioma, which was similar with the research results from Wang YG et al (12), which showed that the EGFR positive expression might be the malignant progress of glioma. Tumor with EGFR positive expression had better activity of cell division and proliferation, and EGFR played an important role in the glioma malignant process.

The results of the present study proved that P53 was negatively correlated with MGMT expression, and the mechanism may be the protection of the tumor cells from high expression of DNA repair enzyme MGMT in tissues on P53 gene DNA. In experiments on mice, Blough (13) found that MGMT expression decreased significantly in P53 gene mutated cells of star glioma cells. Hence, P53 had an important role in the expression and transcription of MGMT gene. More mutual interactions and mechanisms between P53 and MGMT need to be researched. At the same time, the expressions of P53 and EGFR in glioma tissues increased along with the worsening of tumor malignant degree, and they showed positive correlation. It has been proved that P53 and EGFR might participate in the glioma malignant transformation and development. It is possible that P53 mutation induced over-expression of EGFR. However, the specific function of disease occurrence and development of P53, MGMT and EGFR in glioma and the issue of whether P53 could promote expression of MGMT and EGFR need to be further explored.

The RT-PCR results revealed that there was no significant change in the expressions of P53, MGMT and EGFR in glioma tissues and control tissues. Furthermore, because it was very hard to exclude the interference of other tissues and cells, the protein expressions of P53, MGMT and EGFR in various tissues were not detected in the current research. In addition, the immunohistochemical results clearly demonstrated that P53, EGFR and MGMT might be involved in occurrence, development and deterioration of glioma. Further research is necessary to confirm these results.

REFERENCES

1. Ikeguchi M, Makino M, Kaibara N. Telomerase activity and p53 gene mutation in familial polyposis coil. Anticancer Res 2000; 20(5c):3833-37.
2. Hegi ME, Diserens AC, Gorlia T, et al. MGMT gene silencing and benefit from temozolomide in glioblastoma. N Engl J Med 2005; 325(10):997-1003.

3. Ji L, Zhou FM. The correlation of the expression of MGMT and P53 in human brain gliomas with tumor grade or prognosis. Chin J Clin Neurosci 2011; 19(6):588-93.
4. Yuan Q, Matsumoto K, Nakabeppu Y, et al. A comparative immunohistochemistry of O^6-methylguanine-DNA methyltransferase and p53 in diffusely infiltrating astroylomas. Neuropathology 2003; 23(3):203.
5. Horbinski C, Hamilton RL, Lovell C, Burnham J, Pollack IF. Impact of morphology, MIB-1, p53 and MGMT on outcome in pilocytic astrocytomas. Brain Pathol 2010; 20(3):581-8.
6. Sun YH, Zhang YZ, Wang ZC, et al. Relationship between the expression of O^6-methylguanine-DNA methyltransferase in glioma and the survival time og patients. Chinese Journal of Cancer 2004; 23(9):1052-55.
7. Brown RC, Degenhardt B, Kotoula M, Papadopoulous V. Location-dependent role of the human glioma cell peripheral-type benzodiazepine receptor in proliferation and steroid biosynthesis. Cancer Lett 2000; 156(2):125-32.
8. Roger S, Monika EH, Warren PM, et al. Effects of radiotherapy with concom intant and adjuvant temozolomide versus radiotherepy along on survival in glioblastoma in randomized plase study 5-year analysis of the EORTC-NCIC trail. Lancet Oncol 2009; 10(11):459-66.
9. Meert AP, Martin B, Delmotte P, et al. The role of EGFR expression on patient survival in lung cancer: a systematic review with meta-analysis. Eur Respir J 2002; 20(4):975-81.
10. Bhardwaj A, Ganesan N, Tachibana K, Rajapakshe K, Albarracin CT, Gunaratne PH, Coarfa C, Bedrosian I. Annexin A1 preferentially predicts poor prognosis of basal-like breast cancer patients by activating mTOR-S6 signaling. PLoS One 2015; 10(5):e0127678.
11. Xie YQ, Wu XB, Tang SQ. Curcumin treatment alters ERK-1/2 signaling in vitro and inhibits nasopharyngeal carcinoma proliferation in mouse xenografts. Int J Clin Exp Med 2014; 7(1):108-14.
12. Wang YG, Zhan YP, Pan SY, Wang HD, Zhang DX, Gao K, Qi XL, Yu CJ. Hyperbaric oxygen promotes malignant glioma cell growth and inhibits cell apoptosis. Oncol Lett 2015; 10(1):189-95.
13. Blough MD, Zlatescu MC, Cairncross JG, et al. O6-methylguanine-DNA methyltransferase regulation by p53 in astrocytic cell. Cancer Res 2007; 67:580-84.

JOURNAL OF BIOLOGICAL REGULATORS & HOMEOSTATIC AGENTS Vol. 29, no. 4, 859-863 (2015)

LETTER TO THE EDITOR

UNEXPECTEDLY HIGH OCCURRENCE OF *ESCHERICHIA COLI* AND *STAPHYLOCOCCUS AUREUS* ISOLATES FROM RAW MILK IN ILAM, WESTERN IRAN

M. TAHERIKALANI[1], S. HEMATI[2], K. HEIDARZADI[2], Z. MAHDAVI[2], F. GHANBARI[2], M. MOHAMADI[2], S. GHAFOURIAN[2], A.M. VARZI[3], F. AZIZI JALILIAN[4], L. BOGDANOVIC[5] and K. SAKI[6]

[1]Razi Herbal Medicines Research Center and Department of Microbiology, School of Medicine, Lorestan University of Medical Sciences, Khorramabad, Iran; [2]Clinical Microbiology Research Center, Ilam University of Medical Sciences, Ilam, Iran; [3]Department of Immunology, School of Medicine, Lorestan University of Medical Sciences, Khorramabad, Iran; [4]Department of Microbiology, School of Medicine, Hamadan University of Medical Sciences, Hamadan, Iran; [5]Department of Public Health, University of Naples Federico II, Naples, Italy, [6]Department of Psychiatry, School of Medicine, Shahid Beheshti University of Medical Sciences, Tehran, Iran

Received July 19, 2015 – Accepted September 16, 2015

Raw milk contains diverse nutritional components that provide a suitable medium for spoilage and the growth of potentially pathogenic microorganisms. Unpasteurized milk consumption by a large number of people can threaten health and increase public concerns. In this study, sixty-two raw cow's milk samples were collected from the dairy farms of Ilam, Western Iran. All samples were collected in sterilized containers and were transferred via ice boxes to the laboratory. Isolates were then identified by standard methods. Totally, 88.7% (n=55) of samples were contaminated. Our study also showed that *Escherichia coli* had a high prevalence among isolates (43: 69.4%), while *Klebsiella pneumoniae* and *Klebsiella planticola* showed the lowest prevalence (1: 1.6%). *Staphylococcus aureus* was also detected in 17.7% (n=11) of samples. The raw milk microbial contamination is complex. Some of the microorganisms threaten public health via different traits, therefore it is recommended that raw milk consumption should be avoided.

Today, dairy products are the most important part of the human diet (1). Milk composition includes lipids, proteins, carbohydrates, amino acids, vitamins and minerals. This diversity makes it a suitable medium for growth of pathogenic microorganisms (2-4). Recently, food safety activities, such as milk pasteurization and biopreservation techniques were developed to reduce zoonotic pathogens and milk-borne diseases (1, 5, 6).

Staphylococcus aureus, enterotoxigenic coagulase-negative strains, *Salmonella* spp, *Listeria monocytogenes*, pathogenic *E.coli*, *Campylobacter* spp, *Bacillus cereus*, *Clostridium botulinum* and *Pseudomonas* spp are known pathogen bacteria in raw milk (1-3, 7, 8). These isolates also have unfavorable effects on the milk quality and its products (7).

Enterobacteriaceae family including *Salmonella*

Key words: raw milk, Escherichia coli, Staphylococcus aureus

Mailing address: Dr Kourosh Saki,
Department of Psychiatry,
School of Medicine,
Shahid Beheshti,
University of Medical Sciences,
Tehran, Iran
e-mail: kooreshss@gmail.com

0393-974X (2015)

spp, *Yersinia* spp and *Shigella* spp are human pathogens and their presence in milk is associated with low hygienic quality, and contamination through fecal origin, as well as poor cooling conditions such as time and temperature of refrigeration (9).

The other important opportunistic pathogens such as *Klebsiella oxytoca*, *Enterobacter cloacae*, *Klebsiella pneumonia*, *E.coli* and *Pseudomonas,* with high ability to grow in milk should be considered (9). Some psychotropic spp (i.e. *Pseudomonas*) cannot resist heating conditions, but their heat-resistant photolytic and lipolytic enzymes, which are secreted in raw milk, during the cold storage, can withstand pasteurization and ultrahigh temperature treatments (UHT) and alter dairy product qualities (3, 7, 9, 10).

Unpasteurized milk consumption is a major public health issue worldwide (3, 11), therefore, the aim of the present study was to determine the potential microbial pathogens in raw cow's milk, among samples collected from different locations of Ilam, Iran (11).

MATERIALS AND METHODS

Sampling

Sixty-two raw milk samples were collected from dairy farms in Ilam, Iran, from December 2014 to March 2015. All samples were collected in sterilized containers and transferred in an ice box to the Microbiology Laboratory of Ilam University of Medical Sciences.

Microbial evaluation

In case of *Enterobacteriace* spp., the raw milk was transferred into separated 2% brilliant green bile broth (BGBB) tubes and was incubated for 18-24 h at 37°C. Then, the isolates were identified by standard protocols. The Mannitol Salt Agar (Oxoid) was used for the enumeration of *S. aureus*. The plates were incubated at 37°C for 48 h. Yellow colonies were counted and checked for gram and catalase reactions. Also, the isolated colonies were checked for their coagulation on rabbit plasma. Catalase positive Gram negative colonies were spread and cultured on Trypticase Soya Agar slants for further characterization (12).

Statistical analysis

Descriptive results were expressed by percentages, means and standard deviations (SD). To identify any correlation, the c^2 and the Fisher's exact test were used. P values <0.05 were considered statistically significant.

RESULTS

The results demonstrated that 55 (88.7%) samples were contaminated, while in 7 (11.29%) samples no pathogenic bacteria were found. Our findings showed that *E.coli* was the most prevalent pathogen isolated (43: 69.4%), while *K. pneumoniae* and *K. planticola* showed the lowest frequency (1: 1.6%, respectively). *S. aureus* was also identified in 17.7% of all milk samples. These findings demonstrate that there was a significant correlation between existence of *E.coli* isolates and raw milk contamination (P=0.001). The results are summarized in Table I.

DISCUSSION

The contamination control of milk and its products is known as an important proceeding for both economical and health purposes (13). Contamination sources of raw milk were mainly unidentified, but they may be associated with unhealthy animals, milking machines, unclean teats, fecal contaminations, housings, quality of feed and food stuffs, storage conditions (temperature at which milk is stored and the time that elapses between milk production and collection), other non-bovine animals, air, water (used for cleaning utensils and animals), equipment and other environmental sources (3, 4, 13, 14). Therefore, it could be concluded that milk contamination occurs via multiple ways (13).

In this study, we used BGBB media, which is applied for coliform identification and enumeration,

Table I. *Prevalence of bacteria in the raw milk samples.*

Bacterial spp	N (%)		P values
	Positive	Negative	
K. pneumoniae	1 (1.6%)	61 (98.4%)	0.7
K. planticola	1 (1.6%)	61 (98.4%)	0.7
P. aeruginosa	3 (4.8%)	59 (95.2%)	0.498
E. hormaechei	6 (9.7%)	56 (90.3%)	0.325
S.aureus	11 (17.7%)	51 (82.3%)	0.675
E.coli	43 (69.4%)	19 (30.6%)	0.001

but interestingly, after subculturing on the BHI agar we observed *S. aureus* (11, 17.7%). *S. aureus* is known as the most prevalent and economically significant pathogen for intramammary infections in dairy herds and is responsible for approximately 30-40% of all mastitis (15). It is also considered as the third most important food-borne illnesses agent (16, 17). *S. aureus* has been reported as a prevalent pathogen by many other studies (3, 18, 19), which is consistent with our results.

High levels of *Enterobacteriaceae spp* in raw milk are a serious concern, especially in those consumers that use unpasteurized milk. The presences of *Enterobacteriaceae* spp are considered an indicator to assess food microbial quality; however, their high populations may constitute a serious obstacle (20). In agreement with our findings, some previous studies showed high frequency of *Enterobacteriaceae spp* in raw milk samples (Table I). The presence of *Enterobacteriaceae spp* in raw milk may be associated with unhygienic conditions, intestinal tract normal microflora of humans and warm blooded animals (11). The findings of our study demonstrated that *E. coli* was the pathogen which causes the most concern for public health with prevalence of 69.4% (n = 43) in raw milk samples. In accordance with our findings, Pant et al. (2013) showed that 100% of milk samples (50/50) were contaminated with *E.coli*, and Gundogan et al.(2014) also detected *E.coli* in 74% of raw milk samples (21, 22).

E. hormaechei is a new species of the Enterobacteriaceae family within the *E. cloacae* complex and it is collected from human infections such as vascular host tissues infections and sepsis in neonates admitted to intensive care units (23, 24). Surprisingly, in the current study, we identified *E. hormaechei* in 9.7% (n= 6) of raw milk samples.

Studies in the United States revealed 12 confirmed outbreaks of human diseases related to consumption of raw milk between 2002 and 2008. Two outbreaks were caused by verotoxogenic *E.coli*. Furthermore, according to the European Food Safety Authority (EFSA) Report and the European Centre for Disease Prevention and Control (ECDC) report in 2010 (EFSA-ECDC, 2012), 2.6% of milk samples in Belgium and 5.3% in Germany were contaminated with verotoxic *E. coli* strains. Recent studies in the United States also showed that shiga-toxin producing *E.coli* was isolated from 2.4% of milk samples (25-27).

In the present study, *S. aureus* was enumerated from 17.7 % of milk samples. Similarly to our study, Bysteron and colleagues demonstrated that *Staphylococcus* spp were present in 16% of all samples. Moreover, some French and Polish studies have reported the presence of *S. aureus* in raw milk (25-27).

In total, 88.70% (n=55) samples were contaminated with pathogenic bacteria, while 11.29% (n=7) of milk samples resulted negative. In addition, although pasteurization can eliminate raw milk organisms, the previously produced heat-resistant toxins are not eliminated, and can remain active for long periods which contributes further to the contamination of raw milk. (8, 28, 29).

Due to increasing demands for milk and its products, more public concerns about milk-related infections are present, therefore the hygiene issues in all aspects of milk handling, reduction of storage times, effective refrigeration temperatures, methods for reduction of pathogenic and spoilage microbial flora should be administrated seriously (7, 14). In the United States, foodborne diseases cause up to 9,000 deaths and cost about 5 billion dollars annually (15).

Although the prevalence of *Enterobacteriaceae spp* was high among studied samples, the pathogen bacteria such as *Yersinia enterocolitica* or *Salmonella* spp were not detected.

This high prevalence may be influenced by any of factors mentioned above. The development of correct pasteurization techniques and restriction of raw milk consumption is necessary. In order to prevent milk contamination in all production processes, the appropriate training and guidance should be given to farm owners and their workers. Untreated raw milk consumption should be avoided (3).

Finally, despite the beneficial impacts of raw milk or raw milk-derived products, from pathogens that can be found therein there is a significant threat to possible consumers (30).

ACKNOWLEDGEMENTS

We would like to thank all staff working in the Clinical Microbiology Research Center of Ilam University of Medical Sciences for their

collaboration.

REFERENCES

1. Jakobsen RA, Heggebø R, Sunde EB, Skjervheim M. *Staphylococcus aureus* and *Listeria monocytogenes* in Norwegian raw milk cheese production. Food microbiol 2011; 28:492-96.
2. Gündoğan N, Citak S, Turan E. Slime production, DNase activity and antibiotic resistance of *Staphylococcus aureus* isolated from raw milk, pasteurised milk and ice cream samples. Food control 2006; 17:389-92.
3. Chye FY, Abdullah A, Ayob MK. Bacteriological quality and safety of raw milk in Malaysia. Food microbiol 2004; 21:535-41.
4. Hill B, Smythe B, Lindsay D, Shepherd J. Microbiology of raw milk in New Zealand. Int J food microbiol 2012; 157:305-8.
5. Lindqvist R, Sylvén S, Vågsholm I. Quantitative microbial risk assessment exemplified by *Staphylococcus aureus* in unripened cheese made from raw milk. Int J Food Microbiol 2002; 78:155-70.
6. Anas M, Eddine HJ, Mebrouk K. Antimicrobial activity of *Lactobacillus species* isolated from Algerian raw goat's milk against *Staphylococcus aureus*. World J Dairy Food Sci 2008; 3:39-49.
7. Ercolini D, Russo F, Ferrocino I, Villani F. Molecular identification of mesophilic and psychrotrophic bacteria from raw cow's milk. Food Microbiol 2009; 26:228-31.
8. do Carmo LS, Dias RS, Linardi VR, et al. Food poisoning due to enterotoxigenic strains of Staphylococcus present in Minas cheese and raw milk in Brazil. Food microbiol 2002; 19:9-14.
9. Tornadijo M, Garcıa M, Fresno J, Carballo J. Study of Enterobacteriaceae during the manufacture and ripening of San Simon cheese. Food microbiol 2001; 18:499-509.
10. Eneroth Å, Ahrné S, Molin G. Contamination routes of Gram-negative spoilage bacteria in the production of pasteurised milk, evaluated by randomly amplified polymorphic DNA (RAPD). Int Dairy J 2000; 10:325-31.
11. Bali OS, Lajnef R, Felfoul I, Attia H, Ayadi MA. Detection of *Escherichia coli* in unpasteurized raw milk. Int J Agricult Food Sci 2013; 3(2).
12. Dedeke G, Omemu O, Aladesida A, Museliu F. Comparative microbial analysis of earthworm casts collected from Ikenne, Ogun state, Nigeria. Ethiop J Environment Studi Manag 2010; 3(3).
13. Callon C, Gilbert FB, De Cremoux R, Montel M-C. Application of variable number of tandem repeat analysis to determine the origin of *S. aureus* contamination from milk to cheese in goat cheese farms. Food control 2008; 19:143-50.
14. Bonfoh B, Wasem A, Traoré A, et al. Microbiological quality of cows' milk taken at different intervals from the udder to the selling point in Bamako (Mali). Food control 2003; 14:495-500.
15. Peles F, Wagner M, Varga L, et al. Characterization of *Staphylococcus aureus* strains isolated from bovine milk in Hungary. Int J Food microbiol 2007; 18:186-93.
16. Normanno G, Firinu A, Virgilio S, et al. Coagulase-positive Staphylococci and *Staphylococcus aureus* in food products marketed in Italy. Int J Food Microbiol 2005; 98:73-9.
17. André MCD, Campos MRH, Borges LJ, Kipnis A, Pimenta FC, Serafini AB. Comparison of Staphylococcus aureus isolates from food handlers, raw bovine milk and Minas Frescal cheese by antibiogram and pulsed-field gel electrophoresis following SmaI digestion. Food Control 2008; 19:200-207.
18. Gran H, Wetlesen A, Mutukumira A, Rukure G, Narvhus J. Occurrence of pathogenic bacteria in raw milk, cultured pasteurised milk and naturally soured milk produced at small-scale dairies in Zimbabwe. Food Control 2003; 14:539-44.
19. Kanbakan U, Con A, Ayar A. Determination of microbiological contamination sources during ice cream production in Denizli, Turkey. Food Control 2004; 15:463-70.
20. Psoni L, Tzanetakis N, Litopoulou-Tzanetaki E. Microbiological characteristics of Batzos, a traditional Greek cheese from raw goat's milk. Food Microbiol 2003; 20:575-82.
21. Pant R, Nirwal S, Rai N. Prevalence of antibiotic resistant bacteria and analysis of microbial quality of raw milk samples collected from different regions of Dehradun. Prevalence 2013; 5:804-10.

22. Gundogan N, Avci E. Occurrence and antibiotic resistance of *Escherichia coli*, *Staphylococcus aureus* and *Bacillus cereus* in raw milk and dairy products in Turkey. Int J Dairy Technolo 2014; 67:562-9.
23. Sahebekhtiari N, Nochi Z, Eslampour MA, et al. Characterization of *Staphylococcus aureus* strains isolated from raw milk of bovine subclinical mastitis in Tehran and Mashhad. Acta Microbiol Immunol Hung 2011; 58:113-21.
24. Townsend SM, Hurrell E, Caubilla-Barron J, Loc-Carrillo C, Forsythe SJ. Characterization of an extended-spectrum beta-lactamase *Enterobacter hormaechei* nosocomial outbreak, and other Enterobacter hormaechei misidentified as Cronobacter (Enterobacter) sakazakii. Microbiol 2008; 154:3659-67.
25. Pyz-Łukasik R, Paszkiewicz W, Tatara MR, Brodzki P, Bełkot Z. Microbiological quality of milk sold directly from producers to consumers. J Dairy Sci 2015; 98:4294-301.
26. Bystro J, Paszkowska-Kosek K, Molenda J. Occurrence of enterotoxigenic staphylococci in raw milk. Med Weter 2001; 57:645- 48.
27. Oliver SP, Boor KJ, Murphy SC, Murinda SE. Food safety hazards associated with consumption of raw milk. Food-borne Pathog Dis 2009; 6:793-806.
28. Viçosa GN, Moraes PM, Yamazi AK, Nero LA. Enumeration of coagulase and thermonuclease-positive *Staphylococcus spp*. in raw milk and fresh soft cheese: An evaluation of Baird-Parker agar, Rabbit Plasma Fibrinogen agar and the Petrifilm™ Staph Express count system. Food Microbiol 2010; 27:447-52.
29. Eslampour MA, Hovareshti P, Feizabadi MM, et al. Molecular characterization of *Staphylococcus aureus* isolated from bovine mastitis in Iran. Vet Microbiol 2009; 139:207-8.
30. Quigley L, O'Sullivan O, Stanton C, et al. The complex microbiota of raw milk. FEMS Microbiol Rev 2013; 37:664-98.

LETTER TO THE EDITOR

NEGLECTED GIANT SPINOCELLULAR CARCINOMA OF THE LOWER LIP

I. BAKARDZHIEV[1], A.A. CHOKOEVA[2], G.K. MAXIMOV[3], U. WOLLINA[4], T. LOTTI[5], S. GIANFALDONI[6] and G. TCHERNEV[7]

[1]Medical College , Medical University of Varna, Bulgaria; [2]"Onkoderma" Policlinic for Dermatology and Dermatologic Surgery, Sofia, Bulgaria; [3]Department "Medicines Use Control", Sofia, Bulgaria; [4]Department of Dermatology and Allergology, Academic Teaching Hospital Dresden-Friedrichstadt, Dresden, Germany; [5]University of Rome "G. Marconi", Rome, Italy; Department of Biotechnology, Delft University of Technology, Delft, The Netherlands; [6]Division of Dermatology, Department of Critical and Experimental Medicine, University of Pisa, Pisa, Italy; [7]Policlinic for Dermatology and Venereology, Saint Kliment Ohridski University, Medical Faculty, University Hospital Lozenetz, Sofia, Bulgaria

Received August 21, 2015 – Accepted October 5, 2015

Although squamous cell carcinoma (SCC) is the most common type of lip cancer worldwide, its giant form is extremely rare, due to its easy detection and early diagnosis. The survival rate is good if early eradication is performed, as 5-year survival accounts for approximately 80-90%. We present a rare variant of giant form of SCC on the lower lip in a 70-year-old patient, which had been neglected for many years, due to social disadvantages and absence of any resources for adequate medical help, until the tumor caused total inability of administration of food and drink. The recent diagnostic and therapeutic options are considered. Despite well-known etiologic factors regarding squamous cell carcinoma and the newest prognostic factors on tumor differentiation, such as β-catenin abnormal expression, the negative influence of the demographic characteristics of the patient were also in focus. Certain outcast ways of living should be considered as potential risk factors for the development of giant forms of SCC. In addition, an improvement of the quality of life of these patients results as being critical for the prevention of various of risk factors, as well as improving the survival rate in general.

Squamous cell carcinoma (SCC) is the most common type of lip cancer (1). SCC represents more than 90 percent of all head and neck non-melanocytic cancers, as the most affected area is the lower lip, due to occupation-related sun exposure combined with excessive tobacco and alcohol use (1). The prognosis, as well as the risk of recurrence and metastasis rate depends on several factors, including i) treatment modality, ii) prior treatment, iii) location, iv) size, v) depth of invasion, vi) histologic differentiation, vii) histologic evidence of perineural involvement, vii) precipitating factors other than ultraviolet light, and ix) host immunosuppression status (2). Five-year survival rate averages approximately 74% (3). The survival prognosis is usually improved if the tumor is treated at the early stages and when

Key words: giant SCC, lip, diagnostic, management

Mailing address: Assoc. Prof. Georgi Tchernev,
Policlinic for Dermatology and Venereology,
Saint Kliment Ohridski University,
Medical Faculty, University Hospital Lozenetz,
Koziak street 1, 1407 Sofia, Bulgaria
Tel.: +359 885 588 424
e-mail: georgi_tchernev@yahoo.de

0393-974X (2015)

DISCLOSURE: ALL AUTHORS REPORT NO CONFLICTS OF INTEREST RELEVANT TO THIS ARTICLE.

there is a lack of metastasis (3). Males are the predominantly affected gender with distribution ratio male to female 3:1 (2, 3). The incidence of SCC of the lower lip is more common after the 5th or 6th decade, as 74% of the affected patients are smokers (4). Age, absence of family history of cancer, smoking, alcohol consumption, and previous diagnosis of cancer without treatment are associated with a higher incidence of cancer of the lip (4). In addition, Epstein-Barr virus, human papillomavirus (HPV) infection, gastroesophageal reflux disease (GERD), and exposure to paint fumes, plastic by-products, wood dust, asbestos, and gasoline fumes are considered to be in possible association with the incidence of SCC on the lip (2, 4).

Case report

We present the case of a 70-year-old, otherwise healthy male patient, without history of any comorbidities or medication, consulted on an occasion of complaints, presented by itching, burning and tingling on the lower lip. Inability to administer food and fluids was also reported. According to the patient's history, he was a smoker, as well as an excessive user of alcohol for more than 20 years. No history in respect to tumoral diseases was presented. The duration of the complaints was 12-13 years, as the initial symptoms were presented by a small nodule in the middle of the lower lip, which gradually transformed into a tumor-like formation as the result of repetitive manipulation by the patient himself. The patient was socially disadvantaged, homeless, without social security and without any financial resources to seek medical help at the initial stages of the disease. According to the reported history, no family members, nor patient's friends were available to administer any medical care or support earlier. Therefore, the patient initiated a behaviour of repeated manipulation of the already present tumor, until the formation became large enough to hamper the administration of food or drink. Despite social economics disabilities, the patient lives in seaside town which provide excessive sun and wind exposure during the whole year, and the outcast way of living favors the exposure to various risk factors. An exophytic giant tumor in the form of two connected half circles, fully engaging the lower lip in all of its length was clinically established, at the dermatological examination. Highly differentiated squamous cell carcinoma was confirmed histologically after carrying out a mucocutaneous biopsy. Locoregional and distant metastasis were excluded by the conducted screening. Paraclinical and imaging diagnostic examinations were within the normal range. Nonspecific bilateral lymphadenopathy was established by an ultrasound examination and was successfully controlled after intravenous administration of cephalosporin-second generation. Although oral-maxillo-facial reconstruction was planned, the treatment was not performed, because of of the non-appearance of the patient on the appointed day.

DISCUSSION

The histopathological examination of the lower lip carcinomas revealed 63% squamous cell carcinoma, 30% basal cell carcinomas, 5% keratoacanthoma and 2% actinic keratosis (5). Misdiagnosis is rare, due to the typical clinical manifestation and histopathological pattern (1). The prognosis based on the tumor diameter classes in the TNM system seems to be not always specific (6). According to earlier reported scientific findings, tumor thickness, depth of infiltration and grade of malignancy should also be taken into consideration if the prognosis is to be estimated accurately (6). According to some authors' collectives if the level of invasion and the tumor thickness are taken into consideration, a large group of tumors (50%) can be separated: these tumors do not metastasize, even though they are at least 2 mm thick, and they do not infiltrate the subcutaneous tissue (no risk group) (6).

According to recently published results by Barakat C, the expression of β-catenin is an independent prognostic factor for histological grading and tumor differentiation, as the author established β-catenin abnormal expression in 29% of the squamous cells of well differentiated SCC of the lip, 63% of moderately differentiated and 86% of poorly differentiated tumors (7). Therefore he suggests a possible structural association and the role of β-catenin in tumor progression (7).

The majority of lip cancers are easily detected, due to their visible location which facilitates the positive cure rate at the early stages (8). Treatment

options include surgery, radiation, and cryotherapy (freezing with liquid nitrogen), with Mohs technique, as cure rates for early detected lesions could be achieved in nearly 100% of the cases (8).

Surgical treatment for small lesions of the lower lip has a favorable prognosis (5). The successful management of lip cancer includes not only the control of the primary tumours with appropriate surgical margins, but also the subsequent reconstruction which aims to improve the oral phase of swallowing and to prevent possible metastatic spread to the neck (9).

For giant lesions with poor prognosis, aggressive surgical treatment is recommended, such as surgical excision, prophylactic suprahyoid neck dissection, and possible radical neck dissection which are considered as adequate surgical options in such cases (10). Although cancers of the lip have relatively low rates of metastatic spread to nearby lymph nodes and distant sites, the particular parameters of the primary tumor seem to predict the chance of development of local recurrence and regional lymph node metastasis (11). In giant, untreated forms of SCC, as in the presented case, the mortality rate accounts for 15% (8). If spread to local lymph nodes is present, the five-year survival rate decreases to approximately 50% (9). If cervical lymph nodes are affected by metastasis, the survival rate reduces from 90 to 50%, while the survival after recurrent disease is 10% (9). Over 60% of the recurrences result from tumors less than 4 cm in diameter (11). The local recurrence rate is 7 to 20%, but reexcision of the local recurrence provides 75% cure rate (11).

REFERENCES

1. Molnar L, Ronay P, Tapolcsanyi L. Carcinoma of the lip. Analysis of the material of 25 years. Oncology 1974; 29:101-21.
2. Rowe DE, Carroll RJ, Day CL Jr. Prognostic factors for local recurrence, metastasis, and survival rates in squamous cell carcinoma of the skin, ear, and lip. Implications for treatment modality selection. J Am Acad Dermatol 1992; 26(6):976-90.
3. Pietersma NS, de Bock GH, de Visscher JG, Roodenburg JL, van Dijk BA. No evidence for a survival difference between upper and lower lip squamous cell carcinoma. Int J Oral Maxillofac Surg 2015; 44(5):549-54.
4. Ribeiro IL, Medeiros JJ, Rodrigues LV, Valença AM, Lima Neto Ede A. Factors associated with lip and oral cavity cancer. Rev Bras Epidemiol 2015; 18(3):618-29.
5. Calcaianu N, Popescu SA, Diveica D, Lascar I. Surgical attitude in premalignant lesions and malignant tumors of the lower lip. J Med Life 2015; 8(1):109-11.
6. Brantsch KD, Meisner C, Schönfisch B, Trilling B, Wehner-Caroli J, Röcken M, Breuninger H. Analysis of risk factors determining prognosis of cutaneous squamous-cell carcinoma: a prospective study. Lancet Oncol 2008; 9(8):713-20.
7. Barakat C. β-Catenin alterations in squamous cell carcinoma of the lip. Asian Pac J Cancer Prev 2015; 16(13):5187-90.
8. Mohs FE, Snow SN. Microscopically controlled surgical treatment for squamous cell carcinoma of the lower lip. Surg Gynecol Obstet 1985; 160:37-41.
9. Moretti A, Vitullo F, Augurio A, Pacella A, Croce A. Surgical management of lip cancer. Acta Otorhinolaryngol Ital 2011; 31(1):5-10.
10. de Visscher JG, van den Elsaker K, Grond AJ, van der Wal JE, van der Waal I. Surgical treatment of squamous cell carcinoma of the lower lip: evaluation of long-term results and prognostic factors--a retrospective analysis of 184 patients. J Oral Maxillofac Surg 1998; 56(7):814-20.
11. Cruse CW, Radocha RF. Squamous cell carcinoma of the lip. Plast Reconstr Surg 1987; 80(6):787-91.

LETTER TO THE EDITOR

EXPRESSION OF mTOR AND ITS INHIBITORY EFFECT ON CELL PROLIFERATION AND APOPTOSIS OF BREAST CANCER CELLS

XF. CHENG[1], Q. LIU[2], XF. ZHANG[3], HD. ZHAO[1], W. WANG[1] and AJ. CHU[1]

[1]Surgery Department of Galactophore, The First Affiliated Hospital of Henan University of TCM, Zhengzhou City, Henan Province, China; [2]Scientific Bureau, Henan University of TCM, Zhengzhou City, China; [3]Department of Traditional Chinese Medicine and Western Medicine, Henan Cancer Hospital, Zhengzhou City, Henan Province, China

Received May 21, 2015 –Accepted September 23, 2015

The first two authors contributed equally to this work

The aim of this study is to investigate the expression of mTOR in breast cancer and observe the effect of CCI-779 on proliferation and apoptosis of MDA-MB-231 cells. Immunohistochemical staining was used to detect the expression of mTOR protein in breast cancer tissues and MDA-MB-231 cells. MTT assay was used to assess the effect of CCI-779 on proliferation of MDA-MB-231 cells. Annex-inV-FITC/PI assay was utilized to evaluate the effect of CCI-779 on apoptosis of MDA-MB-231 cells. Among the 71 cases of breast cancer tissues, 54.9% were mTOR-positive that exhibited significantly higher expression than the 32 cases of normal tissues (21.9%); mTOR protein was also found to be expressed in MDA-MB-231 cells. The mTOR inhibitor CCI-779 significantly inhibited the proliferation of MDA-MB-231 cells that was dose- and time-dependent. However, CCI-779 was unable to induce apoptosis of MDA-MB-231 cells as demonstrated with AnnexinV-FITC/PI assay. mTOR plays a key role in the initiation and development of breast cancer, and its inhibitor CCI-779 exerts a strong suppressive activity against MDA-MB-231 cells, suggesting its therapeutic potential to treat breast cancer.

Breast cancer is recognized as one of the most common malignant tumors among women worldwide. The incidence has increased significantly in recent years, with younger people being affected, thus demanding intensive attention from the research and clinical community. mTOR belongs to the family of serine-threonine protein kinases, and assumes an important role in regulating cell proliferation and differentiation. In-depth interrogation of the relationship between mTOR and tumorigenesis has become an intensive area of research in oncology in recent years. For example, Suzuki et al. (1) reported robust expression of mTOR in kidney cancer cells, and Sun et al. (2) demonstrated aberrant expression of mTOR in gastric cancer tissues. Clinical administration with the mTOR inhibitor rapamycin can inhibit the proliferation of gastric cancer cells and block the cell cycle. These results together indicated that high expression of mTOR is closely correlated with the development of malignant tumors.

There have been few previous reports studying the relationship between mTOR and breast cancer. With

Key words: breast neoplasm, CCI-779, mTOR, mTOR inhibitor

Mailing address: Dr Xufeng Cheng,
The First Affiliated Hospital,
Henan University of TCM,
No.19, Renmin Road,
Zhengzhou City,
450000, PR China
e-mail: zmeditcxf@163.com

0393-974X (2015)

breast cancer tissues and breast cancer cells as research objects, we used immunohistochemical SP analysis to detect mTOR protein expression in breast cancer tissues and cells. The MTT and AnnexinV-FITC/PI methods were applied to evaluate the influence of mTOR inhibitor CCI-779 on MDA-MB-231 cell proliferation and apoptosis. Our study aimed to explore the relationship between mTOR and breast cancer, to provide new ideas for the treatment of breast cancer, and to offer important references for clinical screening to identify efficacious chemotherapy drugs.

MATERIALS AND METHODS

This study included 71 clinical case specimens of breast cancer with modified radical or surgical treatments in The First Affiliated Hospital of Henan University of TCM and Henan Cancer Hospital from 2012 to 2013. MDA-MB-231 cells were preserved in the Henan Cancer Hospital morphological laboratory. mTOR antibodies were purchased from Beijing Bioss company, China. CCI-779 were purchased from Plizer, China, and MTT were purchased from Sigma-Aldrich Co. LLC., China. RPMI 1640 medium, fetal bovine serum and AnnexinV-FITC/PI apoptosis detection kit were obtained from Beijing Solarbio Technology Co. LTD., China.

Immunohistochemical staining

The immunohistochemical SP method was applied to detect mTOR protein expression in 71 cases of breast cancer and 32 cases of control tissues adjacent to carcinoma. All specimens were fixed with 10% formaldehyde, and then subjected to conventional dehydration, paraffin embedding and serial sectioning. All experiments were carried out in strict accordance with the manufacturer's instructions, namely, DAB chromogenic, gradient ethanol dehydration, xylene transparenting and neutral gum cementing. Samples were then observed under the microscope. PBS (0.01 mol/L) was used as negative control. The pathological image analysis system was utilized to analyze the results.

Cell culture

Breast cancer cell line MDA-MB-231 was cultured at 37°C and 5% CO_2 saturated humidity. The growth medium was 10% of RPMI 1640 supplemented with fetal bovine serum.

Cell immunohistochemistry

Sterilized cover glass was added to the 6-well cell culture plates, and MDA-MB-231 cells were selected in good growth condition. After 48 hours, cells were washed and the cover glass removed, followed by fixation with cold acetone and then immunohistochemical staining. A semi-quantitative integral method was used to analyze the results, and an optical microscope was utilized to consecutively observe any 5 for 400-magnitude vision. Cell quantity was defined as follows: positive cells less than 5% were 0 points, positive cells between 5% and 25% were 1 point, positive cells between 26% and 50% were 2 points, positive cells between 51% and 75% were 3 points, and positive cells more than 75% were 4 points. The degree of dye staining: no dyeing was 0 points, mild staining was 1 point, moderate dyeing was 2 points and heavy staining was 3 points. The positive expression was shown for the multiple integration more than 4 points of the two above figures

The influence of mTOR inhibitors on cell growth using MTT assay

MDA-MB-231 breast cancer cells were selected in the logarithmic phase and subject to trypsin digestion. Cells were counted and seeded with 3×10^3 cells in each well of a 96-well plate, maintained at 37°C and 5% CO_2 humidity in an incubator overnight. Our experiments included a no-treatment blank group, a control group and an experimental group, each group with 5 wells with the remaining wells filled with PBS. mTOR inhibitors CCI-779 was diluted in culture medium to reach the final concentration of 0.1μmol/L, 0.2μmol/L, 0.4μmol/L and 0.8μmol/L, with the duration of inhibitory stimulation being 24 h, 48 h and 72 h. Five mg/ml of MTT 20 μl were then added to each well and maintained for 4 hours. The supernatants were then removed followed by addition of 150 μl DMSO, and incubated at room temperature with gentle shaking for 10 min to dissolve crystallization. The absorbance values were recorded at wavelength of 490 nm. The mean for the same experimental samples were calculated as the results of MDA-MB-231 cells in the drug group. The experiments were repeated three times. According to the following formula, a growth inhibition rate of CCI-779 on MDA-MB-231 cells was calculated under different drug concentrations and different stimulation times. An inhibition rate was determined as A(control group) – A(experiment group)/A(control group)x 100%.

mTOR inhibitors effects on cell apoptosis through AnnexinV-FITC/PI assay

MDA-MB-231 cells were selected during the logarithmic phase and in good condition by trypsin digestion. Cells were then accounted and seeded at 5×10^5 in a 5-well plate with 2 ml per well at 37°C and 5% CO_2 humidity incubator and cultured overnight. Various concentrations of CCI-779 (0μmol/L, 0.1μmol/L, 0.2μmol/L, 0.4μmol/L and 0.8μmol/L) were used to

stimulate MDA-MB-231 cells for 24 h. Cells were then collected. Samples were then subject to flow cytometry for analysis.

Statistical processing

Results were statistically processed by SPSS 13.0. Experimental data were expressed as $\overline{x} \pm s$. Depending upon the specific datasets, *Chi*-squared or Student's *t*-test was carried out. Multiple comparisons were analyzed with analysis of variance (ANOVA). P<0.05 was considered as statistically significant.

RESULTS

Immunohistochemical analysis

We found that mTOR protein was expressed in the cytoplasm and cell membrane as brown or tan particles. Among the 71 specimens of breast cancer, there were 39 mTOR-positive cases with a positive rate of 54.9%. Only 7 of 32 cases of the control tissues adjacent to carcinoma were found to express mTOR protein with a positive rate of 21.9%. Importantly, the comparison between the two groups was statistically significant (P<0.05, Figs. 1, 2). Cell immunohistochemical display showed that the mTOR protein was expressed in breast cancer cells MDA-MB-231.

Growth inhibition of CCI-779 on MDA-MB-231 cells

Results showed that the CCI-779 effectively inhibited the proliferation of MDA-MB-231 cells. Different concentrations CCI-779 at 0.1μmol/L, 0.2μmol/L, 0.4μmol/L, 0.8μmol/L all had an effect

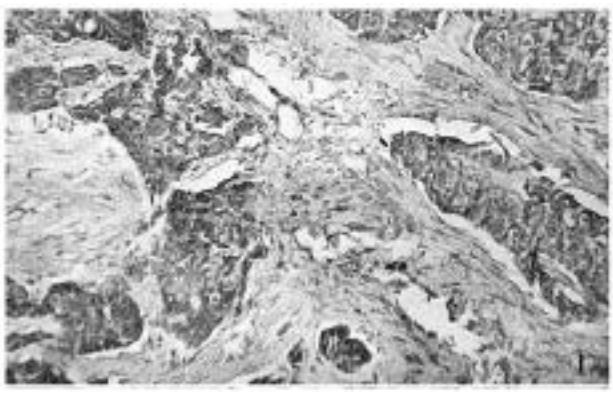

Fig. 1. *mTOR expression in breast cancer tissue as assessed by the SP method.*

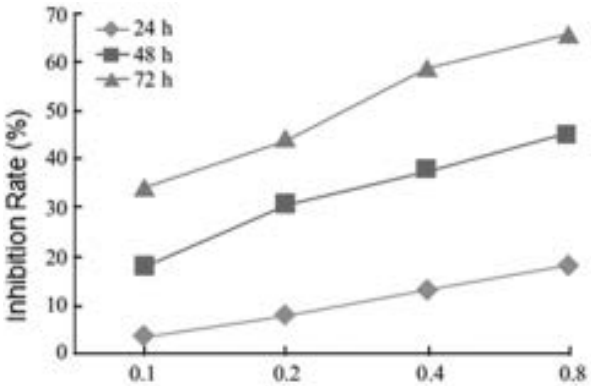

Fig. 3. *Inhibitory effect of CCI-779 on the proliferation of MDA-MB-231 cells.*

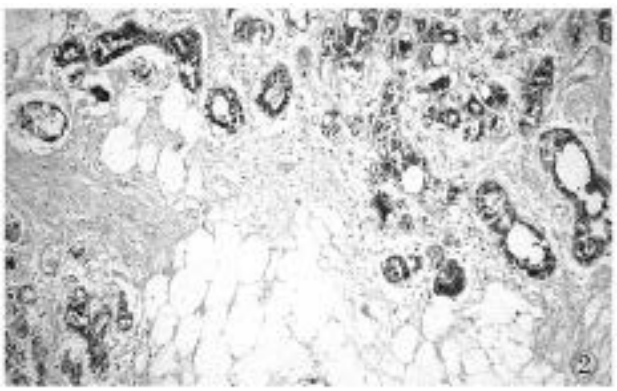

Fig. 2. *mTOR expression in the tissues adjacent to carcinoma as assessed by the SP method.*

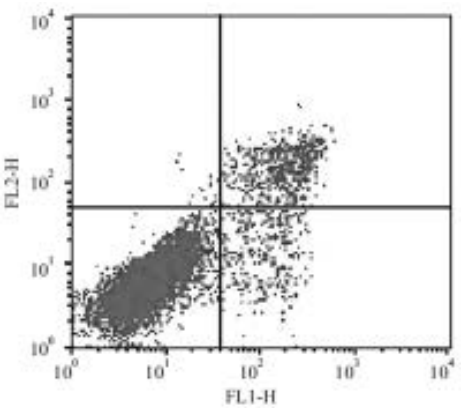

Fig. 4. *Cell apoptosis upon stimulation with 0μmol/L CCI-779.*

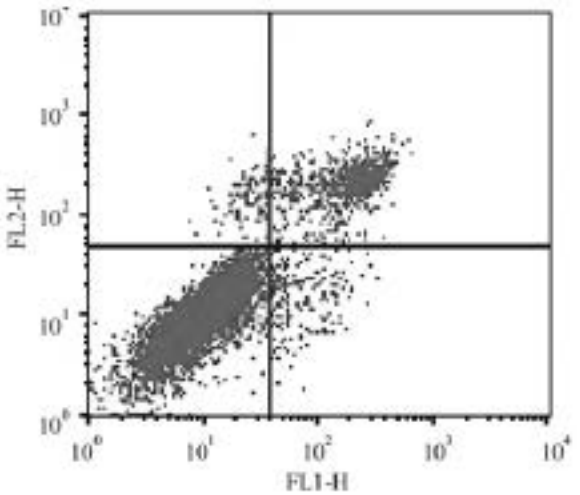

Fig. 5. *Cell apoptosis upon stimulation with 0.8μmol/L CCI-779.*

on MDA-MB-231 cells. Increased concentrations and extended duration of stimulation had a greater inhibitory impact on the MDA-MB-231 cells. The comparison between any two groups showed statistical significance ($P<0.05$, Fig. 3).

Influence of CCI-779 on MDA-MB-231 cell apoptosis

Flow cytometry analysis showed that CCI-779 at different concentrations of 0μmol/L, 0.1μmol/L, 0.2μmol/L, 0.4μmol/L and 0.8μmol/L had a pronounced effect on the MDA-MB-231 cells for 24 hours. The percentages of apoptosis cells were (9.57±1.47)%, (9.71±1.65)%, (9.37±1.52)%, (9.62±1.84)%, and (9.96±1.18)%, respectively. However, there was no statistically significant difference between the groups with different concentrations ($P>0.05$, Figs. 4, 5).

DISCUSSION

Rapid development of molecular biology in recent years has allowed us to gain a deeper understanding of the initiation, development and evolution of breast cancer. However, breakthrough progress in the diagnosis and treatment of breast cancer remains scarce. Therefore, efforts to seek new therapeutic targets and identify efficacious chemotherapy drugs has become the key for establishing clinical treatment of breast cancer.

Initially discovered as the macromolecular protein with conservative evolution, mTOR belongs to the family of serine/threonine protein kinases that play an important role in controlling cell growth and metabolism in various types of cells. Previous studies have consistently implicated the high expression of mTOR in malignant tumor (3) and its strong correlation with tumor formation, invasion, metastasis and prognosis. mTOR serves as a main therapeutic target in cancer. Indeed, Ji et al. (4) identified mTOR expression in cervical cancer. In addition, Munari et al. (5) hypothesized that mTOR was closely related to the development of urothelial carcinoma. Our experiments utlized the immunohistochemical SP method to quantify mTOR expression in 71 cases of breast cancer specimens and 32 cases of control tissues adjacent to carcinoma specimens. We found that mTOR protein expression in breast cancer tissue was significantly higher than that in the tissue adjacent to carcinoma. mTOR protein expression was also identified in breast cancer cells MDA-MB-231, and increased mTOR was connected with the formation of breast cancer. Our results provide new theoretical and experimental basis for clinical application of gene targeting for breast cancer.

Our increasing understanding of the relationship between mTOR and tumors has allowed the development and production of mTOR-specific inhibitors. Intriguingly, Finn (6) reported that mTOR inhibitors were effective when used to treat patients with liver cancer by inhibiting the development of tumor and tumor blood vessels (7). Our experiments were carried out using the MTT method to assess how mTOR inhibitors CCI-779 suppressed growth of breast cancer MDA-MB-231 cells. Our results showed that CCI-779 had a significant inhibitory effect on MDA-MB-231 cell proliferation that was concentration- and time-dependent. Our data indicated that mTOR was the key factor that influences the pathogenesis of breast cancer. Therefore, the mTOR inhibitor CCI-779 likely confers strong resistance to the proliferative activity of breast cancer cells, thus likely serving as a promising drug for the treatment of breast cancer in the future.

The MTT Method confirmed that CCI-779 can inhibit the proliferation of MDA-MB-231 cells. In

order to determine whether apoptosis inhibits the cell growth, we performed experiments to adopt AnnexinV-FITC/PC method to characterize how CCI-799 influences cell apoptosis of MDA-MB-231 cells. The results showed that none of the CCI-779 concentrations tested had any significant influences on cells apoptosis, suggesting that CCI-799 inhibited cell proliferation but not apoptosis pathway. Indeed, previous studies by Chen et al. (8) reported that mTOR inhibitors inhibited tumor cell proliferation and metabolism through the inhibition of vascular endothelial growth factor VEGF signaling pathways. Another study by Chen et al .(9) speculated that mTOR inhibitors suppressed regulatory factors HIF-l in tumor microenvironment, thereby inhibiting tumor cell proliferation. Ying Liu et al. (10) treated gastric cancer cells with mTOR inhibitors, and found arrested cell cycle resulting from elevated p27 expression. The underlying mechanism remains elusive at present, which requires extensive further exploitation. One possible explanation lies in elevated p27 expression that induces cell cycle arrest. In conclusion, we revealed evidence suggesting that mTOR is closely related with malignant formation, development, invasion and metastasis of various tumors. Further studies are necessary to find the evolutionary mechanism of breast cancer, to uncover effective drugs to inhibit breast tumor growth, to open a new avenue for breast cancer, and to improve the efficacy of clinical treatment for breast cancer.

Although it has previously been reported that mTOR plays a critical role in multiple cellular functions, including metabolism, proliferation, growth and survival, we analyzed mTOR expression levels in breast cancer patients by IHC staining assay, and found that the mTOR inhibitor CCI-779 inhibited cell proliferation but did not influence apoptosis, which provides valuable clinical information concerning the relationship between mTOR and breast cancer. Furthermore, although multiple previous papers have shown that mTOR was overexpressed in breast cancer patients, and the application of mTOR inhibitors in breast cancer have been discussed, we further demonstrated that mTOR was closely related to the formation of breast cancer, and CCI-779 has strong activity against MDA-MB-231 cells, implicating CCI-799 as a prospective drug for treatment of breast cancer in the future.

REFERENCES

1. Suzuki K, Mizuno R, Suenaga K, Teruya T, Tanaka N, Kosaka T, Oya M. Bisebromoamide, an extract from lyngbya species, induces apoptosis through ERK and mTOR inhibitions in renal cancer cells. Cancer Med 2013; 2(1):32-39.
2. Sun DF, Zhang YJ, Tian XQ, Chen YX, Fang JY. Inhibition of mTOR signaling potentiates the effects of trichostatin in human gastric cancer cell lines by promoting histone acetylation. Cell Biol In 2014; 38(1):50 -63.
3. Kang LF, Li YH, Zhang XH, et al. The expression and clinical significance of mTOR and elF4E protein in the sample endometrial adenocarcinoma. Chinese J Clinical Exp Path 2011; 27(1):71-74.
4. Ji J, Zheng PS. Activation of mTOR signaling pathway contributes to survival of cervical cancer cells. Gynecol Oncol 2010; 117(1):103-108.
5. Munari E, Fujita K, Faraj S, et al. Dysregulation of mammalian target of rapamycin pathway in upper tract urothelial carcinoma. Hum Pathol 2013; 44(12):2668 -76.
6. Finn RS. Current and future treatment strategies for patients with advanced hepatocellular carcinoma: role of mTOR inhibition. Liver Cancer 2012; 1(3-4):247-56.
7. Potter CS, Wang Z, Silva KA, et al. Chronic proliferative dermatitis in Sharpin null mice: development of an autoinflammatory disease in the absence of B and T lymphocytes and IL4/IL13 signaling. PLoS One 2014; 9(1):e85666.
8. Chen JL, Appelbaum DE, Kocherginsky M, Cowey CL, Rathmell WK, McDermott DF, Stadler WM. FDG-PET as a predictive biomarker for therapy with everolimus in metastatic renal cell cancer. Cancer Med 2013; 2(4):545-52.
9. Chen B, Yuping S, Ni J. Rapamycin decreases survivin expression to induce NSCLC cell apoptosis under hypoxia through inhibiting HIF-1αinduction. Mol Biol Rep 2012; 39(1):185-91.
10. Liu YL, Zhu ZA, Kong QY, et al. Reversal agents of mTOR specific inhibitors RAD001 on drug resistance of SGC7901/DDP cell. Chin J Cli Exp Path 2013; 29(11):1206 -10.

LETTER TO THE EDITOR

EXPRESSION AND DIAGNOSIS OF TRANSIENT RECEPTOR POTENTIAL VANILLOID1 IN UROTHELIUM OF PATIENTS WITH OVERACTIVE BLADDER

H.Y. ZHANG[1], J.F. CHU[1], P. LI[1], N. LI[1] and Z.H. LV[2]

[1]Department of Urology, Yantai Hill Hospital of Yantai City, Shandong, China; [2]Department of Urology, First People's Hospital of Jining, Shandong, China

Received January 29, 2015 – Accepted June 4, 2015

The first two authors contributed equally to this paper

This study was carried out to test expression of transient receptor potential vanilloid1 (TRPV1) in urothelium of female patients with overactive bladder (OAB) and explore clinical significance of TRPV1 in diagnosing female OAB. TRPV1 expression in urothelium of female OAB patients (n=21) and healthy females (n=9) was detected using Strept Avidin-Biotin Complex (SABC), an immunohistochemical method and image analysis system. Relative content of TRPV1 was expressed by average optical density (AOD) and was analyzed through data of urodynamics. Compared to TRPV1 expression in urothelium of healthy females (AOD 0.3658 ± 0.1009), TRPV1 expression in OAB patients was much higher (AOD 0.4834 ± 0.1252) and the difference was significant P<0.05. Observation and comparison in clinic of urodynamic parameters of female patients and healthy females revealed that the former had lower indexes with remarkable differences (P<0.05) such as Qmax, first desire volume (FDV), strong desire volume (SDV), maximum cyst capacity (MCC) and bladder compliance (BC). Thus high expression of TRPV1 in urothelium of female OAB patients is closely correlated to OAB occurrence, showing great importance of improved bladder sensitivity in female OAB occurrence mechanism.

OAB is a common chronic disease of the urinary system and a symptom complex of lower urinary tract. Excluding infection and other pathological changes, urgent urination is a major feature of OAB, frequent urination in daytime and increased urination at night, which is likely to be accompanied (or not) by urgent urinary incontinence. Overactive detrusor is the common performance of OAB in clinical uridynamics, which also performs as functional disorder of bladder urethra (1). More and more studies show that bladder urothelium, mainly functioning as a protective screen, possesses unique attribute of sensation, playing a vital role in detection and transmission of physiological and harmful spikes. Urothelium cells are able to react to external stimulus like physical, chemical, mechanical and heat and are likely to mediate correlation among muscular system urothelium environment and lower nerves of urothelium (2).

Wang Yuliang et al. (3) investigated adult females with OAB in Beijing with the hope to acquire and analyze OAB occurrence and regularity, resulting in 4.7% occurrence rate which increased with aging. Trend of increasing OAB occurrence rate, especially

Key words: OAB, TRPV1, urodynamics, AOD

Mailing address:
Dr Zhonghua Lv,
No.6, Jiankang Road, Jining,
Shandong, 272011, China
e-mail: lkyxkxy@163.com

0393-974X (2015)

among females, has been proved based on various evidence including bad living conditions, therefore this receives increasing attention from specialists and scholars. Abnormal sensory function, abnormal nerve functional and bladder detrusor has instead been the study focus of OAB occurrence mechanism for some time. However, studies on sensory function in recent years have maintained more relevant achievements in physiology, leading to the attention on sensory function of bladder.

Recently found TRPV1 is a non-selective cation channel receptor closely connected to the bladder, TRPV1 is mainly located in peripheral sensory neurons which function in improving intracellular Ca^{2+} and resealing transmitters. For instance, some research cut down TRPV1 antagonist and removed TRPV1 gene from mice through decreasing PH value of esthesioneure, which resulted in improved response of urothelium to vanilloid (4, 5). In the study of bladder disease, differences are found when a TRPV1 gene knockout mouse responds to chemical factor-induced bladder stimulus and inflammatory reaction and TRPV1 expression is increased in nerves and urothelium of OAB patients. The injection of vanilloid in bladder can improve clinical urodynamic parameters and ease pain, which is possibly due to the effect of vanilloid on the desensitization mechanism of bladder nerves. Successful clinical cases with vanilloid treatment show that constant targeted-activation of TRPV1 in urothelium desensitizes urothelium receptor and completely consumes transmitter, which achieves effective treatment of OAB (6, 7).

Based on the above studies, this study detected TRPV1 expression in urothelium of female OAB patients using SABC combined with image analysis system, analyzed and discussed TRPV1 expression in OAB occurrence and development combining clinical urodynamics data, in order to establish OAB occurrence mechanism and offer results for relevant clinical diagnosis.

MATERIALS AND METHODS

Tests were carried out on 21 in-hospital female patients (aged 31 to 62 years, mean 45±2.5) treated from January 2010 to May 2012. Having excluded related pathological changes, urgent urination in accordance with OAB diagnosis criteria was regarded as the major symptom and uncontrolled detrusor contraction was ruled out through clinical urodynamic test. In addition, specimens used for this study were collected from tissues in the bladder trigone.

Anti-rabbit TRPV1 polyclonal antibody was taken as the primary antibody and the second antibody was a ready-to-use SABC kit. A DAB color kit was used for developing color. Phosphate buffer solution (PBS) was used as washing liquid and alcohol and dimethylbenzene in different concentrations were used as dehydration and transparenting agents. Citric acid buffer solution 0.1% was used for antigen retrieval. H_2O_2 carbinol solution 3% was used to inactivate the endogenous peroxidase. Hydrochloric alcohol 1% and haematoxylin were used for rinsing and counterstaining, respectively. Microtome, dryer, refrigerator, light microscope, thermostat oscillator, oven and high-color-defined pathological image analysis system (HPIAS-1000) were the instruments used in this study.

All experimental steps were carried out strictly, according to the manufacturer's instructions; for reference, anti-rabbit TRPV1 polyclonal antibody was replaced by PBS (4).

Result criteria

Cells found with brown particles in membrane or cell organs were confirmed as TRPV1 positive cells; otherwise, negative cells were confirmed. HPIAS-1000 was performed in image analysis and each section was observed and analyzed under 5 random high-power fields (10×40). AOD was taken as quantitive index, TRPV1 in urothelium of OAB patients and healthy females was evaluated followed by overall evaluation based on the above results.

Statistical analysis

Database of patients urodynamic information and staining results were established and SPSS 17.0 software was performed for analyzing obtained data and the results were all expressed as mean ±* MERGEFORMAT standard deviation. AOD of TRPV1 was compared between OAB patients and healthy females while comparison among OAB patients referred to clinical urodynamic data of healthy females; *t*-test was used in parameter; α=0.05 was considered to be significant.

RESULTS

TRPV1 expression in urothelium of female OAB patients and healthy females

As shown in Table I, positive cells of TRPV1 expressed highly in urothelium of OAB patients;

Table I. *TRPV1 expression in urothelium of female OAB patients and healthy females.*

Groups	TRPV1expression and distribution	Color
Urothelium of OAB patients	Distribution as diffused particles in cell membranes or membrane of intracellular organs with high expression	Brown
Urothelium of healthy females	Distribution in cell membranes or membrane of intracellular organs with low expression	Faint yellow

Table II. *Relation between AOD and TRPV1.*

Groups	n	AOD	t	P
Urothelium of OAB patients	21	0.4834±0.1252	2.601	0.015
Urothelium of healthy females	9	0.3658±0.1009		

Table III. *Comparison of clinical urodynamic data between female OAB patients and healthy females.*

Urodynamic data	Female OAB patients	Healthy females	P
Qmax (ml/s)	13.79	22	<0.05
FDV (ml)	108.48	188	<0.05
SDV (ml)	243.67	372	<0.05
MCC (ml)	243.67	580	<0.05
BC (ml/cmH2O)	26.26	119	<0.05
Pdet.Qmax (cmH2O)	27.86	27	<0.05

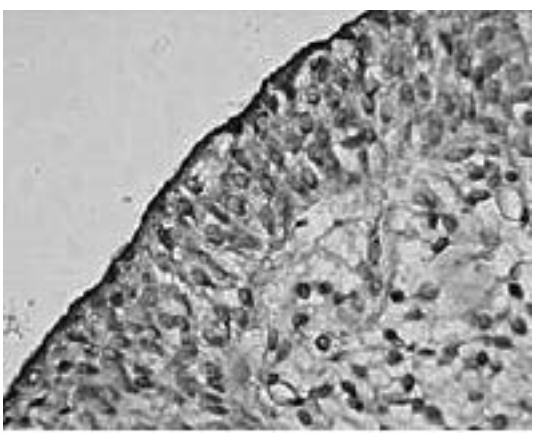

Fig. 1. *TRPV1 expression in female OAB patients (SABC, ×400).*

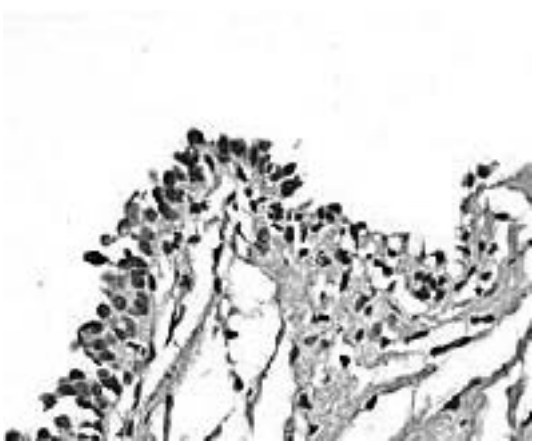

Fig. 2. *TRPV1 expression in healthy females OAB patients (SABC, ×400).*

in particular, the positive cells showed brown and diffused particles which expressed in cell membranes and membrane of intracellular organs (Fig. 1), While for healthy females, TRPV1 showed faint yellow (Fig. 2).

Relation between AOD and TRPV1

Pathological image analysis of TRPV1 in urothelium of OAB patients and healthy females led to higher AOD value of 0.4834±0.1252 in the former and 0.3658±0.1009 in the latter. The comparisons

were statistically significant, P<0.05 (Table II).

Based on urodynamic parameters of healthy females, OAB patients witnessed lower indexes of Qmax, FDV, SDV, MCC and BC and higher index of Pdet. The comparison resulted as being statistically significant (p<0.05) (Table III).

DISCUSSION

OAB has great impact on quality of life due to a high occurrence rate (4). However, there is still a lot to understand about the cause and occurrence mechanism of OAB. To date, OAB determination depends largely on exclusion of infection and other diseases. In past studies OAB was found to be related to damages of the spermatogenic pathway and changes of detrusor structure. It has been reported that abnormality of the bladder sensory function also affects OAB occurrence. Basic studies on urothelium show its various functions such as protective screen and high metabolic activity. Urothelium secretes neurotransmitters and inflammatory factors to mediate the response from sensory nerve fibers of interstitial nucleus in mucous membrane of urinary bladder and cells involved amplify sensory responses and regulate sensory changes of bladder. Moreover, physiological researches prove the significance of bladder sensory function in reflex activity of micturition (8, 9).

Transient receptor potential (TRP) including TRPV1 are located in cell membranes and intracellular membranes. While, in bladder, TRP mainly distributes in primary sensory neurons of urothelium nuclear membrane, which can be activated or sensitized by more than one exogenous and endogenous media. Even in recent studies, over expression of TRPV1 was found to correlate to inflammation and pain occurrence and development. Thus basic and clinical studies support the theory that besides pain perception, TRPV1 also involves in regular reflex activity of micturition and the introduction of urothelium stimulus and signals (10). ATP released by injured cells or inflammatory cells is able to activate P2X and P2Y receptors on primary sensory neurons to induce pain. P2X3 subunits in P2C receptors express in sensory neuron with high selectivity. Studies on antisense oligonucleotides, RNA interference, gene knockout and selective antagonist based on P2X3 indicate that ATP and P2X3 receptors play important roles in the production and maintenance of multiple pains. PGF2, NGF, SP and glutamic acid are all able to strengthen inward currents stimulated by P2X3 receptor agonist, thereby upregulating functions of P2X3 receptors rapidly.

In this study, TRPV1 expressed higher in urothelium of OAB female patients compared to healthy females in accordance with the results of studies conducted by Kai et al. (11, 12) who indicated the importance of TRPV1 in OAB occurrence mechanism. Furthermore, Krhut, et al. (13, 14) found that OAB caused by overactive detrusor rather than improved bladder sensitivity could be effectively treated through TRPV1 antagonist and blocker of cholinergic receptor and (or) adrenergic receptor. This was possibly because some patients suffered from abnormal regulation of sensory nerves. Kuo, et al. (15, 16) perfused PTX intravesically that was sensitive to TRPV1 and improved patients conditions, which in a sense suggested the vital role of bladder hyperesthesia in OAB occurrence mechanism.

Referring to regular indexes, parameters during urine storage period in this study like FDV, SDV and BC were obviously lower, suggesting bladder hyperesthesia occurrence in OAB patients. As for parameters during urination period, Pdet.Qmax was within normal range while Qmax was lower which was likely to be caused by reduced MCC thus patients were considered to experience normal urination. Based on comprehensive analysis of urodynamic data combined with immunohistology, bladder hyperesthesia ranked first in pathogenic factors of OAB. If anti-choline treatment is unable to cure a patient in an effective way, it is advisable to check urodynamic parameters. Once the patient is confirmed with improved bladder hyperesthesia, perfusion of capsaicin, RTX and alidase in bladder is supposed to function on bladder sensitivity reduction to achieve effective treatment. In conclusion, compared to urothelium of healthy females, TRPV1 expression is notably higher in urothelium of OAB patients. With urodynamic parameter changes in urine storage period, over expression of TRPV1 is proved to influence bladder hyperesthesia, the abnormality of bladder sensory function resulting

in OAB occurrence. Over expression of TRPV1 in urothelium of OAB patients is in close correlation to OAB occurrence and development. Thus, reducing sensitivity of bladder by regulating the expression of TRVP1 in urothelium can help to improve the symptoms of OAD patients.

ACKNOWLEDGEMENTS

This study was funded by: Shandong Nature Science Fund Project: ZR2009CL027; Fund Project for Science and Technology Plan of Science and Technology Bureau of Jinan: 20100118; and Medical Fund Project or Academy of Medical Science of Shandong: 201023.

REFERENCES

1. Na YQ, Ye ZQ, Sun G. Guideline on diagnosis and treatment of urological disease in china. Beijing: People's Medical Publishing House 2011; 147-53.
2. Lori B, Karl-Erik A. Urothelial signaling. Physiol Rev 2013; 93(2):653-80.
3. Wang YL, Xu KX, Hu H. Prevalence of overactive bladder and the impact of overactive bladder on quality of life in Beijing adult women. Chinese J Urol 2010; 31(8):550-4.
4. Feng SQ. Expression and clinical significance of transient receptor potential vanilloid type 1 in female patient with overactive bladder. Wuhan: Huazhong University of Science and Technology 2013. http://cdmd.cnki.com.cn/Article/CDMD-10487-1014028853.htm.
5. Birder LA, Nakamura Y, Kiss S, et al. Altered urinary bladder function in mice lacking the vanillaoid receptor TRPV1. Nat Neuros 2002; 5(9):856-60.
6. Charrua A, Cruz CD, Cruz F, et al. Transient receptor potential vanilloid subfamily 1 is essential for the generation of noxious bladder input and bladder over activity in cystitis. J Urol 2007; 177(4):1537-41.
7. Wang ZY, Wang P, Merriam FV, et al. Lack of TRPV1 inhibits cystitis-induced increased mechanical sensitivity in mice. Pain 2008; 139(1):158-67.
8. Lori AB. Nervous network for lower urinary tract function. J Urol 2013; 20(1):4-12.
9. Juszczak K, Thor PJ. The basic neurophysiologic concept of lower urinary tract function -the role of vanilloid TRPV1 receptors of urinary bladder afferent nerve endings. Adv Clin Exp Med 2012; 21(4):417-21.
10. Frias B, Charrua A, Avelino A, et al. Transient receptor potential vanilloid 1 mediates nerve growth factor-induced bladder hyperactivity and noxious input. BJU Int 2012; 110(8b):E422-E8.
11. Li M, Sun Y, Simard J, et al. Increased transient receptor potential vanilloid type 1 (TRPV1) signaling in idiopathic overactive bladder urothelial cells. Neurourl Urodyn 2011; 30(4):606-11.
12. Birder LA, Wolf-Johnston AS, Sun Y, et al. Alteration in TRPV1 and muscarinic (m3) receptor expression and function in idiopathic overactive bladder urothelial cells. Acta Physiologica 2013; 207(1):123-9.
13. Krhut J, Gartner M, Havranek O, et al. Combination therapy with anti-cholinergics and alphablockers for the treatment of overactive bladder in female patients-pilot study. Ceska Gynekol 2009; 74(6):416-20.
14. Charrua A, Cruz CD, Narayanan S, et al. GRC-6211, a new oral specific TRPV1 antagonist, decreases bladder overactivity and noxious bladder input in cystitis animal models. J Urol 2009; 181(1):379-86.
15. Ha US, Park EY, Kim JC. Effect of botulinum toxin on expression of nerve growth factor and transient receptor potential vanilloid 1 in urothelium and detrusor muscle of rats with bladder outlet obstruction-induced detrusor over activity. Urology 2011; 78(3):721.
16. Kissin I, Szallasi A. Therapeutic targeting of TRPV1 by resiniferatoxin, from preclinical studies to clinical trials. Curr Top Med Chem 2011; 11(17): 2159-70.

LETTER TO THE EDITOR

EFFECT AND MECHANISM OF DIHYDROARTEMISININ ON PROLIFERATION, METASTASIS AND APOPTOSIS OF HUMAN OSTEOSARCOMA CELLS

C. TANG[1], PY. AO[2], YQ. ZHAO[1], SZ. HUANG[1], Y. JIN[1], JJ. LIU[1], JP. LUO[1], J. ZHENG[1] and DP. SHI[3]

[1]Department of Orthopedics, People's Hospital of Zhengzhou University and Henan Province People's Hospital, Zhengzhou, Henan, China; [2]Department of Traditional Chinese Orthopedics and Physiotherapy, Traditional Chinese Medicine Hospital of Baoji, Baoji, Shaanxi, China; [3]Department of Radiology, People's Hospital of Zhengzhou University and Henan Province People's Hospital, Zhengzhou, Henan, China

Received July 1, 2015 – Accepted September 22, 2015

Osteosarcoma represents an aggressive type of bone malignancy that poses a significant health threat. The objective of the current study was to analyze the effect and mechanism of dihydroartemisinin (DHA) on the proliferation, metastasis and apoptosis of human osteosarcoma cells. A gradient concentration of DHA (15, 25 and 35 μmol.L^{-1}) was used to stimulate the cells, along with control and Dimethyl sulfoxide (DMSO). The phenotypic outcomes were characterized using MTT assay, clone formation assay, Hoechst 33258 staining assay, luciferase reporter plasmid assay, Western blot and wound healing assay. In addition, IBM SPSS Statistics 18.0 software was applied for statistical analysis and all experimental data were expressed as mean ± s.d. Analysis of variance (ANOVA) was applied to compare the differences among multiple groups. Our results demonstrated that DHA inhibited the proliferation and metastasis of osteosarcoma cells and promoted the apoptosis in the cytomorphosis.

Osteosarcoma originates from the mesenchyme with the potential of becoming osteogenic. Osteosarcoma cells that are actively aberrantly proliferating directly produce neoplastic osteoid tissues or immature bones, which harbor high levels of malignancy and are likely to induce an early pulmonary metastasis (1). The development of neoadjuvant chemotherapy and limb salvage has increased the five-year survival rate to 65%~75%, despite a 40% death rate resulting from pulmonary metastasis (2).

Artemisinin and its derivatives are malarial drugs, which are clinically effective with high recovery rates and low toxicity. These drugs induce impressive outcomes, particularly for cerebral malaria and malignant malaria that exhibit robust tolerance to chloroquine and other drugs, thus enabling therapeutic application (3). Dihydroartemisinin (DHA) is one of the important derivatives of artemisinin, which has a molecular formula of $C_{15}H_{24}O_5$ and a molecular weight of 284.35 with high anti-malarial activity and strong water-solubility. DHA assumes a multifaceted biological function, including and regulating immune responses, suppressing tumor growth, and

Key words: dihydroartemisinin, osteosarcoma, cell proliferation, metastasis, apoptosis

Mailing address: Dr Jia Zheng,
People's Hospital of Zhengzhou University,
No. 7, Weiwu Road ,
Zhengzhou City, 450003, PR China
Tel.: + 8613939061358
Fax: +86 0371-65528998
e-mail: zmeditzj@163.com

0393-974X (2015)

DISCLOSURE: ALL AUTHORS REPORT NO CONFLICTS OF INTEREST RELEVANT TO THIS ARTICLE.

inhibiting proliferation of scars. Notably, when utilized in cancer patients, DHA maintains high anti-tumor activity with minimal collateral damage to normal tissues.

In a study by Zhan Xiaolong et al. (4), it was found that DHA could effectively inhibit the development of colorectal cancer in nude mice with transplanted tumors. Compared with other derivatives, DHA exhibit multiple remarkable merits, including oral assimilation, short response time, wide distribution *in vivo*, quick excretion and metabolism. Interestingly, there have been a large body of studies on regulators that modulate the proliferation and metastasis of osteosarcoma cells. For example, in the paper by Song Guohui et al. (5), the effect of SCUBE3 on osteosarcoma cell growth and its association with prognosis was extensively investigated. Besides, the expression of the SCUBE3 protein in osteosarcoma cells and tissues was found to be significantly increased, which potentially promotes the growth of osteosarcoma cells by perturbing the cell cycle. In the paper by Zhang Xi et al. (6), based on the study concerning how RanBP9 expression influences the proliferation, apoptosis and metastasis of osteosarcoma cells, it was revealed that RanBP9 was highly expressed in osteosarcoma cells. Intriguingly, decreased expression of RanBP led to enhanced proliferation and metastasis of osteosarcoma cells, as well as a lower rate of apoptosis.

Therefore, this paper investigated the effect of DHA on human osteosarcoma cell, and then discussed its effect on the proliferation, metastasis and apoptosis of osteosarcoma cells, and further analyzed the functional mechanism of DHA.

MATERIALS AND METHODS

Materials

Human osteosarcoma cells were purchased from American type culture collection. Cells were cultured in a sterile thermostat incubator at 5% CO_2 and 37C° in complete medium containing 10% fetal bovine serum (FBS) and 1% penicillin or streptomycin (P/S). MTT, DMSO and Trypsin/EDTA solution were also added (Sigma, USA). DHA (Sichuan Sanqi Pharmaceutical Co., Ltd) was dissolved in DMSO to prepare 70mmol/L liquid medicine. DMEM medium, FCS and P/S were all purchased from Thermo Scientific (USA), and Hoechst 33258(C1011) was from Beyotime. Trypsin/EDTA solution (R-001 -100) was purchased from Cascade Biologics. The mouse monoclonal antibody VEGF (C-1) (Art. No. sc-7269), goat polyclonal antibody MMP-9 (C-20) (Art. No. Sc-6840) and mouse monoclonal antibody β Actin (Art. No. sc -47758) were all from Santa Cruz Biotechnology Co., Ltd.

Methods

A total of five groups, including Control (blank control), DMSO (solvent control), and DHA with 15, 25, 35μmol.L^{-1} were studied.

MTT assay

Monolayer adherent cells were obtained in the exponential phase and then digested into single cells with 0.25% Trypsin. Cell suspension was prepared at around 5×106 per/ L. In a 96-well plate, 100 μL cellular suspensions were added to each well; when cells were attached, the following processing steps were carried out based on intended classification (there were 8 parallel wells in each group). Four hours before the conclusion of processing, 0.02mL MTT (5 g·L^{-1}) was added to each well. Four hours later, the absorbance was determined (OD value) at 492 nm, and the cellular survival graph produced. Each experiments was repeated three times.

Clone formation assay

Monolayer adherent cells were obtained in the exponential phase and then digested into single cells with 0.25% Trypsin; cell suspension was prepared with density of 150 per/mL. In a 6-well plate, 1 ml cellular suspension was added to each well. When cells were attached, they were cultured at 37C° and 5% CO_2 and against saturated humidity environment. Ten days later, the culture was terminated and the supernatants then removed. Cells were rinsed gently twice with PBS, and then maintained for 15 min (stationary liquid was made up of Acetic Acid plus Methanol in the ratio of 1:3). The crystal violet living cell staining was conducted for 30 min, and the staining solution was rinsed out slowly and kept air-dried. The clone formation of cells was observed, and the number of clones over 10 cells under a microscope (at low power lens) were counted to calculate the rate of clone formation. This assay was repeated for three independent times, and the equation was used as follows: rate of clone formation/%= the number of clones/ the number of inoculated cells ×100%.

Hoechst 33258 staining

The monolayer adherent cells were obtained in the exponential phase and then digested into single cells with 0.25% Trypsin. Cell suspension was prepared at a density of 5×107 per/L. In a 24-well plate, 0.5 ml cell suspension

was added to each well. Attached cells were dissolved in water at 37C° for 7 min, and then rapidly cooled, followed by centrifugation and removal of the staining solution. Cells were then resuspended in PBS and the blue fluorescence was observed at 450 nm of ultraviolet. Normal control cells and necrotic cells appeared to be light blue, and apoptotic cells appeared to be bright blue; karyopyknosis was observed. This assay was repeated for three times.

Luciferase reporter plasmid assay

The cells were spread in the exponential phase onto a 24-well plate. Attached cells were transfected with 0.3μg reporter plasmid by Lipofectamine 2000. Five hours later, the transfection was terminated and replaced with regular medium. Cells were lysed 24 h later and the luciferase activity was determined according to the manufacturer's instructions. The total protein concentration in lysate was then determined and corrected by the BCA method. This assay was repeated for three times and the mean value obtained as the experimental result.

Western blot

After stimulation with DHA for 24 h, lysates from human 143B osteosarcoma cells were obtained prepared for Western blot with condensed SDS-PAGE protein buffer solution, and then placed in boiling water for 10 min to achieve complete protein denaturation. SDS-PAGE was then performed. This assay was repeated for three times.

Wound healing assay

The individual human 143B osteosarcoma cells were spread in a good growth state at a density of 5×105 per/L into a 6-well plate (1000 μL in each well) and then maintained cell culture for 6~8 h. When the monolayer adhesion grew, a "#" on monolayer cell was marked by a gel pen and the abscission cells gently rinsed out by PBS. DHA was then added in different concentrations and pictures recorded at 0 h, 6 h, 12 h, and 24 h. This assay was repeated for three times.

Statistical analysis

IBM SPSS Statistics 18.0 software was utilized for statistical analysis and all experimental data were expressed as Mean ± SD and differences among multiple groups were analyzed by analysis of variance (ANOVA).

RESULTS

DHA inhibited the proliferation of osteosarcoma cell 143 B

DHA significantly inhibited the activity and survival rate of 143B cell proliferation as demonstrated by MTT assay and crystal violet staining. Upon stimulation with DHA in different concentrations for 24 h, results from the MTT assay on 143B osteosarcoma cells demonstrate the activity of cell proliferation was significantly lower in the experiment group than in the control

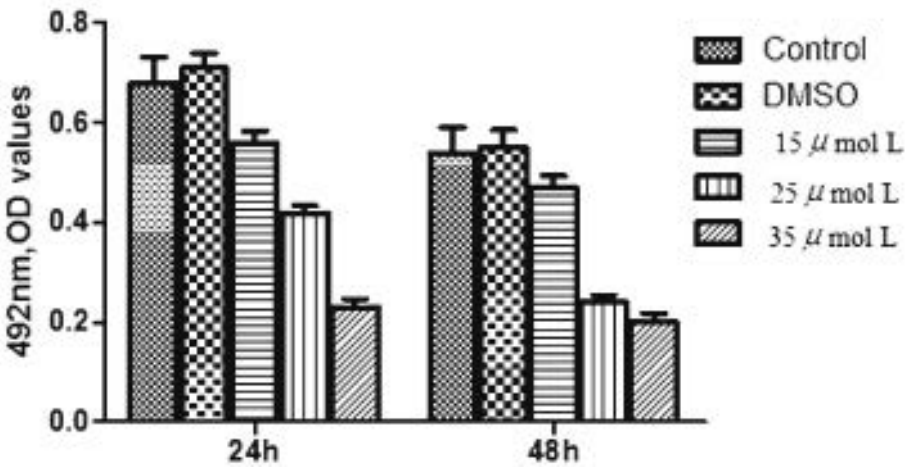

Fig. 1. *Inhibitory effect of DHA on 143B osteosarcoma cell lines (mean ± SD, n=3).*

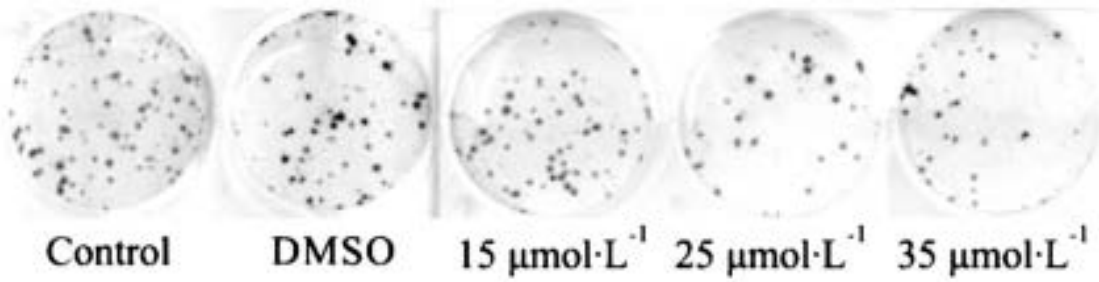

Fig. 2. *Clone formation after DHA stimulation on 143B osteosarcoma cells.*

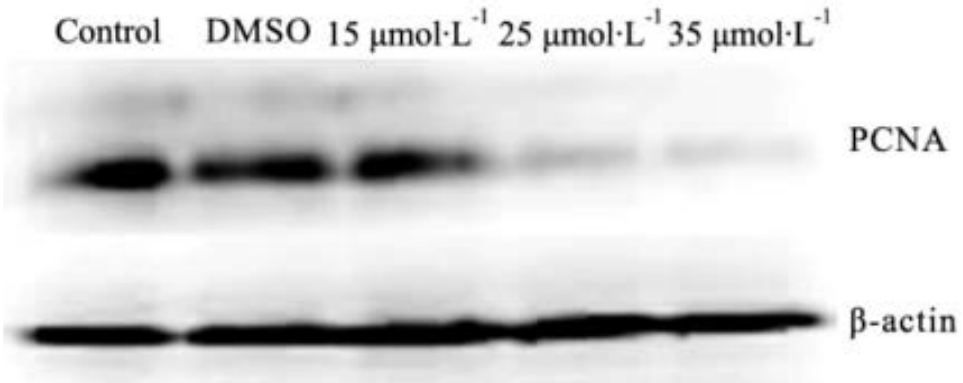

Fig. 3. *Decreased expression of the PCNA protein induced by DHA in 143B cell lines.*

group, suggestion a strong inhibitory role for DHA that depended upon concentration and duration of stimulation (Fig. 1).

Our additional experiments demonstrated that DHA effectively impaired the ability of 143B cells to form clones. This indicated that while DHA significantly inhibited cell proliferation, it also compromised clone formation. The results of clone formation assay showed that the rates of clone formation in these five groups were 0.607, 0.580, 0.453, 0.313, and 0.253, respectively (Fig. 2).

We further discovered that DHA inhibited the expression of PCNA, a key regulator for cell proliferation, which is consistent with an inhibitory role for DHA in regulating the proliferation of human 143B osteosarcoma cells. After stimulation with various concentrations of DHA on 143B human osteosarcoma cells for 24 h, results from Western blots showed a lower expression of PCNA protein (Fig. 3), which failed to promote the function of DNA polymerase δ as accessory protein and thus restricted the DNA synthesis in 143B cells. This provides a potential mechanistic explanation as to how the proliferation of 143B cells was inhibited.

Because the Wnt/β-catenin signal transduction plays a key role in the pathogenesis of a spectrum of human diseases, in particular cancer, we hypothesized that DHA may inhibit the activity of the critical protein factor β-Catenin and thereby modulate the activation of Wnt/β-catenin cascade. Therefore, we constructed a β-Catenin luciferase plasmid (p-Top) and induced adenovirus-mediated Wnt-3a overexpression (positive control). As shown in Fig. 4, Adv-Wnt-3a effectively stimulated the activity of β-Catenin; in contrast, there was only a weak activity of β-Catenin in the experiment group. Together, these results indicated that DHA inhibited the critical protein factor β-Catenin and thus Wnt/β-

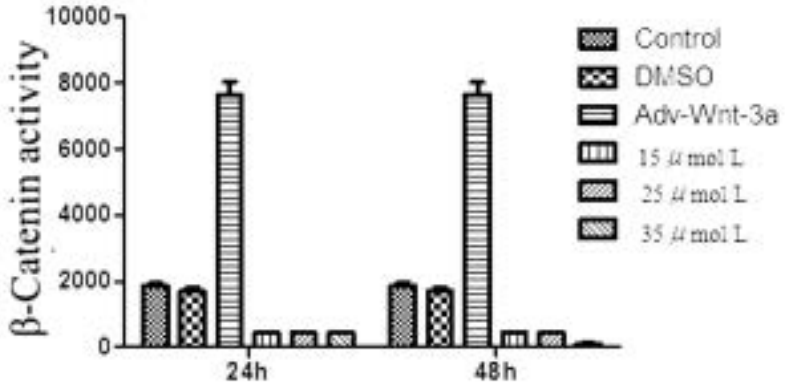

Fig. 4. *Reduced activity of β-Catenin resulting from DHA stimulation in 143B cell lines.*

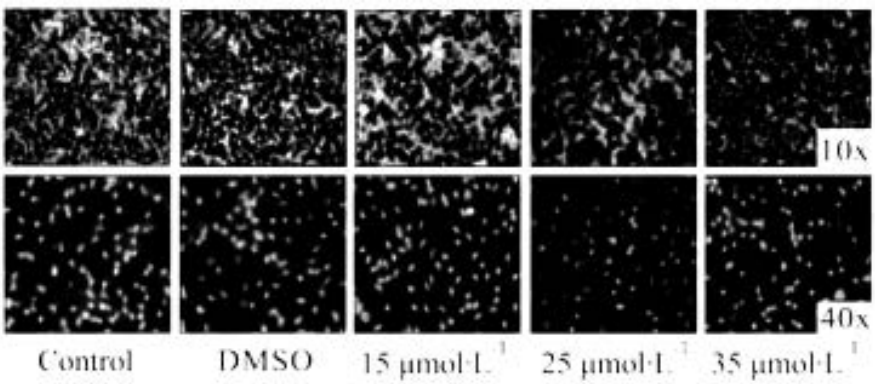

Fig. 5. *Induced apoptosis of 143B osteosarcoma cell lines by DHA as demonstrated by Hoechst 33258 staining.*

catenin signal transduction.

DHA induced the apoptosis of 143B human osteosarcoma cells

Results from Hoechst 33258 apoptosis staining revealed that DHA promoted the apoptosis of 143B cell, as shown in Fig. 5. Upon stimulation with DHA for 24 h, 143B cells adopted a unique pattern that was characterized by uniform nuclei and well-distributed and diffused fluorescence, which appeared to be light blue. Compared with the control group, nuclei from the cells in the experiment group appeared to be much smaller with condensed chromatin and unevenly distributed fluorescence staining, suggestive of active apoptosis. Taken together, these results showed that DHA may induce and promote the apoptosis of 143B human osteosarcoma cells.

A previous study established that DHA induced altered expression of apoptosis-related proteins, such as Bcl-2, Bad and Caspase-3 (7). We therefore assessed the expression of these proteins by Western blots. As demonstrated in Fig. 6, the expression of Bad was increased, which promoted its interaction with Bcl-2 (8) and thus inhibited the anti-apoptotic activity of Bcl-2. Meanwhile, the expression of Caspase-3 was higher, which is in line with the enhanced apoptosis we observed. Therefore, our Western blot results strongly suggest that DHA effectively promotes the apoptosis of 143B cells, which likely results from higher expression of Bad and Capase-3 proteins and attenuated anti-apoptotic activity of the Bcl-2 protein.

DHA inhibited the metastatic activity of 143B human osteosarcoma cells (wound healing assay)

Upon stimulation with DHA for 6 h on 143B cells, we found that the metastatic ability of 143B cells was

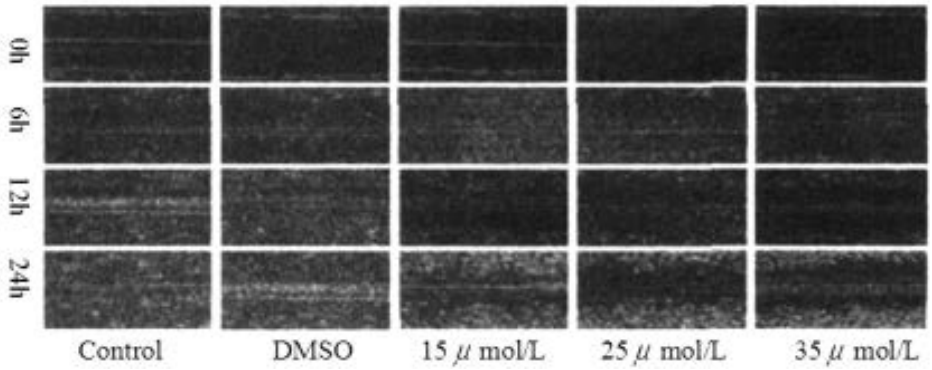

Fig. 6. *Evaluation of metastatic ability of 143B cells in wound healing assay.*

significantly impaired under microscopy, as shown in Fig. 6. Twelve or 24 hours later, the effect becomes much more pronounced, as the cellular movement in the experiment group was significantly downregulated, while the cells in the control group almost completely crossed the wound and achieved a radical recovery These data suggested that DHA effectively inhibits the metastasis of 143B, which becomes much more obvious for a longer period of time.

DISCUSSION

Metastasis represents a particularly life-threatening situation that occurs frequently in human osteosarcoma. Early pulmonary metastasis is especially a prominent challenge in patients with osteosarcoma that results in difficulty in clinical treatment. The development of osteosarcoma is a multi-step complex process that includes altered expression of genes involved in various biological functions (9, 10). DHA exhibited high anti-tumor activity by inhibiting the proliferation of tumor cells, inducing the apoptosis of tumor cells, suppressing the generation of new blood vessels, reversing the drug-resistance of tumor cells and improving its ability to kill tumor cells. DHA has high water-solubility and other clinically useful characteristics, such as being readily assimilated and quick and highly effective excretion and metabolism with less toxicity. In-depth studies uncovered that, in addition to a specific anti-malarial effect, DHA regulates immune and inflammatory responses, and can also inhibit the proliferation of scars. These outstanding features have earned DHA broad attention from the public for clinical use. Our results demonstrated that DHA regulated human osteosarcoma cells by maintaining the expression of related important proteins. However, our study must be interpreted with precaution as the effect of dihydroartemisinin on proliferation, metastasis and apoptosis of osteosarcoma cells needs to be confirmed by animal models or human samples *in vivo*.

In this paper, different concentrations of DHA were used to stimulate 143B human osteosarcoma cell *in vitro*. The MTT assay showed that DHA in all assessed concentrations could inhibit the proliferation of 143B osteosarcoma cells, and the rate of inhibition was dependent on the concentration and duration of DHA used. When the concentration of DHA reached beyond 35 μ mol·L^{-1}, after stimulation for 48 h, there was a significant effect on inhibiting proliferation and clone formation of 143B cells when compared with the control group ($p<0.01$). Furthermore, results from Hoechst 33258 staining assay, luciferase reporter plasmid assay, Western blot and wound healing assay demonstrated that 143B human osteosarcoma cells had high ability of metastasis. Compared with the control group, the DHA experiment group could effectively inhibit the expression of relative proteins and further inhibit the proliferation of osteosarcoma cells.

REFERENCES

1. Kumar RM, Arlt MJ, Kuzmanov A, Born W, Fuchs B. Sunitinib malate (SU-11248) reduces tumour burden and lung metastasis in an intratibial human

xenograft osteosarcoma mouse model. Am J Cancer Res 2015; 5(7):2156-68.
2. Rasalkar DD, Chu WC, Lee V, Paunipagar BK, Cheng FW, Li CK. Pulmonary metastases in children with osteosarcoma: characteristics and impact on patient survival. Pedia Radiol 2011; 41(2):227-36.
3. Talundzic E, Chenet SM, Goldman IF, Patel DS, Nelson JA, Plucinski MM, Barnwell JW, Udhayakumar V. Genetic analysis and species specific amplification of the artemisinin resistance-associated Kelch Propeller Domain in P. falciparum and P. vivax. PLoS One 2015; 10(8):e0136099.
4. Krishna S, Ganapathi S, Ster IC, et al. A Randomised, double blind, placebo-controlled pilot study of oral artesunate therapy for colorectal cancer. EBioMedicine 2014; 2(1):82-90.
5. Herrera CL, Kim DY, Kumar SR, Bryan JN. Peroxisome proliferator activated receptor g protein expression is asymmetrically distributed in primary lung tumor and metastatic to lung osteosarcoma samples and does not correlate with gene methylation. BMC Vet Res 2015; 11(1):230.
6. Wang Z, Sokolovska A, Seymour R, Sundberg JP, Hogenesch H. SHARPIN is essential for cytokine production, NF-kB signaling and induction of Th1 differentiation by dendritic cells. PLoS One 2012; 7(2):e31809.
7. Brigger D, Schläfli AM, Garattini E, Tschan MP. Activation of RARα induces autophagy in SKBR3 breast cancer cells and depletion of key autophagy genes enhances ATRA toxicity. Cell Death Dis 2015; 6:e1861.
8. Ahmad Tali M, Bashir Y, Bhat S, Manzoor F, Bashir N, Geelani S, Rasool J, Waheed Mir A. Pseudotumour cerebri in acute promyelocytic leukemia on treatment with all-trans-retinoic acid (ATRA) - an experience from a tertiary care centre. Malays J Pathol 2015; 37(2):141-44.
9. Strauss SJ, Ng T, Mendoza-Naranjo A, Whelan J, Sorensen PH. Understanding micrometastatic disease and Anoikis resistance in Ewing family of tumors and osteosarcoma. Oncologis 2010; 15(6):627-35.
10. Sampo M, Koivikko M, Taskinen M, et al. Incidence, epidemiology and treatment results of osteosarcoma in Finland-a nationwide population-based study. Acta Oncol 2011; 50(8):1206-14.

LETTER TO THE EDITOR

INFLUENCE OF COLORECTAL CANCER TUMOR SUPPRESSOR GENE CHD5 METHYLATION ON ITS CLINICAL AND PATHOLOGICAL CHARACTERISTICS

JB. LIU, QB. ZHOU, JZ. XU, GX. WANG and WT. YUAN

Colorectum surgery department of the First Affiliated Hospital of Zhengzhou University, Zhengzhou, China

Received June 25, 2015 – Accepted September 25, 2015

Recently, abnormal tumor suppressor gene (TSG) methylation has become a hotspot in the research on colorectal cancer (CRC). This study aimed to explore the influence of CHD5 methylation of CRC TSG on its clinical and pathological characteristics. A total of 40 operation samples as well as corresponding tissue specimens were collected from CRC patients treated in the First Affiliated Hospital of Zhengzhou University from January to December in 2014. CHD5 gene methylation in tissue specimens was detected with methylation specific polymerase chain reaction (MSP); moreover, messenger ribose nucleic acid (mRNA) expression of CHD5 in each tissue was tested using reverse transcription-polymerase chain reaction (RT-PCR), and Western blot was applied to detect the expression of CHD5 protein in those tissues and to analyze the correlation between mRNA and protein of cancer tissue CHD5 as well as the relationship between CHD5 methylation and protein expression. Results revealed that the expression rate of CHD5 methylation in 40 normal mucosal tissues, para-carcinoma tissues, adenoma tissues and CRC tissues was 12.5% (5/40), 22.5% (9/40), 47.5% (19/40) and 72.5% (33/40), respectively. The mRNA expression of CHD5 in the above tissues was 0.225±0.276, 0.169±0.231, 0.147±0.159 and 0.013±0.011 and the protein expression of CHD5 was 0.438±0.205, 0.398±0.180, 0.156±0.1 and 0.024±0.311, respectively. Methylation rate of CHD5 was 87% (20/23) in 23 cases of CHD5 protein loss expression and 52.9% (9/17) in 17 cases of CHD5 protein expression. Results of *chi*-squared test indicated that there was a significant difference in methylation rate ($P < 0.05$), that is, the methylation rate of negatively expressed CHD5 protein was obviously higher than positively expressed protein. Thus, it can be concluded that the CHD5 methylation rate rises gradually in the evolution of CRC, which is related to the occurrence and development of CRC. Furthermore, CHD5 mRNA is positively correlated with protein expression and CHD5 gene methylation is associated with protein loss expression. Therefore, TSG CHD5 methylation of rectal cancer has a great effect in influencing its clinical and pathological features.

Colorectal cancer (CRC), one of the most common malignant tumors in the digestive tract, has the third morbidity and mortality among malignant tumors worldwide (1). In China, morbidity of CRC ranks third and mortality ranks fifth, its mechanism is still unclear, and the commonly used fecal occult blood method is lowly sensitive and specific to early screening and diagnosis of CRC. One third of Chinese patients were in the progressive stage when being confirmed (2). Over the past twenty years, the

Key words CRC, methylation, CHD5, methylation specific PCR

Mailing address:
Dr Weitang Yuan,
colorectum surgery department,
the First Affiliated Hospital, Zhengzhou University, Zhengzhou, 450052, China
e-mail: ywt0284@163.com

0393-974X (2015)

morbidity of CRC has increased notably as diet and lifestyle of Chinese people changed. Abnormal tumor suppressor gene (TSG) methylation leading to TSG inactivation cannot normally transcribe, translate and synthesize tumor-suppressor protein, and also fails to play a role of antitumor effect, so cells are capable of developing monoclonal hyperplasia and forming tumors (3). In recent years, some scholars (4, 5) have found down-regulated or silent expression induced by CHD5 gene methylation is related to a variety of malignant tumors, including CRC. Although China is a low-epidemic area, the incidence of CRC is rising year after year as dietary structure and lifestyle change (6).

This study was designed to explore the role of CHD5 gene methylation in CRC mechanism and its relationship with CRC clinical pathology through detecting the condition of CHD5 gene methylation in the carcinogenic process of CRC, as well as messenger ribose nucleic acid (mRNA) and protein expression of CHD5 gene, so as to discuss the relationship between this gene methylation and the occurrence and development of CRC and clinical and pathological features.

MATERIALS AND METHODS

Specimen collection

From January to December in 2014, cancer tissues, corresponding adjacent para-carcinoma tissues and remote normal tissues, were collected from 40 patients, 21 males and 19 females, aged 46-77 years (average age: 58.28±7.91 years), who had CRC but had not received chemotherapy or radiotherapy. Patients were divided into groups according to clinical and pathological features: age: < 50 years (8 cases), ≥ 50 years (32 cases); tumor site: colon (15 cases), rectum (25 cases); tumor lesion: < 5 cm (12 cases), ≥ 5 cm (28 cases); depth of invasion: submucosa (14 cases), muscular layer (26 cases); differentiated degree: low differentiation (15 cases), moderate and high differentiation (25 cases); tumor node metastasis (TNM) staging: I ~ II stages (22 cases), III ~ IV stages (18 cases); lymph node metastasis: negative (26 cases), positive (14 cases); distant metastasis: negative (28 cases), positive (12 cases). Specimens were frozen in liquid nitrogen immediately after being obtained, and then stored at -80°C. This study was reviewed and approved by the ethics committee of the First Affiliated Hospital of Zhengzhou University and all patients signed informed consent.

Experimental methods

CHD5 gene methylation was tested with methylation specific polymerase chain reaction (MSP) method based on the following steps. Deoxyribose nucleic acid (DNA) was extracted from human colorectal tissues and modified with sodium hydrogen sulfite, and then purified and recycled. The DNA was then used in MSP and methylation specific PCR amplification after modification. Reverse transcription-polymerase chain reaction (RT-PCR) was applied in detecting mRNA. RNA was extracted with Trizol method and identified, and finally reverse transcription and real-time PCR reactions were observed. CHD5 protein expression was detected with Western-blot. Protein was extracted and received sodium dodecyl sulfate polyacrylamide gel electrophoresis (SDS-PAGE) electrophoresis, and then transferred and crossbred.

Statistical analysis

SPSS 13.0 software was applied for statistical analysis, all data were expressed with mean ± SD. One-way analysis of variance, together with Student-Newman-Keuls' test, was used in pairwise comparison, Pearson χ^2 confirmed whether there was a differences between two or more total rates, and Pearson correlation analysis was used to confirm whether there was a correlation between two variables. Difference was considered to be significant if $P < 0.05$.

RESULTS

CHD5 methylation of tissues

Expression rates of CHD5 methylation in 40 normal mucosal tissues, para-carcinoma tissues, adenoma tissues and CRC tissues were 12% (5/40), 22% (9/40), 47% (19/40) and 72% (33/40), respectively. Compared with normal, para-carcinoma and adenoma tissues, the positive rate of CHD5 methylation in cancer tissues was significantly higher ($P < 0.05$), and adenoma tissues had remarkably higher positive CHD5 methylation rate than normal and para-carcinoma tissues ($P < 0.05$), and the differences between normal and para-carcinoma tissues were not statistically significant ($P > 0.05$) (Table I).

CHD5 gene methylation was closely correlated with CRC differentiated degree, staging, lymphatic metastasis and distant metastasis ($P < 0.05$), while having no obvious relationship with age, gender, tumor site, tumor size, tumor pathological pattern or other clinical and pathological characteristics ($P > 0.05$) (Table II).

The condition of CHD5 gene methylation had a correlation with pathological patterns of colorectal adenoma ($P < 0.05$), and the methylation rate of villous adenoma (75%) was higher than tubular (33.3%), tubulovillous (33.3%), and serrate (0%) adenoma tissues. Besides, CHD5 gene methylation was obviously not related to gender, age, adenoma site, adenoma size, number of adenoma or other clinical and pathological parameters ($P > 0.05$).

CHD5 mRNA expression in every tissue

Of 40 normal tissues, para-carcinoma tissues, adenoma tissues and CRC tissues, the mRNA expression of CHD5 was 0.225±0.276, 0.169±0.231,

Table I. *CHD5 methylation rate in four kinds of tissues.*

Tissues	Methylation number	Non-methylation number	Methylation rate/%	P value (corresponding χ^2 value)
Normal tissues	5	35	12	
Para-carcinoma tissues	13	27	22	0.24*(1.38)
Adenoma tissues	19	21	47	0.0 (11.67) 0.0 (5.5)
Cancer tissues	33	7	72	0.0 (29.46) 0.0 (20.05) 0.0 (5.21)

*Note: Δ, *, • and •• indicates P<0.05, compared to cancer tissues, para-carcinoma tissues, normal tissues and adenoma tissues.*

Table II. *Relationship between CHD5 methylation and clinical pathological features of CRC.*

Clinical pathological parameters		N	CHD5			χ^2	P
			Methylation	Non-methylation	Methylation rate (%)		
Gender	Male	21	13	8	61.9	0.001	0.970
	Female	19	14	5	73.7		
Age	< 50	8	5	3	62.5	0.200	0.660
	≥ 50	32	24	8	75.0		
Tumor site	Colon	15	10	5	66.7	0.001	0.970
	Rectum	25	16	9	64.0		
Tumor size	< 5 cm	12	7	5	58.3	0.050	0.820
	≥ 5 cm	28	16	12	57.1		
Differentiated degree	Low	15	12	3	80.0	4.700	0.300
	Moderate + high	25	11	14	44.0		
TNM staging	I + II stages	22	12	10	54.5	4.400	0.030
	III + IV stages	18	16	2	88.9		
Invasion depth	Submucosa	14	8	6	57.1	0.060	0.800
	Muscular layer	26	14	12	53.8		
Lymph node metastasis	With	26	7	19	26.9	5.200	0.020
	Without	14	9	5	64.3		
Distant metastasis	Without	28	6	22	21.4	7.900	0.050
	With	12	10	2	83.3		

Table III. *Correlation of CHD5 methylation and protein expression in CRC tissues.*

Item/No. of cases		CHD5 protein expression /No. of cases		χ^2	P
+		+	-		
Methylation	+	9	20		

0.147±0.159 and 0.013±0.011; and one-way analysis of variance Student-Newman-Keuls (SNK) test demonstrated that differences existed in the mRNA expression of CHD5 in these tissues ($P < 0.05$), showing a downward trend.

CHD5 protein expression in every tissue

The protein expression of CHD5 in 40 normal tissues, para-carcinoma tissues, adenoma tissues and CRC tissues was 0.438±0.205, 0.398±0.180, 0.156±0.100 and 0.024±0.311, respectively; and one-way analysis of variance SNK test indicated that there were differences in the protein expression of CHD5 in the above tissues ($P < 0.05$), showing a downward trend.

Relationship between CHD5 mRNA and protein expression

Pearson correlation analysis on mRNA and protein expression of CHD5 in 40 CRC tissues showed a positive correlation, with a statistical significance ($r = 0.899$, $P < 0.05$). Low or loss of mRNA expression of CHD5 gene was always accompanied with low or loss of protein expression.

Relationship between cancer tissue CHD5 protein expression and CHD5 methylation

After qualitatively detecting the methylation and protein expression of CHD5 in 40 cancer tissues and analyzing their relationships, it was found that the methylation rate of CHD5 was 87% (20/23) in 23 cases of protein expression loss and 52.9% (9/17) in 17 cases of protein expression. *Chi*-squared test results displayed that the difference of methylation was significant ($\chi^2 = 5.673$, $P < 0.05$), that is, negatively expressed CHD5 protein apparently exceeded positively expressed protein in methylation rate (Table III).

DISCUSSION

As the standard of living improves and dietary habits and structures change, rapidly growing morbidity and mortality of CRC seriously threaten people's health. Gene methylation mainly includes high methylation of TSG CpG island and low methylation of whole genome (7, 8), and tumor suppressor gene methylation runs through the whole process of the occurrence and development of CRC, which affects cell cycle, DNA repair, carcinogen metabolism, interactions between cells, cell apoptosis and angiogenesis, etc (9). It has been shown by the present study that CHD5 methylation was capable of causing antitumor effect loss and bringing about CRC through affecting mRNA and protein expression. CHD5 methylation might involve in the evolution of colorectal adenoma – adenocarcinoma. In this way, CHD5 methylation could show a great potential in screening and diagnosing CRC in an early phase. Besides, multiple genes combined with methylation detection could improve the specificity and sensitivity of early CRC diagnosis (10, 11). Patients with low tumor differentiation, lymph node metastasis, distant metastasis and malignant staging developed high CHD5 methylation rate, which predicted a potential of malignancy and could be used for monitoring conditions and estimating prognosis (12 ~ 14).

To sum up, CHD5 methylation rate in CRC is high, and meanwhile, reduced mRNA and protein expression are also observed. CHD5 gene may have incomplete expression due to methylation, leading to occurrence and development of CRC. In addition, CHD5 methylation is closely associated with clinical and pathological features of CRC, and patients with low tumor differentiation, lymph node metastasis, distant metastasis and malignant tumor are more

likely to have methylation.

REFERENCES

1. Ferlay J, Shin HR, Bray F, Forman D, Mathers C, Parkin DM. Estimates of worldwide burden of cancer in 2008: GLOBOCAN 2008. Int J Cancer 2010; 127(12): 2893-917.
2. Kim MS, Lee J, Sidransky D. DNA Methylation markers in colorectal cancer. Cancer Metastasis Rev 2010; 29(1):181-206.
3. Zhao R, Wang NS, Huang HL, Ma WL, Yan QT. CHD5 a tumor suppressor is epigenetically silenced in hepatocellular carcinoma. Liver Int 2014; 34(6):e151-60.
4. Wang J, Chen H, Fu S, Xu ZM, Sun KL, Fu WN. The Involvement of CHD5 Hypermethylation in Laryngeal Squamous Cell Carcinoma. Oral Oncol 2011; 47(7):601-8.
5. Lee JC, Chen MJ, Chang CH, Tiai YF, Lin PW, Lai HS, Wang ST. Plasma amino acid levels in patients with colorectal cancers and liver cirrhosis with hepatocellular carcinoma. Hepato-Gastroenterol 2003; 50 (53):1269-73.
6. Sung JJ, Lau JY, Goh KL, et al. Increasing incidence of colorectal cancer in Asia: implications for screening. Lancet Oncol 2005; 6(11):871-76.
7. Hu WX, Wang TZ, Xu JH, Li HZ. Micro RNA mediates DNA methylation of target genes. Biochem Biophys Res Commun 2014; 444(4):676-81.
8. Weber M, Davies JJ, Wittig D, Oakeley EJ, Haase M, Lam WL, Schubeler D. Chromosome-wide and promoter-specific analyses identify sites of differential DNA methylation in normal and transformed human cells. Nat Genet 2005; 37:853-62.
9. Carmona FJ, Esteller M. Epigenomics of human colon cancer. Mutat Res 2010; 693(1-2):53-60.
10. Tokarz P, Blasiak J. Role of DNA Methylation in colorectal cancer. Postepy Biochem 2013; 59(3): 267-79.
11. Bawson JB, Bapat B. Epigenetic biomarkers in colorectal cancer diagnostics. Expert Rev Mol Diagn 2012; (12):499-509.
12. Zhao R, Yan QT, Lv JY, Huang HL, Zheng WL, Zhang B. CHD5, a tumor suppressor that is epigenetically silenced in lung cancer. Lung Cancer 2012; 76(3):324-31.
13. Koyama H, Zhuang TG, Light JE, Kolla V, Higashi M, McGrady PW, London WB, Brodeur GM. Mechanisms of CHD5 inactivation in neuroblastomas. Clin Cancer Res 2012; 18(6):1588-97.
14. Fujita T, Igarashi J, Okawa ER, et al. CHD5, a tumor suppressor gene deleted from 1p36. 31 in Neuroblastomas. J of the Nat Cancer Inst 2008; 100(13): 940-949.

LETTER TO THE EDITOR

ANGIOGENESIS OF HEPATOCELLULAR CARCINOMA UNDER MULTISLICE SPIRAL CT PLAIN SCAN AND ENHANCED SCAN

A.D. MA[1], Y. ZHANG[1], Z. XUE[1] and K. LI[2]

[1]Department of Radiology, Shandong Jining No.1 People's Hospital, Jining, Shandong, China; [2]Department of Gynaecology and Obstetrics, Affiliated Hospital of Shandong Academy of Medical Sciences, Shandong Academy of Medical Sciences, Shandong, China

Received May 11, 2015 – Accepted July 14, 2015

This study explores the value of 64-layer spinal computed tomography (CT) in diagnosing hepatocellular carcinoma (HCC) through performing dynamic contrast-enhanced scans. The study includes analysis of enhancement presentation of HCC in dynamic contrast-enhanced scan performed by multislice spinal CT (MSCT), comparison of detection rate and positive predictive value of neoplastic foci in subdivided arterial phases and portal venous phases, optimization of optimal scanning scheme for diagnosing HCC and discussion of the value of quantitative indexes such as T-D curve, maximum enhancement rate and clearance rate in diagnosing and identifying HCC. A total of 61 lesions were detected in 40 patients with HCC who were selected from the First People's Hospital, Jining, Shandong, China. Density difference was observed with statistical significance between the solid part of tumor and normal liver in different periods after CT scan and enhanced scan ($H = 45.208$, $P < 0.01$), and difference in the late arterial phase was the most obvious; enhanced peak value mostly appeared in the late arterial phase. In terms of lesion detection rate, the difference of HCC detection rate was statistically significant in early, middle and late arterial phase and early and late portal vein phases ($\chi^2 = 32.910$, $P = 0.001$), and the rate was the highest in the late arterial phase (78.689%). Lesions were divided into 3 cm or less group (small HCC) and over 3 cm group based on the maximum parameter. Detection rate of the late arterial phase was the highest, 85% (3 cm or less) and 75.61% (over 3 cm), respectively. When lesions with high density in arterial phase and/or low density in portal venous phase were considered as positive, and moreover, those confirmed clinically or pathologically were as true positive, we found positive predictive value of the over 3 cm group reached 100% in all phases, but that of 3 cm or less group was the highest (100%) in early and late portal venous phases. Among four scanning schemes involving early, middle and late arterial phases, detection rate of the early and late arterial phases and three arterial phases were consistent, reaching the highest value (3 cm or less group: 90%; the 3 cm over group: 78.049%). This study confirmed that the late arterial phase was the best time to detect abundant blood supplied HCC. The scanning scheme involving double arterial phases (early and late), late portal venous phase and stable phase which can help improve detection rate and correct diagnosis rate of HCC, was thought to be the most effective. Using dynamic enhanced CT examination in the diagnosis of HCC is meaningful

Key words: multi-slice spiral computed tomography, hepatocellular carcinoma, body section photography, dynamic contrast enhancement, multiphase

Mailing address: Dr Zhuang Xue
Department of Radiology,
Shandong Jining No.1 People's Hospital,
Henan Science and Technology
University, Luoyang,
No. 6, Jiankang Road Jining, Shandon 272100, China
e-mail: madsci@163.com

0393-974X (2015)

both in qualitative and quantitative diagnosis. T-D curve, in particular, can intuitively and objectively reflect enhanced characteristics of HCC, and can be used to make a preliminary diagnosis of some atypical liver cancers.

Primary hepatocellular carcinoma (HCC), one of the most common malignant tumors in China, has an increasingly higher incidence rate around the world. At a pathological level, differentiation level of HCC can be divided into high differentiation, medium differentiation and low differentiation. Differentiation level is thought to have important influence on the prognosis of HCC (1-3). Tumor epithelial cells of high differentiated HCC generally show an even or relatively even patchy enhancement, which is generally associated with a tumor of small volume, tiny capillaries, high permeability or blood supply of hepatic sinusoid (4). The innovative Computed Tomography (CT) technology with shorter scanning time and improved scanning mode plays a more and more important function in diagnosis, treatment and prognosis assessment of various diseases (5).

HCC as well as Hepatitis B and liver cirrhosis frequently occur in China and about 100,000 people die of HCC every year. Pathological classification of HCC is regarded as an important factor for formulating treatment strategy and confirming prognosis. Low differentiated tumors increase significantly compared to high differentiated tumors; as the blood supply to liver tumors increases the differentiation level of tumors tends to decrease (6, 7). CT imaging can achieve qualitative separation and quantitative determination of substance by measuring single energy levels and base substance content (8, 9). Additionally, it has been found that, the enhancement mode of spiral CT three-phase dynamic scanning is associated with pathological differentiation levels; the difference of quantity of vascular endothelial growth factor (VEGF) generated by tumors with different differentiation levels leads to significantly different blood supply types to them, which can produce great effect on growth, invasion and metastasis of tumor tissues (10-13).

This study subdivided traditional scanning phases, especially the arterial phase, in view of blood supply characteristics of HCC to explore the detection rate in different phases; additionally, we took efforts to select a high-value scanning schedule combining with the detection rate in early, middle and late arterial phases, thus to improve the accuracy of quality confirmation of HCC, especially the detection rate of small HCC in the early stage.

MATERIALS AND METHODS

Study subjects

Forty primary HCC patients at the department of gastroenterology in the First People's Hospital, Jining, Shandong, China from April 2009 to January 2010, who underwent spiral CT scan and multiphase dynamic enhanced scan, after signing informed consent and clinically or pathologically confirmed as primary HCC, were selected as research subjects. Of 40 patients, 29 were male and 11 were female, with age ranging from 26~81 years (mean age 53.00±13.56 years). In addition, 30 out of 40 patients were found to have chronic hepatitis b and 34 cases had cirrhosis of the liver. Main symptoms included abdominal pain (especially hepatic region), abdominal distension and emaciation and some patients developed jaundice and enclosed mass. They had had the disease for 1 month to 2 years. Abdominal ultrasound indicated liver solid space-occupying lesions. Plasma P value was detected before CT examination (> 100 mu g/l). This study was approved by the ethics committee of the First People's Hospital, Jining, Shandong, China.

Inclusion and exclusion criteria

Patients who were confirmed as HCC by pathology or aspiration biopsy after surgery were included in this study, while patients with HCC who underwent intervention or radiofrequency ablation, patients with recurred HCC or patients with both HCC and cholangiocellular carcinoma were excluded.

CT examination technology

Preparation before scanning: patients had not taken an upper gastrointestinal barium meal or undergone a barium enema examination during the week prior to CT examination and moreover, had not eaten at least 6 h before the examination; only patients who were negative in the iodine allergy test were qualified to receive CT examination; they were orally administrated with 500 ml warm water before examination.

Scanning method: all cases were first CT plain scanned (64-layer Light speed VCT XT machine, GE, USA) for the whole liver, and then injected with 80 ~ 100 ml nonionic contrast agent ultravist (370 mg/ml) through

the middle vein by high pressure injector (Nemoto, Japan) at a speed of 2.5-3 ml/s; then multiphase dynamic enhanced CT examination was performed; enhanced scans of every period were completed while breath was held and the scanning scope was from diaphragm to lower edge of liver; scanning parameters included whole-vision shaft spiral scanning, layer thickness 5 mm, rotational speed 0.5 s / 360°, pitch 1.375:1, width of detector 40 mm (64 × 0.625 rnm); pipe voltage 120 kV, current 120 mA, matrix 512 × 512, 36 cm field of view.

Determination of delay time after injection: delay time of scanning was obtained by studying 20 patients with liver cirrhosis with Smart Prep technology, and early arterial phase was 22-24 s, middle arterial phase was 29-31 s, late arterial was 37 to 39 s, early portal venous phase was 60-65 s, late portal venous phase was 80-85 s and liver balance phase was 150 s.

Observation index of MSCT examination

CT images were reviewed by two experienced radiologists, and information involving lesion demonstration was recorded. Location, number, size, shape and density differences in different parts of the lesions, solid tumor sections, tumor necrosis, tumor capsule, adjacent normal liver tissue and intrahepatic metastasis in different periods, blood supply arteries for tumor, existence of vascular complications such as arterio-venous fistula and portal vein tumor thrombus, invasive degree of tumor to adjacent tissue were observed. The size of lesion was determined by the largest diameter measured on a cross section. Density of lesion in the arterial phases and early and late portal venous phases were classified as low, equivalent and high level, and lesion demonstration in MSCT was scored. The scoring is shown in Table I.

CT value measurement

CT values of intrahepatic lesions which were obviously enhanced in enhanced scanning were measured. In enhanced images of different phases, CT values were measured based on the same area of region of interest (ROI) on the corresponding site. The difference between two CT values was enhanced CT value, which showed tumor enhanced degree. Enhanced CT value below 20 HU was considered as low-grade enhancement, between 20 and 50 HU was as medium enhancement, and more than 50 HU was as high-grade enhancement. A lesion found with no more than 5 HU CT value in different phases was determined to have the same enhancement degree. At the same time, the density of adjacent normal liver tissue was measured and then the density difference of the solid part between normal liver and liver cancer were calculated. Necrosis area, calcified area, tumor capsule and blood vessels within the tumor were thought to be unsuitable to be selected as ROI. The average value of measurements from the three continuous sections was taken as the final measurement result.

Statistical analysis

SPSS13.0 software was used for analyzing CT scanning data of patients clinically or pathologically confirmed as HCC. The density of normal liver and HCC in different phases was compared using rank-sum test. The detection rate and positive predictive value of lesions with a maximum diameter of no more than and more than 3 cm in different arterial phases and portal venous phases were compared respectively. The difference was considered to

Table I. *Scoring for lesion display of MSCT.*

Score	Performance
0	No HCC
1	May have no HCC
2	May have HCC (high density in early, middle and late arterial phases and low density in early and late portal venous phases)
3	Basically confirm HCC (high density in early, middle and late arterial phases and low density in early and late portal venous phases)
4	Confirm HCC

Lesions with 2 points or higher is considered as positive diagnosis; lesions scoring 2 points or higher and clinically or pathologically confirmed are considered as true positive diagnosis; lesions scoring 2 points or higher but not confirmed are considered as false positive diagnosis.

have statistical significance if P<0.05.

RESULTS

A total of 40 patients with HCC underwent CT plain scan and multiphase dynamic enhanced examination, and 61 lesions with diameters ranging from 1.1 to 17.4 cm (average 4.6±0.4 cm) were detected. Of 61 lesions, 20 were 3 cm or less, 15 were less than 5 cm and 26 were 5 cm or more. Density value of the part of normal liver solid and liver tumors were measured and compared. Detailed CT values of them in different phases are shown in Table II. Statistical analysis revealed that density differences of normal livers and liver tumors were statistically significant in different phases (H=45.208, P<0.01).

CT plain scan

CT plain scan results revealed that 34 out of 40 cases had liver cirrhosis, and 61 lesions were found including one which was not observed due to equidensity. The CT plain scan value of lesions ranged from 24.7 to 58.3 HU. Moreover, of 53 with low density, 18 were with even density and 35 were uneven; 7 lesions had a density slightly higher than adjacent liver parenchyma, among which, 4 showed high density due to the existence of fatty liver. Two lesions were observed with high-density calcification. Five lesions were found under liver capsules and some part of them extruded the outline of liver. Relatively small lesions were mostly with even density and clear edged while the opposite resulted for relatively large lesion.

Multiphase dynamic enhanced examination

The CT enhancement degree and enhancement peak distribution were observed and analyzed. Results revealed that, enhancement performance of the 61 lesions was various, i.e., irregular mass-shaped enhancement, sheet enhancement and multiple tubercular enhancement. CT enhancement degree and enhancement peak distribution of lesions in different phases are shown in Table III.

Detection and display of cancer lesion

HCC detection and display of enhanced CT scan

Table II. *Density difference of tumor and normal liver in different scanning phases.*

Scanning phase	Number of lesions (n)	Normal liver (χ±s, HU)	Tumor (χ±s, HU)	Density difference (χ±s, HU)
Plain scan	61	54.347±4.917	45.932±7.293	9.294±7.513
Early arterial phase	61	60.106±6.943	60.632±12.371	10.374±8.069
Middle arterial phase	61	68.663±9.480	77.269±18.986	14.063±13.596
Late arterial phase	61	80.875±16.443	92.846±21.878	19.897±14.702
Early portal venous phase	61	104.289±17.372	91.888±17.129	17.284±13.091
Late portal venous	61	105.938±15.071	87.245±16.507	19.687±12.979
Hepatic balance phase	61	96.028±14.920	80.438±14.063	16.625±10.001

Table III. *CT strengthening degree and the strengthening peak distribution of 61 lesions in different scan phases.*

Scanning phase	Number of lesions (n)	Enhancement peak	Enhancement degree of lesions		
			Low	Middle	High
Plain scan	61	0	46	15	0
Early arterial phase	61	1	20	29	12
Middle arterial phase	61	34	9	25	27
Late arterial phase	61	20	2	37	22
Early portal venous phase	61	6	6	36	19
Late portal venous phase	61	0	6	46	9

Table IV. *HCC display in arterial phases and portal venous phases and comparison of detection rate.*

Scanning phase	Number of lesion (n)	High density	Equi-density	Low density	Number	Detection rate (%)	χ^2	P
Early arterial phase	61	22	10	29	22	36.066		
Middle arterial phase	61	37	5	19	37	60.656		
Late arterial phase	61	48	3	10	48	78.689	32.91	0.001
Early portal venous phase	61	9	7	45	45	73.77		
Late portal venous phase	61	10	5	46	46	75.41		

Table V. *Comparison of HCC detection rate in arterial phases and portal venous phases.*

	Scanning phase	Number of lesions detected (n)	Lesion detection rate (%)	χ^2	P
Lesions 3 cm or less (n=20)	Early arterial phase	8	40.000	11.875	0.018
	Middle arterial phase	13	65.000		
	Late arterial phase	17	85.000		
	Early portal venous phase	15	75.000		
	Late portal venous phase	16	80.000		
Lesions over 3 cm (n=41)	Early arterial phase	14	34.146	21.412	0.023
	Middle arterial phase	24	58.537		
	Late arterial phase	31	75.610		
	Early portal venous phase	30	73.171		
	Late portal venous phase	30	73.171		

were observed and analyzed. It was found that, lesion detection showed up high density in early, middle and late arterial phases while early and late portal venous phases showed low density, which was taken as the determination criteria for positive results. Detailed data are shown in Table IV.

Results demonstrated that, the difference of detection rate in early, middle and late arterial phases and early and late portal venous phases was statistically significant (χ^2= 32.910, P = 0.001). Further comparison between groups showed that, the difference of detection rate of the three arterial phases was also statistically significant (χ^2= 0.043, P = 0.835 > 0.05). Lesions were subdivided into 3 cm and less group and 3 cm and over group based on the maximum diameter.

As shown in Table V, the detection rate of the two kinds of lesions was both statistically significant in early, middle and late arterial phases and early and late portal venous phases; the detection rate of the two kinds of lesions was the highest in the late arterial phase, 85.00% and 75.61%. In depth analysis and comparison found that, the detection rate of lesions of 3 cm or less was statistically significant in

Table VI. *Comparison of positive predictive value of HCC in arterial phases and portal venous phases (%).*

Scanning phase	Lesions 3 cm or less	Lesions over 3 cm	All lesions
	Positive predictive value	Positive predictive value	Positive predictive value
Early arterial phase	88.889	100	95.652
Middle arterial phase	92.857	100	97.368
Late arterial phase	94.444	100	97.959
Early portal venous phase	100	100	100
Late portal venous phase	100	100	100
χ^2	19.87	—	7.241
P	0.001	—	0.124

Table VII. *Comparison of HCC (3 cm or less) detection rate in multiple arterial phases.*

	Scanning phase	Number of lesions detected (n)	Lesion detection rate (%)	χ^2	P
Lesions 3 cm or less (n=20)	Early+middile arterial phase	14	70	19.797	0.002
	Middle+late arterial phase	17	85		
	Early+late arterial phase	18	90		
	Multiple arterial phases	18	90		

the three arterial phases (χ^2=8.756, P=0.013<0.05), as it was in lesions of over 3cm

(χ^2=14.459, P=0.01); however, in the early and late portal venous phases, detection of both kinds of lesions was not statistically significant.

Comparing lesions detected by multiphase dynamic enhanced CT scan, we obtained the number of true positive and false positive lesions. Early, middle and late arterial phases all showed up one false positive lesion. The positive predictive value of lesions in arterial phases and portal venous phases was calculated respectively, as shown in Table VI.

Table VIII. *Comparison of HCC (3 cm or less) detection rate in multiple arterial phases.*

	Scanning phase	Number of lesions detected (n)	Lesion detection rate (%)	χ^2	P
Lesions over 3 cm (n=41)	Early+middle arterial phase	24	58.537	13.818	0.013
	Middle+late arterial phase	32	78.049		
	Early+late arterial phase	32	78.049		
	Multiple arterial phases	32	78.049		

The positive predictive value of lesions of 3 cm or less in arterial phases and portal venous phases was statistically significant (P=0.001), 100% in the early and late portal venous phases; for lesions over 3cm, positive predictive value also reached 100%.

Comparison of detection rate of lesions in multiple arterial phases

To analyze the use of scanning schemes in multiple arterial phases for the detection of lesions, arterial phases (early, middle and late) were divided into four schemes. Detection rate of lesions using different schemes was calculated, and the results are shown in Tables VII and VIII.

Tables VII and VIII revealed that, the detection rate of lesions of 3 cm or less and over 3 cm were both statistically significant using four different schemes. For lesions of 3cm or less, the detection rate obtained by scanning lesions in early and late arterial phases and early, middle and late arterial phases was consistent, reaching the highest value, 90%; for lesions of over 3 cm. The detection rate obtained by scanning lesions in the middle and late arterial phases, early and late arterial phases, and early, middle and late arterial phases were all 78.049%. When compared to scanning performed in the early, middle and late arterial phases separately, early and late arterial phase scanning and multiple arterial phase scanning had the highest detection rate.

Other signs

Of the 40 HCC patients, 29 cases were with portal hypertension, among which, 24 were with splenauxe; 25 cases were with seroperitoneum; 7 cases were observed with tortuously expanded vessel imaging in gastric fundus area, ligamentum hepatogastricum area and hilus lienis area; 1 case was found with umbilical vein recanalization; 9 cases were observed with peritoneal and/or retro-peritoneal lymphadenopathy, among which, 7 cases had lymphadenectasis in hepatic hilar region, portal veins and the ligamentum hepatogastricum area; 5 cases were observed with swollen lymph nodes around the aorta abdominalis; 3 cases were observed with nodular shadows in the adrenal area and the bilateral lung.

DISCUSSION

A new, non-invasive and highly repeatable examination method is urgently needed as less than 20% HCC patients conform to surgical requirements (14). This study selected early and late arterial phase combined scanning and optimized the previous

traditional scanning scheme. Moreover, we confirmed the necessity of portal venous phase scanning, especially late portal venous phase, as it improves the detection rate. To avoid missing non-typical HCC, lesions with enhancement peaks occurring in late portal venous phase in particular, hepatic balance phase was also taken as one of the regular scanning phases. Missed diagnosed HCC and misdiagnosis can be effectively reduced if scanning combining double arterial phases (early and late), portal venous phase (late) and hepatic balance phase is used, where space-occupying lesion are particularly demonstrated. The emergence of the 64-layer spiral CT helps us to obtain such an optimal scanning scheme, which is of great significance to detection, diagnosis and identification of HCC.

In conclusion, enhancement characteristics of CT multi-phase dynamic enhancement scanning is in correlation to the differentiation of HCC; low differentiated liver cancer shows more vessels in the early arterial phase. Enhancement scanning for double arterial phases can provide more information for diagnosis.

REFERENCES

1. Zhou L, Rui JA, Wang SB, Chen SG, Qu Q. Prognostic factors of solitary large hepatocellular carcinoma: the importance of differentiation grade. Eur J Surg Oncol 2011; 37(6):521-25.
2. Jonas S, Bechstein WO, Steinmuller T, et al. Vascular invasion and histopathologic grading determining outcome after liver transplantation for hepatocellular carcinoma in cirrhosis. Hepatol 2001; 33(5):1080-86.
3. Hemming AW, Cattral MS, Reed AI, Van Der Werf WJ, Greig PD, Howard RJ. Liver transplantation for hepatocellular carcinoma in cirrhosis. Ann Surg 2001; 233(5):652-59.
4. Tajima T, Honda H, Taguchi K, Taguchi K, Asayama Y, Kuroiwa T, Yoshimitsu K. Sequential hemodynamic change in hepatocellular carcinoma and dysplastic nodules: CT angiography and pathologic correlation. Am J Roentgenol 2002; 178(4):885-97.
5. Johnson PT, Fishman EK. Computed tomography dataset postprocessing: from data to knowledge. Mt Sinai J Med 2012; 79(3):412-21.
6. Lavisse S, Lejeune P, Rouffiac V, et al. Early quantitative evaluation of a tumor vasculature disruptive agent AVE8062 using dynamic contrast-enhanced ultrasonography. Investive Radiol, 2008; 43(2):100-111.
7. Yao DF, Wu XH, Zhu Y, et al. Quantitative analysis of vascular and othelial growth factor, microvascular density and their clinicopathologic features in human hepatocellular carcinoma. Hepatobil Pancreat Dis Int 2005; 4:220-26.
8. Matsumoto K, Jinzaki M, Tanami Y, Ueno A, Yamada M, Kuribayashi S. Virtual monochromatic spectral imaging with fast kilovoltage switching: improved image quality as compared with that obtained with conventional 120-kVp CT? Radiol 2011; 259(1):257-62.
9. Lv P, Lin XZ, Li J, Li W, Chen K. Differentiation of small hepatichemangioma from small hepatocellular carcinoma: recently introduced spectral CT method. Radiol 2011; 259:720-29
10. Tarhan NC, Hatipoglu T, Ercan E, Bener M, Keles G, Basaran C, Bilezikci B. Correlation of dynamic multidetector CT findings with pathological grades of hepatocellular carcinoma. Diagn Interv Radiol 2011; 17:328-33
11. Kitao A, Zen Y, Matsui O, Gabata T, Nakamura Y. Hepatocaicinogenesis: multistep changes of drainage vessels at CT during arterial portography and hepatic arteriography radiologic-pathologic correlation. Radiol 2009; 252(2):605-14.
12. Laurent V, Corby S, Antunes L. Liver and focal liver contrast: radiologic-pathologic correlation. J Radiol 2007; 88(7-8):1036-47.
13. Bhattachrejee PK, Saito OA, Chiba M, Katsuragawa H, Takasaki K. Detection of hepatocellular carcinoma capsule by contrast-enhanced ultrasound using Levovist: correlations with pathological findings. J Med Ultrasonics 2005; (32):167-72.
14. Tamano M, Kojima K, Akima T, et al. The usefulness of measuring liver stiffness by transient elastography for assessing hepatic fibrosis in patients with various chronic liver diseases. Hepatogastroenterol 2012; 59(115):826-30.

LETTER TO THE EDITOR

IDENTIFICATION OF BENIGN AND MALIGNANT ENDOMETRIAL CANCER WITH TRANSVAGINAL ULTRASONOGRAPHY COMBINED WITH ELASTOGRAPHY AND TISSUE HARDNESS ANALYSIS

Y. ZHANG[1], L. LUO[2] and Q. LUO[1]

[1]Department of Radiology, Shandong JiNing No.1 People's Hospital, Jining, Shandong, China; [2]Department of Gynaecology and Obstetrics, Shandong JiNing No.1 People's Hospital, Jining, Shandong, China

Received May 15, 2015 – Accepted July 20, 2015

This study was designed to explore tissue hardness and distinguish benign and malignant endometrial cancer with the use of transvaginal ultrasonography combined with elastography. Color Doppler ultrasonic diasonograph was used to carry out transvaginal ultrasonography and elastography. Once the nidus was observed, features of the 2D image were analyzed. Then features of elasticity of the uterine cavity in different states were analyzed by elastography, and strain rate ratio was measured. Finally, elasticity scoring (0~5 points) was made. Receiver operating characteristic (ROC) curve was drawn based on elasticity score and strain rate ratio. The area under the elasticity score curve and strain rate ratio curve was 0.761 and 0.852, respectively, and there was no statistically significant difference between them (c^2= 4.663, P>0.05). Then 2.98 was confirmed as the diagnostic cut-off value of benign and malignant lesions, based on strain rate ratio. Ultrasonic elastography as an effective assistance for transvaginal ultrasonography provides more valuable information for confirmation of lesions and offers more accurate evidence for diagnosis of disease in the uterine cavity.

With the constant development of society and increase of diseases, an increasing number of people are concerned for their health and more females pay attention to physical examination. Endometrial cancer has become one of the frequently seen malignant tumors in the female reproductive system, and the number of young people diagnosed with this disease is increasing (1). Though its incidence is lower than cervical cancer in China, endometrial cancer is observed with an incidence rate higher than carcinoma of uterine cervix in some European countries and ranks first of all the gynecologic malignant tumors (2, 3). Ultrasonic testing is a routine gynecological screening program and plays an important function in screening uterine cavity diseases. Transvaginal ultrasonography is able to clearly demonstrate the state, size and blood flow of the uterus in different states. Transvaginal ultrasonography has been widely applied in clinical use as a non-invasive, effective and rapid method of examination (4). However, its feasibility in diagnosing the space occupying lesions in the uterine cavity has not yet been confirmed. During exploration, many authors held that it is of great importance to find

Key words: transvaginal ultrasonography, elastography, tissue hardness, endometrial cancer, space occupying lesions in uterine cavity

Mailing address: Dr Qian Luo,
X-ray Department,
Shandong Jining No.1 People's Hospital,
No.6, Jiankang Road,
Jining, Shandong, 272100, China
e-mail: lq0584@163.com

0393-974X (2015)

a more advanced technical means to improve the diagnosis rate of malignant pathological changes (5-6). In 1991, Ophir et al. (7) proposed ultrasonic elastography which is based on the principle that displacement of tissue is different under certain pressure, due to different elastic coefficients (8-9). Elastography is able to demonstrate the hardness of tissues, thus compensates for the disadvantage of traditional image technologies. Currently, this technology is applied, especially in diagnosis and differential diagnosis of superficial organs such as breast diseases (10-11). In addition, its application in liver and prostate diseases has been initiated, but its application in gynecology is seldom reported. To discuss the diagnostic value of elastography, this study applied it in the diagnosis of different uterine cavity diseases.

MATERIALS AND METHODS

Eighty-eight patients who were treated at the Gynecology Department of the First People's Hospital, Jining, Shandong, China from January 2013 to January 2014 were selected as research subjects. They were all examined by transvaginal ultrasonography combined with elastography. A total of 25 patients were diagnosed to have normal uterine cavity and taken as normal controls (average age 30±2.3 years), and 63 cases were diagnosed with space occupying lesions in the uterine cavity (average age 40±3.1 years). Of these 63 subjects, 28 cases were benign and 35 cases were malignant, all of whom received operative treatment and pathological diagnosis in our hospital. This study was approved by the ethics committee of the First People's Hospital, Jining, Shandong, China and all participants signed informed consent.

In the normal control group, the 25 subjects underwent routine gynecological examination and resulted normal and having no inflammation.

The patients with abnormal vaginal discharge and bleeding were found by ultrasound to have space occupying lesions in the uterine cavity. In addition, it was their first visit and they had not received radiotherapy or chemotherapy previously. The clinical staging and pathological pattern of these patients are summarized in Table I and II, based on FIGO 2000 surgical pathological staging criteria for endometrial cancer.

Examination method

The patients were examined, after emptying the bladder, in the lithotomy position, by a routine 2D scanning of the uterus, adnexa of uterus and pelvic cavity with a vaginal ultrasonic probe. Once a lesion was found, the size, form, internal echo and neighborhood relationship with organs was analyzed through images, to make a preliminary judgment of properties of the lesion.

The area with pathological changes was clearly demonstrated by ultrasound B-mode imaging. The central part of the image was selected as lesion area and adjacent normal tissues were taken as controls. The region of interest was set at an area larger than the lesion area. Then the cervix uterus was slightly pressed by a probe. When the press index was kept between 3 and 4, the hardness of tissues was clearly demonstrated, after which images were taken. Elasticity scoring based on the images determined whether the lesion was benign or malignant.

Elastography

For the elastography, firstly, free-frame elasticity image with a pressure index between 3 and 4, and a sampling range of normal tissue one to two times the size of the lesion area were selected. Elasticity images containing pseudomorphisms were excluded. For every lesion three elasticity images were taken. The elasticity scoring and detection of strain ratio rate was then calculated. Lastly, dynamic images were stored in a PC.

The lesion area and normal tissues were adjusted to the same layer, depth and measuring area. Strain ratio rate was detected on the lesion area and normal tissue selected. The operation was repeated three times and the average value was taken as the final result. The ratio indicated the hardness of lesion compared to normal tissues.

Elasticity images were scored from one to five points based on the coloration. One point meant the lesion area and adjacent tissue were both green; 2 points meant that the lesion area was either green or blue with green dominating; 3 points meant that the lesion area was either green or blue with blue dominating; 4 points meant that the lesion area was totally blue; and 5 points mean that the lesion area, as well as the adjacent tissues, was blue (Fig. 1). Lesions with a score of one or two points were considered as benign while those with a score from three to five points as malignant.

Statistical analysis

Chi-squared test was used to compare sensitivity and specificity of transvaginal ultrasonography, elastography and the combination of both in determining the properties of space occupying lesions in the uterine cavity. SPSS 17.0 software was used for statistical analysis, and the results were expressed as mean ± standard deviation. Receiver operating characteristic (ROC) curve regarding the elasticity score and strain ratio rate for space occupying lesions in the uterine cavity was plotted and the area below the curve was calculated. Values between 0.5 and

0.7, between 0.7 and 0.9 and values of 0.9 signified little diagnostic meaning, relatively large diagnostic meaning and great diagnostic meaning, respectively. $P < 0.05$ indicated differences had statistical significance.

RESULTS

Characteristics of transvaginal ultrasonography and elastography of different space occupying lesions in the uterine cavity

Using transvaginal ultrasonography, the normal uterus displayed the shape of an inverted pear, longitudinally, and was found with a clear outline and smooth surface; the internal part had an even substantial structure, with moderate strength echo, and echo in the uterine body was slightly weaker than the uterine neck; the uterine cavity surrounded by endometrium epithelial with weak echo had linear strong echo; the part at the bottom of the uterus was triangular-shaped and the somatic part was elliptic, transversely; the central part was observed with a strong echo in the endometrium line. Using color Doppler flow imaging (CDFI), mesometrium was observed with no blood flow signal or less blood flow signals (Fig. 2).

The elasticity image demonstrated that the body of the uterus was green and the endometrium epithelial was either green or red.

Endometrial polyp

Using transvaginal ultrasonography, the uterus with polyp was observed with unevenly distributed echo in the endometrium, and one or more flat equal echoes or strong echoes were also found. In addition, two cases were found with little hydrops in the uterine cavity. The outline of the polyp and width of the pedicle were clearly demonstrated. With CDFI, we could see that the blood flow signal entered through the basilar part of the strong echo.

Endometrial polyp was observed in green and a little red in the elasticity image.

Submucous myoma of uterus

Using transvaginal ultrasonography, submucous myoma of the uterus was observed with separated uterine cavity; moderate or weak echo mass was observed between the front and back endometrium epithelial. In addition, its outline was clear and regular. Uneven echo was found to be distributed in the internal part, and strong echo was vortex-like, along with damping in varying degrees. When degenerative necrosis or liquidation occurred, part of the mass was observed with strong echo or liquid echo. With CDFI, dotted or half-ring blood flow

Table I. *Clinical staging of cases with space occupying lesions in uterine cavity.*

FIGO clinical staging	Malignant cases (n)	Benign cases (n)
0		
Ia, Ib, Ic	24	
II	6	
III	4	
IV	1	
	35	28

Table II. *Pathological classification of cases with space occupying lesions in uterine cavity.*

Pathological pattern	Malignant cases (n)	Benign cases (n)
Adenocarcinoma	27	
Adenosquamous carcinoma	7	
Clear cell carcinoma	1	
Polypus		19
Liomyoma		9
	35	28

Table III. *Elasticity scoring of endometrial cancer of different blood flow distribution types (n).*

Types of blood flow distribution	Elasticity level					Total
	I	II	III	IV	V	
Type of sufficient blood flow	0	1	1	7	6	15
Type of insufficient blood flow	1	1	1	7	1	11
Type of no blood flow	0	3	3	2	1	9
Total	1	5	5	16	8	35

Table IV. *Comparison of results obtained pathologically and by transvaginal ultrasonography.*

Transvaginal ultrasonography	Pathologically confirmed results		Total
	Malignant	Benign	
Malignant	19	5	24
Benign	16	23	39
Total	35	28	63

Table V. *Comparison of results obtained by elasticity imaging and pathologically confirmed results (n).*

Elasticity imaging	Pathologically confirmed results		Total
	Malignant	Benign	
Malignant	25	6	31
Benign	10	22	32
Total	35	28	63

Table VI. *Comparison of results obtained by the combination of elasticity imaging and transvaginal ultrasonography and pathologically confirmed results (n).*

The combination of elasticity imaging and transvaginal ultrasonography	Pathologically confirmed results		Total
	Malignant	Benign	
Malignant	31	2	33
Benign	4	26	30
Total	35	28	63

Table VII. *Comparison of results obtained by elasticity imaging and transvaginal ultrasonography (n).*

Elasticity imaging	Transvaginal ultrasonography		Total
	Malignant	Benign	
Malignant	20	11	31
Benign	5	27	32
Total	25	38	63

Table VIII. *Comparison of results obtained by transvaginal ultrasonography and the combination of elasticity imaging and transvaginal ultrasonography (n).*

Combination of elasticity imaging and transvaginal ultrasonography	Transvaginal ultrasonography		Total
	Malignant	Benign	
Malignant	20	19	39
Benign	6	18	24
Total	26	37	63

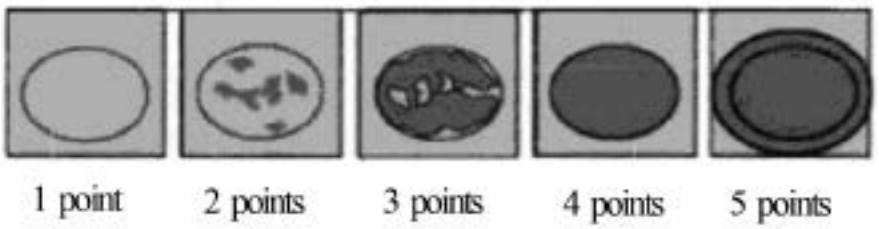

Fig. 1. *Scores for coloration of elasticity images.*

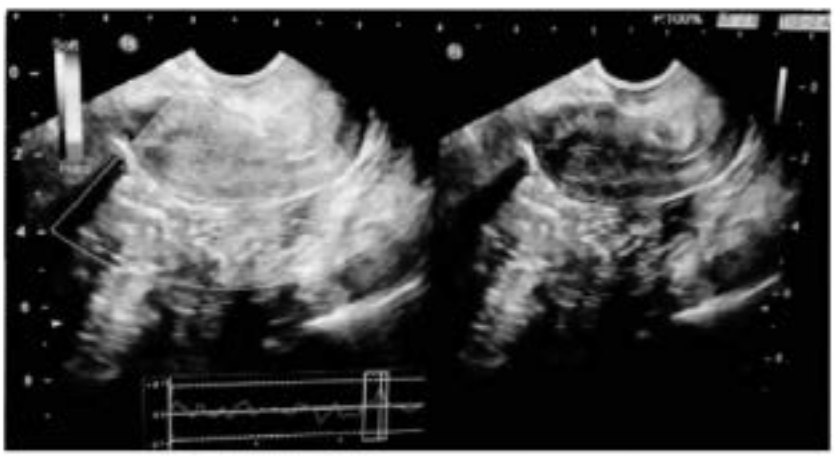

Fig. 2. *2D image and elasticity image of normal uterine cavity.*

signals were observed in and around the mass.

Its elasticity image was characterized by blue-and-green (green dominated) and blue-and-red.

Endometrial cancer

Using transvaginal ultrasonography, the body of the uterus was in a regular shape. Either irregular strong, moderate or weak echo or randomly distributed and uneven dotted and mass-like echo were observed inside. Uterus with hydrops or empyema at the same time was observed with liquid echo area with decreased acoustic transmission. Typically, the uterus with endometrial cancer was observed with low-echo mass, unclear boundary, irregular form and mess echo inside. With CDFI, three kinds of blood flow distribution were found, i.e., sufficient blood flow type (tortuous and strip-shaped blood flow signals were observed inside

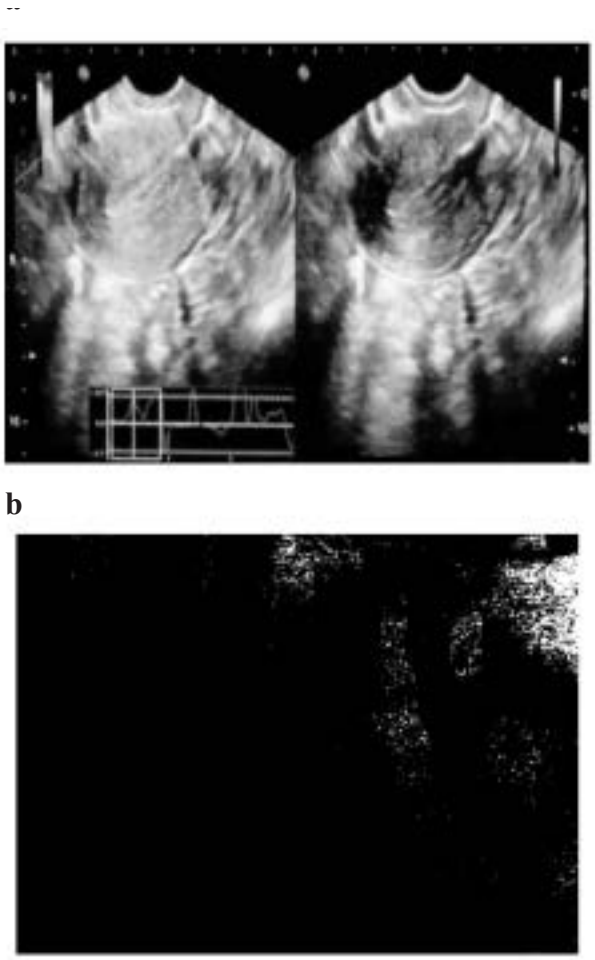

Fig. 3. ***a****) 2D image and elasticity image of endometrial polyp.* ***b****) Pathologically determined endometrial polyp.*

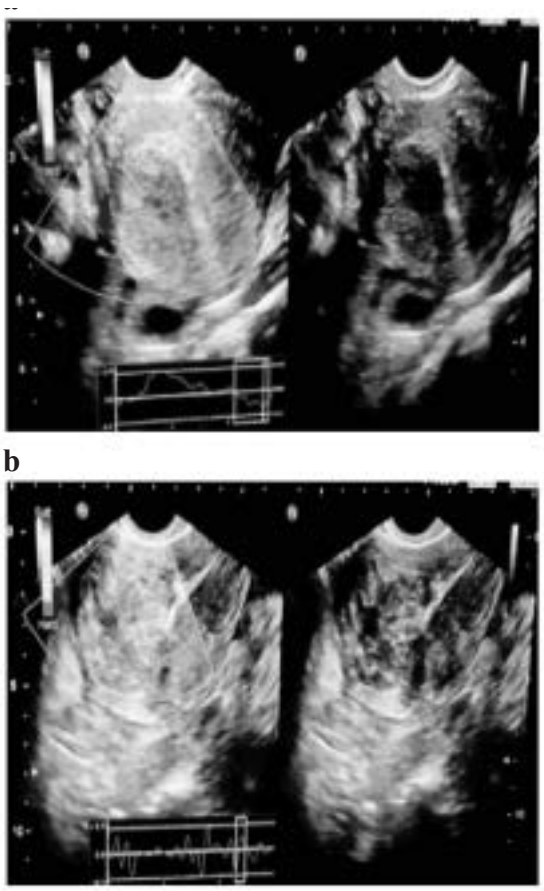

Fig. 4. ***a****) 2D image and elasticity image of submucous myoma of uterus.* ***b****)2D image and elasticity image of submucous myoma of uterus along with partial denaturation.*

and around the nidus), insufficient blood flow type (dotted blood flow signals were observed inside and around the nidus) and no blood flow type (no blood flow signal was observed inside nodus and around). Its elasticity image was characterized by mostly blue or totally blue.

Elasticity scoring of endometrial cancer of different blood flow distribution type

Table III demonstrates that elasticity score did not decrease with the increase of blood flow.

Comparison of diagnosing benign and malignant space occupying lesions in uterine cavity with transvaginal ultrasonography and elastography technology

Specificity and sensitivity of diagnosing space occupying lesions with transvaginal ultrasonography, elasticity scoring and the combination of the two methods was 59% and 79.2%, 68.8% and 80.6%, 86.7% and 93.9%, respectively, as shown in Tables III, IV, V.

Comparison of the results obtained by transvaginal ultrasonography and elastography scoring is shown in Table VI, and differences were found with no statistical significance (c^2= 1.563, P>0.05), while comparison of results obtained by transvaginal ultrasonography and the combination of

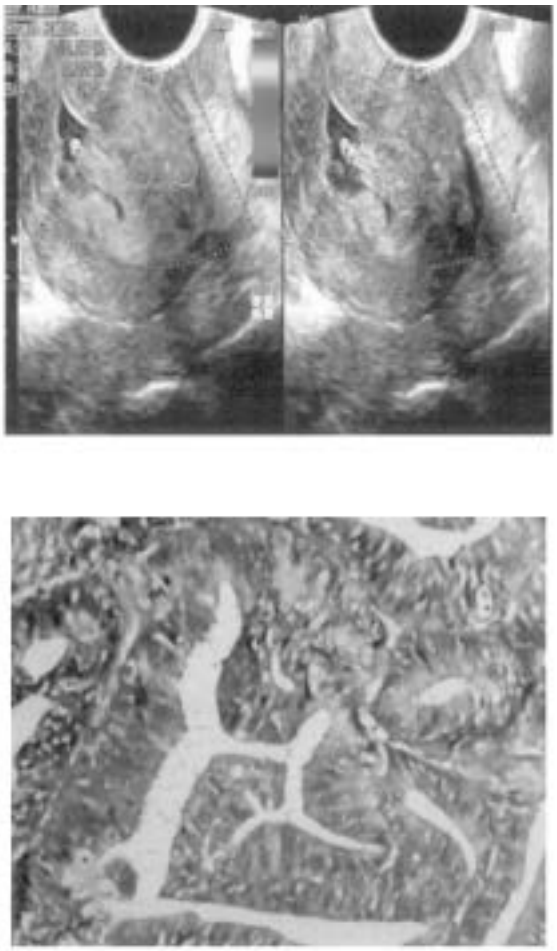

b

Fig. 5. ***a****)2D and elasticity image of endometrial cancer.* ***b****) Pathological determined endometrial cancer.*

elasticity imaging and transvaginal ultrasonography is shown in Table VII, and differences had significant statistical significance (c^2=5.760, P<0.05; c^2=6261, P<0.05).

Comparison of accuracy of diagnosing properties of lesions in uterine cavity with elasticity score and strain rate ratio

ROC curve was drawn based on elasticity score and strain rate ratio. The area of elasticity score and strain ratio curve was 0.761 and 0.852 respectively, and there was no statistically significant difference between them (c^2=4.663, P>0.05). Finally, 2.98 was confirmed as the diagnostic cut-off value of benign and malignant lesions, based on strain rate ratio.

DISCUSSION

Tables II, III and IV demonstrate that transvaginal ultrasound sensitivity was close to elasticity imaging. Diagnosis of disease in the uterine cavity using transvaginal ultrasound combined with elasticity imaging could result as having no statistical significance compared to results obtained by pathological diagnosis. Thus diagnosing disease in the uterine cavity by elasticity imaging had limitations (12). Preliminarily determining the

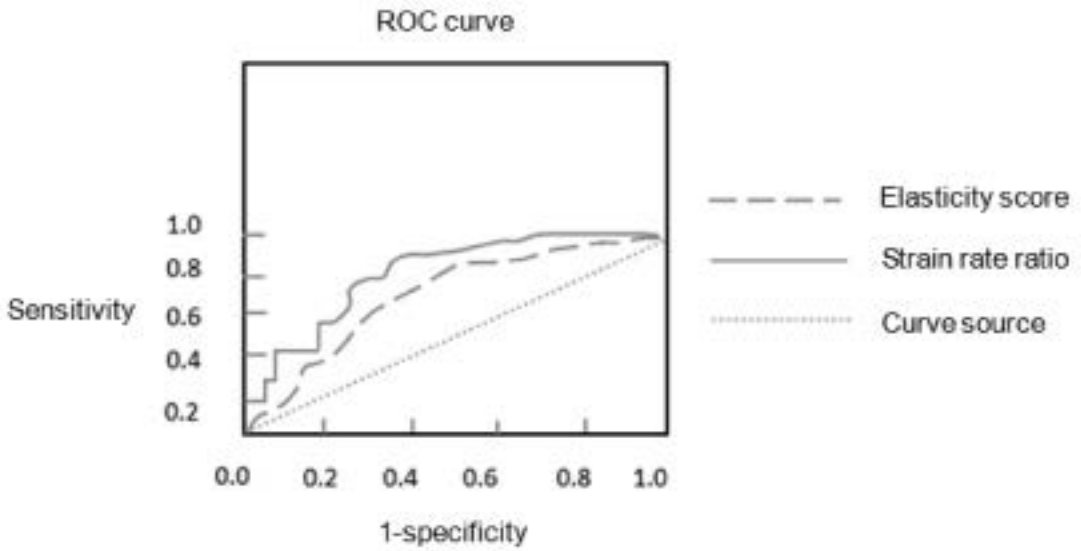

Fig. 6. *ROC curve.*

properties of nidus with transvaginal ultrasonography first and then combining with information displayed by elasticity imaging greatly improved the diagnostic rate and lessened the difference between the results and the gold standard of diagnosis to a large extent. Judging from the demonstration of nidus, we found elasticity imaging was more advantageous than 2D ultrasound. Thus, we believe that elasticity imaging is a beneficial supplement to 2D ultrasound.

Sixty-three cases of space occupying lesions in the uterine cavity were all determined taking 2.98 as a critical point. Finally 35 cases were determined as benign lesion and 28 as malignant lesion. But 9 cases of malignant lesion were mistaken as benign and 5 cases of benign lesion were mistaken as malignant lesion. Though elasticity scoring is easy to be affected by subjective factors of diagnosticians, its advantages were outstanding. For instance, it was convenient and easy to be understood. Strain ratio rate was relatively objective compared with elasticity scoring.

To sum up, elastography needs to be further investigated for its potential application in the diagnosis of disease in the uterine cavity.

REFERENCES

1. Chen J. MRI Signs analysis of endometrial cancer. Chin Imaging J of Integr Trad and Western Med 2011; 9(1):82-83
2. Zhang B, Jiao Y. Review of Diagnosis and Treatment of Endometrial Cancer. Chin J of Clinicians (Electronic Version) 2013; 7(4):1392-95.
3. Wang LQ. Research Progress of Clinical Diagnosis and Treatment of Endometrial Cancer. Chin J of Clin Oncol Rehabil 2012; 19(5):472-74.
4. Epstein E, Di Legge A, Masback A, Lindqvist PG, Kannisto P, Testa AC. Sonographic characteristics of squamous cell cancer and adenocarcinoma of the uterine cervix. Ultrasound Obstet Gynecol 2010; 36(4):512-16.
5. Sun LT, Ning CP, Liu YJ, Wang LD, Kong XC, Tian JW. Is transvaginal elastography useful in pre-operative diagnosis of cervical cancer. Eur J Radiol 2012; 81(8):e888-e92.
6. Hao Hj, Tsujimoto M, Tsubanidto H, Komori S, Hirota S. Immunohistochemical phenotype of the urinary bladder endocervicosis: comparison with normal endocervix and well-differentiated mucinous adenocarcinoma of uterine cervix. Pathol Int 2010; 60(7):528-32.
7. Ophir J, Cespedes I, Ponnekanti H, Yazdi Y, Li X. Elastography: a quantitative method for imaging the elasticity of biological tissues. Ultrasonic Imaging 1991; 13 (2):111-34.
8. Wu YT. Principle, design and application of medical equipment of ultrasound. Beijing: Science and Technical Documentation Press 2012.
9. Vreugdenbrug TD, Willis CD, Mundy L and Hiller JE. A systematic review of elastography, electrical impedance scanning, and digital infrared thermography for breast cancer screening and diagnosis. Breast Cancer Res Treat 2013; 137(3):665-76.
10. Rago TjSantini F, Scutari M, Pinchera A, Vitti P. Elastography: new developments in ultrasound for predicting malignancy in thyroid nodules. J Clin Endocrinol Metab 2007; 92(8):2917-22.
11. Vidal-Casariego A, Lopez-Gonzalez L, Jimenez-Perez A, et al. Accuracy of ultrasound elastopraphy in the diagnosis of thyroid cancer in a low-risk population. Exp Clin Endocrinol Diabetes 2012; 120(10):635-8.
12. Fruscazo A, Schmitz R. Quantitative cervical elastography in pregnancy. Ultrasound Obstet Gynecol 2012; 40(5):612.

LETTER TO THE EDITOR

EFFECT OF MYO-INOSITOL AND ALPHA-LIPOIC ACID ON OOCYTE QUALITY IN POLYCYSTIC OVARY SYNDROME NON-OBESE WOMEN UNDERGOING *IN VITRO* FERTILIZATION: A PILOT STUDY

R. RAGO[1], I. MARCUCCI[2], G. LETO[3], L. CAPONECCHIA[2], P. SALACONE[2], P. BONANNI[2], C. FIORI[2], G. SORRENTI[2] and A. SEBASTIANELLI[2]

[1]Department of Materno Infantile, Unit of Pathophysiology of Reproduction, Sandro Pertini Hospital, Rome Italy; [2]Department of Specialist Medicine, Unit of Andrology and Pathophysiology of Reproduction, S.M Goretti Hospital, Latina, Italy; [3]Department of Experimental Medicine, Sapienza University of Rome, Polo Pontino, Latina, Italy

Received March 30, 2015 – Accepted September 2, 2015

The aim of the present study was to evaluate the effectiveness of the combined administration of myo-inositol and α-lipoic acid in polycystic ovary syndrome (PCOS) patients with normal body mass index (BMI), who had previously undergone intracytoplasmic sperm injection (ICSI) and received myo-inositol alone. Thirty-six of 65 normal-weight patients affected by PCOS who did not achieve pregnancy and one patient who had a spontaneous abortion were re-enrolled and given a cycle of treatment with myo-inositol and α-lipoic acid. For all female partners of the treated couples, the endocrine-metabolic and ultrasound parameters, ovarian volume, oocyte and embryo quality, and pregnancy rates were assessed before and after three months of treatment and compared with those of previous *in vitro* fertilization (IVF) cycle(s). After supplementation of myo-inositol with α-lipoic acid, insulin levels, BMI and ovarian volume were significantly reduced compared with myo-inositol alone. No differences were found in the fertilization and cleavage rate or in the mean number of transferred embryos between the two different treatments, whereas the number of grade 1 embryos was significantly increased, with a significant reduction in the number of grade 2 embryos treated with myo-inositol plus α-lipoic acid. Clinical pregnancy was not significantly different with a trend for a higher percentage for of myo-inositol and α-lipoic acid compared to the myo-inositol alone group. Our preliminary data suggest that the supplementation of myo-inositol and α-lipoic acid in PCOS patients undergoing an IVF cycle can help to improve their reproductive outcome and also their metabolic profiles, opening potential for their use in long-term prevention of PCOS.

Polycystic ovary syndrome (PCOS) is an endocrine disorder affecting 4-12% of women of reproductive age (1). PCOS phenotype derives from the interaction between environmental and genetic factors. PCOS appears to be inherited as a complex, polygenic trait. Several family studies have been conducted with the aim to clarify the genetic aspects of PCOS, but their findings are often conflicting and not conclusive (2). Metabolic features play a key role in the pathogenesis of the syndrome and, according

Key words: myo-inositol, oocyte quality, polycistic ovarian syndrome, ICSI cycles, insulin resistance, alpha-lipoic acid

Mailing address: Dr Annalisa Sebastianelli,
ASL Latina University of Rome, Department of Specialist Medicine,
Unit of Andrology and Pathophysiology of Reproduction
Centre for Sterility in Couples and Gamete Cryopreservation,
S. Maria Goretti Hospital, via G. Reni, 04100 Latina, Italy
Tel./ Fax: +39 07736553799
e-mail: annalisa.sebastianelli@gmail.com

0393-974X (2015)

to recent studies, seem to be the main cause of the syndrome itself. Affected women show an increased prevalence of several comorbidities such as obesity, ovarian dysfunction, dyslipidemia, hypertension, type 2 diabetes mellitus, and cardiovascular disease (3). Several studies have identified insulin resistance (IR) as the fundamental link between these conditions (4).

IR affects 50-80% of the women when PCOS is associated with overweight and obesity, but it is also present in 20% of the women with normal Body Mass Index (BMI) (5-9).

In recent years, myo-inositol, a glucose isomer of inositol, in consideration of its insulin-sensitizing properties (10), has been used either alone or in combination with drugs such as clomiphene and gonadotropins in PCOS patients for the induction of ovulation. Several clinical studies have demonstrated that myo-inositol has a positive effect both on energy metabolism and on oocyte quality of women affected by PCOS who have undergone *in vitro* fertilization (IVF) (11-16). It has also been shown that α–lipoic acid (17), a potent antioxidant enzyme cofactor in the mitochondrial respiratory chain, like myo-inositol, is a substance capable of improving insulin resistance, glycemic control, and lipid profiles and reducing LDL-cholesterol and triglyceride concentrations in PCOS patients with type 2 diabetes (18-19). These molecules exert their insulin-sensitivity effect from within the cell, by promoting Glut-4 translocation to the cell membrane. Therefore, administration of these two substances in PCOS patients, by both modifying the metabolic pathway and reducing oxidative stress, should also improve reproductive outcome by acting on the physiological processes of the recruitment, growth, and maturation of oocytes. The aim of this study was to evaluate the effects of combined administration of myo-inositol and α-lipoic acid on oocyte and embryo quality, and on pregnancy rate in women affected by PCOS with normal BMI, who had previously undergone an intracytoplasmic sperm injection (ICSI) procedure and received myo-inositol alone.

MATERIALS AND METHODS

Selection of patients

The present study was an open and prospective study approved by the Institutional Ethics Committee (reference n.100/13) and all recruited patients provided written informed consent before taking part in the study.

Inclusion criteria were age: 18-42 years; diagnosis of PCOS meeting two parameters of the Rotterdam criteria - sonographic appearance and oligomenorrhea (20); BMI ≤ 24.9 Kg/m^2; no previous pelvic surgery; no tubal or uterine cavity disease by hysterosalpingocontrast sonography investigation (21); no endocrine or genetic disorders; previous IVF cycle with supplementation of myo-inositol only; no azoospermic or cryptozoospermic male partners.

The population enrolled in the present study consisted of 37 of the 65 normal-weight patients affected by PCOS who had previously been subjected to ICSI receiving a supplementation of 4 g of myo-inositol + 400 μg folic acid/day for three months before and during recombinant follicle stimulating hormone (r-FSH) administration, but who did not get pregnant. Three patients with autoimmune thyroiditis and four patients with hyperprolactinemia were excluded. Two IVF cycles were cancelled, and two were suspended due to a 17β-estradiol (17β-E_2) peak >4.000 pg/mL. Eighteen of the 54 patients who underwent an IVF cycle achieved pregnancy (15 ongoing pregnancies and 3 spontaneous abortions). The 36 patients who did not achieve pregnancy and one patient who had an abortion were re-enrolled to undergo a cycle of treatment with 2 g myo-inositol + 800 mg/day α-lipoic acid (Sinopol®, Laborest, Milano, Italy) and compared with the outcomes of previous cycles. After treatment with myo-inositol, we waited six months (the "wash-out period"), a window necessary because the ovary may remain sensitized to a second treatment after three months of treatment (Fig. 1).

For all female partners of treated couples (91 in total), the following endocrine-metabolic and ultrasound parameters were analyzed at the beginning (T0) and after three months of treatment (T3): BMI, total cholesterol, high-density lipoprotein (HDL) and low-density lipoprotein (LDL) cholesterol, triglycerides, fasting plasma glucose (FPG) and fasting insulinemia, follicle-stimulating hormone (FSH), luteinizing hormone (LH), 17β-E_2, prolactin (PRL), thyroid stimulating hormone (TSH), free triiodothyronine (FT3), free thyroxine (FT4), ovarian volume and reserve. For 37 patients, plasma glucose and insulinemia were analyzed at 1 and 2 h after an oral glucose tolerance test (OGTT).

Stimulation protocol

For IVF, the ovulation induction protocol included the "long protocol", involving administration of a GnRH-agonist (Decapeptyl®; Ipsen, Paris, France) on day 21 of the ovarian cycle and r-FSH (Gonal-F®; Merck, Geneva, Switzerland) from day 3 of the following cycle. Thereafter, the r-FSH dose was adapted individually according to the

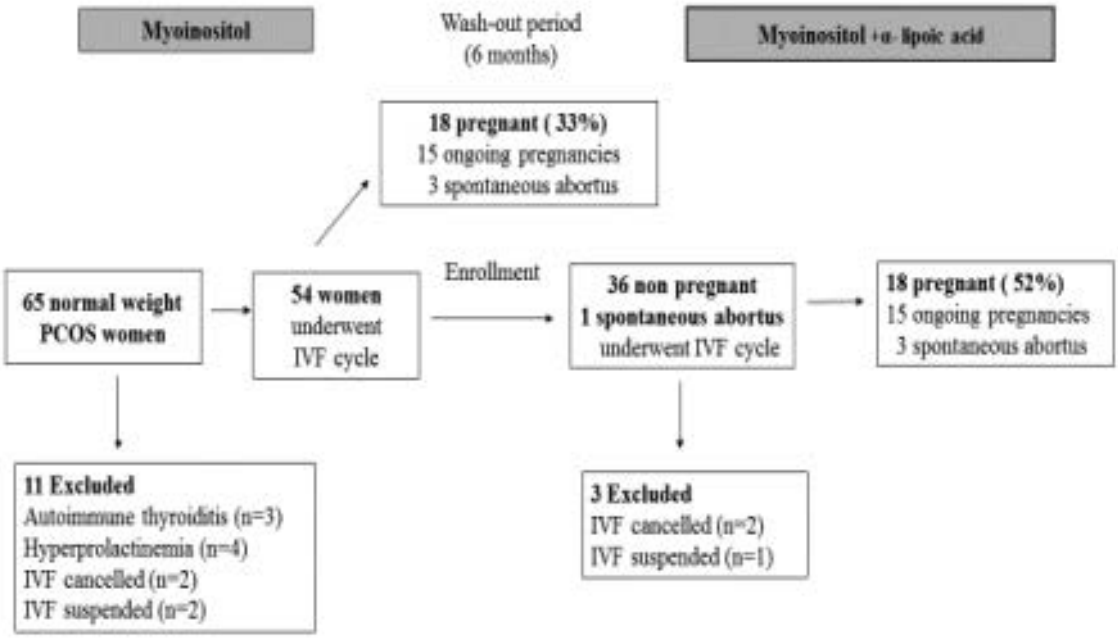

Fig. 1. *Flow chart showing the study design.*

patient's age and BMI. Follicular growth was monitored by ultrasound measurements and serum 17ß-E_2 levels. Ovulation was induced by administration of 10,000 IU human chorionic gonadotrophin (hCG) (Gonasi HP®; IBSA Pharmaceuticals, Italy) when at least one leading follicle had reached a diameter of 18 mm. Follicles were aspirated under neuroleptoanalgesia under transvaginal ultrasound guidance 36 h after hCG administration. The ICSI procedure, oocyte and sperm preparation protocols have been thoroughly described elsewhere (22). With respect to ICSI, briefly, cumulus and corona radiate cells were immediately removed after being retrieved by a short exposure to Hepes–buffer medium (Cook, Limerick, Ireland) containing 10 UI/mL hyaluronidase (Cook, Limerick, Ireland) and gentle aspiration in and out of a Pasteur pipette, and were mechanically cleaned from the remaining surrounding cumulus cells by aspiration using a denuding pipette (Denuding Flexi-Pet; Cook, Limerick, Ireland) with a 140 µm diameter.

Assessment of oocyte and embryo quality

Following the decumulation of the complexes described above, the oocyte, zygote, and embryo morphology were monitored using an inverted microscope equipped with a Hoffman modulation contrast system, and an imaging and archival software. Observation of oocytes was carried out with particular regard to the following parameters: stage of maturity (presence of the first polar body in the perivitelline space (MII stage), presence of germinal vesicles (GV), absence of both (MI stage); size and shape (it is necessary to eliminate the giant oocyte since it has a double set of chromosomes); cytoplasmic characteristics [ooplasma homogeneous or degenerated, (DEG)], presence of vacuoles, presence of plaques of smooth endoplasmic reticulum (SER clusters), presence of plaques of organelles, presence of refractile bodies); and extra-cytoplasmic characteristics (thickness and density of the *pellucida zonae*, size, and presence of granules).

Zygote quality was scored at 16-20 h after ICSI according to the European Society of Human Reproduction and Embryology (ESHRE) guidelines (23). At this stage, regular fertilization, characterized by the formation two pronuclei and two polar bodies, the number and distribution of nucleolar precursor bodies in each pronucleus were assessed. The cleavage rate and embryo morphology were evaluated approximately 44-48 h after ICSI and were classified according to the ESHRE guidelines (23) as follows: a) type1 embryos of excellent quality (regular blastomeres, fragmentation <10%, no multi-nucleation); b) type 2 embryos of good quality (regular blastomeres

Table I. *Baseline characteristics and clinical outcome in 58 women treated with myo-inositol alone.*

Characteristics (N=54 pz)	Myo-inositol	
	T0	T3
Age (years)	35.9 ± 2.8	/
Duration of infertility (years)	2.5 ± 0.9	/
BMI kg/m^2	22.6 ± 2.0	22.0 ± 2.4
Total cholesterol (mg/dL)	180.0 ± 32.6	179.1 ± 31.5
HDL (mg/dL)	51.8 ± 12.1	52.1 ± 12.2
LDL (mg/dL)	100.2 ± 15.3	98.9 ± 14.7
Tryglicerides (mg/dL)	98.7 ± 40.7	96.7 ± 40.2
Basal glycemia (mg/dL)	84.7 ± 9.7	83.8 ± 8.8
Basal insulin (mU/mL)	6.4 ± 2.8	6.3 ± 2.8
Basal FSH (mIU/mL)	6.0 ± 2.0	5.9 ± 1.9
Basal LH (mIU/mL)	7.0 ± 1.8	6.9 ± 1.7
17β-E2 (pg/mL)	46.3 ± 17.8	45.0 ± 16.3
PRL (ng/mL)	12.2 ± 4.7	11.6 ± 4.4
TSH (mIU/L)	1.6 ± 0.5	1.6 ± 0.5
FT3 (pg/mL)	2.6± 0.5	2.8 ± 0.4
FT4 (ng/dL)	1.2 ± 0.3	1.3 ± 0.4
Ovarian volume (cm^3)	10.5 ± 0.3	10.1 ± 0.4
Ovarian reserve (no. follicles)	27.8 ± 3.0	26.8 ± 3.4
Clinical outcome (%) (N = 58pz)		
Stimulation (days)		11 ± 0.4
Total FSH (IU) administration		1483.4 ± 728.5
Clinical pregnancies (%)		18/54 (33.3)
Ongoing pregnancies (%)		15/18 (83.4)
Spontaneous abortion (%)		3/18 (16.6)

Values are expressed as means ± standard deviation (SD) or percentage (%). BMI = Body mass index; HDL = high density lipoprotein, LDL = low-density lipoprotein, FSH = follicle stimulating hormone, LH = luteinizing hormone, 17β-E_2 = 17β-estradiol, PRL = prolactin, TSH = thyroid stimulating hormone, FT3 = free triiodothyronine, FT3 = free thyroxine.

and fragments <25%, multinucleation is not clear); and c) type 3 embryos of poor quality (irregular blastomeres, no fragments >25%, multi-nucleation present).

Luteal phase

Intravaginal administration of 200 mg progesterone twice/daily (Progeffik®, Effik, Italy) was started on the day of transfer, and treatment was performed daily until a serum pregnancy test was carried out.

Determination of pregnancy status

Fifteen days from transfer, the patients underwent plasma assays for ß-human chorionic gonadotrophin (ßhCG). If positive, a clinical pregnancy was determined by the visualization of an embryo with cardiac activity at 6-7 weeks of gestation. Spontaneous abortion was

Table II. *Baseline characteristics in 37 women treated with myo-inositol alone and with myo-inositol plus α-lipoic acid.*

Characteristic (n = 37)	Myo-inositol			Myo-inositol plus α-lipoic acid		
	T0	T3	p value	T0	T3	p value
Age (years)	36.3 ± 2.8	/	/	37.1 ± 2.7	/	/
Duration of infertility (years)	2.5 ± 1.0	/	/	3.5 ± 0.9	/	/
BMI (kg/m^2)	21.9 ± 1.5	21.2 ± 1.3	0.41	22.3 ± 1.5	21.2 ± 1.6	< 0.01
Total cholesterol (mg/dL)	181.8 ± 31.5	180.2 ± 30.0	0.69	179.7 ± 27.1	177.4 ± 27.8	0.51
HDL (mg/dL)	51.9 ± 12.4	51.8 ± 12.6	0.58	51.5 ± 11.4	53.0 ± 11.1	0.08
LDL (mg/dL)	99.7 ± 15.8	98.9 ± 14.7	0.06	99.0 ± 12.1	97.2 ± 10.2	0.39
Triglycerides (mg/dL)	97.9 ± 39.9	98.3 ± 40.5	0.84	98.5 ± 35.8	95.4 ± 33.3	0.16
Basal glycemia (mg/dL)	85.3 ± 10.2	84.4 ± 8.7	0.32	84.5 ± 8.9	83.3 ± 8.5	0.32
Basal insulin (mU/mL)	6.5 ± 2.9	6.5 ± 2.6	0.81	6.6 ± 2.9	6.0 ± 2.4	< 0.01
Basal FSH (mIU/mL)	6.2 ± 1.9	5.7 ± 1.0	0.18	5.6 ± 1.4	6.0 ± 1.9	0.24
Basal LH (mIU/mL)	7.1 ± 1.8	7.1 ± 1.7	0.97	7.0 ± 1.8	6.7 ± 1.9	0.30
17β-E2 (pg/mL)	45.1 ± 17.8	44.1 ± 16.3	0.68	46.6 ± 16.1	44.7 ± 14.5	0.60
PRL (ng/mL)	11.9 ± 4.8	11.4 ± 4.6	0.67	13.1 ± 5.4	12.4± 4.3	0.51
TSH (mIU/L)	1.6 ± 0.5	1.6 ± 0.5	0.32	1.6 ± 0.4	1.71± 0.3	0.26
FT3 (pg/mL)	2.7 ± 0.5	2.9 ± 0.7	0.22	2.7 ± 0.6	2.7± 0.5	0.92
FT4 (ng/dL)	1.2 ± 0.3	1.2 ± 0.4	0.79	1.2 ± 0.3	1.3 ± 0.4	0.17
Ovarian volume (cm^3)	10.6 ± 0.5	10.3± 1.2	0,19	10.9 ± 1.0	9.5 ± 0.8	< 0.001
Ovarian reserve (no. follicles)	27.7± 3.8	26.4 ± 3.5	0.06	27.8 ± 3.6	26.1 ± 1.6	0.06

Values are reported as mean ± standard deviation (SD). BMI = Body mass index, HDL = high density lipoprotein, LDL = low-density lipoprotein, FSH = follicle stimulating hormone, LH = luteinizing hormone, 17β-E_2 = 17β-estradiol, PRL = prolactin, TSH = thyroid stimulating hormone, FT3 = free triiodothyronine, FT4 = free thyroxine.

classified as the loss of the pregnancy between the fifth and twelfth weeks of gestation.

Statistical analysis

All data are presented as the mean ± standard deviation (SD). Mean values of quantitative data were normally distributed, including age, BMI, ovarian reserve and volume, years of infertility, hormonal and retrieved oocytes and the data were compared using the paired Student's *t*-test; qualitative data including parameters

of oocyte score and reproductive outcome (percentage of fertilization, cleavage, pregnancy, implantation, and abortion) were compared using the Fisher's exact test between patients treated with myo-inositol alone and those treated with myo-inositol plus α-lipoic acid. BMI and oocyte maturity, after treatment with a combination of myo-inositol plus α-lipoic acid were correlated using the Pearson's test. The commercial software SPSS (version 11, SPSS Inc. in Chicago, USA) was used for data analysis. Results with $p < 0.05$ were considered significant.

RESULTS

The baseline characteristics and clinical outcome of 58 patients treated with myo-inositol are shown in Table I.

Baseline characteristics of 37 patients treated with supplementation of myo-inositol alone and with supplementation of myo-inositol plus α-lipoic acid are shown in Table II.

We compared parameters from the same patients at four different times. The internal factors (PCOS severity) and external factors (e.g., diet) were constant over time and discontinuation of myo-inositol after three months of treatment returned the patients to pre-treatment conditions. When patients were treated with a supplementation of myo-inositol alone, metabolic and hormonal parameters were similar at T3 compared to T0. Instead, when patients were treated with a supplementation of myo-inositol plus α-lipoic acid, insulin levels, BMI, and ovarian volume which did not change at T3 versus T0 after treatment with myo-inositol alone, were significantly reduced at T3 versus T0, whereas all the other metabolic and hormonal parameters did not change at T3 versus T0. Fig. 2 shows the comparison of trends of insulin values at 0 min, 60 min, and 120 min at T3 *vs* T0 of 37 patients treated with myo-inositol plus α-lipoic acid.

These results showed that the treatment with myo-inositol plus α-lipoic acid for 3 months is effective in significantly reducing the insulin values both at 60 min and at 120 min after the administration of glucose in an OGTT when compared to values at 60 min and 120 min, respectively of T0 (56.0±22.2 *vs* 43.8±20.8; 31.9±19.1 *vs* 21.11±18.0; $p < 0.001$).

Fig. 3 shows the existence of an inverse correlation between BMI and the oocyte maturity. In fact, the decrease of BMI is associated with a

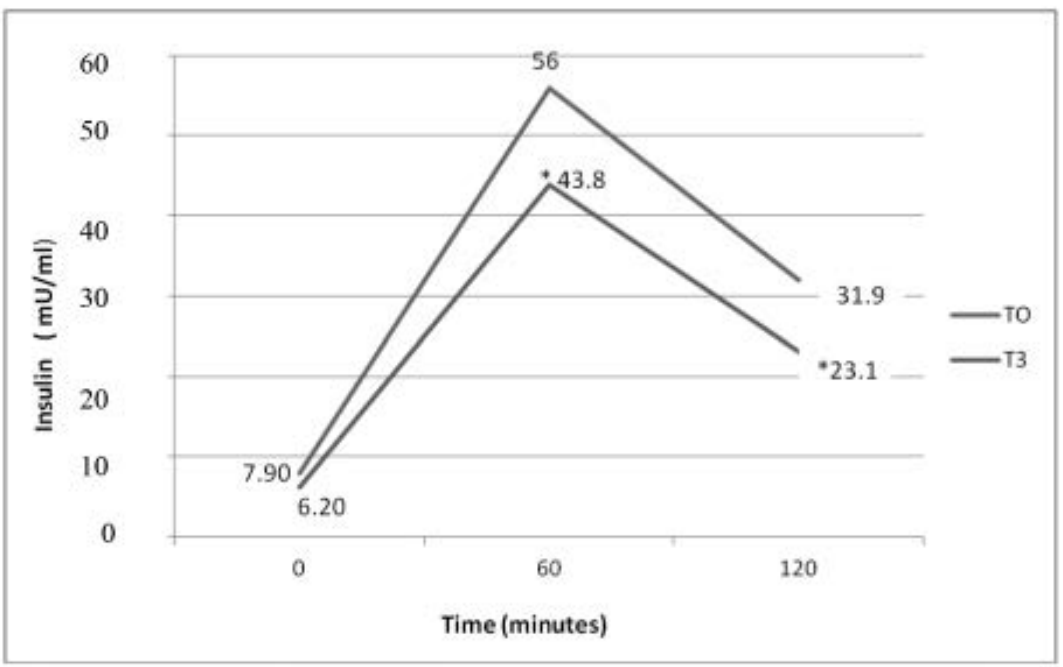

Fig. 2. *Oral glucose tolerance test (OGTT) at T0 and T3 after treatment with myo-inositol plus α-lipoic acid. Note: Comparison of insulin values at 0, 60, and 120 min at T3 vs T0. Paired Student's t-test: *p < 0.001.*

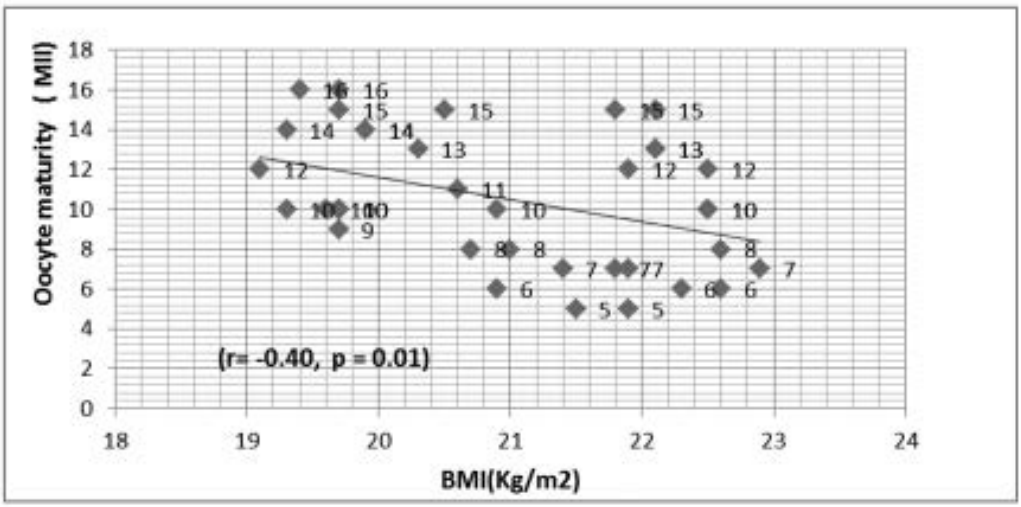

Fig. 3. *Correlation between BMI and oocyte maturity (MII). Note. Parametric Pearson test. 0 < r < 0.3 weak correlation; 0.3 < r < 0.7 moderate correlation; r > 0.7 strong correlation.*

Table III. *Outcome, oocyte maturity and embryo score in 37 women treated with myo-inositol alone and myo-inositol plus α-lipoic acid.*

Characteristic (N = 37)	Myo-inositol	Myo-inositol plus α- lipoic acid	p value
Stimulation (days)	11.6 ± 0.6	10.8 ± 0.6	0.06
FSH (IU) administration	1501.9 ± 676.4	1498.0 ± 698.4	0.96
No. of retrieved oocytes	11.5 ± 4.2	12.0 ± 4.8	0.06
No. of MII oocytes	9.4 ± 3.9	10.9 ± 4.6	0.17
MII/total retrieved oocytes (%)	0.81 ± 0.9	0.87 ± 0.9	< 0.05
No. of GV+DEG	1.01 ± 1.5	0.2 ± 0.4	< 0.001
Fertilization rate (%)	78.9	83.4	0.53
Cleavage rate (%)	95.9	95.5	1.0
No. of embryos transferred	2.6 ± 0.7	2.7 ± 0.4	0.62
Embryo grade 1 (%)	57.7	75. 7	< 0.05
Embryo grade 2 (%)	27.8	18.4	< 0.01
Embryo grade 3 (%)	14.4	7.7	0.11

Values are means ± SD or %. MII = metaphase II; DEG = degenerate oocytes, GV = germinal vesicles.

significant improvement in the number of metaphase II (MII) oocyte retrieved (r = -0.40, $p = 0.01$).

No differences were found between the cycles of the two different treatments in terms of total FSH units administered and the duration of stimulation, respectively (1501.9±676.4 *vs* 1498.0 98.5; $p = 0.961$) and (11.6±0.6 *vs* 10.8±0.6; $p = 0.06$) (Table III).

Two cycles were cancelled, whereas one was suspended due to 17β-E_2 peak >4,000 pg/mL. The mean number of oocytes retrieved did not differ between the two treatments (11.5±4.2 *vs* 12.0±4.8; $p = 0.06$). Whereas in the myo-inositol plus α-lipoic acid group the number of immature oocytes (VG and DEG) not suitable for injection was significantly reduced (0.2±0.4 *vs* 1.0±1.5; $p < 0.001$), with a significantly increased percentage of MII oocytes compared to treatment with myo-inositol alone (0.87±0.9% *vs* 0.81±3.9%; $p < 0.05$). No differences emerged in terms of fertilization and cleavage rate or mean number of transferred embryos between the two different treatments; whereas the number of grade 1 embryos was significantly increased, with a significant reduction of grade 2 embryos (18.4% *vs* 27.8%; $p < 0.01$) by myo-inositol plus α-lipoic acid treatment.

A total of 18 pregnancies were obtained in the myo-inositol plus α-lipoic acid group, with a trend for a higher percentage compared to the myo-inositol alone group (52.0% *vs* 33.3%; $p = 0.07$)

DISCUSSION

Patients affected by PCOS have generally poorer oocyte quality and a state of increased oxidative stress compared to patients who do not have this syndrome (24, 25). We hypothesized that using myo-inositol plus a potent antioxidant such as α-lipoic acid would therefore have a beneficial effect on the PCOS phenotype. The insulin-sensitizing properties and antioxidant capacity of these two substances could produce a positive synergistic effect. We decided to enroll normal-weight women with PCOS for this study because excess body weight interferes negatively on oocyte quality and amplifies the state of oxidative stress (26).

The most common cause of IVF embryo transfer failure is reduced embryo quality; other factors that can have a negative effect include physiological factors, such as ageing and/or pathological factors such as PCOS.

Post-ovulatory oocyte ageing is clearly a prominent issue affecting fecundity; however, the molecular mechanisms that control this process are not well elucidated. Several studies that have assessed factors known to influence the onset of post-ovulatory ageing, specifically highlight the potential role of oxidative stress as the 'initiator' of a cascade of events that generates the aged oocyte phenotype (27), and show how oxidative stress can directly influence the onset of apoptosis in post-ovulatory aged oocytes both *in vitro* and *in vivo* (28, 29).

Nuclear and cytoplasmic oocyte quality are critical for the competence of the embryo upon which medically assisted procreation outcome ultimately depends. The follicular microenvironment is crucial for oocyte quality and this must be taken into account particularly with the use of ovarian stimulation protocols in which many stages of the maturation process of the oocyte are skipped and result in the formation of numerous oocytes with varying degrees of quality.

The data reported in the literature show that myo-inositol is a key component of this follicular environment, and higher concentrations of myo-inositol correlate with a higher quality oocyte (30). In fact, supplementation with myo-inositol in cycles is positively correlated to meiotic progression in mouse germinal vesicle oocytes, enhancing intracellular Ca^{2+} (12), and this could provide an explanation for the higher number of mature oocytes retrieved.

Preliminary data of the few studies in patients with PCOS treated with the addition of myo-inositol to folic acid have shown that this treatment reduces the number of germinal vesicles and degenerate oocytes at the time of pick-up, without compromising the total number of oocytes retrieved (13, 14).

The present study focused on the combination of myo-inositol plus α-lipoic acid in patients with PCOS undergoing ovulation induction. Our data show that a treatment of at least three months with myo-inositol plus α-lipoic acid, compared with myo-inositol alone, reduced germinal vesicles and degenerate oocytes at ovum pick-up without compromising the total number of retrieved oocytes. These patients also had a significant reduction in

insulinemia at the end of treatment.

Lipoic acid has a biological function unique among other natural antioxidants, which has been defined by Halliwell and Gutteridge as "any substance that, when present at low concentrations compared to those of an oxidizable substrate significantly delays or prevents oxidation of the substrate" (31). Common antioxidants are either water-soluble or lipid soluble agents. In contrast, α-lipoic acid has both hydrophilic and hydrophobic properties. Being both water- and fat-soluble means that α-lipoic acid is widely distributed in plants and animals in both cellular membranes and in the cytosol (32), therefore, it can elicit its antioxidant action in both the cytosol and plasma membrane in contrast to vitamin C (which is lipophobic) and vitamin E (which is lipophilic). This could result in a greater number of excellent quality embryos and, consequently, in a more positive trend in the achievement of clinical pregnancy rates as we observed in the group treated with the combination of myo-inositol plus α-lipoic acid.

The insulin-sensitizing properties and antioxidant capacity of these two substances could produce a positive synergistic effect at crucial points of assisted reproductive techniques, such as an enhanced oocyte competence as shown by the data of our study resulting in a significantly increased number of grade 1 embryos and a significant reduction of grade 2 embryos. Not negligible was the positive effect of this combined treatment achieved on metabolic parameters of such patients. In our study, the association between myo-inositol and α-lipoic acid determined a reduction in weight at T3 compared to T0. There was also a significant reduction of insulin values both at 60 min at 120 min after the administration of glucose in an OGTT ($p<0.001$) when compared to values at 60 min and 120 min, respectively, of OGTT performed before treatment (T0), producing a beneficial effect on long-term cardiovascular risk in these patients. It should be emphasized that such supplementation is well tolerated by patients, without any gastrointestinal side effects such as can occur with the use of metformin. This contributes to a better compliance and adherence to therapy by the patient without treatment interruption.

In conclusion myo-inositol plus α-lipoic acid is an effective and well-tolerated treatment. The available data suggest that the supplementation of myo-inositol and α-lipoic acid in PCOS patients, undergoing IVF cycles can help to improve their reproductive outcome and also their metabolic profile, posing however, hypothetical issues about their use in the long-term prevention of cardiovascular disease. The value of this study is limited by the number of subjects evaluated; therefore, further randomized studies are needed to confirm these findings.

REFERENCES

1. Knochenhauer ES, Key TJ, Kahsar-Miller M, Waggoner W, Boots LR, Azziz R**.** Prevalence of the polycystic ovary syndrome in unselected black and white women of the southeastern United States: a prospective study. J Clin Endocrinol Metab 1988; 83:3078-82.
2. Calogero AE, Calabrò V, Catanuso M, Condorelli RA, La Vignera S. Understanding polycystic ovarian syndrome pathogenesis:an updated of its genetic aspects. J Endocrinol Invest 2011; 34:630-44.
3. Ehrmann DA. Polycystic ovary syndrome. N Engl J Med 2005; 352:1223-36.
4. Reaven GM. Banting lecture 1988. Role of insulin resistance in human disease. Diabetes 1988; 37:1595-607.
5. Chang RJ, Nakamura RM, Judd HL, Kaplan SA. Insulin resistance in nonobese patients with polycystic ovarian disease. J Clin Endocrinol Metab 1983; 57:356-9.
6. Holte J, Bergh T, Berne C, Lithell H. Serum lipoprotein lipid profile in women with polycystic ovary syndrome: relation to anthropometric, endocrine and metabolic variables. Clin Endocrinol (Oxf) 1994; 41:463-71.
7. Morales AJ, Laughlin GA, Bützow T, Maheshwari H, Baumann G, Yen SS. Insulin, somatotropic, and luteinizing hormone axes in lean and obese women with polycystic ovary syndrome: common and distinct features. J Clin Endocrinol Metab 1996; 81:2854-64.
8. Morin-Papunen LC, Vauhkoneni I, Koivunen RM, Ruokonen A, Tapanainen JS. Insulin sensitivity, insulin secretion, and metabolic and hormonal parameters in healthy women and women with

polycystic ovarian syndrome. Hum Reprod 2000; 15:1266-74.
9. Ovesen P, Moller J, Ingerslev HJ, Jorgensen JO, Mengel A, Schmitz O, Alberti KG, Moller N. Normal basal and insulin stimulated fuel metabolism in lean women with polycystic ovary syndrome. J Clin Endocrinol Metab 1993; 77:1636-40.
10. Berridge MJ. Inositol triphosphate and calcium signaling mechanisms. Biochim Biophys Acta 2009; 1793:933-40.
11. Chiu TT, Tam PP. A correlation of the outcome of clinical in vitro fertilization with the inositol content and embryotrophic properties of human serum. J Assist Reprod Genet 1992; 9:524-30.
12. Chiu TT, Rogers MS, Briton-Jones C, Haines C. Effects of myo-inositol on the in-vitro maturation ad subsequent development of mouse oocytes. Hum Reprod 2003; 18:408-16.
13. Ciotta L, Stracquadanio M, Pagano I, Carbonaro A, Palumbo M, Gulino F. Effects of myo-inositol supplementation on oocyte's quality in PCOS patients: a double blind trial. Eur Rev Med Pharmacol Sci 2011; 15:509-14.
14. Papaleo E, Unfer V, Baillargeon JP, Fusi F, Occhi F, De Santis L. Myo-inositol may improve oocyte quality in intracytoplasmatic sperm injection cycles. A prospective controlled, randomized trial. Fertil Steril 2009; 91:1750-4.
15. Galletta M, Grasso S, Vaiarelli A, Roseff SJ. Bye-bye chiro-inositol-myo-inositol: true progress in the treatment of polycystic ovary syndrome and ovulation induction. Eur Rev Med Pharmacol Sci 2011; 15:1212-4.
16. Unfer V, Carlomagno P, Rizzo P, Raffone E, Roseff S. Myo-inositol rather than D-chiro-inositol is able to improve oocyte quality in intracytoplasmic sperm injection cycles. A prospective controlled, randomized trial. Eur Rev Med Pharmacol 2001; 15:452-7.
17. Masharani U, Gjerde C, Evans JL, Youngren JF, Goldfine ID. Effect of controlled-release alpha lipoic acid in lean, nondiabetic patients with polycystic ovary syndrome. J Diabetes Sci Technol 2010; 4:359-64.
18. Evans JL, Goldfine ID, Maddux BA, Grodsky GM. Are oxidative stress-activated signaling pathway mediators of insulin resistance and beta-cell dysfunction? Diabetes 2003; 52:1-8.
19. Gambera A, Visenzi C, Fratus C, Bugari G, Iacobello C, Scagliola P, Sartori E. Alternative insulin-sensitizers (Lipoic acid and inositol) in polycystic ovary syndrome (PCOS). Giorn.It.Ost.Gin 2012; 34: 182-3.
20. Rotterdam ESHRE/ASRM - Sponsored PCOS Consensus Workshop Group. Revised 2003 consensus on diagnostic criteria and long-term health risks related to policystic ovary syndrome. Fertil Steril 2004; 81:19-25.
21. Marci R, Marcucci I, Marcucci AA, et al. Hysterosalpingocontrast sonography (HyCoSy): evaluation of the pain perception, side effects and complications. BMC Med Imaging 2013; 13:28.
22. Van De Valde H, Nagy ZP, Joris H, De Vos A, Van Steirteghem AC. Effects of different hyaluronidase concentrations and mechanical procedures for cumulus cell removal on the outcome of intracytoplasmic sperm injection. Hum Reprod 1997; 12:2246-50.
23. Alpha Scientists in Reproductive Medicine and ESHRE Special Interest Group of Embryology. The Istanbul consensus workshop on embryo assessment: proceedings of an expert meeting. Hum Reprod 2011; 26:1270-83
24. Toprak S. Yönem A, Cakir B, Guler S, Azal O, Ozata M, Corakci A. Insulin resistance in nonobese patients with polycystic ovary syndrome. Hormone Research 2001; 55:65-70.
25. Karuputhula NB, Chattopadhayay R, Chakravarty B, Chaudhury K. Oxidative status in granulose cells of infertile women undergoing IVF. Syst Biol Reprod Med 2013; 59:91-8.
26. Pantasri T, Norman RJ. The effects of being overweight and obese on female reproduction: a review. Gynecol Endocrinol 2014; 30:90-4.
27. Lord T, Aitken RJ. Oxidative stress and ageing of the post-ovulatory oocyte. Reproduction 2013; 146:R217-27.
28. Takahashi T, Igarashi H, Kawagoe J, Amita M, Hara S, Kurachi H. Poor embryo development in mouse oocytes aged in vitro is associated with impaired calcium homeostasis. Biol Reprod 2009; 80:493-502.

29. Takahashi T, Takahashi E, Igarashi H, Tezuka N, Kurachi H. Impact of oxidative stress in aged mouse oocytes on calcium oscillations at fertilization. Mol Reprod Dev 2003; 66:143-52.
30. Chiu TT, Rogers MS, Law E, Briton-Jones CM, Cheung LP, Haines CJ. Follicular fluid and serum concentrations of myo-inositol in patients undergoing IVF: relationship with oocyte quality. Hum Reprod 2002; 17:1591-6.
31. Petersen SK, Moreau RF, Smith EJ, Hagen TM. Is alpha-lipoic acid a scavenger of reactive oxygen species in vivo? Evidence for its initiation of stress signaling pathways that promote endogenous antioxidant capacity. IUBMB Life 2008; 60:362-7.
32. Wada H, Shintani D, Ohlrogge J. Why do mitochondria synthesize fatty acids? Evidence for involvement in lipoic acid production. Proc Natl Acad Sci USA 1997; 94:1591-6.

LETTER TO THE EDITOR

SERUM 25-HYDROXYVITAMIN D LEVELS IN CHILDREN WITH RECURRENT TONSILLITIS LIVING IN MILAN

S. TORRETTA[1], P. MARCHISIO[2], E. IOFRIDA[1], P. CAPACCIO[1] and L. PIGNATARO[1]

[1]Department of Clinical Sciences and Community Health, Università degli Studi di Milano, Otorhinolaryngological Clinic, Fondazione IRCCS Ca' Granda Ospedale Maggiore Policlinico, Milan, Italy; [2]Pediatric Clinic, Department of Pathophysiology and Transplantation, Università degli Studi di Milano, Pediatric Highly Intensive Care Unit, Fondazione IRCCS Ca' Granda Ospedale Maggiore Policlinico, Milan, Italy

Received May 13, 2015 – Accepted September 28, 2015

Involvement of 25-hydroxyvitamin D in the etiopathogenesis of tonsillar disease in children is still debated; this study assesses possible differences in serum 25-hydroxyvitamin D levels between 309 Caucasian children (58.1% males; mean age 55.7±31.0 months) living in Milan with a history of recurrent tonsillitis (RT) and healthy controls. Mean serum 25(OH)D levels were significantly reduced in the children with a history of RT (22.0±8.7 ng/mL *vs* 24.6±7.8 ng/mL; p=0.03), and the proportion of children with insufficient or deficient serum 25(OH)D levels was higher in the RT group (81.5% and 6.5% respectively) than in the control group (75.1% and 3.5%) (not significant). The multivariable model created to test the independent association between serum 25(OH)D levels and a history of RT after adjusting for age and season showed that the association was not significant. Our study failed to find any significant reduction in serum 25(OH)D levels after adjustment for age and season in a case series of children with RT in comparison with healthy controls, which suggests that vitamin D does not play a relevant role in the etiology of pediatric tonsillar infections.

In addition to being involved in bone metabolism and calcium homeostasis, vitamin D may also play a role in immunity and infections (1-6). In particular, it has been postulated that 25-hydroxyvitamin D [25(OH)D], the liver hydroxylated isoform that is considered to reflect individual vitamin D status acts as an immunomodulator of both the innate and adaptive immune system by shifting the T helper cell pool towards Th2 status, inducing antimicrobial peptide synthesis, and inhibiting the production of pro-inflammatory cytokines (1, 3-6). It may therefore modulate the incidence and severity of some bacterial and viral infections, as indicated by the findings of clinical studies involving patients with tuberculosis, respiratory tract infections, and otitis media (2, 7-10). However, it is still unclear what impact vitamin D deficiency and insufficiency may have on the prevention and treatment of pediatric respiratory tract infections (10), and the few, mainly retrospective studies of a small case series of patients evaluating the possible effect of reduced serum 25-hydroxyvitamin D levels on the etiopathogenesis

Key words: children, tonsillitis, 25-hydroxyvitamin D

Mailing address: Sara Torretta, MD
Department of Specialist Surgical Sciences,
University of Milan, Fondazione I.R.C.C.S.
Cà Granda Ospedale Maggiore Policlinico,
Via F. Sforza 35, 20122 Milano, Italy
Tel.: +39 0250320245 Fax: +39 0250320248
e-mail: sara.torretta@policlinico.mi.it

0393-974X (2015)

DISCLOSURE: ALL AUTHORS REPORT NO CONFLICTS OF INTEREST RELEVANT TO THIS ARTICLE.

Table I. *Demographic, anamnestic and clinical characteristics of the study population.*

		Groups			
		Recurrent tonsillitis	**Controls**	**p-value**	**Total**
Demographic features	No. of males (%)	66 (61.0)	115 (57.2)	ns	181 (58.6)
	Mean age±SD†	71.4±36.1	51.1±27.8	< 0.01	55.7±31.0
	No. recruited in winter seasons	71 (65.7)	11 (55.2)	< 0.01	182 (58.9)
Clinical features	Mean BMI±SD	16.2±3.0	16.2±2.5	ns	16.2±2.6
	Mean serum 25(OH)D level (ng/mL)	22.0±8.7	24.6±7.8	0.03	24.0±8.1
	No. with serum 25(OH)D level <30 ng/mL (%)	88 (81.5)	151 (75.1)	ns	239 (77.3)
	No. with serum 25(OH)D level < 20 ng/mL (%)	7 (6.5)	7 (3.5)	ns	14 (4.5)
	Mean serum IgE level (IU/mL)	124.0±186.2	125.8±301.8	ns	125.0±259.3
	No. of subjects with increased IgE levels (%)	40 (37.0)	67 (33.3)	ns	107 (34.6)
	Total	108	201	-	309

†: months; SD: standard deviation; BMI: body mass index; ns: not significant; 25(OH)D: 25-hydroxyvitamin D.

Table II. *Relationship between mean serum 25-hydroxyvitamin D levels (ng/mL) and possible confounding factors.*

Confounding factors		**Mean serum 25(OH)D levels±SD**	**p-value**	**SE**	**95%CI**	**R2**
Age		-	<0.01*	0.01	-0.10;-0.03	0.06
Gender	**Male**	24.2±8.4	ns**	-	-	-
	Female	23.7±7.6				
Season+	**Winter**	23.8±7.8	<0.01**	-	-	0.06
	Fall	29.3±10.5				
	Spring	20.8±5.7				
	Summer	31.2±5.7				
Season++	**Winter seasons**	23.4±7.7	<0.01**	-	-	0.05
	Non-winter seasons	29.6±9.8				
BMI		-	ns*	-	-	-
Mean serum IgE level		-	ns*	-	-	-
Decreased serum IgE level	**No**	23.4±7.6	ns**			
	Yes	25.2±8.8	-			

*SD: standard deviation; *: linear regression analysis; **: one-way ANOVA; +: tested as a categorical variable; ++: tested as a dichotomic variable.*
25(OH)D: 25-hydroxyvitamin D.

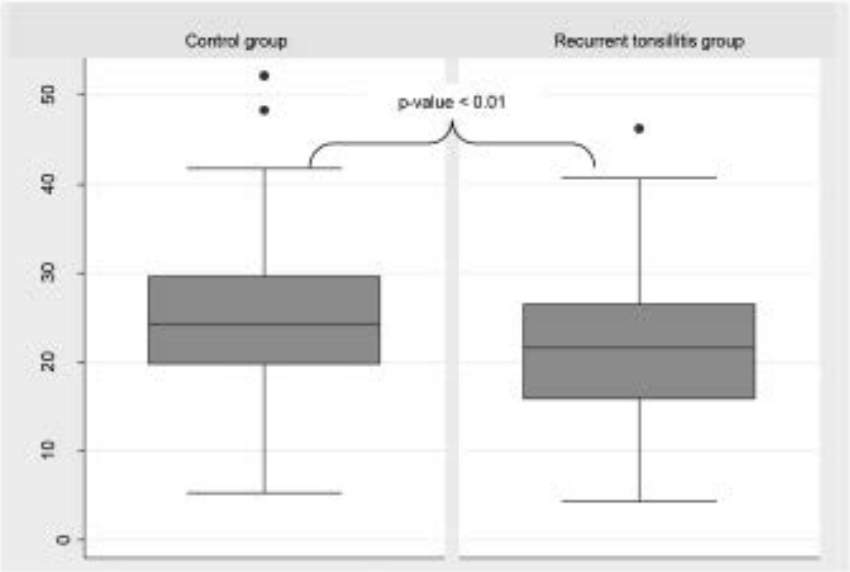

Fig. 1. *Box plots of hydroxyvitamin D levels in children with a history of recurrent tonsillitis and control group. The edges of the box indicate the first and third quartiles, the line inside the box the median value, and the "whiskers" the highest and lowest values.*

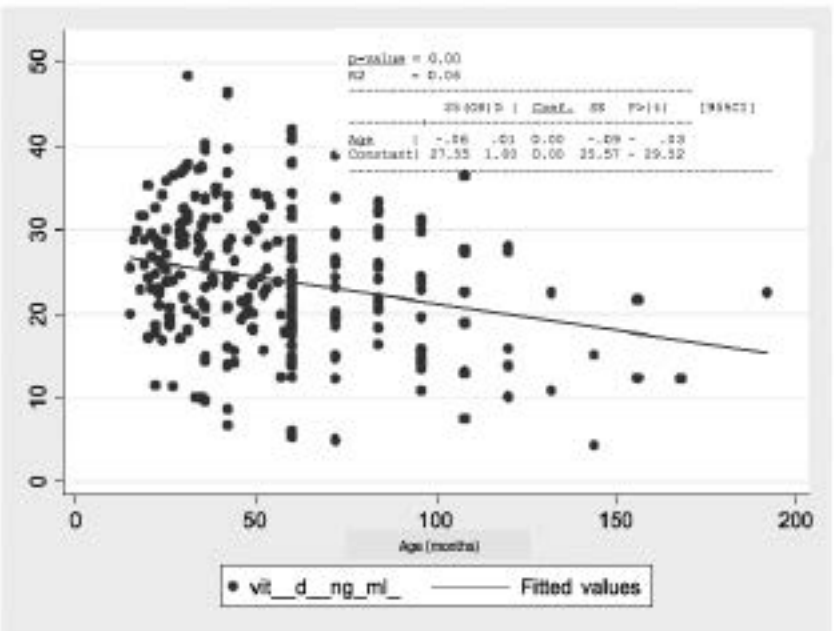

Fig. 2. *Linear relationship between age and mean 25-hydroxyvitamin D levels in the population as a whole (coefficients reported in the insert).*

of chronic tonsillar disease have led to conflicting results (11-14).

We therefore planned a case-control study in order to assess possible differences in serum 25(OH) D levels determined by means of an enzyme-linked immunosorbent assay between a sample of consecutive Caucasian children living in Milan (Italy, latitude 45° 27' N) with a history of recurrent

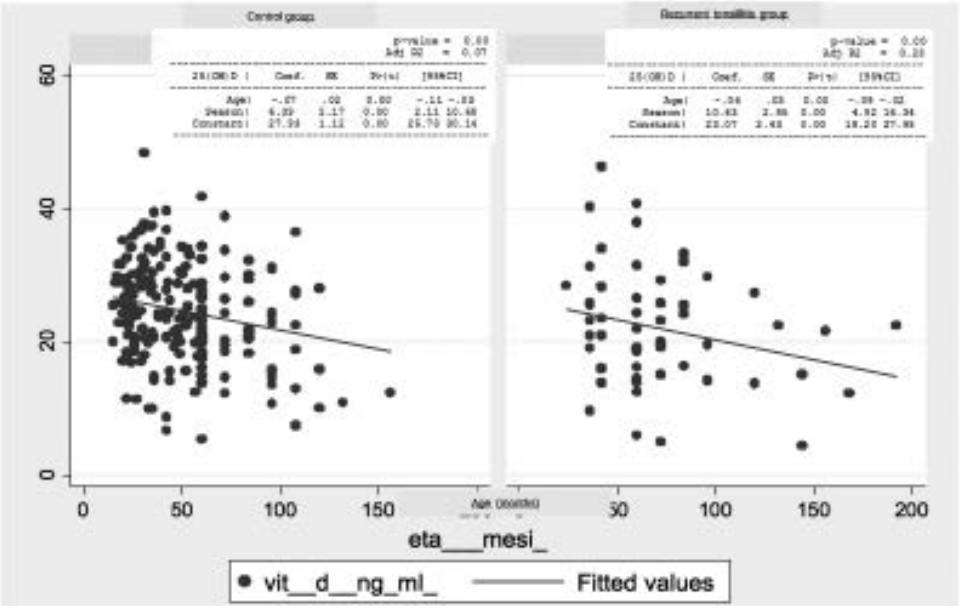

Fig. 3. *Linear relationship between age and mean 25-hydroxyvitamin D levels in patients with a history of recurrent tonsillitis and control group after adjustment for the season (coefficients reported in the insert). Red line corresponding to fitted values in control group is superimposable to the one corresponding to fitted values in the group with a history of recurrent tonsillitis, suggesting that, after adjustment for season, the relationship between age and mean 25-hydroxyvitamin D levels is not influenced by a positive history of recurrent tonsillitis.*

tonsillitis (RT), (documented by medical records and defined as at least seven episodes of acute tonsillitis in the preceding year, or at least five episodes per year for two consecutive years, or at least three episodes per year for three consecutive years or more) (15) and healthy controls. Inclusion criteria were based on those of Paradise (15) as they are considered among the reference criteria in our Italian guidelines (16). Vitamin D insufficiency was defined as serum 25(OH)D levels of <30 ng/mL, and vitamin D deficiency as serum 25(OH)D levels of <20 ng/mL (2).

The final analyses were made using the data relating to a total of 309 children (58.1% males; mean age 55.7±31.0 months): 108 with a history of RT and 201 healthy controls (Table I). Mean serum 25(OH)D levels were significantly reduced (p=0.03) in the children with a history of RT (22.0±8.7 ng/mL *vs* 24.6±7.8 ng/mL) (Fig. 1), and the proportion of children with insufficient or deficient serum 25(OH) D levels was higher in the group with a history of RT (81.5% and 6.5%, respectively) than in the control group (75.1% and 3.5%), although the difference was not significant. There was a significant relationship (p<0.01) between mean serum 25(OH)D levels and age insofar as serum levels decreased with age (Fig. 2); moreover, mean serum 25(OH)D levels were significantly lower in the winter months (23.4±7.7 ng/mL *vs* 29.6±9.8 ng/mL; p<0.01).

The multivariable model created to test the independent association between serum 25(OH) D levels and a history of RT after adjusting for age and season showed that the association was not significant (Fig. 3). Finally, there was no significant relationship between serum 25(OH)D levels and any of the other assessed variables (i.e. gender, BMI, and mean serum IgE levels) (Table II).

These results add to the conflicting findings of the few and mainly retrospective studies of small populations that have been published to date (11-14,

17). Only two prospective, cross-sectional pediatric studies were carried out previously (12, 14). In 2010, Esteitie et al. (14) published a pilot study of 47 children undergoing adenotonsillectomy without finding any between-group difference in serum 25(OH)D levels. However, only 12 of the 47 children had recurrent infections, but it is not clear what the "recurrent infections" were, therefore the results cannot be directly compared with our findings in children with RT. Aydin et al. (12) analysed serum 25(OH) D levels and vitamin D receptor polymorphisms over a 9-month period (autumn, winter, and spring) in 106 children who had undergone tonsillectomy because of recurrent tonsillitis and 127 healthy children, without finding any significant difference between the groups, although the tonsillectomised children had slightly lower serum 25(OH)D levels. They also found that the prevalence of serum 25(OH)D insufficiency was significantly higher in the group with recurrent tonsillitis, which agrees with the albeit non-significant greater prevalence of deficient or insufficient serum 25(OH)D levels observed in children with RT. On the contrary, a study of 54 adults with documented recurrent group A streptococcal tonsillar infections found that they had significantly lower serum 25(OH)D levels than the 50 controls (17). It can be speculated that the discrepancy between this finding and our experience may be related to the different ages of the study subjects. Moreover, all of the patients in Nseir's study had documented recurrent group A streptococcal tonsillar infections, whereas neither we nor that author made an etiological assessment; as the exact mechanisms involved in the antibacterial effect of vitamin D are still unclear and have only been documented in patients with selected bacterial infections (18), a difference in the etiology of the infectious process could at least partially account for the different findings.

In conclusion, our study failed to find any significant reduction in serum 25(OH)D levels after adjustment for age and seasoning in a case series of children with a history of RT based on Paradise criteria (15) in comparison with healthy controls. Our results seem to suggest that vitamin D does not play any role in the etiology of pediatric tonsillar infections, and on this basis, we cannot support the widespread use of vitamin D supplementation as a preventive strategy for children with a history of RT. However, due to our study design we were not able to test the possible evolution of infectious tonsillar disease related to modification in serum 25(OH)D levels over time, and the effect of seasonal fluctuation in serum 25(OH)D levels among tonsillitis-prone children, which would be better addressed by means of cohort studies or randomized controlled trails.

REFERENCES

1. Adams JS, Hewison M. Unexpected actions of vitamin D: new perspectives on the regulation of innate and adaptive immunity. Nat Clin Pract Endocrinol Metab 2008; 8:80-90.
2. Bergman P, Lindh AU, Björkhem-Bergman L, Lindh JD. Vitamin D and respiratory tract infections: a systematic review and meta-analysis of randomized controlled trials. PLoS One 2013; 8:e65835.
3. Charan J, Goyal JP, Saxena D, Yadav P. Vitamin D for prevention of respiratory tract infections: A systematic review and meta-analysis. J Pharmacol Pharmacother 2012; 3:300-303.
4. Gombart AF, Borregaard N, Koeffler HP. Human cathelicidin antimicrobial peptide (CAMP) gene is a direct target of the vitamin D receptor and is strongly up-regulated in myeloid cells by 1,25-dihydroxyvitamin D3. FASEBJ 2005; 19:1067-77.
5. Barlow PG, Svoboda P, Mackellar A, et al. Antiviral activity and increased host defense against influenza infection elicited by the human cathelicidin LL-37. PLoS One 2011; 6:e25333.
6. Jolliffe DA, Griffiths CJ, Martineau AR. Vitamin D in the prevention of acute respiratory infection: Systematic review of clinical studies. J Steroid Biochem Mol Biol 2013; 135:321-29.
7. Marchisio P, Consonni D, Baggi E, et al. Vitamin D supplementation reduces the risk of acute otitis media in otitis-prone children. Pediatr Infect Dis J 2013; 32:1055-60.
8. Esposito S, Baggi D, Bianchini S, Marchisio P, Principi N. Role of vitamin D in children with respiratory tract infection. Int J Immunopathol Pharmacol 2013; 26:1-13.
9. Science M, Maguire JL, Russell ML, Smieja M, Walter SD, Loeb M. Low serum 25-hydroxyvitamin

D level and risk of upper respiratory tract infection in children and adolescents. Clin Infect Dis 2013; 57:392-97.
10. Esposito S, Baggi E, Bianchini S, Marchisio P, Principi N. Role of vitamin D in children with respiratory tract infection. Int J Immunopathol Pharmacol 2013; 26:1-13.
11. Yildiz I, Unuvar E, Zeybek U, et al. The role of vitamin D in children with recurrent tonsillopharyngitis. Ital J Pediatr 2012; 38:25.
12. Aydın S, Aslan I, Yıldız I, et al, Vitamin D levels in children with recurrent tonsillitis. Int J Pediatr Otorhinolaryngol 2011; 75:364-67.
13. Reid D, Morton R, Salkeld L, Bartley J. Vitamin D and tonsil disease--preliminary observations. Int J Pediatr Otorhinolaryngol 2011; 5:261-64.
14. Esteitie R, Naclerio RM, Baroody FM. Vitamin D levels in children undergoing adenotonsillectomies. Int J Pediatr Otorhinolaryngol 2010; 74:1075-77.
15. Paradise JL, Bluestone CD, Bachman RZ, et al. Efficacy of tonsillectomy for recurrent throat infection in severely affected children: results of parallel randomized and nonrandomized clinical trials. N Engl J Med 1984; 310:674-83.
16. Appropriateness and safety of tonsillectomy and/or adenoidectomy. Guildelines. http://www.snlgiss.it/cms/files/LG_en_tonsillectomy_2008.pdf.
17. Nseir W, Mograbi J, Abu-Rahmeh Z, Mahamid M, Abu-Elheja O, Shalata A. The association between vitamin D levels and recurrent group A streptococcal tonsillopharyngitis in adults. Int J Infect Dis 2012; 16:e735-e738.
18. Borella E, Nesher G, Israeli E, Shoenfeld Y. Vitamin D: a new anti-infective agent? Ann NY Acad Sci 2014.

LETTER TO THE EDITOR

TREATMENT WITH TERIPARATIDE MIGHT BE ASSOCIATED WITH CARDIOMETABOLIC CHANGES IN POSTMENOPAUSAL SEVERE OSTEOPOROTIC WOMEN

E. PASSERI[1], E. DOZIO[2], M. MENDOLA[1], E. COSTA[3], F. BANDERA[4], M.M. CORSI ROMANELLI[2,5] and S. CORBETTA[1,2]

[1]Endocrinology Unit, IRCCS Policlinico San Donato, San Donato M.se, Milan, Italy; [2]Department of Biomedical Sciences for Health, University of Milan, Milan, Italy; [3]Clinical Chemistry Laboratory, IRCCS Policlinico San Donato, San Donato M.se, Milan, Italy; [4]Heart Failure Unit, IRCCS Policlinico San Donato, San Donato M.se, Milan, Italy; [5]UOC SMEL-1 Clinical Pathology, IRCCS Policlinico San Donato, San Donato M.se, Milan, Italy

Received March 16, 2015 – Accepted September 22, 2015

Parathormone (PTH) has been suggested to affect the cardiovascular system. Teriparatide (TPT), the hormonally active 1-34 fragment of PTH, provides an anabolic treatment for osteoporosis. The aim of the present study was to evaluate the cardiometabolic effects of 18-month treatment with 20 μg/die teriparatide subcutaneosly. Fourteen women with postmenopausal severe osteoporosis treated with once-daily sc 20 μg TPT (aged 67.6±2.5 years; BMI 27.7±1.0 kg/m^2) and 24 age- and BMI-matched severe osteoporotic women treated with iv yearly 5 mg zoledronate (ZLN) were evaluated at baseline and at 12-18 months of treatment for anthropometric measures, calcium, glucose and lipid metabolic parameters, and assessment of cardiac geometry by conventional echocardiography. TPT was effective in increasing mean lumbar spine bone mineral density with no clinically relevant changes in calcium metabolism parameters. TPT patients experienced an increase of BMI (27.7±1.0 at baseline *vs* 29.0±1.0 kg/m^2 at last evaluation, P=0.005) and mean whole body fat percentage (37.0±2.1 *vs* 40.3±1.9%, P=0.05), associated with increased serum leptin levels (17.3±2.1 *vs* 22.9±3.0 ng/ml; P=0.049). Glucose and lipid parameters were not affected by TPT as well as by ZLN treatment. Furthermore, TPT was associated with a decrease in systolic blood pressure; a decrease in the fractional shortening (41.2±2.3 *vs* 36.9±1.2; P=0.05) and an increase in the relative wall thickness (0.39±0.01 *vs* 0.48±0.01 mm; P=0.002), suggestive for concentric cardiac remodeling, was detected by echocardiographic monitoring. These changes could not be detected in bone active drug-free age- and metabolic-matched controls. In conclusion, long-term TPT therapy might affect cardiometabolic and cardiac geometry parameters in severe osteoporotic women, though changes are not clinically relevant.

Osteoporosis is a highly prevalent chronic disease worldwide and the most serious consequences of this disorder are frailty fractures. Among the burden of medical drugs available for the prevention of the

Key words: postmenopausal osteoporosis, teriparatide, glucose, lipids, cardiac geometry, body weight

Mailing address: Sabrina Corbetta, MD, PhD
Endocrinology Unit,
Department of Biomedical Sciences for Health,
University of Milan, IRCCS Policlinico San Donato,
Piazza Malan 1, 20097 San Donato M.se (MI), Italy
Tel./Fax: +39 02 52774444
e-mail: sabrina.corbetta@unimi.it

0393-974X (2015)

osteoporotic fractures, the fully active, truncated amino-terminal fragment 1-34 of the PTH molecule, named teriparatide, is the unique osteoanabolic agent directly stimulating bone formation to improve bone mass and skeleton microarchitecture.

Evidence indicates that osteoporosis and atherosclerotic cardiovascular diseases have a similar physiopathological and genetic background (1). Recently, interest in the involvement of calcium metabolism key molecules in cardiovascular diseases has been increased, in particular in circulating PTH levels. Patients with primary hyperparathyroidism, whose plasma PTH levels are constantly elevated due to autonomous release from parathyroid tumors, showed significantly increased cardiovascular mortality (2). Besides pathological PTH hypersecretion from parathyroid tumors, circulating PTH levels from normal parathyroid glands have been shown to predict cardiovascular morbidity and mortality (3-5). Clinical studies reported that PTH is associated with hypertension (6), body mass index (BMI) (7), atherogenesis, left ventricular hypertrophy and congestive heart failure (8).

PTH might directly affect the cardiovascular system as PTH receptors are expressed by a variety of cells. In the cells classical target of PTH action, namely osteoblasts and kidney tubular epithelial cells, PTH receptors modulate the osteoanabolic response to PTH and stimulate the phosphate reabsorption, respectively. Functional PTH receptors have been detected also in adult cardiomyocytes, where their activation exerts hypertrophic as well as metabolic effects (8); a direct effect on rat ventricular myocytes has been reported also for teriparatide (9). Finally, PTH receptors are expressed on cell surface of human mesenchymal stem cells, and intermittent treatment with PTH as well as teriparatide inhibits adipocyte differentiation of human bone marrow stromal cells (10, 11); indeed, the effect of PTH on human subcutaneous and visceral adipocytes has never been investigated to date.

Furthermore, treatment with PTH1-84 has been demonstrated to increases the osteoblast-secreted protein osteocalcin, both total and undercarboxylated (12). The undercarboxylated form of osteocalcin has favorable effects on fat and glucose metabolism in mice (13). In human subjects, cross-sectional studies suggested a relevant association of the circulating undercarboxylated osteocalcin with changes in metabolic parameters, such as body weight, fat mass, and plasma glucose levels (14, 15).

Teriparatide is approved for the treatment of severe osteoporosis complicated with vertebral and/or femoral frailty fractures in Italy. It has been reported to be effective and safe for bone metabolism.

The present study aimed to evaluate the effects of long-term once-daily treatment with 20 μg teriparatide on cardiometabolic parameters and left ventricular geometry in women affected with severe post-menopausal osteoporosis.

MATERIALS AND METHODS

Study design and population

This pilot trial was designed as a prospective study with the primary end-point to test the safety of 18-month treatment with teriparatide on the cardiometabolic profile in severe post-menopausal osteoporotic women; the secondary end-point was to test the effect of 18-month treatment with teriparatide on cardiac geometry.

Fourteen Caucasian post-menopausal women (aged 69.1±2.2 years) affected with post-menopausal severe osteoporosis according to the 2011 Italian eligibility criteria for the reimbursement of the treatment with teriparatide (TPT) (≥3 severe vertebral or femoral fractures or severe vertebral/femoral fracture on bisphosphonate therapy) were consecutively enrolled between June 2011 and June 2012 (TPT group). Four patients had never been previously treated with anti-osteoporotic drugs and presented multiple (≥3) severe, according to Genant's classification (16), vertebral fractures, whereas 10 patients were non-responders to bisphosphonate treatment as they experienced vertebral fractures on bisphosphonate administration. All patients received oral calcium (mean 600 mg/die) and cholecalcipherol (mean 1000 UI/die) supplementation. Metabolic and cardiac evaluations were performed at baseline and 6, 12 and 18 months from starting sc 20 μg/die TPT. Bone mineral density (BMD) at lumbar spine and femoral levels was measured by dual-energy X-ray absorptiometry (DEXA) at baseline and after 18 months of treatment.

Control groups were built as follows: group 1) zoledronate (ZLN)-treated post-menopausal women matched for age and body mass index (BMI) (n=24) to compare the effect of TPT on weight, BMI and blood pressure, evaluated at baseline, after 12 and 18 months of treatment (Table I); group 2) anti-osteoporotic drug-free (DF) age-, BMI-, glucose and lipid profiles-matched women referred for endocrine screening and diagnosed

Table I. *Baseline clinical characteristics of severe osteoporotic patients treated with iv 5 mg/year zoledronate (ZLN group) vs sc 20 μg/die teriparatide (TPT group).*

	ZLN group	TPT group	*P*
n	24	14	-
Age, years	69.4±1.1	67.6±2.5	0.30
BMI, kg/m^2	28.0±1.5	27.7±1.0	0.62
Waist circumference, cm	90.8±4.1	91.8±3.7	0.65
Serum calcium, mg/dl	9.3±0.1	9.5±0.1	0.26
Serum PTH, pg/ml	59.1±6.7	50.7±5.6	0.50
Serum ALP, U/l	96.3±9.7	82.8±11.4	0.16
Serum 25OHD, ng/ml	27.3±4.5	34.1±5.1	0.42
Osteoporotic fractures, %	75	100	0.19
L1-L4 BMD, g/cm^2	0.731±0.03	0.769±0.02	0.37
Femoral neck BMD, g/cm^2	0.555±0.02	0.606±0.04	0.34
Total femoral BMD, g/cm^2	0.669±0.02	0.740±0.02	**0.04**

PTH: parathormome; ALP: alkaline phosphatase; 25OHD: 25hydroxyvitamin D3; BMD: bone mineral density.

otherwise healthy (n=11) to exclude the effect of time and blood pressure on cardiac geometry parameters (Table II), evaluated at baseline and at 18-month follow up.

Exclusion criteria for the enrolment of both patients and controls were: liver or heart failure (NYHA class II, III or IV), chronic kidney disease, overt diabetes mellitus, corticosteroid therapy and endogenous hypercortisolism, malignances, poorly controlled hypertension, hypercalcemia and primary hyperparathyroidism, connective autoimmune diseases, anti-estrogenic drugs and any drugs potentially interfering with bone metabolism, including diuretics, active smoke and alcohol consumption.

Written informed consent was obtained from all the participants and the local ethics committee approved the study protocol. The study complied with the Declaration of Helsinki II.

Clinical, biochemical and hormonal assessment

Medical history focusing on co-existing cardiac diseases and risk factors was collected from all participants. Anthropometric measurements, including height, weight, waist and hip circumferences, were obtained at baseline and after 12 and 18 months of treatment. Weight was measured on a standard balance beam scale; height was measured using a calibrated, wall-mounted Harpenden stadiometer. Body mass index (BMI) was calculated. Whole body composition, including body fat mass, was estimated by body bioelectrical impedance analysis (Bodygram Pro 3.0, AKERN, Florence, Italy).

Bone metabolism was investigated in TPT patients and ZLN controls as follows: overnight fasting venous blood samples were collected for determination of serum calcium, phosphate, creatinine and alkaline phosphatase according to routinely used laboratory kits. Serum PTH levels were determined by ElectroChemiLuminescence on an Elecsys 2010 (Roche Diagnostics, Mannheim, Germany). Serum 25OHvitamin D (25OHD) was measured by a chemiluminescent assay (LIAISON® test, DiaSorin Inc., Stillwater, MN, USA). Twenty-four-hour urine calcium and phosphate excretions were also measured.

Metabolic profile was investigated in TPT patients and ZLN/DF controls as follows: overnight fasting

Table II. *Metabolic and cardiac parameters at baseline and at 18-month follow-up in severe osteoporotic patients treated with iv 5 mg/year zoledronate or sc 20 µg/die teriparatide and drug-free controls.*

	ZLN Group (n=24)			TPT Group (n=14)			DF Controls (n=11)		
	Basal	*18 months*	*P*	*Basal*	*18 months*	*P*	*Basal*	*18 months*	*P*
Age, years	69.4±1.1	-	-	67.6±2.5	-	-	69.1±2.2	-	-
MBI, kg/m^2	28.0±1.5	26.5±1.1	0.11	27.7±1.0	29.6±1.0	**0.005**	30.3±0.9	31.3±1.5	0.45
Fat mass, %				37.7±2.1	40.3±1.9	**0.05**	40.4±1.8	38.3±2.5	0.10
Waist circ., cm				91.8±3.4	91.1±3.1	0.71	97.3±3.2	101.2±3.0	0.36
Metabolic parameters									
T-chol, mg/dl	196.8±11.1	219.7±9.0	0.20	211.3±13.7	217.5±14.9	0.81	196.3±18.1	213.2±7.9	0.31
HDL-chol, mg/dl	57.4±3.7	61.2±5.6	0.78	63.2±2.6	63.2±6.7	0.94	64.1±9.4	59.0±4.4	0.47
LDL-chol, mg/dl	125.7±13.2	139.6±12.3	0.82	124.3±12.6	128.6±11.7	0.65	106.1±16.0	123.3±6.9	0.34
Triglycerides, mg/dl	114.3±16.4	134.6±19.5	0.33	119.5±14.8	128.8±18.3	0.22	129.7±18.4	138.8±16.0	0.35
Glucose, mg/dl	102.8±9.1	109.0±8.7	0.25	91.2±2.7	91.6±2.8	0.31	101.6±5.3	103.8±8.4	0.66
HOMA-IR	2.8±0.5	3.2±0.8	0.44	1.9±0.1	1.5±0.4	0.27	3.2±0.8	3.0±0.5	0.80
Cardiac geometry parameters									
Hypertension, %	66	66	1.00	50	50	1.00	64	64	1.00
Grade I DD, %				43	64	0.24	45	45	1.00
Cardiac hypertrophy, %				21	28	0.85	36	27	0.75
CR, %				14	71	**0.01**	36	45	0.56
LVIDd, mm				4.6±0.1	4.7±0.1	0.51	5.1±0.1	4.9±0.1	0.16
LVIDs, mm				2.7±0.1	3.2±0.1	**0.05**	3.2±0.1	3.2±0.1	0.97
FS, %				41.2±2.3	36.9±1.2	**0.05**	36.5±2.9	35.5±2.6	0.36
RWT, mm				0.39±0.01	0.48±0.01	**0.002**	0.40±0.2	0.42±0.02	0.38
LVMI index, g/m^2				97.9±7.2	110.8±8.0	0.27	125.6±6.5	110.7±4.8	0.18
LVEF, %				62.5±1.6	62.4±1.2	1.00	61.5±2.6	58.9±1.6	**0.03**
IVSd, mm				1.09±0.1	1.35±0.2	0.55	1.10±0.1	1.02±0.1	0.11
IVSs, mm				1.45±0.1	1.45±0.1	1.00	1.50±0.1	1.48±0.1	0.46
PWTd, mm				0.87±0.07	1.14±0.04	**0.05**	1.10±0.03	1.04±0.05	0.45
PWTs, mm				1.54±0.04	1.50±0.06	0.34	1.50±0.1	1.54±0.09	0.61
LAD, mm				3.5±0.2	3.8±0.1	0.95	3.9±0.1	3.9±0.1	0.98

ZLN: zoledronate treated; TPT: teriparatide treated; DF: drug free; Waist circ.: waist circumference; T-chol: total cholesterol; HDL-chol: HDL cholesterol; LDL-chol: LDL cholesterol; HOMA-IR: homeostasis assessment model insulin resistance; DD: dyastolic dysfunction; CR: concentric remodeling (RWT: relative wall thickness >0.45); LVIDd: left ventricular internal diameter in diastole; LVIDs: left ventricular internal diameter in systole; FS: fractional shortening; RWT: relative wall thickness; LVMI index: left ventricular mass index; LVEF: left ventricular ejection fraction; IVSd: diastolic interventricular septal thickness; IVSs: systolic interventricular septal thickness; PWTd: diastolic posterior wall thickness; PWTS: systolic posterior wall thickness; LAD: left atrial diameter.

serum total cholesterol, HDL cholesterol, triglycerides, glucose and insulin were measured by routinely used laboratory kits. LDL-cholesterol was calculated with the Freidewald *formula*. The insulin resistance index HOMA (Homeostasis Model Assessment) was calculated (17). Plasma samples from TPT patients were snap-frozen for the determination of leptin and adiponectin according to the manufacturer's instructions (Human Leptin ELISA kit R&D Systems®, CV% intra-assay: 3.3 ng/ml, inter-assay 5.4 ng/ml; Human total adiponectin Quantikine ELISA Kit R&D Systems®, CV% intra-assay: 4.7 µg/ml, inter-assay 6.9 µg/ml).

Echocardiographic assessment

Transthoracic Doppler echocardiography was performed for all TPT patients and DF controls at baseline and at the end of 18 months of treatment with daily teriparatide (TPT group) or at the end of 18 months of follow-up (DF group) with a GE Vivid 7, using conventional transducer of 1.5-4.0 MHz; all images were analyzed by a single investigator blinded to all clinical data. Measurements were taken by standard two-dimensional protocols according to European guidelines (18). Left ventricular diameter at end-diastole (LVDd) and at end-systole (LVDs), fractional shortening (FS), end-diastolic LV volume (LVEDV), end-systolic LV volume (LVESV) and ejection fraction (EF) were measured. As index of hypertrophy, left ventricular mass (LVM) was calculated according to the ASE (American Society of Echocardiography) recommendation and LVM

index (LVMI) was calculated as LVM divided by body surface area (m^2). The relative wall thickness (RWT) was calculated as 2x posterior wall thickness/LVDd.

Statistical analysis

Data are expressed as mean±standard error of mean (SE). Categorical data are presented as percentages and compared by Fisher's exact test. Normal distribution of continuous variables was tested. Comparisons of continuous variables between patients and controls groups were performed by Student's *t*-test or Mann-Whitney U-test, as appropriate. Comparison at different timing of TPT treatment in osteoporotic patients was performed using One-way ANOVA for repeated measurements versus basal conditions corrected for multiple comparisons by the Dunnett test. Bivariate associations between the biochemical parameters were tested by Pearson product moment correlation. Correlations with BMI values, which failed to pass normality tests, were analysed using Spearman correlation test. A P value ≥0.05 was considered significant. Statistical analysis was performed using PRISM 6.1.

RESULTS

Effects of 18 months teriparatide (TPT) treatment on calcium metabolism

The administration of TPT was associated with a mild not significant increase in serum calcium levels within the normal range (mean +0.3 mg/dl at 18 months) (Fig. 1), while no symptoms or signs of hypercalcemia, namely dehydration, polyuria and kidney stones, were recorded. Similarly, 24-hour mean renal calcium excretion showed an increase not reaching statistical significance (mean increase 50 mg/24 hours at 18 months). Serum phosphate (3.9±0.1 *vs* 3.2±0.2 mg/dl) and urine phosphate excretion levels (0.64±0.12 *vs* 1.34±0.78 g/24h) showed a trend to decrease and increase, respectively, at 18 months of treatment, though these differences were not statistically significant. As expected, serum PTH levels progressively decreased (50.7±5.6 *vs* 30.4±6.4 pg/ml, *P*=0.01; baseline *vs* 18 months of TPT) and alkaline phosphatase levels, a marker of bone turnover, increased (82.8±11.4 *vs* 114.3±16 pg/ml, *P*=0.01; baseline *vs* 18 months of TPT) (Fig. 1). Vitamin D status was optimal (>30 ng/ml) in all patients at the beginning of treatment and monitoring of cholecalcipherol replacement therapy confirmed serum 25OHD levels persistently above 30 ng/ml throughout the 18 months of treatment.

Effects of 18-month TPT treatment on bone mineral density

Mean bone mineral density (BMD) at lumbar spine (L1-L4) significantly increased at 18 months of TPT treatment (0.769±0.02 *vs* 0.815±0.02 g/cm^2, P=0.04). Moreover, mean femoral neck BMD showed a mild trend of increase (0.606±0.04 *vs* 0.622±0.03). No frailty fractures at any site were reported and no patient experienced a decrease in body height greater than 2 cm.

Effects of 18-month TPT treatment on body composition

Compared to the zoledronate (ZLN)-treated control group (28.5±1.9 at 12 months, 26.5±1.1 at 18 months *vs* 28.0±1.5 kg/m^2 at baseline, P>0.05), TPT treated patients showed a progressive increase of BMI (28.0±1.0 at 12 months, 29.6±1.0 kg/m^2 at 18 months, *vs* 27.7±1.0 at baseline, P=0.005), with a mean weight gain of 1.6 Kg. Mean waist circumferences were unaffected by TPT treatment, while mean body fat mass percentage increased (37.7±2.1% at baseline *vs* 40.3±1.9% at 18 months; P=0.05). Serum adiponectin and leptin levels were evaluated: as expected, basal serum adiponectin levels negatively correlated with body weight (r=-0.46, P=0.04) and basal serum leptin levels positively correlated with BMI (r=0.41, P=0.05) and with body fat mass (r^2=0.38, P=0.02). Eighteen-month TPT treatment did not exert any significant effect on serum adiponectin levels (13.8±1.2 *vs* 16.6±2.6 mg/ml), while serum leptin levels significantly increased in most TPT-treated patients from mean serum leptin levels 17.3±2.1 ng/ml at baseline to 22.9±3.0 ng/ml after 18 months (P=0.049). Although no significant correlation between leptin levels and BMI or body fat mass could be detected after 18 months of TPT treatment, body weight gain and consensus leptin level increases were observed in 10 out of 14 patients (71%).

Effects of 18-month TPT treatment on glucose and lipid metabolic parameters

We further evaluated the effect of TPT on metabolic parameters: serum glucose and insulin levels, as well as the calculated insulin-resistance index HOMA-IR were unaffected by TPT treatment (Table II). Similarly,

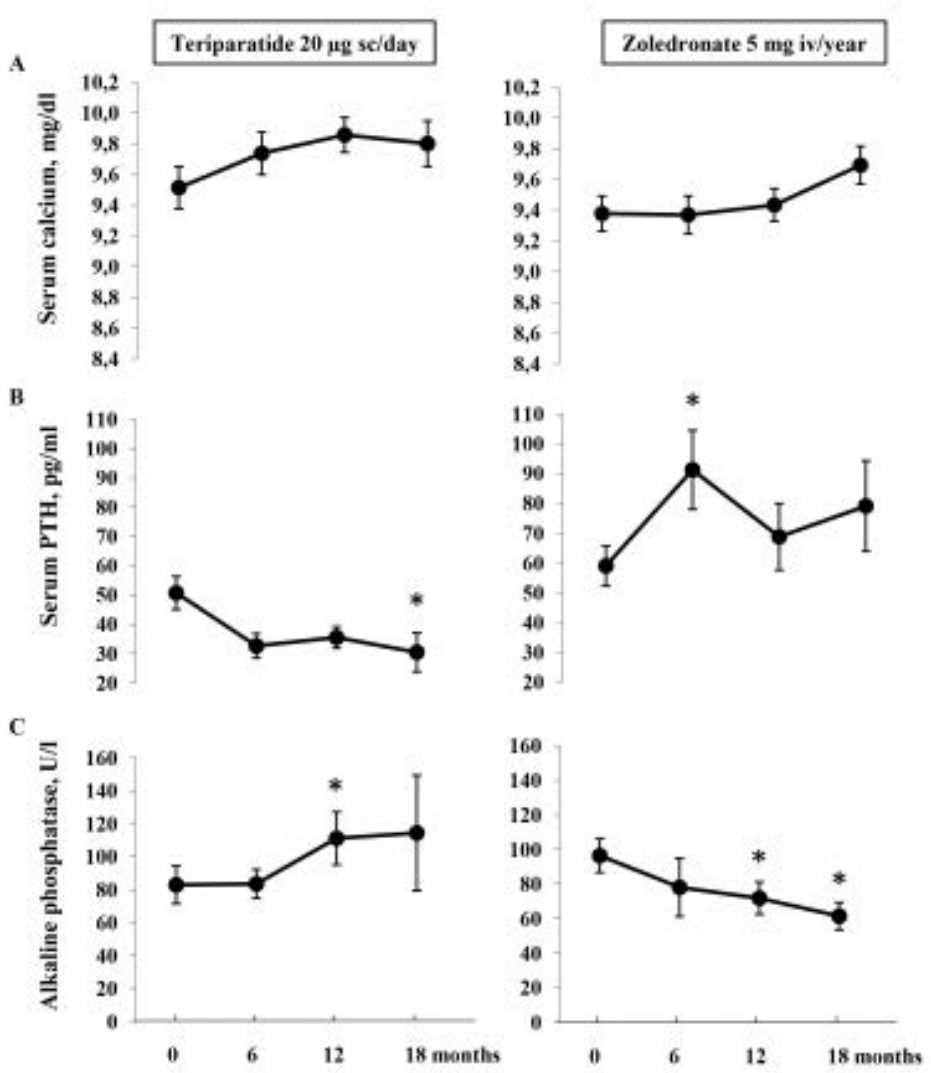

Fig. 1. *Changes in serum calcium (**A**), serum PTH (**B**) and serum total alkaline phosphatase levels (**C**) in patients treated with 20 µg/die sc teriparatide (left diagrams) and with 5 mg/year iv zoledronate (right diagrams). * P<0.05.*

the lipid profile, namely serum total cholesterol, LDL cholesterol, HDL cholesterol and triglycerides, did not show significant variations (Table II).

Effects of 18-month TPT treatment on blood pressure levels

At baseline, 50% of TPT patients, 66% of ZLN controls and 64% of drug-free (DF) healthy controls had arterial blood hypertension well controlled with anti-hypertensive drugs. Ambulatory blood pressure monitoring identified a significant reduction of systolic pressure levels at 18 months of TPT treatment (140.7±6.0 *vs* 128.2±4.0 mmHg, P=0.04), while in ZLN and DF control groups blood pressure was unaffected (130.5±2.3 *vs* 128.7±3.9 mmHg, and 131.4±4.5 *vs* 128.8±4.1 mmHg, respectively).

Effects of 18-month TPT treatment on cardiac geometry parameters

Echocardiographic examination in TPT patients

and DF-matched controls excluded cardiac valvular or septal defects and showed that at baseline, 43% of TPT patients and 45% of DF controls showed grade 1 diastolic dysfunction (E/A<1), while cardiac hypertrophy occurred in 21% of TPT patients and 36% of DF controls. None showed echocardiographic signs of previous ischemic damage. All TPT patients had an ejection fraction > 55% at baseline, while two patients showed LVMI>95 g/m^2 and three patients had an RWT>0.45 suggesting the presence of LV hypertrophy (Table II).

Cardiac performance parameters were evaluated: ejection fraction did not change after TPT treatment (Table II), though fractional shortening (FS) significantly diminished at 18 months of treatment (41.2±2.3 *vs* 36.9±1.2%; P=0.05). As far as parameters of cardiac geometry were concerned, atrial diameters were not affected by TPT treatment, while posterior wall thickness (PWTd) and relative wall thickness (RWT) significantly increased after 18 months of TPT treatment (0.87±0.07 *vs* 1.14±0.04 mm, P=0.05; 0.39±0.01 *vs* 0.48±0.01 mm, P=0.002), and LVMI showed a trend to increase though not statistically significant (Table II). To exclude the effects of age progression and hypertension on cardiac parameters, results were compared with those recorded in DF controls matched for age, prevalence of hypertension, glucose and lipid profiles and fat mass. FS and RWT did not vary in DF control subjects at 18 months of follow-up (Table II), although the left ventricular ejection fraction (LVEF) significantly decreased.

DISCUSSION

To our knowledge this is the first study investigating *in vivo* the cardiometabolic effects of long-term once-daily PTH1-34/TPT treatment in severe osteoporotic post-menopausal women. In the present study the treatment with TPT for 18 months was confirmed to be effective in increasing lumbar BMD and clinically ineffective on parameters of calcium metabolism. Besides these expected effects, TPT treatment was associated with a mild increase of BMI, whole body fat mass and circulating leptin levels, a reduction of systolic arterial blood pressure and modified US parameters of left ventricular geometry towards a concentric remodeling.

Postmenopausal severe osteoporotic patients treated with TPT experienced a mild weight gain at 12 and 18 months of treatment that could not be detected in post-menopausal osteoporotic women treated with zoledronate. This specific effect of TPT was associated with increased whole body fat mass and increased circulating leptin levels. Leptin is primarily secreted from adipocytes, and the levels of circulating leptin are positively correlated with percentage of body fat. Therefore, the TPT induced increases in circulating leptin levels suggest an impairment of the subcutaneous or visceral adipocytes. The increase in weight and body fat mass might have a positive clinical mean as cross-sectional studies in the general adult population showed that body fat is positively associated with bone mineral density. Adiposity has a known osteoprotective effect on bone: the gain in BMD at the lumbar spine from an incremental rise of BMI in postmenopausal women was 1.5-fold higher than in pre-menopausal women and the inhibition of osteoclastic bone resorption is responsible at least in part for the positive effect of high BMI on BMD (19).

The weight and whole body fat mass gain were not associated with impairment of glucose as well as with lipid parameters. Therefore, TPT might influence the subcutaneous adipose tissues, which are known as the main source of leptin (20), rather than the metabolically active visceral fat. The lack of TPT effect on visceral fat, estimated by waist circumference in the present study, supports this hypothesis. Absence of TPT effects on glucose homeostasis and insulin sensitivity was in agreement with previously published data (21, 22), although *in vitro* data reported that PTH decreases insulin-induced glucose transport, thus promoting insulin resistance (23).

In the present study, postmenopausal women with severe osteoporosis often experienced cardiovascular comorbidities such as arterial blood hypertension, grade 1 diastolic dysfunction and left ventricular hypertrophy. Monitoring of the cardiovascular parameters during treatment with TPT showed the occurrence of a significant reduction in the mean systolic arterial blood pressure, a finding not detected in the follow-up of women treated with zoledronate, which might be explained by the known vasodilatatory effect of PTH (24, 25). The

reduction of systolic blood pressure did not require an adjustment of the anti-hypertensive drugs, and no lipothymia was reported. Moreover, the sequential evaluation of cardiac parameters by conventional echocardiography identified changes in parameters of cardiac performance, namely FS, and cardiac geometry, namely PWTd and RWT. TPT treatment was associated with a decrease of FS, an estimate of myocardial contractility, and with increases of RWT and LVMI. This cardiac pattern is suggestive of concentric remodeling (26) and is in agreement with *in vitro* data demonstrating a direct hypertrophic effect of PTH on cardiomyocytes (8). It is worth noting that increasing body fat has been reported to be significantly related to an increase in posterior wall thickness, relative wall thickness, LV mass, and decreased fractional shortening also in asymptomatic females (27), changes similar to those detected after long-term TPT treatment in postmenopausal severe osteoporotic women. Indeed, these changes in cardiac geometry did not correspond to clinically relevant events.

Subcutaneous TPT administration raises the circulating TPT concentrations for about 4 hours (28) and is able to induce the anabolic effect of PTH. Data obtained from the present study are closer to those from *in vitro* and *in vivo* studies with acute PTH administration than to data obtained from clinical studies on patients with hyperparathyroidism or in the general population, where likely PTH secretion is variably impaired.

This observational, prospective, controlled study is limited by the small size of the investigated series. Admittedly, enrolled patients and controls showed a high prevalence of cardiovascular comorbidities, limiting the extension of the results to the general population treated with TPT. Finally, cardiac geometry should be evaluated more appropriately by magnetic resonance, the sensitivity of which is greater than conventional ecocardiography in detecting wall thickness changes.

In conclusion, TPT was confirmed to be an effective anti-osteoporotic treatment with no adverse effects on calcium, glucose, or lipid metabolisms although there was a small increase in body weight and fat mass. TPT might also affect systolic blood pressure and cardiac concentric hypertrophy correlated parameters in severe osteoporotic patients with known cardiac comorbidities.

ACKNOWLEDGEMENTS

This work was supported by the IRCCS Policlinico San Donato Ricerca Corrente Fund.

REFERENCES

1. Baldini V, Mastropasqua M, Francucci CM, D'Erasmo E. Cardiovascular disease and osteoporosis. J Endocrinol Invest 2005; 28:69-72.
2. Yu N, Donnan PT, Leese GP. A record linkage study of outcomes in patients with mild primary hyperparathyroidism: the Parathyroid epidemiology and Audit Research Study (PEARS). Clin Endocrinol 2011; 75:169-76.
3. Hagström E, Ingelsson E, Sundström J, et al. Plasma parathyroid hormone and risk of congestive heart failure in the community. Eur J Heart Fail 2010; 12:1186-92.
4. Wannamethee SG, Welsh P, Papacosta O, Lennon L, Whincup PH, Sattar N. Elevated parathyroid hormone, but not vitamin D deficiency, is associated with increate risk of heart failure in older men with and without cadiovascular disease. Circ Heart Fail 2014; 7:732-39.
5. Hagström E, Ahlström T, Ärnlöv J, Larsson A, Melhus H, Hellman P, Lind L. Parathyroid hormone and calcium are independently associated with subclinical vascular disease in a community-based color. Atherosclerosis 2015; 238:420-26.
6. Jorde R, Svartberg J, Sundsfjord J. Serum parathyroid hormone as a predictor of increase in sistolic blood pressure in men. J Hypertens 2005; 23:1639-44.
7. Kamycheva E, Sundsfjord J, Jorde R. Serum parathyroid hormone level is associated with body mass index. The 5th Tromso study. Eur J Endocrinol 2004; 151:167-72.
8. Andersson P, Rydberg E, Willenheimer R. Primary hyperparathyroidism and heart disease – a review. Eur Heart J 2004; 25:1776-87.
9. Liu X, Xie R, Liu S. Rat parathyroid hormone 1-34 signals through the MEK/ERK pathway to induce cardiac hypertrophy. J Int Med Res 2008; 36:942-50.
10. Rickard DJ, Wang FL, Rodriguez-Rojas AM, Wu Z,

Trice WJ, Hoffman SJ, Votta B, Stroup GB, Kumar S. Intermittent treatment with parathyroid hormone (PTH) as well as a non-peptide small molecule agonist of the PTH1 receptor inhibits adipocyte differentiation in human bone marrow stromal cells. Bone 2006; 39:1361-72.

11. Cohen A, Stein EM, Recker RR, et al. Teriparatide for idiopathic osteoporosis in premenopausal women: a pilot study. J Clin Endocrinol Metab 2013; 98:1971-81.
12. D'Amelio P, Sassi F, Buondonno I, et al. Effect of intermittent PTH treatment on plasma glucose in osteoporosis: a randomized trial. Bone 2014; 76:177-84.
13. Lee NK, Sowa H, Hinoi E, et al. Endocrine regulation of energy metabolism by the skeleton. Cell 2007; 130:456-69.
14. Kanazawa I, Yamaguchi T, Yamauchi M, Yamamoto M, Kurioka S, Yaho S, Sugimoto T. Serum undercarboxylated osteocalcin was inversely associated with plasma glucose level and fat mass in type 2 diabetes mellitus. Osteoporosis Int 2011; 22:187-94.
15. Schafer AL, Sellmeyer DE, Schwartz AV, et al. Change in undercaboxylated osteocalcin is associated with changes in body weight, fat mass, and adiponectin: parathyroid ormone (1-84) or alendronate therapy in postmenopausal women with osteoporosis (the PaTH study). J Clin Endocrinol Metab 2011; 96:E1982-89.
16. Genant HK, Wu CY, Van Kuijk C, Nevitt MC. Vertebral fracture assessment using a semiquantitative technique. J Bone Miner Res 1993; 8:1137-48.
17. Matthews DR, Hosker JP, Rudenski AS, Naylor BA, Treaher DF, Turner RC. Homeostasis model assessment: insulin resistance and beta-cell function from fasting plasma glucose and insulin concentrations in man. Diabetologia 1985; 28:412-19.
18. Lang RM, Bierig M, Devereux RB, Flachskampf FA, Foster E, Pellikka PA, Picard MH, Roman MJ, Seward J, Shanewie J, Solomon S, Spencer KT, St John Sutton M, Stewart W; American Society of Echocardiography's Nomenclature and Standards Committee; Task Force on Chamber Quantification; American College of Cardiology Echocardiography Committee; American Heart Association; European Association of Echocardiography, European Society of Cardiology. Recommendations for chamber quantification. Eur J Echocardiogr 2006; 7:79-108.
19. Puntus T, Schneider B, Meran J, Peterlik M, Kudlacek S. Influence of age and gender on associations of body mass index with bone mineral density, bone turnover markers and circulating calcium-regulating and bone-active sex hormones. Bone 2011; 49:824-29.
20. Wronska A, Kmiec Z. Structural and biochemical characteristics of various white adipose tissue depots. Acta Physiol 2012; 205:194-208.
21. Anastasilakis AD, Goulis DG, Koukoulis G, Kita M, Slavakis A, Avramidis A. Acute and chronic effect of teriparatide on glucose metabolism in women with established osteoporosis. Exp Clin Endocrinol Diabetes 2007; 115:108-11.
22. Anastasilakis AD, Efstathiadou Z, Plevraki E, Koukoulis GN, Slavakis A, Kita M, Avramidis A. Effect of exogenous intermittent recombinant human PTH 1-34 administration and chronic endogenous parathyroid hormone excess on glucose homeostasis and insulin sensitivity. Horm Metab Res 2008; 40:702-707.
23. Chang E, Donkin SS, Teegarden D. Parathyroid hormone suppresses insulin signaling in adipocytes. Mol Cell Endocrinol 2009; 307:77-82.
24. Saglikes Y, Massry SG, Iseki K, Nadler JL, Campese VM. Effect of PTH on blood pressure and response to vasoconstrictor agonists. Am J Physiol 1985; 248:F674-81.
25. Jespersen B, Randløv A, Abrahamsen J, Fogh-Andersen N, Olsen NV, Kanstrup IL. Effects of PTH(1-34) on blood pressure, renal function, and hormones in essential hypertension: the altered pattern of reactivity may counteract raised blood pressure. Am J Hypertens 1997; 10:1356-67.
26. Katz DH, Beussink L, Sauer AJ, Freed BH, Burke MA, Shah SJ. Prevalence, clinical characteristics, and outcome associated with eccentric versus concentric left ventricular hypertrophy in heart failure with preserved ejection fraction. Am J Cardiol 2013; 112:1158-64.
27. Lai YH, Liu CC, Kuo JY, Hung TC, Wu YJ, Yeh HI, Bulwer BE, Hung CL. Independent effects of body fat and inflammatory markers on ventricular geometry, midwall function, and atrial remodeling. Clin Cardiol 2014; 37:172-77.

28. Lindsay R, Nieves J, Henneman E, Shen V, Cosman F. Subcutaneous administration of the amino-terminal fragment of human parathyroid hormone-(1-34): kinetics and biochemical response in estrogenized osteoporotic patients. J Clin Endocrinol Metab 1993; 77:1535-39.

LETTER TO THE EDITOR

NOSE-BRONCHI LINK: DOES AN ASTHMA MARCH EXIST?

S. BARBERI[1], L. BERNARDO[1], M. BELLASIO[1], F. FERRARA[1], S. TOSI[1] and G. CIPRANDI[2]

[1]Department of Pediatrics, Fatebenefratelli Hospital, Milan, Italy; [2]Department of Medicine, IRCCS-AOU San Martino, Genoa, Italy

Received May 13, 2015 – Accepted September 24, 2015

Allergic rhinitis is considered a strong risk factor for the onset of asthma. However, few studies have addressed this issue from a functional point of view. In this work the close link between upper and lower airways is highlighted, suggesting that spirometry should be precociously performed on patients with allergic rhinitis.

Allergic rhinitis is characterized by an IgE-mediated inflammatory response of the nose to allergen exposure (1). Several trials have demonstrated a close link between allergic rhinitis and asthma (2-5). Allergic rhinitis may also be considered a relevant risk factor for the onset of asthma (6).

Asthma is characterized by a reversible airflow obstruction, bronchial inflammation, and hyperreactivity. Asthma diagnosis is based on clinical and functional evaluation. Spirometry is mandatory in asthmatic patients and GINA guidelines propose the forced expiratory volume/1 second (FEV_1) as gold standard lung function measurement to evaluate bronchial obstruction (www.ginasthma.com). Spirometric parameters have been recently well standardized and their interpretation is commonly recognized (7, 8). In addition, reversibility of airflow obstruction is considered the main pathophysiological characteristic of asthma and is pathognomonic for asthma. This reversibility may be spontaneous or induced by drugs, such as bronchodilators. The bronchodilation test is usually prescribed to demonstrate the reversibility of bronchial obstruction and so it allows a sure asthma diagnosis.

Pathophysiological considerations

Several studies, some from more than 30 years ago, have demonstrated that asthmatic patients, mainly children, often may have normal FEV_1 values when clinically stable. In this regard, in a comparison study of asthma severity based on symptom frequency with FEV_1, it was found that the mean FEV_1 was 95.1% of predicted values in children with mild persistent asthma, 90.2% in those with moderate persistent asthma, and 83.8% in those with severe persistent asthma (9). Moreover, small airways are deeply involved in the pathogenesis of asthma. Even though there is no direct marker for obstruction/inflammation of small airways, it has been proposed that the forced expiratory flow at 25% and 75% of the pulmonary volume (FEF_{25-75}) might be a more sensitive parameter to determine a small airway obstruction rather than FEV_1 (10). It has been demonstrated that the value of FEF_{25-75} is useful in predicting airway responsiveness, as it may also be a more sensitive indicator of chronic airflow obstruction than FEV_1, as well as a risk

Key words: allergic rhinitis, FEF_{25-75}, BHR, sensitisations

Mailing address:
Giorgio Ciprandi, M.D.
Largo R. Benzi 10,
16132 Genoa, Italy
Tel.: +39 10 35331820
Fax: +39 10 3538664
e-mail: gio.cip@libero.it

0393-974X (2015)

DISCLOSURE: ALL AUTHORS REPORT NO CONFLICTS OF INTEREST RELEVANT TO THIS ARTICLE.

factor for the persistence of respiratory symptoms in children suffering from allergic asthma. Also, it has to be considered that subjects with mild asthma and normal FEV_1 may show impaired FEF_{25-75} only (11).

Evidence

In this regard, it has been demonstrated that both $FEV_{1,}$ and mainly FEF_{25-75} may be impaired in patients suffering from allergic rhinitis and perceiving nasal symptoms alone (12). Allergic rhinitis may therefore be considered as the first step of a possible progression towards asthma. Indeed, in the revised version of the WHO document on "the impact of allergic rhinitis on asthma" (ARIA), the role is clearly underlined of allergic rhinitis as a risk factor for asthma development and/or worsening (13). Moreover, the last American guidelines on rhinitis reported that a reduced FEF_{25-75} (i.e. <65% of predicted) may be a marker of early bronchial pathology in patients with allergic rhinitis (14). In addition, a new concept has been recently demonstrated: the duration of allergic rhinitis is *per se* a risk factor for inducing spirometric impairment (15), bronchial hyperreactivity (BHR) (16), and positive response to a bronchodilation test (17). On the other hand, it has been recently reported that an initial airflow obstruction may be also documented in patients with recent onset of allergic rhinitis (18).

However, the possible definition of a progression from allergic rhinitis to asthma has not been deeply investigated. In this regard, allergic rhinitis and asthma could be frequently associated and allergic rhinitis may precede asthma onset which, indeed, has been considered as a a risk factor (19). It has been previously demonstrated that patients with allergic rhinitis alone may frequently show impaired, such as <65% of predicted, FEF_{25-75} values (20). The duration of allergic rhinitis may be considered a relevant risk factor for a bronchial involvement; in fact, it has been reported that the duration of allergic rhinitis is associated with impaired spirometry (15), BHR (16), and positive response to bronchodilation test (17). To date, there are very few studies that have evaluated the progression from rhinitis to asthma (22-24). In this regard, it will be interesting to know whether a nose-bronchi link exists in the elderly, as well as whether there are any differences that can be related to the gender of the subjects.

On the other hand, it has to be noted that allergen immunotherapy may prevent asthma onset in AR patients as demonstrated by the PAT study (25)

Therefore, from a clinical point of view it is relevant to evaluate the type of sensitisation and the duration of nasal symptoms in each patient with moderate-severe persistent allergic rhinitis. In addition, the concept has to be considered that allergic rhinitis frequently precedes the onset of asthma: therefore, we could interpret this phenomenon as an "asthmatic march", such as a progression from nose to bronchi of the allergic inflammation.

Conclusion

FEF_{25-75} may be regarded as a marker of early bronchial involvement in patients suffering from recent allergic rhinitis. Therefore, it is recommended to precociously perform spirometry in patients presenting with allergic rhinitis to individuate those predisposed to evolve into asthma.

REFERENCES

1. Van Cauwenberger P, De Belder T, Vermeiren J, Kaplan A Global resources in allergy (GLORIA): allergic rhinitis and conjunctivitis. Clin Exp All Rev 2003; 3:46-50.
2. Bugiani M, Carosso A, Migliore E, Piccioni P, Corsico A, Olivieri M, et al. Allergic rhinitis and asthma comorbidity in a survey of young adults in Italy. Allergy 2005; 60:165-70.
3. Asher I. ISAAC International Study of Asthma and Allergies in Childhood. Pediatr Pulmonol 2007; 42:100.
4. Braunstahl GJ, Kleinjan A, Overbeek SE, Prins JB, Hoogsteden HC, Fokkens WJ. Segmental bronchial provocation induces nasal inflammation in allergic rhinitis patients. Am J Respir Crit Care Med 2000; 161:2051-7.
5. Braunstahl GJ, Overbeek SE, Fokkens WJ, et al. Segmental bronchoprovocation in allergic rhinitis patients affects mast cell and basophil numbers in nasal and bronchial mucosa. Am J Respir Crit Care Med 2001; 164:858-65.
6. Plaschke PP, Janson C, Norrman E et al. Onset and remission of allergic rhinitis and asthma and the relationship with atopic sensitization and smoking.

Am J Respir Crit Care 2000; 162:920-4.
7. Pellegrino R, Viegi G, Brusasco V, et al. Interpretative strategies for lung function tests. Eur Respir J 2005; 26:948-68.
8. Miller MR, Hankinson J, Brusasco V, Burgos R, Casaburi R, Coates R, et al. Standardisation of spirometry. Eur Respir J 2005; 26:319-38.
9. Bacharier LB, Mauger DT, Lemanske RF, Schend V, Sorkness C, Strunk RC. Classifying asthma severity in children: is measuring lung function helpful? J Allergy Clin Immunol 2002; 109:S266
10. Bjermer L Past and future perspectives in the asthma treatment. Resp Med 2001;95:703-19
11. Lipworth BJ, Clark DJ Effects of airway calibre on lung delivery of nebulised salbutamol. Thorax 1997; 52:1016-21.
12. Ciprandi G, Cirillo I, Vizzaccaro A, Tosca MA, Passalacqua G, Pallestrini E, et al. Seasonal and perennial allergic rhinitis: is this classification adherent to real life? A population based study. Allergy 2005; 60:882-87.
13. Bousquet J, Khaltaev N, Cruz AA, Denburg J, Fokkens WJ, Togias A, et al. Allergic Rhinitis and its Impact on Asthma (ARIA) 2008 Update (in collaboration with the World Health Organization, GA2LEN and AllerGen). Allergy 2008; 63:S8-160.
14. Wallace DV, Dykewicz MS. The diagnosis and management of rhinitis: An updated practice parameter. J Allergy Clin Immunol 2008; 122:S1-84.
15. Ciprandi G, Cirillo I, Pistorio A. Impact of allergic rhinitis on asthma: effects on spirometric parameters. Allergy 2008; 63:255-60.
16. Cirillo I, Pistorio A., Tosca MA, Ciprandi G. Impact of allergic rhinitis on asthma: effects on bronchial hyperreactivity. Allergy 2009; 64:439-44.
17. Ciprandi G, Cirillo I, Pistorio A, La Grutta S, Tosca MA. Impact of allergic rhinitis on asthma: effects on bronchodilation test. Annals Allergy Asthma Immunol 2008;101:42-6.
18. Bousquet PJ, Combescure C, Neukirch F, Klossek JM, Mechin H, Daures JP, Bousquet J. Visual analog scales can assess the severity of rhinitis graded according to ARIA guidelines. Allergy 2007; 62:367-72.
19. American Thoracic Society. Guiedelines for Methacholine and Exercise Challenge Testing 1999. Am J Resp Crit Care Med 2000; 161:309-29.
20. Simons FER What's in a name? The allergic rhinitis-asthma connection. Clin Exp All Rev 2003; 3:9-17.
21. Ciprandi G, Cirillo I, Klersy C, Marseglia GL, Vizzaccaro A, Pallestrini E, Tosca MA Role of FEF^{25-75} as an early marker of bronchial impairment in patients with seasonal allergic rhinitis. Am J Rhinol 2006; 20:641-7.
22. Guerra S, Sherrill DL, Martinez FD, Barbee RA. Rhinitis as an independent risk factor for adult-onset asthma. J Allergy Clin Immunol 2002; 109:419-25.
23. Shaaban R, Zureik M, Soussan D, et al. Rhinitis and onset of asthma: a longitudinal population-based study. Lancet 2008 20; 372(9643):1049-57.
24. Ciprandi G, Cirillo I, Klersy C, Castellazzi AM, Barberi S, Marseglia GL. Nasal decongestion test in allergic rhinitis: definition of responder. Int Immunopharm 2007; 7(3):372-4.
25. Moller C, Dreborg S, Ferdousi HA, et al. Pollen immunotherapy reduces the development of asthma in children with seasonal rhinoconjunctivitis (the PAT-study). J Allergy Clin Immunol 2002; 109:251-6.

JOURNAL OF BIOLOGICAL REGULATORS & HOMEOSTATIC AGENTS Vol. 29, no. 4, 945-951 (2015)

LETTER TO THE EDITOR

THE ROLE OF HYALURONIC ACID IN PATIENTS AFFECTED BY GLENOHUMERAL OSTEOARTHRITIS

G. DI GIACOMO and N. DE GASPERIS

Orthopedic Department, Concordia Hospital for "Special Surgery", Rome, Italy

Received March 12, 2015 – Accepted October 7, 2015

Persistent shoulder pain is a highly prevalent problem, due to different pathologies, that is frequently associated with limited range of motion and decreased function. The correct diagnosis can lead to the best treatment for each pathology. In this study we tried to understand what could be the role of hyaluronic acid and its effective benefit in patients affected by mild-to-moderate glenohumeral osteoarthritis. From January 2013 to June 2014, we prospectively followed-up 61 consecutive patients with shoulder osteoarthritis degrees I, II, and III. We divided the patients into 2 homogeneous groups: 31 patients in the first group treated with 5 intra-articular injections of Hyalgan 20mg/2ml and a specific physiotherapy program, and 30 patients in the second group treated only with physical therapy. The mean follow-up examination was carried out 5.2 months after the beginning of the therapy for both groups. The statistical analysis revealed a significant difference (P<0.05) between the two groups in terms of pain reduction and improvement in the activities of daily living. The present study demonstrates the greater and long-lasting efficacy of a five-injection treatment with hyaluronic acid (Hyalgan 20mg/2ml) combined with a physical therapy program in comparison with physical therapy only in patients affected by glenohumeral osteoarthritis degree I, II or III.

Persistent shoulder pain is a highly prevalent problem that is frequently associated with limited range of motion (ROM) and decreased function (1, 2). It can have different etiologies, including glenohumeral osteoarthritis (OA), rotator cuff tear or tendinitis, adhesive capsulitis and subacromial bursitis (3). The key point for an efficient treatment of a painful shoulder is a correct diagnosis based on the patient's history and a careful objective examination supported by X-Ray (anteroposterior view on the scapular plane) and MRI study (4). A correct diagnosis can lead to the best treatment for each pathology, that is very different especially between degenerative (glenohumeral OA) and inflammatory (adhesive capsulitis or subacromial bursitis), even if both are characterized by the same symptoms such as pain and loss of ROM. The treatment of these two groups of pathologies generally includes the use of oral analgesics, physical therapy and intra-articular injections with corticosteroids or hyaluronic acid (HA) aimed at reducing the pain and restoring the ROM of the shoulder, but no standardized protocols are available in clinical practice and literature data are contrasting (3-7). Analgesics and non-steroidal anti-inflammatory drugs are not always effective and may be associated with substantial side effects, particularly in elderly patients (8-10). In this study we assessed the potential role of HA and its effective

Key words: hyaluronic acid, glenohumeral osteoarthritis, shoulder

Mailing address: Giovanni Di Giacomo MD,
Dipartimento di Ortopedia,
Concordia Hospital for "Special Surgery"
Via delle Sette Chiese 90
00145 Rome, Italy
Tel. +39065126439 Fax +39065136655
email: concordia@iol.it

0393-974X (2015)

DISCLOSURE: ALL AUTHORS REPORT NO CONFLICTS OF INTEREST RELEVANT TO THIS ARTICLE.

benefit in patients affected by mild to moderate glenohumeral OA (degree I, II, or III). Patients with glenohumeral OA are usually elderly people (between 60 and 70 years old) who describe the origin of the pain as traumatic or spontaneous (11, 12). In these patients the X-ray and the MRI usually show the typical aspect of OA like joint space narrowing, sclerosis of subchondral bone and osteophytosis**.** It was postulated that intra-articular injections of HA (Hyalgan, molecular weight 500-730 kDa) would be beneficial for the treatment of persistent shoulder pain in patients with glenohumeral OA due to the specific characteristics of Hyalgan able to restore synovial fluid properties in this degenerative pathology (11, 13-18). The aim of this study was to evaluate the effects of the treatment with intra-articular injections of HA combined with a physical therapy program in patients affected by shoulder OA degrees I, II, or III, in terms of reduction of shoulder pain and improvement in ROM. Other clinical data on previous experience of OA of the shoulder with HA viscosupplementation are missing.

MATERIALS AND METHODS

In this open-label study, we prospectively followed-up 61 consecutive patients, with shoulder OA degree I, II, or III, seen in our unit from January 2013 to June 2014. All patients signed an informed consent to be part of the study. The study obtained approval from the Ethics Committee of the Concordia Hospital for Special Surgery Rome (approval n° 1/2013).

All patients were carefully evaluated and selected with clinical selection criteria. Inclusion criteria were patients with good general conditions and shoulder OA degree I, II, o III, showing the typical aspect of OA at the standard X-ray studies (antero-posterior view, internal and external rotation view, lateral view) such as joint space narrowing, subchondral bone sclerosis and osteophytosis. Exclusion criteria were concomitant rotator cuff lesions, previous shoulder surgery, previous humeral head fracture, metabolic diseases and poor general condition. Patients with OA degree IV with surgical indications (shoulder arthroplasty) were not included in this study.

The "Constant score" functional scoring systems was calculated for all 61 patients before treatment. On the basis of the expected difference between groups in the Constant variable, we calculated the sample size for each group, setting the p value at <0.05 and the minimum power of the study at 80% (Fig. 1). Patients were then randomly allocated to two different homogeneous groups, 31 patients for the first group (case group) and 30 patients for the second group (control group).

Of the 31 patients belonging to the case group, 15 were males and 16 were females. The mean age of the patients was 62.5 years (range 49 to 82 years). There were 21 right shoulders and 10 left shoulders. The dominant side was treated in 16 patients (51.6%). All patients referred having shoulder pain for several months (average 8.2 months); 9 of the patients (29%) had mild pain, 19 (61.3%) had moderate pain and 3 (9.7%) severe pain; 7 (22.6%) of our patients had been involved in trauma, 24 (77.4%) of the patients had a spontaneous pain. All the patients had a reduced ROM: mean active forward elevation was 150.2°, mean external rotation with the arm at the side was 23.2°. The mean Constant Score was 78.2. All the patients showed OA signs at the X-ray examination. Of the 31 patients, 16 (51.6%) had OA degree I, 12 (38.7%) had OA degree II, and 3 (9.7%) had OA degree III.

Of the 30 patients belonging to the control group, 11 were males and 19 were females. The mean age of the patients was 65.5 years (range 49 to 83 years). There were 16 right shoulders and 14 left shoulders. The dominant side was treated in 14 patients (46.7%). All patients had experienced shoulder pain for several months (average 10.6 months); 6 of the patients (20%) had mild pain, 17 (56.7%) had moderate pain and 7 (23.3%) severe pain; 3 (10%) of our patients had been involved in trauma, 27 (90%) of the patients had a spontaneous pain. All the patients had a reduced ROM: mean active forward elevation was 142.2°, mean external rotation with the arm at the side was 24°. The mean Constant Score was 70.8. All the patients showed OA signs at the X-ray examination. Of the 30 patients, 15 (50%) had OA degree I, 10 (33.3%) had OA degree II, and 5 (16.7%) had OA degree III.

The treatment for patients belonging to the first group was performed by 5 intra-articular injections with Hyalgan 20mg/2ml (molecular weight 500-730 kDa), 1 injection every 15 days, and a specific physiotherapy program for patients belonging to the first group; on the other hand, patients belonging to the second group were treated with physical therapy only. The mean follow-up examination was performed 5.2 months after the beginning of the therapy for both groups, with halfway clinical examination every month.

The physical therapy program, performed with a professional therapist, had a 3-month duration with a frequency of 3 days every week. The program consisted of passive capsular stretching for recovery of ROM, isometric exercises for deltoid, rotator cuff and scapulo-thoracic muscles, isotonic exercises for scapulo-thoracic muscles (closed kinetic chain), and hydrokinesis therapy.

At the final follow-up examination we determined the

functional status, ROM and pain of the treated shoulder by means of the Constant score.

Statistical analysis was performed by STATISTICA 7.0 software (StatSoft Inc,T ulsa, OK, USA). The database was constituted of 61 patients with glenohumeral OA defined by the ROM (forward elevation and external rotation) and by the Constant score functional scoring systems (scale 0-100). The distribution of subjects along the three variables (forward elevation, external rotation and Constant score) before the treatment, verged on normality ($P>0.05$; Shapiro-Wilk = 0.945, 0.951 and 0.961, respectively). Thus, patients were divided in two different groups of treatment and were evaluated before and after the two different kinds of treatment. Variables were considered as continuous and a one-way ANOVA was performed for repeated measures and scheduled post-hoc tests (Tukey's test; $P<0.05$) between the two groups and within the same group.

RESULTS

The mean follow-up for all the patients was 5.2 months after the beginning of the treatment (range 4-6 months). At the final clinical examination of patients belonging to the case group (average 98 days after the 5th intra-articular injection with Hyalgan) the mean active forward elevation was 168.2° (gain of 18°), and the mean external rotation with the arm at the side was 30.8° (gain of 7.6°). Patients also showed a relevant reduction in level of pain and a significant improvement in daily activities. The mean Constant score after the treatment with Hyalgan was 91.6 points, 13.4 points more than the initial score (Table I). No side effects were found in patients treated with Hyalgan intra-articular injections.

At the final clinical examination of patients belonging to the control group (average 156 days after the beginning of treatment) the mean active forward elevation was 150° (gain of 7.8°), and the mean external rotation with the arm at the side was 28.5° (gain of 4.5°). Patients also showed a lower level of pain and moderate improvement in daily activities. The mean Constant score after physiotherapy only was 79 points, 8.2 points more the initial score (Table I).

The ANOVA for repeated measures for the Constant score revealed a significant effect of the treatments between groups ($F_{1,59}= 11.705$; $P<0.05$) and within groups ($F_{1,59}= 19.076$; $P<0.05$). As shown in Fig. 2, there was no difference between groups before the treatment (78.2±2.2 and 70.8±2.2 for the case group and control group, respectively), while there was a significant effect after the treatment (91.6±1.9 and 79.0±2.0 for case group and control group, respectively).

Similar results were obtained for the forward elevation movement. In this case, the ANOVA for repeated measure showed a significant effect between groups ($F_{1,59}= 9.746$; $P<0.05$) and within groups ($F_{1,59}= 27.547$; $P<0.05$). As shown in Fig. 3, there was no difference before the treatments between the two groups (150.2±3.1 and 142.2±3.1 for the case group and control group, respectively), while for the Constant score, after the different treatments there was a significant difference between groups (168.2±3.0 for the case group and 150.0±3.0 for control group,

Table I. *Means and standard deviation for case and control group, before (t0) and after (t1) the therapy.*

	Control	Case	Range
Const $_{t0}$	70.8 ± 15.3	78.2 ± 7.7	42 – 95
Const $_{t1}$	79 ± 14.5	91.6 ± 6.5	52 – 99
Elevation $_{t0}$	142.2 ± 22.2	150 ± 10.4	100 – 175
Elevation $_{t1}$	150 ± 20.9	168 ± 10.5	120 – 180
Extra $_{t0}$	24 ± 5.9	23.2 ± 7	10 – 35
Extra $_{t1}$	28.5 ± 7.9	30.8 ± 5.8	20 – 45

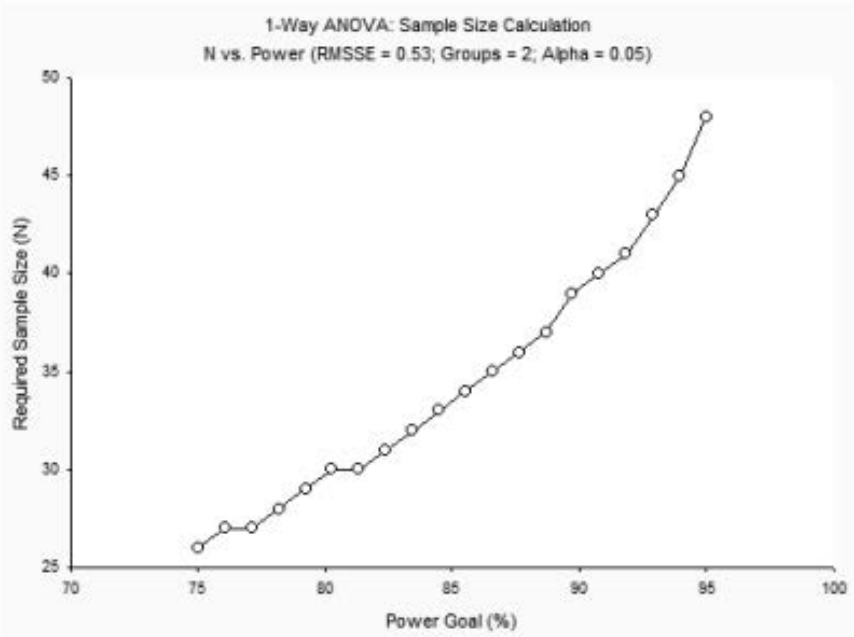

Fig. 1. *Sample size calculation as function of the power of the study.*

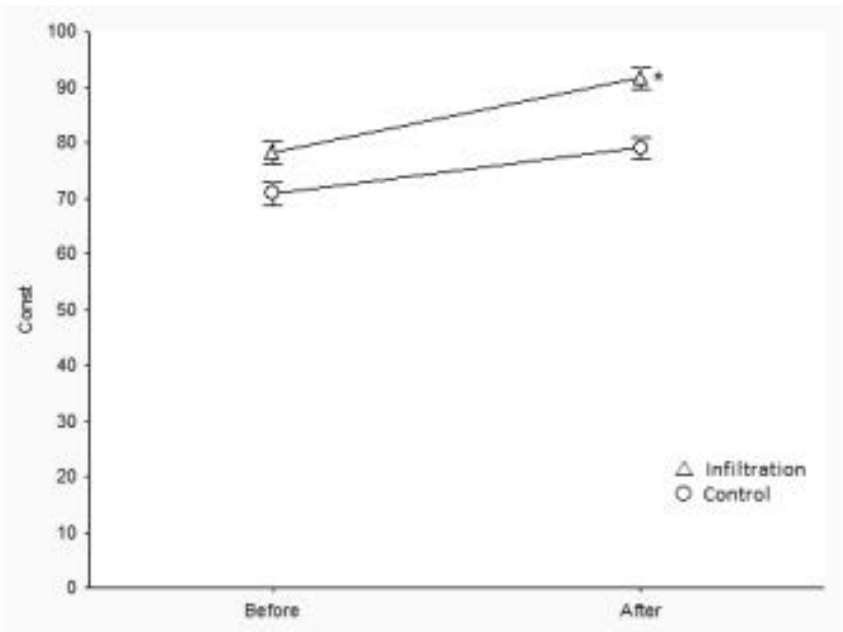

Fig. 2. *Constant score in case and control groups, before and after the treatment. Spreads represent standard error. *Indicates a significative difference between groups (P<0.05; Tukey's post-hoc test).*

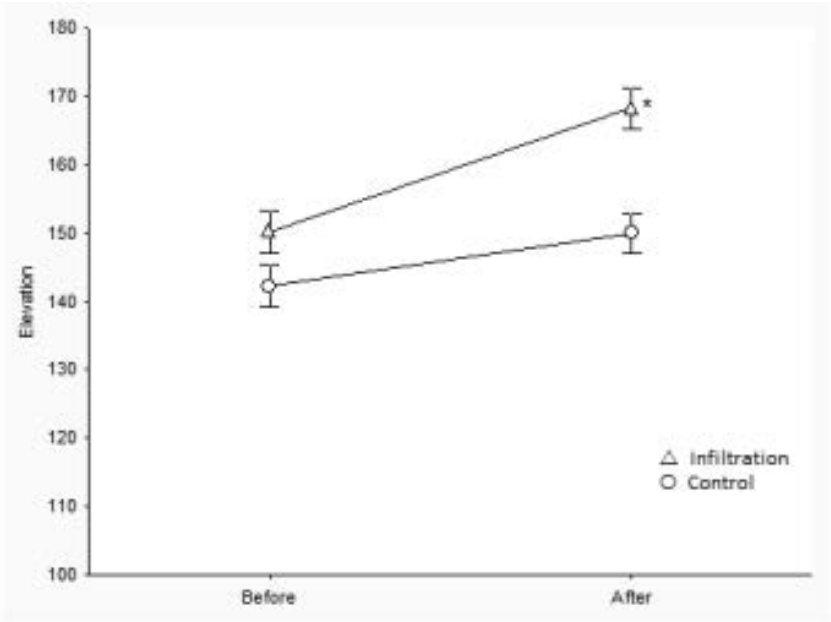

Fig. 3. *Grades of forward elevation movement evaluated in case and control groups, before and after the treatment. Spreads represent standard error. *Indicates a significative difference between groups (P<0.05; Tukey's post-hoc test).*

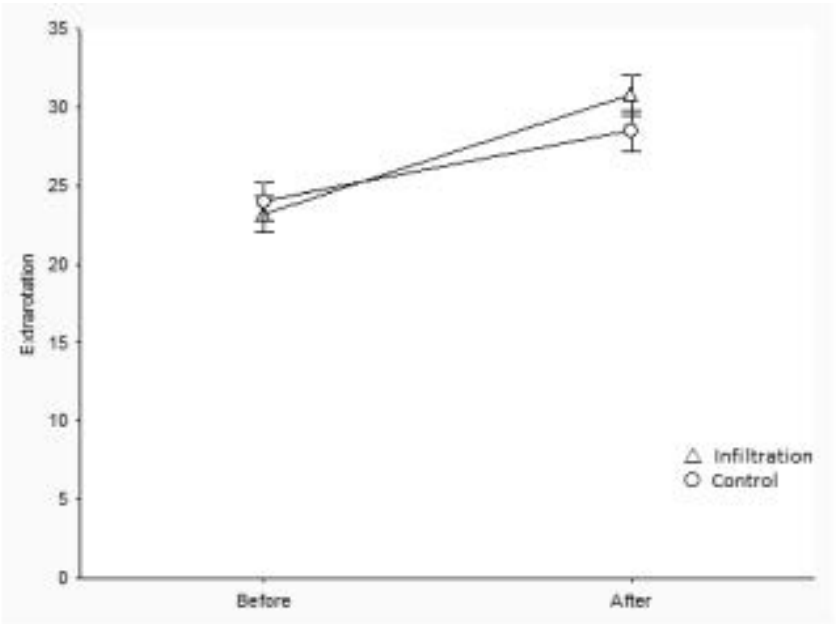

Fig. 4. *Grades of external rotation movement evaluated before and after treatment in the case and control groups. Spreads represent standard error. No significant differences between groups.*

respectively). Differently, in the evaluation of the external rotation movement, the performed statistical analysis did not show a significant difference between groups ($F_{1,59}$= 0.221; P=0.64). There was a significant effect only within groups ($F_{1,59}$= 8.046; P<0.05). The effect is reported in Fig. 4.

DISCUSSION

The aim of this study was to evaluate the effects of the treatment with intra-articular injections of HA combined with a physical therapy program in patients affected by shoulder OA degree I, II, or III, in terms of reduction of shoulder pain and improvement in ROM. To do this we evaluated two different kinds of treatment: 5 intra-articular injections with HA (Hyalgan 20mg/2ml) associated with physical therapy rehabilitation versus physical therapy only treatment.

The role of HA in patients affected by shoulder OA is controversial in literature. Kwon et al., in a multicenter, randomized, double-blind, placebo-controlled trial, showed that only patients without concomitant shoulder pathologies, treated with intra-articular injections of HA, had a statistically significant improvement in terms of pain (14). Also Merolla et al., in a retrospective controlled trial, found that patients affected by mild to moderate glenohumeral OA had significant pain reduction and satisfaction, for up to 6 months, after treatment with intra-articular injections of HA (18). On the other hand, Colen et al., in a systematic review published in 2014, showed that intra-articular injections with HA have a good efficacy at follow-up compared to baseline but the difference in efficacy between HA and placebo did not reach the minimal clinically important difference at any time points of the follow-up (19).

This study showed a significant decrease of shoulder pain (P<0.05) within the two groups, treated with the two different procedures. Furthermore, this study showed a significant difference in the degree of shoulder pain (P<0.05) between the two groups of patients. This supports the concept that patients treated with intra-articular injections with HA associated with physical therapy benefit from a greater and long-lasting positive effect compared to patients that received physical therapy only treatment (mean follow-up 5.2 months).

Similarly, this study showed a significant improvement in forward elevation (P<0.05) within the two groups. The improvement resulted significant also between the two groups. Also in this case the study showed that patients treated with intra-articular injections with HA and physical therapy received a greater benefit compared to patients who received physical therapy only treatment in terms of improvement in ROM in forward elevation. This could be probably due to the large reduction of shoulder pain.

On the other hand, even if there was also a significant improvement in the external rotation movement within the two groups (P<0.05), it appeared to be non-significant between the two groups.

This adds clarity to literature data and supports our hypothesis that intra-articular injections of HA are beneficial for the treatment of patients with glenohumeral OA (degree I, II or III), with a significant reduction of shoulder pain and a partial recovery of ROM, resulting in improvement in the activities of daily living, due to the specific characteristics of Hyalgan able to restore synovial fluid properties in this degenerative pathology (11, 13-18).

This study has some limitations. The first limitation is the possible concomitant inflammation of the long head of the biceps or the rotator cuff, very frequent in patients affected by glenohumeral OA, that could influence the results of the treatment in terms of pain. In addition, the second limitation is that we did not consider the scapular morphology that could partially influence the shoulder ROM.

In conclusion, the present study demonstrates the greater and long-lasting efficacy of a five-injection treatment with HA (Hyalgan 20mg/2ml) combined with a physical therapy program in patients affected by mild to moderate glenohumeral OA (degree I, II or III), in terms of reduction of shoulder pain and improvement in daily activities, compared to alternative treatments such as physical therapy only.

REFERENCES

1. Chakravarty K, Webley M. Shoulder joint movement and its relationship to disability in the elderly. J

Rheumatol 1993; 20:1359-61.
2. Steinfeld R, Valente RM, Stuart MJ. A commonsense approach to shoulder problems. Mayo Clin Proc 1999; 74:785-94.
3. Andrews JR. Diagnosis and treatment of chronic painful shoulder: review of nonsurgical interventions. Arthroscopy 2005; 21:333-47.
4. Calis M, Demir H, Ulker S, Kirnap M, Duygulu F, Calis HT. Is intraarticular sodium hyaluronate injection an alternative treatment in patients with adhesive capsulitis? Rheumatol Int 2006; 26:536–540.
5. Carfagno DG, Ellenbecker TS. Osteoarthritis of the glenohumeral joint. Phys Sportsmed 2002; 30(4):19-30.
6. Blaine T, Moskowitz R, Udell J, et al. Treatment of persistent shoulder pain with sodium hyaluronate: a randomized, controlled trial. J Bone Joint Surg Am 2008; 90:970-9. doi:10.2106/JBJS.F.01116.
7. Brander VA, Gomberawalla A, Chambers M, Bowen M, Nuber G. Efficacy and safety of hylan G-F 20 for symptomatic glenohumeral osteoarthritis: a prospective, pilot study. PM R 2010; 2(4):259-67. doi: 10.1016/j.pmrj.2010.02.010.
8. American College of Rheumatology. Recommendations for the medical management of osteoarthritis of the hip and knee: 2000 update. American College of Rheumatology Subcommittee on Osteoarthritis Guidelines. Arthritis Rheum 2000; 43:1905-15.
9. Singh G. Recent considerations in nonsteroidal anti-inflammatory drug gastropathy. Am J Med 1998; 105:31S-38S.
10. Jordan K, Arden N, Doherty M, Bannwarth B, Bijlsma J, Dieppe P, Gunther K. EULAR Recommendations 2003: an evidence based approach to the management of knee osteoarthritis: Report of a Task Force of the Standing Committee for International Clinical Studies. Including Therapeutic Trials (ESCISIT). Ann Rheum Dis 2003; 62:1145-55.
11. Sinusas K. Osteoarthritis: diagnosis and treatment. Am Fam Physician 2012; 85(1):49-56.
12. Menge TJ, Boykin RE, Byram IR, Bushnell BD. A comprehensive approach to glenohumeral arthritis. South Med J 2014; 107(9):567-73.
13. Balazs EA, Denlinger JL. Viscosupplementation: a new concept in the treatment of OA. J Rhematol 1993; 1:85-87.
14. Kwon YW, Eisenberg G, Zuckerman JD. Sodium hyaluronate for the treatment of chronic shoulder pain associated with glenohumeral osteoarthritis: a multicenter, randomized, double-blind, placebo-controlled trial. J Shoulder Elbow Surg 2013; 22(5):584-94.
15. Colen S, Haverkamp D, Mulier M, van den Bekerom MP. Hyaluronic acid for the treatment of osteoarthritis in all joints except the knee: what is the current evidence? BioDrugs 2012; 26(2):101-12.
16. Gu Q, Zhou N, Shanghai J. Research progress of viscosupplementation. Zhongguo Xiu Fu Chong Jian Wai Ke Za Zhi 2011; 25(6):755-60.
17. Abate M, Pulcini D, Di Iorio A, Schiavone C. Viscosupplementation with intra-articular hyaluronic acid for treatment of osteoarthritis in the elderly. Curr Pharm Des 2010; 16(6):631-40.
18. Merolla G, Sperling JW, Paladini P, Porcellini G. Efficacy of Hylan G-F 20 versus 6-methylprednisolone acetate in painful shoulder osteoarthritis: a retrospective controlled trial. Musculoskelet Surg 2011; 95(3):215-24.
19. Colen S, Geervliet P, Haverkamp D, Van Den Bekerom MP. Intra-articular infiltration therapy for patients with glenohumeral osteoarthritis: A systematic review of the literature. Int J Shoulder Surg 2014; 8(4):11.

LETTER TO THE EDITOR

PERISURGICAL AND INTRA-REHABILITATIVE SALIVARY STEROID HORMONE PROFILES IN BICOMPARTMENTAL ARTHROPLASTY

S. PEREGO[1], D. GRASSO[1], B.D. BODINI[2], F. CAVAIANI[2], C. DE SANTIS[2], N. URSINO[3], C. PELOSI[2], G. BANFI[1,4] and G. LOMBARDI[1]

[1]Laboratory of Experimental Biochemistry and Molecular Biology, I.R.C.C.S. Istituto Ortopedico Galeazzi, Milan, Italy; [2]O.U. Rehabilitation, 1st Division – Clinical Orthopaedic Rehabilitation, I.R.C.C.S. Istituto Ortopedico Galeazzi, Milan, Italy; [3]O.U. Reconstructive Joint Surgery and Orthopaedic Surgery (C.A.S.C.O.), I.R.C.C.S. Istituto Ortopedico Galeazzi, Milan, Italy; [4]Vita-Salute San Raffaele University, Milan, Italy

Received June 29, 2015 – Accepted October 7, 2015

The first two authors contributed equally to the work

Sex hormones play a role in pain perception, a key variable in evaluating the progression and treatment of osteoarthritis. The aim of this study was to determine the relationship between salivary concentrations of four steroid hormones and functional/clinical outcomes after hip and knee arthroplasty. Saliva samples were collected from 24 otherwise healthy patients with osteoarthritis before surgery, on admission to rehabilitation, and at hospital discharge. Salivary concentrations of testosterone, 17β-estradiol, dehydroepiandrosterone (DHEA), and cortisol were immunoassayed. Changes in hormone levels were compared with clinical outcomes, as assessed by functional independence measure (FIM®), Barthel Index (BI), and visual analog scale for pain (VAS) scores. Changes in testosterone levels were significantly inversely correlated with VAS (r= -0.53, p=0.043) and FIM® and BI scores in all patients (r= -0.30, p= 0.043, and r= -0.35, p=0.031, respectively). The testosterone to cortisol ratio was inversely correlated with BI scores in all patients (r= -0.30, p=0.040), and in the men (r= -0.55, p=0.005) and the women (r= -0.28, p=0.042) when analyzed separately. Changes in salivary testosterone concentrations closely correlated with clinical outcome measurements for total hip and knee arthroplasty. Clinical outcome after arthroplasty was generally better among the men.

Sex hormones are physiologically involved in pain sensation. Estrogens, for example, modulate the perception of peripheral pain possibly through estrogen receptor alpha (ER-α) and G protein-coupled receptor 30 (GPR30) expressed in primary afferent neurons (1, 2). Lipopolysaccharide (LPS)-induced toll-like receptor (TLR)-4 activation in the spinal cord has been found to induce allodynia in male, but not female, mice mediated through the actions of testosterone, as demonstrated by gonadectomy and hormone replacement therapy (HRT) (3). Although experimental animal models of pain have suggested dose- and sex-dependent effects of gonadal hormones (4), the sex hormone-

Key words: arthroplasty, saliva, steroid hormones, pain, rehabilitation

Mailing address: Dr Giovanni Lombardi,
Laboratory of Experimental Biochemistry
& Molecular Biology,
I.R.C.C.S. Istituto Ortopedico Galeazzi,
Via Riccardo Galeazzi, 4 20161, Milano, Italy
Tel.: +39 02 66214068 Fax: +39 02 66214068
e-mail: giovanni.lombardi@grupposandonato.it

0393-974X (2015)

DISCLOSURE: ALL AUTHORS REPORT NO CONFLICTS OF INTEREST RELEVANT TO THIS ARTICLE.

dependent pathways modulating pain in humans are still unknown.

Pain is a key variable in evaluating the progression of osteoarthritis (OA), indications for arthroplasty, and rehabilitation outcome after total hip and knee replacement for primary OA (5). Hormonal response to surgery and rehabilitation is particularly relevant in open surgeries such as hip and knee arthroplasty which require adequate response for good recovery (6).

Although sex hormones are involved in pain modulation, no research to date has correlated hormone profiles with pain during the perioperative period in patients undergoing total knee (TKA) or hip (THA) arthroplasty. Amory and coworkers reported that in elderly men receiving TKA, pre-operative supraphysiological testosterone administration improved the ability to stand, walk, and climb stairs in the immediate postoperative period (day 3) without further complications (7). Since hormone levels in saliva provide a direct measure of the biologically active (free) fraction of steroid hormone present, saliva analysis is being increasingly used for diagnosing and monitoring health and disease status (8). The aim of this study was to determine whether a relationship exists between the clinical rehabilitation outcome after TKA and THA and the changes in salivary steroid hormone levels measured during the perioperative period.

MATERIALS AND METHODS

Study population

For this pilot study 30 patients were recruited between March and July 2013. Two patients voluntarily withdrew and salivary samples from 4 patients were unsuitable for analysis. The final study population comprised 24 patients (12 men and 12 women) with hip or knee OA and referred for THA or TKA. Inclusion criteria were: age between 45 and 80 years, menopause (for women) not treated with HRT, good general health status. Exclusion criteria were comorbidities and glucocorticoid or steroid treatment within 1 month before the beginning of the study. Comorbidity was excluded at presurgical examination on the basis of Charlson Index scores (range, 0 to 2, median 0) (9) and American Society of Anesthesiology (ASA) risk index scores (range, 1 to 3, aggregate score 2) (10).

Postoperative analgesia was provided as in routine clinical practice, except for steroids. Standard analgesia was offered with paracetamol (maximum 2 g/day) when the visual analog scale (VAS) for pain was ≥ 4 and ketorolac (maximum 30 mg/day) when the VAS was ≥ 6.

The study protocol was approved by the hospital internal review board and all patients gave their informed consent for saliva sampling and use of data. Table I presents the anthropometrical and clinical characteristics of the study population.

Saliva sampling and steroid hormone determination

After rinsing with mouthwash, fasting unstimulated saliva samples were collected between 8:00 and 10:00 a.m. before surgery (day 1, T0), on admission to the rehabilitation unit (day 4, T1), and at hospital discharge (day 10, T2). Saliva was collected in polypropylene low-steroid absorbing tubes (Sali-tubes, DRG® Instruments GmbH, Marburg, Germany) and stored at -20°C until assayed. After centrifugation of samples to eliminate particulate material, testosterone, 17β-estradiol, dehydroepiandrosterone (DHEA), and cortisol were assayed by polyclonal antibodies-based competitive ELISA (DRG® Instruments GmbH) on a Dynex DSX® automated ELISA system (Dynex Technologies, Chantilly, VA, USA) following the manufacturer's instructions. Sensitivity, maximum intra-assay (CV_w %) and inter-assay (CV_b %) coefficients of variation were: 1.9 pg/mL, 13.8%, 9.6% for testosterone; 0.4 pg/mL, 6.9%, 4.3% for estradiol; 2.2 pg/mL, 8.0%, 4.7% for DHEA; and 0.537 ng/mL, 4.52%, 7.47% for cortisol.

Pain indices and clinical response

A pain VAS was administered as a self-report immediately before saliva sampling. Patients were asked to rate their pain intensity by placing a mark on a 100-mm horizontal line with anchor words at either end ("no pain" and "worst possible pain") (11). Physical rehabilitation outcome measures (T1 to T2) were the Functional Independence Measure (FIM™) and the Barthel Index (BI). The FIM™ instrument comprises 18 items (13 motor-sphincteric and 5 cognitive) and the BI 10 items. Both scales assess performance of daily activities, from complete dependence (1) to complete independence (7 items in the FIM™; 10 in the BI). The maximum scores are 126 for the FIM™ and 100 for the BI (12, 13).

Statistical analysis

Statistical analysis was performed using GraphPad Prism v5.0 software (GraphPad Software Inc., LaJolla, CA, USA) according to Simundic (14). Data are described as the median (5^{th} to 95^{th} percentile). Medians were compared over the 3 time points using Friedman's test with Dunn's correction. Coupled comparisons were performed using a two-tailed Wilcoxon signed-rank test (paired data) and two-tailed Mann-Whitney

U test (unpaired data). Median (range) values (i.e., the difference in hormone levels between two time points) in the men and the women were compared with a two-tailed Mann-Whitney U test. Correlation analysis (two-tailed Spearman's rank correlation test) defined the relationships between changes in hormone levels and clinical scores. The significance level was set at 0.05.

RESULTS

Anthropometrical features

The median body mass index (BMI, weight in kilograms divided by the square of height in meters) and age were similar in the male and female groups (p=0.468 and p=0.840, respectively) (Table I). The median body weight, although slightly different, did not reach statistical significance (p=0.055). The age and body weight of patients undergoing TKA or THA were similar (p=0.725 and p=0.141, respectively). The BMI was higher in the TKA patients (p=0.035). The female to male ratio was higher in the TKA group (6:10) than in the THA group (6:14).

Pain indices and clinical response

Overall, the VAS pain scores decreased from 6.50 (1.25-10.00) at T0 to 4.50 (1.00-8.00) at T1 and to 3.50 (0.25-7.00) at T2 (Fig. 1) (p=0.033 for T0 *vs* T1; p=0.007 for T0 *vs* T2). The baseline VAS scores for the men and the women were similar at T0 (p=0.467); the VAS scores for the men were lower at T1 (p=0.003) and T2 (p=0.002) than for the women; the VAS scores at T1 (p=0.027) and T2 (p=0.010) were significantly lower than at T0 for the men but not for the women. The VAS scores for the TKA and THA patients were similar.

Overall, the FIM™ score increased from 92.0 (73.5-105.5) to 123.0 (116.3-125.0) and the BI score from 59.5 (43.5-75.7) to 98.0 (95.2-100.0) (p <0.001 for both measures). The differences remained statistically significant when the scores for the men and the women were analyzed separately (p <0.001). However, while the FIM™ scores for the men and the women were similar at both time points, the median BI for the men [64.5 (43.0-78.0)] was higher than for the women [57.5 (45.0-66.0)] (p=0.031) at T1. The FIM™ and the BI scores for the TKA and THA patients were significantly different at T1 as compared with T2 (p <0.001), whereas the median scores were similar in the TKA and THA patients at each time point (Fig. 2).

Steroid hormone profile

Salivary cortisol levels increased from 3.03 (1.07-5.80) ng/mL before surgery (T0) (p <0.001) to 4.730 (2.48-7.80) ng/mL after surgery (T1), and then returned to baseline values at T2 [3.48 (1.50-7.20) ng/mL] (p=0.002). Unlike other hormones, because cortisol concentrations are not sex-dependent, their values can be compared between males and females. The trends were similar between the sexes and comparable to the whole cohort, as were the range of

Table I. *Anthropometrical and clinical characteristics of the study population at recruitment.*

	Age (years)	Weight (kg)	BMI (Kg/m^2)	Surgical Indication	
				TKA (n)	THA (n)
All (n= 24)	66.7 (49.43-78.23)	72.50 (43.25-96.75)	26.00 (17.50-31.75)	9	15
Stratification by Sex					
	Age (years)	**Weight (kg)**	**BMI (Kg/m^2)**	**Surgical Indication**	
				TKA (n)	**THA (n)**
Males (n= 12)	67.0 (48.9-74.9)	75.00 (69.00-98.00)	26.00 (22.00-30.00)	4	8
Females (n= 12)	66.7 (51.0-78.7)	70.50 (39.00-80.00)	27.00 (16.00-32.00)	6	6

*Patients are presented as the whole population and stratified by sex or by surgical indication (total knee arthroplasty [TKA] and total hip arthroplasty [THA]). Age, weight, and BMI are shown as median (5th to 95th percentile). Asterisks indicate significant differences in the comparison of the same parameter between two different categories (two-tailed unpaired Mann-Whitney test; *: p< 0.05).*

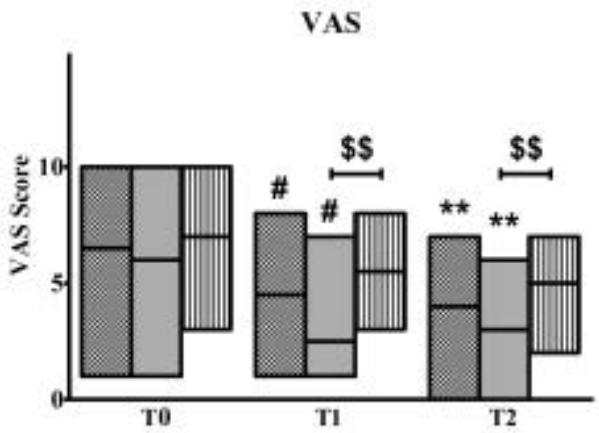

Fig. 1. *Pain VAS scores recorded during the perisurgical period. The figure shows the changes in VAS scores between the day before the surgery (T0), on postoperative day 4 (T1, first day of rehabilitation), and postoperative day 10 (T2, before hospital discharge) for the whole population (dotted), the men (oblique lines), and the women (vertical lines). Superscript symbols indicate statistically significant differences (#: T1 vs. T0; *: T2 vs T0) within the same cohort; significant differences between the sexes at the same time point are indicated by "$".*

changes in cortisol levels. In the women, the cortisol levels at T2 were higher than at T0 (p=0.028), although lower than those measured at T1 (p=0.009).

Estradiol levels increased from 1.63 (0.03-15.38) pg/mL] before surgery (T0) to 5.00 (0.24-21.75) pg/mL after surgery (T1) and then decreased to 3.20 (0.30-17.60) pg/mL at T2, with a statistically significant difference in values noted only between T0 and T1 (p=0.030). The difference was significant for the men (p=0.010 for T1 vs. T0; p=0.043 for T0 *vs* T2). The range of changes in estradiol levels between the time points was similar for both the men and the women.

Overall, salivary testosterone increased from 17.54 (1.11-75.06) pg/mL before surgery (T0) to 21.60 (2.62-74.12) pg/mL at T1 and then decreased to 9.23 (0.51-31.66) pg/mL at T2. There was a significant difference between the median values at T1 and at T2 and between the median value at T0 and at T2 (p=0.002 and p=0.011, respectively) but not between T0 and T1 (p=0.907). Testosterone levels in the women remained unchanged but decreased in the men from 34.55 (16.21-81.64) pg/mL at T0 to 29.06 (14.16-82.81) pg/mL at T1 and to 13.52 (1.21-33.29) pg/mL at T2 (p=0.409 for T1 *vs* T0; p=0.007 for T2 *vs* T1; p=0.003 for T2 *vs* T0). The median range of change in testosterone levels in the men and the women was similar (T0 *vs* T1) but the differences were significantly greater in the men (p=0.020 for T1 *vs* T2; and p=0.007 for T0 *vs* T2).

DHEA concentrations increased from 84.0 (17.3-304.5) pg/mL at T0 to 94.5 (23.3-319.5) pg/mL at T1 and then decreased to 61.5 (19.0-535.0) pg/mL at T2 in the men; in the women it increased from 61.5 (13.0-282.0) pg/mL at T0 to 90.0 (32.0-583.0) pg/mL at T2 (p=0.043). The median range of change between T0 and T1 was similar in the men and the women but was significantly greater in the men between T1 and T2 (p=0.030) and between T0 and

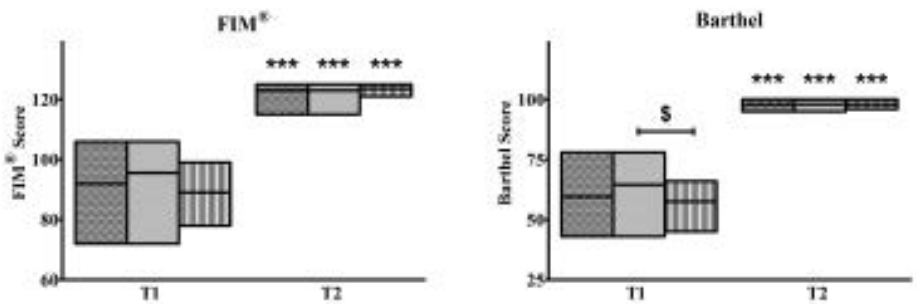

Fig. 2. *Clinical indices before surgery and at the end of rehabilitation. The figure shows the changes in FIM™ and BI scores between the day before surgery (T0) and postoperative day 10 (T2, before hospital discharge) in the whole population (dotted), the men (oblique lines), and the women (vertical lines). Superscript symbols indicate statistically significant differences (*: T2 vs T0) within the same cohort; significant differences between the sexes at the same time point are indicated by "$".*

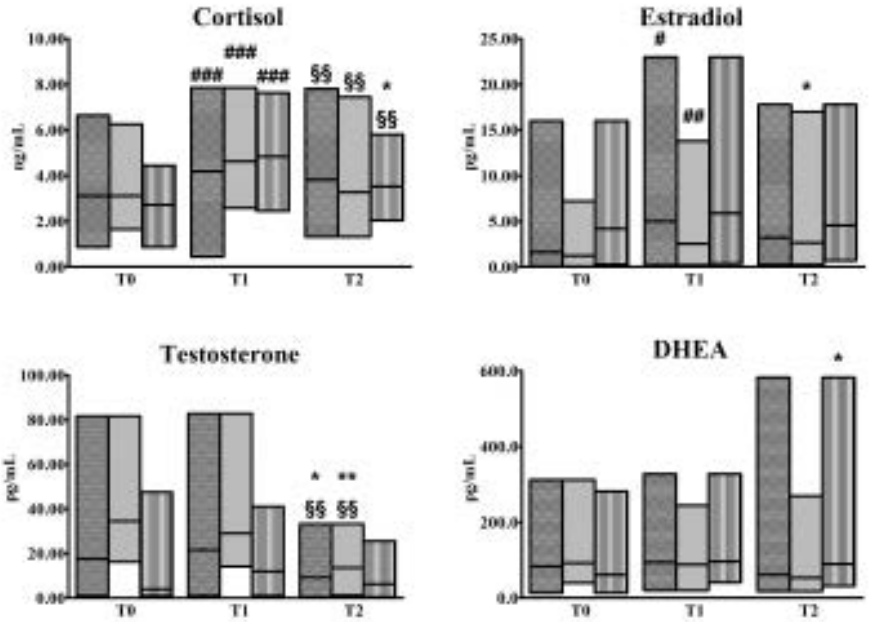

Fig. 3. *Changes in salivary hormone levels during the perisurgical period. The figure shows the changes in concentrations of salivary cortisol, estradiol, testosterone, and DHEA between the day before surgery (T0), postoperative day 4 (T1, first day of rehabilitation), and postoperative day 10 (T2, before hospital discharge) in the whole population (dotted), the men (oblique lines), and the women (vertical lines). Superscript symbols indicate statistically significant differences (#: T1 vs T0; §: T2 vs T1; *: T2 vs T0).*

T2 (p=0.004).

Overall, the testosterone to cortisol ratio decreased from 6.33 (0.35-26.31) at T0 to 4.72 (0.57-63.85) at T1 and to 1.88 (0.14-12.24) at T2. The difference was significant only between T1 and T2 (p=0.035) for all patients but not when stratified by sex. Of note was the wide range in inter-individual variability in the salivary concentrations of estradiol, testosterone, and DHEA (Fig. 3).

Correlations

Among the women, salivary cortisol concentrations were directly correlated with the changes in the FIM™ (r= 0.50, p=0.011) and BI (r= 0.50, p=0.015) scores between T1 and T2; the correlations were not significant for the study population as a whole, nor for the men. An inverse correlation between changes in estradiol levels and BMI was observed for the men (r= -0.38, p=0.024) but not with the changes in the other clinical indices. Overall, changes in testosterone levels were significantly directly correlated with changes in VAS scores (r= -0.53, p=0.043) and among both the men (r= -0.67, p=0.0011) and the women (r= -0.39, p=0.044). Changes in testosterone concentration were inversely correlated with changes in FIM™ and BI scores in the whole population (r= -0.30, p=0.043 and r= -0.35, p=0.031, respectively), among the men (r= -0.58, p=0.003, and r= -0.62, p=0.001, respectively) and the women (r= -0.30, p=0.043, and r= -0.29, p=0.040, respectively). No correlations with changes in DHEA were noted. There was a significant inverse relationship between the testosterone to cortisol ratio and the BI scores for the whole population (r= -0.30, p=0.040), the men (r= -0.55, p=0.005), and the women (r= -0.28, p=0.042).

DISCUSSION

The aim of this study was to determine whether a relationship exists between changes in the salivary concentrations of four steroid hormones

and functional/clinical rehabilitation outcomes after TKA or THA. The pain VAS scores for the men were significantly lower than those recorded for the women, irrespective of type of surgery (TKA or THA). This result was reflected in a better improvement in the BI scores for the men. Moreover, an inverse correlation was observed between the changes in testosterone levels and the improvement in clinical indices (VAS, FIM™, and BI scores) in the whole population as well as in the male and the female subgroups.

Saliva is increasingly used in research for monitoring health and disease status and as an easily accessible diagnostic fluid in clinic practice (8). It provides a noninvasive and stress-free alternative to serum and an effective (and cost-saving) technique for serial monitoring (15, 16). However, salivary diagnostics has several important limitations: i) although concentrations of some hormones in whole saliva correlate well with plasma concentrations, systemic and local conditions can directly or indirectly modify the filtering, secretory, and metabolic activities of the salivary glands; ii) the amounts of circulating molecules produced by the salivary glands differ as a result; and iii) oral acute and chronic conditions affect the production/secretion of numerous analytes in saliva (8). Moreover, while enzymes involved in steroid hormone synthesis are expressed in salivary glands, their biologic relevance is still unclear (8).

The salivary and serum levels of testosterone and cortisol are strongly correlated. Salivary hormone concentrations more accurately reflect their blood free levels, i.e., the biologically active fractions (17). In the bloodstream, steroid hormones are mainly bound to albumin and sex-hormone binding globulin (ShBG, 95–98%) (15).

In rehabilitation after open surgery, the availability of a practical monitoring tool is desirable: blood losses and liquid infusions, very common in such types of surgery, can mask substantial variations in blood parameters. Saliva analysis can overcome this problem since the concentration of hormones present in saliva is little influenced by plasma volume changes (18). Testosterone is reduced in hypercortisolemia, a typical feature of stressful conditions such as major surgeries (i.e., hip arthroplasty). Hypercortisolemia is one of the main causes of muscle strength loss (19) and possibly rehabilitation failure. Our findings show that hypercortisolemia after surgery was accompanied by an increase in testosterone levels (also in DHEA and estradiol) which tended to normalize during the course of rehabilitation.

Although their effect on bone and muscle metabolism is clear (20), the molecular link between steroid hormones and inflammation is not known. DHEA inhibits cytokine expression, e.g., interleukin (IL)-6, by directly inhibiting NF-κB (nuclear factor-κB). As IL-6 potently activates the hypothalamic-pituitary-axis (HPA), a possible therapeutic value of DHEA in inflammation has been hypothesized. Moreover, decreased DHEA downregulates the levels of sex hormones, which have modulatory effects on arthritis (21). We found that DHEA followed the same trend as estradiol and testosterone without, however, reaching statistical significance (probably owing to the wide range in inter-individual variability).

The role of cortisol in mediating inflammation and pain is well known (22). Trauma-related injuries activate the HPA axis to produce cortisol which, in turn, increases the expression of T-helper 2 (Th2) phenotype in lymphocytes which impairs cell-mediated immunity function. Depression of cell-mediated immunity, particularly after surgery, predisposes patients to infections (23) which could be prevented by close monitoring of (salivary) cortisol levels.

The immunomodulating role of estrogens is poorly understood. Estrogens can exert either pro- or anti-inflammatory effects, although their proinflammatory effect is predominant in injury and trauma (24). Many pain conditions that are prevalent in women are chronic. Contrary to popular view, experimental studies clearly indicate that women have lower pain thresholds, higher pain ratings, and reduced pain tolerance than men. Evidence suggests that female gonadal hormones modulate pain by modulating responses in primary afferents, dorsal horn neurons, and supraspinal sites (25). The association between pain symptoms and the reproductive cycle in women suggests a role for estrogens/progesterone in the sex-related differences in pain perception. Testosterone, the major male sex hormone, is thought to protect men from chronic musculoskeletal pain (26). Our clinical data corroborate these observations in TKA/THA.

We show that, unlike the non-significant decrease observed in the females, in males the higher salivary testosterone concentrations, alone, or together with low estradiol levels are associated with a better clinical response to surgery and rehabilitation. Our findings provide further evidence for a relationship between the sex hormone profile and recovery potential after tissue damage.

The findings from this cohort pilot study suggest the usefulness of molecular analysis of salivary testosterone and cortisol concentrations measured both as single values and in ratio to each other, in the evaluation of clinical rehabilitation outcomes in men and women undergoing TKA and THA.

The main limitation of this study was the small, heterogeneous study population composed of otherwise healthy OA patients. Comorbidities were excluded on the basis of the Charlson index and ASA scores to understand the hormone response to surgery and rehabilitation. Studies on larger cohorts are needed to confirm the usefulness of salivary testosterone in monitoring clinical response during the perisurgical period and rehabilitation in middle-aged patients undergoing knee or hip arthroplasty.

The main findings of this study are:

i)a better clinical response to TKA/THA was observed among the men in an otherwise healthy population of patients with OA;

ii) a significant indirect relationship exists between changes in salivary testosterone concentrations and indices of clinical response (FIM®, BI);

iii) a significant direct relationship between male testosterone levels and decreases in pain VAS scores suggest the usefulness of monitoring these parameters in future larger studies;

iv) saliva is an easily accessible sample matrix that may provide a useful noninvasive diagnostic tool in rehabilitation after knee or hip replacement.

ACKNOWLEDGEMENTS

This research was funded by the Italian Ministry of Health.

REFERENCES

1. Lu Y, Jiang Q, Yu L, Lu ZY, Meng SP, Su D, Burnstock G, Ma B. 17beta-estradiol rapidly attenuates P2X3 receptor-mediated peripheral pain signal transduction via ERalpha and GPR30. Endocrinology 2013; 154:2421-33.
2. Ji Y, Tang B, Traub RJ. Spinal estrogen receptor alpha mediates estradiol-induced pronociception in a visceral pain model in the rat. Pain 2011; 152:1182-91.
3. Sorge RE, LaCroix-Fralish ML, Tuttle AH, et al. Spinal cord Toll-like receptor 4 mediates inflammatory and neuropathic hypersensitivity in male but not female mice. J Neurosci 2011; 31:15450-54.
4. Aloisi AM, Affaitati G, Ceccarelli I, et al. Estradiol and testosterone differently affect visceral pain-related behavioural responses in male and female rats. Eur J Pain 2010; 14:602-7.
5. Horlocker TT. Pain management in total joint arthroplasty: a historical review. Orthopedics 2010; 33:14-9.
6. Perazzo P, Vigano M, De Girolamo L, Verde F, Vinci A, Banfi G, Romagnoli S. Blood management and transfusion strategies in 600 patients undergoing total joint arthroplasty: an analysis of pre-operative autologous blood donation. Blood Transfus 2013; 11:370-6.
7. Amory JK, Chansky HA, Chansky KL, Camuso MR, Hoey CT, Anawalt BD, Matsumoto AM, Bremner WJ. Preoperative supraphysiological testosterone in older men undergoing knee replacement surgery. J Am Geriatr Soc 2002; 50:1698-701.
8. Pfaffe T, Cooper-White J, Beyerlein P, Kostner K, Punyadeera C. Diagnostic potential of saliva: current state and future applications. Clin Chem 2011; 57:675-87.
9. Charlson ME, Pompei P, Ales KL, MacKenzie CR. A new method of classifying prognostic comorbidity in longitudinal studies: development and validation. J Chronic Dis 1987; 40:373-83.
10. Judge A, Cooper C, Arden NK, Williams S, Hobbs N, Dixon D, Gunther KP, Dreinhoefer K, Dieppe PA. Pre-operative expectation predicts 12-month post-operative outcome among patients undergoing primary total hip replacement in European orthopaedic centres. Osteoarthritis Cartilage 2011; 19:659-67.
11. Bijur PE, Silver W, Gallagher EJ. Reliability of the visual analog scale for measurement of acute pain.

Acad Emerg Med 2001; 8:1153-7.
12. Wade DT, Collin C. The Barthel ADL Index: a standard measure of physical disability? Int Disabil Stud 1988; 10:64-7.
13. Linacre JM. FIM levels as ordinal categories. J Outcome Meas 2000; 4:616-33.
14. Simundic AM. Practical recommendations for statistical analysis and data presentation in Biochemia Medica journal. Biochem Med 2012; 22:15-23.
15. Papacosta E, Nassis GP. Saliva as a tool for monitoring steroid, peptide and immune markers in sport and exercise science. J Sci Med Sport 2011; 14:424-34.
16. Gatti R, De Palo EF. An update: salivary hormones and physical exercise. Scand J Med Sci Sports 2011; 21:157-69.
17. Arregger AL, Contreras LN, Tumilasci OR, Aquilano DR, Cardoso EM. Salivary testosterone: a reliable approach to the diagnosis of male hypogonadism. Clin Endocrinol 2007; 67:656-62.
18. Grasso D, Corsetti R, Lanteri P, Di Bernardo C, Colombini A, Graziani R, Banfi G, Lombardi G. Bone-muscle unit activity, salivary steroid hormones profile, and physical effort over a 3-week stage race. Scand J Med Sci Sports 2015; 25:70-80.
19. Ferrando AA, Wolfe RR. Restoration of hormonal action and muscle protein. Crit Care Med 2007; 35:S630-4.
20. Zofkova I. Hormonal aspects of the muscle-bone unit. Physiol Res 2008; 57(S1):S159-69.
21. Niissalo S, Hukkanen M, Imai S, Tornwall J, Konttinen YT. Neuropeptides in experimental and degenerative arthritis. Ann N Y Acad Sci 2002; 966:384-99.
22. Riad M, Mogos M, Thangathurai D, Lumb PD. Steroids. Curr Opin Crit Care 2002; 8:281-4.
23. Marik PE, Flemmer M. The immune response to surgery and trauma: Implications for treatment. J Trauma Acute Care Surg 2012; 73:801-8.
24. Straub RH. The complex role of estrogens in inflammation. Endocr Rev 2007; 28:521-74.
25. Traub RJ, Ji Y. Sex differences and hormonal modulation of deep tissue pain. Front Neuroendocrinol 2013; 34:350-66.
26. Cairns BE, Gazerani P. Sex-related differences in pain. Maturitas 2009; 63:292-6.

JOURNAL OF BIOLOGICAL REGULATORS & HOMEOSTATIC AGENTS Vol. 29, no. 4, 961-967 (2015)

LETTER TO THE EDITOR

DENTAL PULP IN MATURE REPLANTED HUMAN TEETH: MORPHOLOGICAL ALTERATIONS AND METALLOPROTEINESES-2 AND -9, ANNEXIN-5, BCL-2 AND iNOS MODULATION

A. LEONE[1-2], A. ANGELOVA VOLPONI[2], ML. UZZO[1], GF. SPATOLA[1], A. JURJUS[3] and V. VANDEVSKA–RADUNOVIC[4]

[1]Department of Experimental Biomedicine and Clinical Neurosciences, Section of Histology, University of Palermo, Palermo, Italy; [2]Department of Craniofacial Development and Stem Cell Biology, King's College, London, UK; [3]Department of Anatomy, Cell Biology and Physiology, American University of Beirut, Beirut Lebanon; [4]Department of Orthodontics, Institute of Clinical Dentistry, University of Oslo, Oslo, Norway

Received June 24, 2015 – Accepted October 5, 2015

All authors share the same authorship

Tooth replantation, as a treatment concept, has been subject to controversies regarding the mechanism as well as the various parameters underlying this process. This work aimed to study time-related changes in the pulp of replanted mature human premolars through the changes in the levels of certain factors involved in the underlying mechanisms of pulpal tissue healing after replantation. Eleven experimental mature teeth were extracted, immediately replanted in the original socket and left without any other intervention for 1, 2, 3 and 12 weeks before re-extraction. Three premolars served as control. All specimens were subject to histological analysis and the levels of MMP-2, MMP-9, Annexin V, iNOS and BCL-2 (anti-apoptotic family) were analyzed employing immunohistochemistry. The results showed degradation of the extracellular matrix (ECM), inflammatory cell infiltrate, loss in pulpo-dentine interface and loss of odontoblasts in the dental pulp tissue. This was accompanied by increase over time of MMP-9, Annexin V, iNOS and a decrease of BCL-2 and MMP-2, suggesting that apoptosis increased throughout the experimental period.

Dental pulp is a connective tissue that is well vascularized and innervated, capable of limited repair after trauma and/or noxious stimuli (1). Tooth replantation and transplantation are clinical procedures where pulpal tissues undergo temporal disruption of their vascular and neural supply. The initial pulpal reaction may be inflammation, degeneration of the osteoblast layer and in most severe cases, necrosis (2, 3). However, under favorable conditions, the pulpal tissues may demonstrate revascularization, re-innervation, and formation of reparative dentin. (4-6).

Matrix metalloproteinases (MMP's) are endopeptidases that take part in the degradation

Key words: dental pulp, replanted teeth, morphological alteration

Mailing address: Dr Angelo Leone
BioNec , Section of Histology and Embryology
School of Medicine, University of Palermo
Via del Vespro, 129
90127 Palermo - Italy
Tel +39 0916553581
e-mail: angelo.leone@unipa.it

0393-974X (2015)

DISCLOSURE: ALL AUTHORS REPORT NO CONFLICTS OF INTEREST RELEVANT TO THIS ARTICLE.

of extracellular matrix (ECM) components and mediate tissue remodeling in hard tissues such as bone (7). They have been identified in clinically healthy and inflamed pulp tissues (8), suggesting that they participate in the regulation of inflammatory mediators (9). Moreover, vascular cell apoptosis, proliferation, and angiogenesis can also be moderated by MMPs (10), changes that follow the pulp tissue reaction to teeth replantation. In a previous study, we showed that decrease of metalloproteinase activity after orthodontic traction may be an impediment to the regeneration of the ECM and the restoration of dental pulp structure (11).

A well-known hallmark of apoptosis, particularly in the early events, is Annexin V (12). Annexin V is involved in the process of apoptosis following tooth development (13), where apoptosis occurs at different stages of the development as a physiological event. The control of apoptosis as a process is influenced by the interplay between members of the B-cell lymphoma 2 (BCL-2) family, indicating these factors as players in the physiological control of apoptosis (14). BCl-2 is considered to be an anti-apoptotic member of the BCL-2 family and is shown to be an important factor for preventing apoptosis of odontoblasts and promoting dentin damage repair (15).

When a cascade of an immune response is triggered as a consequence of an injury or a noxious factor, the cells of the immune system produce nitric oxide (NO), a short lived highly reactive free radical with cytotoxic properties damaging host tissue. It has been recognized that NO causes induction of apoptosis in human dental pulps (16-18) and was indicated as a factor in the production of tertiary dentin by odontoblasts (19).

The purpose of this study was to investigate time-related changes in the pulp of replanted human premolars through the expression and distribution of MMPs, NO, Annexin V and BCl-2.

MATERIALS AND METHODS

Collection of the material was performed at the Department of Orthodontics, University of Oslo, according to the procedure described in detail by Breivik and Kvam (20). The material was obtained from twelve girls (age: 10.2-19.7 years) and twelve boys (age: 10.2-13.3 years) where extractions of teeth (two or four premolars) were needed as part of their orthodontic treatment. Experimental teeth were extracted and immediately replanted into the original socket, marked as time point zero (T0) and left without any other intervention for 1, 2, 3 and 12 weeks before re-extraction (T1). Each subject had one premolar extracted as a control at T1. The teeth were fixed in 4% paraformaldehyde (PFA), embedded in paraffin and sectioned at 5 μm thick sections for further analysis. Approximately half of the sections were stained with haematoxylin and eosin (H&E) and used for histological evaluation in previous studies (3, 21). The rest of the sections were stored at room temperature and some of them used for immunohistochemical analysis in this study.

In this investigation, a total of fourteen mature teeth were used: eleven teeth representing 1 (n=2), 2 (n=2), 3 (n=4) and 12 (n=3) weeks after replantation and three control teeth. The slides were dewaxed and rehydrated by sequential immersion in a graded series of alcohols and transferred into water for 5 min. To inhibit any endogenous peroxidase activity, the slides were treated for 5 min with peroxidase quenching solution in hydrated incubation enclosure at room temperature. Subsequently, the slides were transferred to PBS (Na2HP04 , KH2P04, KCl, NaCl pH 7.4 - 7.6) at room temperature. The following protocol was realized using Histostain®-Plus 3rd Gen IHC Detection Kit with DAB chromogen as substrate (Invitrogen). After rinsing with PBS for 4 min, the sections were incubated with a blocking solution for 10 min and then incubated overnight at 4°C with rabbit anti-mouse MMP-9, full-length polyclonal antibody (Chemicon Intemational) diluted 1:100, mouse anti-human MMP-2 monoclonal antibody (Millipore, USA) diluted 1:100, rabbit monoclonal anti Annexin V antibody (Genetex Inc.) diluted 1:100, rabbit monoclonal Anti iNOS antibody (Genetex Inc.) diluted 1:100, mouse monoclonal anti BCL-2 clone 100 antibody (Millipore) diluted 1:100.

After incubation, slides were washed with PBS for 5 min and the sections were incubated with biotinylated secondary antibody for 20 min at room temperature. Unbound antibody was removed by washing (2x with PBS, 5 min each), followed by Streptavidin-Peroxidase conjugate for 10 min. To reveal the reaction DAB chromogen in substrate buffer was added for 5 min and stopped in distilled water. The slides were removed from the water and mounted with one drop of aqueous mounting medium (DAKO, Faramount). Negative controls were performed by omission of primary antibody, and by incubating sections with antiserum saturated with homologous antigen. Finally, the sections were observed with Leica Laborlux S microscope.

Image analysis

The immunohistochemical specimens were examined

using a Leica DM1000 Microscope (Leica Microsystem GmbH Wetzlar, Germany) with a Leica digital photographic system. Each sample was analyzed with double-blind system and two different operators. Moreover, the results were compared to an image analysis obtained from TIFF files. Adobe Photoshop CS6 extended (Adobe System Inc, San Jose, CA, USA) was used to elaborate images and perform an image analysis (22, 23). The images were analyzed in CMYK color profile, using the yellow channel for a best linear response to color intensity (24). All the images, converted in a gray scale inverted images, were analyzed and a range of 0-255 value was detected, where 0 marked the maximum black value and 255, marked the maximum white value. The colorimetric analysis was performed for the entire pulp tissue surface and the values were expressed in the following scale range: "+" (0-50); "++" (51-100); "+++" (101-150); "++++" (151-200); "+++++" (2001-255) (24).

RESULTS

Control teeth

Teeth stained with H&E (Fig. 1 A1), exhibit normal histological features of well organized connective pulp tissue (P) with visible blood vessels (BV) and tubular dentin (D). Distinct odontoblast layer (Ob) was present adjacent to the pulp-dentin border. Immunohistochemical staining did not show particular accumulation, showing homogeneous distribution throughout the pulp tissue (Fig. 1 B1-F1).

Quantitatively, the expression of MMP-2 and BCL-2 was strongest, while MMP-9, Annexin V and iNOS showed low colorimetric staining (Table I).

1-3 weeks

The results obtained from teeth extracted 1, 2 and 3 weeks after replantation were similar in histological changes, accumulation pattern and quantitative expression of the markers. Therefore, these time points were treated as one experimental group. The pulp tissue (P) showed irregular fibrous matrix, loss of normal vasculature and abnormal odontoblast layer (Fig. 1 A2). The pulp-dentine junction showed areas of interruption (arrows) with infiltration of inflammatory cells (circled areas). Some vacuolization was present (Fig. 1 E2 *asterisk) next to the pulp-dentin junction.

Immunohistological analysis revealed homogeneous distribution of immunopositive cells throughout the pulp tissue, with no particular accumulation (Fig. 1 B2, C2, E2, F2), except for the Annexin V (Fig. 1 D2), where more positive cells (arrows) were present in the odontoblast area (Ob) next to the pulp-dentine junction.

The intensity of the staining for MMP-2 and BCL2 was decreased compared to the control group, while the opposite was observed for MMP-9, Annexin V and iNOS (Table I).

12 weeks

The pulp was highly vacuolated, particularly evident next to the enamel-dentin junction with possible fluid accumulation in the interface (Fig. 1 A3 * asterisk area). Edema and inflammatory cells were visible throughout the pulp tissue (Fig. 1 A3), as well as red blood cells. The odontoblast layer was lost and gap was evident in the pulp-dentine junction area (Fig. 1 A3, D3, F3-square), leaving no clear alignment or histological features of odontoblasts.

Immunopositive cells for MMP 2, MMP9, iNOS and BCl2 were distributed throughout the pulp tissue, with no particular accumulation (Fig. 1 B3, C3, E3, F3), while Annexin V (Fig. 1 D3), positive cells (arrows) were more present in the odontoblast area (Ob) next to the pulp-dentine junction.

The intensity of the staining for MMP-9, Annexin V and iNOS was similar to the previous experimental periods, and higher than the control teeth. BCL2 showed further decrease in staining, while no changes were observed in MMP-2 (Table I).

DISCUSSION

Replantation of teeth is followed by a series of reactive alterations of dental pulp tissue. This is

Table I. *Quantification of colorimetric staining.*

	0	3 week	12 week
MMP2	+++	+	+
MMP9	+	++	+++
ANNEXINA V	+	+++	++
iNOS	+	+++	+++
BCL2	+++	++	+

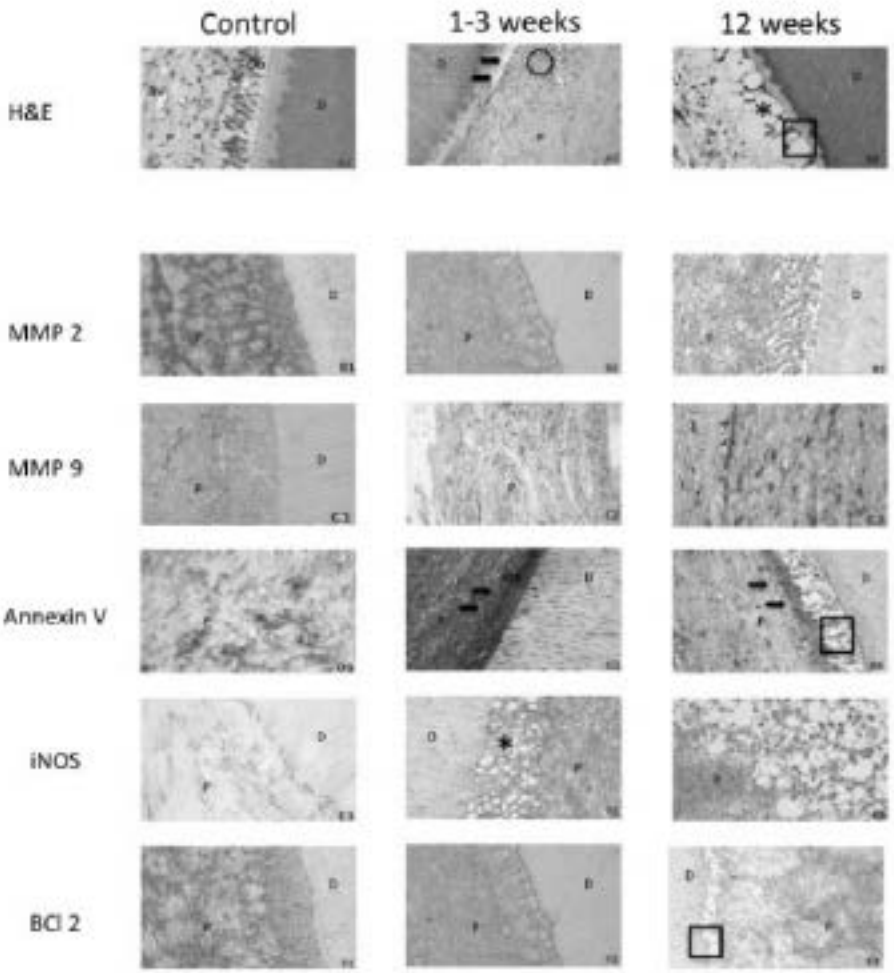

Fig. 1. *Histological alterations and expression of different markers of dental pulp tissue in human replanted teeth at different time points.* ***A)*** *H&E staining of dental pulp tissue in control (A1) shows normal histological features of the dental pulp tissue (P), visible blood vessels (BV) and tubular dentin (D). Distinct odontoblast layer (Ob) was adjacent to the pulp-dentin border. Replanted teeth after 1-3 weeks (A2) showed irregular fibrous matrix in the pulp tissue (P), loss of normal vasculature and abnormal odontoblast layer. (The pulp-dentine junction showed areas of interruption (arrows) with infiltration of inflammatory cells (circle areas). At 12 weeks (A3), the pulp (P) was highly vacuolated, particularly evident next to the enamel-dentin junction with possible fluid accumulation in the interface (* asterisk area). The odontoblast layer was lost and gap was evident in the pulp-dentine junction area (square).* ***B)*** *The immunohistochemical reaction of MMP-2. Decrease in the difference between Control (B1), 1-3 weeks (B2) and 12 weeks (B3) time points was noticeable. There is a significant decrease of MMP-2 with time in parallel to an increase of vacuolization of the pulp.* ***C)*** *Immunohistochemical reaction of MMP-9. Note the significant increase in MMP-9 stain after 1-3 weeks (C2) compared to Control (C1). MMP-9 continued to increase with time (C3).* ***D)*** *Immunohistochemical reaction of Annexin V. There was noticeable increase in Annexin V positive cells in time from Control (D1) to 1-3 weeks (D2), where there was a significant positive staining in the odontoblast layer (Ob), (arrows). This decreased in the 12 weeks group (D3-arrows), followed by noticeable gap at pulp-dentin junction (square).* ***E)*** *Immunohistochemical reaction of induced nitric oxide (iNOS). The immunopositive cells increased through time (E1-E3) with vacuolisation in the pulp-dentin junction starting at 1-3 weeks time point (D2-asterisk).* ***F)*** *Immunohistochemical reaction of BCL-2. The BCl-2 expression decreased through time (F1-3), with more evident gap in the pulp dentin junction (D3-square), indicating advanced degenerating changes in the dental pulp at this time point. (Images taken at x400).*

due to the severed vascular and nerve supply that accompanies the procedure and consequently triggers inflammatory and degenerative changes in the dental pulp (3). Subsequent healing of the pulp takes place in a high percentage of replanted immature teeth, but also, to a lesser extent, in mature teeth (6). A number of investigations have attempted to examine the underlying biological mechanisms determining the healing process, but the majority is descriptive and almost exclusively carried out on animal teeth (25-28). Therefore this histological material provides a unique opportunity to study the time-related pulpal tissue changes after replantation of mature human teeth.

A previous study showed that degradation of dental pulp tissue, losing its anatomical "order" and disturbances in the odontoblastic layer, as well as severed vascularization of the dental pulp tissue was noticeable within 3 weeks of replantation of mature human premolars (3). This was confirmed in the present study, where the histological appearance of the pulp was noticeably different from that of the control teeth showing signs of inflammation and partial loss of the normal odontoblastic layer. Such a reaction was aggravated by a later time point (12 weeks), leading to more dramatic changes due to inflammatory reaction followed by fibrosis and vacuolization of the dental pulp tissue, loss of a distinct odontoblast layer and a consequent degeneration of the dental pulp tissue. There was a loss of distinct blood vessels, usually present in a healthy pulp tissue, but a presence of blood cells, as a consequence of bleeding, was noticeable.

In order to study the main mechanisms that underlie the changes, we assumed the role of inflammation and apoptosis as being main processes following the replantation of teeth, causing changes in the dental pulp tissue.

Inflammatory cells infiltrated the pulp tissue after 3 weeks and increased more by 12 weeks. This was followed by an increase in MMP-9 through the different time points, as a result of degradation of the extracellular matrix. The present results confirm the data of previous reports on the increase in MMP-9 during inflammatory processes (29, 30).

On the other hand, there was less presence of MMP-2 in the dental pulp with the progression of time. Although this observation was in contradiction to previous reports (8), it was in accordance with other studies where MMP-2 was proposed to be able to release active Tumor Growth Factor β 2 (TGF-β 2) during noxious stimulated conditions (such as caries), which can then stimulate diverse repair processes (31).

Further studies focusing on TGF-β 2 and other factors such as Tissue Inhibitors of Metalloproteinases (TIMPS) may explain the results, as these inhibitors might act ambiguously at times, favoring the activation, or inhibiting the MMP-2 (8, 32).

The observed morphological alterations of the pulp tissue suggested an increase in apoptosis. This has been confirmed by an increase in Annexin V, well-known hallmark of apoptosis (12), and the decrease in the anti-apoptosis protein BCL-2, recently indicated as an important factor where its over expression can prevent odontoblastic apoptosis and promote dentin damage repair (15). Annexin V increased from day zero (+1) to week 3 (+3) then decreased (+2) by 12 weeks when necrotic changes were detected.

The increase in apoptosis is closely connected to the inflammatory processes and response of the dental pulp, confirmed and influenced by the increase of MMP-9 and iNOS which were increased over time. iNOS is a recognized mediator and regulator of the inflammatory response (16). NO is produced by nitric oxide synthase (NOS) which is abundantly expressed in human dental pulp cells and can be cytotoxic to these cells. It induces apoptosis and increases the number of Annexin V positive human dental pulp cells. It was suggested that NO induces apoptosis of human dental pulp cells (HDPC's) through the mitochondria dependent pathway (18). This NO-induced apoptosis could be influenced by modulation of BCl-2 (an anti-apoptotic BCL-2 family) in human dental pulp cells (17). Further studies including these factors might contribute to better understanding of the cascade of events that follow the triggering of the apoptosis. In addition, phagocytosis of the apoptotic odontoblasts and other pulp cells by scavenger cells may result in decrease of Annexin V level over time.

In our study we have shown a steady decrease in time in BCL-2, explaining the most obvious histological change in the dental pulp tissue - the loss of odontoblastic layer. BCl-2 has been indicated

as one of the important factors to promote dentin damage repair, when BCl-2 overexpression prevented artificial cavity-induced odontoblast apoptosis (15).

A study of the periodontal membrane proliferation, possible stem cell migration and the following changes could help in elucidating the homeostasis of renewing tooth tissues and maintaining a balance between cell proliferation, cell differentiation, and cell death (33).

In conclusion, the spectrum of histological alterations in replanted mature teeth indicate an ongoing inflammatory process depicted by the inflammatory cell infiltration leading to (i) ECM degradation through the increase and maintenance of high levels of MMP-9, (ii) increase in apoptosis, expressed by the increase of Annexin V and decrease of BCL-2, (iii) the loss of odontoblast layer, and (iv) eventually necrosis by 12 weeks of replantation. This study of mature human replanted teeth has its own limitations due to the small number of teeth and lack of long-term data. Furthermore, tracking the histological changes in the periodontal ligament might provide valuable data, however this was not possible in the present material.

REFERENCES

1. Smith AJ. Pulpal responses to caries and dental repair. Caries Res 2002; 36:223-32.
2. Rungvechvuttivittaya S, Okiji T, Suda H. Responses of macrophage-associated antigen-expressing cells in the dental pulp of rat molars to experimental tooth replantation. Arch Oral Biol 1998; 43:701-10.
3. Fiane JE, Breivik M, Vandevska-Radunovic V. A histomorphometric and radiographic study of replanted human premolars. Eur J Orthod 2014; 36(6):641-8.
4. Skoglund A, Tronstad L, Wallenius K. A microangiographic study of vascular changes in replanted and autotransplanted teeth of young dogs. Oral Surg Oral Med Oral Pathol Oral Radiol Endod 1978; 45:17-28.
5. Kvinnsland I, Heyeraas KJ, Byers MR. Regeneration of calcitonin gene-related peptide immunoreactive nerves in replanted rat molars and their supporting tissues. Arch Oral Biol 1991; 36:815-26.
6. Andreasen JO, Paulsen HU, Yu Z, Bayer T, Schwartz O. A long-term study of 370 autotransplanted premolars. Part II. Tooth survival and pulp healing subsequent to transplantation. Eur J Orthodont 1990; 12:14-24.
7. Paiva KB, Granjeiro JM. Bone tissue remodeling and development: focus on matrix metalloproteinase functions. Arch Biochem Biophys 2014; 561:74-87.
8. Accorsi-Mendonça T, Nogueira Leal Silva EJ, Marcaccini AM, Gerlach RF, Roncato Duarte KM, Souza Pardo AP, Peres Line SR, Zaia AA. Evaluation of gelatinases, tissue inhibitor of matrix metalloproteinase-2, and myeloperoxidase protein in healthy and inflammed human dental pulp tissue. J Endod 2013; 39(7):879-82.
9. Gusman H, Santana RB, Zehnder M. Matrix metalloproteinase levels and gelatinolytic activity in clinically healthy and inflamed human dental pulps. Eur J Oral Sci 2002; 110 (5):353-7.
10. Li Z, Chen Q, Jin M, Yang F, Zhu J, Xiao Q, Zhang L. Matrix metalloproteinases: inflammatory regulators of cell behaviors in vascular formation and remodeling. Mediators Inflamm 2013; doi: 10.1155/2013/928315.
11. Leone A, Mauro A, Spatola GF, et al. MMP-2, MMP-9, and iONS Expression in Human Dental Pulp Subjected to Orthodontic Traction. Angle Orthod 2009; 79:1119-25.
12. Marder LS, Lunardi J, Renard G, et al. Production of recombinant human annexin V fed-batch cultivation. BMC Biotechnol 2014; 14(1):14-33.
13. Bronckers AL, Goei SW, Dumont E, Lyaruu DM, Wöltgens JH, Van Heerde WL, Reutelingsperger CP, Van den Eijnde SM. In situ detection of apoptosis in dental and periodontal tissues of the adult mouse using annexin-V-biotin. Histochem Cell Biol 2000; 113(14):293-301.
14. Czabotar PE, Lessene G, Strasser A, Adams JM. Control of apoptosis by the BCL-2 protein family: implications for physiology and therapy. Nat Rev Mol Cell Biol 2014; 15(1):49-63.
15. Zhang W1, Ju J. Odontoblast-targeted Bcl-2 overexpression promotes dentine damage repair. Arch Oral Biol 2012; 57(3):285-92.
16. Korhonen R, Lahti A, Kankaanranta H, Moilanen E. Nitric oxide production and signaling in inflammation. Curr Drug Targets Inflamm Allergy 2005; 64:749-74.

17. Park SY, Jeong YJ, Kim SH, Jung JY, Kim WJ. Epigallocatchin gallate protects against nitric oxide-induced apoptosis via scavenging ROS and modulating the Bcl-2 family in human dental pulp cells. J Toxicol Sci 2013; 38(3):371-8.
18. Park MY, Jeong YJ, Kang GC, Kim SH, Chung HJ, Jung JY, Kim WJ. Nitric oxide-induced apoptosis of human dental pulp cells is mediated by the mitochondria-dependent pathway. Korean J Physiol Pharmacol 2014; 18(1):25-32.
19. Yasuhara R, Suzawa T, Miyamoto Y, Wang X, Takami M, Yamada A, Kamijo R. Nitric oxide in pulp cell growth, differentiation, and mineralization. J Dent Res 2007; 86(2):163-68.
20. Breivik M, Kvam E. Evaluation of histologic criteria applied for description of pulp reactions in replanted human premolars. Scand J Dent Res 1977; 85:392-95.
21. Breivik M. Human odontoblast response to tooth replantation. Eur J Orthod 1981; 3:95-108.
22. Lehr HA, Mankoff DA, Corwin D, Santeusanio G, Gown AM. Application of photoshop-based image analysis to quantification of hormone receptor expression in breast cancer. J Histochem Cytochem 1997; 45(11):1559-65.
23. Kirkeby S, Thomsen CE. Quantitative immunohistochemistry of fluorescence labelled probes using low-cost software. J Immunol Methods 2005; 301(1-2):102-13.
24. Pham NA, Morrison A, Schwock J, Aviel-Ronen S, Iakovlev V, Tsao MS, Ho J, Hedley DW. Quantitative image analysis of immunohistochemical stains using a CMYK color model. Diagn Pathol 2007; 27:2-8.
25. Öhman A. Healing and sensitivity to pain in young replanted human teeth. An experimental and histological study. Odontol Tidsk 1965; 73:166-227.
26. Ohshima H, Nakakura-Ohshima K, Yamamoto H, Maeda T. Alteration in the expression of heat shock protein (Hsp) 25-immunoreactivity in the dental pulp of rat molars following tooth replantation. Arch Histol Cytol 2001; 64:425-37.
27. Schwartz O, Andreasen J O. Allo- and autotransplantation of mature teeth in monkeys: a sequential time-related histoquantitative study of periodontal and pulpal healing. Dent Traumatol 2002; 18:246-61.
28. Ogawa R, Saito C, Jung H S, Ohshima H. Capacity of dental pulp differentiation after tooth transplantation. Cell Tissue Res 2006; 326:715-24.
29. Leone A, Uzzo ML, Rappa F, Abdallah Hajj Hussien I, Gerbino A, Spatola GF, Jurjus A. Immunohistochemical expression of apoptotic factors, cytokeratins, and metalloproteinase-9 in periapical and epithelialized gingival lesions. Folia Histochem Cyto 2012; 50(4):497-503.
30. Tsai CH, Chen YJ, Huang FM, Su YF, Chang YC. The upregulation of matrix metalloproteinase-9 in inflamed human dental pulps. Journal Endod 2005; 31(12):860-62.
31. Charadram N1, Farahani RM, Harty D, Rathsam C, Swain MV, Hunter N. Regulation of reactionary dentin formation by odontoblasts in response to polymicrobial invasion of dentin matrix. Bone 2012; 50(1):265-75.
32. Nakata K1, Yamasaki M, Iwata T, Suzuki K, Nakane A, Nakamura H. Anaerobic bacterial extracts influence production of matrix metalloproteinases and their inhibitors by human dental pulp cells. J Endod 2000; 26(7):410-13.
33. Sato K, Muramatsu T, Tsuchiya Y, Masaoka T, Enokiya Y, Hashimoto S, Shimono M. Proliferation, migration and apoptosis of periodontal ligament cells after tooth replantation. Oral Dis 2010; 16:263-8.

JOURNAL OF BIOLOGICAL REGULATORS & HOMEOSTATIC AGENTS Vol. 29, no. 4, 969-976 (2015)

LETTER TO THE EDITOR

AIRBORNE NITRIC OXIDE AND NASAL CYTOLOGY IN PATIENTS WITH CHRONIC RHINOSINUSITIS AND NASAL POLYPS

S. TORRETTA, M. CAPPADONA, D. CAIROLI and L. PIGNATARO

Department of Clinical Sciences and Community Health, Fondazione IRCCS Ca` Granda Ospedale Maggiore Policlinico, Università degli Studi di Milano, Milan, Italy

Received July 21, 2015 – Accepted October 14, 2015

Nitric oxide (NO) is involved in eosinophilic inflammation. The fraction of exhaled nitric oxide (FENO) is increased in chronic rhinosinutis with nasal polyps (CRSwNP), whereas nasal NO (nNO) is reduced in chronic rhinosinutis. Nasal cytology can detect eosinophilic inflammation in CRSwNP. We aimed to describe the baseline rhinocytological characteristics and NO (FENO and nNO) levels in patients with CRSwNP, and assess their possible correlations. This longitudinal study involved 37 consecutive adult outpatients with CRSwNP and 36 healthy controls. They underwent a complete clinical otolaryngological assessment, measurement of FENO and nNO levels, and nasal scraping in order to collect material for nasal cytology. Disease severity was evaluated by means of endoscopic and Lund-Mackay radiological scores. Median FENO level was higher (p <0.001) in CRSwNP (28.3 ppb, 95%CI 13.0-33.6 ppb) than in the controls (7.5 ppb, 95%CI 6.1-8.9 ppb). Median nNO levels were lower (255.7, 95%CI 199.7-311.6 *vs* 385.5, 95%CI 345.0-425.9 ppb; p <0.001), and were lower in the patients with severe endoscopic obstruction (p=0.05). Lund-Mackay scores positively correlated with median FENO levels (R=0.11; p=0.05), and inversely with median nNO levels (R=-0.31; p=0.04). Metachromatic nasal cytotypes were more prevalent among CRSwNP patients who had previously undergone surgery (p=0.05). The number of metachromatic elements in the patients with CRSwNP positively correlated with their median FENO levels (R=0.24; p=0.002). Our results confirm the dynamic interplay between the upper and lower airways in patients with CRSwNP. FENO/nNO and nasal cytology can be useful for detecting and monitoring nasal inflammation in CRSwNP.

Nitric oxide (NO) is a biological messenger, produced by the ciliated human epithelium and inflammatory cells such as eosinophils and macrophages, which is increased during airway inflammation (1). Measurement of the fraction of exhaled NO (FENO; i.e. the orally exhaled NO produced by the lower airways) has become a standardised, non-invasive, time- and cost-effective means of diagnosing and therapeutically managing patients with asthma and lower airway disease, because it has been reported that FENO levels increase in the case of eosinophilic airway inflammation (2) and they seem to correlate with its extent (3). As chronic rhinosinusitis with nasal polyps (CRSwNP) is characterised by conspicuous eosinophilic inflammation and Th2 polarization (4) and epidemiological studies (5) have shown that asthma co-exists in at least 34% of cases, FENO

Key words: nitric oxide, nasal cytology, rhinosinusitis, polyposis, eosinophils

Mailing address: Sara Torretta, MD
Department of Clinical Sciences and Community Health,
University of Milan, Fondazione I.R.C.C.S. Cà Granda,
Ospedale Maggiore Policlinico,
Via F. Sforza 35, 20122 Milano, Italy
Tel.: +39 0250320245 Fax: +39 0250320248
e-mail: sara.torretta@gmail.com

0393-974X (2015)

DISCLOSURE: ALL AUTHORS REPORT NO CONFLICTS OF INTEREST RELEVANT TO THIS ARTICLE.

levels are generally increased in patients with CRSwNP (6, 7). On the other hand, it has been reported that various respiratory tract diseases are characterised by altered levels of nasal NO (nNO); i.e.: NO produced by the mucosa of the paranasal sinuses, which can be measured by aspirating the air in the nasal cavities (8). As reduced nNO levels have been described in patients with cystic fibrosis and primary ciliary dyskinesia, nNO measurement is currently considered a reliable means of screening chronic lung disease (8). Reduced nNO levels have also been reported in patients with CRSwNP or acute and chronic rhinosinusitis without nasal polyps (CRSsNP) (6, 9). Nasal cytology has been introduced as a fast, repeatable and inexpensive means of diagnostically managing rhinosinusitis, and is capable of assessing the presence and number of metachromatic elements suggesting Th2 activation (10, 11).

The aim of this study was to describe the baseline rhinocytological characteristics and NO (FENO and nNO) levels of consecutive adult outpatients with CRSwNP and otherwise healthy candidates for elective ENT surgery (septoplasty, turbinoplasty, or salivary gland or laryngeal surgery for benign diseases), and to assess the possible correlations between nasal cytotypes and FENO or nNO levels, and between these parameters and other clinical and radiological characteristics. All of the patients underwent a complete ENT examination, including flexible fibre nasal endoscopy (Olympus ENF-P4, Olympus Corporation, Japan): the severity of nasal polyposis was endoscopically graded (Fig. 1), with severe endoscopic nasal obstruction being defined as

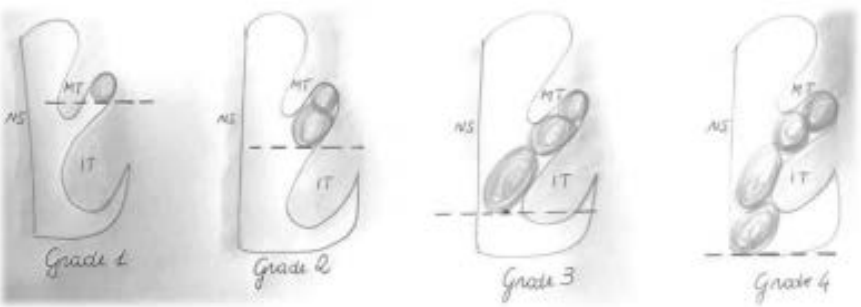

Fig. 1. *Endoscopic classification.*

Table I. *Demographic and clinical characteristics.*

	CRSwNP (n=37)	Controls (n=36)	p-value	Total (n=73)
No. of males (%)	23 (62.2)	20 (55.6)	n.s.	43 (58.9)
Median age (95%CI), years	51.5 (47.5-55.5)	48.0 (34.6-45.4)	n.s.	46.0 (23.0-72.0)
No. with allergy (%)	20 (54.0)	14 (38.9)	n.s.	34 (46.6)
No. with asthma (%)	22 (59.5)	18 (50.0)	n.s.	40 (54.8)
No. previously undergoing ESS (%)	24 (64.9)	-	-	-
Median SNOT-20 score (95%CI) [19]	16 (0-41)	-	-	-
Median Lund score (95%CI) [18]	8 (2-11)	-	-	-
Median FENO (95%CI), ppb	28.3 (13.0-33.6)	7.5 (6.1-8.9)	< 0.001	9.3 (3-41.2)
Median nNO (95%CI), ppb	255.7 (199.7-311.6)	385.5 (345.0-425.9)	< 0.001	299.1 (78.0-610.3)
No. with pathological nasal cytotype (%)	26 (70.3)	15 (41.7)	0.02	41 (56.2)
No. with metachromatic nasal cytotype (%)	21/28 (75.0)	9/13 (69.2)	n.s.	30 (73.2)

CRSwNP: chronic rhinosinutis with nasal polypos; FENO: fraction of exhaled nitric oxide; nNO: nasal nitric oxide; ESS: endoscopic sinus surgery; 95%CI: 95% confidence interval; ppb: parts per billion

an endoscopic score of ≥3, and scored using Lund-Mackay's radiological classification (12).

The standardised Sino-nasal Outcome Test (SNOT-20) (13) questionnaire was filled in by all of the patients in order to evaluate the subjective burden of the disease and its impact on their quality of life. In accordance with the international guidelines (14), FENO and nNO were measured in parts per billion (ppb) using a single-breath on-line method at constant flow by means of a dedicated chemiluminescence analyser (CDL 88 sp, Ecomedics, Dürnten, Switzerland). Nasal cytology was performed uing scrapings collected during anterior rhinoscopy from the middle portion of the inferior turbinate using a disposable nasal mucosa curette (Rhino-probe™, Arlington Scientific, Inc., Springville, UT, USA). The cellular material was examined under a light microscope using Meltzer and Jalowayski's semi-quantitative grading (15). Normal smears contain only epithelial cells and rare neutrophils; the pathological nasal cytotypes were defined on the basis of cell predominance as follows: i) an eosinophilic form (nasal eosinophils >20% of total cells); ii) a mast cell form (nasal mast cells >10% of total cells); iii) a neutrophilic form (nasal neutrophils >50% of the total cells without any bacterial or fungal element); and iv) a mixed eosinophilic–mast cell form (eosinophils >20% and mast cells >10% of the total cells) (16).

The descriptive analysis was based on the data obtained from 73 subjects (median age 46 years, 95%CI 23-72; 58.9% males): 37 with CRSwNP and 36 controls (Table I). All the patients or their legal guardians gave their informed consent to partecipate in the study; the study was approved by our local Ethics Commitee, according to the declaration of Helsinki.

The median FENO level was significantly higher ($p<0.001$) in the patients with CRSwNP (28.3 ppb, 95%CI 13.0-33.6 ppb) than in the controls (7.5 ppb; 95%CI= 6.1-8.9 ppb), and median nNO levels were significantly lower (255.7 ppb, 95%CI 199.7-311.6 ppb *vs* 385.5 ppb, 95%CI 345.0-425.9 ppb; $p<0.001$) (Fig. 2, a and b). Pathological nasal cytotypes were more frequently detected among patients with CRSwNP (26/37, 70.3% *vs* 15/36, 41.7%; p 0.02), as were metachromatic nasal cytotypes (21/28, 75.0% *vs* 9/13, 69.2%; p = n.s.) (Table I). Median FENO levels were significantly higher in patients with asthma (27.9 ppb, 95%CI 11.3-34.9 ppb) than in

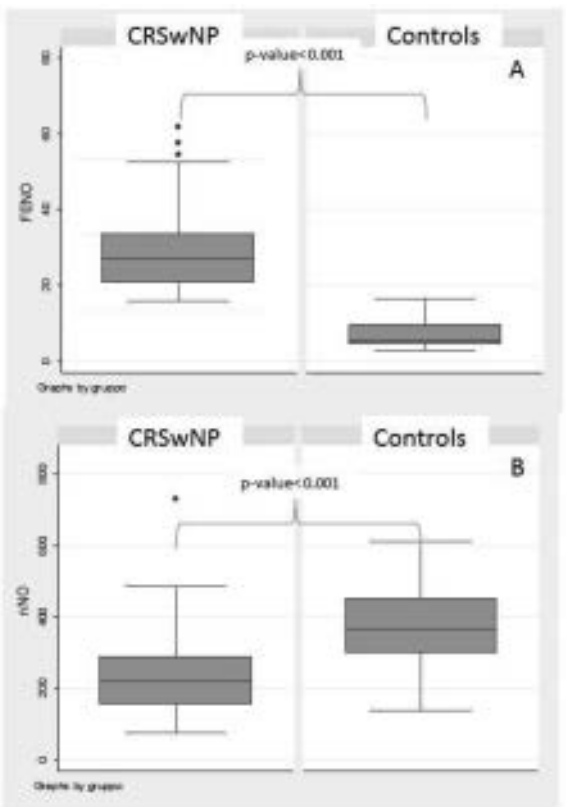

Fig. 2. *Median FENO (**a**) and nNO (**b**) levels in patients with CRSwNP and controls.*

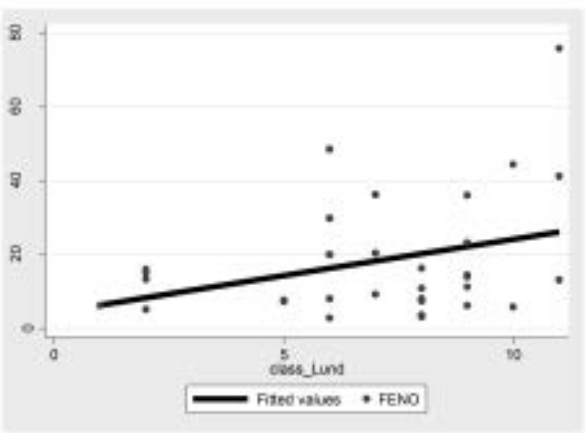

Fig. 3. *Correlation between Lund-Mackay score (18) and median FENO levels.*

Table II. *Median nNO in the whole population according to confounders.*

Variable		Median nNO (95%CI), ppb
Asthma	Yes	252.5 (188.9-316.2)
	No	348.6 (304.2-393.1)
	p-value	0.02
Rhinorrea	Yes	252.2 (170.0-280.4)
	No	350.6 (187.5-513.7)
	p-value	0.005
Hyposmia	Yes	226.2 (171.1-281.2)
	No	362.6 (186.2-539.0)
	p-value	0.04
Severe endoscopic nasal obstruction	Yes	166.2 (98.6-233.7)
	No	284.4 (215.3-353.6)
	p-value	0.05

nNO: nasal nitric oxide; 95%CI: 95% confidence interval; ppb: parts per billion

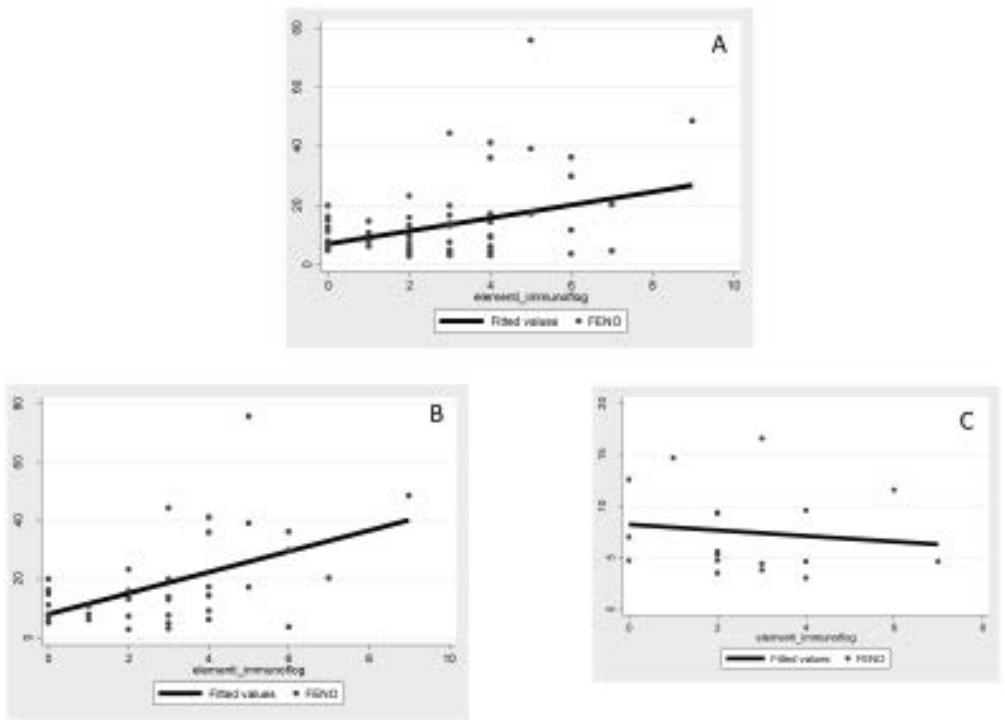

Fig. 4. *Correlation between median FENO levels and the number of pathological cell elements in the nasal smears of the population as a whole (**a**), the patients with CRSwNP (**b**), and the controls (**c**).*

those without (10.8 ppb, 95%CI 7.7-13.9; p=0.02), and they positively correlated with Lund-Mackay's scores (R=0.11; p=0.05) (Fig. 3). There were no other significant associations. Median nNO levels were significantly lower in patients with concomitant asthma (p=0.02), in patients with symptoms of nasal impairment such as rhinorrhea (p=0.05) and hyposmia (p=0.04), and in those with severe endoscopic nasal

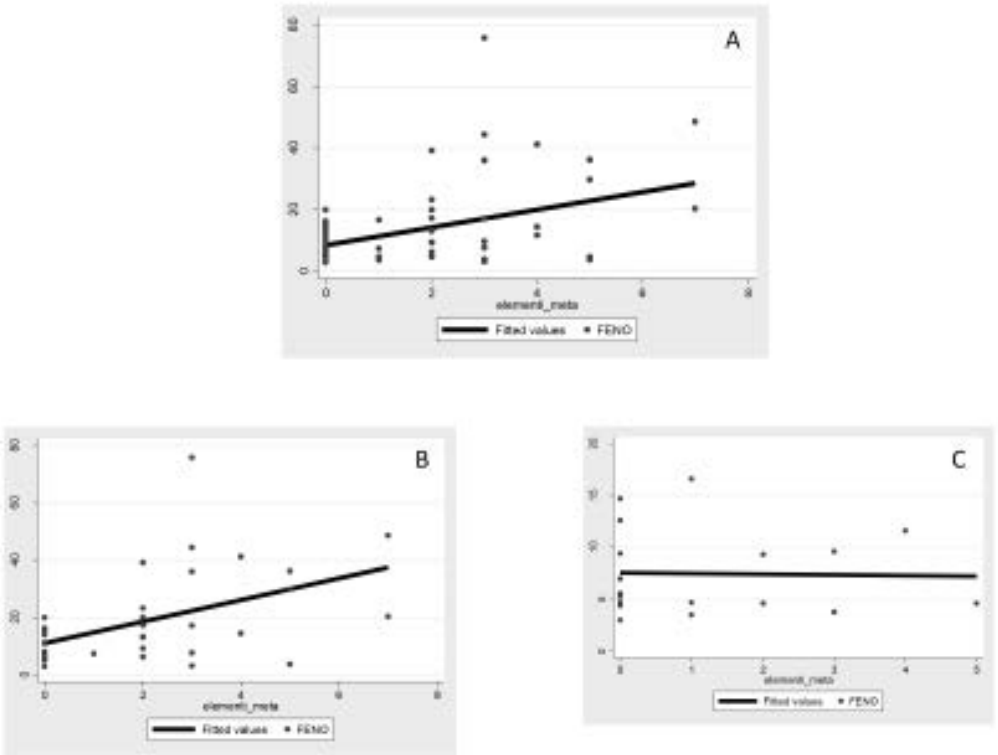

Fig. 5. *Correlation between median FENO levels and the number of metachromatic elements in the nasal smears of the population as a whole (**a**), the patients with CRSwNP (**b**), and the controls (**c**).*

Table III. *Median FENO and nNO levels according to nasal cytotype.*

Dependent variable	Independent variable		CRSwNP	Controls	Whole population
Median FENO (95% CI), ppb	Pathologic nasal cytotype	Yes	20.3 (13.8-26.8)	7.4 (5.8-9.0)	13.7 (10.1-17.4)
		No	11.1 (7.2-15.0)	8.1 (5.1-11.1)	9.8 (7.2-12.4)
		p-value	n.s.	n.s.	n.s.
	Metachromatic nasal cytotype	Yes	23.9 (16.1-31.8)	7.6 (5.5-9.7)	16.6 (11.5-21.7)
		No	10.1 (7.4-12.8)	7.4 (5.5-9.3)	8.6 (7.0-10.2)
		p-value	0.007	n.s.	0.007
Median nNO (95% CI), ppb	Pathologic nasal cytotype	Yes	261.1 (191.1-331.0)	405.5 (363.9-447.1)	334.5 (291.0-378.0)
		No	236.1 (155.8-316.5)	285.6 (162.6-408.6)	257.3 (197.1-317.6)
		p-value	n.s.	0.02	n.s.
	Metachromatic nasal cytotype	Yes	275.3 (184.3-366.3)	429.0 (374.2-483.9)	344.5 (285.5-403.4)
		No	226.9 (178.0-275.8)	341.9 (284.7-399.1)	289.6 (247.9-331.3)
		p-value	n.s.	0.03	n.s.

CRSwNP: chronic rhinosinutis with nasal polypos; FENO: fraction of exhaled nitric oxide; nNO: nasal nitric oxide; 95%CI: 95% confidence interval; ppb=parts per billion

obstruction (p=0.05) (Table II). There was also a significant inverse correlation between median nNO levels and Lund-Mackay's scores (R=-0.31; p=0.04). There were no other significant associations. There were no significant associations between the pathological nasal cytotypes and the patients' clinical characteristics, but metachromatic cytotypes were more prevalent among the patients with CRSwNP who had previously undergone surgical treatment (17/24, 70.8% *vs* 5/13, 38.5%; p=0.05).

The higher the median FENO levels, the higher the number of pathological cell elements in the nasal smears of the population as a whole (R=0.13; p<0.001) (Fig. 4a), but the group analyses showed that this association was only significant in patients with CRSwNP (R=0.26; p=0.001) (Fig. 4, b and c). Median FENO levels were higher in patients with pathological nasal cytotypes in the population as a whole (p=n.s.) and in the CRSwNP group (p=n.s.), but not in the control group (p=n.s.) (Table III). The higher the median FENO levels, the higher the number of metachromatic elements in the nasal smears of the population as a whole (R=0.17; p<0.001) (Fig. 5a) but, once again, the group analyses showed that this association was only significant in patients with CRSwNP (R=0.24; p=0.002) (Fig. 5, b and c). Median FENO levels were higher in patients with metachromatic nasal cytotypes in the population as a whole (p=0.007) and in the CRSwNP group (p=0.007), but no differences were detected in the control group (p=n.s.) (Table III).

There was no correlation between median nNO levels and the number of pathological cell elements in the nasal smears of the population as a whole or in either group, and comparisons between the patients with and without pathological nasal smears showed that the difference in their median nNO levels was significant only in the control group (p=0.02), and not in the CRSwNP group (p=n.s.) or in the population as a whole (p=n.s.) (Table III). Median nNO levels did not correlate with the number of metachromatic elements in the population as a whole or in either group, and comparisons between the patients with and without metachromatic elements showed that the difference in their median nNO levels was significant only in the control group (p=0.03), and not in the CRSwNP group (p=n.s.) or in the population as a whole (p=n.s.) (Table III).

DISCUSSION

Our findings confirm that gaseous airborne NO is impaired in patients with CRSwNP and are in line with those of previous studies (6, 7), and support the widely accepted "one airway, one disease" theory (17) based on the concept of the unification and dynamic interplay between the upper and lower airways. Under these conditions, NO may act as an aerocrine messenger linking the sino-nasal district and the lungs and enhance pulmonary oxygenation uptake (18). Our data also confirm previous findings (19) that FENO levels correlate with the presence of lower airway disease as median FENO levels were higher in patients with concomitant asthma, and showed a significant relationship with clinical obstruction as FENO levels directly correlated with the Lund-Mackay's scores (12). In addition, reduced nNO levels correlated with the presence of symptoms of nasal impairment, and median nNO levels inversely correlated with Lund-Mackay's scores, confirming previous experiences (6, 9). The biological significance of NO within the sino-nasal district is still unclear, but it is thought that nNO is involved in vasodilation (thus inducing mucosal swelling during rhinitis), and that it increases mucociliary beat frequency thus positively affecting paranasal mucociliary clearance (20). There is also some evidence that it plays an antiviral and bacteriostatic role in the local host defence system (21). The paradoxically low nNO concentration in CRSwNP patients may therefore be related to the sinus entrapment of NO as a result of the ostial obstruction caused by polyps, mucosal oedema and secretion retention, rather than a decreased sinusal production. The most frequently detected pathological nasal cytotype was characterised by the presence of metachromatic elements (i.e. eosinophils and/or mast cells), which were found in about 70% of our CRSwNP patients. This is in line with the findings of Gelardi et al. (10). We also found that metachromatic nasal cytotypes were more prevalent among CRSwNP patients who had previously undergone surgical treatment, thus confirming some evidence suggesting an increased risk of clinical relapse in patients with eosinophilic and mast cell elements (11). Median FENO levels significantly correlated with the presence of metachromatic elements in the

nasal smears of the population as a whole and the patients with CRSwNP. On the other hand, there was no significant relationship between nNO and nasal cytotypes in patients with CRSwNP, but significantly increased nNO levels correlated with the presence of metachromatic elements in the controls. To the best of our knowledge, these associations have never been tested before, but authors (22) investigating the possible relationship between sputum eosinophilia and FENO levels, found that sputum eosinophilia was more prevalent among patients with CRSwNP than those with CRSsNP, and positively correlated with increased FENO levels. On the basis of these findings, it can be speculated that the correlation between median FENO levels and the number of metachromatic elements in nasal smears further indicates that sino-nasal inflammatory diseases cause an inflammatory reaction in the lower airway leading to increased FENO production regardless of the co-existence of asthma, and it suggests the presence of an ubiquitous metachromatic inflammatory pattern in the airways of patients with CRSwNP. The absence of any association between nNO levels and the number of metachromatic elements in the nasal smears of patients with CRSwNP seems to suggest that impaired sinus ostium patency and mucociliary clearance (indirectly evaluated by nNO) does not correlate with nasal inflammation (evaluated by means of nasal cytology); however, this discrepancy may be partially attributable to the fact that the real intra-sinusal NO concentration is actually unknown, as ostial obstruction due to the presence of inflammatory tissue rich in metachromatic elements results in intra-sinusal NO entrapment and makes the measured nNO certainly underestimated (23). Therefore, metachromatic elements should be more correctly comparable not to nNO, but to the real intrasinusal NO.

In conclusion, the correlations between airborne NO concentrations and nasal cytology in patients with CRSwNP confirm the "one airway, one disease" theory and the dynamic interplay between the upper and lower airways. FENO/nNO measurements and nasal cytology seem to be useful means of detecting and monitoring nasal inflammation in patients with CRSwNP, and could also be hypothetically considered a guide to the treatment of chronic airway diseases.

REFERENCES

1. Williamson PA, Vaidyanathan S, Clearie K, M Stewart, Lipworth BJ. Relationship between fractional exhaled nitric oxide and nasal nitric oxide in airways disease. Ann Allergy Asthma Immunol 2010; 105:162-7.
2. Alving K, Weitzberg E, Lundberg JM. Increased amount of nitric oxide in exhaled air of asthmatics. Eur Respir J 1993; 6:1368-70.
3. Berry MA, Shaw DE, Green RH, Brightling CE, Wardlaw AJ, Pavord ID. The use of exhaled nitric oxide concentration to identify eosinophilic airway inflammation: an observational study in adults with asthma. Clin Exp Allergy 2005; 35:1175-9.
4. Van Zele T, Claeys S, Gevaert P, Van Maele G, Holtappels G, Van Cauwenberge P, Bachert C. Differentiation of chronic sinus diseases by measurement of inflammatory mediators. Allergy 2006; 61:1280-9.
5. Annesi-Maesano I. Epidemiological evidence of the occurrence of rhinitis and sinusitis in asthmatics. Allergy 1999; 54:7-13.
6. Jeong JH, Yoo HS, Lee SH, Yoon HJ, Kim SH. Nasal and exhaled nitric oxide in chronic rhinosinusitis with polyps. Am J Rhinol Allergy 2014; 28:e11-6.
7. Guida G, Rolla G, Badiu I, et al. Determinants of exhaled nitric oxide in chronic rhinosinusitis. Chest 2010; 137:658-64.
8. Balfour-Lynn IM, Laverty A, Dinwiddie R. Reduced upper airway nitric oxide in cystic fibrosis. Arch Dis Child 1996; 75:319-22.
9. Dabholkar YG, Saberwal AA, Velankar HK, Shetty AK , Chordia NP, Budhwani SR. Correlation of nasal nitric oxide measurement with computed tomography findings in chronic rhinosinusitis. Indian J Otolaryngol Head Neck Surg 2014; 66:92-6.
10. Gelardi M, Russo C, Fiorella ML, Fiorella R, Ciprandi G. Inflammatory cell types in nasal polyps. Cytopathology 2010; 21:201-3.
11. Gelardi M, Fiorella R, Fiorella ML, Russo C, Soleti P, Ciprandi G. Nasal-sinus polyposis: clinical-cytological grading and prognostic index of relapse. J Biol Regul Homeost Agents 2009; 23:181-8.
12. Lund VJ, Mackay IS. Staging in rhinosinusitus. Rhinology 1993; 31:183-4.

13. Piccirillo JF, Merritt MG Jr, Richards ML. Psychometric and clinimetric validity of the 20-Item Sino-Nasal Outcome Test (SNOT-20). Otolaryngol Head Neck Surg 2002; 126:41-7.
14. American Thoracic Society; European Respiratory Society. ATS/ERS recommendations for standardized procedures for the online and offline measurement of exhaled lower respiratory nitric oxide and nasal nitric oxide, 2005. Am J Respir Crit Care Med 2005; 171:912-30.
15. Meltzer EO, Jalowayski AA. Nasal cytology in clinical practice. Am J Rhinol 1988; 2:47-54.
16. Ellis AK, Keith PK. Nonallergic rhinitis with eosinophilia syndrome and related disorders. Clin Allergy Immunol 2007; 19:87-100.
17. Bachert C, Vignola AM, Gevaert P, Leynaert B, Van Cauwenberge P, Bousquet J. Allergic rhinitis, rhinosinusitis, and asthma: one airway disease. Immunol Allergy Clin North Am 2004; 24:19-43.
18. Lundberg JO, Lundberg JM, Settergren G, K Alving, Weitzberg E. Nitric oxide, produced in the upper airways, may act in an 'aerocrine' fashion to enhance pulmonary oxygen uptake in humans. Acta Physiol Scand 1995; 155:467-8.
19. Kharitonov SA, Yates D, Springall DR, Buttery L, Polak J, Robbins RA, Barnes PJ. Exhaled nitric oxide is increased in asthma. Chest 1995; 107:156S-157S.
20. Jain B, Rubinstein I, Robbins RA, Leise KL, Sisson JH. Modulation of airway epithelial cell ciliary beat frequency by nitric oxide. Biochem Biophys Res Commun 1993; 191:83-8.
21. Moncada S, Palmer RM, Higgs EA. Nitric oxide: physiology, pathophysiology, and pharmacology. Pharmacol Rev 1991; 43:109-42.
22. Wang W, Huang KW, Wu BM, Wang YJ, Wang C. Correlation of eosinophil counts in induced sputum and fractional concentration of exhaled nitric oxide and lung functions in patients with mild to moderate asthma. Chin Med J 2012; 125:3157-60.
23. Suojalehto H, Vehmas T, Lindström I, et al. Nasal nitric oxide is dependent on sinus obstruction in allergic rhinitis. Laryngoscope 2014; 124:E213-8.

LETTER TO THE EDITOR

MICROBIOLOGICAL INVESTIGATION OF MEDICATION-RELATED OSTEONECROSIS OF THE JAW: PRELIMINARY RESULTS

V. CRINCOLI[1], A. BALLINI[2], M. DI COMITE[2], L. TETTAMANTI[3], M.F. COSCIA[2], F. MASTRANGELO[4] and D. DE VITO[2]

[1]Department of Interdisciplinary Medicine, University of Bari Aldo Moro, Bari, Italy [2]Department of Base Medical Sciences, Neurosciences and Sense Organs, University of Bari Aldo Moro, Bari, Italy; [3]Department of Oral Science, Insubria University of Varese, Varese, Italy; [4]Unit of Dentistry, IRCCS San Raffaele Scientific Institute, Vita e Salute San Raffaele University, Milano, Italy

Received September 7, 2015 – Accepted October 28, 2015

Medication-related osteonecrosis of the jaw (MRONJ) is a well-recognized severe complication of bisphosphonate (BPs) treatment in patients with osteoporosis or metastatic cancer. Microbiological infection has been hypothesized as a contributing factor to bisphosphonate related osteonecrosis of the jaw (BRONJ). Despite infection being present in BRONJ patients, there is no clear data as to whether infection plays a role in the pathophysiology. Moreover, microbial cultures have not been helpful in directing therapy because specific pathogens have not been identified. The objective of this study was to determine the bacterial colonization of jawbone and identify the bacterial phylotypes associated with BRONJ. Twenty oncologic patients, aged 48-87 years (average age 70.65±8.86 years) with BRONJ were enrolled in this study and underwent three different microbiological samplings. Overall, 60 samples were obtained from oral mucosa, necrotic bone fragments and fistula drainage. The same procedure was performed for the laboratory culture of all these specimens. No significant differences regarding either gram+ and gram– species (*Chi*-squared= 0.1642; p = 0.6854) or aerobes and anaerobes bacteria (*Chi*-squared= 3.084; p = 0.0791) were found. Compared to other sampling techniques, the oral swab allowed to obtain valuable microbial data in order to recognize pathogens responsible for the infection and to outline a focused antimicrobial therapy.

Osteonecrosis of the jaw (ONJ) is a severe bone disease that affects both jaws.

ONJ associated with bisphosphonate treatment has been referred to by several acronyms including BRONJ (bisphosphonate-related ONJ), BRON (bisphosphonate-related osteonecrosis), BON (bisphosphonate osteonecrosis), BAONJ (bisphosphonate-associated ONJ), and simply ONJ (1-3). In 2014, the American Association of Oral and Maxillofacial Surgeons suggested a nomenclature change from BRONJ to Medication-related osteonecrosis of the jaw (MRONJ) to accommodate the growing number of gnathic osteonecrosis cases associated with other antiresorptive (denosumab)

Key words: medication-related osteonecrosis of the jaw (MRONJ), microbial flora, bone biopsy, fistula drainage, oral mucosa

Mailing address: Dr Andrea Ballini,
Department of Basic Medical Science,
Neurosciences and Sense Organs,
University of Bari Aldo Moro,
P.zza Giulio Cesare, 11, 70124, Bari, Italy
Tel/fax: +39 0803430657
e-mail: andrea.ballini@me.com

0393-974X (2015)

and antiangiogenic therapies (1).

The location of MRONJ is more often mandibular than maxillary (2:1 ratio), but can appear in both jaws (4, 5). In one review of 368 reported cases, 65% of ONJ was manifested in the mandible, 26% in the maxilla, and 9% in both (3). BRONJ is clinically diagnosed when the three following conditions are met: i) current or previous treatment with bisphosphonates (BPs), ii) persistent exposure of necrotized bone in the maxillofacial region for 8 weeks or longer, iii) no past medical history of radiotherapy for the jaw bone (4). The 8-week duration is consistent with the time frame in which most trauma, extractions and oral surgical procedures would have resulted in soft tissue closure and exposed bone would no longer be present (5, 6).Woo et al. (3) assumed that bisphosphonate-related osteonecrosis develops only in the jaw bones because, unlike other bones in the body, they are not sufficiently protected. On one hand, an important fact is that they are protected from possible intraoral trauma only by thin mucosa and periosteum (7). On the other hand, the presence of teeth in the jaw bone is a prerequisite which facilitates penetration of microbiota and development of intra□osseous infections via deep caries complications and the periodontium (8). Colonization has been reported in varying frequencies ranging from as low as 39% to as high as 100% (9).

On the basis of the hypothesis of microbial biofilms in ONJ secondary to BPs therapy (7-11), in the present study a microbiological investigation of the BRONJ lesions evaluating three different samples was performed. This was to assess whether one of these investigative techniques was more accurate and reliable than the others in selecting the microbial species colonizing the BRONJ lesions, with the aim to provide an appropriate antibiotic therapy to the bacterial species responsible for the BRONJ infection.

MATERIALS AND METHODS

Twenty oncologic patients with BRONJ, aged 48-87 years (average age 70.65±8.86 years) were enrolled in this study (14 females and 6 males) at the University Hospital of Bari, Italy. In order to minimize the operator's bias, surgical procedures were performed by only one operator, maintaining the same equipment in all performed surgical procedures. All patients gave informed consent and the study was carried out according to the Declaration of Helsinki.

Inclusion criteria were: patients who were undergoing, or who had undergone treatment with BPs, and were diagnosed with BRONJ according to the definition provided by the American Society for Bone and Mineral Research (ASBMR task force) (12) or patients with sites who had failed to heal for 8 weeks or longer despite continuous treatment with antimicrobial drugs from the time of first diagnosis. Exclusion criteria were: patients who had been given radiotherapy according to the definition provided by the American Association of Oral and Maxillofacial Surgeons (AAOMS) (4) and patients who had neoplastic involvement of the jaw.

The diagnosis of BRONJ was confirmed in all patients after clinical examination, including medical history, physical, and oral examinations, and radiographic examination by orthopantomogram, computed tomography (CT), and bone scan. The patients' personal information, type of bisphosphonate taken, together with doses, duration of use, and indicationa for use were recorded. The sites and sizes of the exposed necrotic bone, the presence of infection and pain, and the extension of lesions were also recorded, as were coexisting conditions including those patient-related (diabetes, obesity, and renal failure) and iatrogenic factors (use of steroids and chemotherapy).

Sampling methods

Sixty samples of different organic material were obtained by using 3 different sampling techniques:

a) 20 oral swabs (OS), using sterile dry mouth cotton swab were rubbed and rolled into osteonecrotic lesions;

b) 20 samples of purulent exudates (EX), from secreting fistulas, aspirated by a 19 Gauge needle in 10 cc sterile syringes;

c) 20 necrotic bone fragments (NBF), at least of 5 mm in diameter, removed by bone forceps during surgery and quickly inserted in a hermetic test-tube containing sterile saline solution.

Culture technique

The same procedure was performed for the culture of all the different specimens. Samples were immediately submerged in a culture medium containing thioglycolic acid after test tube heating at 80°C and water-cooling. Subsequent to the addition of liquid paraffin (mineral oil), the test tube was closed and incubated at 37°C for up to 5 days. An aliquot of the samples was then taken from the bottom of the test tubes and was placed on a Petri dish filled with Columbia II Agar Base.

The plates were placed in a GENbag system, which

Table I. *Data of patients in treatment with bisphosphonates.*

Patient number	*Sex*	*Age*	*Underlying disease*	*Bisphosphonate*	*Treatment duration (in month)*	*Tooth Extraction (Y/N)*	*Site of bone necrosis*
1	M	68	Multiple Myeloma	Zoledronate	12	Y	Right mandible
2	M	71	Multiple Myeloma	Zoledronate	12	Y	Maxilla (medial) Mandible (medial)
3	F	59	Multiple Myeloma	Pamidronate Zoledronate	96 12	Y	Right maxilla
4	M	48	Prostate cancer	Zoledronate	36	Y	Left mandible
5	M	76	Prostate cancer	Pamidronate Zoledronate	24 48	Y	Maxilla (medial)
6	F	70	Breast cancer	Zoledronate	36	Y	Left maxilla
7	F	66	Breast cancer	Zoledronate	24	Y	Right maxilla
8	F	78	Multiple Myeloma	Alendronate	72	Y	Left mandible
9	F	65	Breast cancer	Zoledronate	24	Y	Right mandible
10	F	68	Multiple Myeloma	Zoledronate	36	N	Left maxilla
11	M	61	Prostate cancer	Zoledronate	5	Y	Mandible (medial)
12	F	77	Thyroid cancer	Zoledronate	60	Y	Right mandible
13	F	79	Prostate cancer	Risedronate	48	Y	Mandible (medial)
14	F	87	Breast cancer	Alendronate	24	Y	Left mandible
15	F	81	Breast cancer	Zoledronate	18	Y	Right maxilla
16	F	73	Lung cancer	Zoledronate	36	Y	Left maxilla
17	F	66	Multiple Myeloma	Zoledronate	24	Y	Right Maxilla
18	M	65	Multiple Myeloma	Zoledronate	18	Y	Left maxilla
19	F	73	Multiple Myeloma	Zoledronate	30	Y	Mandible (medial)
20	F	82	Multiple Myeloma	Zoledronate	24	Y	Mandible (medial)

allowed to create an atmosphere fit for the culture of bacteria which require the presence of CO_2 to survive, and then a second sample incubation at 37°C for up to 72 h was carried out. Finally, after Gram staining of colonies, an examination by optical inverted microscope (Nikon Eclipse TS100-F) was carried out. Panels for the final identification of group and species were placed in the MicroScan Walkaway 40 (Dade Behring) for overnight incubation and were read automatically by the instrument.

Data collection

The microbial species isolated through each sampling design were divided into two groups according to the following criteria: a) gram-positive, gram-negative, fungi; b) aerobes, anaerobes, fungi. The percentage distribution of the different microbiota was then evaluated in each sampling technique and the results were compared to each other.

Statistical analysis

Statistical significance was assessed by *Chi*-squared test with Yates correction, with 95% confidence level ($p<0.05$). (PRISM version 5.0 - GraphPad Software, inc.1994-2007).

RESULTS

Data on the number of patients in treatment with BPs, and data on the three groups of microbiota detected are reported respectively in Table I and Table II. The percentage distribution of microbial flora (Fig. 1) showed a prevalence of Gram-positive in respect to Gram-negative bacteria in all the three sampling designs. The *Chi*-squared test with Yates correction showed no significant differences regarding gram-positive and gram-negative species colonizing the OS and NBF (*Chi*-squared= 0.1642; p = 0.6854).

The EX microbiological analysis testified a remarkable increase of gram-positive to detriment of gram-negative species (*Chi*-squared=11.15 *p =

Table II. *Microbiotica isolated.*

ORAL SWAB							
	Gram +			Gram -		Fungi	
streptococci α - hemolytic	Streptococcus mitis	9		Neisserie	2	Candida kefyr	1
	Streptococci α - hemolytic	3		Moraxella catarrhalis	1	Candida albicans	2
streptococci β - hemolytic	Streptococcus milleri	3	enterobacteria	Escherichia coli	1		
	Streptococcus agalactiae	1		Citrobacter Freundii complex	1		
	Streptococcus sanguis	2		Serratia marcescens	0		
	Streptococcus bovis	0	anaerobes	Veillonella parvula	1		
staphylococci	Staphylococcus epidermidis	2		Mobiluncus	1		
enterobacteria	Enterococcus faecalis	2		Fusobacterium	6		
	Bacillus cereus	1		Fusobacterium nucleatum	1		
anaerobes	Actinomyces viscosus	1					
	Actinomyces spp.	1		Fusobacterium necrophorum	1		
	Lactobacillus spp.	5					
	Bifidobacterium dentium	4		Bacteroides	2		
TOTAL		34	TOTAL		17	TOTAL	3

EXUDATES							
	Gram +			Gram -		Fungi	
streptococci α - hemolytic	Streptococcus mitis	7		Neisserie	1	Candida kefyr	0
	Streptococci α - hemolytic	0		Moraxella catarrhalis	0	Candida albicans	0
streptococci β - hemolytic	Streptococcus milleri	2	enterobacteria	Escherichia coli	1		
	Streptococcus agalactiae	0		Citrobacter Freundii complex	0		
	Streptococcus sanguis	2		Serratia marcescens	0		
	Streptococcus bovis	0	anaerobes	Veillonella parvula	0		
staphylococci	Staphylococcus epidermidis	3		Mobiluncus	0		
enterobacteria	Enterococcus faecalis	2		Fusobacterium	0		
	Bacillus cereus	0		Fusobacterium nucleatum	0		
anaerobes	Actinomyces viscosus	0					
	Actinomyces spp.	1		Fusobacterium necrophorum	0		
	Lactobacillus spp.	2					
	Bifidobacterium dentium	1		Bacteroides	0		
TOTAL		20	TOTAL		2	TOTAL	0

NECROTIC BONE FRAGMENT							
	gram +			gram -		fungi	
streptococci α - hemolytic	Streptococcus mitis	8		Neisserie	0	Candida kefyr	0
	Streptococci α - hemolytic	0		Moraxella catarrhalis	0	Candida albicans	0
streptococci β - hemolytic	Streptococcus milleri	3	enterobacteria	Escherichia coli	0		
	Streptococcus agalactiae	1		Citrobacter Freundii complex	0		
	Streptococcus sanguis	0		Serratia marcescens	1		
	Streptococcus bovis	1	anaerobes	Veillonella parvula	2		
staphylococci	Staphylococcus epidermidis	4		Mobiluncus	0		
enterobacteria	Enterococcus faecalis	1		Fusobacterium	6		
	Bacillus cereus	0		Fusobacterium nucleatum	1		
anaerobes	Actinomyces viscosus	0					
	Actinomyces spp.	0		Fusobacterium necrophorum	1		
	Lactobacillus spp.	4					
	Bifidobacterium dentium	6		Bacteroides	2		
TOTAL		28	TOTAL		13	TOTAL	0

0.003). Statistical analysis of gram-positive and gram-negative prevalence in the EX showed significant differences when compared to the OS (*Chi*-square= 15.56; °p< 0.0001) to NBF (*Chi*-squared = 13.56; **“**p= 0.0002). Besides, the histogram of their percentage distribution (Fig. 2) showed similar values for aerobes and anaerobes in OS and NBF. Aerobes appeared to prevail with regard to anaerobic bacteria in OS and EX’ samplings, whereas they tend to equalize anaerobes in NBF. Fungi were poorly represented and totally absent in EX and NBF. The statistical analysis appeared to confirm this trend: the *Chi*-squared Test with Yates’ correction showed no significant differences concerning aerobes and anaerobic bacteria present in the OS and in NBF (*Chi*-squared= 3.084; p = 0.0791). Anaerobes resulted outstandingly reduced

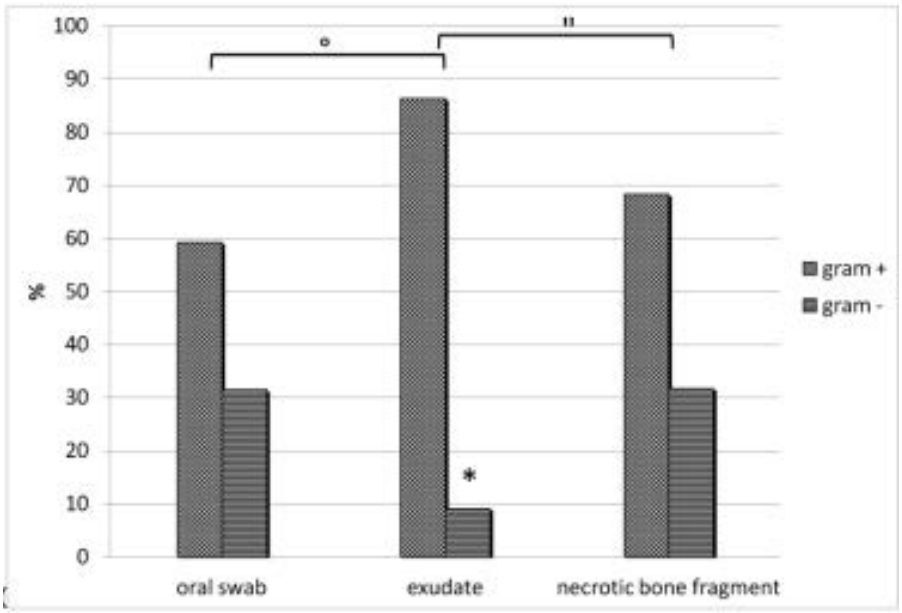

Fig. 1. *Gram-positive and gram-negative distribution. The microbiota isolated were divided into two groups: gram-positive and gram-negative. The histogram shows their quantitative distribution into the three distinct types of samples. Statistical significance was assessed by Chi-squared test with Yates' correction, with 95% confidence level ($p<0.05$).*

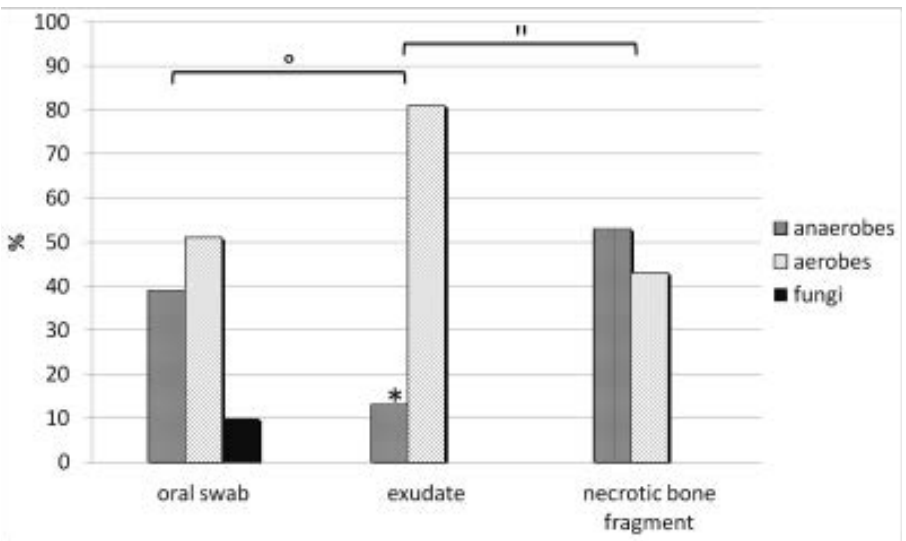

Fig. 2. *Anaerobes, aerobes and fungi distribution. The microbiota isolated were divided into three groups: anaerobes, aerobes and fungi. The histogram shows their quantitative distribution into the three distinct types of samples.*

in favor of aerobic bacteria in EX (*Chi*-squared=10.23 *p = 0.003) in respect to OS (Chi-squared= 17.3; °p < 0.0001) or NBF (*Chi*-squared= 33.92; “p < 0.0001).

DISCUSSION

Despite the strong clinical correlation between jaw necrosis and bisphosphonate therapy, a definitive causal relationship has yet to be established. In fact, epithelialization is an essential step in the management of BRONJ because alveolar bone exposure in BRONJ exposes the bone to the unique infectious microenvironment of the oral cavity. A biofilm forms on the exposed bone surface, and *Actinomyces* facilitate the adherence of other microflora, which results in a heterogeneous population of bacteria primed for the development of persistent infection (10).

Favia et al. (13) observed with scanning laser microscopy that the BP-induced remodeling leaves cavities of bone isolated from marrow, resulting in both necrosis and subsequent infection from colonizing bacteria. The above-mentioned report overwhelmingly supports the presence of infection (81.6% with inflammatory infiltrate and 80.3% with bacterial colonization) in the setting of osteonecrosis (85.1%). However, these findings do not exclude the possibility that concurrent colonization and/or infection may be present during and even facilitate BP remodeling of bone. Sporadic cases of osteomyelitis of the jaws supported by *Staphylococcus aureus* are described in literature (14, 15), but they are attributable to a previous transcutaneous bone exposure, caused, for example, by traumas (16).

Although the sample size was small, results from the present preliminary investigation showed that the overlying infection on the BRONJ is caused by an assorted microbial flora different from that of the above-cited forms of osteomyelitis. In fact, by using different sampling techniques, *Staphylococcus aureus* was not isolated in any patient, which indicated that there may be other oral bacteria which can trigger bone infection in BRONJ. We can speculate that the reported triple check procedure, in our opinion, gives more reliability to the results. The three sampling techniques, furthermore, showed different advantages and disadvantages.

The EX sampling appeared an invasive procedure requiring a good professional capability, but it is practicable only in the presence of secreting fistulas. NBF sampling could be performed only in patients destined to surgery. The OS proved to be a non-invasive and economic technique, easily feasible in all patients affected by BRONJ, that allows to obtain valuable microbial data in order to recognize pathogens responsible for the infection, to take account of their sensitivity to antibiotics and to outline a focused antimicrobial therapy.

Our initial hypothesis, based on the belief that anaerobe insulation was easier from close environments, such as inner bones or fistulas rather than from oral lesions, therefore appears to be wrong. This could be explained by technical problems of suction of the suppurative material. The sampling of EX gave one negative response, due to the insufficient amount of the purulent material aspirated from secreting fistula. These data, however, could be partially altered by a short exposure to oxygen, although the sampling procedure was optimized. Our microbial findings could be explained by an “internal” via of diffusion of the infection, that is, the oral cavity, with its mucosa and saliva, without skin involvement. However, the long-term outcome needs better assessment, and according to recent research and evidence-based dentistry (17, 18), further studies should address this issue.

REFERENCES

1. Medication-Related Osteonecrosis of the Jaw - 2014 Update. American Association of Oral and Maxillofacial Surgeons. http://www.aaoms.org/docs/position_papers/mronj_position_paper.pdf?pdf=MRONJ-Position-Paper (Accessed on October 26, 2015).
2. Raffaelli L, Scaramuzzo L, Rossi Iommetti P, Graci C, Maccauro G, Manicone PF. Jaw osteonecrosis related to bisphosphonate treatment of bone metastasis. J Biol Regul Homeost Agents 2010; 24:115-21.
3. Woo SB, Hellstein JW, Kalmar JR. Narrative [corrected] review: bisphosphonates and osteonecrosis of the jaws. Ann Intern Med 2006; 144:753-61. Erratum in: Ann Intern Med 2006; 145 :235.
4. Ruggiero SL, Dodson TB, Assael LA, Landesberg

R, Marx RE, Mehrotra B; American Association of Oral and Maxillofacial Surgeons position paper on bisphosphonate-related osteonecrosis of the jaws--2009 update. J Oral Maxillofac Surg 2009; 67:2-12

5. Vahtsevanos K, Kyrgidis A, Verrou E, et al. Longitudinal cohort study of risk factors in cancer patients of bisphosphonate-related osteonecrosis of the jaw. J Clin Oncol 2009; 27:5356-62.
6. Yoneda T, Hagino H, Sugimoto T, et al. Bisphosphonate-related osteonecrosis of the jaw: position paper from the Allied Task Force Committee of Japanese Society for Bone and Mineral Research, Japan Osteoporosis Society, Japanese Society of Periodontology, Japanese Society for Oral and Maxillofacial Radiology, and Japanese Society of Oral and Maxillofacial Surgeons. J Bone Miner Metab 2010; 28:365-83.
7. Sedghizadeh PP, Kumar SK, Gorur A, Schaudinn C, Shuler CF, Costerton JW. Identification of microbial biofilms in osteonecrosis of the jaws secondary to bisphosphonate therapy. J Oral Maxillofac Surg 2008; 66:767-75.
8. Tsurushima H, Kokuryo S, Sakaguchi O, Tanaka J, Tominaga K. Bacterial promotion of bisphosphonate-induced osteonecrosis in Wistar rats. Int J Oral Maxillofac Surg 2013; 42:14818-7.
9. Hinson AM, Smith CW, Siegel ER, Stack BC Jr. Is bisphosphonate-related osteonecrosis of the jaw an infection? A histological and microbiological ten-year summary. Int J Dent 2014; Article ID: 452737.
10. Wei X, Pushalkar S, Estilo C, et al. Molecular profiling of oral microbiota in jawbone samples of bisphosphonate-related osteonecrosis of the jaw. Oral Dis 2012; 18:602-12.
11. Mawardi H, Giro G, Kajiya M, et al. A role of oral bacteria in bisphosphonate-induced osteonecrosis of the jaw. J Dent Res 2011; 90:1339-45.
12. Khosla S, Burr D, Cauley J, et al. Bisphosphonate-associated osteonecrosis of the jaw: report of a task force of the American Society for Bone and Mineral Research. J Bone Miner Res 2007; 22:1479-91.
13. Favia G, Pilolli GP, Maiorano E. Histologic and histomorphometric features of bisphosphonate-related osteonecrosis of the jaws: an analysis of 31 cases with confocal laser scanning microscopy. Bone 2009; 45:406-13.
14. Carlson ER, Basile JD. The role of surgical resection in the management of bisphosphonate-related osteonecrosis of the jaws. J Oral Maxillofac Surg 2009; 7:85-95.
15. Otto S, Hafner S, Mast G, ET AL. Bisphosphonate-related osteonecrosis of the jaw: is pH the missing part in the pathogenesis puzzle? J Oral Maxillofac Surg 2010; 1158-61.
16. Scattarella A, Ballini A, Grassi FR, et al. Treatment of oroantral fistula with autologous bone graft and application of a non-reabsorbable membrane. Int J Med Sci 2010; 7:267-271
17. Katsarelis H, Shah NP, Dhariwal DK, Pazianas M. Infection and medication-related osteonecrosis of the jaw. J Dent Res 2015; 94:534-9
18. Ballini A, Capodiferro S, Toia M, Cantore S, Favia G, De Frenza G, Grassi FR. Evidence based dentistry: what's new? Int J Med Sci 2007; 4:174-8.

JOURNAL OF BIOLOGICAL REGULATORS & HOMEOSTATIC AGENTS Vol. 29, no. 4, 985-990 (2015)

LETTER TO THE EDITOR

ARTHRITIS AND OSTEOPOROSIS: PATHOGENETIC CORRELATIONS IN FUNCTION OF ARTHROPLASTY

L. MOLFETTA and B. SERIOLO

School of Medical and Pharmaceutical Sciences, Research Centre on Osteoporosis and Osteoarticular Diseases (CROPO) University of Genoa, Genoa, Italy

Received March 4, 2015 – Accepted October 23, 2015

Osteoarthritis is being increasingly characterised as an inflammatory incoming and recurrent disease, with the specific symptoms of inflammation at every stage of the disease. With regard to the pathogenesis over time, the degenerative and inflammatory components are combined and lead to osteocartilaginous degeneration. Such deterioration involves other joint tissues as well as the subchondral bone tissue, the suffering of which is the key event of the beginning and progression of OA; its involvement concerns the same pathogenetic mechanisms and the same chemical mediators of the chondropathy. The increase in joint inflammatory events leads to suspect the onset or the worsening of the osteometabolic disorder, which is documented by the MR as "bone edema" or as algodystrophic syndrome. The pain appears both while moving and resting and with signs of inflammation. The treatment of OA requires drugs, such as paracetamol, selective and nonselective NSAIDs and opiates, for pain control. Treatment should ensure the pharmacological control of the pain related to the osteometabolic juxta-articular alteration, through bisphosphonates, favouring those which can control bone loss, inflammation and pain.

Osteoarthritis (OA) is a complex and mainly degenerative disease, resulting from the loss of the physiological balance between degenerative and restorative phenomena of the joint cartilage. Over time OA involves all the joint components, and in particular the subchondral bone, with a gradual joint mechanical unbalance until the global failure of the joint (1). The progression of the disease determines disability and deterioration of the quality of life and is the main cause of muscle-skeletal pain (2).

With regard to the pathogenesis over time, the degenerative and inflammatory components are combined and lead to osteocartilaginous degeneration (3).

Cartilage is certainly the target-tissue of the disease; its complete wear requires a prosthetic replacement to suppress the local and general dysfunctional-pain condition and to restore its function. The pathogenetic mechanisms of chondropathy are well known; the disruption of the cartilage structure and the alteration of its mechanobiology are caused by cytokines (IL-1beta, IL-17, IL-18, TNF, etc.) which accentuate the catabolic phase of the tissue (4). Incoming biochemical changes caused, for example, by traumas and micro-traumas occur before the typical radiographic alterations related to the clinical signs. Despite attempted restoration, the tissue damage becomes structural over time, with the loss of the mechanobiological competence of the hyaline cartilage. Such degeneration involves other

Key words: arthritis, inflammation, subchondral bone, bone edema, clodronate

Mailing address:
Prof. Luigi Molfetta,
School of Medical and Pharmaceutical Sciences,
Research Center on Osteoporosis and Osteoarticular Diseases,
Via L.B. Alberti 4,
16132, Genova, Italy
e-mail: Prof.molfetta@gmail.com

0393-974X (2015)

joint tissues as well as the subchondral bone tissue, the suffering of which is the key event of the onset and progression of OA (5). Radin and Paul state that it is the subchondral bone, and not the cartilage, which plays the main role of shock absorber, so that it suffers microfractures that can be observed at the onset of the OA (6, 7) with an increase of the bone turnover (8) and a decrease of the secondary mineralisation for the benefit of osteoformation processes (9). Westcott et al. even documented that the osteoblasts release factors which are responsible for the cartilage degradation, highlighting the close pathogenetic correlation (10).

Arthritis and inflammation

OA is being increasingly characterised as an inflammatory incoming and recurrent disease, with the specific symptoms of inflammation at every stage of the disease (1). The synovial fluid often shows an increase of both mononuclear cells and Ig and complement levels, while the synovial membrane shows the typical modification of inflammation, such as cellular hyperplasia with infiltrations of inflammatory cells in the subepithelial tissue; the histomorphology of the synovial membrane of these joints resembles the synovium of patients with early rheumatoid arthritis (RA) (11).

Albeit free from blood vessels and therefore excluded from any immunological surveillance, the cartilage expresses an important immunological reactivity, which explains the condition of chronic inflammation, induced by the production and release of inflammatory cytokines, chemokines, nitric oxide and prostaglandins and destructive enzymes, in a macro-etiological framework of traumatic events, of functional overload, of ageing, of associated pathogenic conditions, etc. A vicious circle (degradation, cytokines, inflammation, release of antigenic factors, etc.) develops, making the inflammatory process chronic, and increasing the catabolic moment of the joint cartilage for an uneven activation of the intra-articular cytokinetic network (12).

Finally, the role of chemokines, prostaglandins and leukotrienes (eicosanoids) in the pathogenesis of inflammation is well known. Chemokines take part in the pathogenic cascade in OA, as well as in RA, for an inappropriate activation of the chemokine network.

Prostaglandins E2 (PGE2) appear in the osteoarthritic tissues in significant quantities because of the presence of cyclooxygenases 2 (COX-2), which leads to the overproduction of prostaglandin E2(PGE2). This results in the important role of the NSAIDs in anti-COX/PGE2 function, at least in the early stages of the OA. The metalloproteinases deteriorate all the components of the pH-neutral cartilage matrix (13).

This disease process is characterised as autoimmune when the damage of the cartilage causes the release of certain cartilage antigens, which are exposed to the immune system. A situation of immunisation was shown in rats, using type II collagen, heterologous and homologous, with the onset of destructive inflammatory polyarthritis. Chondrocytes have particular antigens which reveal and "expose" themselves in case of extracellular matrix degradation(14). This was then confirmed by the results of histomorphological studies of OA, which highlighted mononuclear cellular infiltrations and lymphocytic aggregates in the synovial membrane, and the deposit of antibodies and immune complexes in the arthritic cartilage (15).

Pain of OA

The three main signs of the disease are pain, deformity, and disability, which may appear with different grading and timing according to the patient's general and local context.

Pain is the main symptom of OA, the characteristics of which correlate the two pathogenic moments of the disease - mechanical and inflammatory - that intersect each other and vary over time. Rigidity, muscle weakness, deformity, etc. are associated to and are important to "identify" pain and its origin and to plan the treatment at the moment of assessment. Pain correlates the global assessment of damage, joint deformity, muscle atrophy and inflammation. The latter is caused by different mechanisms, such as the presence of micro-crystals of hydroxyapatite, the unveiling of cartilage antigens or the phagocytosis of fragments of degradation. When evident, it is expressed by redness, heat, swelling and pain during palpation; nevertheless, there may be a sub-acute condition of inflammation, less striking and so persistent as to become an underhand moment of

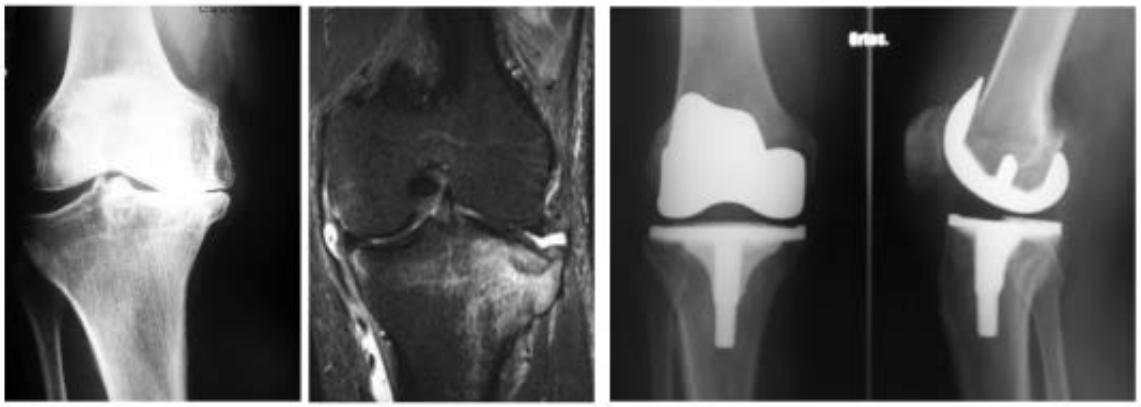

Fig. 1. *Patient with osteoarthritis of the right knee with initial algodystrophy, operated by two-compartment arthroplasty.*

worsening of the cartilage degeneration and of an early extra-cartilage damage, like the one affecting, for example, the bone (16). In the course of OA, the role of the subchondral bone becomes increasingly important, since it is a co-participant in the chondropathy and an evident trace in the radiographic staging of the disease, with a reduction of the joint line, osteophytosis, geodes and modifications of the mineral density. Radiographies are, therefore, useful to stage OA, especially if it is post-traumatic; they accompany the clinical diagnosis that is the pain and its anatomical-pathological counterpart.

In the lower limb, joint pain depends on load (start of the movement, standing position and/or prolonged walking or running, change of position). The pain evaluation index (VAS, Womac, Lequesne) (17) assesses and qualifies the pain itself, while a precise identification of signs and symptoms to the diseased joint is necessary for its classification, excluding its extra-articular origin (bursitis or periarthritis, enthesitis, etc.). It is nevertheless difficult to outline pain and its pathogenesis rigidly, since the evolutionary stages have a variable trend, the axial joint deviation makes it more localised, the involvement of various tissues makes it all-encompassing and the presence of inflammation changes its profile.

Bone juxta-articular disease in OA

The participation of the subchondral bone in the disease process of OA generally occurs in more advanced stages; its involvement concerns the same pathogenetic mechanisms and chemical messengers of chondropathy and it is possible to recognise a first instance (secondary to the chondropathy) of sclerotic reactivity, defined as relating to the elementary mechanical compensation to the compartmental mechanical-biological deficit of the chondropathy, and a second moment of osteometabolic damage, of failure and inflammatory concomitant participation in the disease which becomes, therefore, osteocartilaginous (18). This evolution modifies and generally increases the intensity of pain.

In the stage of sclerotic reactivity, pain is characterised as nociceptive, mechanical in its main essence, remitting with rest, with a good response to the analgesic treatment. In the stage of osteometabolic suffering, pain varies in terms of intensity, site, type, duration and functional counterpart. A joint undergoes micro-damage with consequent accumulation of structural alterations which lead to both a reduction in cartilage thickness and an increase of the subchondral turnover; the latter becomes the main characteristic of the arthritic process in which the cartilage takes part (19, 20). This is accompanied by bone tissue loss rate that increases with ageing (21).

The increase in articular inflammatory events induces to suspect the onset or the worsening of the osteometabolic damage, which is documented by the Magnetic Resonance (MR) as “bone oedema”, or as algodystrophic syndrome (Fig. 1). Pain appears both

while moving and at rest, and is accompanied by signs of inflammation (22).

In prosthetic replacement, the diseased cartilage is removed, while the cancellous bone pain persists and influences the subsequent bone-growth and periprosthetic bone-remodelling, i.e. the complex biological process which translated the primary stability into secondary biological stability and which realises the so-called periprosthetic osseointegration.

Periprosthetic bone-stock

The prosthesis replaces seriously damaged joint surfaces to restore a compromised motor function. The prosthetic components must be permanently fixed to the contiguous joint epiphysis with acrylic cement, which guarantees the fixation, the adhesion and the primary stability of the components; the fixation may also occur without cement, in which case the bone is the "biological cement" that guarantees the adhesion, the fixation and, therefore, the primary press-fit stability with the cancellous or cortical bone (23).

The metabolic condition of the bone at the moment of surgery influences the post-surgical restoration. This consists of a first moment of bone-growth with the post-surgical restoring osteogenesis. Subsequently, the newly formed bone tissue, which varies in terms of intensity and time according to the different sites around the prosthesis, becomes "mechanically able", adapting its micro- and macro-structure to the peculiar mechanical needs of the joint site (bone-remodelling) (24). The whole process of "osseointegration" is preceded by a phase of bone mineral density (BMD) reduction due to the mechanical stress on the interface. This decrease of the BMD ranges from 3% (Fig. 2) to over 15% in the first quarter of the year, then regaining arithmetically within the following 24 months (25).

The interpretation of this data is mechanical and related to the stress-shielding. The difference of Young's modulus of elasticity between bone and metallic prosthetic components generates a transfer of stress to the interface during the loading phase, a temporary negative biological reaction, of adjustment with subsequent compensation within at least 24 months, according to the age of the patient, the gender and the type of prosthesis. Moreover, the different Gruen zones, for example in the hip, express a specific bone loss in function of their biomechanical role, at high turnover (Gruen zones 1-7), of mechanical stability (zones 2 and 6) and of centralising (zones 3 and 5) (26).

The use of acrylic cement reduces the phenomenon impacts, delimiting the periprosthetic bone loss, especially in the femoral hip prosthesis (27). Periprosthetic bone loss correlates initial bone stock, rasping damage, and, primarily, mechanical stress, as shown by Leichtle et al. (28). The characteristics of the prosthesis in the hip, for example, affect the higher mineral density loss in the straight stems, for a more invasive transmission of stress of the anatomic stems (29). Even years after, the bone remodelling leads to the differentiation of the greater remodelling Gruen zones, such as zones 1 and 7, by reason of the peculiar stress transmitted (29). The decrease in the periprosthetic BMD must always be compared to the age of the patient and to the pre-surgical bone stock. In each patient, this characteristic datum dissociates itself from the BMD assessed in other sites, such as the spinal column and the wrist and, therefore, it does not express the patient's general osteometabolic condition. The use of antiresorptive drugs reduces the periprosthetic loss due to stress shielding, as shown in the Literature (30) and in experimental models in rats; in particular, clodronate has an effect of control of the inflammation in the experimental rheumatoid arthritis of rats, interfering with polymorphnucleates and reducing the cartilage damage (31).

Protection of long time osteointegration

The bone-prosthesis osteointegration over time is the function of various variables related to the host bone, the types of implantation (adhesion, fixation, and primary stability), the mechanical characteristics of the prosthetic components (straight, anatomic, cemented, non-cemented stem), and the patient (weight, job, stress, drugs, etc.). The components of the implantation cause a continuous transfer of stress to the interface directly with the bone or through the acrylic cement. The mechanical stimulus is constantly translated into a biological stimulus, on the back of the osteocytes, the mechanical transducers which recognise any kind of stress induced in the bone. A bone-prosthesis relation, if kept within certain physiological limits, leads to a "new normality" condition of the replaced joint without pain and with

an optimal joint function (36).

If, at the time of the implantation or over time, the interaction bone-prosthesis becomes pathological, it will cause a loss in stability. The macro-movements to the interface cause the loss of the bone-ingrowth and a radiolucency that is a fibrous ingrowth causing mobilisation of the prosthesis and, therefore, pain. The management of the post-surgical bone-growth is therefore necessary as a premise for a following positive remodelling. Today, pharmacological help to the periprosthetic osteogenesis is considered to be necessary immediately after the surgery. In this sense, bisphosphonates showed a positive action; clodronate, in particular over the last 15 years, has established its antiresorptive role, with an analgesic and anti-inflammatory action that fits very well with the post-surgical moment, when bone-loss, reactive inflammation and pain co-occur in the treated joint (32).

CONCLUSIONS

Alterations in OA cannot be considered just as a mechanical phenomenon, and chondropathy cannot be considered as an expression of a simple functional overload. The arthritic joint goes through phases of severe inflammation, especially in the advanced stages of its natural history. In this course, the juxta-articular bone is involved in the pathogenesis of the disease; the initial mechanical reaction (sub-chondral sclerosis) phase is followed by a phase of real osteometabolic alteration, which leads to a decrease in the BMD, visible in the x-ray as a bone oedema until the real compartmental or total joint algodystrophy.

Today the pharmacological management of OA focuses on drugs for pain control, such as paracetamol, selective and nonselective NSAIDs and opiates. Treatment should ensure the pharmacological control of the pain related to the osteometabolic juxta-articular alteration, through the bisphosphonates, fostering those which can control bone loss, inflammation and pain (38). For a complete treatment of arthritis in all its aspects, it is therefore necessary to consider, in the approach to the prosthetic surgery of a severely arthritic joint, the metabolic damage of the juxta-articular bone. In this way, the joint is appropriately prepared for the prosthetic replacement which will involve a further immediate post-surgical decrease of the BMD, causing higher "biological fatigue" in the course of the periprosthetic osseointegration.

REFERENCES

1. Altman R, Asch E, Bloch D, et al. Development of criteria for the classification and reporting of osteoarthritis, classification of osteoarthritis of the knee. Arthritis Rheum 1986; 29:1039.
2. Gray ML, Pizzanelli AM, Grodzinsky AJ, et al. Mechanical and physiolgical determinants of the chondrocyte biosynthetic response. J Orthop Res 1988; 6:777-92.
3. Creamer P, Hochberg MC. Osteoarthritis. Lancet 1997; 350:503-9.
4. Murphy G, Hembry RM, Heghes CE, et al. Role and regulation of metalloproteinases in connective tissue turnover. Biochem Soc Trans 1990; 18:812-5.
5. Adami S, Viapiana O. Pathophysiology of osteoarthritis: perspectives. Reumatismo 2001; 53:18-25.
6. Radin EL, Paul IL. Does cartilage compliance reduce skeletal impact loads? The relative force attenuating properties of articular cartilage, synovial fluid, periarticular soft tissue and bone. Arthritis Rheum 1970; 13:139-44.
7. Fazzalari NL. Trabecular microfractures. Calcif Tissue Int 1993; 53(S1):S143-S47.
8. Campion GV, Delms PD, Dieppe PA. Serum and synovial fluid osteocalcin levels in joints disease. Br J Rheum 1989; 28:393-98.
9. Parfitt AM. Skeletal heterogeneity and the purposes of bone remodelling. In: Marcus R, Feldman D, Kelsey J (eds). Osteoporosis. Academic Press, San Diego, CA, USA. 1996; Chapter 12 pp 315-29.
10. Westacott CI, Webb GR, Warnock MG, et al. Alteration of cartilage metabolism by cells from osteoarthritic bone. Arthritis Rheum 1997; 40:1282-91.
11. Kwan Tat S, Lajeunesse D, Pelletier JP, Martel-Pelletier J. Targeting subchondral bone for treating osteoarthritis: what is the evidence? Best Pract Res Clin Rheumatol 2010; 24:51-70.
12. Kapoor M, Martel-Pelletier J, Lajeunesse D, et al. Role of proinflammatory cytokines in the pa-

thophysiology of osteoarthritis. Nat Rev Rheumatol 2011; 7:33-42.
13. Murphy G, Hembry RM, Heghes CE, et al. Role and regulation of metalloproteinases in connective tissue turnover. Biochem Soc Trans 1990; 18:812-3.
14. Breedveld FC, Dnesius-Trentham R, De Sousa M, Trentham DE. Collagen arthritis in the rats is initiated by cd4+ T cells and can be amplied by iron. Cell Immunol 1989; 21:1-12.
15. Yuan GH, Masuko-Hongo K, Kato T, Nishioka K. Immunologic intervention in the pathogenesis of osteoarthritis. Arthritis Rheum 2003; 48:602-11.
16. Viapiana O, Povino MR, Liuzza S, Troplini S, Adami S. Artrosi: fisiopatologia e nuove indicazioni terapeutiche. GIBIS 2009; 10 (2):5-18.
17. Salaffi F, Stancati Q. Scale di valutazione e malattie reumatiche, Mattioli Editore,Parma, 2001.
18. Bettica P, Cline G, Hart DJ, et al. Evidence for increased bone resorption in patients with progressive knee osteoarthritis: longitudinal results from the Chingford study. Arthritis Rheum 2002; 46:3178-84.
19. Peterson IF, Boegard T, Dahlstrom J et al. Bone scan and serum markers of bone and cartilage in patients with knee pain and osteoarthritis. Osteoarthritis Cartilage 1998; 6:33-9.
20. Dieppe P. Osteoarthritis: time to shift the paradigm. BMJ 1999; 318:1299-300.
21. Burger H, van Daele PL, Odding E, et al. Association of radiographically evident osteoarthritis with higher bone mineral density and increased bone loss with age. Arthritis Rheum 1996; 39:81-86.
22. Roemer FW, Eckstein F, Hayashi D, Guermazi A. The role of imaging in osteoarthritis. Best Pract Res Clin Rheumatol 2014; 28(1):31-60.
23. Molfetta L. La chirurgia protesica delle grandi articolazioni. Reumatologo 2003; 56:29-33
24. Chang CY, Huang AJ, Palmer WE. Radiographic evaluation of hip implants. Semin Musculoskelet Radiol 2015; 19(1):12-20.
25. Smolders JM, Pakvis DF, Hendrickx BW, Verdonschot N, van Susante JL. Periacetabular bone mineral density changes after resurfacing hip arthroplasty versus conventional total hip arthroplasty. A randomized controlled DEXA study. J Arthroplasty 2013; 28(7):1177-84.
26. Molfetta L. Palermo A, Monteforte P, Bianchi G, Pipino F. DEXA analysis of Antega total hip prosthesis. J Orthop Traumatol 2000; 1:17-21.
27. Vidovic D, Matejcic A, Punda M, et al. Periprosthetic bone loss following hemiarthroplasty:a comparison between cemented and cementless hip prosthesis. Injury 2013; 44 (S3):S62-6.
28. Leichtle UG, Leasure J, Martini F, Leichtle CI. Immediate changes of bone density caused by the implantation of a femoral stem--a DEXA study. Hip Int 2011; 21(6):706-12.
29. Grochola LF, Habermann B, Mastrodomenico N, Kurth A. Comparison of periprosthetic bone remodelling after implantation of anatomic and straight stem prostheses in total hip arthroplasty. Arch Orthop Trauma Surg 2008; 128(4):383-92.
30. Zeng Y, Lai O, Shen B, et al. A systematic review assessing the effectiveness of alendronate in reducing periprosthetic bone loss after cementless primary THA. Orthopedics 2011; 34(4).
31. Bendele AM, Hulman JF. Spontaneous cartilage degeneration in guinea pigs. Arthritis Rheum 1988; 31:561-5.
32. Bhandari M, Bajammal S, Guyatt GH, et al. Effect of bisphosphonates on periprosthetic bone mineral density after total joint arthroplasty: a meta analysis. J Bone Joints Surg (A) 2005; 87(2):293-301.

JOURNAL OF BIOLOGICAL REGULATORS & HOMEOSTATIC AGENTS Vol. 29, no. 4, 991-997 (2015)

LETTER TO THE EDITOR

BEHAVIOUR OF DENTAL PULP STEM CELLS ON DIFFERENT TYPES OF INNOVATIVE MESOPOROUS AND NANOPOROUS SILICON SCAFFOLDS WITH DIFFERENT FUNCTIONALIZATIONS OF THE SURFACES

M. MARRELLI[1,2,3*], G. FALISI[4*], A. APICELLA[5*], D. APICELLA[1,2], M. AMANTEA[1,3], A. CIELO[6], L. BONANOME[6], F. PALMIERI[2], L. SANTACROCE[7*], S. GIANNINI[6], E. DI FABRIZIO[9], C. RASTELLI[4*], M. GARGARI[8*], G. CUDA[10*], F. PADUANO[2*] and M. TATULLO[1,2,4*]

[1]Unit of Maxillofacial Surgery, Calabrodental, Crotone, Italy; [2]Tecnologica Research Institute, Biomedical Section, Crotone, Italy; [3]Marrelli Hospital, Cancer Surgery Unit, Crotone, Italy; [4]Department of Life, Health and Environmental Sciences, School of Dentistry, University of L'Aquila, L'Aquila, Italy; [5]Department of Architecture and Industrial Design, Second University of Naples, Italy; [6]Private practice in Rome; [7]Department JSGEM, University of Bari - Section of Taranto, Italy; [8]Department of Clinical Sciences and Translational Medicine, University of Rome "Tor Vergata", Rome, Italy; [9]BioNEM Laboratory, Department of Experimental and Clinical Medicine, Magna Græcia University of Catanzaro, Salvatore Venuta Campus, Catanzaro, Italy; Physical Science & Engineering Division, King Abdullah University of Science and Technology (KAUST), Thuwal, Kingdom of Saudi Arabia; [10]Department of Experimental and Clinical Medicine, Magna Græcia University of Catanzaro, Salvatore Venuta Campus, Catanzaro, Italy

Received September 3, 2015 – Accepted October 22, 2015

[*] These Authors equally contributed to this research

Dental pulp stem cells (DPSCs) are stem cells found in the dental pulp. The ability of DPSCs to differentiate towards odontoblastic and osteoblastic phenotype was reported first in the literature, then in the following years, numerous studies on odontogenesis were carried out, starting from mesenchymal stem cells isolated from tissues of dental and oral origin. The aim of this research was to evaluate the behaviour of DPSCs grown on silicon nanoporous and mesoporous matrices and differentiated towards the osteogenic phenotype, but also to investigate the use of DPSCs in pilot studies focused on the biological compatibility of innovative dental biomaterials. Twenty-eight silicon samples were created with standardized procedures. These scaffolds were divided into samples made of silicon bulk, nanoporous silicon, mesoporous silicon, nanoporous silicon functionalized with (3-Aminopropyl) Trimethoxysilane (APTMS) and methanol (MeOH), nanoporous silicon functionalized with (3-Aminopropyl) Trimethoxysilane (APTMS)/toluene, mesoporous silicon functionalized

Key words: regenerative medicine, mesenchymal stem cells, dental pulp stem cells, silicon scaffolds, nanoporous scaffolds, mesoporous scaffolds

Mailing address: Dr. Marco Tatullo, PhD
Scientific Director,
Tecnologica Research Institute,
Biomedical Section,
Stem Cells Unit, Str. E. Fermi,
88900 Crotone, Italy
e-mail: marco.tatullo@tecnologicasrl.com

0393-974X (2015)

DISCLOSURE: ALL AUTHORS REPORT NO CONFLICTS OF INTEREST RELEVANT TO THIS ARTICLE.

with (3-Aminopropyl) Trimethoxysilane (APTMS) and methanol (MeOH) andmesoporous silicon functionalized with (3-Aminopropyl) Trimethoxysilane (APTMS)/toluene. DPSC proliferation on the tested silicon scaffolds was analyzed at 3 and 5 days. The assay showed that DPSCs proliferated better on mesoporous scaffolds functionalized with APTMS/toluene compared to a silicon one. These results show that the functionalization of silicon scaffold with APTMS/toluene supports the growth of DPSCs and could be used for future applications in tissue engineering.

The regeneration of dental and bone tissues represents a continuous incentive to develop new performing biomaterials capable of restoring the morphology and the physiology of the damaged tissues. An ideal scaffold for dental and bone tissues engineering must be biocompatible, and should promote the cell adhesion and proliferation, but it should also promote cell differentiation and mineralization of the extracellular matrix, in order to replace the hard tissues which form the main part of the bone and the tooth (1).

Dental pulp stem cells (DPSCs) are stem cells isolated from the dental pulp and mainly originate from the neural crests. DPSCs express several surface markers such as CD44, STRO-1, CD90, CD105, CD106, CD146 and CD27; they also express embryonic stem cell markers, such as Oct-4, and Nanog, and they are able to differentiate into osteogenic, chondrogenic, myogenic, odontogenic, adipogenic and neurogenic lineage, according to their embryonic origin (2-5).

The pulpal tissue hosts a variable number of DPSCs; although the percentage is typically assessed around 1% of the whole cell population these cells can be found in many zones of the dental pulp, but the coronal zone has been reported to be the richest in adult dental pulp stem cells. The niches of DPSCs are likely to be activated after a stimulus of different typology, as a trauma or a deep bacterial contamination of the above dentinal tissue (6).

The ability of DPSCs to differentiate toward odontoblasts and osteoblasts has been investigated by numerous studies on odontogenesis starting from cells from tissues of dental origin (2), however this ability was also used for testing the biological compatibility of innovative dental materials. Different studies initially assessed the ability of stem cells from dental pulp tissue to grow and to differentiate on different scaffolds and materials.

Porous silicon is an innovative material with a well known degree of biocompatibility, it is biodegradable and shows a highly modifiable surface. Silicon-based scaffolds have been investigated to better understand the interaction of several cell lines with different geometrical features of the scaffold surface. It has been demonstrated that mesoporous silicon substrates, with an average pore size ranging between ~5 and ~20 nm, are able to support a good cell adhesion, making interesting and promising the future studies on porous silicon substrates for evaluating cell behaviour on them (7).

The aim of this research was to evaluate the *in vitro* behavior of DPSCs differentiated towards the osteogenic phenotype, grown on silicon nanoporous and mesoporous scaffolds: these scaffolds have been also functionalized with (3-Aminopropyl) Trimethoxysilane (APTMS) and methanol (MeOH) or with APTMS and toluene, among the most common chemicals able to link silicon matrices and to support cell adhesion on the surface; in this way, it has been possible to determine the best functionalization protocol sustaining DPSC proliferation.

MATERIALS AND METHODS

Cell culture

DPSCs were isolated by enzymatic digestion of dental pulp tissue. Dental pulp was harvested from premolar teeth previously extracted for orthodontic therapy. Human dental pulp tissue was obtained from 2 healthy volunteers, 33±2 years of age, who provided written informed consent at the Calabrodental dental clinic (Crotone, Italy). The study was carried out according to guidelines of the internal Ethics Committee. DPSCs were cultured in α-MEM, 20% (Fetal Bovinum Serum) FBS and 1% penicillin/streptomycin. Protocol was performed as previously described and validated (8, 9).

Cell counting

To determine the population doubling (PD) rate, cells isolated from human dental pulp were initially seeded at the density of 150 x 10^3 cells/ 6-well in culture medium. At each passage cells were re-plated at the initial density and cultures were extended until passage 11. The following

formula was applied: $PD = [log_{10}(N) - log_{10}(N_S)] / log_{10}(2)$, where N is the harvested cell number and N_S is the initial plated cell number (15). Cumulative population doublings (cPD) index for each passage was obtained by the sum of the PD of each passage to the PD of the previous passages.

Flow cytometric analysis

Cells at passage 4 were trypsinized, resuspended and aliquoted at 500,000/100 µl PBS onto a FACS tube. Each aliquot was incubated with saturating concentrations of fluorochrome conjugated antibodies on ice for 30 min. At the end of incubation, the tube was centrifuged at 200 g for 5 min and inverted onto a paper towel to drain the supernatant. The cells were washed twice and 0.5 ml of PBS was added to each tube. The samples were kept on ice and in the dark until running on FACS. CD73-FITC, CD90-PE, CD105-APC, CD13-PE, CD29-APC, CD44-FITC and CD45-APC-H7 (Becton Dickinson - BD) antibodies were used for our analysis. Samples were analyzed with FACSCanto II instruments (BD) and data were analyzed by using FlowJo software (Tree Star).

In vitro osteogenic differentiation

Cells at passage 4 were plated at 1 x 10^4 cells/96 well. The next day, growth medium was replaced by osteogenic medium [α-MEM] (Sigma), 20% FBS (Invitrogen) 0.2 mM L-ascorbic acid-2-phosphate (Sigma), 100 nM dexamethasone (Sigma), 10 mM β-glicerophosphate (Sigma), 100 U/ml penicillin, 0.1 mg/ml streptomycin, 0.25 mg/ml amphotericin B. α-MEM supplemented with 10% FBS was used in the control group. Cells isolated from dental pulp, growing in osteogenic medium for 3 weeks, were washed once with PBS and fixed with 4% paraformaldehyde (Sigma) for 15 min at RT. After washing thrice with PBS, aqueous solution of 5 mg/ml Alizarin red S (Sigma) was added to the cells for 30 min. Then, cells were washed thrice with H_2O for 5 min each wash and were analyzed by microscopy.

Production of silicon scaffolds

Twenty-eight silicon samples were made with standardized procedures, and were divided into the following typologies:

4 samples made of silicon bulk,

4 samples made of not functionalized nanoporous silicon,

4 samples made of not functionalized mesoporous silicon,

4 samples made of nanoporous silicon functionalized with APTMS/MeOH,

4 samples made of nanoporous silicon functionalized with APTMS/toluene,

4 samples made of mesoporous silicon functionalized with APTMS/MeOH,

4 samples made of mesoporous silicon functionalized with APTMS/toluene.

The production and the functionalization of the porous silicon scaffolds were carried out starting from crystalline silicon, by means of an anodizing process; specifically, an electrolysis process was induced by the fluoridric acid.

The electrochemical functionalizations were obtained in a cell, made of Teflon and containing a solution made by fluoridric acid together with methanol. This process allowed to obtain a precise control of the superficial porosity of the silicon, in order to achieve mesoporous silicon with a porosity ranging from 2 to 50 nanometers, as well as nanoporous silicon with a porosity lower than 2 nanometers.

The silicon utilized for our studies showed a resistivity between 5 and 10 Ω/cm, and a thickness standardized at 500 micron for all the samples: anodizing process left only 5 min, followed by 5 min of rinses with distilled water, EtOH and pentane. Silicon samples, measuring 1cm x 1cm, were cut with a precision instrument, an optimal shape to transfer them into the 24-well tissue culture plates.

Functionalization of the silicon scaffolds

Silicon samples, obtained as above described, were functionalized with 3-Aminopropyltrimethoxysilane (APTMS), by 2 different protocols:

Protocol 1: the sample is put for 2 h into a solution with 5% APTMS diluted in MeOH at room temperature. At the end of the chemical reaction, the sample is subjected to 2 different washes: the first one with acetone for 30 s, the second one with MeOH for 40 seconds. Finally, the sample is dried for 2 h at 100°C.

Protocol 2: the sample is put for 5 min into a solution with 5 mM APTMS diluted in toluene at room temperature. At the end of the chemical reaction, the sample is subjected to 2 different washes: the first one with acetone for 30 s, the second one with MeOH for 40 s. Finally, the sample is dried for 2 h at 100°C.

Cell proliferation

Fifty thousand DPSCs were cultured on different silicon scaffolds measuring 1cm x 1cm, as previously described .

Cells were directly seeded onto the scaffolds allocated in 100 µl of culture medium. The cells were left on the scaffolds for 3 h and then 900 µl of culture medium was added to every well. The day following this procedure, further 1 ml of culture medium was added: cell count was performed at 3 and 5 days, by Trypan blue. Only vital

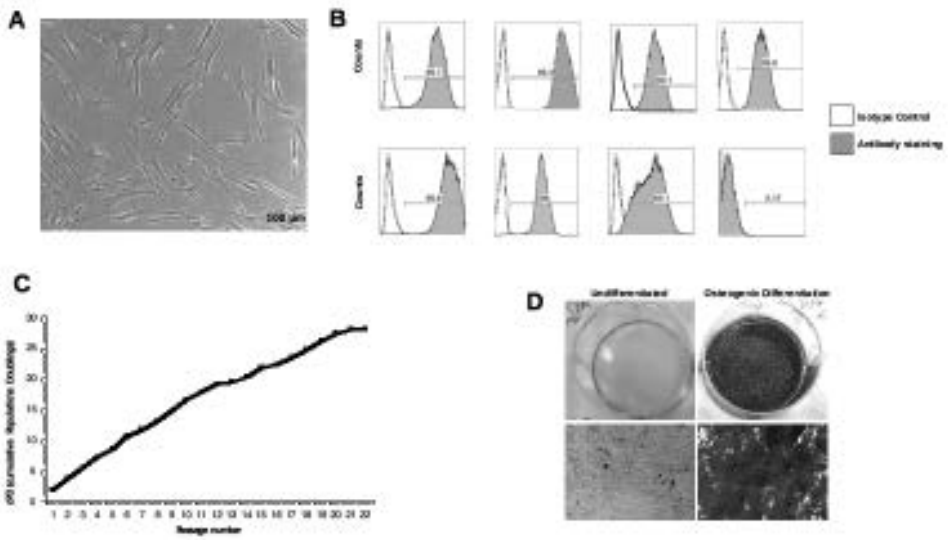

Fig. 1. *Morphological characterization, cell surface markers, growth and osteogenic differentiation of DPSCs.* ***A)*** *Morphological appearance of human DPSCs at passage 4.* ***B)*** *Immunophenotype of DPSCs at passage 4. Results reported forward and side scatter and in each plot, X-axis shows relative fluorescence and Y-axis the number of events. Histograms show isotype control (white peaks) versus specific antibody staining (grey peaks) and the percentage of cells positive for selected molecules.* ***C)*** *Cumulative population doublings (cPD) of cells isolated from oral cyst. The number of population doublings was calculated as follows: PD = [$\log_{10}(N) - \log_{10}(N_s)$] / $\log_{10}(2)$, where N is the harvested cell number and Ns is the initial plated cell number. Cumulative population doublings (cPD) index for each passage was obtained by adding the PD of each passage to the PD of the previous passages.* ***D)*** *Mineralized deposit identified by Alizarin Red staining in DPSCs grown in osteogenic medium for 3 weeks.*

cells were considered in our cell count. Every experiment was performed in triplicate.

Cell visualization in the scaffolds

After 48 h from the seeding, scaffolds containing cells at passage 4 were fixed in 3.7% formaldehyde (Sigma-Aldrich) for 30 min at room temperature. Subsequently, samples were mounted in ProLong Gold antifade reagent containing DAPI (Invitrogen, Carlsbad, CA, USA) and analyzed using a confocal microscope (Leica, TCS SP5 II).

Statistical analysis

Results were expressed as the mean ± standard deviations of three separate experiments. The significance of differences between groups was evaluated by one-way analysis of variance (ANOVA) followed by Student's *t*-test. Analyses were conducted using the GraphPad Prism software (San Diego, CA, USA), and differences were considered significant if $P < 0.05$ (*).

RESULTS

Morphological analysis of DPSCs indicated the presence of cells with large, flattened, or fibroblast-like shape (Fig. 1A). Prior to seeding DPSCs onto silicon scaffolds, flow cytometry was performed to confirm the mesenchymal surface marker expression of the cells. DPSCs were positive for MSC markers CD13, CD29, CD44, CD73, CD90, CD105 and CD146 and negative for the hematopoietic marker CD45 (Fig. 1B). Moreover, evaluation of proliferation rates by measuring cell viability at various time points indicated that DPSCs had a good proliferation rate (Fig. 1C).

Long-term cultures (3 weeks) of cells grown in the presence of osteogenic media demonstrated the capacity to form Alizarin Red-positive condensed nodules with high levels of calcium covering the

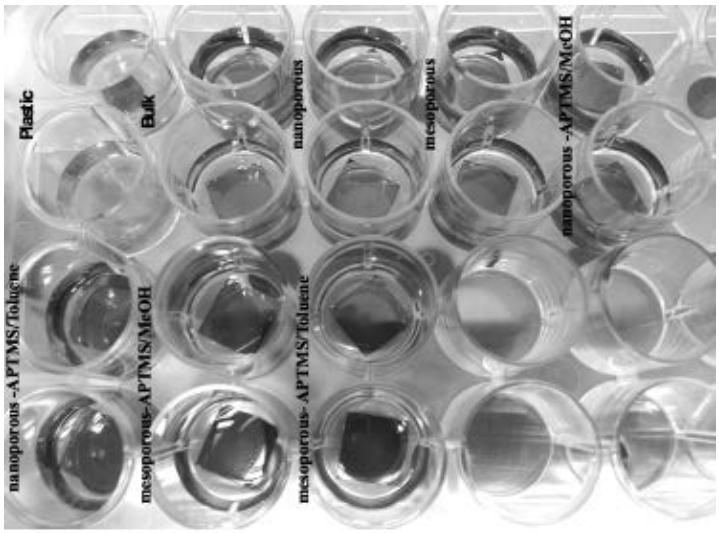

Fig. 2. *DPSCs growing on the scaffold surfaces.*

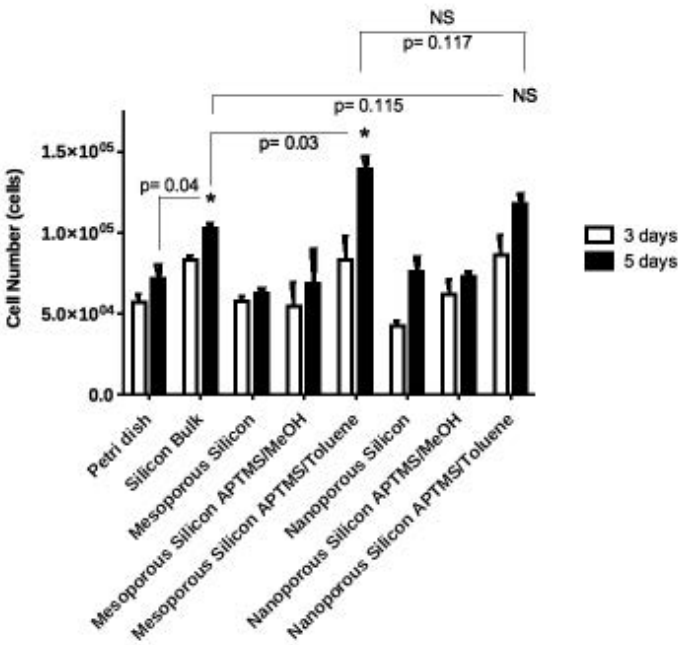

Fig. 3. *Cell proliferation of DPSCs on scaffolds of silicon at 3 and 5 days. The control is DPSCs grown on culture plates and silicon not worked (bulk). The mean with the standard deviation was represented. Statistical significance was assessed by Student's t-test analysis (p values provided, N.S. not significant).*

entire wells (Fig. 1D). The deposits were randomly scattered throughout the adherent layer as single mineralized zones. No mineralisation was evident without induction. These data demonstrated the osteogenic potential of DPSCs. To evaluate DPSC proliferation on the different silicon scaffolds, cells were cultured on them for 3 and 5 days. In the early analysis of our plates, we already observed that at day 1 a small amount of DPSCs was detached from the surface of not-functionalized scaffolds, although we

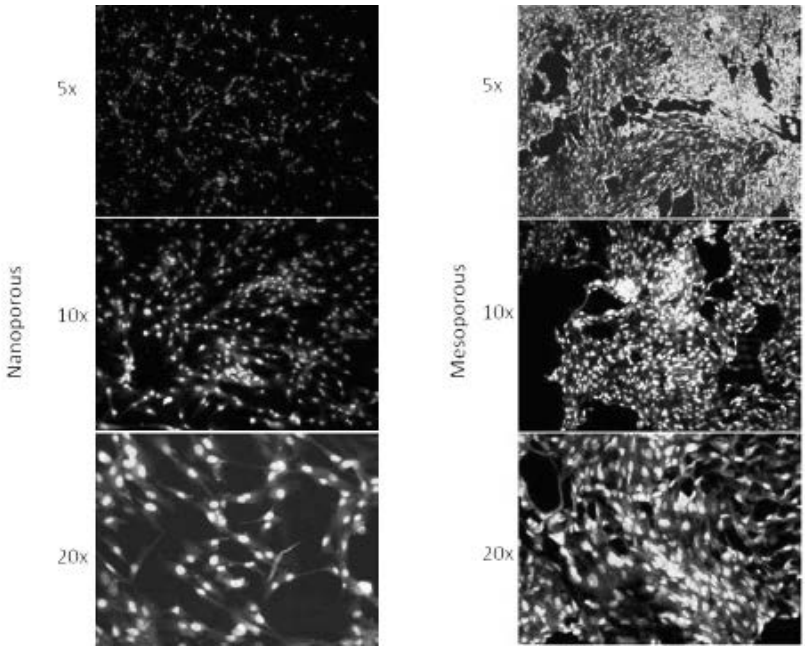

Fig. 4. *Cell-seeded scaffolds. After seeding in the scaffolds, distribution and interaction of the cells were analyzed. Here, cells are presented in white (DNA: 4',6-diamidino-2-phenylindole (DAPI). DPSCs on Nanoporous and Mesoporous silicon scaffolds functionalized with APTMS /Toluene at 5-10-20x magnification. The Mesoporous scaffolds showed the best performances.*

checked the correct adhesion of DPSCs on scaffolds already after 3 h from the cell seeding.

A lower cell detachment was observed on scaffolds functionalized with APTMS/MeOH. The best cell adhesion was achieved on mesoporous and nanoporous scaffolds functionalized with APTMS/ toluene. Moreover, bulk silicon also showed a good cell adhesion on its surface.

DPSC proliferation on the tested silicon scaffolds (Fig. 2) was analyzed at 3 and 5 days: the proliferation assay showed that DPSCs were grown better on silicon bulk than on petri dish (Fig. 3). Moreover, DPSCs seemed to better proliferate onto mesoporous and nanoporous scaffolds functionalized with APTMS/toluene at day 5, compared with the silicon bulk (Fig. 3). However, only DPSCs seeded on mesoporous silicon scaffolds functionalized with APTMS/toluene had a significantly higher proliferation rate compared to silicon bulk.

Although statistically significant difference was not observed between proliferation of DPSCs seeded on mesoporous and nanoporous silicon functionalized with APTMS/toluene, cells seemed to grown better on mesoporous silicon functionalized with APTMS / toluene (Fig. 3). This result was confirmed by DAPI staining as shown in Fig. 4.

In conclusion, these preliminary results suggest that mesoporous silicon-made scaffolds functionalized with APTMS/toluene are able to better induce cell proliferation of DPSCs.

DISCUSSION

The recent literature reported a research by Zhang et al. (1) who tested the ability of DPSCs to grow and differentiate on several scaffolds made from different materials, such as collagen, sintered ceramic and titanium where they demonstrated that DPSCs were able to grow and differentiate into osteocytes, producing a mineralized matrix. The selection of the best material to use for the construction of scaffolds is an important element for obtaining an optimal regeneration of dental tissues (1). The characteristics of the biomaterials can affect cell proliferation and differentiation, therefore, the choice of the biomaterials is crucial to ensure the

quality of the process of formation of new dental tissues from DPSCs.

We compared the effects of different types of silicon scaffolds on DPSC proliferation. Our results showed that DPSCs proliferate more effectively on silicon scaffolds in comparison to petri dish. Moreover, the results indicate that DPSCs grown on mesoporous silicon functionalized with APTMS/toluene showed a higher proliferation rate than cultures on silicon bulk. However, there was no statistically significant difference in the cell proliferative index between nanoporous silicon functionalized with APTMS/toluene and silicon bulk.

This result clearly indicates that silicon scaffolds with different porosity offer a superior performance in supporting cell growth than a common tissue culture plate (TCP).

These assessments are quite new, thus no existing literature is focused on this specific topic.

It would be interesting to further investigate whether the mesoporous silicon scaffolds functionalized with APTMS/toluene are able to promote a higher osteoblast differentiation, if compared to bulk silicon and to the culture plate.

Finally, our study suggests that the material we have verified to be the best-performer can be also an excellent culture substrate for mesenchymal stem cells to use for tissue engineering applications.

REFERENCES

1. Zhang H, Liu S, Zhou Y, et al. Natural mineralized scaffolds promote the dentinogenic potential of dental pulp stem cells via the mitogen activated protein kinase signaling pathway. Tissue Eng part A 2012; 187:677-91.
2. Bluteau G, Luder HU, De Bari C, Mitsiadis TA. Stem cells for tooth engineering. Eur Cell Mater 2008; 16:1-9.
3. Zhang W, Walboomers XF, van Kuppevelt TH, Daamen WF, Bian Z, Jansen JA. The performance of human dental pulp stem cells on different three-dimensional scaffold materials. Biomaterials 2006; 27:5658.
4. Zhang W, Walboomers XF, Wolke JG, Bian Z, Fan MW, Jansen JA. Differentiation ability of rat postnatal dental pulp cells in vitro. Tissue Eng 2005; 11:357.
5. Yu J, Deng Z, Shi J, Zhai H, Nie X, Zhuang H, Li Y, Jin Y. Differentiation of dental pulp stem cells into regular-shaped dentin-pulp complex induced by tooth germ cell conditioned medium. Tissue Eng 2006; 12:3097.
6. Huang GT, Gronthos S, Shi S. Mesenchymal stem cells derived from dental tissues vs. those from other sources: Their biology and role in regenerative medicine. J Dent Res 2009; 88:792-806.
7. Gentile F, La Rocca R, Marinaro G, et al. Differential cell adhesion on mesoporous silicon substrates. ACS Appl Mater Interfaces 2012 27; 4(6):2903-11.
8. Marrelli M, Paduano F, Tatullo M. Cells isolated from human periapical cysts express mesenchymal stem cell-like properties. Int J Biol Sci 2013; 9:1070-78.
9. Tatullo M, Marrelli M, Shakesheff KM, White LJ. Dental pulp stem cells: function, isolation and applications in regenerative medicine. J Tissue Eng Regen Med 2014; doi: 10.1002/term.1899

JOURNAL OF BIOLOGICAL REGULATORS & HOMEOSTATIC AGENTS Vol. 29, no. 4, 999-1005 (2015)

LETTER TO THE EDITOR

HYALURONIC ACID-BASED MEDICAL DEVICE AND ORAL DISORDERS: CAN IT BE USED IN PAEDIATRIC DENTISTRY?

S. D'ERCOLE[1], A. NANUSSI[2], M. TIERI[1], D.F. BARATTINI[3] and D. TRIPODI[1]

[1]Unit of Paediatric Dentistry, Medical, Oral and Biotechnological Sciences, University "G. D'Annunzio" Chieti-Pescara, Italy; [2]Gnato-posturology and cranio-facial pain therapy, Hospital "San Gerardo di Monza", University Milan-Bicocca, Italy; [3]Opera Consulting Srl, Timisoara, Romania

Received May 27, 2015 – Accepted October 22, 2015

Due to its physical and biological characteristics and safety profile, hyaluronic acid is very widely used in numerous clinical conditions, ranging from its best-known use in cosmetic surgery (as a filler and for its ability to promote tissue regeneration and therefore minimise scarring) to lesser-known fields such as ophthalmic surgery, major abdominal surgery (where it is used to prevent the complication of adhesion bands) and intra-articular use. Studies were recently published in which this type of device was also used in paediatric patients for the management of inflammatory disorders of the oral cavity and teething symptoms. As this is a highly topical field for dentists, we felt it would be useful to review the efficacy and safety of the device in the paediatric population treated, and analyse any discrepancies with the results obtained in the adult population. The preparations of hyaluronic acid used in pediatric dentistry, thanks to their anti-inflammatory and angiogenic properties, proved to be very effective in therapy of oral diseases in children. Further clinical research is needed to confirm the effectiveness of these products to dispel doubts about any side effects.

Hyaluronic acid (HA), a polysaccharide found in the connective tissue of vertebrates, is a polymer of glucuronic acid and N-acetyl glucosamine, a member of the family of high-molecular-weight glucosamines. It is one of the main constituents of the extracellular connective tissue matrix of the skin, joints, eyeballs and other tissues, including periodontal tissues. Unlike other glucosamines, the synthesis of which takes place at intracellular level in the endoplasmic reticulum, HA is biosynthesised in the inner portion of the cell plasma membranes by three different synthases: HAS1, HAS2 and HAS3 (1). HAS1 and HAS2 synthesise high-molecular-weight HA, whereas HAS3 generates low-molecular-weight HA; this information is very important, because the two forms appear to be involved in different functions. In humans, the half-life of HA ranges between one and seventy days, depending on the tissue concerned, and its breakdown mainly takes place in the liver and kidneys, to which it is conveyed through the lymphatic system under physiological conditions (2). In healthy tissue, HA is present in the form of a high-molecular-weight polymer, although fragments of HA with a lower molecular weight may accumulate following a trauma or wound. Each of these polymers possesses specific characteristics,

Key words: hyaluronic acid, teething, paediatric patients

Mailing address: Dr Simonetta D'Ercole,
Unit of Paediatric Dentistry,
Medical, Oral and Biotechnological Sciences
University "G. d'Annunzio" Chieti-Pescara,
Via dei Vestini, 31
66100 Chieti, Italy
e-mail: simonetta.dercole@virgilio.it

0393-974X (2015)

DISCLOSURE: ALL AUTHORS REPORT NO CONFLICTS OF INTEREST RELEVANT TO THIS ARTICLE.

Table I. *Studies regarding the use of high-molecular-weight HA in dentistry.*

Study ID	Design	Patients	Treatment	Efficacy Parameters	Outcome
Mesa FL, 2002	Randomized Double-blind Split mouth placebo-controlled	28 adult pat 13 F 8 M Mean age 44,5 years Periodontal disease	HA gel bid for 1 month	Gingival papilla biopsy; grade of inflammatory infiltrate; Proliferation antigen Ki-67	% Pat with moderate-intense inflammatory infiltrate Control: 61.9% HA:28.4% Sign reduction in proliferation index in epithelium (276 vs 514 p= 0.003) and fibroblasts (1.46 vs 3.22 p=0.05) Mean depth of pockets increased with PL (from 2.84 to 3.05 mm), remained the same(2.71) with HA
Jentsch H, 2003	Randomized Double-blind Controlled vs placebo Parallel groups	50 Age: verum mean 29.5+11.00 placebo mean 30.6 +10.1 plaque-induced gingivitis	Twice daily additionally to oral hygiene for a 3-week	API Turesky index, PBI peroxidase, lysozyme	From day 4: API ($p<0.011$). From day 7: PBI ($p<0.001$). Significant decreases vs placebo in peroxydase and lysozyme after 7, 14 and 21 days (P 0.034 and <0.001)
Xu Y, 2004	Randomized Controlled Split mouth vs no treatment	20 Age 28-70 years Chronic parodontitis	Supra- and subgingival scaling Root smoothing + treatment HA 0.2% gel instilled subgingivally Once weekly for 6 weeks	Plaque index (PI) Sulcus-fluid-flow-rate (SFFR) Sulcus bleeding index (SBI) Probing depth (ST) Attachment loss (AL)	After 3 months all parameters had improved in both groups ($p<0.001$). The regression in SFFR was sign faster with HA than without ($p<0.001$).
Pistorius A, 2005	Randomized Controlled Vs no treatment Parallel groups	60 (40 HA, 20 controls) (30 M, 30 F) Age 16-59 years Gingivitis	HA spray for 7 days	Plaque index API Sulcus bleeding index SBI Papilla bleeding index PBI Gingival crevicular fluid flow rate CFFR	API no change. SBI diminished by 22.5% on day 3-4 and a further 10% by day 7 with HA; it diminished by 6.5% with PL. PBI and CFFR improved significantly with HA (from 1.58 to 0.67); from 13.0 to 6.6), no sign change with PL

ranging from the metabolic inertia of stabilised HA used as a filler to the marked biological properties exhibited, in particular, by the polymers with a lower molecular weight (3). HA performs numerous functions, some of which are associated with its ability to trap water in its molecular structure, in quantities far exceeding its own weight. This property of HA ensures the optimum bodily distribution of fluids in the tissues, through which low-molecular-weight nutrients originating from the capillary flow are freely diffused, and at the same time slows the transit of substances with a higher molecular weight in direct proportion to their molecular weight. As a result of these characteristics HA performs a major role in homeostasis, participating in tissue fluid regulation and the passage of molecules through the interstitial compartment, and simultaneously acting as a barrier in the intra-tissue diffusion of macromolecules and harmful external substances. The particular viscosity of HA also suggests that

it may act during skeletal movements as an ideal lubricant, allowing the articular surfaces to glide and reducing the loads on them; important analgesic effects appear to be specifically due to this viscosity (4). Finally, much of the elasticity and stability of the extracellular collagen matrix is associated with the presence of HA. In view of its physicochemical characteristics, HA has a protective effect on the skin and mucosa due to its film-forming component, and that special property provides excellent bioadhesion, unlike other substances not containing HA which slide off immediately after application (5).

HA is a polymer consisting of a molecule of two sugars repeated numerous times; in nature, the length of the chain therefore varies considerably, and both low- and high-molecular-weight polymers can be simultaneously present, where the former act in a radically different way from the latter. There is no codified and accepted distinction regarding the limits according to which a given HA-based product can be correctly defined as belonging to the oligosaccharides or as low- or high-molecular-weight HA, because when a product is manufactured the exact value of the molecular weight is not determined, only a range. It therefore appears more correct to distinguish between products based on HA with a high or low molecular weight on the basis of their ranges, and their consequent specific characteristics and properties; in fact, products containing low-molecular-weight HA perform an angiogenic action, whereas those with high molecular weight mainly perform tissue reconstruction activities. Due to its particular characteristics (biocompatibility, biodegradability, low immunogenicity and viscoelasticity) and its versatile properties, it has been suggested that HA could be an ideal substance for some medical and cosmetic applications (6).

DISCUSSION

Hyaluronic acid in dentistry

The introduction of professional HA-based products in dentistry is recent. Gingival tissue contains about 0.8% HA under normal physiological conditions, while the percentage rises to 2.1% in the same tissue under conditions of hyperplasia. These data indicate the important relationship between HA and the proliferation of connective tissue cells (7). Studies conducted on animals have demonstrated that the application of HA at the wound site leads to increased reconstruction and healing of the damaged, exposed pulp tissue, due to the more rapid formation of the fibrin clot and to anti-inflammatory activity at cell level. More rapid differentiation of fibroblasts and osteoblasts and dentine repair has also been observed (8). It has also been demonstrated that the accelerated repair due to increased HA production may be associated with growth factor of platelet origin, which is known to exercise a proliferative action on the gingival fibroblasts (5). It has also been found that the marked bacteriostatic effect of HA may inhibit the localisation of pathogenic organisms in the periodontal pockets (9). The osteoinductive power of high-molecular-weight HA had already been postulated in a study conducted with transmission electron and scanning microscopes on the healing of wounds induced in the femur of the rat. After mechanically inducing standardised bone wounds in rats, the authors filled some of the cavities with an HA-based preparation (10). Other research has also been conducted to evaluate the possible use of HA as a support for periodontal treatment. In particular, it has been demonstrated that increased HA production in the periodontal ligament, induced by basic fibroblast growth factor (bFGF), promotes the formation of new cement and periodontal wound healing (11).

On the basis of knowledge of the regularisation role performed by HA in tissues in which an inflammatory process is in progress, clinical trials have been conducted in dentistry, in particular in gingivitis (12), post-surgical treatment of incisions of the buccal cavity (13), and various pathological periodontal conditions (14, 15).

Despite their heterogeneity, due to the different types of HA used in view of its above-mentioned intrinsic characteristics, the dose administered and the administration route, these studies represent an important confirmation of the therapeutic possibilities of HA in stopping bleeding, reducing swelling and promoting healing of damaged tissues. Finally, one study has indicated the potential of HA to modulate matrix synthesis and increase cell growth in gum lesions (16), while other studies have postulated the use of HA in surgical debridement to increase the weight of bone tissue (14). These clinical results are

therefore strongly indicative of the possible use of HA-based film-forming devices in the treatment of numerous conditions of the oral cavity (5).

For use in clinical practice, as already mentioned, it is important to distinguish between the low- and high-molecular-weight types of HA, as the biological behaviour of the molecule changes considerably with variation in weight. However, this distinction is not always stated in the preparations available on the market, because it requires a standardisation that is difficult and expensive to achieve in a manufacturing process. The table below summarises some important studies published in the literature regarding the use of high-molecular-weight HA in dentistry (Table I).

Studies conducted by Jentsch and Mesa (12, 17) were randomized, double-blind, and placebo-controlled, while the two remaining (15, 18) were controlled to no treatment.

When evaluating the efficacy of the product, the usual indicators of periodontal inflammation were generally used, such as redness, swelling and bleeding, evaluated with scores; in only one study, a randomised double-blind trial conducted on 28 subjects with a clinical history of periodontitis (17), was the primary efficacy parameter a gingival biopsy, used to evaluate the degree of inflammatory infiltrate and the expression of antigen Ki-67 proliferation, measured by immunohistochemical techniques. From the histological standpoint, it was found that HA reduced the level of inflammation and the extent of inflammatory infiltrate, and that the mechanisms underlying those activities are probably associated with a barrier effect against bacteria, the bond between HA and *Treponema denticola*, transmembrane cell signal inhibition induced by the CD44 membrane receptors, and a reduction in the expression of proliferation antigen Ki-67. From the clinical standpoint, these studies also agree that HA-based products reduce the degree of inflammation compared with a placebo or no treatment. This finding is particularly important in periodontal disease because it can prevent the formation of periodontal pockets, which are considered to be one of the agents that lead to loss of the tooth over time.

The efficacy of HA in treating pain was evaluated in a randomised, double-blind, placebo-controlled clinical trial (19). The trial was conducted on a population of 120 patients suffering from recurrent aphthous stomatitis (RAS), a very common inflammatory disorder of the oral cavity (which affects about 20% of the population), characterised by severe pain. Treatment with corticosteroids and antimicrobials for prophylactic purposes is required in the most severe cases, but treatment usually involves drugs (such as anaesthetics) to reduce pain, and/or medicaments that produce a barrier able to protect the tissue against aggression by external agents. The use of HA to treat this disorder was suggested in view of its ability to form a barrier covering the ulcer, thereby reducing pain and facilitating healing. The HA-based gel, administered two or three times a day for 7 days, rapidly reduced pain and the average number of new ulcers. Similar results were obtained in a mirror study to the preceding one (randomised, double-blind and placebo-controlled) conducted on 124 patients suffering from oral lichen planus (OLP), a chronic inflammatory disorder involving the mucosa of the oral cavity, especially in middle-aged women (20). It is believed to be caused by an immune response to antigens in the oral epithelium, which justifies the use of topical steroids as the most common treatment. HA was applied 4-5 times a day for 28 days. The sensation of pain significantly decreased from the first application of HA (which did not occur in the placebo group), and the average size of the area of ulceration/erosion was also reduced ($p<0.05$).

Hyaluronic acid in paediatric dentistry

A study of Farronato (21) did not merely involve verifying the already recognised anti-oedema and anti-inflammatory action of the fluid formulation of HA, but also analyzed its differential efficacy between children who wore fixed braces and those with no orthodontic treatment. This led to the observation that after the application of HA, there was a marked percentage decrease in Bleeding On Probing (BOP) index in all subjects treated (from 21.64±11.07 to 7.87±5.59), and also in the sub-group of 43 subjects who wore braces (from 20.59±11.25 to 8.33±6.14). In this study cited, a total of 200 children were treated with these products based on high-molecular-weight HA, which always exhibited a high level of safety, a factor of crucial importance for use in small children.

Teething is a physiological condition frequently

associated with inflammation of the gingival mucosa; it primarily presents with the eruption of the deciduous teeth at a crucial stage of the child's growth (from 3 months to about 3 years of age) and, in a less perceptible form, the eruption of the permanent teeth (after 6 years of age). Teething involves the classic array of symptoms, including irritability, hypersalivation, diarrhoea, gingivitis, low appetite, insomnia, skin rashes, coughing and vomiting (22). Apart from folk remedies and homeopathic products, for which only retrospective cohort studies exist (23), those symptoms are generally treated with topical agents based on anaesthetics (mainly lidocaine and benzocaine) and salicylates. Lidocaine is a local anaesthetic which is rapidly absorbed through the mucosa, thus bringing rapid, albeit temporary, pain relief; however, it should be borne in mind that prescriptions of products containing lidocaine for children under six years of age should be extremely limited, and they should never be prescribed if the patient's case history indicates that sensitivity is suspected (24). The use of analgesics containing benzocaine is not considered by the American Academy of Pediatrics (AAP) to be an advisable therapeutic strategy for teething in children under two years of age (25). It is also known that the active ingredients used in these medicaments could potentially inhibit the child's pharyngeal reflex, leading to a risk of suffocation. The AAP also notes that the use of topical analgesics can give rise to local reactions, convulsions and acquired methaemoglobinaemia (25). Salicylates can be classed as minor analgesics, and are similar to lidocaine in that they rapidly penetrate the mucosa, leading to fast pain reduction. The therapeutic advantage compared with lidocaine lies in their anti-inflammatory and antipyretic properties, which also give rise to a reduction in swelling (26). Some authors (27) state that although Reye's syndrome is specific to aspirin used in cases of viral infections, many paediatricians and pharmacists advise against the use of salicylates for teething. Frequent topical applications of salicylates to the oral mucosa can produce chemical burns (28). Finally, Paynter and Alexander (29) reported a case of infantile salicylate poisoning following repeated, incongruous administration by the mother of a teething gel containing salicylates.

In view of the properties demonstrated in other disorders of the oral cavity (protection of the mucosal surface; reduction of swelling and consequently pain; reduction of inflammation) the use of HA-based products to treat teething and the correlated symptoms has been proposed. In this context, the use of HA-based medical devices would guarantee therapeutic efficacy while not containing pharmacological ingredients (and therefore excluding systemic absorption of the product and ensuring absence of toxicity after swallowing), while anti-inflammatories and local anaesthetics could be reserved for the most severe cases, under strict medical supervision.

Rosu et al. (30) performed a study with an HA-based product for teething symptoms conducted on 18 children, aged between 6 and 36 months, and a subsequent comparative study in which 48 subjects were treated for 7 days (24 with HA and 24 with 0.33% lidocaine and 0.10% cetylpyridinium chloride). The children presented the following symptoms: pain, swelling and redness; they did not have subcutaneous mucosal lacerations, and had not used local anaesthetics and/or anti-inflammatory drugs. This study confirms that the HA-based product can be considered a useful therapeutic tool for the treatment of teething in infants and the results demonstrated that the reduction in symptoms (pain, swelling and redness) was significantly greater in the patients who used HA than in the control group.

CONCLUSIONS

The rapid change in the oral cavity during paediatric age requires fast renewal of periodontal tissues. HA, a polysaccharide naturally occurring in the oral mucosa, plays an essential role in maintaining the functional balance required for intercellular exchange. The preparations of hyaluronic acid used in paediatric dentistry, thanks to their anti-inflammatory and angiogenic properties, proved to be very effective in therapy of oral diseases in children. Future research will be based on the use of hyaluronic acid preparations as an adjuvant in the treatment of various forms of gingivitis in children. Further clinical research is needed to confirm the effectiveness of these products and to dispel doubts about any side effects.

REFERENCES

1. Itano N, Kimata K. Mammalian hyaluronan synthases. IUBMB Life 2002; 54(4):195-9.
2. Fraser JR, Laurent TC, Laurent UB. Hyaluronan: its nature, distribution, functions and turnover. J Intern Med 1997; 242(1):27-33.
3. McDonald J, Camenisch TD. Hyaluronan: genetic insights into the complex biology of a simple polysaccharide. Glycoconj J 2002; 19(4-5):331-9.
4. Balazs EA. Analgesic effect of elastoviscous hyaluronan solutions and the treatment of arthritic pain. Cells Tissues Organs 2003; 174(1-2):49-62.
5. Dahiya P, Kamal R. Hyaluronic Acid: a boon in periodontal therapy. N Am J Med Sci 2013; 5(5):309-15.
6. Liao YH, Jones SA, Forbes B, Martin GP, Brown MB. Hyaluronan: pharmaceutical characterization and drug delivery. Drug Deliv 2005; 12(6):327-42.
7. Suresh R, Puvanakrishnan R, Dhar SC. Alterations in human gingival glycosaminoglycan pattern in inflammation and in phenytoin induced overgrowth. Mol Cell Biochem 1992; 115(2):149-54.
8. Sasaki T, Kawamata-Kido H. Providing an environment for reparative dentine induction in amputated rat molar pulp by high molecular-weight hyaluronic acid. Arch Oral Biol 1995; 40(3):209-19.
9. Pirnazar P, Wolinsky L, Nachnani S, Haake S, Pilloni A, Bernard GW. Bacteriostatic effects of hyaluronic acid. J Periodontol 1999; 70(4):370-4.
10. Sasaki T, Watanabe C. Stimulation of osteoinduction in bone wound healing by high-molecular hyaluronic acid. Bone 1995; 16(1):9-15.
11. Shimabukuro Y, Ichikawa T, Takayama S, et al. Fibroblast growth factor-2 regulates the synthesis of hyaluronan by human periodontal ligament cells. J Cell Physiol 2005; 203(3):557-63.
12. Jentsch H, Pomowski R, Kundt G, Göcke R. Treatment of gingivitis with hyaluronan. J Clin Periodontol 2003; 30(2):159-64.
13. Galli F, Zuffetti F, Capelli M, Fumagalli L, Parenti A, Testori T, Esposito M. Hyaluronic acid to improve healing of surgical incisions in the oral cavity: a pilot multicentre placebo-controlled randomised clinical trial. Eur J Oral Implantol 2008; 1(3):199-206.
14. Engström PE, Shi XQ, Tronje G, Larsson A, Welander U, Frithiof L, Engstrom GN. The effect of hyaluronan on bone and soft tissue and immune response in wound healing. J Periodontol 2001; 72(9):1192-200.
15. Xu Y, Höfling K, Fimmers R, Frentzen M, Jervøe-Storm PM. Clinical and microbiological effects of topical subgingival application of hyaluronic acid gel adjunctive to scaling and root planing in the treatment of chronic periodontitis. J Periodontol 2004; 75(8):1114-8.
16. Haase HR, Bartold PM. Enamel matrix derivative induces matrix synthesis by cultured human periodontal fibroblast cells. J Periodontol 2001; 72(3):341-8.
17. Mesa FL, Aneiros J, Cabrera A, Bravo M, Caballero T, Revelles F, del Moral RG,O'Valle F. Antiproliferative effect of topic hyaluronic acid gel. Study in gingival biopsies of patients with periodontal disease. Histol Histopathol 2002; 17(3):747-53.
18. Pistorius A, Martin M, Willershausen B, Rockmann P. The clinical application of hyaluronic acid in gingivitis therapy. Quintessence Int 2005; 36(7-8):531-8.
19. Nolan A, Baillie C, Badminton J, Rudralingham M, Seymour RA. The efficacy of topical hyaluronic acid in the management of recurrent aphthous ulceration. J Oral Pathol Med 2006; 35(8):461-5.
20. Nolan A, Badminton J, Maguire J, Seymour RA. The efficacy of topical hyaluronic acid in the management of oral lichen planus. J Oral Pathol Med 2009; 38(3):299-303.
21. Farronato G, Tremolati M, Ceschel G, Falciola L. Hyaluronic Acid in the management of gingivitis in young patients. International Tissue Care Symposium. Abst, September 3, 2002, Frankfurt am Mein.
22. Noor-Mohammed R, Basha S. Teething disturbances; prevalence of objective manifestations in children under age 4 months to 36 months Med Oral Patol Oral Cir Bucal 2012; 17(3): e491–4.
23. Thompson EA, Bishop JL, Northstone K. The use of homeopathic products in childhood: data generated over 8.5 years from the Avon Longitudinal Study of Parents and Children(ALSPAC). J Altern Complement Med 2010; 16(1):69-79.
24. Balit CR, Lynch AM, Gilmore SP, Murray L,

Isbister GK. Lignocaine and chlorhexidine toxicity in children resulting from mouth paint ingestion: a bottling problem. J Paediatr Child Health 2006; 42(6):350-3.

25. American Academy of Pediatrics. Teething Care and Anticipatory Guidance. https://www2.aap.org/oralhealth/pact/ch2_sect5.cfm. Accessed July 16, 2015.
26. Jones M. Teething in children and the alleviation of symptoms. J Fam Health Care 2002; 12(1):12-3.
27. Steward M. Infant care. Teething troubles. Community Outlook 1988; 11:27-8.
28. Sapir S, Bimstein E. Cholinsalicylate gel induced oral lesion: report of case. J Clin Pediatr Dent 2000; 24(2):103-6.
29. Paynter AS, Alexander FW. Salicylate intoxication caused by teething ointment. Lancet 1979; 2(8152):1132.
30. Rosu S, Montanaro F. A single site, open non controlled study of efficacy and tolerability of two formulations of the medical device Gengigel Baby gel (0.2% Hyaluronic Acid) in the topical treatment of teething in infants. Medicine in Evolution 2012; 17(2):409-15

JOURNAL OF BIOLOGICAL REGULATORS & HOMEOSTATIC AGENTS Vol. 29, no. 4, 1007-1011 (2015)

LETTER TO THE EDITOR

MEDICAL TREATMENT OF JOINT PROSTHESIS: INDICATION, OPPORTUNITIES AND LIABILITY PROFILES

L. MOLFETTA[1], C. TROMPETTO[2] and E. SILVESTRI[3]

[1]Research Center on Osteoporosis and Osteoarticular Diseases, School of Medical and Pharmaceutical Sciences, University of Genoa, Italy; [2]Neurosciences Department, School of Medical and Pharmaceutical Sciences, University of Genoa, Italy; [3]Department of Radiology and Interventional Ultrasound, Evangelical Hospital International, Genoa, Italy

Received March 12, 2015 – Accepted November 11, 2015

Orthopaedic specialists should completely and sequentially manage osteoarthritis, from the onset to the prosthesis, with no attitude of resignation, complying with national and international Guidelines (GLs) and abiding by the criteria of appropriateness of drugs, rehabilitation and orthopaedic device prescription, in line with the ethics of the medical profession. The GLs are a paper that rationalises the quantity of existing information for a disease, without abusing the decision of the doctor; a large volume of scientific knowledge is concentrated in a format that is easily accessible to doctors when carrying out their work. The use of drugs has taken on a connotation of a rational and multifactorial choice, rather than an accidental and incremental choice - inspired only by safety, rather than efficacy criteria. The Notes compiled by the Italian Medicines Agency - a legal instrument to define the reimbursability of medicines and, therefore, an instrument for managing pharmaceutical expenditure – are, in reality, a means to guarantee the appropriateness of the use of medicines, orienting the therapeutic choices according to established Guidelines. In the specific case of osteoarthritis, the knowledge of the GLs is the most appropriate and complete approach towards the disease, in the context of its pathogenetic complexity in its natural history. Moreover, pharmacological treatment of the subchondral osteometabolic damage becomes necessary when documented by magnetic resonance or a scintigraphy; the bone-related pain cannot be challenged through symptomatic analgesic treatment alone.

Osteoarthritis (OA) requires a multi-purpose medical treatment, aimed both at controlling pain and other related symptoms, through the management of all the pathogenetic (mechanical and inflammatory) components which cause it, and at postponing the final stage of the implantation (1). Orthopaedic specialist should completely and sequentially manage the disease, from the onset to the prosthesis, with no attitude of resignation, complying with national and international Guidelines and biding by the criteria of appropriateness of drugs, rehabilitation and orthopaedic device prescription, in line with the ethics of the medical profession. In fact, patients require the specialist to provide them with a global overview on arthritic disease, a thoughtful prognostic judgement concerning its development, educational

Key words: osteoarthritis, guidelines, subchondral bone, antiresorptives, professional liability

Mailing address:
Prof. Luigi Molfetta,
Orthopedics and Traumatology Center,
School of Medicine and Pharmaceutical Sciences
Via L.B. Alberti 4
16132, Genova, Italy
e-mail: prof.molfetta@gmail.com

0393-974X (2015)

DISCLOSURE: ALL AUTHORS REPORT NO CONFLICTS OF INTEREST RELEVANT TO THIS ARTICLE.

advice and, finally, prescriptions of drugs and other therapeutic aids as effective as possible (2).

Guidelines on osteoarthritis

Before the advent of evidence-based medicine, which led to the drafting of the national and international Guidelines (GLs), the treatment of arthritis relied exclusively on the specialist's individual competence and on the specific approach of his/her specialisation; the disease was considered almost in function of the surgical therapy by the orthopaedist, mainly using rehabilitation resources by the physiatrist and using pharmacological resources by the rheumatologist (3). The patient was mainly directed towards one of the three therapies and could take advantage of the "integrated" treatment only by involving more specialists. Therefore, the therapy was sectional and fragmentary, with the risk of losing a chance of appropriate treatment for the specific clinical moment; the early indication for a tibial osteotomy in a constitutional varus knee, free from chondropathy, made this surgery effectively preventive; the only control of pain caused the chondropathy over years, changing a decisive surgical intervention into a procrastinating intervention (4). At the end of the '90s, the GLs were considered, in the first instance, as a duty, an instrument for raising objections against the work of the doctor. A valuable instrument of update, knowledge, work, clinical governance, indicator of quality, pertinence, efficacy and cheapness of the performances was included in everyday practice. Thanks to the GLs, the scientific vision of OA became totalising, trans-specialised, cancelling the specialists' "race for patient". The GLs have been defined as "recommendations systematically developed to support physicians and patients in deciding the proper management of specific clinical conditions" (5). They are the result of a multidisciplinary, multi-specialized and critical interpretation of the multiple available information, in order to orient the clinical practice for every clinical need via diagnostic-therapeutic decision-making instruments. The GLs are a paper that rationalises the quantity of existing information for a disease, without abusing the decision of the doctor; a large volume of scientific knowledge is concentrated in a format that is easily accessible to doctors when carrying out their work. The use of drugs has taken on a connotation of a rational and multifactorial choice, rather than an accidental and incremental choice - inspired only by safety, rather than efficacy criteria (6).

Therefore, International Scientific Societies, European League Against Rheumatism(EULAR), American College of Rheumatology (ACR) and American Academy of Orthopaedic Surgeons (AAOS) drew up the GLs on OA, through an analysis carried out by specialists; a deep analysis of the literature was carried out with the stringent requirements of the real evidence, drawing the appropriate conclusions on the effectiveness of the available therapies. Different levels of recommendation were identified and the best scientific path was suggested, always in respect of the specific choice of the doctor for every patient.

EULAR GLs, in particular, were published in three documents, in 2003, 2004 and 2007, for OA of the knee, the hip and the hand, respectively (7-9). They were summarised in 10 points, from the educational-behavioural aspects, to the indication of the different classes of drugs and of the rehabilitation devices, and, finally, to the surgical indication. The EULAR GLs were transposed in Italy through two documents of Consensus, related to OA of the knee and the hip, in order to adapt some technical elements, such as the dose of paracetamol (limited to 3g/die) (10). In the Italian Consensus it was underlined that pain, in addition to the degenerative-mechanical factor, was also the expression of an inflammatory state; the inflammation involved all the joint tissues and even the subchondral bone, able to characterise the worsening of the disease, without suggesting the osteometabolic treatment (11).

National healthcare system notes on arthritis

The Notes carried out by the Italian Medicines Agency - a legal instrument to define the reimbursability of medicines and, therefore, an instrument for managing pharmaceutical expenditure – are, in reality, a mean to guarantee the appropriateness of the use of medicines, orienting the therapeutic choices according to established GLs. AIFA Notes, more than other regulations, are inspired to the criteria of evidence-based medicine, that is based on random and multiple clinical trial results. The Notes are periodically reviewed

by the Drug Authority in order to modernise the indications with regard to the new evidence in the scientific Literature concerning efficacy and safety (12). Therefore, the Ministry Notes concerning the prescribability and reimbursability of drugs by the National Healthcare System have a double purpose: confirm the indication of a molecule, restating what was verified and established about its distribution agreement and, secondly, allow free drugs only for the actual carriers of the specific disease. Therefore, unlike the GLs, the Ministry Note combines the indication and the economic criteria. Note 66 of AIFA states the reimbursability of the NSAIDs for osteoarthritis in the phase of pain or inflammation, besides the connectivity arthropathies, neoplastic pain and acute attacks of gout.

Comprehensive treatment of OA

EULAR GLs for knee and hip arthritis provide three sequential steps for pain management, in relation to the response to the therapy itself. Therefore, paracetamol (dose ≤ 3 g/day, even in addition to other drugs for OA and a good safety profile), NSAIDs (non-selective or COX-2 inhibitors, topical or systemic) and opiates (with or without paracetamol) have been placed in reference to the clinical response of pain management (7-9). Symptomatic slow-acting drugs for OA (SYSADOA) support the previous ones and have scientific evidence only for the knee, despite a certain scepticism in prescribing them (10).

The ACR GLs concern hand, hip and knee OA cumulatively (6). Tramadol or oral (COX-2 inhibitors included) or topical NSAIDs - the latter especially for elder patients - are recommended for hand OA. As for knee and hip OA, besides paracetamol, oral or topical NSAIDs are recommended, in particular COX-2 inhibitors, the greater selectivity and gastrointestinal safety of which is highlighted, combined with proton pump inhibitors in patients with gastrointestinal symptoms or gastrointestinal bleeding during the year prior to treatment; opiates are not mentioned for the long-term treatment, while intra-articular injections of corticosteroids and hyaluronan are recommended in patients with an inadequate response to the initial therapy (13).

AAOS GLs for OA of the knee, published in 2013, recommend tramadol (strongly recommended) or NSAIDs (oral or topical), both COX-2 inhibitors and non-selective, depending on the patient (14).

During 10 years of use of the GLs, clinical experience made it necessary to replace and complete the therapeutic options for pain in OA, since it is not possible to disregard the inflammatory component characterising the natural course of the disease (15). The involvement of the juxta-articular subchondral bone is considered the main event of the arthritic process at onset and, especially, in the development of OA. The subchondral bone may go through a first stage of mechanical reaction (subchondral sclerosis) and a phase of real osteometabolic alteration, which leads to a BMD decrease, well expressed in the joint magnetic resonance (MR) with bone oedema or real compartmental algodystrophy. (16). The pharmacological management of OA, currently focusing on drugs for pain such as paracetamol, selective and non-selective NSAIDs and opiates, must involve the pharmacological control of pain that is related to the juxta-articular osteometabolic alteration, through bisphosphonates, favouring the ones that can control the bone loss, inflammation and pain.

Ethical and professional profile

With regard to responsibility, there is an increase in the legal actions against members of the medical profession, with a nearly exclusive economic importance. This incites the exponential increase so much as to create an autonomous sub-system on civil liability (17) in the legal system, stating a substantial and procedural 'favour' towards the patient, considered as the weaker party in the relationship of care and assistance. The physician adopts a defensive stance, almost unconscious, both in the diagnostic path (tests, advice, investigations) and, especially, in the choice of treatment. Defensive medicine is not the antidote against judicial harassment, but it becomes "another chapter" of judicial attention. In the specific case of arthritis, the GLs are the most appropriate and complete approach towards the disease, in the context of its pathogenetic complexity in its natural history. Moreover, the pharmacological treatment of the subchondral osteometabolic damage becomes necessary when documented by an MR or scintigraphy. The bone-related pain cannot be challenged through the symptomatic analgesic treatment alone, therefore, the use of antiresorptive

bisphosphonates may find indication, being in reality a local or compartment joint osteoporosis (18). The use of clodronate combines the antiresorptive and analgesic and/or anti-inflammatory effectiveness, healing BMD loss and joint pain for the metabolic component (19). The control of the loss of the local juxta-articular mineral density contributes to prepare the joint for the implantation of the prosthesis and for the post-surgical osteogenesis, avoiding "biological fatigue" of the bone during periprosthetic osseointegration (20, 21).

In the Code of Ethics related to "Diagnostic Investigations and Therapeutic Treatments" art. 12 states that "The prescription of a diagnostic investigation and/or a therapy involves the professional and ethical responsibility of the physician and follows a detailed diagnosis or, at least, a founded diagnostic suspicion. The physician has autonomy in the planning, choice and application of every diagnostic and therapeutic aid, even during hospitalisation, but the patient is free to refuse, taking the responsibility on himself. Prescriptions and treatments must follow updated and tested scientific achievements in order to use the resources correctly, always for the benefit of the patient. The physician must have an adequate knowledge of the nature and effect of drugs, their indications, contraindications, interactions and predictable individual reactions, as well as characteristics of use of the diagnostic and therapeutic means (22).

In conclusion, in arthritis, it is not convenient, correct or appropriate to divide the various components of the disease (pain, osteometabolic pathology, functional deficit) assigning each one to a different specialist without a coordination, as prescribed in the Code of Conduct and tacitly required by the patient who entrusts him/herself to our care. The "extrapolation of pain" from the pathogenetic and clinical context of the patient with OA and his/her "isolated" treatment, defined pain management, leads the physician away from the spirit of the Guidelines, with consequent loss of the therapeutic unity belonging to the orthopaedic-rheumatology-physiatry field.

REFERENCES

1. Creamer P, Hochberg MC. Osteoarthritis. Lancet 1997; 350:503-9.
2. Viapiana O, Povino MR, Liuzza S, Troplini S, Adami S. Artrosi: fisiopatologia e nuove indicazioni terapeutiche. GIBIS 2009; 10(2):5-18.
3. Sackett DL, Rosemberg WMC, Muir Gray LA, et al. Evidence based medicine: what it is and what it isn't. BMJ 1996; 312:71-77
4. Brouwer RW, Huizinga MR, Duivenvoorden T, et al. Osteotomy for treating knee osteoarthritis. Cochrane Database Syst Rev accessed 2014 Dec 13.
5. Plebani M, Trenti T. eds. Praticare il governo clinico: qualità, efficacia e professionalità in medicina. Centro Scientifico Editore, Torino, 2002.
6. Woolf SH, Grol R, Hutchinson A, et al. Potential benefits, limitations, and harms of clinical guidelines. BMJ 1999; 318:527-30.
7. K M Jordan, N K Arden, M Doherty, et al. EULAR Recommendations 2003: an evidence based approach to the management of knee osteoarthritis: Report of a Task Force of the Standing Committee for International Clinical Studies Including Therapeutic Trials (ESCISIT). Ann Rheum Dis 2003; 62:1145-55.
8. Zhang W, Doherty M, Arden N, et al. EULAR evidence based recommendations for the management of hip osteoarthritis: report of a task force of the EULAR Standing Committee for International Clinical Studies Including Therapeutics (ESCISIT). Ann Rheum Dis 2004; 64:669-81.
9. Zhang W, Doherty M, Leeb BF, et al. EULAR evidence based recommendations for the management of hand osteoarthritis – report of a task force of the EULAR Standing Committee for International Clinical Studies Including Therapeutics (ESCISIT). Ann Rheum Dis 2007; 66:377-88.
10. Punzi L, Canesi B, Carrabba M. et al. Consensus italiana sulle raccomandazioni dell'EULAR 2003 per il trattamento dell'artrosi del ginocchio. Reumatismo 2004; 56(3):190-201.
11. Bhandari M, Bajammal S, Guyatt GH et al. Effect of Bisphosphonates on Periprosthetic Bone Mineral Density After Total Joint Arthroplasty: a meta analysis. J Bone Joints Surg (A) 2005; 87(2):293-301.
12. Genovese U, Mariotti P, Zoja R. Le Linee guida e la responsabilità sanitaria. Maggioli Editore, Rimini,

2013.

13. Hochberg MC, Altman RD, Toupin K. et al. American College of Rheumatology 2012 Recommendations for the Use of Nonpharmacologic and Pharmacologic Therapies in Osteoarthritis of the Hand, Hip, and Knee. ACR Arthritis Care Res 2012; 64:465-74.
14. American Accademy of Orthopaedic Surgeons. Treatment of osteoarthritis of the knee.Evidence-based-Guideline, 2nd Edition, 2013.
15. Bianchi G, Molfetta L, Saggini R, Italian survey on the use of anti-inflammatory drugs in Osteoarthritis. Int J Immunopatholand Pharmacol 2014; 27(4):467-71.
16. Roemer FW, Eckstein F, Hayashi D, Guermazi A. The role of imaging in osteoarthritis. Best Pract Res Clin Rheumatol 2014; 28(1):31-60.
17. Introna F. Responsabilità professionale medica e gestione del rischio. Riv It Med Leg 2007; 3:666-73.
18. Ji WP, Wang XL, Ma MQ, Lan J, Li H. Prevention of early bone loss around the prosthesis by administration of anti-osteoporotic agents and influences of collared and non-collared femoral stem prostheses on early periprosthetic bone loss. Eur J Orthop Surg Traumatol 2013; 23(5):565-71.
19. Carbone LD, Nevitt MC, Wildy K, et al. The relationship of antiresorptive drug use to structural finding and symptoms of knee osteoarthritis. Arthritis Rheum 2004; 50 (11):3516-25.
20. Prieto-Alhambra D, Javaid MK, Judge A, et al. Association between bisphosphonate use and implant survival after primary total arthroplasty of the knee or hip: population based retrospective cohort study. BMJ 2011; 343:d7222. doi: 10.1136/bmj.d7222.
21. Hilding M, Aspenberg P. Postoperative clodronate decreases prosthetic migration: 4-year follow-up of a randomized radiostereometric study of 50 total knee patients. Acta Orthop 2006; 77(6):912-6
22. Mariotti P, Serpetti A, Ferrario A, Zoja R, Genovese U. La medicina difensiva, Maggioli Editore, Rimini, 2011.

JOURNAL OF BIOLOGICAL REGULATORS & HOMEOSTATIC AGENTS Vol. 29, no. 4, 1013-1015 (2015)

LETTER TO THE EDITOR

BIOPHYSICAL STIMULATION AND THE PERIPROSTHETIC BONE: IS THERE A RATIONALE IN THE USE OF PULSED ELECTROMAGNETIC FIELDS AFTER A HIP OR KNEE IMPLANT?

L. MASSARI[1], R. OSTI[1], V. LORUSSO[1], S. SETTI[2] and G. CARUSO[1]

[1]*Orthopaedic Institute of University, Ferrara, Italy*; [2]*IGEA Spa, R&D Department, Carpi(MO), Italy*

Received March 4, 2015 - Accepted November 17, 2015

The biophysical stimulation of bone and cartilage, using Pulsed ElectroMagnetic Fields (PEMF), covers many different aspects of bone formation and/or cartilage repair, such as healing of delayed or non-union of fracture, bone necrosis, osteocartilagineous defects. To date there are no specific data on the effects of PEMFs in osteointegration of prosthetic implants but there are some papers that denote clinical advantages, in terms of early recovery, in patients treated with these procedures. Considering these clinical applications, PEMF stimulation around hip or knee joint implants could be useful to reduce the bone oedema, pain and to reduce excessive bone reabsorption around the femoral stems.

The effect of Pulsed ElectroMagnetic Fields (PEMF) on the bone and the cartilage is the subject of many studies, most of which consider the positive effect of this biophysical stimulation in the bone healing processes (1-3). *In vitro* and *in vivo* animal studies demonstrated that PEMFs enhance the fibrous callus formation and the osteoblastic activity during osteogenesis (4).

Electric and magnetic stimulation of the osteogenesis began with the study of Fukada and Yasuda (5) followed by that of Bassett and Becker (2).

Bone has two different types of electrical signal: one type after a mechanical stimulus and one type at rest without mechanical stimuli. Both types of electrical signals have been considered as local factors controlling the bone modelling/remodelling phenomena and the bone healing processes. Since the beginning of studies on the electrical properties of bone, authors considered that the ability to bring these signals from the outside into the bone could be of clinical interest, especially in cases of altered healing processes (6-11).

At present there are three methods to electrically stimulate bone:

a) continuous currents directly applied into the bone using implanted electrodes (faradic systems);

b) alternate currents induced from the outside using Pulsed ElectroMagnetic Fields (PEMF) (inductive systems);

c) alternate currents induced from the outside using pure electrical fields (capacitive systems).

The capacitive and inductive systems are non-invasive; in particular the inductive methods do not need direct contact between the machine and the skin of the patient.

Several papers highlight the efficacy of PEMFs in the healing of delayed union or non-union of fractures (12-17). These are conditions in which there is a delay in the healing processes and PEMFs give the

Key words: biophysical stimulation bone, pulsed electromagnetic fields, total hip arthroplasty, total knee arthroplasty

Mailing address: Prof. L. Massari,
Orthopaedic Institute of University,
Via Aldo Moro 8,
44124 Ferrara, Italy
Tel.: +390532237110
Fax: +390532757463
e-mail: msl@unife.it

0393-974X (2015)

DISCLOSURE: ALL AUTHORS REPORT NO CONFLICTS OF INTEREST RELEVANT TO THIS ARTICLE.

possibility to recover and restart the process in order to heal the fracture. For these reasons the possibility to use PEMF to stimulate the periprosthetic bone is an intriguing option for orthopaedic surgeons, both for primary and especially for revision cases. To date, we have no definitive indications for the use of PEMF to enhance periprosthetic osseointegration or to avoid periprosthetic bone remodelling, but several papers are present in the literature regarding the analgesic effects of PEMF stimulation in painful or loose hip prostheses.

Rispoli and coll. (18) affirmed that electrical stimulation can be useful in case of painful hip prostheses. Kennedy and coll. (19) affirmed that PEMF treatment could be useful in delaying the prosthetic revision. Konrad and coll. (20), considering 24 patients with non-infected loosed femoral implants, affirmed that PEMFs are useful in treating pain and functional limitations. They also found better aspects in bone scans examinations, but not in radiographic imaging.

Pipino and Molfetta (21) confirmed that PEMFs could enhance osseointegration in the uncemented revision, especially in cases in which the Wagner trans-femoral approach had been used. In these cases PEMF could accelerate the healing of the femoral bone windows. Dallari and coll. (22), in a double-blind clinical and densitometric study on the effects of PEMF in hip revisions with trans-femoral approaches, denoted that the periprosthetic bone grew better in the stimulated group compared to the placebo group, and also the clinical aspects, measured with the Merle d'Aubignè score, were significantly higher in the stimulated group.

Recently, a double-blind study (23) on the use of PEMF after knee prosthesis demonstrated that biophysical stimulation permits to reduce post-operative pain and the use of drugs against pain and that the improvement continues also after 3 post-operative years.

In conclusion, the data from the literature and the great amount of experimental and clinical experience on the use of PEMF in situations in which there is a lack of bone healing processes (delayed or non-union of fractures, femoral head necrosis, etc.) confirm that biophysical stimulation can be useful in the treatment of periprosthetic bone problems, such as pain, oedema, flogosis and probably also in cases of excessive bone remodeling in the early phases.

REFERENCES

1. Bassett CAL, Becker RO. Generation of electric potentials in bone in response to mechanical stress. Science 1962; 137:1063-64.
2. Bassett CAL, Mitchell SN, Sawnie R. Pulsing electromagnetic field treatments in ununited fractures and failed arthrodeses. JAMA 1982; 247:623-28.
3. Bassett CAL, Valdez MG, Hernandez E. Modification of fracture repair with selected pulsing electromagnetic fields. J Bone Joint Surg Am 1982; 64A:888-95.
4. Cane' V, Botti P, Soana S. Pulsed magnetic fields improve osteoblast activity during the repair of an experimental osseous defect. J Orthop Res 1993; 11:664.
5. Fukada E, Yasuda I. On the piezoelectric effect of bone. J Phys Soc Japan 1957; 12:121-28.
6. Friedenberg ZB, Andrews ET, Smolenski BI, Pearl BW, Brighton CT. Bone reaction to varying amounts of direct current. Clin Obstet Gynecol 1970; 131:894-99.
7. Becker RO, Murray DG. The electrical control system regulating fracture healing in amphibians. Clin Orthop 1970; 73:169-209.
8. Borgens RB. Endogenous Ionic Currents Traverse Intact And Damaged Bone. Science 1984; 225:478-82.
9. Chiabrera A, Grattarola M, Parodi G, Marcer M. Interazione tra campo elettromagnetico e cellule. Le Scienze 1984; 192:78-94.
10. frost HM. The biology of fracture healing: an overview for clinicians. Part I and II. Clin Orthop 1989; 248:283-309.
11. Behari J. Electrostimulation and bone fracture healing. Biomed Mater Eng 1991; 18:235-54.
12. Hinsenkamp M, Ryaby J, Burny F. Treatment Of non-union by pulsing electromagnetic field: European multicenter study of 308 cases. Reconstr Surg Traumatol 1985; 19:147-51.
13. Frykman GK, Taleisnik J, Peters G, et al. Treatment of nonunited scaphoid fractures by pulsed electromagnetic field and cast. J Hand Surg [Am]

1986; 11:344-49.
14. Sharrard WJ. A double-blind trial of pulsed electromagnetic fields for delayed union of tibial fractures. J Bone Joint Surg Br 1990; 72(3):347-55.
15. Traina GC, Fontanesi G, Costa P, et al. Effect of electromagnetic stimulation on patients suffering from nonunion. A retrospective study with a control group. J Bioelectricity 1991; 10:101-17.
16. Cebriàn JL, Gallego P, Francès A, et al. Comparative study of the use of electromagnetic fields in patients with pseudoarthrosis of tibia treated by intramedullary nailing. Int Orthop 2010; 34:437-40.
17. Assiotis A, Sachinis NP, Chalidis BE. Pulsed electromagnetic fields for the treatment of tibial delayed unions and nonunions. A prospective clinical study and review of the literature. J Orthop Res 2012; 7:24.
18. Rispoli FP, Corolla FM, Mussner R. The use of low frequency pulsing electromagnetic fields in patients with painful hip prosthesis. J Bioelectricity 1988; 7:181-87.
19. Kennedy WF, Roberts GC, Zuege RC, Dicus WT. use of pulsed electromagnetic fields in the treatment of loosened cemented hip prostheses: a double blind trial. Clin Orthop, 1993; 286:198-205.
20. Konrad K, Sevcic K, Foldes K, Piroska E, Molnar E. Therapy with pulsed electromagnetic fields in aseptic loosening of total hip prostheses: a prospective study. Clin Rheumatol 1996; 15:325-28.
21. Pipino F, Molfetta L. I C.E.M.P. nella Chirurgia Di Riprotesizzazione Dell'anca. In Traina GC, Pipino F, Massari L, Molfetta L, Cadossi R "Modulazione Biofisica Della Osteogenesi Mediante Campi Elettromagnetici Pulsanti", Walberti Ed. Lugo (RA), 1999; p. 103-14.
22. Dallari D, Fini M, Giavaresi G, Del Piccolo N, Stagni C, Amendola L, Rani L, Gnudi S, Gidino R. Effects of pulsed electromagnetic stimulation on patients undergoing hip revision prostheses: a randomized prospective double-blind study. Bioelectomagnetics 2009; 30:423-30.
23. Moretti B, Notarnicola A, Moretti L, Setti S, De Terlizzi F, Pesce V, Patella V. I-ONE therapy in patients undergoing total knee arthroplasty: a prospective, randomized and controlled study. BMC Musculoskelet Disord 2012; 13:88.

LETTER TO THE EDITOR

ALKALINE PHOSPHATASE LEVEL IN GINGIVAL CREVICULAR FLUID DURING TREATMENT WITH QUAD-HELIX

A. DELLI MAURI[1], M. PETRINI[2], D. VITALE[2], S. TECCO[2], F. FESTA[2], E. BARBATO[1] and G. SPOTO[2]

[1]Department of Head and Neck Pathology, University Sapienza, Rome, Italy;
[2]Department of Medical, Oral and Biotechnological Sciences, University G. d'Annunzio, Chieti-Pescara, Italy

Received April 1, 2015 – Accepted October 21, 2015

The aim of this work is to assess the level of the human alkaline phosphatase enzyme (ALP) during palatal expansion with Quad-Helix (QH) appliance. A total of twenty-two orthodontic patients characterized by contraction of the upper jaw, that needed application of a QH in order to treat their condition, were included in this study. Gingival crevicular fluid (GCF) was collected at four different times: before cementation (T0), after two weeks (T1), after four weeks (T2) and after one year (T3) from application of QH. In each patient maxillary first molars, right (UM-right) and left (UM-left), which were connected with bands to QH, were used for testing; first lower molars were used as Controls (LM-right, LM-left). Data show that ALP level in tension sites was proportional to the average increase of the inter-molar distance; on the contrary, the enzymatic level in compression sites was characterized by an inverse trend. The only exception to this phenomenon was recorded after one year (T3), when the increase of ALP level in both sites of tension and compression was ascribed to a mild inflammation due to bacterial plaque accumulation. The level of ALP in control sites was constant for the whole period of observation. The described ALP fluctuations in accordance with the inter-molar distance increment, shows that the main action of QH on bone remodelling was exerted during the fourth week (T2); for this reason, the monitoring of this enzyme could be used as a marker of effective function of the QH appliance.

Quad Helix (QH) is an orthodontic appliance that has four active helix springs, connected to the first upper molars via bands, which expand the upper arch by acting on the teeth. The QH generates orthodontic transverse forces up to 5 N, inducing a dental and a skeletal effect of slow palatal expansion (1, 2). In young patients, sutures easily open to allow expansion under light forces regardless of expander type, so the QH seems equally effective for the Haas and the Hyrax appliances for posterior cross-bite correction, inter-molar expansion, and inter-molar angulation (3, 4). Boysen et al. studied the three-dimensional evaluation of dentoskeletal changes after posterior cross-bite correction by QH in 34 children (5). They found that QH causes greater expansion and buccal translation of teeth, whereas the removable expander gives more buccal tipping and long-term relapse. Frank et al. found that QH in young patients exerted a 6:1 ratio between the orthodontic and the orthopaedic expansion (6). In

Key words: quad helix, alkaline phosphatase (ALP), bone metabolism, orthodontics

Mailing address: Prof Giuseppe Spoto,
Full Professor of Dental Material and Medical Chemistry,
University G. d'Annunzio,
Via dei Vestini, 31 66100 Chieti, Italy
Tel.: +39 0871 355 4066 Fax: +39 0871 355 4375
e-mail: spoto@unich.it

0393-974X (2015)

DISCLOSURE: ALL AUTHORS REPORT NO CONFLICTS OF INTEREST RELEVANT TO THIS ARTICLE.

young patients, Slow Maxillary Expansion (SME) is said to provide the maximum rate at which the midface sutures can adapt, with minimum tearing and hemorrhaging compared with Rapid Maxillary Expansion (RME) (7). Nevertheless, during the treatment by means of RME the clinician can appreciate on a day-by-day basis the effectiveness of the expander; on the contrary, the SME, due to the very small and continuous changes, does not permit such clinical evaluation. A viable option is represented by the monitoring of tissue remodeling through the quantification of alkaline phosphatase level in gingival crevicular fluid (GCF), which represents a consolidated and repeatable method in orthodontic research (8). GCF is an exudate, the constituents of which are derived from a variety of sources, including microbial dental plaque, host inflammatory cells, host tissues and serum. During orthodontic tooth movement, the early response of periodontal tissues to mechanical stress is an acute inflammatory reaction.

Mechanical stress from orthodontic appliances is believed to induce cells in the periodontal ligament (PDL) to form biologically active substances, such as enzymes and cytokines, responsible for connective tissue remodelling. Bone remodelling, that occurs during orthodontic tooth movement, is a biologic process involving an acute inflammatory response in periodontal tissues (9). In hard bony tissues alkaline phosphatase is implicated in the process of mineralization; consequently, forces deriving from the orthodontic treatment affect its level, which is significantly greater in dental sites of tension than in sites of compression (10). As a result of orthodontic force application, ALP produced in the periodontium diffuses into gingival crevicular fluid (GCF). However its level in GCF can be influenced by alveolar bone turnover events and therefore reflects metabolic changes in the periodontium (10). Biochemical analysis of the GCF has provided a non-invasive model for investigating the cellular response of the underlying PDL during orthodontic tooth movement *in vivo* (11). The repeatability of gingival crevicular fluid collection and the quantification of biomarkers, like alkaline phosphatase level, has been demonstrated (8). However, there are no studies in literature on the monitoring of QH treatment through the collection of GCF and the ALP quantification. The objective of this study is to assess whether the GCF-ALP could be used as a marker of active bone remodelling during QH treatment.

MATERIALS AND METHODS

Twenty-two orthodontic patients (plus one patient who dropped out from the study), 14 females and 8 males, (age range 11-21 years, mean, 15.5), were included in the study. Informed consent was received from the patients to participate in the study. In order to eliminate the variability given by dental eruption in ALP level, only subjects who had completed permutation were included in the study, because the variability of the anatomical structures is smaller in permanent dentition than during the mixed one.

The following inclusion criteria were observed: permanent dentition; a contraction of the upper jaw treatable by the appliance of a QH mounted on cemented bands on the maxillary first molars; good general health; no use of anti-inflammatory drugs during the month preceding the study; probing depth values not exceeding 3 mm in the whole dentition; no radiographic evidence of periodontal bone loss; and full-mouth plaque score and a full-mouth bleeding score less than or equal to 20% (after probing with a 20-g controlled force probe).

Clinical treatment

All subjects received repeated oral hygiene instructions for the use of toothbrush, dental floss, and inter-dental brush during two months preceding the baseline. All participants underwent professional oral hygiene with ultrasonic instruments. In each patient, maxillary first molars, right (UM-right) and left (UM-left), which were connected with bands to QH, were used for the testing (Test group); first lower molars were used as Controls (LM-right, LM-left).

The QH was activated before cementation so that the bands did not match up perfectly with the molars, but they exceeded inter-molar distance by a half-labial cusp. Activation was then repeated once after a period of 3 months from the cementation and it was made extraorally. In total, two activations of Quad Helix were carried out. Strength of 400 g for an 8 mm of activation was used, as suggested by many studies concerning the QH appliance (12, 13). The appliance was stabilized in the mouth giving a radicolo-buccal activation torque of approximately 45° and a distal rotation activation torque of approximately 40°.

Gingival crevicular fluid (GCF) collection

Each crevicular site included in the study was isolated with cotton rolls. Before the GCF collection,

any supragingival plaque was removed with cotton pellets, and a gentle air stream was directed toward teeth surface for 5 seconds to dry the area. GCF was collected with standardized sterile endodontic paper tips sized 30 (Inline; Torino, Italy) inserted 1 mm into the gingival crevice mesio-buccal sites and left *in situ* for 30 seconds. Care was taken to avoid mechanical injury. Samples were taken immediately before QH cementation (T0), and then 2 weeks (T1), 4 weeks (T2), and 1 year (T3) after its cementation.

Alkaline phosphatase activity assay

Following collection, paper points were transferred into plastic vials. GCF total volume was determined for each sample as previously described (14). ALP level was assayed with a spectrophotometer at 405 nm (model 8453, Hewlett Packard; Waldgrohn, Germany) (14). The paper tips used for sampling were incubated at 30°C, with less than 0.5°C fluctuation, for 20 min in a substrate containing p-nitrophenyl phosphate (10 mmol/L), carbonate buffer (pH 10.2 +/- 0.1 at 30°C), mannitol (200 mmol/L), and $MgCl_2$ (3 mmol/L), to a total volume of 1.0 mL. One of the by-products of ALP hydrolysis of p-nitrophenyl phosphate, p-nitrophenol, was monitored in order to indirectly quantify the ALP level. The rate of increase in absorbance at 405 nm was detected by a UV/vis-spectrophotometer as the p-nitrophenol formed.

We used 18.45 as conversion factor in order to quantify, into enzyme level units, the GCF ALP starting from the millimolar absorbance of the p-nitrophenol (1 U =1 μmol of p-nitrophenol released per minute at 30°C). Final results were reported as total ALP level (mUnits/sample). During the experimental period the QH was clinically inspected to ensure a correct function and avoid problems to the palatal mucosa.

Statistical analysis

Statistical analysis was carried out by using Statview 5.0 Software, (SAS Institute, Cary, NC, USA). ANOVA for repeated measures and Fisher PLSD's analysis were followed by post hoc tests, Bonferroni–Dunn methods.

RESULTS

The ALP level in sites of tension (Fig. 1) and compression (Fig. 2) of Tests and Controls were evaluated and compared with the average increments

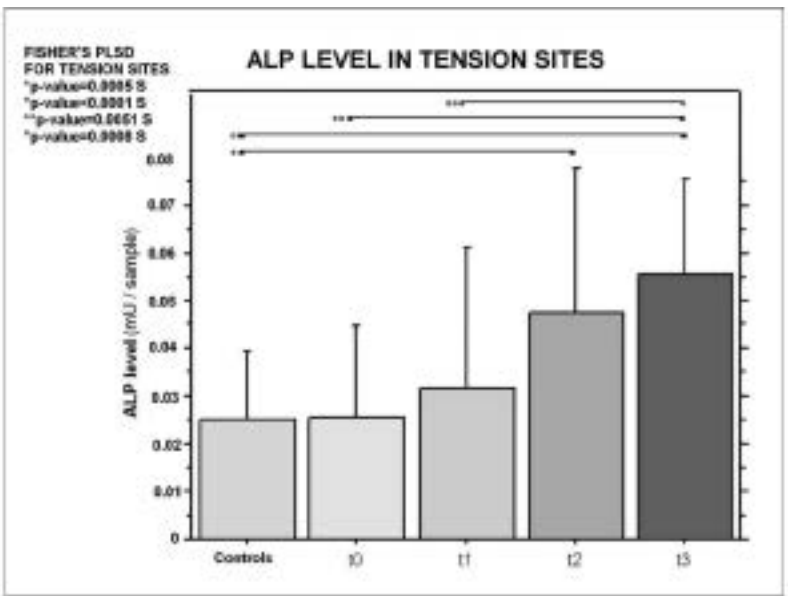

Fig. 1. *ALP level in GCF from tension and control sites related to the time span of application of the Quad Helix. ALP level in Control sites remained constant during the whole treatment. On the contrary the enzymatic activity in sites of tension increased during the whole application of the Quad Helix; statistically significant differences were found between T0, T2 and T3 (Significance < 0.005). Considering that between T2 and T3 only a small increment of the inter-molar distance occured, (also because the last activation of Quad Helix was carried out in the third month), the Authors believe that the increment of ALP in test sites, but not in controls could be expression of neutrophilic ALP, produced as a consequence of inflammation due to the plaque retention of the appliance.*

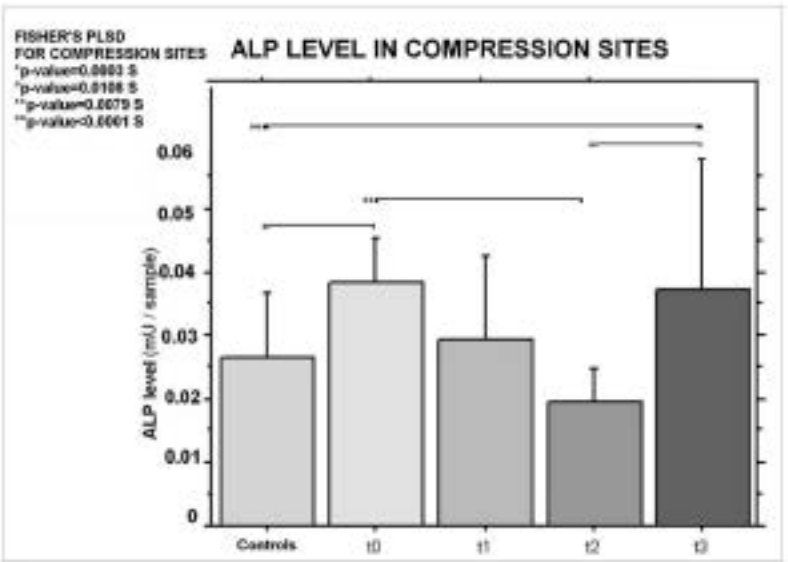

Fig. 2. *ALP level in GCF from compression and control sites related to the time span of application of the Quad Helix. ALP level in Control sites remained constant during the whole treatment. On the contrary the enzymatic activity in sites of compression were characterized by the decrement of ALP activity between T0 and T2, but in the last part of the application of Quad Helix, between T2 and T3, the level increased. Considering that during this period only a small increment of the inter-molar distance occurs, (also because the last activation of Quad Helix was carried out in the third month), the Authors believe that the increment of ALP in test sites, but not in controls could be expression of neutrophilic ALP, produced as a consequence of inflammation due to the plaque retention of the appliance.*

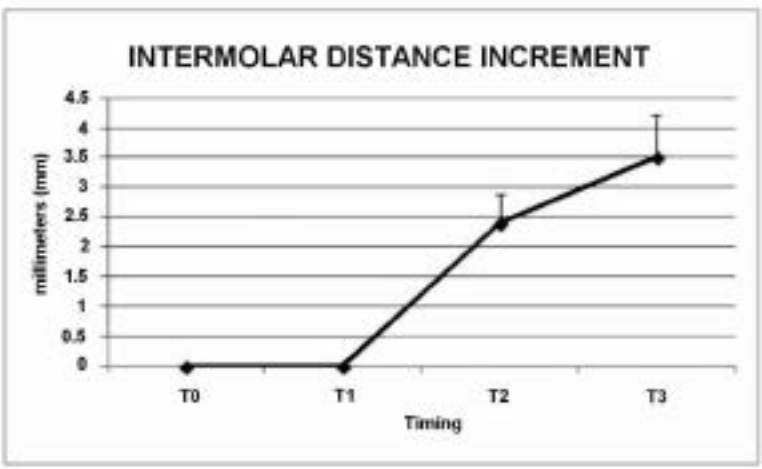

Fig. 3. *Average variation of the inter-molar distance as a function of the timing. The maximum increment of this measurement, occured between T1 and T2.*

of the inter-molar distance of the patients (Fig. 3). Average values were statistically analyzed and described. The ALP level in sites of tension were directly correlated with the increment of the inter-molar diameter. Between T0 and T1 the inter-molar diameter remained constant, indeed at this point there was only a slight decrease in the average levels of ALP in compression sites, and a slight increase in ALP level was detected in tension sites. However, all the variations detected between T0 and T1 were not statistically significant. At T2, the upper dental arch showed an average expansion value of 2.4 mm +/- 0.5 as inter-molar diameter (Fig. 3).

This expansion resulted in a reduction of ALP level in sites of compression (Fig. 2); statistically significant differences were found between T0 and T2, p-value=0.0003. On the contrary, the level of the enzyme had greatly increased in tension sites (p-value=0.0005). At T3, a mean increase of inter-molar distance of 3.5 +/- 0.7 mm was registered in respect to T0, before cementation (Fig. 3). However, the average expansion measured between four weeks (T2) and one year (T3) was 1.1 mm. At this stage, a slight increase of ALP level was found in tension sites, with a p-value < 0.0001 between T0 and T3; p=0.0008 between T1 and T3. No statistically significant differences in ALP level were found between T2 and T3 in tension sites. Contrarily, with regard to the ALP level in sites of compression, a sharp increase was found at T3 and there were statistically significant differences with T1 and T2.

DISCUSSION

ALP levels were detected in patients with permanent dentition during the active palatal expansion via QH. The monitoring of tissue remodeling through the use of biomarkers represents a new frontier in orthodontic research as well as clinical practice. Few studies have been focused on the dosage-effect relationship between mechanical stimuli and cellular reaction or, in other words, the optimal *in vitro* stress magnitude; 1.0 g/cm^2 of compressive force seems to significantly increase the expression of bone morphogenetic proteins (BMPs) (15). The objective of the study was to assess the reliability of this biomarker to verify the effectiveness of the QH treatment. In fact, orthodontic forces alter the PDL (periodontal ligament) vascularity and blood flow, resulting in local synthesis and release of various key molecules, such as neurotransmitters, cytokines, growth factors, colony-stimulating factors, and arachidonic acid metabolites (16). These molecules can evoke many cellular responses by various cell types in and around teeth, providing a favorable microenvironment for tissue deposition or resorption (17). One of these mediators is the bone ALP, which is synthesized by osteoblasts and acts as an initiator of bone matrix biomineralization (18, 19). It is essential for bone deposition, indeed it hydrolyzes nonorganic pyrophosphate, which is a potent inhibitor of the mineralization processes (20, 21). ALP activity in control sites remained constant during the whole treatment with QH. On the contrary, test sites were characterized by a fluctuation of the enzyme level (Fig 2) that seemed to be directly correlated to the inter-molar increment (Fig 1). At T1, no palatal expansion or tooth movement were recorded, according to the lag phase of approximately 21 days that occurs before tooth movement (22).

At this stage the fluctuation of ALP levels underwent only moderate changes, both at tension and compression Test sites. However, there were no significant differences between Test and Control (Fig. 2). The ALP level significantly changed at T2, that corresponded to an average expansion of 2.4 mm +/- 0.5 of inter-molar diameter. The increment of ALP level in tension sites and the decrement in compression ones agrees with Takimoto's study (23). He studied the fluctuation of ALP level in PDL of rats subjected to orthodontic forces. After one day, alkaline phosphatase was moderate on the tension side and slight on the pressure side of cervical regions. At the third day alkaline phosphatase was detected as strongly increased in the tension site. In the five-day experiment, numerous osteoblasts and calcifying periodontal ligaments adjacent to the alveolar bone showed the strongest acid and alkaline phosphatase level. In another histological study it was observed that in marginal tensional areas cell proliferation occured between 36 and 50 h and lasted for 10 days or 3 weeks (6). Moreover, a longitudinal study, realized by Insoft in 1996, on three female subjects in orthodontic treatment, found that ALP peaked between the first and third weeks, followed

by an increase in acid phosphatase between the third and sixth weeks (24). A recent study examined the changes of ALP activities in GCF during rapid palatal expansion in thirty-eight patients within an age range similar to the one in the present study (25). ALP level significantly increased from 7-day activation to 28-day retention in the control and experimental group, and there was statistically significant difference between the control and the experimental group in retention from 7 days to 28 days. The Authors believe that the increment of ALP activity in compression sites at T3 in respect to Control ones reflects the higher susceptibility to inflammation, due to anatomical reasons and to the augmented plaque accumulation promoted by the presence of QH. Indeed, the emergence of Steno's duct predisposes the upper arch to higher plaque and calculus accumulation (26, 27). This hypothesis is in agreement with the literature; in fact GCF ALP also reflects the periodontal status. In fact,ALP is also produced by neutrophils as a consequence to bacterial infections (28).

An increase of ALP can be associated to inflammation and subgingival microbiological changes, which can occur as a consequence of plaque accumulation, after orthodontic appliance placement (29, 30). Furthermore, ALP fluctuations at T3 cannot be correlated with QH forces, because the last activation of the appliance had been performed at the 3rd month and a less relevant increment of inter-molar distance occurred during this period (between T2 and T3).

In conclusion, the results suggest that: ALP monitoring associated to QH allows to appreciate the smallest and continuous changes that cannot be detected by a clinical evaluation; the main action of the Qh was exerted during the fourth week: the maximum intermolar distance and ALP increment in tension sites and its decrease in compression ones were recorded; on the contrary, the concomitant peak of ALP level in both tension and compression sites, that does not happen in sites of Control, is the expression of neutrophilic ALP, due to inflammation caused by the plaque accumulation increased by the presence of the appliance; ALP level during treatment with QH, associated with adequate control of oral hygiene, could be used as a marker of the effective action of the appliance; and the GCF ALP monitoring might represent an instrument for clinicians to evaluate dento-alveolar development and could also be used for settling forensic disputes. However, further specific studies are needed to confirm this field of application.

ACKNOWLEDGEMENTS

The Authors would like to thank Drs Maurizio Ferrante, Paolo Trentini and Lorenzo Barassi for the revision of the paper.

REFERENCES

1. Reitan K. The initial tissue reaction incident to orthodontic tooth movement as related to the influence of function; an experimental histologic study on animal and human material. Acta Odontol Scand Suppl 1951; 1-240.
2. Shundo I, Kobayashi Y, Endo T. Short-term treatment effects of quad-helix on maxillomandibular expansion in patients with maxillary incisor crowding. Odontology 2012;76-86. doi: 10.1007/s10266-011-0028-z.
3. Huynh T, Kennedy DB, Joondeph DR, Bollen AM. Treatment response and stability of slow maxillary expansion using Haas, hyrax, and quad-helix appliances: a retrospective study. Am J Orthod Dentofacial Orthop 2009; 136:331-9.
4. Bell RA. A review of maxillary expansion in relation to rate of expansion and patient's age. Am J Orthod 1982; 81:32-7.
5. Boysen B, La Cour K, Athanasiou AE, Gjessing PE. Three-dimensional evaluation of dentoskeletal changes after posterior cross-bite correction by quad-helix or removable appliances. Br J Orthod 1992; 19(2):97-107.
6. Frank SW, Engle GH. The effects of the maxillary quad-helix appliance expansion on cephalometric measurements in growing orthodontic patients. Am J Orthod Dentofacial Orthop 1982; 878-89.
7. Huynh T, Kennedy DB, Joondeph DR, Bollen AM. Treatment response and stability of slow maxillary expansion using Haas, hyrax, and quad-helix appliances: a retrospective study. Am J Orthod Dentofacial Orthop 2009; 136:331-9. doi: 10.1016/j.ajodo.2007.08.026.

8. Perinetti G, Di Leonardo B, Di Lenarda R, Contardo L. Repeatability of gingival crevicular fluid collection and quantification, as determined through its alkaline phosphatase activity: implications for diagnostic use. Journal of Periodontal Res 2013; 48:98-104.
9. Nishijima Y, Yamaguchi M, Kojima T, Aihara N, Nakajima R, Kasai K. Levels of RANKL and OPG in gingival crevicular fluid during orthodontic tooth movement and effect of compression force on releases from periodontal ligament cells in vitro. Orthod Craniofac Res 2006; 9:63-70.
10. Batra P, Kharbanda O, Duggal R, Singh N, Parkash H. Alkaline phosphatase activity in gingival crevicular fluid during canine retraction. Orthod Craniofac Res 2006; 9:44-51.
11. Uitto VJ. Gingival crevice fluid—an introduction. Periodontol 2000 2003; 31:9-11.
12. Bell RA, LeCompte EJ. The effects of maxillary expansion using a quad-helix appliance during the deciduous and mixed dentitions. Am J Orthod 1981; 79:152-61.
13. Chaconas SJ, Alba y Levy JA. Orthopedic and orthodontic applications of the quad-helix appliance. Am J Orthod 1977; 72:422-28.
14. Spoto G, Fioroni M, Rubini C, Tripodi D, Di Stilio M, Piattelli A. Alkaline phosphatase activity in normal and inflamed dental pulps. J Endod 2001; 27(3):180-2.
15. Mitsui N, Suzuki N, Maeno M, Yanagisawa M, Koyama Y, Otsuka K, Shimizu N. Optimal compressive force induces bone formation via increasing bone morphogenetic proteins production and decreasing their antagonists production by Saos-2 cells. Life Sci 2006; 78:2697-706.
16. Krishnan V, Davidovitch Z. Cellular, molecular, and tissue-level reactions to orthodontic force. Am J Orthod Dentofacial Orthop 2006; 129:469.e1-32.
17. Davidovitch Z, Nicolay OF, Ngan PW, Shanfeld JL. Neurotransmitters, cytokines and the control of alveolar bone remodeling in orthodontics. Dent Clin North Am 1988; 32:411-35.
18. Aubin J.E. Regulation of osteoblast formation and function. Rev End Met Dis. 2001; 2:81-94.
19. Ramirez-Yanez GO, Symons AL. Prostaglandin E2 affects osteoblast biology in a dose-dependent manner: an in vitro study. Arch Oral Biol 2012; 57:1274-81.
20. Coleman JE. Structure and mechanism of alkaline phosphatase. Ann Rev Biophys Biomol Struct 1992; 21:441-83.
21. Judex S, Gupta S, Rubin C. Regulation of mechanical signals in bone. Orthod Craniofac Res 2009; 12:94-104.
22. Iwasaki LR, Haack JE, Nickel JC, Morton J. Human tooth movement in response to continuous stress of low magnitude. Am J Orthod Dentofacial Orthop 2000; 117:175-83.
23. Takimoto K, Deguchi T, Mori M. Histochemical detection of acid and alkaline phosphatases in periodontal tissues after experimental tooth movement. J Dent Res 1968; 47:340.
24. Insoft M, King GJ, Keeling SD. The measurement of acid and alkaline phosphatase in gingival crevicular fluid during orthodontic tooth movement. Am J Orthod Dentofacial Orthop 1996; 109:287-96.
25. Wei FL, Wang CL, Liu DX, Guo J, Ke HF, Guo XX. Changes of aspartate aminotransferase and alkaline phosphatase activities in gingival crevicular fluid during rapid palatal expansion. Shanghai Kou Qiang Yi Xue 2007; 16:168-71.
26. Volpe AR, Kupczak LJ, King WJ. In vivo calculus assessment, Part III: scoring techniques, rate of calculus formation, partial mouth exams vs. full mouth exams in intra-examiner reproducibility. Periodontics 1967; 5:184-93.
27. Trombelli L. Susceptibility to gingivitis: a way to predict periodontal disease? Oral Health Prev Dent 2004; 2:265-9.
28. Karlsson A, Khalfan L, Dahlgren C, Stigbrand T, Follin P. Neutrophil alkaline phosphatase activity increase in bacterial infections is not associated with a general increase in secretory vesicle membrane components. Infect Immun 1995; 911-6.
29. Perinetti G, Paolantonio M, D'Attilio M, D'Archivio D, Tripodi D, Femminella B, Festa F, Spoto G. Alkaline phosphatase activity in gingival crevicular fluid during human orthodontic tooth movement. Am J Orthod Dentofacial Orthop 2002; 122:548-56.
30. Perinetti G, Varvara G, Salini L, Tetè S. Alkaline phosphatase activity in dental pulp of orthodontically treated teeth. Am J Orthod Dentofacial Orthop 2005; 128:492-6.